frontiers | Research Topics

Modulation of the immune system by bacteria: From evasion to therapy

Edited by
Marina De Bernard, Maria Kaparakis-Liaskos and Mario M. D'Elios

Published in
Frontiers in Immunology

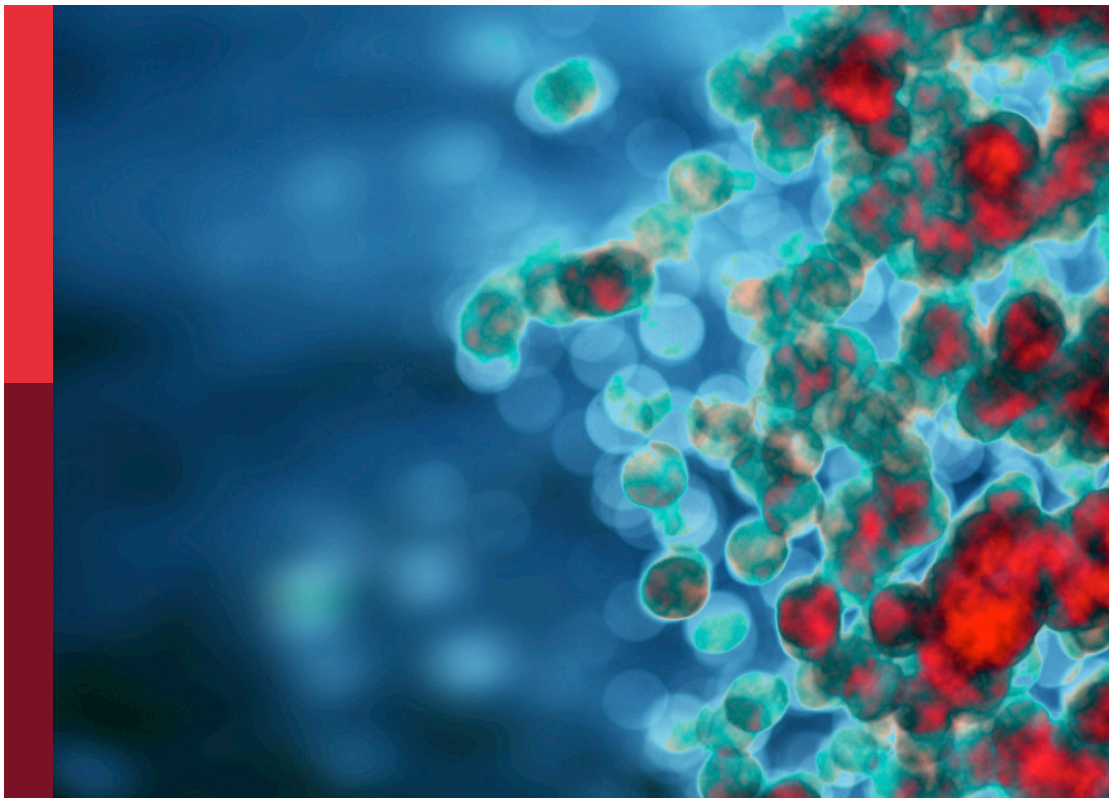

FRONTIERS EBOOK COPYRIGHT STATEMENT

The copyright in the text of individual articles in this ebook is the property of their respective authors or their respective institutions or funders. The copyright in graphics and images within each article may be subject to copyright of other parties. In both cases this is subject to a license granted to Frontiers.

The compilation of articles constituting this ebook is the property of Frontiers.

Each article within this ebook, and the ebook itself, are published under the most recent version of the Creative Commons CC-BY licence. The version current at the date of publication of this ebook is CC-BY 4.0. If the CC-BY licence is updated, the licence granted by Frontiers is automatically updated to the new version.

When exercising any right under the CC-BY licence, Frontiers must be attributed as the original publisher of the article or ebook, as applicable.

Authors have the responsibility of ensuring that any graphics or other materials which are the property of others may be included in the CC-BY licence, but this should be checked before relying on the CC-BY licence to reproduce those materials. Any copyright notices relating to those materials must be complied with.

Copyright and source acknowledgement notices may not be removed and must be displayed in any copy, derivative work or partial copy which includes the elements in question.

All copyright, and all rights therein, are protected by national and international copyright laws. The above represents a summary only. For further information please read Frontiers' Conditions for Website Use and Copyright Statement, and the applicable CC-BY licence.

ISSN 1664-8714
ISBN 978-2-83252-022-2
DOI 10.3389/978-2-83252-022-2

About Frontiers

Frontiers is more than just an open access publisher of scholarly articles: it is a pioneering approach to the world of academia, radically improving the way scholarly research is managed. The grand vision of Frontiers is a world where all people have an equal opportunity to seek, share and generate knowledge. Frontiers provides immediate and permanent online open access to all its publications, but this alone is not enough to realize our grand goals.

Frontiers journal series

The Frontiers journal series is a multi-tier and interdisciplinary set of open-access, online journals, promising a paradigm shift from the current review, selection and dissemination processes in academic publishing. All Frontiers journals are driven by researchers for researchers; therefore, they constitute a service to the scholarly community. At the same time, the *Frontiers journal series* operates on a revolutionary invention, the tiered publishing system, initially addressing specific communities of scholars, and gradually climbing up to broader public understanding, thus serving the interests of the lay society, too.

Dedication to quality

Each Frontiers article is a landmark of the highest quality, thanks to genuinely collaborative interactions between authors and review editors, who include some of the world's best academicians. Research must be certified by peers before entering a stream of knowledge that may eventually reach the public - and shape society; therefore, Frontiers only applies the most rigorous and unbiased reviews. Frontiers revolutionizes research publishing by freely delivering the most outstanding research, evaluated with no bias from both the academic and social point of view. By applying the most advanced information technologies, Frontiers is catapulting scholarly publishing into a new generation.

What are Frontiers Research Topics?

Frontiers Research Topics are very popular trademarks of the *Frontiers journals series*: they are collections of at least ten articles, all centered on a particular subject. With their unique mix of varied contributions from Original Research to Review Articles, Frontiers Research Topics unify the most influential researchers, the latest key findings and historical advances in a hot research area.

Find out more on how to host your own Frontiers Research Topic or contribute to one as an author by contacting the Frontiers editorial office: frontiersin.org/about/contact

Modulation of the immune system by bacteria: From evasion to therapy

Topic editors

Marina De Bernard — University of Padua, Italy

Maria Kaparakis-Liaskos — La Trobe University, Australia

Mario M. D'Elios — University of Siena, Italy

Citation

De Bernard, M., Kaparakis-Liaskos, M., D'Elios, M. M., eds. (2023). *Modulation of the immune system by bacteria: From evasion to therapy*. Lausanne: Frontiers Media SA. doi: 10.3389/978-2-83252-022-2

Table of contents

frontiers | Frontiers in Immunology

TYPE Editorial
PUBLISHED 04 January 2023
DOI 10.3389/fimmu.2022.1112427

Check for updates

OPEN ACCESS

EDITED AND REVIEWED BY
Ian Marriott,
University of North Carolina at Charlotte, United States

*CORRESPONDENCE
Marina de Bernard
marina.debernard@unipd.it

SPECIALTY SECTION
This article was submitted to Microbial Immunology, a section of the journal Frontiers in Immunology

RECEIVED 30 November 2022
ACCEPTED 20 December 2022
PUBLISHED 04 January 2023

CITATION
de Bernard M, Kaparakis-Liaskos M and D'Elios MM (2023) Editorial: Modulation of the immune system by bacteria: From evasion to therapy. *Front. Immunol.* 13:1112427. doi: 10.3389/fimmu.2022.1112427

COPYRIGHT
© 2023 de Bernard, Kaparakis-Liaskos and D'Elios. This is an open-access article distributed under the terms of the Creative Commons Attribution License (CC BY). The use, distribution or reproduction in other forums is permitted, provided the original author(s) and the copyright owner(s) are credited and that the original publication in this journal is cited, in accordance with accepted academic practice. No use, distribution or reproduction is permitted which does not comply with these terms.

Editorial: Modulation of the immune system by bacteria: From evasion to therapy

Marina de Bernard[1]*, Maria Kaparakis-Liaskos[2] and Mario Milco D'Elios[3]

[1]Department of Biology, University of Padova, Padova, Italy, [2]Department of Microbiology, Anatomy, Physiology and Pharmacology, School of Agriculture, Biomedicine and Environment, La Trobe University, Melbourne, VIC, Australia, [3]Department of Molecular and Developmental Medicine, University of Siena, Siena, Italy

KEYWORDS

bacterial mechanisms, bacteria elicited trained immunity, T cells, anti-microbial therapeutics, bacteria-based therapeutics

Editorial on the Research Topic
Modulation of the immune system by bacteria: From evasion to therapy

This Research Topic examines how bacterial pathogens avoid or inactivate host defenses in order to survive within a host. Numerous tactics are employed by bacteria, such as modulating cell surfaces, secreting proteins that inhibit or degrade host immune factors, and even mimicking host molecules to mediate pathogenesis. Knowledge of the mechanisms utilized by pathogens to mediate disease may be advantageous for developing medical treatments aimed at eliminating infection-causing bacteria from humans. Furthermore, understanding how some bacterial factors tune the immune system may facilitate the development of targeted therapies. In this editorial we provide an overview of the exciting and diverse contents of this research topic, spanning multiple aspects of microbiology and immunology.

One-half of the world's population is colonized by *Helicobacter pylori*, a Gram-negative bacterial pathogen that is able to persist and establish chronic infection (1). The tight association of *H. pylori* with gastric cancer is established (2). Deng et al., elegantly review the effects of *H. pylori* on the microenvironment of gastric cancer, which may impair cancer immune surveillance or change the stroma of the tumor, thus promoting carcinogenesis both locally and systemically. The role of the immunomodulatory activity of *H. pylori* in favoring the onset and progression of gastric cancer (3) represents only one side of the coin. The other side is the potential application of some bacterial factors produced by the pathogen, such as the *H. pylori* neutrophil activating protein (HP-NAP), as adjuvants. This topic is extensively discussed by Codolo et al. in a review fully devoted to HP-NAP, a miniferritin with immune modulatory properties, that is becoming a promising biological therapeutic tool for the treatment of allergies and solid tumors.

The possibility that immune synapse formation between an antigen-presenting cell and a T lymphocyte might be a direct target of bacterial virulence factors is emerging as a

novel means of immune evasion. Capitani and Baldari offer an overview of the evidence that has recently accumulated to support this notion.

It is established that pathogens that cause chronic inflammation promote tumorigenesis (4), but it is also true that bacteria may display tumor-targeting properties and can activate the immune system to exert anti-tumor effects (5). Decades have passed since *Bacille Calmette-Guérin* (BCG), an attenuated strain of *Mycobacterium bovis*, has been approved by the FDA as a treatment for bladder cancer. However, recently, there has been a substantial increase in the number of studies focusing on the application of bacteria as cancer therapeutics. Tang et al. present an up-to-date review of the role of bacteria in anti-cancer immunity and their use in immunotherapy as carriers of therapeutic agents. The advantages of using unmodified bacteria in comparison to engineered bacteria in immunotherapy are also discussed.

Mycobacterium tuberculosis, the etiologic agent of tuberculosis, remains a significant global public health burden (6). Despite being developed nearly a century ago, BCG remains the only licensed vaccine against tuberculosis (7). Opportunities to leverage knowledge regarding the immunology of *M. tuberculosis* infection to improve treatments and vaccines are growing as our understanding of host responses to *M. tuberculosis* infection increases. The findings that the mycobacterial acyl carrier protein (AcpM), a key protein involved in mycolic acid production (8), is a mycobacterial effector capable of modulating macrophage functions broaden our understanding of this pathogen. AcpM upregulates miR-155-5p to prevent the activation of the transcription factor EB (TFEB), which regulates the expression of the autophagy and lysosomal genes in macrophages, and it enhances the survival of intracellular mycobacteria by preventing phagosome-lysosome fusion (Paik et al.).

The pathophysiology of brucellosis and *M. tuberculosis* infection share several characteristics. Despite the possibility of its occurrence during the treatment of *M. tuberculosis* infection, immune reconstitution inflammatory syndrome (IRIS) has never been documented in brucellosis patients. According to a case study described by Qu et al., IRIS can happen when treating *Brucella*. A persistent parasitic infection is brought on by the pathogen's infection of macrophages and ability to elude clearance mechanism. Mitroulis et al., taking advantage of *in vitro* and *ex vivo* approaches, describe the expression pattern of genes in the immune cell population, when they first encounter *Brucella*, throughout the sickness, and following a successful cure.

Comparatively examining immune responses to nine uropathogens in bladder infection, Li et al. list the similarities and differences between them. The findings lead the authors to suggest that various microbial bladder infections should adopt matching immunomodulatory therapies, and that distinct microbial illnesses may also make use of the same immunomodulatory intervention if they share the same potent therapeutic targets.

A crucial element of innate immunity is represented by NOD-like receptors (NLR) which act as intracellular sensors for bacteria. In their discussion of the many strategies employed by bacterial pathogens to elude detection by NLRs and eventually interfere with the development of host defense, Kienes et al. highlight how bacterial infections and their products activate NLRs to induce inflammation and illness. The possibility that NLRs, which operate by recruiting and activating caspases into inflammasomes, might be subverted by bacterial factors to alleviate inflammasome-driven diseases is also discussed.

Despite the fact many Gram-negative pathogens produce outer-membrane vesicles (OMVs) that contain immunogenic cargo, the presence of immunostimulatory molecules in OMVs produced by commensal organisms has only recently been recognized. In the study of Gilmore et al., it is reported that the cargo associated with OMVs produced by the intestinal commensal *Bacteroides fragilis* can activate host innate immune receptors such as Toll-like receptors (TLR)-2, TLR4, TLR7, and nucleotide oligomerization domain (NOD)-like receptor NOD1, whereas *B. fragilis* bacteria could only activate TLR2, suggesting that *B. fragilis* OMVs may facilitate immune crosstalk at the gastrointestinal epithelial surface.

A technique called fecal microbiota transplantation (FMT) is utilized to directly modify the recipient's gut microbiota. FDA authorized the use of FMT in 2013 for the treatment of recurrent and resistant Clostridium difficile infection and FMT therapy has been applied beyond gastrointestinal disorders to also include extra-gastrointestinal diseases ever since (9). According to the notion that the microbiota is crucial for intestinal homeostasis in all vertebrates, intestinal bacteria-free birds (IBF) exhibit lower body weights and inferior immunological, metabolic, antioxidant, and intestinal absorption capacities than bacteria-bearing birds. The transplantation of fecal bacteria of birds from the control group into the intestines of IBF birds reshapes the intestinal immune function and metabolism (Li et al.).

Immune checkpoint inhibitors (ICIs) have been used to treat a variety of malignancies, and the results have been astounding (10). The most popular ICIs are antibodies that target the programmed cell death protein 1 (PD-1). These ICIs operate by preventing the interaction between the PD-1 receptor on T cells and the PD-L1 ligand on tumor cells, which allows T cells to detect and destroy tumor cells (11). Most colorectal cancer (CRC) patients do not react to anti-PD-1 therapy because the tumor microenvironment lacks sufficient tumor-infiltrating lymphocytes (Bai et al.). Using a mouse model of CRC, it was demonstrated that treatment with FMT plus anti-PD-1 antibodies improved survival and tumor control in mice compared to treatment with anti-PD-1 therapy or FMT alone (Huang et al.).

An updated viewpoint on autotransporter (AT) proteins, the central part of a molecular nano-machine that transports cargo proteins through the outer membrane of Gram-negative bacteria, is provided by Clarke et al. By expanding the knowledge of the connections between structure and function of ATs, the study gives insights into the variety of ATs that may direct future research aimed at addressing several open questions about autotransporters.

In order to shed light on the protective mechanism underpinning vibriosis resistance in fish, Zhou et al. employed genomic, transcriptomic, and experimental methods. This work provides essential genetic resources for breeding and controlling infectious diseases in fish culture.

Hormones may modulate host responses to pathogens and dysmetabolic conditions. It has been recently reported that in obese patients chronic low-grade inflammation is driven by the CD300e antigen (12). Brettle et al. elegantly review the interactions between sex hormones, gut microbiome, and intestinal inflammation in obesity. The epidemiology, etiology, and outcomes of obesity and its associated metabolic problems clearly exhibit sexual dimorphisms, with females frequently experiencing more protection than males. This defense has mostly been credited to variations in fat distribution and the female sex hormone estrogen. More recently, changes in gut microbiota and intestinal immune system have also been linked to the sexual dimorphisms of obesity.

Males were generally more susceptible to *Nocardia* infection and disease than females. However, Han et al. by investigating the interplay between estradiol and immune response to *Nocardia*, demonstrated increased severity in *Nocardia*-infected female mice compared to male mice with increased mortality, elevated lung bacterial loads, and an exaggerated pulmonary inflammatory response that was mimicked in ovariectomized female mice supplemented with 17β-estradiol. Authors underlines the importance to include and separately evaluate both sexes in the future research on *Nocardia* immune responses.

Collectively, the wide-ranging studies and reviews presented in this research topic highlight the multiple mechanisms whereby bacterial pathogens promote disease and reveal novel insights and targets to combat bacterial infections and bacterial-mediated pathologies. On the other hand, the amount of evidence supporting the use of bacterial-derived bioactive materials for therapeutic purposes has been steadily increasing. Accordingly, the present collection includes critical findings on the great potential of bacterial organisms and their active components in the biomedical field, especially in cancer therapy.

Author contributions

MdB, MK-L, MMDE: Prepared and discussed about this Research Topic, invited authors, revised their manuscripts, and handled their revisions. All authors contributed to the article and approved the submitted version.

Conflict of interest

The authors declare that the research was conducted in the absence of any commercial or financial relationships that could be construed as a potential conflict of interest.

Publisher's note

All claims expressed in this article are solely those of the authors and do not necessarily represent those of their affiliated organizations, or those of the publisher, the editors and the reviewers. Any product that may be evaluated in this article, or claim that may be made by its manufacturer, is not guaranteed or endorsed by the publisher.

References

1. Salama NR, Hartung ML, Müller A. Life in the human stomach: Persistence strategies of the bacterial pathogen helicobacter pylori. *Nat Rev Microbiol* (2013) 11 (6):385–99. doi: 10.1038/nrmicro3016

2. Wroblewski LE, Peek RM, Wilson KT. Helicobacter pylori and gastric cancer: Factors that modulate disease risk. *Clin Microbiol Rev* (2010) 23(4):713–39. doi: 10.1128/CMR.00011-10

3. Moyat M, Velin D. Immune responses to helicobacter pylori infection. *World J Gastroenterol* (2014) 20(19):5583–93. doi: 10.3748/wjg.v20.i19.5583

4. Greten FR, Grivennikov SI. Inflammation and cancer: Triggers, mechanisms, and consequences. *Immunity* (2019) 51(1):27–41. doi: 10.1016/j.immuni.2019.06.025

5. Duong MT-Q, Qin Y, You S-H, Min J-J. Bacteria-cancer interactions: Bacteria-based cancer therapy. *Exp Mol Med* (2019) 51(12):1–15. doi: 10.1038/s12276-019-0297-0

6. *Global tuberculosis report 2020*. Available at: https://www.who.int/publications-detail-redirect/9789240013131.

7. Calmette A. Preventive vaccination against tuberculosis with b c g and the lübeck casualties. *J Am Med Assoc* (1931) 96(1):58–9. doi: 10.1001/jama.1931.02720270060030

8. Kremer L, Nampoothiri KM, Lesjean S, Dover LG, Graham S, Betts J, et al. Biochemical characterization of acyl carrier protein (AcpM) and malonyl-CoA: AcpM transacylase (mtFabD), two major components of mycobacterium tuberculosis fatty acid synthase II. *J Biol Chem* (2001) 276(30):27967–74. doi: 10.1074/jbc.M103687200

9. Wang J-W, Kuo C-H, Kuo F-C, Wang Y-K, Hsu W-H, Yu F-J, et al. Fecal microbiota transplantation: Review and update. *J Formosan Med Assoc = Taiwan Yi Zhi* (2019) 118 Suppl 1:S23–31. doi: 10.1016/j.jfma.2018.08.011

10. Shiravand Y, Khodadadi F, Kashani SMA, Hosseini-Fard SR, Hosseini S, Sadeghirad H, et al. Immune checkpoint inhibitors in cancer therapy. *Curr Oncol (Toronto Ont.)* (2022) 29(5):3044–60. doi: 10.3390/curroncol29050247

11. Topalian SL, Hodi FS, Brahmer JR, Gettinger SN, Smith DC, McDermott DF, et al. Safety, activity, and immune correlates of anti-PD-1 antibody in cancer. *New Engl J Med* (2012) 366(26):2443–54. doi: 10.1056/NEJMoa1200690

12. Coletta S, Trevellin E, Benagiano M, Romagnoli J, Della Bella C, D'Elios MM, et al. The antigen CD300e drives T cell inflammation in adipose tissue and elicits an antibody response predictive of the insulin sensitivity recovery in obese patients. *J Inflammation (London England)* (2022) 19(1):21. doi: 10.1186/s12950-022-00318-7

frontiers in Immunology

ORIGINAL RESEARCH
published: 02 March 2022
doi: 10.3389/fimmu.2022.858609

Estradiol Aggravate *Nocardia farcinica* Infections in Mice

*Lichao Han[1], Xingzhao Ji[2,3], Xueping Liu[4], Shuai Xu[1], Fang Li[5], Yanlin Che[4], Xiaotong Qiu[1], Lina Sun[1] and Zhenjun Li[1]**

[1] State Key Laboratory of Infectious Disease Prevention and Control, National Institute for Communicable Disease Control and Prevention, Chinese Center for Disease Control and Prevention, Beijing, China, [2] Department of Pulmonary and Critical Care Medicine, Shandong Provincial Hospital Affiliated to Shandong First Medical University, Jinan, China, [3] Shandong Key Laboratory of Infections Respiratory Disease, Shandong Provincial Hospital Affiliated to Shandong First Medical University, Jinan, China, [4] School of Laboratory Medicine and Life Sciences, Wenzhou Medical University, Wenzhou, China, [5] Department of Medical, Tibet University, Lhasa, China

Males are generally more susceptible to *Nocardia* infection than females, with a male-to-female ratio of 2 and higher clinical disease. 17β-Estradiol has been implicated in affecting the sex-based gap by inhibiting the growth of *N. brasiliensis* in experiments, but the underlying mechanisms have not yet been fully clarified. In the present study, however, we report increased severity in *N. farcinica* IFM 10152-infected female mice compared with male mice with increased mortality, elevated lung bacterial loads and an exaggerated pulmonary inflammatory response, which was mimicked in ovariectomized female mice supplemented with E2. Similarly, the overwhelming increase in bacterial loads was also evident in E2-treated host cells, which were associated with downregulating the phosphorylation level of the MAPK pathway by binding the estrogen receptor. We conclude that although there are more clinical cases of *Nocardia* infection in males, estrogen promotes the survival of the bacteria, which leads to aggravated inflammation in females. Our data emphasize the need to include and separately analyze both sexes in future studies of *Nocardia* to understand the sex differences in immune responses and disease pathogenesis.

Keywords: *Nocardia farcinica*, sex difference, 17β-estradiol, estrogen receptor, MAPK

OPEN ACCESS

Edited by:
Mario M. D'Elios, University of Florence, Italy

Reviewed by:
Mario Salinas-Carmona, Autonomous University of Nuevo León, Mexico
Nagaja Capitani, University of Siena, Italy

***Correspondence:**
Zhenjun Li
lizhenjun@icdc.cn

Specialty section:
This article was submitted to Microbial Immunology, a section of the journal Frontiers in Immunology

Received: *20 January 2022*
Accepted: *10 February 2022*
Published: *02 March 2022*

Citation:
Han L, Ji X, Liu X, Xu S, Li F, Che Y, Qiu X, Sun L and Li Z (2022) Estradiol Aggravate Nocardia farcinica Infections in Mice. Front. Immunol. 13:858609. doi: 10.3389/fimmu.2022.858609

INTRODUCTION

Nocardia is a saprophytic gram-positive bacillus that usually manifests as an opportunistic infection in both immunocompetent and immunocompromised hosts. It is mainly transmitted through the respiratory tract to cause lung abscesses but also through wound or blood transmission to cause skin and central nervous system infections (1, 2).

The genus *Nocardia* currently contains more than 100 species, and clinically, the primary recognized human pathogens include *N. farcinica*, *N. cyriacigeorgica*, *N. brasiliensis* and *N. asteroides*. Nocardiosis has been reported at all ages, and the incidence of males with isolated nocardiosis is significantly higher than that of females worldwide (3, 4), such as in Mexico (5), the United States (6, 7), Canada (8), France (9), Spain (10), Australia (11, 12) and China (13).

However, there is no clear explanation for this sex predominance. One of the most common explanations is that men's distinct lifestyle- and agriculture-related professions lead to increased

exposure to *Nocardia* (14, 15), considering the widespread distribution of this organism, especially in soil, decaying vegetation, fresh water and salt water (1). In addition, the presence of estrogen might also contribute to the sex difference observed (16). As a sex steroid hormone, estrogen exerts a broad spectrum of biological effects by binding to estrogen receptor alpha (ERα) or ERβ (17). Estrogen, primarily 17β-estradiol (E2), regulates cellular function in diverse cell types, including macrophages, dendritic cells (DCs), granulocytes, and lymphocytes. It is important to mention here that E2 has divergent effects on inflammation controls. It diminishes the severity of infections by some pathogens, whereas it enhances susceptibility to other pathogens (18, 19). This aroused our interest in further investigating the role and mechanism of E2 in *Nocardia* infection.

Given the sex hormone and genetic and physiological differences between the sexes, males and females differ in their immune responses to infection with many respiratory pathogens. Often overlooked in animal experiments is the fact that the sex and hormonal status of an individual can regulate inflammatory responses and the development of immunopathology during *Nocardia* infection. In the present study, we sought to use sex-based and E2-manipulated mouse models of *N. farcinica* IFM 10152 infection to clarify the efficiency of E2 in inflammation and bacterial clearance. The underlying mechanisms by which E2 affects *Nocardia* infection were then initially elucidated at the cellular level. The ultimate goal of this study was to improve the understanding of the mechanism of sex differences in inflammatory lung diseases associated with *Nocardia* infection and provide evidence for optimizing clinical preventive measures and treatments for each sex.

MATERIALS AND METHODS

Mice and Ethics Statement

Female and male C57BL/6 mice (6–8 weeks of age) were purchased from SPF Biotechnology Co., Ltd. (Beijing, China) and bred under specific pathogen-free conditions according to the guidelines. All procedures were approved by the Ethics Review Committee of the National Institute for Communicable Disease Control and Prevention at the Chinese Center for Disease Control and Prevention.

Bacteria and Infection of Mice

N. farcinica IFM 10152 was purchased from the German Resource Centre for Biological Materials. Bacteria were grown in BHI broth (Oxoid Ltd, Hants, UK) at 37°C to exponential phase before experiments. Female and male C57BL/6 WT mice were injected intraperitoneally with a uniform bacterial suspension (100 μl) containing approximately 2×10^8 colony-forming units (CFU), and mortality was assessed for 14 consecutive days. For inflammatory studies, 1×10^7 CFU of *N. farcinica* IFM 10152 (50 μl) or 50 μl PBS was intranasally infected under anesthesia.

Weight and Body Temperature

Mouse weight and body temperature were quantified immediately prior to *N. farcinica* IFM 10152 infection and 1 day post-infection. Mice were weighed to hundredth of a gram accuracy, and body temperature was monitored with an Animal Thermometer (KEW, Nanjing, China), which steadily assesses rectal temperature to the nearest 0.1°C in 3–5 seconds.

Bronchoalveolar Lavage Fluid and Lung Homogenates Sample Collection

After the mice were sacrificed by cervical dislocation, pulmonary bronchoalveolar lavage fluid (BALF) was obtained through 3 successive lavages of the bronchi with 1 mL of ice-cold PBS under a sterile environment, and the protein content was assessed using Bradford reagent (TIANGEN, Beijing, China) following the manufacturer's instructions. Whole lung and spleen tissue was collected and homogenized in 1 ml of PBS. For enumerating bacterial counts, serial dilutions of homogenate were plated on BHI agar plates, and the number of *N. farcinica* IFM 10152 CFUs was counted after 48 hours of incubation at 37°C.

Lung Histopathology

Lungs were fixed in 4% paraformaldehyde overnight, embedded in paraffin and cut into 5-μm sections. Slides were stained using hematoxylin and eosin and then viewed using a biological microscope (Nikon, Eclipse Ci-L, Japan) according to the manufacturers' instructions.

Cytokine Measurements

For time course experiments, animals were randomly assigned to be euthanized at 1, 7, or 14 days. Supernatants from lung homogenates were used to measure IL-4, IL-6, IL-10, IL-12, TNF-α and IFN-γ by quantitative ELISA (BD OptEIA™, San Diego, CA, USA). The assays were conducted as recommended by the manufacturer, and all cultures were processed in triplicate.

Growth Curve

To examine the direct effect of E2 on *N. farcinica* IFM 10152 growth, E2 at different concentrations (10 nM, 50 nM, 250 nM) was added to the growth curve plate at 37°C. The OD_{600} value was tested half an hour for 48 hours using an automatic growth curve analyzer (Bioscreen, Finland).

Ovariectomy and Estrogen Treatment

Ovaries of 6-week-old female mice were removed through bilateral incisions over the dorsum under anesthesia. For the sham operation, the ovaries were identified, and an equal volume of paraovarian adipose tissue was removed. Ten days after incisions were sutured, mice were injected subcutaneously with 100 μL of sesame seed oil with or without 100 ng of E2 (Sigma, St. Louis, MO) at 10:00 am for ten consecutive days before *N. farcinica* IFM 10152 infection. Then, E2 concentrations in serum were measured at 1 day postinfection using a Mouse E2 ELISA kit (MEIMIAN, Wuhan, China). Bacterial burden and protein content were determined as described above.

Cell Isolation and Culture

Primary alveolar macrophages were obtained by centrifuging BALF and were resuspended in phenol-free DMEM (BBI, Shanghai, China) supplemented with 10% fetal bovine serum (FBS; Gibco, USA). After 2 hours of incubation in the cell culture dishes at 37°C, the supernatant was discarded, and the adherent cells obtained were cultured with new medium. The mouse and human cell lines RAW264.7 and A549 (National Infrastructure of Cell Line Resource, Beijing, China) were cultured in phenol-free DMEM with 10% FBS at 37°C. In each experiment, wells were washed three times with PBS and seeded with or without 50 nM E2 at 37°C for 16–18 h in a CO_2 incubator before infection, and the cell suspension containing *N. farcinica* IFM 10152 was treated at an MOI of 10:1.

Adhesion and Invasion

For the adhesion assay, A549 and RAW264.7 cells were seeded into 24-well microplates with or without round glass coverslips at a density of 3×10^5 cells per well. After 1 h postinfection at 37°C, for electron microscopic observation, cells were washed three times with PBS and then fixed with methanol for 8 min at room temperature. After methanol was removed, cells were stained with Giemsa stain solution and left for 30 min at room temperature. Coverslips were then washed and removed from the petri plate and examined using an Echo Revolve Generation 2 (ECHO, USA). For bacterial adhesive determination, cells were washed twice with PBS to eliminate extracellular bacteria and lysed with 1 ml of H_2O to disrupt the cells and release the intracellular bacteria. Finally, cell lysates were serially diluted 10-fold for CFU determination and plated on BHI agar plates.

For the invasion assay, A549 and RAW264.7 cells were incubated in a 24-well microplate at a density of 3×10^5 cells per well, and primary alveolar macrophages were incubated at a density of 3×10^4 cells per well. After 1 h of infection, cells were washed twice with PBS to eliminate extracellular bacteria and incubated in DMEM containing 50 μg/ml amikacin (20) and 2% FBS. For bacterial survival determination, cell lysates were plated on BHI agar plates after serially diluted. After 48 h of incubation, the colonies were counted.

Cytotoxicity Assay

Cytotoxicity assays of the E2-treated group and control group at 8 h postinfection were conducted using a CytoTox 96® Non-Radioactive Cytotoxicity Assay (Promega, Madison, USA) as previously described (21). The absorbance data at 490 nm were collected using a microplate reader (BioTek, USA) according to the manufacturer's instructions.

Estrogen Receptor Antagonist

To block estrogen receptors, RAW264.7 cells were pretreated for 1 h at 37°C with the ER antagonist ICI 182780 (which blocks both nuclear and nonnuclear ERs, APEBixo, USA), the ERα-specific antagonist MPP (APEBixo, USA) or the ERβ-specific antagonist PHTPP (APEBixo, USA) prior to E2 exposure. CFU determination in RAW 264.7 cells was counted as described before.

Western Blot Analysis

For Western blot analysis, whole-cell extracts were harvested using RIPA lysis buffer (strong) (CWBIO, Beijing, China) containing protease inhibitor cocktail (CWBIO, Beijing, China) and phosphatase inhibitor cocktail (CWBIO, Beijing, China) at 30 min, 60 min, and 120 min postinfection, separated by SDS–PAGE and transferred onto PVDF membranes (Millipore, Darmstadt, Germany). Subsequently, the membranes were incubated with primary antibodies against monoclonal mouse anti-β-actin (1:4000, TransGen, China), rabbit anti-p-p44/42 MAPK (1:1000, CST, USA), rabbit anti-p-SAPK/JNK (1:1000, CST, USA) or rabbit anti-p-p38 (1:1000, CST, USA) overnight, followed by incubation with HRP-conjugated goat anti-rabbit IgG (1:1000, Beyotime, China) or HRP-conjugated goat anti-mouse IgG (1:4000, ZSGB-BIO, China). Finally, the bands were visualized using Amersham® Hyperfilm® ECL™ and MP Autoradiography Films (GE Healthcare).

MAPK Inhibitor

To block MAPK signaling, RAW264.7 cells were pretreated for 1 h at 37°C with inhibitors of 20 μM p38 (SB 203580, Sigma, USA), 20 μM ERK (PD 98059, Sigma, USA) or 20 μM JNK (SP 600125, Sigma, USA) prior to E2 exposure. CFU determination was counted as described before.

Statistical Analysis

Survival and growth curves were analyzed using GraphPad Prism 9.0.0. Group means and standard deviations (SDs) were analyzed by Student's *t* test. Grayscale values of protein bands were analyzed by Image J. For all tests, difference was considered statistically significant if the *p* value is less than 0.05.

RESULTS

Female Mice Show Higher Mortality From *N. farcinica* Infection Than Male Mice

Following *N. farcinica* IFM10152 inoculation, female mice died significantly earlier than male mice, with survival differences noted as early as 24 h post-infection (**Figure 1A**). While 90% of male mice were able to survive, only 50% of female mice survived for 14 consecutive days.

Female Mice Show Increased Disease Severity Upon *N. farcinica* Infection

To determine potential differences in lung infection and inflammation between sexes, we further established a nonlethal acute pneumonia model in age-matched C57BL/6 female and male mice with 1×10^7 CFU *N. farcinica* IFM 10152 by intranasal infection. At 24 h postinfection, we observed that female mice had decreased body weight (4.04% decrease vs. 2.32%, **Figure 1B**) and increased body temperature (0.7°C increase vs. 0.1°C, **Figure 1C**) compared with male mice. Except for the dramatic physical changes, female mice had more abundant protein content than male mice in their airways ($P < 0.05$), as a sign of lung injury (**Figure 1D**). Consistent with the poor

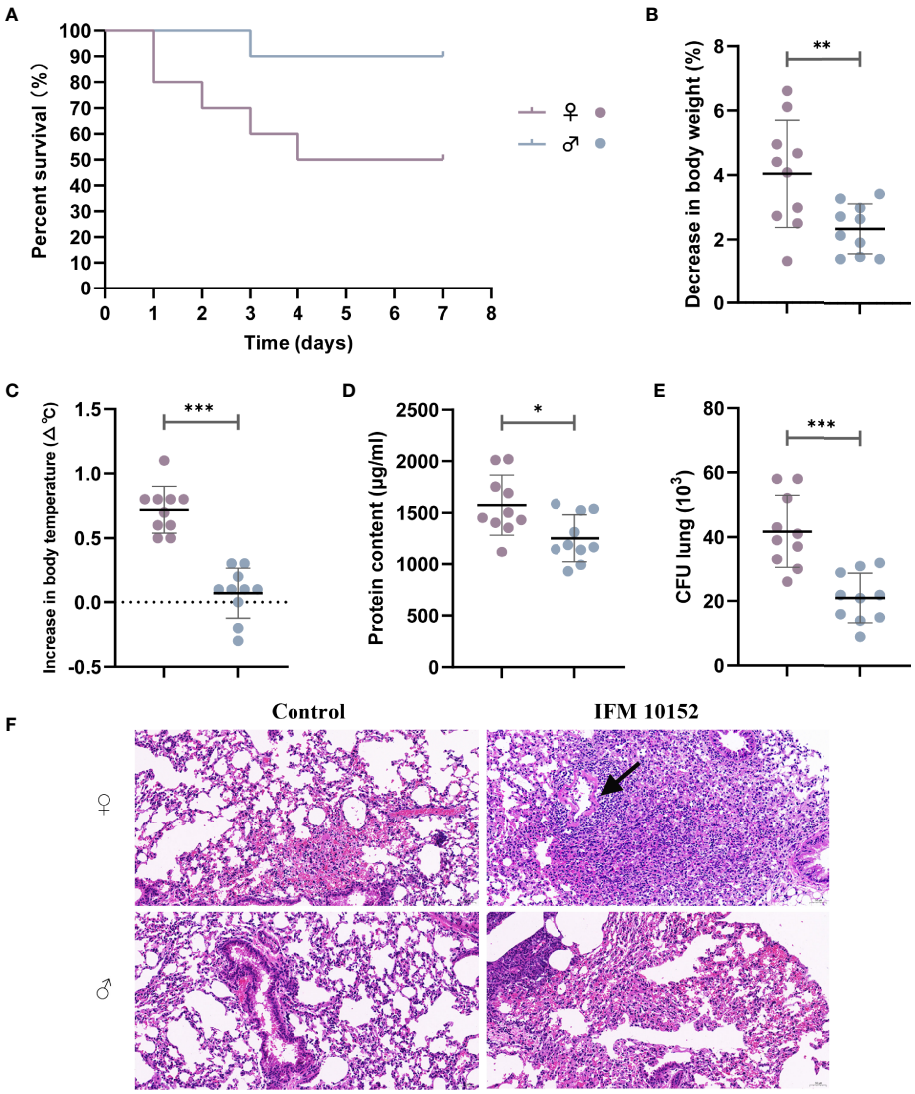

FIGURE 1 | Female mice are more susceptible to *N. farcinica* infection. **(A)** Female mice (n = 10) and male mice (n = 10) were injected intraperitoneally with 2×10^8 CFU (100 μl) of *N. farcinica* IFM 10152, and mortality was assessed for 14 days until no additional deaths were observed. **(B–F)** Female mice (n = 12) and male mice (n = 12) were infected intranasally with 1×10^7 CFU (50 μl) for 24 hours, and control groups were infected with 50 μl of PBS. **(B)** Change in body weight of mice. **(C)** Change in body temperature. **(D)** Protein content in BALF. **(E)** Bacterial burden in lung homogenates. **(F)** Representative H&E-stained lung sections of mice. Scale bars: 100 μm. Each point represents a mouse. Lines display means with SEM. Data are from 3 independent experiments. *$P < 0.05$, **$P < 0.01$, and ***$P < 0.001$.

prognosis, female mice displayed a higher bacterial burden in lung tissue ($P < 0.001$) than male mice (**Figure 1E**), but no bacteria were found in the spleen tissue in either male or female mice (data not shown).

Examination of lung histopathology revealed exacerbated pathology in the *N. farcinica* IFM 10152-infected female mice compared with male mice (**Figure 1F**). The lungs of infected female mice showed marked thickening of the alveolar wall with large amounts of lymphocyte, neutrophil and macrophage infiltration, and some necrotic cell debris and hemorrhaging were also observed in the bronchial lumen. In addition, there was also evidence of inflammatory cells infiltrating into a ring around the vessel, forming a vascular sleeve (**Figure 1F**; black arrow). Male mouse-infected lungs showed evidence of lymphocyte and neutrophil infiltration, as well as slight thickening of the alveolar wall. And no obvious necrotic cell debris and vascular sleeves were observed in the bronchial lumen.

Female Mice Display Higher Cytokine Production in Response to Respiratory *N. farcinica* IFM 10152 Infection

The production of cytokines by innate immune cells can also differ between the sexes in response to different stimuli, including bacterial infections. Analysis of the cytokine levels in the lung supernatant showed that at 1, 7 and 14 days postinfection, female mice had significantly elevated cytokine production

levels (IL-4, IL-6, IL-10, IL-12, TNF-α and IFN-γ) in response to *N. farcinica* IFM 10152 compared with male mice, although all cytokines showed a decreasing trend during the days(**Figure 2**). These massive cytokine levels, which persisted for more than two weeks, are likely a consequence of the poor prognosis in the female mice.

E2 Cannot Alter the Growth Curve of *N. farcinica* IFM 10152

Sex steroid hormones have been described to directly influence bacterial growth and metabolism. To test whether E2 could exert a direct effect on *N. farcinica* IFM 10152 growth, bacteria were grown in brain-heart infusion agar (BHI), with and without E2. Under the conditions tested, we found no quantitative change in the growth of *N. farcinica* IFM 10152, regardless of E2 concentration (**Figure 3A**).

Treatment With E2 Increases Ovariectomized Female Mouse Susceptibility to *N. farcinica* IFM 10152 Lung Infection

Having identified no direct effect of E2 on *N. farcinica* IFM 10152 growth, we sought to determine whether E2 impacted the host inflammatory response. Female mice were sham ovariectomized (supplemented with sesame seed oil) or ovariectomized (supplemented with sesame seed oil or E2 at physiological doses) prior to challenge with *N. farcinica* IFM 10152. The results showed that serum E2 levels in female mice decreased significantly after ovariectomization but increased after exogenous E2 supplementation (**Figure 3B**). The E2 effect was confirmed by measuring the protein content in BALF and counting the bacterial burden in lung tissues. Concordant with the changes in E2 levels, E2-treated ovariectomized

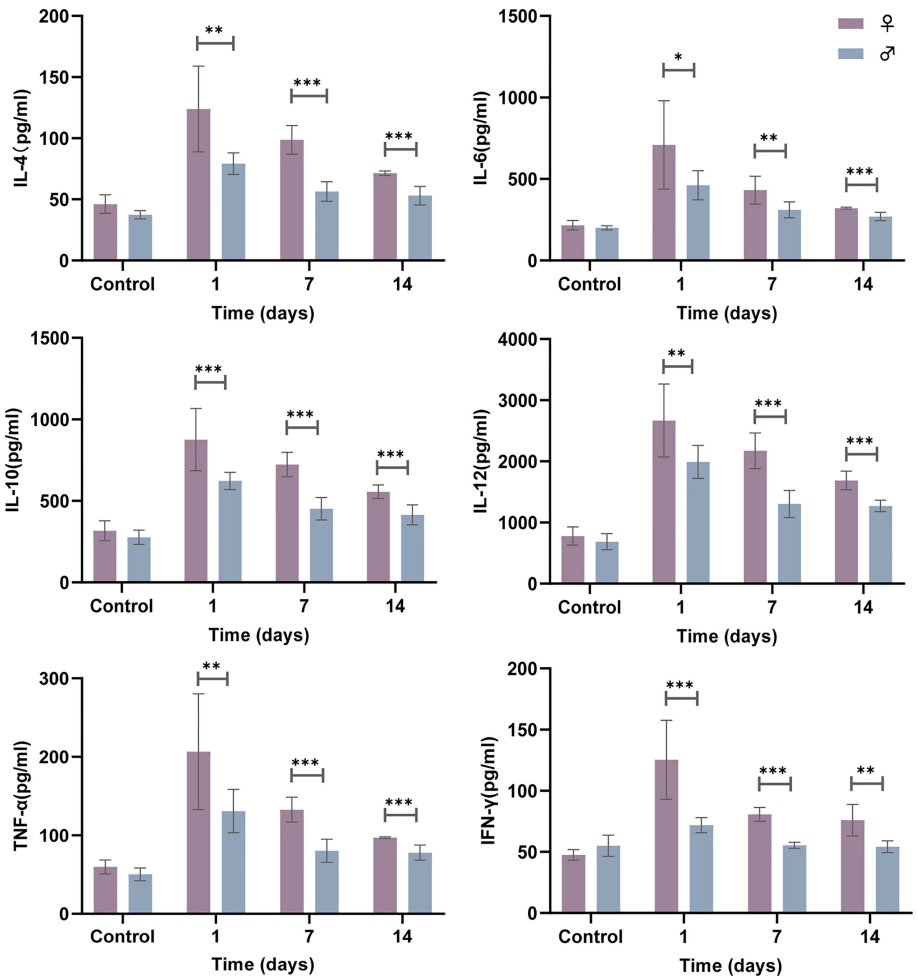

FIGURE 2 | Female mice display higher cytokine production following *N. farcinica* IFM 10152 infection. Female mice (n = 32) and male mice (n = 32) were infected intranasally with 1×10^7 CFU (50 μl) for 1, 7, and 14 days, or 50 μl PBS for 1 day, and cytokine levels (IL-4, IL-6, IL-10, IL-12, TNF-α and IFN-γ) in the lung supernatant were measured by ELISA. Lines display means with SEM. Data are from 2 independent experiments. $^*P < 0.05$, $^{**}P < 0.01$, and $^{***}P < 0.001$.

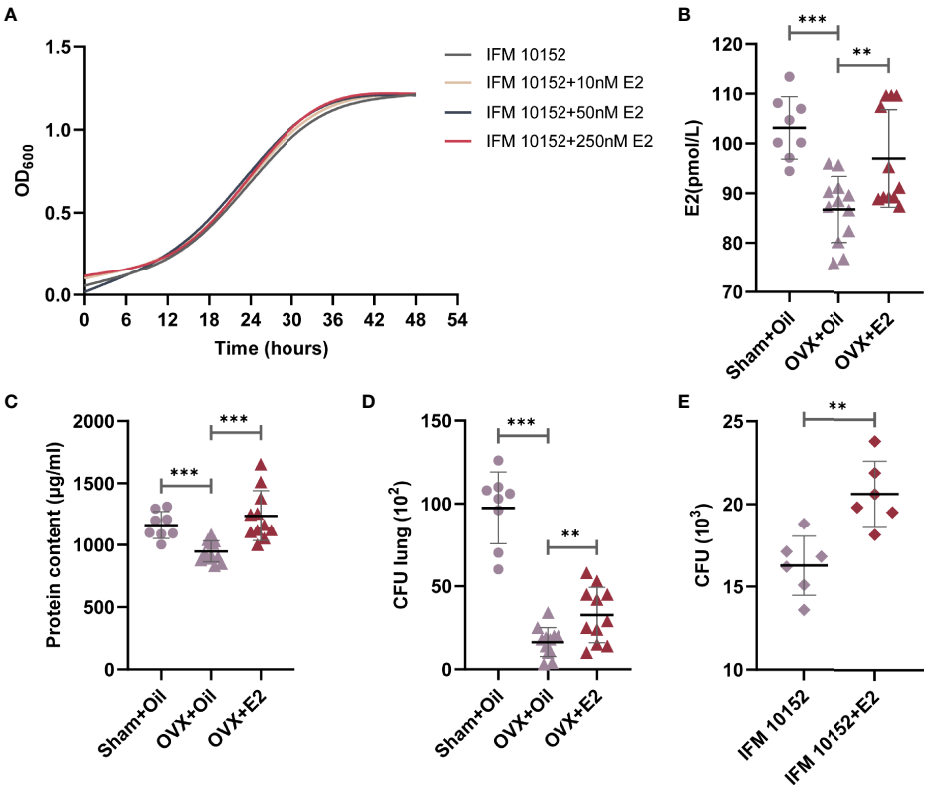

FIGURE 3 | E2 supplementation increases ovariectomized female mouse susceptibility to *N. farcinica* IFM 10152 lung infection. **(A)** Growth curve of *N. farcinica* IFM 10152 in BHI with 10 nM, 50 nM, and 250 nM for 48 hours. **(B–D)** Female mice were treated with sham ovariectomy with sesame seed oil (n=8), ovariectomy with sesame seed oil (n = 12), or ovariectomy with E2 (n = 12) prior to challenge with *N. farcinica* IFM 10152. **(B)** E2 levels in serum. **(C)** Protein content in BALF. **(D)** Bacterial burden in lung homogenates. **(E)** Bacterial survival in alveolar macrophages treated with or without E2. Lines display means with SEM. Data are from 2 independent experiments. $^{**}P < 0.01$, and $^{***}P < 0.001$.

mice had a significant increase in protein content compared with oil-treated ovariectomized mice, which was essentially the same as that of oil-treated sham ovariectomized mice (**Figure 3C**). Furthermore, the lung bacterial burden of ovariectomized mice was significantly higher after supplementation with E2, although it was still significantly lower than that of sham ovariectomized mice (**Figure 3D**). These data demonstrated that ovariectomized mice supplemented with E2 exhibited impaired bacterial clearance compared to oil-treated ovariectomized mice.

E2 Contributes to the Growth of *N. farcinica* IFM 10152 in Alveolar Macrophages

Previous studies established that *Nocardia* grew as a facultative intracellular parasite in cultured alveolar macrophages (21, 22). We next determined the direct effects of E2 on *N. farcinica* IFM 10152 growth in alveolar macrophages by seeding *N. farcinica* IFM 10152 into phenol-free DMEM containing FBS with 50 nM E2 for 6 hours. The results showed that E2-treated cells had more *N. farcinica* CFUs in plates than controls (**Figure 3E**).

E2 Facilitates Adhesion and Invasion of *N. farcinica* IFM 10152 Into Host Cells Dependent on Nuclear Estrogen Receptors

To further evaluate the effect of E2 on *N. farcinica* IFM 10152 growth in cells, A549 and RAW 264.7 cells were imaged by electron microscopy after 1 h of infection. The results showed that *N. farcinica* IFM 10152 adhered and proliferated better in the E2-treated group than in the control group (**Figures 4A, B**). As such, the bacterial burden of *N. farcinica* IFM 10152 in the E2-treated groups was higher than that in the control group at 6, 12 and 24 h postinfection (**Figure 4C**). In addition, we observed that the cytotoxicity of *N. farcinica* IFM 10152 was significantly higher in the E2-treated group than in the control group in both A549 and RAW264.7 cells (**Figure 4D**). To determine whether the difference in cells treated with E2 versus vehicle was ER-specific, RAW 264.7 cells were seeded and supplemented with three ER antagonists. The increased bacterial burden in E2-supplemented RAW 264.7 cells was attenuated in the presence of ICI 182,780, MPP and PHTPP (**Figure 4E**). Taken together, these findings support a specific role for nuclear ERs in the impact of E2 on promoting *N. farcinica* IFM 10152 infection.

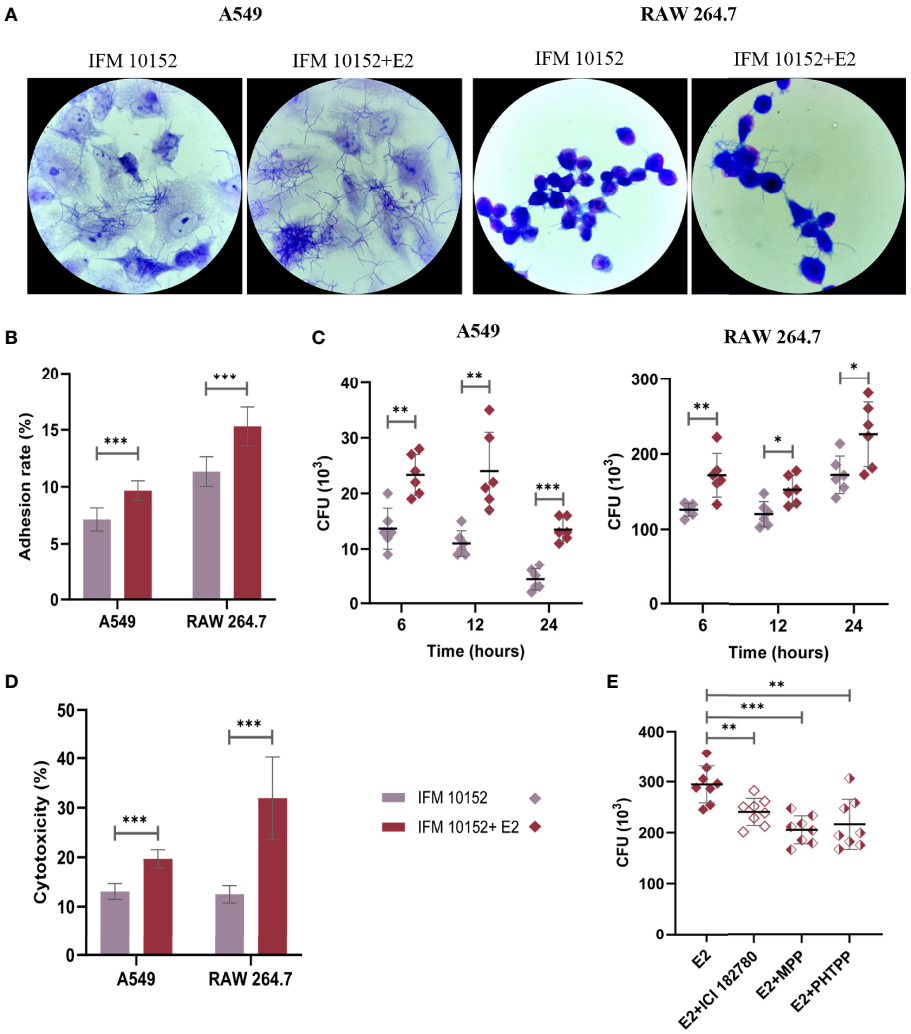

FIGURE 4 | E2 facilitates adhesion and invasion of *N. farcinica* IFM 10152 into host cells through ERα and ERβ signaling. **(A–E)** A549 and RAW 264.7 cells were treated with or without 50 nM E2 for 16–18 h prior to *Nocardia* infection. Electron microscopic observation **(A)** and adhesion rate **(B)** of bacterial strains to A549 (left) and RAW 264.7 (right) cells after 1 h of infection. **(C)** Invasion of bacterial strains into A549 (left) and RAW 264.7 (right) cells after 6, 12, and 24 h of infection. **(D)** The cytotoxicity of *N. farcinica* IFM 10152 to A549 and RAW 264.7 cells after 8 h of infection. **(E)** Bacterial survival in RAW 264.7 cells treated with ICI 182780, MPP or PHTPP. Lines display means with SEM. Data are from 3 independent experiments. $^{*}P < 0.05$, $^{**}P < 0.01$, and $^{***}P < 0.001$.

E2 Promotes Bacterial Survival by Downregulating the Phosphorylation Level of the MAPK Pathway

To elucidate the mechanisms by which E2 promotes *Nocardia* survival in host cells, we examined mitogen-activated protein kinase (MAPK) activation in response to *N. farcinica* IFM 10152 infection. The results showed that the E2-treated group downregulated the phosphorylation levels of ERK (p-ERK), JNK (p-JNK), and p38 (p-p38) compared to the control group in both A549 and RAW 264.7 cells (**Figures 5A–D**). Then, we detected the relationship between bacterial survival in cells and the MAPK signaling pathway with MAPK inhibitors. The results showed increased bacterial survival in the SB 203580- and SP 600125-treated groups, although there was no detectable difference between the PD 98059-treated and control groups (**Figure 5E**). These results indicate that E2 promotes bacterial survival by inhibiting activation of the MAPK-mediated inflammatory response.

DISCUSSION

Sex differences in immunity to respiratory pathogens are evident in humans and experimental rodent models (23). The roles of sex differences and sex hormones have been investigated in experimental models of infection and inflammation with varied results. For many inflammatory-mediated pulmonary diseases, including *Mycobacterium tuberculosis* (24) and

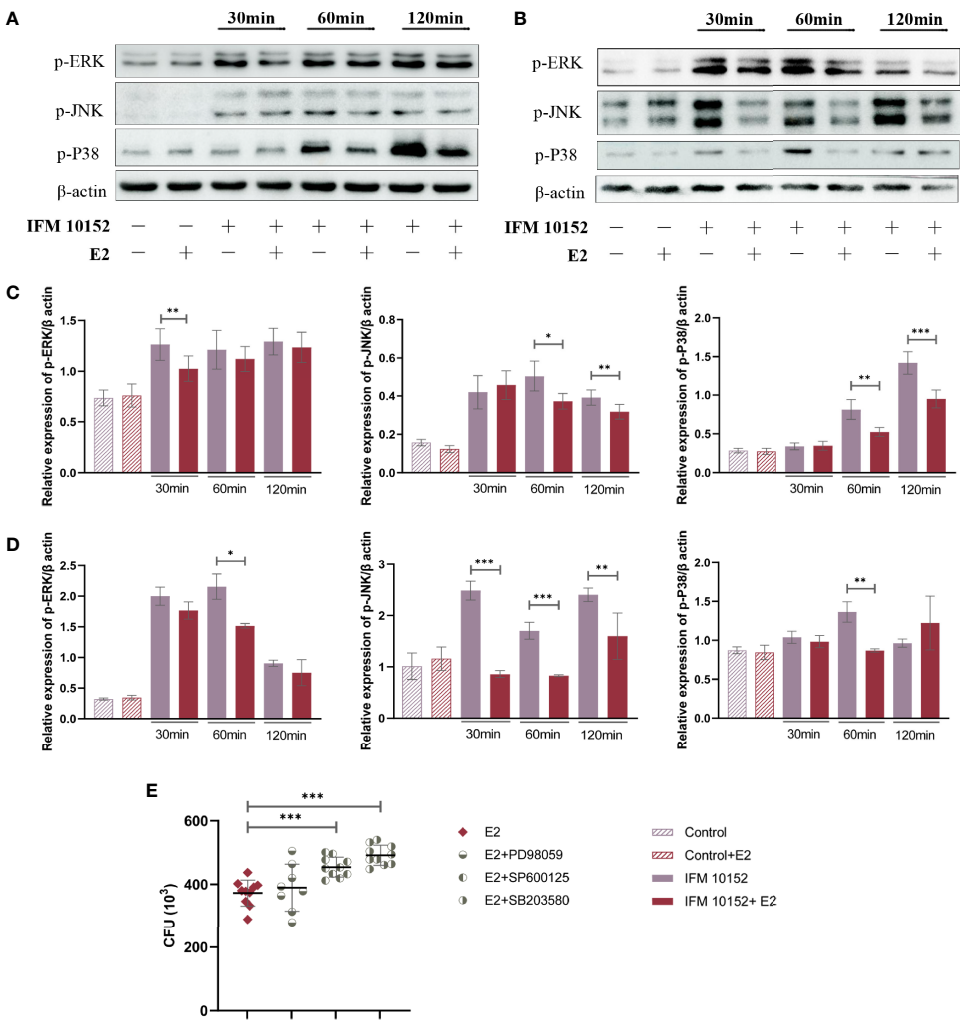

FIGURE 5 | E2 promotes bacterial survival by downregulating the MAPK signaling pathway. A549 **(A)** and RAW 264.7 **(B)** cells were treated with or without 50 nM E2 for 16–18 h prior to *Nocardia* infection. Western blot analysis of the phosphorylation levels of ERK (p-ERK), JNK (p-JNK), and p38 (p-p38) after 30, 60, and 120 minutes of infection. The relative expression of each protein in A549 **(C)** and RAW 264.7 **(D)** cells was analyzed by Image J. **(E)** Bacterial survival in RAW 264.7 cells treated with 20 μM PD 98059, 20 μM SP 600125, or 20 μM SB 203580. Lines display means with SEM. Data are from 3 independent experiments. $^{*}P < 0.05$, $^{**}P < 0.01$, and $^{***}P < 0.001$.

Streptococcus pneumoniae (25), male mice are more susceptible than female mice. However, female mice are more likely to be hospitalized and/or die following infection with other respiratory pathogens, including *Pseudomonas aeruginosa* (26, 27) and *Acinetobacter baumannii* (28).

Given the current importance now placed on utilizing both males and females in research, we designed an innate immune response model of *N. farcinica* IFM 10152 respiratory tract infection in male and female mice. The results showed significantly higher mortality in female mice infected with a lethal dose of *N. farcinica*. Similarly, infection with a nonlethal dose resulted in worse outcomes in female mice than in male mice. The data from the present study illustrate that female mice displayed unstable physical changes, severe lung damage, elevated inflammatory cytokine responses and overall lower bacterial clearance in the lungs after 24 h of infection. In addition, we observed that cytokines in the lung supernatant of female mice were higher than those of male mice for 2 weeks after infection. These massive cytokine levels increase body temperature and excessive inflammatory response, which may be associated with poor prognosis in female mice. These data support and extend the hypothesis that although there is a higher prevalence of *Nocardia* infection in males, females tend to suffer a poor outcome.

Previous studies have focused mostly on sex differences in the incidence of *Nocardia* infection, but little attention has been given to sex differences in prognosis. We observed higher mortality for females than males in some well-documented reports. Rafiei N et al. (29) studied 10 males and 10 females with *Nocardia* infection in Queensland from 1997 to 2015. After

years of follow-up, it was found that the death toll of females was six, which was higher than that of males (two). Sex differences in disease outcome are likely mediated by multiple factors, including sex hormones, glucocorticoids and sex chromosomal genes (30). E2 has been shown to have both proinflammatory and anti-inflammatory roles in host resistance to pathogen infections (18, 19). In the present study, ovariectomized female mice shared a lower bacterial burden in the lungs than sham ovariectomized female mice, and exogenous administration of E2 increased the bacterial burden in ovariectomized female mice, which indicates that E2 can directly or indirectly impair the ability of *Nocardia* clearance in mice. Moreover, although the E2 level in E2-treated ovariectomized female mice essentially reached normal levels, the bacterial burden in the lungs was still significantly lower than that in sham ovariectomized female mice, which indicates the difficulty in reproducing natural E2 function *via* manipulation *in vivo*. Similarly, we observed that E2 can bind nuclear ER-α and ER-β to promote the invasion of *Nocardia* into host cells, resulting in severe cellular damage. However, a previous study showed that E2-treated mice can effectively inhibit the growth of bacterial grains after plantar pad infection with *N. brasiliensis*, demonstrating the protective effect of E2 in mice (16). These different results could be due to the differences in the experimental subjects and experimental approaches, such as the *Nocardia* strains used and/or stimuli employed.

In most respiratory diseases, in general, the severity of symptoms was related to the innate immune response triggered during the early period of infection (31). MAPKs are key factors mediating cellular activities such as cell differentiation, stress responses, apoptosis, and immune defenses to many external stimuli (32). Our observations indicate that E2 can significantly downregulate the phosphorylation level of the MAPK pathway. Further research also showed that downregulation of the MAPK signaling pathway was conducive to bacterial survival in host cells. These data provide evidence that downregulation of the MAPK signaling pathway is one of the mechanisms by which E2 promotes the survival of *N. farcinica*.

In the present study, we demonstrated that the differential susceptibility to *Nocardia*–induced pneumonia between sexes is partly based on E2. Our data provide evidence for determining the specific therapeutic target for sex hormone manipulation. Sex-based differences need to be taken into account in subsequent research and in the understanding of nocardiosis. Ongoing work in our laboratory is further elucidating the difference in antibody production between male and female mice following *Nocardia* infection and then delineating the underlying mechanism from the perspective of humoral immunity.

CONCLUSION

Despite the higher prevalence of *Nocardia* infection in males, females tend to suffer a poor outcome with increased mortality, elevated lung bacterial loads and an exaggerated pulmonary inflammatory response. 17β-Estradiol can promote bacterial survival by downregulating the host MAPK signaling pathway, which is one of the mechanisms responsible for this sex difference.

DATA AVAILABILITY STATEMENT

The original contributions presented in the study are included in the article/supplementary material. Further inquiries can be directed to the corresponding author.

ETHICS STATEMENT

The animal study was reviewed and approved by Ethics Review Committee of the National Institute for Communicable Disease Control and Prevention at the Chinese Center for Disease Control and Prevention.

AUTHOR CONTRIBUTIONS

LH: Conceptualization, Investigation, Writing - original draft. XJ: Methodology, Writing - review & editing. XL: Methodology, Writing - review & editing. SX: Investigation, Data curation. FL: Investigation, Data curation. YC: Software, Resources. XQ: Software, Resources. LS: Formal analysis, Validation. ZL: Supervision, Writing - review & editing, funding acquisition. All authors contributed to the article and approved the submitted version.

FUNDING

This work was supported by National Key Research and Development Program of China (grant number: 2019YFC1200601 and 2019YFC1200700), and National Natural Science Foundation of China (grant number: 82073624).

ACKNOWLEDGMENTS

We thank American Journal Experts (AJE) for its linguistic assistance during the preparation of this manuscript.

REFERENCES

1. Brown-Elliott BA, Brown JM, Conville PS, Wallace RJ Jr. Clinical and Laboratory Features of the Nocardia Spp. Based on Current Molecular Taxonomy. *Clin Microbiol Rev* (2006) 19(2):259–82. doi: 10.1128/CMR.19.2.259-282.2006
2. Wilson JW. Nocardiosis: Updates and Clinical Overview. *Mayo Clin Proc* (2012) 87(4):403–7. doi: 10.1016/j.mayocp.2011.11.016
3. Ambrosioni J, Lew D, Garbino J. Nocardiosis: Updated Clinical Review and Experience at a Tertiary Center. *Infection* (2010) 38(2):89–97. doi: 10.1007/s15010-009-9193-9
4. Martínez-Barricarte R. Isolated Nocardiosis, an Unrecognized Primary Immunodeficiency? *Front Immunol* (2020) 11:590239:590239. doi: 10.3389/fimmu.2020.590239
5. López-Martínez R, Méndez-Tovar LJ, Bonifaz A, Arenas R, Mayorga J, Welsh O, et al. Actualización De La Epidemiología Del Micetoma En México.

Revisión De 3,933 Casos [Update on the Epidemiology of Mycetoma in Mexico. A Review of 3933 Cases]. *Gac Med Mex* (2013) 149(5):586–92. Spanish.
6. Hamdi AM, Fida M, Deml SM, Abu Saleh OM, Wengenack NL. Retrospective Analysis of Antimicrobial Susceptibility Profiles of Nocardia Species From a Tertiary Hospital and Reference Laboratory, 2011 to 2017. *Antimicrob Agents Chemother* (2020) 64(3):e01868–19. doi: 10.1128/AAC.01868-19
7. Schlaberg R, Fisher MA, Hanson KE. Susceptibility Profiles of Nocardia Isolates Based on Current Taxonomy. *Antimicrob Agents Chemother* (2014) 58(2):795–800. doi: 10.1128/AAC.01531-13
8. Tremblay J, Thibert L, Alarie I, Valiquette L, Pépin J. Nocardiosis in Quebec, Canada, 1988-2008. *Clin Microbiol Infect* (2011) 17(5):690–6. doi: 10.1111/j.1469-0691.2010.03306.x
9. Lebeaux D, Bergeron E, Berthet J, Djadi-Prat J, Mouniée D, Boiron P, et al. Antibiotic Susceptibility Testing and Species Identification of Nocardia Isolates: A Retrospective Analysis of Data From a French Expert Laboratory, 2010-2015. *Clin Microbiol Infect* (2019) 25(4):489–95. doi: 10.1016/j.cmi.2018.06.013
10. Minero MV, Marín M, Cercenado E, Rabadán PM, Bouza E, Muñoz P. Nocardiosis at the Turn of the Century. *Medicine* (2009) 88(4):250–61. doi: 10.1097/MD.0b013e3181afa1c8
11. McGuinness SL, Whiting SE, Baird R, Currie BJ, Ralph AP, Anstey NM, et al. Nocardiosis in the Tropical Northern Territory of Australia, 1997-2014. *Open Forum Infect Dis* (2016) 3(4):ofw208. doi: 10.1093/ofid/ofw208
12. Georghiou PR, Blacklock ZM. Infection With Nocardia Species in Queensland. A Review of 102 Clinical Isolates. *Med J Aust* (1992) 156 (10):692–7. doi: 10.5694/j.1326-5377.1992.tb121509.x
13. Yi M, Wang L, Xu W, Sheng L, Jiang L, Yang F, et al. Species Distribution and Antibiotic Susceptibility of *Nocardi*a Isolates From Yantai, China. *Infect Drug Resist* (2019) 12:3653–61. doi: 10.2147/IDR.S232098
14. Zijlstra EE, van de Sande WWJ, Welsh O, Mahgoub ES, Goodfellow M, Fahal AH. Mycetoma: A Unique Neglected Tropical Disease. *Lancet Infect Dis* (2016) 16(1):100–12. doi: 10.1016/S1473-3099(15)00359-X
15. Fatahi-Bafghi M. Nocardiosis From 1888 to 2017. *Microb Pathog* (2018) 114:369–84. doi: 10.1016/j.micpath.2017.11.012
16. Hernandez-Hernandez F, Lopez-Martinez R, Mendez-Tovar LJ, Manzano-Gayosso P. *Nocardia Brasiliensis: In Vitro* and *In Vivo* Growth Response to Steroid Sex Hormones. *Mycopathologia* (1995) 132(2):79–85. doi: 10.1007/BF01103779
17. Fuentes N, Silveyra P. Estrogen Receptor Signaling Mechanisms. *Adv Protein Chem Struct Biol* (2019) 116:135–70. doi: 10.1016/bs.apcsb.2019.01.001
18. Robinson DP, Lorenzo ME, Jian W, Klein SL. Elevated 17β-Estradiol Protects Females From Influenza a Virus Pathogenesis by Suppressing Inflammatory Responses. *PloS Pathog* (2011) 7(7):e1002149. doi: 10.1371/journal.ppat.1002149
19. Tsuyuguchi K, Suzuki K, Matsumoto H, Tanaka E, Amitani R, Kuze F. Effect of Oestrogen on Mycobacterium Avium Complex Pulmonary Infection in Mice. *Clin Exp Immunol* (2001) 123(3):428–34. doi: 10.1046/j.1365-2249.2001.01474.x
20. Cercenado E, Marín M, Sánchez-Martínez M, Cuevas O, Martínez-Alarcón J, Bouza E. *In Vitro* Activities of Tigecycline and Eight Other Antimicrobials Against Different *Nocardia* Species Identified by Molecular Methods. *Antimicrob Agents Chemother* (2007) 51(3):1102–4. doi: 10.1128/AAC.01102-06
21. Han L, Ji X, Xu S, Fan S, Wang C, Wei K, et al. Microbiological Profile of Distinct Virulence of Nocardia Cyriacigeorgica Strains *In Vivo* and *In Vitro*. *Microb Pathog* (2020) 142:104042. doi: 10.1016/j.micpath.2020.104042
22. Davis-Scibienski C, Beaman BL. Interaction of Nocardia Asteroides With Rabbit Alveolar Macrophages: Association of Virulence, Viability, Ultrastructural Damage, and Phagosome-Lysosome Fusion. *Infect Immun* (1980) 28(2):610–9. doi: 10.1128/iai.28.2.610-619.1980
23. Kadel S, Kovats S. Sex Hormones Regulate Innate Immune Cells and Promote Sex Differences in Respiratory Virus Infection. *Front Immunol* (2018) 9:1653. doi: 10.3389/fimmu.2018.01653
24. Hertz D, Dibbern J, Eggers L, von Borstel L, Schneider BE. Increased Male Susceptibility to Mycobacterium Tuberculosis Infection Is Associated With Smaller B Cell Follicles in the Lungs. *Sci Rep* (2020) 10(1):5142. doi: 10.1038/s41598-020-61503-3
25. Yang Z, Huang YC, Koziel H, de Crom R, Ruetten H, Wohlfart P, et al. Female Resistance to Pneumonia Identifies Lung Macrophage Nitric Oxide Synthase-3 as a Therapeutic Target. *Elife* (2014) 3:e03711. doi: 10.7554/eLife.03711
26. Wang Y, Cela E, Gagnon S, Sweezey NB. Estrogen Aggravates Inflammation in Pseudomonas Aeruginosa Pneumonia in Cystic Fibrosis Mice. *Respir Res* (2010) 11(1):166. doi: 10.1186/1465-9921-11-166
27. Abid S, Xie S, Bose M, Shaul PW, Terada LS, Brody SL, et al. 17β-Estradiol Dysregulates Innate Immune Responses to *Pseudomonas Aeruginosa* Respiratory Infection and Is Modulated by Estrogen Receptor Antagonism. *Infect Immun* (2017) 85(10):e00422–17. doi: 10.1128/IAI.00422-17
28. Pires S, Peignier A, Seto J, Smyth DS, Parker D. Biological Sex Influences Susceptibility to Acinetobacter Baumannii Pneumonia in Mice. *JCI Insight* (2020) 5(7):e132223. doi: 10.1172/jci.insight.132223
29. Rafiei N, Peri AM, Righi E, Harris P, Paterson DL. Central Nervous System Nocardiosis in Queensland: A Report of 20 Cases and Review of the Literature. *Medicine* (2016) 95(46):e5255. doi: 10.1097/MD.0000000000005255
30. Arnold AP. The Organizational-Activational Hypothesis as the Foundation for a Unified Theory of Sexual Differentiation of All Mammalian Tissues. *Horm Behav* (2009) 55(5):570–8. doi: 10.1016/j.yhbeh.2009.03.011
31. Chamekh M, Deny M, Romano M, Lefèvre N, Corazza F, Duchateau J, et al. Differential Susceptibility to Infectious Respiratory Diseases Between Males and Females Linked to Sex-Specific Innate Immune Inflammatory Response. *Front Immunol* (2017) 8:1806. doi: 10.3389/fimmu.2017.01806
32. Cho SSL, Han J, James SJ, Png CW, Weerasooriya M, Alonso S, et al. Dual-Specificity Phosphatase 12 Targets P38 MAP Kinase to Regulate Macrophage Response to Intracellular Bacterial Infection. *Front Immunol* (2017) 8:1259. doi: 10.3389/fimmu.2017.01259

Conflict of Interest: The authors declare that the research was conducted in the absence of any commercial or financial relationships that could be construed as a potential conflict of interest.

Publisher's Note: All claims expressed in this article are solely those of the authors and do not necessarily represent those of their affiliated organizations, or those of the publisher, the editors and the reviewers. Any product that may be evaluated in this article, or claim that may be made by its manufacturer, is not guaranteed or endorsed by the publisher.

Copyright © 2022 Han, Ji, Liu, Xu, Li, Che, Qiu, Sun and Li. This is an open-access article distributed under the terms of the Creative Commons Attribution License (CC BY). The use, distribution or reproduction in other forums is permitted, provided the original author(s) and the copyright owner(s) are credited and that the original publication in this journal is cited, in accordance with accepted academic practice. No use, distribution or reproduction is permitted which does not comply with these terms.

frontiers | Frontiers in Immunology

REVIEW
published: 10 June 2022
doi: 10.3389/fimmu.2022.911783

Current Status and Future Directions of Bacteria-Based Immunotherapy

Quan Tang[1,2], *Xian Peng*[1], *Bo Xu*[3,4], *Xuedong Zhou*[1,2], *Jing Chen*[1,2*] *and Lei Cheng*[1,2*]

[1] State Key Laboratory of Oral Diseases, National Clinical Research Center for Oral Diseases, West China Hospital of Stomatology, Sichuan University, Chengdu, China, [2] Department of Operative Dentistry and Endodontics, West China Hospital of Stomatology, Sichuan University, Chengdu, China, [3] Cancer Institute, Xuzhou Medical University, Xuzhou, China, [4] Center of Clinical Oncology, Affiliated Hospital of Xuzhou Medical University, Xuzhou, China

With the in-depth understanding of the anti-cancer immunity, immunotherapy has become a promising cancer treatment after surgery, radiotherapy, and chemotherapy. As natural immunogenicity substances, some bacteria can preferentially colonize and proliferate inside tumor tissues to interact with the host and exert anti-tumor effect. However, further research is hampered by the infection-associated toxicity and their unpredictable behaviors *in vivo*. Due to modern advances in genetic engineering, synthetic biology, and material science, modifying bacteria to minimize the toxicity and constructing a bacteria-based immunotherapy platform has become a hotspot in recent research. This review will cover the inherent advantages of unedited bacteria, highlight how bacteria can be engineered to provide greater tumor-targeting properties, enhanced immune-modulation effect, and improved safety. Successful applications of engineered bacteria in cancer immunotherapy or as part of the combination therapy are discussed as well as the bacteria based immunotherapy in different cancer types. In the end, we highlight the future directions and potential opportunities of this emerging field.

Keywords: immunotherapy, bacterial therapy, engineered bacteria, synthetic biology, microbiology.

OPEN ACCESS

Edited by:
Marina De Bernard,
University of Padua, Italy

Reviewed by:
Rong Xiu Li,
Shanghai Jiao Tong University, China
Li Zhang,
Nanjing General Hospital of Nanjing Military Command, China
Nicoletta Cieri,
Dana–Farber Cancer Institute, United States

***Correspondence:**
Jing Chen
sallychen.jc@gmail.com
Lei Cheng
chenglei@scu.edu.cn

Specialty section:
This article was submitted to Microbial Immunology, a section of the journal Frontiers in Immunology

Received: *03 April 2022*
Accepted: *12 May 2022*
Published: *10 June 2022*

Citation:
Tang Q, Peng X, Xu B, Zhou X, Chen J and Cheng L (2022) Current Status and Future Directions of Bacteria-Based Immunotherapy. Front. Immunol. 13:911783. doi: 10.3389/fimmu.2022.911783

1 INTRODUCTION

In recent decades, the comprehensive cancer treatment including surgery, radiotherapy, and chemotherapy has improved the overall survival rate and quality of life for numerous cancer patients; however, intractable problems such as unforeseen side effects, inaccurate curative efficiency, and high recurrence tendency still exist, necessitating the development of better intervention strategies (1).

Immunotherapy which utilizes agents to reactivate or boost immune surveillance appeals to be a novel and promising strategy for cancer treatment in recent years (2). Some of the therapeutic drugs such as interferon-α (IFN-α) for hairy cell leukemia (3), interleukin-2 (IL-2) for metastatic renal cancer and metastatic melanoma (4) have been approved by the US Food and Drug Administration (FDA), and has achieved certain remission in some patients. However, the short therapeutic duration of IFN-α (5) and the high toxicity and relatively low response rate of IL-2 (6) were reported. In 2011, ipilimumab, a monoclonal antibody that bind to cytotoxic T lymphocyte antigen 4 (CTLA4), was approved for advanced melanoma (7), which introduced the significant immune checkpoint inhibitor and ushered in a new age of immunotherapy. A series of other checkpoints

such as programmed cell death protein-1 (PD-1), programmed cell death-ligand 1 (PD-L1) and lymphocyte activation gene-3 (LAG-3) have also been identified to promote tumor immune escape and tumorigenesis. Therefore, inhibitors against these targets have been extensively developed and approved by the FDA for various cancer therapies, which significantly improved the survival rate of the advanced cancer patients in some clinical practices (8). However, the "cold" tumor microenvironment (TME) (9, 10) which is characterized by lacking of infiltrating immune cells or with exhausted immune cells compromises immune checkpoint blockade therapy and accounts for the non-responsiveness of some cancer patients, necessitating the development of improved immunotherapeutic strategies.

Tracing back to the origin of the modern immunotherapy, bacteria have been utilized as medication to treat incurable cancers. William Coley injected heat-inactivated *Streptococcus* and *Serratia marcescens* (known as Coley's toxins) into malignant tissues and observed the ablation of sarcomas in the nineteenth century (11). Following further investigation, the researchers discovered that the toxins could trigger the activity of the immune system against tumors (12), thus William Coley was honored as the father of immunotherapy (13). Progressively, the interactions between bacteria and the immune system in the context of cancer has extensively developed the field of immunotherapy around the globe. A successful example, Bacillus Calmette–Guérin (BCG), which is a live attenuated strain of *Mycobacterium tuberculosis* variant *bovis* originally designed as a vaccine for tuberculosis (14), has been approved by the FDA for the treatment of bladder cancer (15). But further development of this biological therapy was stalled due to the infection-associated toxicity and the insufficient comprehension of tumor immunity at the time (16).

During the recent years, studies have also demonstrated the existence of intratumoral bacteria and the immune modulation roles of microbiota, indicating that the tumor tissue is a complex of bacteria interacting with tumor cells and the host (17). Bacteria involve into almost all biological aspects of cancer, though the effect is two-sided. Pathogens including *Helicobacter pylori, Fusobacterium nucleatum*, and *Staphylococcus aureus* can cause the chronic inflammation and contribute to the tumorigenesis (18–20). Probiotics and some certain species of bacteria can induce direct cell apoptosis which show promising characteristic to serve as anti-cancer preparations (21, 22). The recent study demonstrated the intracellular bacteria in breast cancer contributed the lung metastasis *via* the cytoskeleton remodeling which indicating that targeting the intracellular bacteria might be a therapeutic choice (23). Bacteria also involved into the anti-cancer drug metabolism, like chemotherapeutic drug gemcitabine was disintegrated by intratumoral bacteria in pancreatic ductal adenocarcinoma (24). Bacteria derived HLA-bound peptides showed immunogenic properties which could be further studied (25). These days, with the in-depth understanding of TME and the rapid advancement of microbiology, nanotechnology and recombinant DNA technology, reprograming bacteria and building genetic circuits that can control their behavior are now becoming conceivable, making bacterial therapy a new hotspot in current cancer research and treatment development (26–28). As the genome information of a large number of bacteria has been successfully deciphered, *Escherichia coli* and *Salmonella typhimurium* (29), have evolved into highly editable engineered microorganisms that can be artificially endowed with diverse traits to facilitate them become sophisticated weapons against cancer.

This review will focus on the role of bacteria in anti-cancer immunity, as well as the present practice of employing bacteria as carriers or therapeutic agents in immunotherapy. The benefits of unmodified bacteria in immunotherapy will be discussed first, followed by engineered bacteria as enhanced treatment strategies. And the application of engineered bacteria in combined immunotherapy as well as the roles of bacteria-based immunotherapy in specific tumors are also discussed.

2 THE NATURAL ADVANTAGES OF BACTERIA

Bacteria show tumor-targeting properties, and their surface structure or metabolites can also activate the immune system to exert anti-tumor effects. Therefore, bacteria are blessed with inherent advantages to function as therapeutic agent or carriers in tumor immunotherapy. This section will highlight the chemotaxis of bacteria to tumors and the immune activation effect.

2.1 Tumor-Targeting Properties of Bacteria

The vasculature in tumor tissue is generally chaotic and irregular, leading to insufficient diffusion of oxygen and nutrients (30). As a result, the central region of tumors is often presented as a hypoxic environment with necrotic tissues, where the oxygen pressure is as low as 7-28mmHg, while it is 40-60mmHg for normal tissues (31). Studies have found that this central area could provide a safe haven for some obligate and facultative anaerobes to colonize and proliferate after systemic administration (32). Zheng *et al.* reported that the number of *S. typhimurium* in the tumor site reached 1×10^{10}CFU/g after intravenous administration for 3 days, and the ratio of tumor to normal organ bacteria exceeds 10000:1 (33). Shi *et al.* also found that *Bifidobacterium* could be detected inside the tumor sites one week after systemic administration, while remained undetectable in the lung (34). On the contrast, traditional chemotherapeutic drugs that solely rely on the passive distribution and limited permeability, are poorly accessible to these necrotic areas with sparse blood vessels through systemic administration, which leads to the relapse of tumors since the dormant but viable cancer cells still reside in the center zone (35). Therefore, bacteria are capable of colonizing the tumor core, the deepest and most difficult region to target for other types of agents.

The mechanism by which bacteria migrate to tumor sites remains to be fully elucidated. Some studies suggest that the disorganized vasculature in malignant tissues, preferential colonization and reproduction of bacteria in TME are the main factors endowing bacteria with tumor chemotaxis (36). When attenuated bacteria were injected intravenously, most of the

bacteria were cleared by the oxygen-rich environment and immune cells in the physiological tissues, however, the motility of bacteria prompts them to cross the vascular system and disperse themselves to the hypoxic area in the center of the tumor, where the hypoxic environment and the nutrients released by the necrotic cancer cells promote the massive proliferation of the anaerobic bacteria. Meanwhile, the local immunosuppressive microenvironment also prevents them from being cleared in the early colonization stage (37), during which process, TNF-α and its induced hemorrhagic necrosis play an important role. Leschner *et al.* found that injection of *S. typhimurium* into tumor tissue increased TNF-α levels in circulatory system and induced increased local hemorrhage. As the bacteria flowed out of the blood vessels, they were trapped in the irregular vasculature, resulting in its colonization in tumors. When the researchers neutralized TNF-α in the blood, the blockage of blood flow and the reduction of bacterial colonization were observed (38), further verifying the role of TNF-α.

2.2 Immune Activation Properties of Bacteria

Hypoxia, as a hallmark for TME, also leads to the suppressive function of local immune cells (39, 40). With the tumor development, the uncontrolled proliferation of cancerous cells deprives the oxygen and nutrients from immune cells (41). The immune cells therefore tend to be exhausted, present a suppressive phenotype by secreting pro-cancer cytokines and chemokines and fail to respond the anti-cancer signals. However, bacteria derived molecules such as peptidoglycan, lipopolysaccharide (LPS), and lipoteichoic acid can provide strong immune stimuli signals. They mainly bind to pattern recognition receptors (PRRs) expressed by innate immune cells such as dendritic cells (DCs) and macrophages to induce significant migration of immune cells, stimulate the immune system to recognize and kill tumor cells (42). For instance, *Salmonella* LPS can increase the expression of IL-1β and exert the anti-tumor effect through the inflammasome and the Toll-like receptor 4 (TLR4)-mediated signaling pathway (43). As a structure of some Gram-negative bacteria, flagella can promote the expression of various pro-inflammatory cytokines, NO, H_2O_2, and chemokines by binding to Toll-like receptor 5 (TLR5) on dendritic cells (44), enhance the tumoricidal effect mediated by $CD8^+$ T cells and down-regulate the suppressive function of Treg cells (45). Studies have shown that *Bifidobacterium* could stimulate stimulator of interferon genes (STING) and increases cross-priming of DCs (34). In addition to enhancing anti-tumor immunity by promoting the secretion of immune active factors, studies have shown that *Salmonella* can lead to up-regulation of connexin 43 (Cx43) expression in melanoma cells, mediating the formation of gap junctions between tumor cells and adjacent dendritic cells. Through this structure, tumor cells can present antigenic peptides to dendritic cells to activate the killing effect of cytotoxic T cells (46, 47). Si *et al.* also reported that oral administration of *Lactobacillus rhamnosus* GG increased tumor infiltrating DCs and promoted recruitment of CD8+ T cells through the type I IFN signaling.

Various cells such as macrophages and myeloid-derived suppressor cells (MDSCs) play important roles in the formation of the immunosuppressive microenvironment, which represents a therapeutic regimen for manipulating these cells to reverse the suppressive TME (48, 49). Certain components of bacteria can mediate the phenotypic transformation of immune cells. For example, macrophages make up a considerable percentage of immune cells and play an important role in immune regulation. According to their surface chemicals and functionalities, they are split into two subtypes. Anti-tumor macrophages mediate phagocytosis, release pro-inflammatory cytokines, whereas pro-tumor macrophages secrete anti-inflammatory cytokines, mediate tumor angiogenesis (50). Studies have found that flagellin can mediate the transformation of pro-tumor macrophages to anti-tumor macrophages, transforming the immunosuppressive microenvironment into an immunocompetent environment (33). Researchers has also reported that a variety of *Lactobacillusi* species promoted anti-tumor M1-like polarization through the TLR2 signaling pathway (51, 52). In addition, MDSCs exist in the blood of cancer patients and have a strong inhibitory effect on T cells and NK cells. Studies have found that *Listeria* can infect MDSCs, reduce the content of MDSCs in the blood, and promote the remaining MDSCs to secrete IL-12, switching to an immunocompetent phenotype (53). In addition, a reduction in tumor growth was observed in animal models treated with *Listeria*, suggesting that *Listeria* can inhibit tumors by acting on MDSCs.

3 ENGINEERING BACTERIA FOR THERAPEUTIC IMPROVEMENT

The chemotactic colonization of bacteria at tumor sites, as well as their immunogenicity, makes them ideal candidates for immunotherapy. It has been reported that several bacteria were detected inside the tumor tissues and intratumoral delivery of probiotics can promote the anti-tumor immunity (34, 54), providing a theoretical foundation for the use of microbes in tumor treatment. In recent years, with the development of synthetic biology, material science and gene editing tools, bacteria engineering has become possible. The tumor targeting properties, therapeutic effects, and safety performance can be further improved by different ways of modifying and transforming. Following studies listed in **Table 1** and also shown in **Figure 1**, summarizes excellent prospects of engineered bacteria with 3 aspects of improved properties.

3.1 Engineered Bacteria Improve Tumor Tropism

It is critical to take the tumor-targeting abilities into consideration when designing therapeutic agents, which accounts for not only the healing effect but also the elimination of off-target damage. When it comes to the improvement of tumor tropism of engineered bacteria, it may be just as crucial to hinder their survival in normal tissues as it is to boost their accumulation in tumor sites.

3.1.1 Construction of Auxotrophic Strain and Inducible Promoter

The construction of auxotrophic mutants is a strategy to improve bacteria targeting property. Based on the difference

TABLE 1 | Engineered bacteria for the enhanced therapeutic outcome.

Improvement	Strain	Mechanism	Cancer model	Ref
Enhanced tumor tropism	*S. typhimurium* A1	Leu/Arg-dependent auxotrophy	PC-3 human prostate cancer	(55)
	S. typhimurium SF104	Mutant of *aroA* gene	CT26 mouse colon cancer RenCa mouse renal cancer	(56)
	E. coli Nissle 1917	Thymidine and diaminopimelic acid auxotrophy	B16-F10 mouse melanoma EL4 mouse T-cell lymphoma A20 mouse B-cell lymphoma 4T1 mouse breast cancer CT26 mouse colon cancer	(57)
	S. typhimurium YB1	Place *asd* gene under a hypoxia conditioned promoter	MDA-MB-231 human breast cancer	(58)
	S. typhimurium VNP20009	Express CEA-specific antibody	MC38 mouse colon cancer	(59)
	S. typhimurium SL3261	Express CD20-targeting antibody	B16-F10 mouse melanoma MCA203 mouse fibrosarcoma CT26 mouse colon cancer Namalwa or Karpas299 human lymphoma	(60)
	S. typhimurium ΔppGpp	Display peptides that bind to αvβ3 integrin	MCF7, MDA-MB-231 human breast cancer MDA-MB-435, M21, M21L human melanoma U87MG human glioblastoma ASPC-1 human pancreatic cancer CT26 mouse colon cancer 4T1 mouse breast cancer MC38 mouse colon cancer	(61)
	L. lactis NZ9000	Display the binding protain of EpCAM and HER2	/	(62)
	S. typhimurium VNP20009	Bind aptamers to the bacterial surface	4T1 mouse breast cancer H22 mouse hepatocellular carcinoma	(63)
Immune modulation	*S. typhimurium* VNP20009	Production of IL-18	CT26 mouse colon cancer D2F2 mouse breast cancer	(64)
	S. typhimurium BRD509	Production of IFN-γ	B16-F10 mouse melanoma	(65)
	L. lactis NZ9000	Production of anti-CTLA-4 single chain fragment variable	/	(66)
	E. coli Nissle 1917	Production of STING-agonist cyclic di-AMP	B16-F10 mouse melanoma EL4 mouse T-cell lymphoma A20 mouse B-cell lymphoma 4T1 mouse breast cancer CT26 mouse colon cancer	(57)
	E. coli Nissle 1917	Production of PD-L1 and CTLA-4 nanobodies	CT26 mouse colon cancer A20 mouse B-cell lymphoma	(67)
	E. coli Nissle 1917	Production of PD-L1 and CTLA-4 nanobodies in a thermal sensitive manner	A20 mouse B-cell lymphoma	(68)
	E. coli	Production of nanobody antagonist of CD47	A20 mouse B-cell lymphoma 4T1 mouse breast cancer B16-F10 mouse melanoma	(69)
	E. coli Nissle 1917	Increase intratumoural concentrations of L-arginine	MC38 mouse colon cancer	(70)
	S. oneidensis MR-1	Reduce intratumoural concentrations of lactate	CT26 mouse colon cancer	(71)
Improved safety	*S. typhimurium* VNP20009	Deletion in the *msbB* and *purI* gene	B16-F10 mouse melanoma LOX human melanoma DLD-1 human colon cancer	(72)
	S. typhimurium ΔppGpp	Deletion in the *relA* and *spoT* gene	/	(73)
	L. monocytogenes 10403S	Mutant of *PrfA* gene	/	(74)
	L. monocytogenes ΔactA/ΔinlB	Deletion in the act*A* and *inlB* gene	CT26 mouse colon cancer	(75)
	E. coli Nissle 1917	Dynamic and tunable regulation of the bacterial surface		

(Continued)

TABLE 1 | Continued

Improvement	Strain	Mechanism	Cancer model	Ref
			CT26 mouse colon cancer 4T1 mouse breast cancer	(76)
	S. typhimurium SL1344	Incorporation of synchronized lysis circuit	MC26 mouse colon cancer	(77)
	E. coli Nissle 1917	Integrate synchronized lysis circuit into genome	CT26 mouse colon cancer A20 mouse B-cell lymphoma	(67)

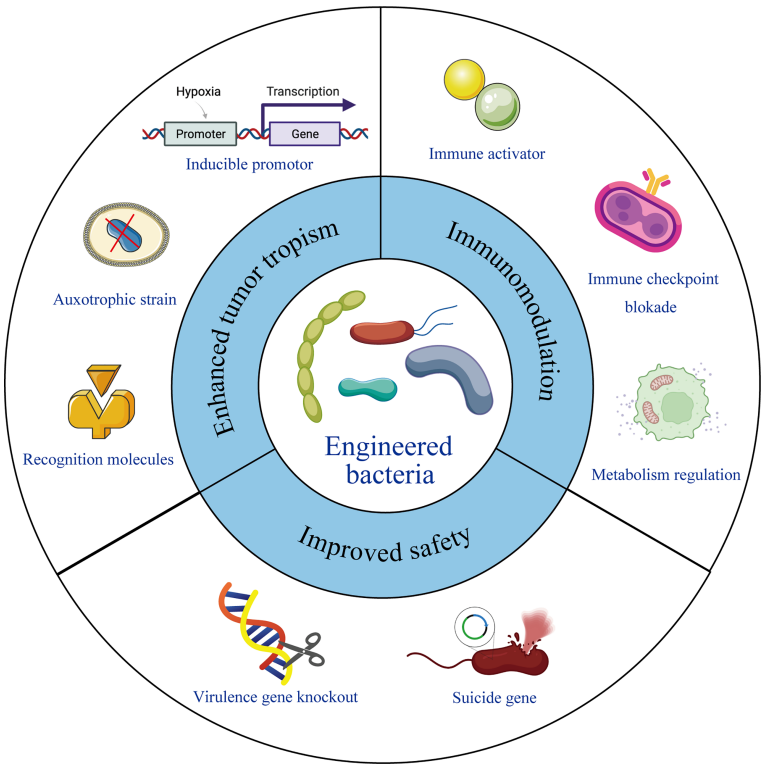

FIGURE 1 | Engineering bacteria for therapeutic improvement. Under modern microbiology, nanotechnology and recombinant DNA technology, bacteria can be engineered with enhanced tumor tropism, significant immunomodulation and improved safety profile, leading to reformed therapeutic outcome.

of nutrients contained in normal tissues and tumor sites, mutants can be designed to be only able to colonize and survive in tumor tissues. Among them, Salmonella A1 and SF104 are examples of successful application. Salmonella A1 is an auxotrophic strain of leucine and arginine (55), while Salmonella SF104 shows the need for aromatic amino acids with the mutation of the gene *aroA* (56), both of which can make the bacteria unable to enrich in normal tissues, but can specifically accumulate in tumor sites. *E. coli* Nissle was also designed by Leventhal *et al.* to include two auxotrophies (*thy*A and *dap*A) which result in its inability to survive outside the TME and in its inability to reproduce within the TME, respectively (57).

The essential gene *asd* of Salmonella, which mediates the synthesis of diaminoacrylic acid (DAP), an important component of the cell wall of Gram-negative bacteria, is placed under a hypoxia-inducible promoter by Yu *et al.* In normal tissues, the synthesis of DAP is blocked, without the supply of exogenous DAP, the bacteria will be lysed. However, the gene *asd* can be expressed in tumor sites with hypoxic environment, which enables Salmonella to colonize and survive in tumors. To further reduce off-target effects, they also placed the expression of inhibitory antisense RNA against *asd* under an aerobic-inducible promoter, and finally the strain showed 1000-fold enrichment in tumor sites compared to other organs (58). In addition, exogenous substances or stimuli, such as L-arabinose (78), acetylsalicylic acid (79), radiation stimulation (80), etc., can also regulate the expression of essential bacterial genes under the corresponding inducible promoters, which is beneficial to ensure specific proliferation at the tumor sites.

3.1.2 Modification Tumor-Related Recognition Molecules

Engineering synthetic adhesins tailored to bind specified cancer-expressed molecules such as neoantigens or other molecules abundant in cancer cells can improve some bacteria's natural affinity for tumors. Bereta *et al.* observed increased bacterial aggregation at tumor sites by expressing a specific single-chain antibody fragment for carcinoembryonic antigen (CEA) on *S. typhimurium* VNP20009 (59); Massa *et al.* increased bacteria's invasiveness against $CD20^+$ lymphoma, while reducing non-specific aggregation by binding anti-CD20 antibody to the surface of Salmonella (60). αvβ3 integrin is overexpressed in a variety of malignant tumors. By fusing arginine-glycine-aspartate peptides to bacterial outer membrane protein A, Park *et al.* enabled the bacteria to specifically bind to αvβ3 integrins and observed significant antitumor effects in xenogeneic melanoma and breast cancer transplant models (61). Epithelial cell adhesion molecule (EpCAM) and human epidermal growth factor receptor 2 (HER2) are transmembrane glycoprotein receptors associated with colorectal cancer. Plavec *et al.* successfully observed the co-localization of bacteria and tumor cells by displaying the binding protein of EpCAM and HER2 on the surface of *Lactococcus lactis* and making the bacteria express the infrared fluorescent protein for imaging, while on cells that did not express the corresponding molecule, no bacterial binding was observed (62). In addition, an aptamer is an oligomeric nucleic acid that can specifically bind to a certain molecule and has similar ligand-receptor binding characteristics with the target molecule. By binding the aptamer AS1411 to the surface of *S. typhimurium* VNP20009, Geng *et al.* observed nearly 2-fold and 4-fold enrichment after 12 and 60 hours in 4T1 and H22 tumor-bearing mouse models compared to unmodified bacteria, showing the enhanced targeting performance of this bacterium (63).

3.2 Engineered Bacteria Regulate the Immune Microenvironment

It has been stated that several fundamental components of bacteria are able to alter the immune system of the human body. However, to obtain greater immune regulatory effects, the engineered bacteria can be designed to load or express exogenous immunotherapeutic medications for enhanced anti-tumor efficacy.

3.2.1 Delivery of Immune-Activating Agents

Given that bacteria preferentially colonize malignant regions and naturally stimulate innate immune cells, bacteria-based therapy can provide a baseline level of immune activation in tumor tissues. Immune activators can effectively reform the immunosuppressive microenvironment of tumors and are one of the commonly used therapeutic agents for immunotherapy, which mainly include cytokines, tumor antigens and other substances. Cytokines own the ability to promote the activation and proliferation of immune cells, and the delivery of cytokines through engineered bacteria are blessed with the characteristics of high specificity and low side effects. Loeffler *et al.* used attenuated *S. typhimurium* to synthesize IL-18. By increasing the infiltration of $CD3^+/CD4^+$ T cells and $DX5^+$ NK cells in the tumor area, the expression of cytokines such as IL-1β, TNF-α, IFN-γ, GM-CSF were increased, and the anti-tumor effect was also observed (64). Yoon *et al.* also genetically modified Salmonella to express and secrete IFN-γ, thereby activating NK cells and mediating direct killing of cancer cells (65). Stimulator of interferon genes (STING) is another immune activating agent that can initiate tumor-specific T cell responses by activating antigen-presenting cells, producing type I interferons, and mediating antigen cross-presentation to cytotoxic T cells (81). Leventhal *et al.* expressed the STING agonist cyclic adenosine diphosphate through non-pathogenic *E. coli* Nissle, and observed the expression of type I interferon and various proinflammatory cytokines such as TNF-αIL-6IL-1βGM-CSF were up-regulated after intratumorally injection (57). The strain caused robust tumor eradication and long-term immunological memory in mice with tumors that were sparsely infiltrated by T cells, making treated mice resistant to tumor relapses. Tumor antigens are often used to make tumor vaccines to enhance immunity and activate immune cells to kill cancer cells. Tumor vaccines using bacteria as carriers have also been vigorously developed, exhibiting promising application prospects (82, 83). The human papillomavirus type 16 oncoprotein E7 (HPV-16 E7) plays a key role in the pathogenesis of cervical cancer and is required for host cell immunization. It is reported that oral administration of *L. lactis* expressing HPV-16 E7 protein could lead to significant delay of E7-expressing tumor growth, with significant increase in the numbers of E7-specific $CD4^+$T helper and $CD8^+$T cell, indicating that this bacteria-based vaccine provided profound protective effects against tumor cell challenge (84). A phase I clinical trial of this oral vaccine is also underwent to verify its safety and immunogenicity (85).

3.2.2 Delivery of Immune Checkpoint Inhibitors

Immune checkpoint therapy has been approved by FDA for the treatment of clinical cancer patients, and has achieved certain clinical results in the treatment of melanoma (7), non-small cell lung cancer (86), etc. The main mechanism of these drugs is to block the immunosuppressive state mediated by cancer cells and relieve the immune tolerance state (87). Monoclonal antibodies against PD-1, PD-L1 and CTLA4 have been widely used. Namai *et al.* successfully expressed human anti-CTLA4 antibody in *L. lactis* by genetic modification, and confirmed its recognition and binding to human CTLA4 by ELISA (66). Gurbatri *et al.* also used a combination of anti-PD-L1 and anti-CTLA4 therapy. The team transformed high-copy plasmids carrying anti-PD-L1 antibodies and anti-CTLA4 antibodies into engineered *E. coli* to achieve controllable expression of PD-L1 and CTLA4 antagonists in tumor sites. And the decrease in the number of Treg cells and the increase in the number of $CD4^+$ and $CD8^+$ T cells have been observed through immunophenotyping studies, indicating that the immunosuppressive microenvironment at this site has been reversed (67). To achieve the selective release of therapeutic agents at the tumor regions, Shapiro *et al.* further manufactured strains that produced tumor-suppressing anti-PD-L1 and anti-CTLA4 antibodies only when heated to a trigger temperature of 42-43°C by introducing a temperature-

actuated genetic state switch. Since the normal human body temperature is 37°C, these strains do not express anti-tumor nanobodies after systemic administration. Instead, they grow inside tumors until a triggering temperature is reached by the utilization of focused ultrasound (68).

CD47 is an anti-phagocytic receptor that overexpressed in multiple cancer types. Chowdhury *et al.* delivered anti-CD47 antibodies by engineering *E. coli* to activate dendritic cells in the TME and increase the phagocytosis of cancer cells, which also promoted the cross-presentation of tumor antigens, activated infiltrating T cells, and achieved rapid tumor regression (69).

3.2.3 Regulation of Metabolic Pathways of Tumor Immune Cells

L-arginine is critical for anti-tumor T cell responses (88), yet low availability of L-arginine in malignant tissues contributes to low T cell responses and the poor efficacy of immune checkpoint inhibition therapy. The Canale team found that the local concentration of L-arginine could not be maintained by injecting a saturated solution of L-arginine into the tumor, so the team leveraged engineered *E. coli* Nissle 1917 to continuously convert the metabolic waste ammonia into L-arginine in the tumor sites, which effectively increased the intratumoral L-arginine concentration and enhanced the T cell response. And a synergistic effect with anti-PD-L1 therapy was also observed, exerting a stronger antitumor effect (70). As studies has revealed that lactate could be responsible for tumor invasion (89), targeting lactate metabolism is a feasible therapeutic strategy. Chen *et al.* fabricated a biohybrid material with significant lactate exhaustion property, in which manganese dioxide nanoflowers as electron receptor was modified onto the surface of *Shewanella oneidensis*. Therefore, the extracellular lactate serves as electron donor to ensure a sustained effect of downregulating the lactate level by the coupling of bacterial respiration with tumor metabolism, which result in inhibited tumor progression (71).

3.3 Engineered Bacteria Improve Safety

Although bacteria exhibit excellent anti-tumor characteristics, their potential toxicity is a major stumbling block to their application. The safety profile of living bacteria preparations, on the other hand, represents a crucial need for their clinical translation. To make full use of bacteria to fight against cancer, researchers have made tremendous efforts to construct a large number of attenuated engineered strains to improve their safety performance.

3.3.1 Virulence-Related Gene Knockout

The immunogenic bacterial surface molecule contribute as main virulence of bacteria, which indicates that modification (such as genetic knockout) of these surface antigens represent a major approach to circumvent toxicity of living pathogen. For instance, ppGpp (guanosine 5'-diphosphate-3'-diphosphate) is a signaling molecule involved in the expression of virulence genes. By knocking out the *relA* and *spoT* genes, the synthesis of ppGpp was blocked, resulting in a 10^5-10^6-fold increase in its LD50 compared to wild strains (73). The bacteria with disordered ppGpp synthesis also showed good antitumor activity due to its ability to induce the secretion of pro-inflammatory factors IL-1β, IL-18, and TNF-α (37). In addition, LPS of Gram-negative bacteria is a potent stimulator for inducing TNF expression and is one of the main causes of sepsis. On the other hand, as the outermost structure of the cell envelop, LPS is also an important barrier and defense agent and is essential for their survival and efficient tumor colonization. VNP20009 is a safe strain of *Salmonella* with deletion of *msbB* and *purI* genes (72), in which *msbB* knockout leads to myristoylation of lipid A in LPS, reducing the ability to induce TNF secretion and greatly reducing its virulence (90). However, the structural changes of lipid A also reduced its therapeutic effect. In clinical trials, the tumor colonization and antitumor activity in human patients were not effectively exhibited (91), suggesting the apparent trade-off between bacterial virulence and antitumor activity. To maintain the balance between safety and anti-tumor efficacy, Frahm *et al.* observed that the attenuated bacteria exerted good therapeutic effects by integrating the LPS biosynthesis gene into the araBAD locus of the bacterial chromosome with the regulation of arabinose-inducible promoter (92). To step further, Harimoto *et al.* realized a dynamic and tunable regulation of the bacterial surface by constructing an inducible synthetic gene circuit that modulates the programmed expression of bacterial surface capsular polysaccharide. In this way, the bacterial surface virulence molecular is hided and shielded from the immune system, which turn out to show enhanced bacterial survival and colonization and a ten-fold increase in systemically injectable tolerated dose *in vivo*, showing an improved safety profile (76).

In addition to modifying virulence molecules, aiming at the escape ability and invasiveness of bacteria is also a major measure for attenuation. *Listeria* is a vaccine strain mainly used to express tumor antigens, whose virulence factor can be deleted by knocking out the *prfA* gene (74). Unfortunately, in this way, *Listeria* cannot escape from the phagosome, which prevents the carried tumor antigens from entering the cytoplasm for processing. To address this issue, the strain was designed to express low levels of PrfA and *Listeria* hemolysin O to improve its immunogenicity, which showed that the reformed strain is endowed with great potential in expressing tumor antigens as well as delivering other therapeutic drugs (93). CRS-207, a *Listeria* strain with two virulence genes *actA* and internalin B knocked out, exhibited reduced spreading and invasive abilities. And its colonization level decreased by 1000 times compared to common strains (75), thus the application security is guaranteed.

3.3.2 Suicide Gene

To avoid the infinite proliferation of bacteria in the body, strategies must be adopted to programmatically limit the proliferation level to maintain the stability of the microecology. Din *et al.* designed a synchronized lysis circuit (SLC) into which a phage φX174 cleavage gene E was integrated. This method takes advantage of the colony effect of natural bacteria. When the bacterial proliferation reaches a threshold density, the bacteriophage-derived lysis factor is produced, diffuses to neighboring cells and triggers lysis. This releases the intracellular therapeutic drugs, while a small number of

surviving bacteria continue to reproduce to maintain the dynamic balance of local bacterial populations (77). Still, a major disadvantage of this approach is its dependence on plasmids, which may lead to recombination, mutation and loss during the growth cycle. As to make the circuit more stable, Gurbatri *et al.* integrated the gene circuit into the genome of *E. coli*. Although a certain number of copies of quorum sensing genes was lost, the results showed that this method has better effect than the original system (67).

4 APPLICATION OF ENGINEERED BACTERIA IN COMBINED IMMUNOTHERAPY

It has been shown that bacteria can function as immunotherapeutic agents to enhance the anti-tumor immunity. As combination therapy is a widely used strategy to improve the overall effect, bacteria-based immunotherapy has also been served as a part of combination with chemotherapy, radiotherapy, photodynamic therapy and photothermal therapy. In this section, we summarize the latest practices of bacteria being recruited as part of the combined therapy, where bacteria exhibited synergistic effect of activating the immune system, synthesizing or protecting the anti-cancer drugs to enhance anti-tumor effect.

4.1 Combined With Chemotherapy

Traditional chemotherapy suffers from a lack of specific delivery to malignant tissue and significant drug systemic exposure, which commonly results in dose-limiting toxicity. Applying engineered bacteria to act as drug delivery system for controlled drug release, as well as utilize their immunogenicity for immune modulation has gained much research attention. Ektate *et al.* attached low-temperature sensitive liposomes onto the membrane of *Salmonella*, which mediated the triggered release of doxorubicin inside colon cancer cells with the help of high intensity focused ultrasound (HIFU) heating, resulting in efficient drug delivery in both the cytoplasm and the nucleus of cancer cells. Moreover, the strain also polarized macrophages to anti-tumor M1 phenotype, enriched Th1 cells population with high production of TNF-α, and decreased expression of IL-10, thus exhibiting enhanced therapeutic effects in a combined chemo-immunotherapy manner (94). For some highly malignant tumor types, chemotherapeutic drugs alone show limited enhanced survival benefits, such as gemcitabine for the treatment of pancreatic ductal adenocarcinoma, thus calling for additional approaches. To reform the poorly immunogenic TME of pancreatic ductal adenocarcinoma, Gravekamp *et al.* delivered tetanus toxoid protein, which act as a neoantigen reactivating preexisting memory T cells that were generated during childhood vaccinations, into tumor cells by attenuated *Listeria*, which could selectively delivered to tumor regions with the help of MDSCs (53). The tetanus toxoid induced attraction of CD4 T cells, with increased production of IFNγ, perforin, and granzyme B in the TME, while gemcitabine was used to reduce immune suppression in the TME, which resulted in reduced tumor burden by 80% compared to untreated mice (95).

Besides leveraging living bacteria, bacterial outer membrane vesicles (OMVs), which are naturally produced from Gram-negative bacterial membranes during growth process, have recently emerged as immunotherapeutic agents for a variety of biomedical applications. Chen *et al.* encapsulated drug-loaded polymeric micelles into bacterial outer membrane vesicles, where the bacterial component could activate the immune response while the loaded tegafur exert both chemotherapeutic and immunomodulatory effect to ablate cancer cells. As a result, this strategy showed substantial improvement in tumor regression, survival extension and remarkable inhibition of pulmonary metastasis (96).

4.2 Combined With Radiotherapy

Bacterial-assisted radiotherapy represent as a new approach for tumor treatment. Although few studies has applied bacteria to improve radiotherapy, this field might be developed as a new viable method in clinical radiation oncology. In a study by Jiang *et al.*, the therapeutic effect of combining *E. coli* with radiotherapy was investigated, which revealed significant tumor shrinkage in a colon tumor model under 21 Gy of radiation and *E. coli* with the production of cytolysin A (97). Similarly, engineered *S. typhimurium* carrying imaging probes and therapeutic agents for tumor imaging and treatment in a combination of radiotherapy demonstrated greater remission. As a result, the bacteria carrying cytolysin A combined with radiotherapy cause more tumor remission as compared to bacterial therapy alone (98). In a recent study, an integrated nanosystem for sensitizing radiation was established using modified *E. coli* and Bi_2S_3 nanoparticles. The bacteria might invade tumor locations and overexpress the cytolysin A protein to switch the cell cycle from a radioresistant to a radiosensitive state. At the same time, Bi_2S_3 nanoparticles may improve radiation sensitivity by causing intracellular production of reactive oxygen species (ROS) and DNA damage (99).

After radiotherapy, tumors release a considerable number of tumor antigens, which can be taken up and presented by DCs, leading to specific adaptive immune responses. However, in the immunosuppressive TME, the number of DCs is typically low and they are usually remaining in a state of dysfunction, which indicate that intratumoral antigens are often poorly recognized and presented. As a result, increasing the number of DCs and boosting their function in tumors are major study topics. Wang *et al.* injected *Salmonella* coated with antigen-adsorbing cationic polymer nanoparticles into tumor tissues, which can capture the antigen released after radiotherapy and transport them out of the tumor core to activate the surrounding DCs in tumor marginal tissues owing to the bacteria's mobility. As a result, large increases in activated DCs *in vitro* and extended survival in multiple tumor mice models *in vivo* were observed, showing the enhanced systemic antitumor effects (100).

4.3 Combined With Photodynamic Therapy and Photothermal Therapy

As standard tumor therapies suffer from unspecific killing effect and complicated surgery, photodynamic therapy and

photothermal therapy have emerged as new therapeutic options due to their non-invasiveness, high specifity and excellent spatial and temporal control. Recently, numerous studies have attempted to employ bacteria as carrier to load the therapeutic agents of PDT and PTT, in order to leverage the tumor-targeting and immunoactivating properties of bacteria.

PDT relies on the conversion of local oxygen molecules into ROS to mediate the killing effect on cancer cells. But the local hypoxic environment of the tumor causes insufficient production of ROS, thus compromising the therapeutic effect of PDT. Liu *et al.* integrated photosensitizer-coated nanoparticles onto the surface of photosynthetic bacteria *Synechococcus*. Under 660nm laser irradiation, photosynthetic bacteria continued to produce oxygen, which ensured the production of ROS and enhanced the effect of photodynamic therapy. *Synechococcus*, as immunogenic bacteria, also activate local immunity by upregulating the expression of MHC class II molecules and IL-12. At the same time, this treatment method induces immunogenic apoptosis by up-regulating calreticulin on the cell surface, and has shown a good therapeutic effect in triple-negative breast cancer model (101).

Other researchers have also tried to combine bacteria with PTT. Indocyanine green (ICG) was bound to the surface of *S. typhimurium* strain YB1 by Liu *et al.* This stratery resulted in a 14-fold increase of the enrichment of the modified strain within tumors, as well as perfect photothermal conversion. In addition to significantly killing the tumor in the central hypoxic area, this method also effectively kills tumor cells in the peripheral area with normal oxygen perfusion, showing better anti-tumor efficacy (102). Chen *et al.* integrated the photothermal agent polydopamine on the surface of *Salmonella* and observed that the engineered bacteria exhibited unaffected tumor-targeting ability and activated local immunity by promoting the production of TNF-α and IL-4 (103). The research team further improved the strategy and realized an innovative triple therapy by combining the immune checkpoint inhibitor AUNP-12 (an anti-PD-1 peptide). Through the application of phospholipid phase separation gel, the team improved the short retention time of the peptide antagonist AUNP-12, and achieved a sustained release effect of the therapeutic drug at the tumor site for up to 42 days. This triple therapy showed a more pronounced antitumor effect than bacterial therapy alone and showed potent inhibition of advanced melanoma (104). However, these studies require the multistep synthesis of nanoparticles and complicated genetic manipulations of bacteria. Reghu *et al.* established a simple modification method by designing nanoparticle-functionalized nonpathogenic natural bacteria. To be more specific, they engineered *Bifidobacterium bifidum* with ICG-encapsulating Cremophor EL nanoparticles by simple incubation and washing processes while maintaining the bacterial natural properties. Under near infrared light induction, the functionalized bacteria showed superior antitumor effect by laser-driven photothermal conversion and the excess TNF-α expression with the assistance of macrophages (105). Similarly, Yang *et al.* apply non-pathogenic natural purplep synthetic bacteria *Rhodopseudomonas palustris* in cancer theranostics without complicated chemical functionalization and genetic manipulation, which are blessed with tumor-targeting abilities, excellent heat and ROS production, resulting in drastic tumor elimination (106).

5 THE ROLE OF BACTERIA-BASED IMMUNOTHERAPY IN DIFFERENT CANCER TYPES

Different types of cancer have their unique biological behaviors, their response to the immune modulation also varies. Here, we summarized the immune related bacteria therapies according to their application in different cancer types. The therapeutic agents and the effect on tumor and the microenvironment were discussed in details, which were also summarized in **Table 2**.

5.1 Colon Cancer

The colon cancer is considered to be highly associated with the gut microbiota (120). Nowadays, emerging studies have demonstrated that the dysbiosis of gut microbiome poses adverse effects on the epithelial cells and eventually lead to the induction of colon cancer. Therefore, probiotics, which specifically suppress the colonization of certain pathogenic bacteria and reverse the dysbiosis of gut microbiome caused by antibiotic usage, have been reported to maintain the balance of intestinal microbiota and exert preventive effects against colon cancers (121). Sun *et al.* reported that oral administration of *L. rhamnosus* Probio-M9 could modulate the gut microbiota in which the relative abundance of beneficial bacteria was increased, and contributed to the recovery of antibiotic-disrupted gut microbiota. Moreover, synergistic effect of this probiotic therapy was discovered when coupled with the anti-PD-1 treatment, in which significant tumor inhibition was observed as compared to the anti-PD-1 treatment alone (107). Similarly, Fu *et al.* also found that intratumoral accumulation of *Bifidobacterium* facilitated anti-CD47 therapy *via* STING signaling (34). These studies pose valid evidence to support that the outcome of immune checkpoint blockade therapy relies on the host's gut microbiota (122). Probiotics are also blessed with protective effects against the tumorigenesis. In an orthotopic colon cancer model induced by azoxymethane, oral intake of *L. acidophilus*, and *B. bifidum* probiotics were reported to inhibit the colon lesions by about 57% and 27% respectively. Moreover, *L. acidophilus* treated mice exhibited improved serum levels of IFN-γ, IL-10, $CD4^+$ and $CD8^+$ cells, manifesting a better protective effects (108).

As a growing number of therapeutic targets have been identified, the idea of genetically engineering bacteria to combat a specific pathogenic process is gaining much attention. Indoleamine 2,3-dioxygenase (IDO), which is an immune check point protein contributing to the immunosuppressive TME, is related to the poor prognosis of colon cancer patients. Melstrom *et al.* successfully reduced the IDO levels by employing *S. typhimurium* which delivers inhibitory small hairpin (sh)RNA targeting IDO. The treatment resulted in significant delayed tumor progression in CT26 and MC38 colon cancer models, where enhanced neutrophils

TABLE 2 | The role of bacteria-based immunotherapy in different cancer types.

Cancer type	Bacterium	Immune modulation effects	Ref
Colon cancer	*L. rhamnosus*	Restore the antibiotic-disrupted gut microbiota and synergize with anti-PD-1 therapy	(107)
	Bifidobacterium	Facilitate anti-CD47 therapy *via* STING signaling	(34)
	L. acidophilus	Improved serum levels of IFN-γ, IL-10, $CD4^+$ and $CD8^+$ cells	(108)
	S. typhimurium	Reduce intratumoral levels of IDO, increase tumor infiltration of neutrophils	(109)
	S. typhimuriumS	Inhibition of Stat3 combined with siRNA against PD-1	(110)
Lung cancer	*L. monocytogenes*	Enhanced function of CD8+ T cell and regulation effcets on Treg cells and MDSCs	(111)
	B. bifidum	Increased secretion of IFN-γ and IL-12, enhanced lymphocyte proliferation and $CD8^+$ T cell responses	(112)
	L. casei	Increased production of IL-2	(113)
	L. lactis	Recombinant strain with IL-17A cytokine secretion	(114)
Melanoma	*L. monocytogenes*	Increased infiltration of $CD4^+$ and $CD8^+$ T cells	(115)
	L. monocytogenes	Elicit profound $CD8^+$ T cells responses and synergize with immune checkpoint blockade	(116, 117)
Breast cancer	*S. typhimurium*	Elevated percentage of $CD3^+CD4^+$ T cells and increased production of IFN- γ and TNF-α	(63)
	E. coli	Local delivery of CD47 antagonist and activation of tumor-infiltrating T cells	(69)
Lymphoma	*E. coli*	Local delivery of PD-L1 and CTLA-4 nanobodies	(67)
	E. coli	Local delivery of CD47 antagonist and activation of tumor-infiltrating T cells	(69)
Prostate cancer	*S. typhimurium*	Induce Th1 immune responses and tumor protective immunity	(118)
Cervical cancer	*L. monocytogenes*	Induction of Th1 immunity, enhanced lymphocyte proliferation and specific CTL activity	(119)
Pancreatic cancer	*L. monocytogenes*	Reactivate the preexisting memory T cells by delivery of tetanus toxoid	(95)

infiltration was observed, indicating the innate immune response was efficiently elicited (109). The overwhelming activation of signal transduction and transcription activator 3 (Stat3) is reported to promote tumorigenesis *via* various mechanisms. By combining the inhibitor of Stat3 (nifuroxazide) with *S. typhimurium* carrying small interfering RNA against PD-1, Feng *et al.* discovered a synergistic antitumor effect on colon cancer, where potent anti-tumor immunity was strongly elicited (110).

5.2 Lung Cancer

It has been shown that a number of probiotics are blessed with anti-tumor efficacy through immunological regulation. To investigate the underlying mechanism, Ghaemi *et al.* demonstrated that intravenous injection of *B. bifidum* led to increased secretion of IFN-γ and IL-12, enhanced lymphocyte proliferation and $CD8^+$ T cell responses as compared to oral administration in a HPV-induced TC-1 mouse lung cancer model (112). Similarly, by using the same cancer model, *L. casei* BL23 was discovered to exert anti-tumor effect by IL-2 signaling pathway, with the involvement of T cells and NK cells (113). Moreover, recombinant strain of *L. lactis* that secreted biologically active IL-17A cytokine was also established, which made 26% of treated mice tumor-free in the TC-1 tumor challenge (114).

To obtain vigorous anti-tumor immunity, simultaneously targeting both the costimulatory and inhibitory receptor-ligands of the immune system can be a promising strategy. In support of this idea, agonist antibody to glucocorticoid-induced tumor necrosis factor receptor-related protein (GITR) which acts as a costimulatory target that promotes effector function has been combined with a *L. monocytogenes*-based vaccine which significantly regulates the suppressive cells including Treg cells and MDSCs. In a mouse model bearing subcutaneous TC-1 lung tumor, this combined therapy resulted in tumor eradication in 60% of treated mice, which could be attributed to the enhanced function of $CD8^+$ T cell, reduced ratio of Treg/$CD4^+$ cell and the regulation to MDSCs (111).

5.3 Melanoma

Melanoma represents as the most aggressive type of skin cancer with a high tendency to progress into the metastatic stage, which may attribute to the notable competency to evade the immune recognition. Therefore, potentiating the immune attack against melanoma is a viable strategy. Poliseno *et al.* has reported that attenuated *L. monocytogenes* could kill various melanoma cells *in vitro*, regardless of their stage and genetic status, which may overcome therapeutic challenge caused by the high degree of heterogeneity. By establishing genetically engineered mice susceptible to primary and metastatic melanoma, the team further assessed the anti-tumor activity of this strain *in vivo*, which resulted in impaired growth of the primary tumor as well as reduction of the metastatic burden. Moreover, increased infiltration of $CD4^+$ and $CD8^+$ T cells was detected, suggesting that the immune responses were effectively augmented (115). To step further, *L. monocytogenes* expressing tumor-associated antigen was successfully constructed, which elicited profound $CD8^+$ T cells responses and subsequently protected about 70% mice from B16F10 melanoma. When combined with immune checkpoint blockade therapy (anti-PD-1, anti-PD-L1, and anti-CTLA-4), significant tumor remission was observed, indicating that anti-tumor immunity induced by *L. monocytogenes* vaccination could be further enhanced with immune checkpoint blockade therapy (116). To better safeguard the application of live strains used in immunocompromised cancer patients, listeriolysin O, which is responsible for the biological activities of *L. monocytogenes* related to the anti-tumor effect, was encapsulated into gold nanoparticles to generate a safer preparation. Similarly, the ability of inducing $CD8^+$ T cells responses was successfully maintained, and a synergism coupled with anti-PD-1 or anti-CTLA-4 was also detected (117).

5.4 Breast cancer

Only a few studies have reported the bacteria-based immunotherapeutic platforms targeting the unique characteristics in breast cancer. Min *et al.* has shown that *S. typhimurium* displaying the RGD peptide could specifically bind

to cancer cells overexpressing αvβ3 integrin, including breast cancer cells. In a mouse model of human breast cancer (MDA-MB-231 cell line), significant tumor regression and prolonged survival of mice receiving intravenous injection of the modified strain were detected, in which the therapeutic effect relied largely on the tumor-specific accumulation following administration (61). Similarly, aptamers which promoted the colonization of bacteria inside tumor areas were also conjugated to *S. typhimurium* VNP20009 by Tan et al, which manifested excellent anti-tumor efficacy in 4T1 tumor-bearing mouse models. Moreover, the percentage of $CD3^+CD4^+$ T cells and the production of IFN- γ and TNF-α ware significantly elevated, suggesting strong immune response triggered by this bacterial agent (63). In another mouse model of triple negative breast cancer, impaired tumor growth and notable reduction in lung metastasis were reported in mice treated with *E. coli* encoding nanobody antagonist of CD47 (69).

5.5 Other Types of Cancers

Recently, immunotherapy, especially the immune checkpoint blockade therapy, has gained encouraging achievements in the treatment of lymphoma (123), and utilizing bacteria to delivery therapeutic antibody also attracts research attention. Danino *et al.* has investigated the anti-tumor activity of *E. coli* expressing both anti-PD-L1 and anti-CTLA-4 antibodies against advanced lymphoma in a mouse model with a larger initial volume (about 200 to 700 mm^3), in which impaired growth or complete clearance was observed (67). Similarly, *E. coli* expressing CD47 antagonist was reported to exert durable anti-tumor efficacy of the established A20 tumors. Moreover, the treated mice obtained resistance when tumors cells were reinjected subcutaneously (69).

Inducing systemic immune responses by certain antigens overexpressed by cancer cells is a potent therapeutic method for metastatic cancer treatment. For instance, *S. typhimurium* carrying a plasmid encoding prostate stem cell antigen was successfully established, which induced Th1 immune responses and resulted in 50% of treated mice tumor-free over the challenge of TRAMPC1 mouse prostate cancer cells (118). Recombinant *L. monocytogenes* expressing HPV16-E7 was also demonstrated to generate protective effect in immunized mice against cervical cancer, where induction of Th1 immunity, enhanced lymphocyte proliferation and specific CTL activity were observed as compared to control group (119). Therefore, more therapeutic modalities targeting certain antigens displayed by specific tumors are yet to be further developed. For certain cancer type with low immunogenicity and low expression of neoantigen such as pancreatic ductal adenocarcinoma, Gravekamp *et al.* has designed a platform to deliver the immunogenic tetanus toxoid protein by *L. monocytogenes*. In this method, the tetanus toxoid acted as an alternative neoantigen to awaken the preexisting memory T cells generated in childhood vaccination, thus turning

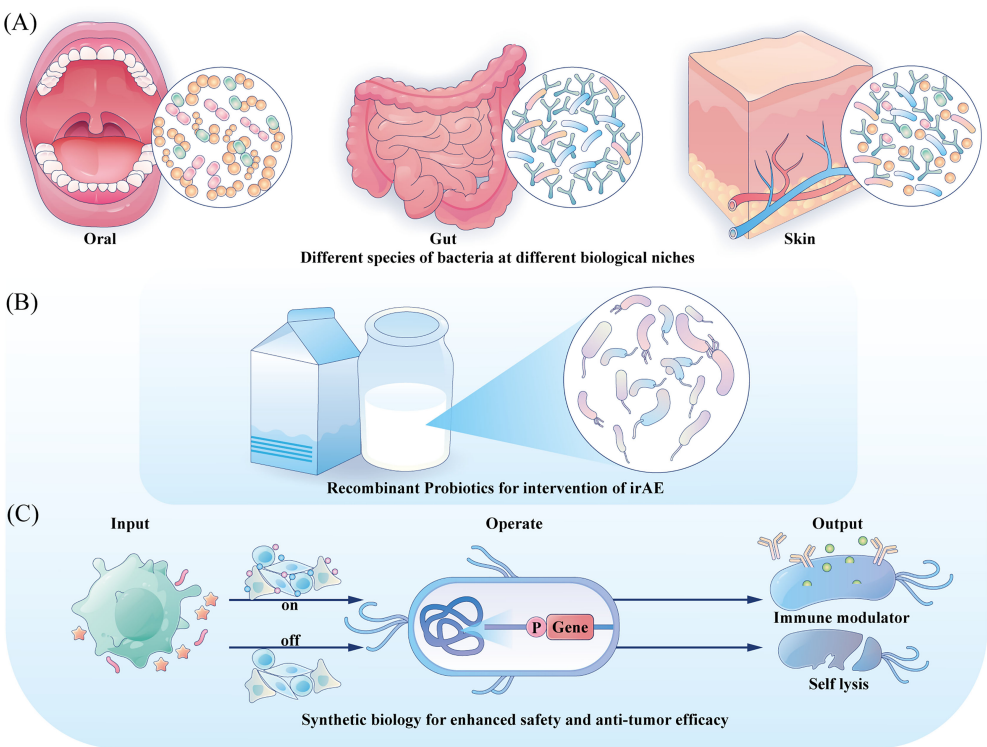

FIGURE 2 | Directions for future engineering. **(A)** Engineering the commensal bacteria at their original ecology with enhanced anti-tumor prospects to provide precise treatment strategy. **(B)** For irAE, probiotics could be developed with anti-inflammation characteristic and serve as local mediators. **(C)** Integration gene circuits could manipulate the bacteria to sense different input information and provide different outputs, tuning the treatment intensity and controlling the bacteria fate.

the cold TME into a highly immunological environment, which eventually resulted in over 80% reduction of tumor growth and metastasis when coupled with the treatment of gemcitabine (95).

6 PERSPECTIVES AND PROSPECTS

Different human body niches reside distinct microbiota communities and bacteria often perform different roles in different ecological sites. It is aware that bacteria being in the wrong place within the body can be quite hazardous. For example, *E. coli*, as a typical resident in the intestine, can cause infection once entering the urethra (124), abdominal cavity (125), and other regions of the body (126). Due to the in-depth understanding of the interaction between microorganisms and tumors, utilizing specialized bacteria for distinct tumor types can not only avoid infection, but also exert a regulatory influence on the local microecology. Shisssss *et al.* found that oral administration of *Akkermansia marcescens* can produce a synergistic effect with IL-2 therapy, and a good therapeutic effect was observed in a mouse model of colorectal cancer (127). Similarly, Zheng *et al.* reported that oral squamous cell carcinoma patients with higher levels of bacteria of the genus *Peptostreptococcus* presented higher probability of long-term survival. To upregulate the levels of *Peptostreptococcus*, subcutaneous injection of an adhesive hydrogel incorporating silver nanoparticles alongside the intratumoral delivery of the bacterium *P. anaerobius* was adopted, which manifested enhanced anti-tumor responses and synergized with the anti-PD-1 therapy. Therefore, In the future, commensal bacteria at different body sites can be specifically developed to exert therapeutic effects for the tumors at their according locus.

Currently, immune therapy exhibited immune-related adverse events (irAEs) such as colitis, fatigue, rash, endocrine disturbance, and hepatotoxicity (128, 129), which can be attributed to off-target effects of therapeutic drugs as well as dose-dependent toxicity. Relying on the precise regulation of the targeting properties of engineered bacteria, specific release of drugs at the tumor site can be achieved, which is beneficial to reduce the occurrence of adverse reactions related to immunotherapy. Besides, plenty of commensal probiotics such as Lactic acid bacteria, has exhibited benefits for the prevention of colitis and moderation of diarrhea, indicating that it is a promising choice to employ engineered probiotics to alleviate some adverse reactions (130).

Decades have passed since the first trial of utilizing BCG as medication for bladder cancer, and relentless practices have also been undergoing to investigate its involvement in cancer therapy beyond bladder cancer (131). Besides BCG, other bacterial preparations such as modifed *S. typhimurium* stains are also in the preclinical or clinical trial stage to better verify their safety and therapeutic effects (132). As bacteria are complex and viable therapeutic agents, some uncontrollable mutations during their proliferation may bring potential toxicity. And their inherent virulence can also lead to complex infections in immuno compromised cancer patients. However, the rapid advances in synthetic biology are making it possible to program a desired bacterial behavior through the introduction of synthetic gene circuits, which are composed of an input module detecting biotic signals, an operation module computing transmitted signal and an output module generating the desired cellular response, resulting in a safer application profile and enhanced anti-tumor efficacy (27). Directions for future engineering are illustrated in **Figure 2**.

AUTHOR CONTRIBUTIONS

QT and JC constructed figures and wrote the manuscript. LC revised the paper. All authors contributed to the article and approved the submitted version.

FUNDING

This work was supported by the National Natural Science Foundation of China 81870759 (LC), 82071106 (LC), the Research Funding from West China School/Hospital of Stomatology Sichuan University, No. RCDWJS2022-5 (to JC), and the Research Funding from West China School/Hospital of Stomatology Sichuan University, No. RCDWJS2021-19 (to LC).

ACKNOWLEDGMENTS

The authors would like to acknowledge Sabina Muend for the language improvement.

REFERENCES

1. Miller KD, Nogueira L, Mariotto AB, Rowland JH, Yabroff KR, Alfano CM, et al. Cancer Treatment and Survivorship Statistics, 2019. *CA: Cancer J Clin* (2019) 69(5):363–85. doi: 10.3322/caac.21565
2. Topalian SL, Weiner GJ, Pardoll DM. Cancer Immunotherapy Comes of Age. *J Clin Oncol* (2011) 29(36):4828. doi: 10.1200/JCO.2011.38.0899
3. Quesada JR, Hersh EM, Manning J, Reuben J, Keating M, Schnipper E, et al. Treatment of Hairy Cell Leukemia with Recombinant Alpha Interferon. *Blood* (1986) 68 (2):493–97. doi: 10.1182/blood.V68.2.493.493
4. Rosenberg SA. Il-2: The First Effective Immunotherapy for Human Cancer. *J Immunol* (2014) 192(12):5451–8. doi: 10.4049/jimmunol.1490019
5. Ahmed S, Rai KR. Interferon in the Treatment of Hairy-Cell Leukemia. *Best Pract Res Clin Haematol* (2003) 16(1):69–81. doi: 10.1016/S1521-6926(02)00084-1
6. Rosenberg SA, Lotze MT, Muul LM, Leitman S, Chang AE, Ettinghausen SE, et al. Observations on the Systemic Administration of Autologous Lymphokine-Activated Killer Cells and Recombinant Interleukin-2 to Patients With Metastatic Cancer. *New Engl J Med* (1985) 313(23):1485–92. doi: 10.1056/NEJM198512053132327
7. Hodi FS, O'Day SJ, McDermott DF, Weber RW, Sosman JA, Haanen JB, et al. Improved Survival With Ipilimumab in Patients With Metastatic Melanoma. *New Engl J Med* (2010) 363(8):711–23. doi: 10.1056/NEJMoa1003466
8. Ribas A, Wolchok JD. Cancer Immunotherapy Using Checkpoint Blockade. *Science* (2018) 359(6382):1350–5. doi: 10.1126/science.aar4060
9. Appleton E, Hassan J, Chan Wah Hak C, Sivamanoharan N, Wilkins A, Samson A, et al. Kickstarting Immunity in Cold Tumours: Localised Tumour Therapy Combinations With Immune Checkpoint Blockade. *Front Immunol* (2021) 12:4319. doi: 10.3389/fimmu.2021.754436

10. Gerard C, Delyon J, Wicky A, Homicsko K, Cuendet MA, Michielin O. Turning Tumors From Cold to Inflamed to Improve Immunotherapy Response. *Cancer Treat Rev* (2021) 101:102227. doi: 10.1016/j.ctrv.2021.102227
11. Coley WB. The Treatment of Malignant Tumors by Repeated Inoculations of Erysipelas: With a Report of Ten Original Cases. *1. Am J Med Sci (1827-1924)* (1893) 105(6):487.
12. Karbach J, Neumann A, Brand K, Wahle C, Siegel E, Maeurer M, et al. Phase I Clinical Trial of Mixed Bacterial Vaccine (Coley's Toxins) in Patients With Ny-Eso-1 Expressing Cancers: Immunological Effects and Clinical Activity. *Clin Cancer Res* (2012) 18(19):5449–59. doi: 10.1158/1078-0432.CCR-12-1116
13. Dobosz P, Dzieciątkowski T. The Intriguing History of Cancer Immunotherapy. *Front Immunol* (2019) 10:2965. doi: 10.3389/fimmu.2019.02965
14. Calmette A. Preventive Vaccination Against Tuberculosis With Bcg. *SAGE Publications* (1931) 96:58–9. doi: 10.1001/jama.1931.02720270060030
15. Lamm DL, Thor DE, Harris SC, Reyna JA, Stogdill VD, Radwin HM. Bacillus Calmette-Guerin Immunotherapy of Superficial Bladder Cancer. *J Urol* (1980) 124(1):38–42. doi: 10.1016/S0022-5347(17)55282-9
16. Rius-Rocabert S, Llinares Pinel F, Pozuelo MJ, García A, Nistal-Villan E. Oncolytic Bacteria: Past, Present and Future. *FEMS Microbiol Lett* (2019) 366(12):fnz136. doi: 10.1093/femsle/fnz136
17. Sepich-Poore GD, Zitvogel L, Straussman R, Hasty J, Wargo JA, Knight R. The Microbiome and Human Cancer. *Science* (2021) 371(6536):eabc4552. doi: 10.1126/science.abc4552
18. Cao L, Zhu S, Lu H, Soutto M, Bhat N, Chen Z, et al. Helicobacter Pylori–Induced Rasal2 Through Activation of Nuclear Factor-Kb Promotes Gastric Tumorigenesis *Via* B-Catenin Signaling Axis. *Gastroenterology* (2022) 162:1716–31. doi: 10.1053/j.gastro.2022.01.046
19. Krueger A, Zaugg J, Chisholm S, Linedale R, Lachner N, Teoh SM, et al. Secreted Toxins From Staphylococcus Aureus Strains Isolated From Keratinocyte Skin Cancers Mediate Pro-Tumorigenic Inflammatory Responses in the Skin. *Front Microbiol* (2022) 12:789042.
20. Queen J, Domingue JC, White JR, Stevens C, Udayasuryan B, Nguyen TT, et al. Comparative Analysis of Colon Cancer-Derived Fusobacterium Nucleatum Subspecies: Inflammation and Colon Tumorigenesis in Murine Models. *Mbio* (2022) 13(1):e02991–21. doi: 10.1128/mbio.02991-21
21. Garbacz K. Anticancer Activity of Lactic Acid Bacteria. *Semin Cancer Biol* (2022) S1044–579X(21):00306–0. doi: 10.1016/j.semcancer.2021.12.013
22. Wang T, Wang P, Ge W, Shi C, Xiao G, Wang X, et al. The Probiotic Companilactobacillus Crustorum Mn047 Alleviates Colitis-Associated Tumorigenesis *Via* Modulating the Intestinal Microenvironment. *Food Funct* (2021) 12(22):11331–42. doi: 10.1039/D1FO01531A
23. Fu A, Yao B, Dong T, Chen Y, Yao J, Liu Y, et al. Tumor-Resident Intracellular Microbiota Promotes Metastatic Colonization in Breast Cancer. *Cell* (2022) 185:1356–72. doi: 10.1016/j.cell.2022.02.027
24. Geller LT, Barzily-Rokni M, Danino T, Jonas OH, Shental N, Nejman D, et al. Potential Role of Intratumor Bacteria in Mediating Tumor Resistance to the Chemotherapeutic Drug Gemcitabine. *Science* (2017) 357 (6356):1156–60. doi: 10.1126/science.aah5043
25. Kalaora S, Nagler A, Nejman D, Alon M, Barbolin C, Barnea E, et al. Identification of Bacteria-Derived Hla-Bound Peptides in Melanoma. *Nature* (2021) 592(7852):138–43. doi: 10.1038/s41586-021-03368-8
26. Yin T, Diao Z, Blum NT, Qiu L, Ma A, Huang P. Engineering Bacteria and Bionic Bacterial Derivatives With Nanoparticles for Cancer Therapy. *Small* (2021) 18:2104643. doi: 10.1002/smll.202104643
27. Cubillos-Ruiz A, Guo T, Sokolovska A, Miller PF, Collins JJ, Lu TK, et al. Engineering Living Therapeutics With Synthetic Biology. *Nat Rev Drug Discovery* (2021) 20(12):941–60. doi: 10.1038/s41573-021-00285-3
28. Rodrigo-Navarro A, Sankaran S, Dalby MJ, del Campo A, Salmeron-Sanchez M. Engineered Living Biomaterials. *Nat Rev Mater* (2021) 6(12):1175–90. doi: 10.1038/s41578-021-00350-8
29. Guo Y, Chen Y, Liu X, Min J-J, Tan W, Zheng JH. Targeted Cancer Immunotherapy With Genetically Engineered Oncolytic Salmonella Typhimurium. *Cancer Lett* (2020) 469:102–10. doi: 10.1016/j.canlet.2019.10.033
30. Jain RK. Normalizing Tumor Microenvironment to Treat Cancer: Bench to Bedside to Biomarkers. *J Clin Oncol* (2013) 31(17):2205. doi: 10.1200/JCO.2012.46.3653
31. West C, Slevin F. Tumour Hypoxia. *Clin Oncol* (2019) 31(9):595–9. doi: 10.1016/j.clon.2019.06.008
32. Taniguchi SI, Fujimori M, Sasaki T, Tsutsui H, Shimatani Y, Seki K, et al. Targeting Solid Tumors With Non-Pathogenic Obligate Anaerobic Bacteria. *Cancer Sci* (2010) 101(9):1925–32. doi: 10.1111/j.1349-7006.2010.01628.x
33. Zheng JH, Nguyen VH, Jiang S-N, Park S-H, Tan W, Hong SH, et al. Two-Step Enhanced Cancer Immunotherapy With Engineered Salmonella Typhimurium Secreting Heterologous Flagellin. *Sci Trans Med* (2017) 9 (376):eaak9537. doi: 10.1126/scitranslmed.aak9537
34. Shi Y, Zheng W, Yang K, Harris KG, Ni K, Xue L, et al. Intratumoral Accumulation of Gut Microbiota Facilitates Cd47-Based Immunotherapy *Via* Sting Signaling. *J Exp Med* (2020) 217(5):e20192282. doi: 10.1084/jem.20192282
35. Fluegen G, Avivar-Valderas A, Wang Y, Padgen MR, Williams JK, Nobre AR, et al. Phenotypic Heterogeneity of Disseminated Tumour Cells Is Preset by Primary Tumour Hypoxic Microenvironments. *Nat Cell Biol* (2017) 19 (2):120–32. doi: 10.1038/ncb3465
36. Forbes NS, Munn LL, Fukumura D, Jain RK. Sparse Initial Entrapment of Systemically Injected Salmonella Typhimurium Leads to Heterogeneous Accumulation Within Tumors. *Cancer Res* (2003) 63(17):5188–93.
37. Kim J-E, Phan TX, Nguyen VH, Dinh-Vu H-V, Zheng JH, Yun M, et al. Salmonella Typhimurium Suppresses Tumor Growth *Via* the Pro-Inflammatory Cytokine Interleukin-1β. *Theranostics* (2015) 5(12):1328. doi: 10.7150/thno.11432
38. Leschner S, Westphal K, Dietrich N, Viegas N, Jablonska J, Lyszkiewicz M, et al. Tumor Invasion of Salmonella Enterica Serovar Typhimurium Is Accompanied by Strong Hemorrhage Promoted by Tnf-A. *PloS One* (2009) 4(8):e6692. doi: 10.1371/journal.pone.0006692
39. Chouaib S, Noman M, Kosmatopoulos K, Curran M. Hypoxic Stress: Obstacles and Opportunities for Innovative Immunotherapy of Cancer. *Oncogene* (2017) 36(4):439–45. doi: 10.1038/onc.2016.225
40. Denko NC. Hypoxia, Hif1 and Glucose Metabolism in the Solid Tumour. *Nat Rev Cancer* (2008) 8(9):705–13. doi: 10.1038/nrc2468
41. Zhang L, Romero P. Metabolic Control of Cd8+ T Cell Fate Decisions and Antitumor Immunity. *Trends Mol Med* (2018) 24(1):30–48. doi: 10.1016/j.molmed.2017.11.005
42. Zitvogel L, Ayyoub M, Routy B, Kroemer G. Microbiome and Anticancer Immunosurveillance. *Cell* (2016) 165(2):276–87. doi: 10.1016/j.cell.2016.03.001
43. Phan TX, Nguyen VH, Duong MTQ, Hong Y, Choy HE, Min JJ. Activation of Inflammasome by Attenuated Salmonella Typhimurium in Bacteria-Mediated Cancer Therapy. *Microbiol Immunol* (2015) 59(11):664–75. doi: 10.1111/1348-0421.12333
44. Vijay-Kumar M, Aitken JD, Kumar A, Neish AS, Uematsu S, Akira S, et al. Toll-Like Receptor 5-Deficient Mice Have Dysregulated Intestinal Gene Expression and Nonspecific Resistance to Salmonella-Induced Typhoid-Like Disease. *Infect Immun* (2008) 76(3):1276–81. doi: 10.1128/IAI.01491-07
45. Sfondrini L, Rossini A, Besusso D, Merlo A, Tagliabue E, Mènard S, et al. Antitumor Activity of the Tlr-5 Ligand Flagellin in Mouse Models of Cancer. *J Immunol* (2006) 176(11):6624–30. doi: 10.4049/jimmunol.176.11.6624
46. Chang WW, Lai CH, Chen MC, Liu CF, Kuan YD, Lin ST, et al. Salmonella Enhance Chemosensitivity in Tumor Through Connexin 43 Upregulation. *Int J Cancer* (2013) 133(8):1926–35. doi: 10.1002/ijc.28155
47. Saccheri F, Pozzi C, Avogadri F, Barozzi S, Faretta M, Fusi P, et al. Bacteria-Induced Gap Junctions in Tumors Favor Antigen Cross-Presentation and Antitumor Immunity. *Sci Trans Med* (2010) 2(44):44ra57–7. doi: 10.1126/scitranslmed.3000739
48. Mantovani A, Marchesi F, Malesci A, Laghi L, Allavena P. Tumour-Associated Macrophages as Treatment Targets in Oncology. *Nat Rev Clin Oncol* (2017) 14(7):399–416. doi: 10.1038/nrclinonc.2016.217
49. Zhang P, Guan H, Yuan S, Cheng H, Zheng J, Zhang Z, et al. Targeting Myeloid Derived Suppressor Cells Reverts Immune Suppression and Sensitizes Braf-Mutant Papillary Thyroid Cancer to Mapk Inhibitors. *Nat Commun* (2022) 13(1):1–18. doi: 10.1038/s41467-022-29000-5
50. Cassetta L, Pollard JW. Targeting Macrophages: Therapeutic Approaches in Cancer. *Nat Rev Drug Discovery* (2018) 17(12):887–904. doi: 10.1038/nrd.2018.169
51. Wang B, Wu Y, Liu R, Xu H, Mei X, Shang Q, et al. Lactobacillus Rhamnosus Gg Promotes M1 Polarization in Murine Bone Marrow-Derived Macrophages by Activating Tlr2/Myd88/Mapk Signaling Pathway. *Anim Sci J* (2020) 91(1):e13439. doi: 10.1111/asj.13439
52. Rocha-Ramírez LM, Hernández-Ochoa B, Gómez-Manzo S, Marcial-Quino J, Cárdenas-Rodríguez N, Centeno-Leija S, et al. Evaluation of

Immunomodulatory Activities of the Heat-Killed Probiotic Strain Lactobacillus Casei Imau60214 on Macrophages *in Vitro*. *Microorganisms* (2020) 8(1):79. doi: 10.3390/microorganisms8010079
53. Chandra D, Jahangir A, Quispe-Tintaya W, Einstein M, Gravekamp C. Myeloid-Derived Suppressor Cells Have a Central Role in Attenuated Listeria Monocytogenes-Based Immunotherapy Against Metastatic Breast Cancer in Young and Old Mice. *Br J Cancer* (2013) 108(11):2281–90. doi: 10.1038/bjc.2013.206
54. Bullman S, Pedamallu CS, Sicinska E, Clancy TE, Zhang X, Cai D, et al. Analysis of Fusobacterium Persistence and Antibiotic Response in Colorectal Cancer. *Science* (2017) 358(6369):1443–8. doi: 10.1126/science.aal5240
55. Zhao M, Yang M, Li X-M, Jiang P, Baranov E, Li S, et al. Tumor-Targeting Bacterial Therapy With Amino Acid Auxotrophs of Gfp-Expressing Salmonella Typhimurium. *Proc Natl Acad Sci* (2005) 102(3):755–60. doi: 10.1073/pnas.0408422102
56. Felgner S, Frahm M, Kocijancic D, Rohde M, Eckweiler D, Bielecka A, et al. Aroa-Deficient Salmonella Enterica Serovar Typhimurium Is More Than a Metabolically Attenuated Mutant. *MBio* (2016) 7(5):e01220–16. doi: 10.1128/mBio.01220-16
57. Leventhal DS, Sokolovska A, Li N, Plescia C, Kolodziej SA, Gallant CW, et al. Immunotherapy With Engineered Bacteria by Targeting the Sting Pathway for Anti-Tumor Immunity. *Nat Commun* (2020) 11(1):1–15. doi: 10.1038/s41467-020-16602-0
58. Yu B, Yang M, Shi L, Yao Y, Jiang Q, Li X, et al. Explicit Hypoxia Targeting With Tumor Suppression by Creating an "Obligate" Anaerobic Salmonella Typhimurium Strain. *Sci Rep* (2012) 2(1):1–10. doi: 10.1038/srep00436
59. Bereta M, Hayhurst A, Gajda M, Chorobik P, Targosz M, Marcinkiewicz J, et al. Improving Tumor Targeting and Therapeutic Potential of Salmonella Vnp20009 by Displaying Cell Surface Cea-Specific Antibodies. *Vaccine* (2007) 25(21):4183–92. doi: 10.1016/j.vaccine.2007.03.008
60. Massa PE, Paniccia A, Monegal A, De Marco A, Rescigno M. Salmonella Engineered to Express Cd20-Targeting Antibodies and a Drug-Converting Enzyme Can Eradicate Human Lymphomas. *Blood J Am Soc Hematol* (2013) 122(5):705–14. doi: 10.1182/blood-2012-12-474098
61. Park S-H, Zheng JH, Nguyen VH, Jiang S-N, Kim D-Y, Szardenings M, et al. Rgd Peptide Cell-Surface Display Enhances the Targeting and Therapeutic Efficacy of Attenuated Salmonella-Mediated Cancer Therapy. *Theranostics* (2016) 6(10):1672. doi: 10.7150/thno.16135
62. Plavec TV, Mitrović A, Perišić Nanut M, Štrukelj B, Kos J, Berlec A. Targeting of Fluorescent Lactococcus Lactis to Colorectal Cancer Cells Through Surface Display of Tumour-Antigen Binding Proteins. *Microb Biotechnol* (2021) 14(5):2227–40. doi: 10.1111/1751-7915.13907
63. Geng Z, Cao Z, Liu R, Liu K, Liu J, Tan W. Aptamer-Assisted Tumor Localization of Bacteria for Enhanced Biotherapy. *Nat Commun* (2021) 12 (1):1–12. doi: 10.1038/s41467-021-26956-8
64. Loeffler M, Le'Negrate G, Krajewska M, Reed JC. Il-18-Producing Salmonella Inhibit Tumor Growth. *Cancer Gene Ther* (2008) 15(12):787–94. doi: 10.1038/cgt.2008.48
65. Yoon W, Park YC, Kim J, Chae YS, Byeon JH, Min S-H, et al. Application of Genetically Engineered Salmonella Typhimurium for Interferon-Gamma–Induced Therapy Against Melanoma. *Eur J Cancer* (2017) 70:48–61. doi: 10.1016/j.ejca.2016.10.010
66. Namai F, Murakami A, Ueda A, Tsukagoshi M, Shigemori S, Ogita T, et al. Construction of Genetically Modified Lactococcus Lactis Producing Anti-Human-Ctla-4 Single-Chain Fragment Variable. *Mol Biotechnol* (2020) 62:572–9. doi: 10.1007/s12033-020-00274-8
67. Gurbatri CR, Lia I, Vincent R, Coker C, Castro S, Treuting PM, et al. Engineered Probiotics for Local Tumor Delivery of Checkpoint Blockade Nanobodies. *Sci Trans Med* (2020) 12(530):eaax0876. doi: 10.1126/scitranslmed.aax0876
68. Abedi MH, Yao MS, Mittelstein DR, Bar-Zion A, Swift MB, Lee-Gosselin A, et al. Ultrasound-Controllable Engineered Bacteria for Cancer Immunotherapy. *Nat Commun* (2022) 13(1):1–11. doi: 10.1038/s41467-022-29065-2
69. Chowdhury S, Castro S, Coker C, Hinchliffe TE, Arpaia N, Danino T. Programmable Bacteria Induce Durable Tumor Regression and Systemic Antitumor Immunity. *Nat Med* (2019) 25(7):1057–63. doi: 10.1038/s41591-019-0498-z
70. Canale FP, Basso C, Antonini G, Perotti M, Li N, Sokolovska A, et al. Metabolic Modulation of Tumours With Engineered Bacteria for Immunotherapy. *Nature* (2021) 598(7882):662–6. doi: 10.1038/s41586-021-04003-2
71. Chen QW, Wang JW, Wang XN, Fan JX, Liu XH, Li B, et al. Inhibition of Tumor Progression Through the Coupling of Bacterial Respiration With Tumor Metabolism. *Angewandte Chemie Int Edition* (2020) 59(48):21562–70. doi: 10.1002/anie.202002649
72. Clairmont C, Lee K, Pike J, Ittensohn M, Low K, Pawelek J, et al. Biodistribution and Genetic Stability of the Novel Antitumor Agent Vnp20009, a Genetically Modified Strain of Salmonella Typhimuvium. *J Infect Dis* (2000) 181(6):1996–2002. doi: 10.1086/315497
73. Na HS, Kim HJ, Lee H-C, Hong Y, Rhee JH, Choy HE. Immune Response Induced by Salmonella Typhimurium Defective in Ppgpp Synthesis. *Vaccine* (2006) 24(12):2027–34. doi: 10.1016/j.vaccine.2005.11.031
74. Freitag NE, Rong L, Portnoy DA. Regulation of the Prfa Transcriptional Activator of Listeria Monocytogenes: Multiple Promoter Elements Contribute to Intracellular Growth and Cell-To-Cell Spread. *Infect Immun* (1993) 61(6):2537–44. doi: 10.1128/iai.61.6.2537-2544.1993
75. Brockstedt DG, Giedlin MA, Leong ML, Bahjat KS, Gao Y, Luckett W, et al. Listeria-Based Cancer Vaccines That Segregate Immunogenicity From Toxicity. *Proc Natl Acad Sci* (2004) 101(38):13832–7. doi: 10.1073/pnas.0406035101
76. Harimoto T, Hahn J, Chen Y-Y, Im J, Zhang J, Hou N, et al. A Programmable Encapsulation System Improves Delivery of Therapeutic Bacteria in Mice. *Nat Biotechnol* (2022), 1–11. doi: 10.1038/s41587-022-01244-y
77. Din MO, Danino T, Prindle A, Skalak M, Selimkhanov J, Allen K, et al. Synchronized Cycles of Bacterial Lysis for *in Vivo* Delivery. *Nature* (2016) 536(7614):81–5. doi: 10.1038/nature18930
78. Loessner H, Endmann A, Leschner S, Westphal K, Rohde M, Miloud T, et al. Remote Control of Tumour-Targeted Salmonella Enterica Serovar Typhimurium by the Use of L-Arabinose as Inducer of Bacterial Gene Expression *in Vivo*. *Cell Microbiol* (2007) 9(6):1529–37. doi: 10.1111/j.1462-5822.2007.00890.x
79. Royo JL, Becker PD, Camacho EM, Cebolla A, Link C, Santero E, et al. *In Vivo* Gene Regulation in Salmonella Spp. By a Salicylate-Dependent Control Circuit. *Nat Methods* (2007) 4(11):937–42. doi: 10.1038/nmeth1107
80. Nuyts S, Theys J, Landuyt W, Van Mellaert L, Lambin P, Anné J. Increasing Specificity of Anti-Tumor Therapy: Cytotoxic Protein Delivery by Non-Pathogenic Clostridia Under Regulation of Radio-Induced Promoters. *Anticancer Res* (2001) 21(2A):857–61.
81. Corrales L, Glickman LH, McWhirter SM, Kanne DB, Sivick KE, Katibah GE, et al. Direct Activation of Sting in the Tumor Microenvironment Leads to Potent and Systemic Tumor Regression and Immunity. *Cell Rep* (2015) 11 (7):1018–30. doi: 10.1016/j.celrep.2015.04.031
82. Toussaint B, Chauchet X, Wang Y, Polack B, Gouëllec AL. Live-Attenuated Bacteria as a Cancer Vaccine Vector. *Expert Rev Vaccines* (2013) 12 (10):1139–54. doi: 10.1586/14760584.2013.836914
83. Le DT, Wang-Gillam A, Picozzi V, Greten TF, Crocenzi T, Springett G, et al. Safety and Survival With Gvax Pancreas Prime and Listeria Monocytogenes–Expressing Mesothelin (Crs-207) Boost Vaccines for Metastatic Pancreatic Cancer. *J Clin Oncol* (2015) 33(12):1325. doi: 10.1200/JCO.2014.57.4244
84. Mohseni AH, Razavilar V, Keyvani H, Razavi MR, Khavari-Nejad RA. Oral Immunization With Recombinant Lactococcus Lactis Nz9000 Expressing Human Papillomavirus Type 16 E7 Antigen and Evaluation of Its Immune Effects in Female C57bl/6 Mice. *J Med Virol* (2019) 91(2):296–307. doi: 10.1002/jmv.25303
85. Mohseni AH, Taghinezhad-S S, Keyvani H. The First Clinical Use of a Recombinant Lactococcus Lactis Expressing Human Papillomavirus Type 16 E7 Oncogene Oral Vaccine: A Phase I Safety and Immunogenicity Trial in Healthy Women Volunteers. *Mol Cancer Ther* (2020) 19(2):717–27. doi: 10.1158/1535-7163.MCT-19-0375
86. Herbst RS, Baas P, Kim D-W, Felip E, Pérez-Gracia JL, Han J-Y, et al. Pembrolizumab Versus Docetaxel for Previously Treated, Pd-L1-Positive, Advanced Non-Small-Cell Lung Cancer (Keynote-010): A Randomised Controlled Trial. *Lancet* (2016) 387(10027):1540–50. doi: 10.1016/S0140-6736(15)01281-7

87. Auslander N, Zhang G, Lee JS, Frederick DT, Miao B, Moll T, et al. Robust Prediction of Response to Immune Checkpoint Blockade Therapy in Metastatic Melanoma. *Nat Med* (2018) 24(10):1545–9. doi: 10.1038/s41591-018-0157-9
88. Grzywa TM, Sosnowska A, Matryba P, Rydzynska Z, Jasinski M, Nowis D, et al. Myeloid Cell-Derived Arginase in Cancer Immune Response. *Front Immunol* (2020) 11:938. doi: 10.3389/fimmu.2020.00938
89. Lee DC, Sohn HA, Park Z-Y, Oh S, Kang YK, K-m L, et al. A Lactate-Induced Response to Hypoxia. *Cell* (2015) 161(3):595–609. doi: 10.1016/j.cell.2015.03.011
90. Low KB, Ittensohn M, Le T, Platt J, Sodi S, Amoss M, et al. Lipid a Mutant Salmonella With Suppressed Virulence and Tnfα Induction Retain Tumor-Targeting *in Vivo*. *Nat Biotechnol* (1999) 17(1):37–41. doi: 10.1038/5205
91. Toso JF, Gill VJ, Hwu P, Marincola FM, Restifo NP, Schwartzentruber DJ, et al. Phase I Study of the Intravenous Administration of Attenuated Salmonella Typhimurium to Patients With Metastatic Melanoma. *J Clin Oncol: Off J Am Soc Clin Oncol* (2002) 20(1):142. doi: 10.1200/JCO.2002.20.1.142
92. Frahm M, Felgner S, Kocijancic D, Rohde M, Hensel M, Curtiss IIIR, et al. Efficiency of Conditionally Attenuated Salmonella Enterica Serovar Typhimurium in Bacterium-Mediated Tumor Therapy. *MBio* (2015) 6(2):e00254–15. doi: 10.1128/mBio.00254-15
93. Wood LM, Paterson Y. Attenuated Listeria Monocytogenes: A Powerful and Versatile Vector for the Future of Tumor Immunotherapy. *Front Cell Infect Microbiol* (2014) 4:51. doi: 10.3389/fcimb.2014.00051
94. Ektate K, Munteanu MC, Ashar H, Malayer J, Ranjan A. Chemo-Immunotherapy of Colon Cancer With Focused Ultrasound and Salmonella-Laden Temperature Sensitive Liposomes (Thermobots). *Sci Rep* (2018) 8(1):1–12. doi: 10.1038/s41598-018-30106-4
95. Selvanesan BC, Chandra D, Quispe-Tintaya W, Jahangir A, Patel A, Meena K, et al. Listeria Delivers Tetanus Toxoid Protein to Pancreatic Tumors and Induces Cancer Cell Death in Mice. *Sci Trans Med* (2022) 14(637):eabc1600. doi: 10.1126/scitranslmed.abc1600
96. Chen Q, Bai H, Wu W, Huang G, Li Y, Wu M, et al. Bioengineering Bacterial Vesicle-Coated Polymeric Nanomedicine for Enhanced Cancer Immunotherapy and Metastasis Prevention. *Nano Lett* (2019) 20(1):11–21. doi: 10.1021/acs.nanolett.9b02182
97. Jiang S-N, Phan TX, Nam T-K, Nguyen VH, Kim H-S, Bom H-S, et al. Inhibition of Tumor Growth and Metastasis by a Combination of Escherichia Coli–Mediated Cytolytic Therapy and Radiotherapy. *Mol Ther* (2010) 18(3):635–42. doi: 10.1038/mt.2009.295
98. Liu X, Jiang S, Piao L, Yuan F. Radiotherapy Combined With an Engineered of Salmonella Typhimurium Inhibits Tumor Growth in a Mouse Model of Colon Cancer. *Exp Anim* (2016) 65:16–0033. doi: 10.1538/expanim.16-0033
99. Pan P, Dong X, Chen Y, Zeng X, Zhang X-Z. Engineered Bacteria for Enhanced Radiotherapy Against Breast Carcinoma. *ACS Nano* (2022) 16:801–12. doi: 10.1021/acsnano.1c08350
100. Wang W, Xu H, Ye Q, Tao F, Wheeldon I, Yuan A, et al. Systemic Immune Responses to Irradiated Tumours Via the Transport of Antigens to the Tumour Periphery by Injected Flagellate Bacteria. *Nat Biomed Eng* (2022) 6(1):44–53. doi: 10.1038/s41551-021-00834-6
101. Liu L, He H, Luo Z, Zhou H, Liang R, Pan H, et al. *In Situ* Photocatalyzed Oxygen Generation With Photosynthetic Bacteria to Enable Robust Immunogenic Photodynamic Therapy in Triple-Negative Breast Cancer. *Adv Funct Mater* (2020) 30(10):1910176. doi: 10.1002/adfm.201910176
102. Chen F, Zang Z, Chen Z, Cui L, Chang Z, Ma A, et al. Nanophotosensitizer-Engineered Salmonella Bacteria With Hypoxia Targeting and Photothermal-Assisted Mutual Bioaccumulation for Solid Tumor Therapy. *Biomaterials* (2019) 214:119226. doi: 10.1016/j.biomaterials.2019.119226
103. Chen W, Wang Y, Qin M, Zhang X, Zhang Z, Sun X, et al. Bacteria-Driven Hypoxia Targeting for Combined Biotherapy and Photothermal Therapy. *ACS Nano* (2018) 12(6):5995–6005. doi: 10.1021/acsnano.8b02235
104. Chen W, Guo Z, Zhu Y, Qiao N, Zhang Z, Sun X. Combination of Bacterial-Photothermal Therapy With an Anti-Pd-1 Peptide Depot for Enhanced Immunity Against Advanced Cancer. *Adv Funct Mater* (2020) 30(1):1906623. doi: 10.1002/adfm.201906623
105. Reghu S, Miyako E. Nanoengineered Bifidobacterium Bifidum With Optical Activity for Photothermal Cancer Immunotheranostics. *Nano Lett* (2022) 22:1880–8. doi: 10.1021/acs.nanolett.1c04037
106. Yang X, Komatsu S, Reghu S, Miyako E. Optically Activatable Photosynthetic Bacteria-Based Highly Tumor Specific Immunotheranostics. *Nano Today* (2021) 37:101100. doi: 10.1016/j.nantod.2021.101100
107. Gao G, Ma T, Zhang T, Jin H, Li Y, Kwok L-Y, et al. Adjunctive Probiotic Lactobacillus Rhamnosus Probio-M9 Administration Enhances the Effect of Anti-Pd-1 Antitumor Therapy *Via* Restoring Antibiotic-Disrupted Gut Microbiota. *Front Immunol* (2021) 12. doi: 10.3389/fimmu.2021.772532
108. Agah S, Alizadeh AM, Mosavi M, Ranji P, Khavari-Daneshvar H, Ghasemian F, et al. More Protection of Lactobacillus Acidophilus Than Bifidobacterium Bifidum Probiotics on Azoxymethane-Induced Mouse Colon Cancer. *Probiotics Antimicrob Proteins* (2019) 11(3):857–64. doi: 10.1007/s12602-018-9425-8
109. Phan T, Nguyen VH, D'Alincourt MS, Manuel ER, Kaltcheva T, Tsai W, et al. Salmonella-Mediated Therapy Targeting Indoleamine 2, 3-Dioxygenase 1 (Ido) Activates Innate Immunity and Mitigates Colorectal Cancer Growth. *Cancer Gene Ther* (2020) 27(3):235–45. doi: 10.1038/s41417-019-0089-7
110. Zhao T, Feng Y, Guo M, Zhang C, Wu Q, Chen J, et al. Combination of Attenuated Salmonella Carrying Pd-1 Sirna With Nifuroxazide for Colon Cancer Therapy. *J Cell Biochem* (2020) 121(2):1973–85. doi: 10.1002/jcb.29432
111. Shrimali R, Ahmad S, Berrong Z, Okoev G, Matevosyan A, Razavi GSE, et al. Agonist Anti-Gitr Antibody Significantly Enhances the Therapeutic Efficacy of Listeria Monocytogenes-Based Immunotherapy. *J Immunother Cancer* (2017) 5(1):1–9. doi: 10.1186/s40425-017-0266-x
112. Abdolalipour E, Mahooti M, Salehzadeh A, Torabi A, Mohebbi SR, Gorji A, et al. Evaluation of the Antitumor Immune Responses of Probiotic Bifidobacterium Bifidum in Human Papillomavirus-Induced Tumor Model. *Microb Pathogen* (2020) 145:104207. doi: 10.1016/j.micpath.2020.104207
113. Jacouton E, Michel M-L, Torres-Maravilla E, Chain F, Langella P, Bermúdez-Humarán LG. Elucidating the Immune-Related Mechanisms by Which Probiotic Strain Lactobacillus Casei Bl23 Displays Anti-Tumoral Properties. *Front Microbiol* (2019) 9:3281. doi: 10.3389/fmicb.2018.03281
114. Jacouton E, Torres Maravilla E, Boucard A-S, Pouderous N, Pessoa Vilela AP, Naas I, et al. Anti-Tumoral Effects of Recombinant Lactococcus Lactis Strain Secreting Il-17a Cytokine. *Front Microbiol* (2019) 9:3355. doi: 10.3389/fmicb.2018.03355
115. Vitiello M, Evangelista M, Di Lascio N, Kusmic C, Massa A, Orso F, et al. Antitumoral Effects of Attenuated Listeria Monocytogenes in a Genetically Engineered Mouse Model of Melanoma. *Oncogene* (2019) 38(19):3756–62. doi: 10.1038/s41388-019-0681-1
116. Gilley RP, Dube PH. Checkpoint Blockade Inhibitors Enhances the Effectiveness of a Listeria Monocytogenes-Based Melanoma Vaccine. *Oncotarget* (2020) 11(7):740. doi: 10.18632/oncotarget.27490
117. Terán-Navarro H, Calderon-Gonzalez R, Salcines-Cuevas D, García I, Marradi M, Freire J, et al. Pre-Clinical Development of Listeria-Based Nanovaccines as Immunotherapies for Solid Tumours: Insights From Melanoma. *Oncoimmunology* (2019) 8(2):e1541534. doi: 10.1080/2162402X.2018.1541534
118. Ahmad S, Casey G, Cronin M, Rajendran S, Sweeney P, Tangney M, et al. Induction of Effective Antitumor Response After Mucosal Bacterial Vector Mediated DNA Vaccination With Endogenous Prostate Cancer Specific Antigen. *J Urol* (2011) 186(2):687–93. doi: 10.1016/j.juro.2011.03.139
119. Duan F, Chen J, Yao H, Wang Y, Jia Y, Ling Z, et al. Enhanced Therapeutic Efficacy of Listeria-Based Cancer Vaccine With Codon-Optimized Hpv16 E7. *Hum Vaccines Immunother* (2021) 17(6):1568–77. doi: 10.1080/21645515.2020.1839291
120. Dahmus JD, Kotler DL, Kastenberg DM, Kistler CA. The Gut Microbiome and Colorectal Cancer: A Review of Bacterial Pathogenesis. *J Gastrointest Oncol* (2018) 9(4):769. doi: 10.21037/jgo.2018.04.07
121. Piewngam P, Zheng Y, Nguyen TH, Dickey SW, Joo H-S, Villaruz AE, et al. Pathogen Elimination by Probiotic Bacillus *Via* Signalling Interference. *Nature* (2018) 562(7728):532–7. doi: 10.1038/s41586-018-0616-y
122. Sivan A, Corrales L, Hubert N, Williams JB, Aquino-Michaels K, Earley ZM, et al. Commensal Bifidobacterium Promotes Antitumor Immunity and Facilitates Anti–Pd-L1 Efficacy. *Science* (2015) 350(6264):1084–9. doi: 10.1126/science.aac4255

123. Li F, Chen Y, Pang M, Yang P, Jing H. Immune Checkpoint Inhibitors and Cellular Treatment for Lymphoma Immunotherapy. *Clin Exp Immunol* (2021) 205(1):1–11. doi: 10.1111/cei.13592
124. Lupo F, Ingersoll MA, Pineda MA. The Glycobiology of Uropathogenic E. Coli Infection: The Sweet and Bitter Role of Sugars in Urinary Tract Immunity. *Immunology* (2021) 164(1):3–14. doi: 10.1111/imm.13330
125. Brook I. Microbiology and Management of Abdominal Infections. *Digest Dis Sci* (2008) 53(10):2585–91. doi: 10.1007/s10620-007-0194-6
126. Geibel M, Schu B, Callaway A, Gleissner C, Willershausen B. Polymerase Chain Reaction-Based Simultaneous Detection of Selected Bacterial Species Associated With Closed Periapical Lesions. *Eur J Med Res* (2005) 10(8):333.
127. Shi L, Sheng J, Chen G, Zhu P, Shi C, Li B, et al. Combining Il-2-Based Immunotherapy With Commensal Probiotics Produces Enhanced Antitumor Immune Response and Tumor Clearance. *J Immunother Cancer* (2020) 8(2):e000973. doi: 10.1136/jitc-2020-000973
128. Postow MA, Sidlow R, Hellmann MD. Immune-Related Adverse Events Associated With Immune Checkpoint Blockade. *New Engl J Med* (2018) 378 (2):158–68. doi: 10.1056/NEJMra1703481
129. Tang L, Wang J, Lin N, Zhou Y, He W, Liu J, et al. Immune Checkpoint Inhibitor-Associated Colitis: From Mechanism to Management. *Front Immunol* (2021) 12. doi: 10.3389/fimmu.2021.800879
130. Wang X, Fukui H, Ran Y, Xu X, Ebisutani N, Nakanishi T, et al. Probiotic Bifidobacterium Bifidum G9-1 Has a Preventive Effect on the Acceleration of Colonic Permeability and M1 Macrophage Population in Maternally Separated Rats. *Biomedicines* (2021) 9(6):641. doi: 10.3390/biomedicines9060641
131. Mukherjee N, Julián E, Torrelles JB, Svatek RS. Effects of Mycobacterium Bovis Calmette Et Guérin (Bcg) in Oncotherapy: Bladder Cancer and Beyond. *Vaccine* (2021) 39(50):7332–40. doi: 10.1016/j.vaccine.2021.09.053
132. Liang K, Liu Q, Li P, Luo H, Wang H, Kong Q. Genetically Engineered Salmonella Typhimurium: Recent Advances in Cancer Therapy. *Cancer Lett* (2019) 448:168–81. doi: 10.1016/j.canlet.2019.01.037

Conflict of Interest: The authors declare that the research was conducted in the absence of any commercial or financial relationships that could be construed as a potential conflict of interest.

Publisher's Note: All claims expressed in this article are solely those of the authors and do not necessarily represent those of their affiliated organizations, or those of the publisher, the editors and the reviewers. Any product that may be evaluated in this article, or claim that may be made by its manufacturer, is not guaranteed or endorsed by the publisher.

Copyright © 2022 Tang, Peng, Xu, Zhou, Chen and Cheng. This is an open-access article distributed under the terms of the Creative Commons Attribution License (CC BY). The use, distribution or reproduction in other forums is permitted, provided the original author(s) and the copyright owner(s) are credited and that the original publication in this journal is cited, in accordance with accepted academic practice. No use, distribution or reproduction is permitted which does not comply with these terms.

frontiers | Frontiers in Immunology

ORIGINAL RESEARCH
published: 23 June 2022
doi: 10.3389/fimmu.2022.884615

Fecal Microbiota Transplantation Reshapes the Physiological Function of the Intestine in Antibiotic-Treated Specific Pathogen-Free Birds

Peng Li, Mingkun Gao, Bochen Song, Yan Liu, Shaojia Yan, Jiaqi Lei, Yizhu Zhao, Guang Li, Tahir Mahmood, Zengpeng Lv, Yongfei Hu and Yuming Guo *

State Key Laboratory of Animal Nutrition, College of Animal Science and Technology, China Agricultural University, Beijing, China

The topic about the interactions between host and intestinal microbiota has already caught the attention of many scholars. However, there is still a lack of systematic reports on the relationship between the intestinal flora and intestinal physiology of birds. Thus, this study was designed to investigate it. Antibiotic-treated specific pathogen-free (SPF) bird were used to construct an intestinal bacteria-free bird (IBF) model, and then, the differences in intestinal absorption, barrier, immune, antioxidant and metabolic functions between IBF and bacteria-bearing birds were studied. To gain further insight, the whole intestinal flora of bacteria-bearing birds was transplanted into the intestines of IBF birds to study the remodeling effect of fecal microbiota transplantation (FMT) on the intestinal physiology of IBF birds. The results showed that compared with bacteria-bearing birds, IBF birds had a lighter body weight and weaker intestinal absorption, antioxidant, barrier, immune and metabolic functions. Interestingly, FMT contributed to reshaping the abovementioned physiological functions of the intestines of IBF birds. In conclusion, the intestinal flora plays an important role in regulating the physiological functions of the intestine.

Keywords: antibiotic-treated, bacteria, bird, intestine, fecal microbiota transplantation

OPEN ACCESS

Edited by:
Mario M. D'Elios,
University of Florence, Italy

Reviewed by:
Nagaja Capitani,
University of Siena, Italy
Wu Shugeng,
Feed Research Institute (CAAS), China

***Correspondence:**
Yuming Guo
guoyum@cau.edu.cn

Specialty section:
This article was submitted to Microbial Immunology, a section of the journal Frontiers in Immunology

Received: *26 February 2022*
Accepted: *18 May 2022*
Published: *23 June 2022*

Citation:
Li P, Gao M, Song B, Liu Y, Yan S, Lei J, Zhao Y, Li G, Mahmood T, Lv Z, Hu Y and Guo Y (2022) Fecal Microbiota Transplantation Reshapes the Physiological Function of the Intestine in Antibiotic-Treated Specific Pathogen-Free Birds. Front. Immunol. 13:884615. doi: 10.3389/fimmu.2022.884615

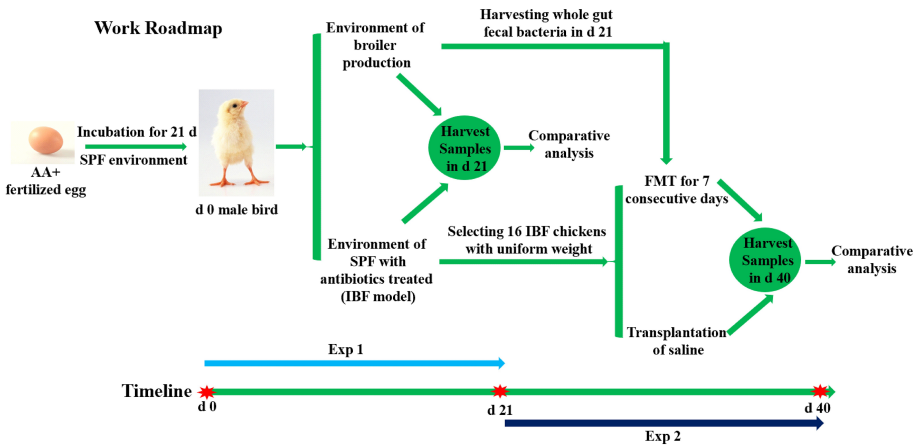

GRAPHICAL ABSTRACT |

INTRODUCTION

The intestine is not only involved in absorbing nutrients in the diet, but also protects the host from infection by pathogenic microorganisms. In addition, the intestine is considered to be the largest immune organ (1). A healthy intestine is one that is equipped with a complete barrier structure, powerful absorption and immune functions, and a healthy microbial population (2). The intestinal flora plays an extremely important role in maintaining intestinal health. Some scholars believe that by regulating the physiological functions of the intestine, such as the absorption and transport of nutrients, immunity, and the secretion of hormones, the intestinal flora establishes a connection circuit with the brain, which regulates the emotions and behaviors of the host (3, 4). The influence of the intestinal flora on the immune function is particularly important. A study suggested that 80% of the immune response in the intestine was induced by the intestinal flora (5). Simultaneously, the genetic factors and health status of the host also affect the composition of the intestinal flora (6). The cross-talk between the intestinal bacteria and the intestine is closely related to the health of the host. The mechanism is extremely complex, and that complexity is precisely what has caught the attention of scholars.

Specific pathogen-free (SPF) and germ-free animal models are considered to be effective tools for studying the relationship between the intestinal flora and host. A study suggested that cecal swelling, intestinal wall atrophy, and decreased intestinal macrophage counts were typical characteristics of sterile mice (7). Based on the SPF bird model, studies found the critical time period for the maturation and establishment of the intestinal flora was 14-28 days of age (8), and *Lactobacillus plantarum* contributed to alleviating necrotizing enteritis induced by *Clostridium perfringens* (9). Additionally, allicin has been shown to play a potential role against avian reticuloendothelial virus (REV) by blocking the ERK/MAPK pathway (10). The breeding of germ-free animals is difficult, and the breeding conditions are harsh. Therefore, some scholars have used antibiotics to treat SPF mice in the early stages of life, and found that the intestines of the mice were almost sterile (11). Many scholars hypothesized that antibiotic-treated SPF animals could be used for germ-free animal models (12). Fecal microbiota transplantation (FMT) technology is an effective method to study the effects of specific intestinal floras on the host. Studies suggested that FMT was useful for the intestinal development of newborn birds (13), the egg-laying performance of law-laying hens (14), and reducing the difference in the structure of the intestinal flora in the newborn birds (15). In addition, FMT could prevent birds from the developing infection with *Salmonella* (16), and relieve the intestinal inflammation in mice (17). Although some studies about FMT conducted on SPF birds provide useful information, the work is very scarce. Moreover, there remains a lack of systematic reports on the difference in intestinal physiology between germ-free and bacteria-bearing birds.

In the present study, an intestinal bacteria-free bird (IBF) model was constructed by using a combination of antibiotics to treat the intestinal flora of SPF birds in the early stages of life. Then, the differences in intestinal absorption, barrier, antioxidant, immune and metabolic functions between IBF and bacteria-bearing birds were systematically evaluated. In addition, based on the IBF model, the whole intestinal fecal bacteria of bacteria-bearing birds were transplanted into IBF birds, and the effect of FMT on the intestinal physiology of IBF birds was studied. This study aimed to reveal the relationship between the resident bacteria in the intestine and the intestinal physiological function of birds.

MATERIALS AND METHODS

Animal and Diet

The animal experiment was carried out at the Poultry Experiment Base of China Agricultural University (Hebei, China). 410 SPF

fertilized AA+ eggs were placed in a SPF hatching room for 21 days of incubation. After the newborn birds were sexed, sixty healthy male birds with uniform weight were selected for follow-up tests. The birds were equally divided into three groups, with 20 birds in each. One group of birds was fed in a normal breeding environment with bacteria (Control), and birds in the other two groups were reared in two isolation barrier systems (Tianjin Jinghang Purification Air Conditioning Company, China) to construct the intestinal bacteria-free bird (IBF) model. The ration formula was formulated based on the nutritional requirements standard of Chinese broilers (NY/T33-2004) (**Table 1**). After the feed was prepared, it was sterilized by radiation (cobalt source, 25K, China Institute of Atomic Energy, Beijing). The drinking water of IBF birds was sterilized (121°C, 103.4 kPa, 15 min), and an antibiotic combination (1 g/L ampicillin, 1 g/L metronidazole, 1 g/L neomycin, and 0.5 g/L vancomycin) was added to the water. The birds in the control group received drinking water without antibiotics. Additionally, all birds had free access to feed, and the cage size, temperature, and lighting conditions were controlled uniformly. At the end of 21 days, 10 birds with uniform body weight from the control group and one group of IBF birds were selected to fast for 8 hours, and then, a 10% D-xylose solution (1 mL/kg BW) was administered orally. One hour later, blood was collected from the underwing vein, and then, these birds were injected intravenously with 50 mg/kg BW sodium pentobarbital, and quickly slaughtered after anesthesia to harvest samples for analysis.

Fecal Microbiota Transplantation

At the end of 21 days, the remaining 10 birds in the control group were slaughtered to obtain whole intestinal chyme to prepare a fecal bacterial suspension. Briefly, the whole intestinal chyme was collected and placed into a 500 mL beaker, and 2 times the volume of normal saline was added and mixed. The mixed liquid was passed through 10-, 18-, 35-, and 60- mesh sieves, and the last filtrate was passed through a 60- mesh sieve three times. The filtrate was centrifuged at 6,000×g for 15 min at 4°C, the pellet was resuspended in sterile normal saline containing 20% glycerol. The prepared bacterial suspension was placed in a refrigerator at 4°C. Sixteen birds with uniform body weight from the remaining IBF birds described above were selected and randomly divided into two treatment groups, with eight birds each. The birds in the FMT group (IBF-FMT) were treated by fecal bacterial transplantation for one week (1 mL/day per bird, the bacterial solution concentration was 1×10^8 CFU/mL), and the birds in the IBF group (IBF-CTR) were given an equal volume of normal saline. Two weeks after the end of FMT, all birds were selected to fasted for 8 hours, and then, the blood and samples were collected according to the method described above. The animal testing procedure was described in the Work Roadmap (**Graphical Abstract**).

TABLE 1 | Test diet composition and nutrition level (air-dry basis).

Ingredients	Contents(%)	Nutritional parameters	Levels[c]
Corn (7.8% pro)	62.644	ME MC/kg	3.016
Dephenolized cottonseed protein (50% pro)	16.200	Crude protein %	21.621
corn gluten meal (51.3% pro)	13.800	Lysine%	1.268
Corn oil	2.000	Methionine%	0.634
CaHPO4	1.980	Calcium %	1.160
Limestone powder	1.100	Total phosphorus %	0.822
L-Lysine HCl (78%)	0.790	Available phosphorus %	0.463
NaCl	0.350	Methionine+Cystine %	0.954
Trace minerals[b]	0.300	Threonine %	0.844
Choline chloride (50%)	0.300	Tryptophan %	0.246
DL-Methionine	0.250		
Threonine	0.140		
Tryptophan	0.080		
Sandaquin	0.030		
multi-vitamins[a]	0.020		
Phytase-5000	0.016		
Total	100		

[a]Vitamin premix (provided per kilogram of feed) the following substances: vitamin A, 12,500 IU; vitamin D3, 2,500 IU; vitamin K3, 2.65 mg; vitamin B1, 2 mg; vitamin B2, 6 mg; vitamin B12, 0.025 mg; vitamin E, 30 IU; biotin, 0.0325 mg; folic acid, 1.25 mg; pantothenic acid, 12 mg; niacin, 50 mg. [b]Trace element premix (provided per kilogram of feed) the following substances: copper, 8 mg; zinc, 75 mg; iron, 80 mg; manganese, 100 mg; selenium, 0.15 mg; iodine, 0.35 mg. [c]Calculated value based on the analysis of experimental diets.

Serum D-Xylose, DAO, and Cytokine Levels

The blood was centrifuged at 3000 ×g and 4°C for 15 min to separate the serum for later use. The Kits purchased from Nanjing Jiancheng Institute of Biological Engineering (Jiangsu, China) were used to determine the levels of D-xylose and DAO in serum. ELISA kits (IDEXX Laboratories Inc., Weatbrook, Maine, USA) were used to analyze the serum levels of TNF-α, IL-10, IL-1β, IL-4 and IFN-γ.

Intestinal Morphology, sIgA and Antioxidant Related Enzymes Levels

Sections of the jejunum and ileum approximately 1 cm in length were collected and suspended in a 4% paraformaldehyde solution, and then, the intestinal tissues were stained with periodic acid-Schiff to prepare sections. The method of Wagner et al. (1999) (18) was used to measure the height of intestinal villi (VH) and the depth of crypts (CD), and the ratio of the VH to CD was calculated. At the same time, the number of goblet cells on 100 μm of villi was counted. A tissue homogenate was prepared at a ratio of the weight of the ileal mucosa sample to the volume of physiological saline = 1:9, and then centrifuged at 3000 ×g and 4°C for 15 min to separate the supernatant for later use. A chicken sIgA ELISA kit (Bethyl Laboratories Inc., Montgomery, TX, USA) was used to detect the level of ileal sIgA. Kits purchased from Nanjing Jiancheng Institute of Biological Engineering were used to determine the contents of superoxide dismutase (SOD), total antioxidant capacity (T-AOC), and malondialdehyde (MDA) in the ileum.

Lymphocyte Analysis of the Ileum

An approximately 3 cm segment of the ileum was taken 1 cm behind the yolk antrum, after the chyme was washed out the intestine was cut into a muddy rough shape in a prechilled calcium and magnesium-free D-Hank's solution. The treated intestine was moved into a 50 mL centrifuge tube, and five milliliters of separation solution (D-Hank's solution with 5%

FCS, 1 mmol/L DTT, 10 mmol/L HEPES, and 2 mmol/L EDTA) was added into it and shaken for 15 min at 250 r/min and 37°C. After that, the mixture was passed through a 200-mesh cell sieve, the cells on the sieve were collected in a new 50 mL centrifuge tube. Five milliliters of digestion solution (D-Hank's without calcium and magnesium supplemented with 5% FCS, 0.15% collagenase VIII, and 100 KU/L DNase I) was added to the centrifuge tube and shaken for 45 min at 250 r/min and 37°C. The mixture was passed through a 300-mesh cell sieve, and the filtrate was collected in a 7 mL centrifuge tube. The mixture was centrifuged at 4°C and 400 × g for 10 min to harvest cells and resuspend it into 2 mL of RPMI-1640. Next, 3.3 mL of separation solution was added to a clean 10 mL centrifuge tube, and the cell suspension was carefully transferred to the surface of the separation liquid. The mixture was centrifuged at 4°C and 3000 × g for 30 min, and the white blood cell layer was carefully transferred into a clean 10 mL centrifuge tube. 2 mL of red blood cell lysate was added to the tube and incubated for 5 min. The mixture was centrifuged at 4°C and 3000 × g for 10 min, and 3 mL of D-Hank's solution was added to the tube to resuspend the cells. After repeating the above centrifugation step, the supernatant was discarded, the cells were resuspended in 2 mL of RPMI-1640, and then, the cell concentration was adjusted to 1×10^7 cells/mL. According to the method of Li, et al. (19), the percentages of Bu-1^+, macrophage, $CD3^+$, $CD4^+$, $CD8^+$ lymphocytes were detected and subsequently calculated. The result is expressed as a percentage.

Gene Expression Level

The jejunum and ileum were collected in RNase-free cryotubes, quickly put into liquid nitrogen, and then stored at -80°C. A 100 mg sample was added to a 1.5 mL centrifuge tube with 1 mL of TRIzol (Invitrogen Life Technologies, Carlsbad, USA) extraction solution, and then, the total RNA was extracted according to the kit instructions (Takara, Dalian, China). After the purity of the total RNA was determined, reverse transcription was performed using an M-MLV cDNA kit (Invitrogen Life Technologies). The reverse transcription product was diluted 1:1 and then subjected to real-time polymerase chain reaction (RT-PCR). Briefly, RT-PCR analysis of gene expression was performed using the primers listed in **Supplementary Table 2**, and SYBR® Premix Ex Taq™ (Takara, Dalian, China) on an Applied Biosystems 7500 Fast Real-Time PCR System (Foster City, CA, USA). The PCR conditions were as follows: 5°C for 2 min, 95°C for 10 min, and 40 cycles of denaturation at 95°C for 15 sec and renaturation at 60°C for 1 min. Finally, the reaction was terminated at 72°C for 10 min. Amplification products were verified by melting curves, agarose gel electrophoresis, and direct sequencing. The results were analyzed by the cycle threshold (CT) method from Fu et al. (2010) (20).

Microbial Sequencing and Analysis

The ileal and cecal chyme of the control and the IBF-FMT group were collected and then sequenced and analyzed according to the method described by Zhang et al. (2018) (21). Briefly, a fecal bacterial DNA extraction kit (QIAamp Fast DNA Stool Mini Kit, Qiagen Company, Germany) was used to harvest microbial DNA from ileal and cecal chyme. A NanoDrop 2000 (Thermo Scientific, Waltham, MA, USA) was used to determine the concentration of DNA, and 1% agarose gel electrophoresis was used to assess the purity of DNA in the samples. The common primers 338 F (5'-ACTCCTACGGGAGGCAGCA-3') and 806 R (5'-GGACTACHVGGGTWTCTAAT-3') targeting the V3-V4 region of the 16S rDNA gene were used to amplify bacterial DNA, and then, the PCR products were purified, quantified and homogenized to construct a sequencing library. A TruSeq® DNA PCR-free sample preparation kit was used for library construction, and the constructed library was quantified by a Qubit and Q-PCR. After the library was qualified, it was sequenced on a system using a HiSeq2500 PE250. The 16S rRNA gene amplicon sequencing results were submitted to the Sequence Read Archive of the NCBI (accession number: PRJNA810526). Sequencing analysis was completed by Beijing Nuohe Zhiyuan Bio-Information Technology Co., Ltd. QIIME software (Qiime2-2019.7, Nature Biotechnology) was used to generate species abundance tables for different taxonomic levels. Based on OTU analysis, the relative abundances of bacteria at the phylum and genus levels were analyzed, and a column chart of the relative abundances of bacteria was drawn.

Non-Targeted Metabolomics Research

The ileal chyme was collected and stored at -80°C. The metabolites in chyme were used for metabolome sequencing and analysis according to the method of Lu et al. (2019) (22). Briefly, 0.1 g of sample was added to precooled 80% formaldehyde, mixed, and then incubated at -20°C for 60 min. The mixture was centrifuged at 4°C and 14,000 × g for 20 min, and the supernatant was vacuum-dried. Sixty percent formaldehyde buffer was used to dissolve the dried metabolite particles, and then, LC–MS/MS analysis was performed. A 16-min linear gradient was used to inject the sample into a Hypersil Gold column (100 × 2.1 mm, 1.9 μm; Thermo Fisher Scientific) at a flow rate of 0.3 mL/min. The eluents for positive polarity mode were eluent A (0.1% formic acid in water) and eluent B (methanol). The eluents for negative polarity mode were eluent A (5 mmol/L ammonium acetate, pH 9.0) and eluent B (methanol). The solvent gradient settings were as follows: 2% B for 1.5 min, 2-100% B to 12.0 min, 100% B to 14.0 min, 100-2% B to 14.1 min, and 2% B to 16.0 min. The AQ Exactive HF-X mass spectrometer (Thermo Fisher Scientific) was operated in positive/negative polarity mode, with a spray voltage of 3.2 kV, a capillary temperature of 320°C, a sheath gas flow rate of 35 arb, and an auxiliary gas flow rate of 10 arb.

The original files obtained by mass spectrometry were imported into Compound Discoverer 3.1 (Thermo Fisher Scientific) software for analysis. The sequencing analysis was commissioned by Beijing Nuohe Zhiyuan Biological Information Technology Co., Ltd. After the qualitative and quantitative results for metabolites were obtained, the data were subjected to quality control to ensure the accuracy and reliability of the results. Metabolites were analyzed by the multivariate statistical analysis partial least squares discriminant analysis (PLS-DA) method to reveal the differences in the metabolic patterns of different groups. Hierarchical clustering analysis (HCA) and metabolite correlation analysis were used to reveal the

relationships between metabolites. Finally, functional analysis was used to explain the biological significance of metabolites.

Data Analysis

The independent sample T test in SPSS 23.0 software (SPSS Inc., Chicago, IL) was used to analyze the data. The results were shown as the mean ± standard deviation. $P < 0.05$ was considered a significant difference between groups. GraphPad Prism 8.0 software was used to draw figures.

RESULTS

FMT Reshaped the Intestinal Bacteria Structure of IBF Chickens

The fecal PCR electrophoresis bands of the control and IBF-FMT group at 1500 bp were bright, and there were no bands in the IBF and the IBF-CTR group (**Supplementary Figure 1**). Additionally, the results of gram staining of the fecal bacterial suspension were consistent with the PCR results. Although we could not determine whether the intestinal tract of the IBF chickens was absolutely sterile, the number of bacteria was at least extremely low. The results also showed that FMT was successful. The weekly test for environmental bacteria showed that there were no bacteria in the growth environment of the birds during the trial. However, due to improper access management of the staff, there was a white mold on the bacterial culture plate used for the detection of environmental bacteria on the day of sampling at the end of the trial (**Supplementary Figure 2**). We believed that it had no effect on the analysis of the study results.

The ileal and cecal bacterial composition of the control and the IBF-FMT group were compared and analyzed. In the control group, the ileal bacteria were mainly related to Firmicutes, Bacteroides, Proteobacteria, *Lactobacillus*, and *Staphylococcus* (**Figures 1A, C**). The cecal was dominated by Firmicutes, Bacteroides, Proteobacteria, *Alistipes*, and *Staphylococcus* (**Figures 1E, G**). Previous results showed that there were almost no bacteria in the intestines of IBF birds. Whole intestinal fecal bacteria of the birds in the control group were transplanted into the intestines of IBF birds, and the composition and structure of the main bacteria in the ileum and cecum of the birds in the IBF-FMT group were similar to the control group (**Figures 1B, D, F, H**). The results showed that FMT could reshape a complete intestinal bacteria structure in the intestine of IBF birds.

FMT Reshaped the Intestinal Absorption, Barrier and Antioxidant Functions of IBF Chickens

Compared with the control group, the IBF chickens had smaller body weight, bursa of fabric and thymus mass index (**Supplementary Figure 3**). The villus height (VH), the ratio of villus height to crypt depth (VH/CD), the number of villus goblet cells, and the mRNA levels of *Mucin-2* and *ZO-1* in the jejunum and ileum of IBF birds were lower than those of the control group (**Figures 2A–C**) (**Supplementary Figure 4**). The gene transcription levels in the jejunum, such as those of aquaporin-8 (*AQP-8*), potassium inwardly rectifying channel subfamily J member 13 (*KCNJ13*), transient receptor potential cation channel subfamily V member 6 (*TRPV6*), and solute carrier family 7 member 7 (*SLC7A7*), of IBF birds were lower than those of birds in the control group, as were the catalase (CAT) and superoxide dismutase (SOD) contents and total antioxidant capacity (T-AOC) in the ileum. In addition, the level of diamine oxidase (DAO) in the serum of IBF birds was higher, and the level of D-xylose was lower than that of the control birds (**Figures 2D–F**). The above evidence showed that the intestinal absorption, barrier and antioxidant functions of IBF birds were weaker than those of the control birds.

To gain more insight, we conducted the FMT on IBF birds, and found FMT elevated the thymus mass index, the VH, VH/CD, number of villus goblet cells, and mRNA level of *Mucin-2* in the jejunum and ileum compared with the IBF-CTR group (**Figures 2G–I**) (**Supplementary Figure 4**). Additionally, the transcription levels of genes in the jejunum, such as *AQP-8*, *KCNJ13*, *TRPV6*, and *SLC7A7*, and the levels of SOD and T-AOC in the ileum were up-regulated by FMT, as was the serum D-xylose level (**Figures 2J–L**). These findings indicated that FMT contributed to improving the intestinal absorption, barrier and antioxidant functions of IBF chickens. This ability might be the reason why we found that the body weight of the birds in the IBF-FMT group was 130 g higher than that of the birds in the IBF-CTR group (**Supplementary Figure 3**).

FMT Reshaped the Intestinal Immune Function of IBF Chickens

The proportion of $CD3^+$ and $CD4^+$ T cells in the ileum of IBF birds were lower, while the proportion of $CD8^+$ T cells was higher than control group (**Figure 3A**) (**Supplementary Figure 5**). It seemed that $CD8^+$ T cells played a key role in immune defense with the removal of intestinal bacteria. Additionally, the levels of serum IL-1β and IL-10, the level of secreted immunoglobulin A (sIgA), and the gene transcription levels in the ileum, such as lysozyme (*LYZ*), *IL-4*, *IL-8*, *IL-10*, interferon-γ (*IFN-γ*), and transforming growth factor β (*TGF-β*) were lower (**Figures 3B–D**). These evidences suggested that the intestinal flora was closely related to the immune function of the intestinal mucosa of host. To gain further insight, the whole intestinal fecal bacteria from chickens in control group was transplanted into the intestine of IBF birds, and found FMT raised the ratio of $CD3^+$, $CD4^+$ T cells, and B lymphocytes. In addition, the transcription levels of *IL-4*, *IL-8*, *IL-10*, and *IFN-γ* in the ileum, and the levels of serum IL-4, IL-10, and IFN-γ were also increased by FMT (**Figures 3E–H**) (**Supplementary Figure 6**). These evidences illuminated us that FMT was helpful for improving the poor development of intestinal immune function in IBF birds. In fact, this further confirmed the importance of intestinal flora for the immune function of intestine.

FMT Reshaped the Intestinal Metabolic Function of IBF Chickens

The compositions of metabolites in the intestinal chyme of IBF birds and control were different. Specifically, there were 214 metabolites were downregulated, and 94 metabolites were

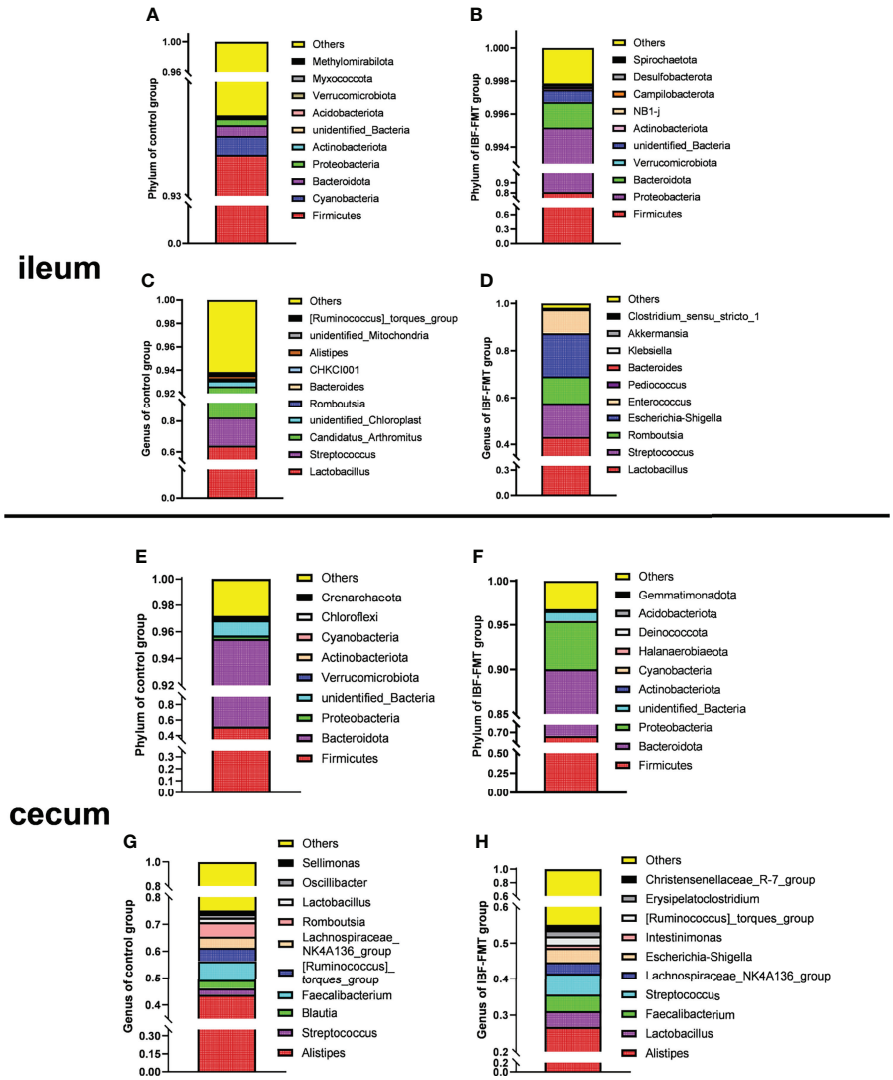

FIGURE 1 | The comparative analysis of intestinal flora structure in control and IBF-FMT group. The main bacteria structure at the phylum and genus level in the ileum (n= 9) and cecum (n= 9) of control group were shown in panels **(A, C)** and panels **(E, G)**, respectively. Based on the IBF bird model, the whole intestinal flora of chickens in the control group were transplanted into the intestine of the chickens of IBF-FMT group, and the main bacteria structure at the phylum and genus level in the ileum (n= 7) and cecum (n= 8) of IBF-FMT group were shown in panels **(B, D)** and panels **(F, H)**, respectively.

upregulated (**Figure 4**). KEGG analysis showed that these differentially abundant metabolites were mainly enriched in the global and overview maps, the amino acid, vitamin and cofactor, nucleotide, and lipid metabolism pathways. At the same time, differentially abundant metabolites were mainly enriched in the cell membrane transport and protein translation pathways (**Supplementary Figure 7**). With intestinal bacteria cleared, the intestinal metabolic function was severely affected, and these changes involved the metabolism of almost all nutrients. Interestingly, we transplanted the fecal bacteria of the birds in the control group into the intestines of IBF birds and found that the levels of 51 metabolites that were downregulated in the IBF group versus the control group were upregulated by FMT treatment, and that the levels of 18 of the upregulated metabolites were downregulated (**Figure 5**) (**Supplementary Figures 9**, **10**). Additionally, FMT reversed the abovementioned changes in the metabolic pathways in the intestines of IBF birds (**Supplementary Figure 8**). The results demonstrated that bacteria in the intestine participated in the entire process of dietary nutrient metabolism, and that FMT helped reshape the intestinal metabolic function of IBF birds. A schematic representation of the relationship between the intestinal flora and the function of the intestinal physiology was described in **Figure 6**.

DISCUSSION

The nutrients in the diet are metabolized by intestinal bacteria to produce short-chain fatty acids (SCFAs), functional amino acids,

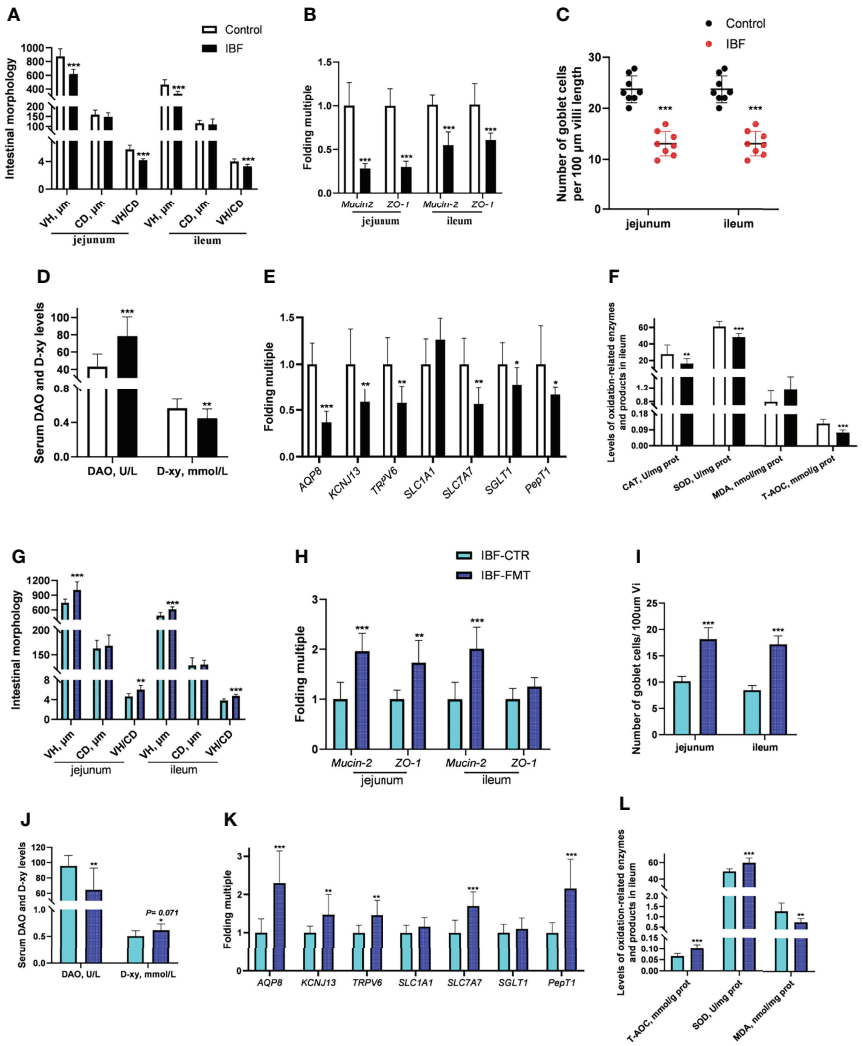

FIGURE 2 | Effects of FMT on intestinal barrier, absorption and antioxidant function in IBF chickens. The results of the comparative study of control and IBF chickens were shown in panels **(A–F)** [as to panels **(A–C)**, n= 8. Additionally, panels **(D–F)**, n= 10], and the comparison results between IBF-CTR and IBF-FMT chickens were shown in panels **(G–L)** (n= 8). Among them, VH= villi height, CD= crypt depth, VH/CD= the ratio of VH to CD, DAO= diamine oxidase, D-xy= D-xylose, CAT= catalase, SOD= superoxide dismutase, MDA= malondialdehyde, and T-AOC= total antioxidant capacity. Additionally, *means that the data tends to be different ($0.05< P< 0.1$), **represents a significant difference ($0.001< P< 0.05$), and ***represents an extremely significant difference ($P< 0.001$), the same below.

vitamins and other functional substances, which improve the digestion and absorption of nutrients by intestinal epithelial cells and promote intestinal development (23–25). Intestinal bacteria can also directly regulate the absorption of nutrients by intestinal epithelial cells. A study found that intestinal bacteria regulated the transport and absorption of lipids in intestinal epithelial cells by regulating the expression of a circadian transcription factor (NFIL3) (26). In the present study, the mRNA levels of intestinal nutrient transporters in the intestine of IBF birds were lower than those of birds with bacteria in the intestine. The results were similar to the findings of previous studies on mice (7). Some scholars have evaluated the absorption function of the intestine by measuring the absorption capacity of D-xylose in piglets under fasting conditions (27). In our study, the level of serum D-xylose in IBF birds was lower than that in control birds. This evidence indicated that the intestinal absorption function of IBF birds was weak and served as a reason that the body weight of the birds was lighter. Intestinal bacteria are involved in the secretion of mucin and contribute to intestinal barrier function (28), and a high level of DAO in serum is regarded as one of the markers of intestinal barrier damage (7). In the present study, the number of goblet cells and the mRNA level of *Mucin-2* in the intestine of IBF birds were less than those of control birds, and the serum DAO level was higher. As a result, we found that the intestinal morphology of IBF birds was worse than that of the control birds. A study suggested that when the fecal bacteria of birds with high feed conversion efficiency (FCR) were transplanted into the intestines of birds with low FCR, the feed intake and body weight

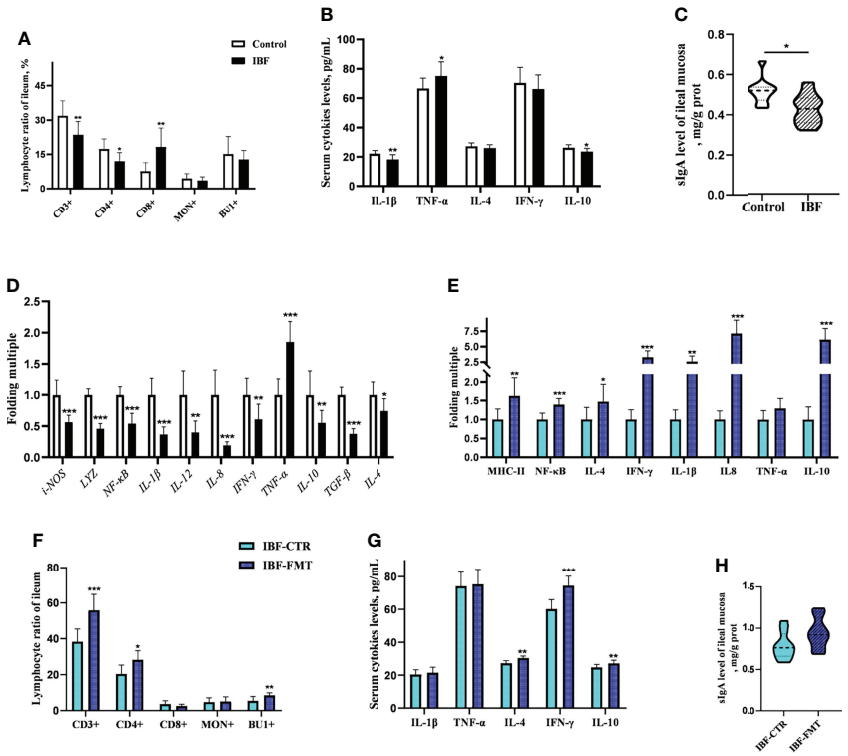

FIGURE 3 | Effects of FMT on intestinal immune function in IBF chickens. The results of the comparative study of control and IBF chickens were shown in panels **(A–D)** (n= 10), and the comparison results between IBF-CTR and IBF-FMT chickens were shown in panels **(E–H)** (n= 8). Among them, * means that the data tends to be different (0.05< P< 0.1), ** represents a significant difference (0.001< P< 0.05), and *** represents an extremely significant difference (P< 0.001), the same below.

of the birds were increased (29). A study also suggested that FMT was beneficial to the intestinal absorption and barrier functions of birds (30). In this study, we found that FMT improved the intestinal morphology and the mRNA levels of intestinal nutrient transporter genes of IBF birds. Our findings lead us to conclude that FMT could reshape the intestinal absorption and barrier functions of IBF birds.

With antibiotic treatment in early life, the intestines become highly sensitive to stress, and a large number of inflammatory factors and oxygen free radicals are produced accordingly (31). We found that the levels of SOD, CAT and the T-AOC in the intestines of IBF birds were lower than those in the intestines of control birds. This finding demonstrated that intestinal bacteria might play a significant role in improving antioxidant function. Studies have found that FMT could improve the antioxidant function of newborn and weaned piglets (32, 33) and relieve oxidative stress caused by acute lung injury in mice (34). To gain further insight, IBF birds were transplanted with the whole intestinal fecal bacteria of the birds in the control group in this study. Interestingly, FMT raised the level of SOD and the T-AOC in the intestine of IBF birds, and decreased the level of MDA. On the basis of these results, we concluded that intestinal bacteria were essential for the antioxidant capacity of the host.

Intestinal bacteria and their metabolites are necessary not only for immune homeostasis but also for determining the host's susceptibility to many diseases. The stable structure of the intestinal bacterial community participates in shaping the immune function of the intestinal mucosa. Once the structure of the intestinal flora is destroyed, immune homeostasis becomes unbalanced (2, 35). A study suggested that intestinal bacteria were involved in regulating the maturation and differentiation of $CD4^+$ and Treg T cells, and maintaining intestinal immune homeostasis (36). In the present study, the number of T and B lymphocytes in the ileum of IBF birds was lower than that of control birds. Notably, the proportion of $CD4^+$ T cells in the ileum of IBF birds was lower than that of the control birds, while the proportion of $CD8^+$ T cells was higher. $CD4^+$ T cells are regarded as important "helpers" of the immune system and are involved in maintaining the body's immune homeostasis. The decrease in the proportion of $CD4^+$ T cells indicated that the body was in a state of immunosuppression. $CD8^+$ T cells directly participate in killing infected cells, and an increase in their proportion is common in immunosuppression (37). Our findings led us to conclude that IBF birds were in an immunosuppressed state and that $CD8^+$ T cells might play an important role in the process of immune defense. Cytokines are involved in regulating the body's immune homeostasis, and the proper expression of proinflammatory factors such as IL-1β, TNF-α, and IL-6 activates the immune system. Once overexpressed, this cytokine expression causes inflammation (38). Anti-inflammatory factors such as IL-4 and IL-10 participate in immune tolerance and

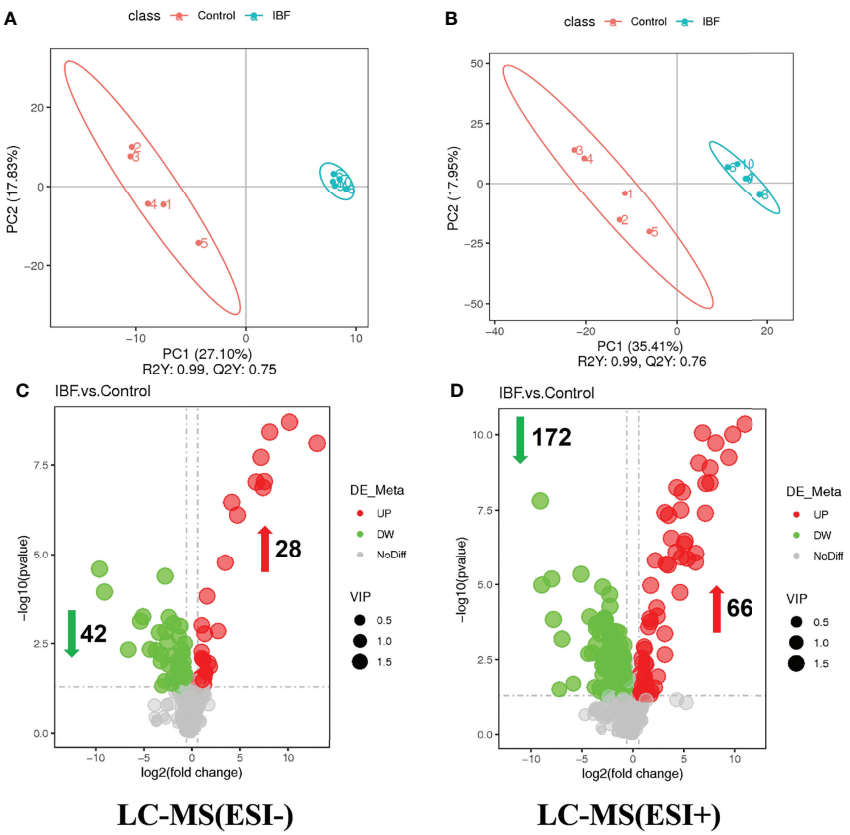

FIGURE 4 | Comparison of ileal chyme metabolome between the birds in IBF and control group. The analysis of panel **(A)** and panel **(B)** were based on the discriminant analysis of partial least squares (PLS-DA). The results in anion mode were showed in panel **(A)** and panel **(C)**, and the results of cation mode were arranged in panel **(B)** and panel **(D)**, n= 5.

antibody synthesis (39). In the present study, the levels of serum IL-1β, IL-10 and the mRNA levels of ileal cytokines were lower in IBF birds than in control birds. The decrease in the levels of these cytokines seemed to be related to the decrease in the number of intestinal immune cells. A study suggested that intestinal bacteria stimulated the secretion of sIgA by promoting the proliferation of intestinal dendritic cells (40). sIgA helps prevent pathogen colonization of the intestinal mucosa, and sIgA is considered to be the main immune barrier that maintains the homeostasis of the symbiotic flora (41). In the present study, the level of ileal sIgA and the weight index of immune organs in IBF birds were lower than those in control birds. These findings further proved that intestinal bacteria played a critical role in regulating the immune function of the host. This finding was consistent with previous study (1, 5, 42).

Studies have suggested that FMT reshaped local and systemic immune development in sterile mice (43), and relieved intestinal flora disorder and immune stress caused by antibiotic abuse (44, 45). In this study, the fecal bacteria of bacteria-bearing birds were transplanted into IBF birds, and found FMT increased the weight of immune organs and the levels of intestinal immune cells and cytokines in IBF birds. This result indicated that FMT reshaped the immune function of IBF birds. A study suggested that transplantation of the whole intestinal flora helped bacteria from different intestinal segments colonize the corresponding locations (46). The commensal bacteria in the intestine provide colonization resistance against pathogenic bacteria by competing for niches and nutrients and metabolizing bacteriocins, SCFAs and other bactericidal substances. This activity contributes to maintaining the homeostasis of the intestinal environment (47). In the present study, the fecal bacteria from birds with bacteria in the control group were transplanted into the intestines of IBF birds, and it was found that the intestinal bacteria of IBF birds could be shaped into a flora structure that was similar to that of the control birds. This evidence indicated that FMT shaped the structure of the intestinal bacteria of IBF birds. This finding was consistent with a previous study in sterile mice (48). On the basis of our findings, it could be concluded that FMT shaped the immune function of the intestine by reshaping the structure of the intestinal bacterial community.

The genes encoding metabolic enzymes carried by the gut microbiota are far more abundant than those of the host, so the gut microbiota is equipped with powerful metabolic capabilities. Diets and host-derived substrates, such as polysaccharides, bile acids and choline, are independently metabolized by intestinal bacteria on the one hand as well as jointly metabolized by the host in coordination (49, 50). Studies have suggested that intestinal bacteria help maintain the metabolic homeostasis of

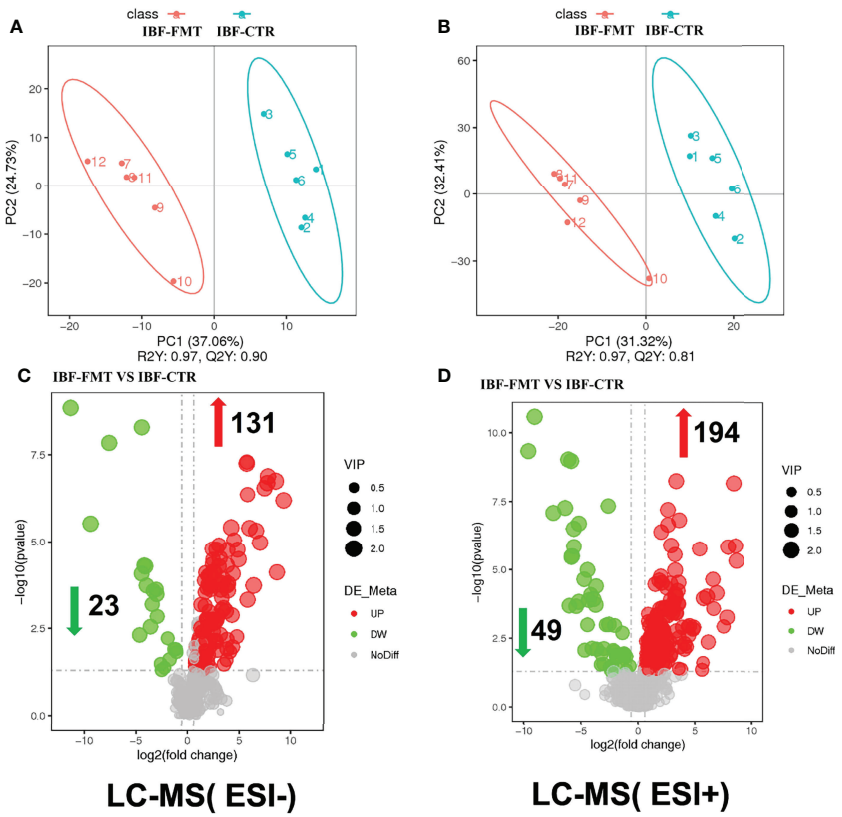

FIGURE 5 | Comparison of ileal chyme metabolome between the birds in IBF-CTR and IBF-FMT group. The analysis of panel **(A)** and panel **(B)** were based on the discriminant analysis of partial least squares (PLS-DA). The results in anion mode were showed in panel **(A)** and panel **(C)**, and the results of cation mode were arranged in panel **(B)** and panel **(D)**, n=6.

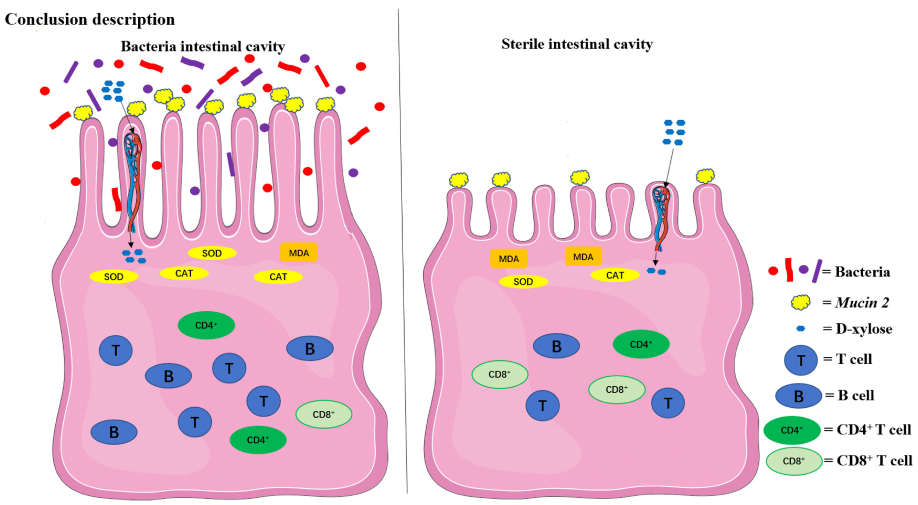

FIGURE 6 | The relationship between the intestinal flora and the function of the intestinal physiology in the present study. The intestinal physiology of the chicken with bacteria in the intestine was described on the left and the IBF on the right. FMT reshaped the physiological function of the intestine in IBF chicken. SOD, superoxide dismutase; CAT, catalase; MDA, malondialdehyde.

the host. The imbalance of intestinal bacteria leads to abnormal metabolism of metabolites such as branched-chain amino acids, hormones, vitamins, and SCFAs, which gives rise to the development of host diseases (51). To clarify the specific metabolic pathways that involve intestinal bacteria, the ileum chyme of IBF and bacteria-containing birds was analyzed by metabolomics. The metabolic pathways of almost all nutrients changed as the intestinal bacteria were cleared. Among them, amino acid, vitamin and cofactor, nucleotide, lipid and other metabolic pathways were most enriched. Some scholars believe that carbohydrates in diets fermented by intestinal bacteria mainly produce SCFAs such as butyric acid, acetic acid and propionic acid, which could be used as energy sources by the intestinal epithelial cells of the host and contribute to intestinal immune function (52). SCFAs, long-chain polyunsaturated fatty acids (PUFAs), bile acids and some methylamine-containing substances, such as choline, lecithin and L-carnitine, are considered to be products of intestinal bacteria metabolizing dietary lipids. These substances play an important role in regulating intestinal absorption, barrier, and immune functions (53). Additionally, intestinal bacteria participate in regulating the energy metabolism of the host by regulating the metabolism of vitamins, especially B and K vitamins (54). A study suggested that intestinal bacteria also regulate intestinal physiology by improving the metabolism of amino acids such as aromatic amino acids and branched-chain amino acids (55). In the present study, the abovementioned differentially enriched metabolic pathways were reshaped by FMT. This evidence led us to conclude that intestinal bacteria were involved in the metabolic process of almost all nutrients in the host, helping maintain normal intestinal physiology. Our findings also illuminated us that FMT might reshape the physiology of the host's intestine by reshaping the structure of the intestinal bacterial community and metabolic pathways.

CONCLUSION

Antibiotic treatment of SPF birds in the early stages of life could be used to construct an intestinal bacteria-free bird model. Intestinal bacteria participated in the regulation of intestinal absorption, barrier, antioxidant, immune and metabolic functions. FMT reshaped the physiology of the host's intestine by reshaping the structure of the intestinal bacterial community and metabolic pathways.

DATA AVAILABILITY STATEMENT

The original contributions presented in the study are publicly available. This data can be found here: https://www.ncbi.nlm.nih.gov/search/all/?term=PRJNA810526.

ETHICS STATEMENT

The animal study was reviewed and approved by Animal Ethics Committee of China Agricultural University, Beijing, China.

AUTHOR CONTRIBUTIONS

YG and PL designed the study, PL wrote the manuscript. PL, MG, YL, BS, SY, JL, YZ, and GL collected and analyzed experimental results. TM, ZL, YH, and YG participated in the writing and revision of the manuscript. All authors contributed to the data interpretation and approved the final version of the manuscript.

FUNDING

This project was funded by the China Agriculture Research System program (CARS-41-G11).

ACKNOWLEDGMENTS

The authors acknowledge Dr. Tahir and American Journal Experts (http://www.aje.com) for its linguistic assistance.

SUPPLEMENTARY MATERIAL

The Supplementary Material for this article can be found online at: https://www.frontiersin.org/articles/10.3389/fimmu.2022.884615/full#supplementary-material

Supplementary Figure 1 | The results of PCR and gram staining about the whole intestinal chyme mixture. According to the standard of China's sterile animal living environment and fecal specimen testing standards (GB/T 14926.41-2001), six samples of each treatment were randomly selected for PCR analysis. The primer sequence was 27F: 5'-AGAGTTTGATCCTGGCTCAG-3', 1492R: 5'- TACGGYTACCTTGTTACGACTT-3'. The result was shown above **(A, B)**, and the NC represented the PCR results of RNA-free water. Then, the intestinal chyme of all birds in each treatment were mixed separately, and three samples from the mixture were randomly selected for gram stain observation. The results were shown in **(C–F)**, among them, the gram-positive bacteria were stained purple, and the red ones represented the gram-negative bacteria.

Supplementary Figure 2 | The results of sedimentation bacteria in SPF environment. According to the standard of China's sterile animal living environment and fecal specimen testing standards (GB/T 14926.41-2001), Different corners of the SPF environment were selected for sedimentation bacteria detection every week, and feeding management staff wear isolation equipment for work every day.

Supplementary Figure 3 | Effects of FMT on the body weight, organ mass index. The comparison results of control and IBF group were shown in **(A, B)**. The comparison results of IBF-CTR and IBF-FMT group were arranged in **(C, D)**. Among them, * means that the data tends to be different ($0.05< P< 0.1$), ** represents a significant difference ($0.001< P< 0.05$).

Supplementary Figure 4 | Effects of FMT on intestinal morphology and the number of goblet cells. The purple dots attached to the intestinal villi represents goblet cells, the picture magnification was 400 times, n= 8.

Supplementary Figure 5 | The flow cytometry analysis results of intestinal immune cells between IBF birds and control. Our analysis steps for flow cytometry results were as follows. At first, we use the CD45 ring gate to eliminate the interference of red blood cells. In the gate of $CD45^+$, T lymphocytes were labeled with $CD3^+$ and their ratios were obtained, and then B lymphocytes and monocytes were labeled with $Bu1^+$ and Mon^+, and their ratios were obtained. In the gate of $CD3^+$, the ratios of $CD4^+$ and $CD8^+$ T cell were obtained, the same below.

Supplementary Figure 6 | The flow cytometry analysis results of intestinal immune cells between the birds in IBF-control and IBF-FMT group. The flow cytometry analysis process was the same as **Supplementary Figure 5**.

Supplementary Figure 7 | The pathway enrichment of differential metabolites based on KEGG between IBF birds and control. The results in the negative ion mode were arranged on the left, and the results in the positive ion mode were displayed on the other side, n=5.

Supplementary Figure 8 | The pathway enrichment of differential metabolites based on KEGG between IBF-CTR birds and IBF-FMT. The results in the negative ion mode were arranged on the left, and the results in the positive ion mode were displayed on the other side, n=6.

Supplementary Figure 9 | The differential metabolites of ileal chyme in anion mode between the birds in IBF-CTR and IBF-FMT group. Substances that were up- or down-regulated by IBF compared with the control group were reshaped by FMT, and these substances were marked by red arrows.

Supplementary Figure 10 | The differential metabolites of ileal chyme in cation mode between the birds in IBF-CTR and IBF-FMT group. Substances that were up- or down-regulated by IBF compared with the control group were reshaped by FMT, and these substances were marked by red arrows.

REFERENCES

1. Pickard JM, Zeng MY, Caruso R, Nunez G. Gut Microbiota: Role in Pathogen Colonization, Immune Responses, and Inflammatory Disease. *Immunol Rev* (2017) 279:70–89. doi: 10.1111/imr.12567
2. Burrello C, Garavaglia F, Cribiu FM, Ercoli G, Lopez G, Troisi J, et al. Therapeutic Faecal Microbiota Transplantation Controls Intestinal Inflammation Through IL10 Secretion by Immune Cells. *Nat Commun* (2018) 9:5184. doi: 10.1038/s41467-018-07359-8
3. Chaucheyras-Durand F, Durand H. Probiotics in Animal Nutrition and Health. *Benef Microbes* (2010) 1:3–9. doi: 10.3920/BM2008.1002
4. Muller PA, Schneeberger M, Matheis F, Wang P, Kerner Z, Ilanges A, et al. Microbiota Modulate Sympathetic Neurons *via* a Gut-Brain Circuit. *Nature* (2020) 583:441–6. doi: 10.1038/s41586-020-2474-7
5. Gill SR, Pop M, Deboy RT, Eckburg PB, Turnbaugh PJ, Samuel BS, et al. Metagenomic Analysis of the Human Distal Gut Microbiome. *Science* (2006) 312:1355–9. doi: 10.1126/science.1124234
6. Dai D, Wu SG, Zhang HJ, Qi GH, Wang J. Dynamic Alterations in Early Intestinal Development, Microbiota and Metabolome Induced by in Ovo Feeding of L-Arginine in a Layer Chick Model. *J Anim Sci Biotechnol* (2020) 11:19. doi: 10.1186/s40104-020-0427-5
7. Schmidt F, Dahlke K, Batra A, Keye J, Wu H, Friedrich M, et al. Microbial Colonization in Adulthood Shapes the Intestinal Macrophage Compartment. *J Crohns Colitis* (2019) 13:1173–85. doi: 10.1093/ecco-jcc/jjz036
8. Xi Y, Shuling N, Kunyuan T, Qiuyang Z, Hewen D, ChenCheng G, et al. Characteristics of the Intestinal Flora of Specific Pathogen Free Chickens With Age. *Microb Pathog* (2019) 132:325–34. doi: 10.1016/j.micpath.2019.05.014
9. Xu T, Chen Y, Yu L, Wang J, Huang M, Zhu N. Effects of Lactobacillus Plantarum on Intestinal Integrity and Immune Responses of Egg-Laying Chickens Infected With Clostridium Perfringens Under the Free-Range or the Specific Pathogen Free Environment. *BMC Vet Res* (2020) 16:47. doi: 10.1186/s12917-020-2264-3
10. Wang L, Jiao H, Zhao J, Wang X, Sun S, Lin H. Allicin Alleviates Reticuloendotheliosis Virus-Induced Immunosuppression *via* ERK/Mitogen-Activated Protein Kinase Pathway in Specific Pathogen-Free Chickens. *Front Immunol* (2017) 8:1856. doi: 10.3389/fimmu.2017.01856
11. Le Roy T, Debedat J, Marquet F, Da-Cunha C, Ichou F, Guerre-Millo M, et al. Comparative Evaluation of Microbiota Engraftment Following Fecal Microbiota Transfer in Mice Models: Age, Kinetic and Microbial Status Matter. *Front Microbiol* (2018) 9:3289. doi: 10.3389/fmicb.2018.03289
12. Yoon H, Schaubeck M, Lagkouvardos I, Blesl A, Heinzlmeir S, Hahne H, et al. Increased Pancreatic Protease Activity in Response to Antibiotics Impairs Gut Barrier and Triggers Colitis. *Cell Mol Gastroenterol Hepatol* (2018) 6:370–88. doi: 10.1016/j.jcmgh.2018.05.008
13. Yin Y, Lei F, Zhu L, Li S, Wu Z, Zhang R, et al. Exposure of Different Bacterial Inocula to Newborn Chicken Affects Gut Microbiota Development and Ileum Gene Expression. *Isme J* (2010) 4:367–76. doi: 10.1038/ismej.2009.128
14. Wang Y, Xu L, Sun X, Wan X, Sun G, Jiang R, et al. Characteristics of the Fecal Microbiota of High- and Low-Yield Hens and Effects of Fecal Microbiota Transplantation on Egg Production Performance. *Res Vet Sci* (2020) 129:164–73. doi: 10.1016/j.rvsc.2020.01.020
15. Donaldson EE, Stanley D, Hughes RJ, Moore RJ. The Time-Course of Broiler Intestinal Microbiota Development After Administration of Cecal Contents to Incubating Eggs. *Peerj* (2017) 5:e3587. doi: 10.7717/peerj.3587
16. Varmuzova K, Kubasova T, Davidova-Gerzova L, Sisak F, Havlickova H, Sebkova A, et al. Composition of Gut Microbiota Influences Resistance of Newly Hatched Chickens to Salmonella Enteritidis Infection. *Front Microbiol* (2016) 7:957. doi: 10.3389/fmicb.2016.00957
17. Strati F, Pujolassos M, Burrello C, Giuffre MR, Lattanzi G, Caprioli F, et al. Antibiotic-Associated Dysbiosis Affects the Ability of the Gut Microbiota to Control Intestinal Inflammation Upon Fecal Microbiota Transplantation in Experimental Colitis Models. *Microbiome* (2021) 9:39. doi: 10.1186/s40168-020-00991-x
18. Wagner U, Burkhardt E, Failing K. Evaluation of Canine Lymphocyte Proliferation: Comparison of Three Different Colorimetric Methods With the 3H-Thymidine Incorporation Assay. *Vet Immunol Immunopathol* (1999) 70:151–9. doi: 10.1016/s0165-2427(99)00041-0
19. Li P, Zhao Y, Yan S, Song B, Liu Y, Gao M, et al. Soya Saponin Improves Egg-Laying Performance and Immune Function of Laying Hens. *J Anim Sci Biotechnol* (2022) 12:126. doi: 10.1186/s40104-021-00647-2
20. Fu WJ, Stromberg AJ, Viele K, Carroll RJ, Wu G. Statistics and Bioinformatics in Nutritional Sciences: Analysis of Complex Data in the Era of Systems Biology. *J Nutr Biochem* (2010) 21:561–72. doi: 10.1016/j.jnutbio.2009.11.007
21. Zhang B, Lv Z, Li Z, Wang W, Li G, Guo Y. Dietary L-Arginine Supplementation Alleviates the Intestinal Injury and Modulates the Gut Microbiota in Broiler Chickens Challenged by Clostridium Perfringens. *Front Microbiol* (2018) 9:1716. doi: 10.3389/fmicb.2018.01716
22. Lu J, Zhang X, Liu Y, Cao H, Han Q, Xie B, et al. Effect of Fermented Corn-Soybean Meal on Serum Immunity, the Expression of Genes Related to Gut Immunity, Gut Microbiota, and Bacterial Metabolites in Grower-Finisher Pigs. *Front Microbiol* (2019) 10:2620. doi: 10.3389/fmicb.2019.02620
23. Sergeant MJ, Constantinidou C, Cogan TA, Bedford MR, Penn CW, Pallen MJ. Extensive Microbial and Functional Diversity Within the Chicken Cecal Microbiome. *PloS One* (2014) 9:e91941. doi: 10.1371/journal.pone.0091941
24. Shakouri MD, Iji PA, Mikkelsen LL, Cowieson AJ. Intestinal Function and Gut Microflora of Broiler Chickens as Influenced by Cereal Grains and Microbial Enzyme Supplementation. *J Anim Physiol Anim Nutr (Berl)* (2009) 93:647–58. doi: 10.1111/j.1439-0396.2008.00852.x
25. Beckmann L, Simon O, Vahjen W. Isolation and Identification of Mixed Linked Beta -Glucan Degrading Bacteria in the Intestine of Broiler Chickens and Partial Characterization of Respective 1,3-1,4-Beta -Glucanase Activities. *J Basic Microbiol* (2006) 46:175–85. doi: 10.1002/jobm.200510107
26. Wang Y, Kuang Z, Yu X, Ruhn KA, Kubo M, Hooper LV. The Intestinal Microbiota Regulates Body Composition Through NFIL3 and the Circadian Clock. *Science* (2017) 357:912–6. doi: 10.1126/science.aan0677
27. Zhao D, Wu T, Yi D, Wang L, Li P, Zhang J, et al. Dietary Supplementation With Lactobacillus Casei Alleviates Lipopolysaccharide-Induced Liver Injury in a Porcine Model. *Int J Mol Sci* (2017) 18:2535. doi: 10.3390/ijms18122535
28. Jakobsson HE, Rodriguez-Pineiro AM, Schutte A, Ermund A, Boysen P, Bemark M, et al. The Composition of the Gut Microbiota Shapes the Colon Mucus Barrier. *EMBO Rep* (2015) 16:164–77. doi: 10.15252/embr.201439263
29. Siegerstetter SC, Petri RM, Magowan E, Lawlor PG, Zebeli Q, O'Connell NE, et al. Fecal Microbiota Transplant From Highly Feed-Efficient Donors Shows Little Effect on Age-Related Changes in Feed-Efficiency-Associated Fecal Microbiota From Chickens. *Appl Environ Microbiol* (2018) 84:e02330–17. doi: 10.1128/AEM.02330-17
30. Metzler-Zebeli BU, Siegerstetter SC, Magowan E, Lawlor PG, CN O, Zebeli Q. Fecal Microbiota Transplant From Highly Feed Efficient Donors Affects Cecal Physiology and Microbiota in Low- and High-Feed Efficient Chickens. *Front Microbiol* (2019) 10:1576. doi: 10.3389/fmicb.2019.01576
31. Scott NA, Andrusaite A, Andersen P, Lawson M, Alcon-Giner C, Leclaire C, et al. Antibiotics Induce Sustained Dysregulation of Intestinal T Cell

Immunity by Perturbing Macrophage Homeostasis. *Sci Transl Med* (2018) 10: eaao4755. doi: 10.1126/scitranslmed.aao4755
32. Xiang Q, Wu X, Pan Y, Wang L, Cui C, Guo Y, et al. Early-Life Intervention Using Fecal Microbiota Combined With Probiotics Promotes Gut Microbiota Maturation, Regulates Immune System Development, and Alleviates Weaning Stress in Piglets. *Int J Mol Sci* (2020) 21:503. doi: 10.3390/ijms21020503
33. Hu L, Geng S, Li Y, Cheng S, Fu X, Yue X, et al. Exogenous Fecal Microbiota Transplantation From Local Adult Pigs to Crossbred Newborn Piglets. *Front Microbiol* (2017) 8:2663. doi: 10.3389/fmicb.2017.02663
34. Tang J, Xu L, Zeng Y, Gong F. Effect of Gut Microbiota on LPS-Induced Acute Lung Injury by Regulating the TLR4/NF-kB Signaling Pathway. *Int Immunopharmacol* (2021) 91:107272. doi: 10.1016/j.intimp.2020.107272
35. Levy M, Blacher E, Elinav E. Microbiome, Metabolites and Host Immunity. *Curr Opin Microbiol* (2017) 35:8–15. doi: 10.1016/j.mib.2016.10.003
36. Zeuthen LH, Fink LN, Frokiaer H. Epithelial Cells Prime the Immune Response to an Array of Gut-Derived Commensals Towards a Tolerogenic Phenotype Through Distinct Actions of Thymic Stromal Lymphopoietin and Transforming Growth Factor-Beta. *Immunology* (2008) 123:197–208. doi: 10.1111/j.1365-2567.2007.02687.x
37. Pellicci DG, Koay HF, Berzins SP. Thymic Development of Unconventional T Cells: How NKT Cells, MAIT Cells and Gammadelta T Cells Emerge. *Nat Rev Immunol* (2020) 20:756–70. doi: 10.1038/s41577-020-0345-y
38. Smith AJ, Humphries SE. Cytokine and Cytokine Receptor Gene Polymorphisms and Their Functionality. *Cytokine Growth Factor Rev* (2009) 20:43–59. doi: 10.1016/j.cytogfr.2008.11.006
39. O'Garra A, Vieira P. T(H)1 Cells Control Themselves by Producing Interleukin-10. *Nat Rev Immunol* (2007) 7:425–8. doi: 10.1038/nri2097
40. Kelly D, Campbell JI, King TP, Grant G, Jansson EA, Coutts AG, et al. Commensal Anaerobic Gut Bacteria Attenuate Inflammation by Regulating Nuclear-Cytoplasmic Shuttling of PPAR-Gamma and RelA. *Nat Immunol* (2004) 5:104–12. doi: 10.1038/ni1018
41. Papp M, Sipeki N, Vitalis Z, Tornai T, Altorjay I, Tornai I, et al. High Prevalence of IgA Class Anti-Neutrophil Cytoplasmic Antibodies (ANCA) Is Associated With Increased Risk of Bacterial Infection in Patients With Cirrhosis. *J Hepatol* (2013) 59:457–66. doi: 10.1016/j.jhep.2013.04.018
42. Kim D, Kim YG, Seo SU, Kim DJ, Kamada N, Prescott D, et al. Nod2-Mediated Recognition of the Microbiota Is Critical for Mucosal Adjuvant Activity of Cholera Toxin. *Nat Med* (2016) 22:524–30. doi: 10.1038/nm.4075
43. Satoh-Takayama N, Kato T, Motomura Y, Kageyama T, Taguchi-Atarashi N, Kinoshita-Daitoku R, et al. Bacteria-Induced Group 2 Innate Lymphoid Cells in the Stomach Provide Immune Protection Through Induction of IgA. *Immunity* (2020) 52:635–49. doi: 10.1016/j.immuni.2020.03.002
44. Avila P, Michels M, Vuolo F, Bilesimo R, Burger H, Milioli M, et al. Protective Effects of Fecal Microbiota Transplantation in Sepsis Are Independent of the Modulation of the Intestinal Flora. *Nutrition* (2020) 73:110727. doi: 10.1016/j.nut.2020.110727
45. An L, Wuri J, Zheng Z, Li W, Yan T. Microbiota Modulate Doxorubicin Induced Cardiotoxicity. *Eur J Pharm Sci* (2021) 166:105977. doi: 10.1016/j.ejps.2021.105977
46. Baruch EN, Youngster I, Ben-Betzalel G, Ortenberg R, Lahat A, Katz L, et al. Fecal Microbiota Transplant Promotes Response in Immunotherapy-Refractory Melanoma Patients. *Science* (2021) 371:602–9. doi: 10.1126/science.abb5920
47. Kamada N, Chen GY, Inohara N, Nunez G. Control of Pathogens and Pathobionts by the Gut Microbiota. *Nat Immunol* (2013) 14:685–90. doi: 10.1038/ni.2608
48. DeFilipp Z, Peled JU, Li S, Mahabamunuge J, Dagher Z, Slingerland AE, et al. Third-Party Fecal Microbiota Transplantation Following Allo-HCT Reconstitutes Microbiome Diversity. *Blood Adv* (2018) 2:745–53. doi: 10.1182/bloodadvances.2018017731
49. Tremaroli V, Backhed F. Functional Interactions Between the Gut Microbiota and Host Metabolism. *Nature* (2012) 489:242–9. doi: 10.1038/nature11552
50. Nicholson JK, Holmes E, Kinross J, Burcelin R, Gibson G, Jia W, et al. Host-Gut Microbiota Metabolic Interactions. *Science* (2012) 336:1262–7. doi: 10.1126/science.1223813
51. Zierer J, Jackson MA, Kastenmuller G, Mangino M, Long T, Telenti A, et al. The Fecal Metabolome as a Functional Readout of the Gut Microbiome. *Nat Genet* (2018) 50:790–5. doi: 10.1038/s41588-018-0135-7
52. Koh A, De Vadder F, Kovatcheva-Datchary P, Backhed F. From Dietary Fiber to Host Physiology: Short-Chain Fatty Acids as Key Bacterial Metabolites. *Cell* (2016) 165:1332–45. doi: 10.1016/j.cell.2016.05.041
53. Schoeler M, Caesar R. Dietary Lipids, Gut Microbiota and Lipid Metabolism. *Rev Endocr Metab Disord* (2019) 20:461–72. doi: 10.1007/s11154-019-09512-0
54. LeBlanc JG, Chain F, Martin R, Bermudez-Humaran LG, Courau S, Langella P. Beneficial Effects on Host Energy Metabolism of Short-Chain Fatty Acids and Vitamins Produced by Commensal and Probiotic Bacteria. *Microb Cell Fact* (2017) 16:79. doi: 10.1186/s12934-017-0691-z
55. Heianza Y, Sun D, Li X, DiDonato JA, Bray GA, Sacks FM, et al. Gut Microbiota Metabolites, Amino Acid Metabolites and Improvements in Insulin Sensitivity and Glucose Metabolism: The POUNDS Lost Trial. *Gut* (2019) 68:263–70. doi: 10.1136/gutjnl-2018-316155

Conflict of Interest: The authors declare that the research was conducted in the absence of any commercial or financial relationships that could be construed as a potential conflict of interest.

Publisher's Note: All claims expressed in this article are solely those of the authors and do not necessarily represent those of their affiliated organizations, or those of the publisher, the editors and the reviewers. Any product that may be evaluated in this article, or claim that may be made by its manufacturer, is not guaranteed or endorsed by the publisher.

Copyright © 2022 Li, Gao, Song, Liu, Yan, Lei, Zhao, Li, Mahmood, Lv, Hu and Guo. This is an open-access article distributed under the terms of the Creative Commons Attribution License (CC BY). The use, distribution or reproduction in other forums is permitted, provided the original author(s) and the copyright owner(s) are credited and that the original publication in this journal is cited, in accordance with accepted academic practice. No use, distribution or reproduction is permitted which does not comply with these terms.

frontiers | Frontiers in Immunology

MINI REVIEW
published: 29 June 2022
doi: 10.3389/fimmu.2022.944139

HP-NAP of *Helicobacter pylori*: The Power of the Immunomodulation

Gaia Codolo[1], *Sara Coletta*[1], *Mario Milco D'Elios*[2*] *and Marina de Bernard*[1*]

[1] Department of Biology, University of Padova, Padova, Italy, [2] Department of Experimental and Clinical Medicine, University of Firenze, Firenze, Italy

The miniferritin HP-NAP of *Helicobacter pylori* was originally described as a neutrophil-activating protein because of the capacity to activate neutrophils to generate oxygen radicals and adhere to endothelia. Currently, the main feature for which HP-NAP is known is the ability to promote Th1 responses and revert the immune suppressive profile of macrophages. In this review, we discuss the immune modulating properties of the protein regarding the *H. pylori* infection and the evidence that support the potential clinical application of HP-NAP in allergy and cancer immunotherapy.

Keywords: HP-NAP, *Helicobacter pylori*, inflammation, allergy, cancer, therapy

OPEN ACCESS

Edited by:
Laurel L. Lenz,
University of Colorado, United States

Reviewed by:
Mohanraj Ramachandran,
Uppsala University, Sweden
Qiaozhen Kang,
Zhengzhou University, China

***Correspondence:**
Marina de Bernard
marina.debernard@unipd.it
Mario Milco D'Elios
mariomilco.delios@unifi.it

Specialty section:
This article was submitted to Microbial Immunology, a section of the journal Frontiers in Immunology

Received: *14 May 2022*
Accepted: *31 May 2022*
Published: *29 June 2022*

Citation:
Codolo G, Coletta S, D'Elios MM and de Bernard M (2022) HP-NAP of Helicobacter pylori: The Power of the Immunomodulation. Front. Immunol. 13:944139. doi: 10.3389/fimmu.2022.944139

INTRODUCTION

Bacteria have two types of ferritin-like molecules, the heme binding bacterioferritins (Bfr) and the non-heme binding bacterial ferritins (Ftn) (1, 2). Both are composed of 24 identical or similar subunits that form a roughly spherical protein containing a large hollow centre that acts as an iron-storage cavity with the capacity to accommodate up to 4000 iron atoms.

In 1992, Almirón and colleagues discovered a starvation-inducible protein that was strongly bound to chromosomal DNA in starved cultures of *Escherichia coli*. The protein was called Dps, as in DNA-binding protein from starved cells (3). Later, *in vivo*, and *in vitro* assays showed that Dps protected DNA during oxidative stress, by sequestering iron and by physically binding the DNA (4), although the latter activity was not demonstrated for all Dps, subsequently identified (5). Dps proteins are ubiquitous in bacteria and, to date, 76 members have been discovered in 57 organisms (6). Their sequence closeness to members of the bacterial ferritin family (7) suggested that Dps represent a new type of ferritin that takes part in a general prokaryotic approach for tackling oxidative stress. In 1998 the first crystal structure of a Dps protein was published (8). The structure proved that Dps is an analogue of ferritins. Dps monomers have essentially the same protein fold (four helix bundle) as the ferritin monomer, and they pack in a dodecameric hollow sphere which closely resembles the packing of ferritin monomers. According to their size which is smaller than that of Bfr and Ftn, Dps can store 500 atoms of iron (9).

Several names and abbreviations have been used to describe miniferritins, depending on the biochemical feature that was being studied: the most common are Dps, for their DNA-binding properties, which is often used interchangeably with miniferritin, and NAP (from neutrophil-activating protein), a term used for the first time referring to the miniferritin of *Helicobacter pylori* because of its capacity to activate neutrophils to produce oxygen radicals and adhere to endothelia (10).

The discovery that miniferritins had an impact on the function of host immune cells besides their role in protecting bacterial DNA from oxidizing radicals, has given the impetus to numerous studies on Dps proteins produced by pathogenic bacteria, such as *Borrelia burgdorferi* (NapA), *Treponema pallidum* (TpF1), *Helicobacter cinaedi* (CAIP). What emerged is that Dps proteins are major determinants in the pathogenesis of chronic inflammatory diseases because of a robust immune modulatory activity (11–14). Among the miniferritins produced by pathogenic bacteria, the most studied is certainly NAP, also called HP-NAP, produced by *H. pylori*.

This minireview summarizes the current state of knowledge on HP-NAP. We address the biological features of this Dps, highlighting the ability of promoting inflammation and dictating the profile of the adaptive immune response, as crucial in the pathogenesis of *H. pylori*-associated diseases. On the other hand, we also emphasize that it is because of its powerful and specific action on the immune system that HP-NAP has a significant potential utility in clinical practice.

HP-NAP IN *H. PYLORI* INFECTION

H. pylori infection is mostly acquired during childhood and often persists for life in the infected host. Depending on geographical region and economic development, the prevalence of *H. pylori* infection in adults has been found to range from 24% to 73% among populations, with a global prevalence estimate of around 50% (15). Although most infected individuals remain asymptomatic, bacteria colonization of the gastric mucosa may cause the development of various clinical conditions such as peptic ulcers, chronic gastritis and gastric adenocarcinomas, and mucosa-associated lymphoid tissue lymphomas (16). The common feature that underlies *H. pylori*-associated disorders is the generation of an inflammatory milieu that the bacterial infection elicits in the gastric mucosa. The strong recruitment of neutrophils, monocytes/macrophages, but most of all, T helper 1 (Th1) lymphocytes whose homing in the inflamed tissue is needed to potentiate the killing potential of macrophages, one would expect to be the best arsenal to fight the bacterium. On the contrary, if left untreated, the infection persists and the inflammatory status that becomes chronic lays the foundation for the development of severe diseases.

Among several virulence factors which cooperate in promoting and maintaining inflammation, HP-NAP is probably the most active. Released by the bacterium in proximity to the gastric epithelial monolayer, HP-NAP can cross the epithelium and activate monocytes/macrophages and mast cells which represent the first line of defense, to release pro-inflammatory cytokines, i.e. TNF-α, IL-6, IL-12 and IL-23 (17, 18). HP-NAP also increases the synthesis of tissue factor (TF) and the secretion of the inhibitor-2 of the plasminogen activator in mononuclear cells (19). The coordinate expression of pro-coagulant and antifibrinolytic activities is expected to favor fibrin deposition and contribute to the inflammatory reaction elicited by *H. pylori* in the gastric mucosa. Once in the stomach wall, HP-NAP directly promotes the recruitment of leukocytes with a path resembling that adopted by the chemokine CXCL8 (20): following transcytosis through endothelial cells, a sizable amount of HP-NAP remains bound to the luminal face of the endothelium (**Figure 1**). How the luminal surface presentation of the protein occurs remains an open issue, but in this form HP-NAP encounters rolling leukocytes, up-regulates the expression of β2 integrins and induces a conformational change of these adhesion receptors, resulting in an increased affinity of them for the endothelial partner (21). This event, which is crucial for the tight adhesion of leukocytes to the endothelium, precedes extravasation. Under HP-NAP stimulation, recruited cells release pro-inflammatory cytokines and chemokines that contribute to the maintenance of inflammation by further recruiting additional neutrophils, monocytes, and lymphocytes (18, 22, 23). Several studies suggest that HP-NAP may interact with at least two receptors on the plasma membrane of leukocytes. The engagement of Toll-like receptor (TLR)-2 (18) is crucial for the production of cytokines, whereas the interaction with a G protein-coupled receptor is mainly linked to burst activation, adhesion, and chemotaxis of leukocytes (22). The evidence that the latter effects are abrogated by inhibiting p38-MAPK, suggested a role for the kinase in the signaling cascade (21, 24).

Despite the pro-inflammatory role of HP-NAP is established, the deletion of the *napA* gene does not abrogate the capacity of *H. pylori* to stimulate the production of TNF-α, IL-6, and CXCL8 by mononuclear cells, suggesting that other factors than HP-NAP are involved. On the contrary, bacteria which do not produce HP-NAP are unable to elicit the release of the Th1-polarizing cytokine IL-12 by the same cells, an event that occurs following the engagement of TLR-2 by the miniferritin (18).

In vivo in the antrum *H. pylori* infection causes a predominant activation of Th1 cells with production of IFN-γ and elevated expression of IL-12, IL-18, IL-17 and TNF-α (25–28). A considerable number of Th cells in the stomach mucosa of *H. pylori*-infected individuals display significant proliferation in response to HP-NAP (18, 25). According to the evidence that HP-NAP can create an IL-12-rich environment, antigen-specific gastric Th cells produce large amounts of IFN- γ and TNF-α and have a powerful cytotoxic activity in response to HP-NAP stimulation, indicating a polarized Th1/T cytotoxic 1 (Tc1) effector phenotype (18).

Collectively, these findings show that the *in vitro* and *in vivo* actions of HP-NAP are highly correlated and identify the bacterial protein as responsible for driving the Th response in the gastric antrum of patients affected by *H. pylori*. The skewing of the gastric T-cell response towards a Th1 profile, characterized by huge IFN-γ production and activation of a cytolytic program, is expected to lead to gastric damage (**Figure 1**). Moreover, the high levels of TF, IFN-γ, and TNF-α might result in procoagulant activity and in gastric functional alteration, such as increased gastrin secretion and pepsinogen release, respectively (25).

HP-NAP AS THERAPEUTIC TOOL

In view of the evidence that HP-NAP possesses a unique capacity to modulate the immune response, numerous researchers have

been motivated to verify the application potential of the miniferritin as therapeutic agent. *In vivo* studies using a recombinant form of HP-NAP has been carried out in mouse model of diseases where a Th2 response is detrimental or where the induction of a Th1 and Tc1 cytotoxic immune response is beneficial, such as allergy and cancer.

Th2 Responses

Allergic disorders, (i.e., allergic rhinitis, asthma and atopic dermatitis-AD) are Th2-mediated inflammatory diseases characterized by local infiltration of eosinophils and elevated allergen-specific IgE serum level (29, 30).

The administration of HP-NAP in a mouse model of ovalbumin (OVA)-induced allergic asthma, revealed the potent inhibitory effect of the protein on the airway eosinophil infiltration and on the Th2 bronchial inflammation, resulting in a great reduction of total serum IgE paralleled by the increase of IL-12 plasma levels (31). A similar effect was achieved in the same mouse model by injecting a plasmid encoding a protein chimera formed by HP-NAP and a soluble form of IL-4 receptor a chain, working as decoy receptor to block the IL-4 released by eosinophils and Th2 cells (32), and after orally administrating spores of *Bacillus subtilis* as a vehicle to deliver HP-NAP fused to the cholera toxin B subunit, widely used to induce peripheral immunological tolerance to co-administered antigens (33).

The capability of HP-NAP to counteract the Th2 immune responses was confirmed in a mouse model of AD (34). AD is characterized by an imbalance between Th1 and Th2 cells which results in increased production of IL-4 and IgE, and local recruitment of eosinophils (35). Intra peritoneal injection of HP-NAP significantly attenuated the secretion of IgE and IL-4 and alleviated the AD symptoms, such as erythema and swelling (**Figure 2A**).

Th2 cells not only regulate allergic disorders but are also involved in the immune response to helminth infections (36). Treatment of mice infected with the intestinal parasite *Trichinella spiralis* with HP-NAP resulted in a consistent reduction of the type 2 immune response, as revealed by the reduced eosinophil infiltration and the drop of IgE serum levels (37).

Cancer

Cancer immunotherapy has revolutionized the field of oncology by prolonging survival of patients with rapidly fatal cancers (38). Among the variety of strategies that have become routine in the clinical practice there is the induction of Th1/Tc1 immune response with massive IFN-γ production (39). Based on the capacity to generate an IL-12-enriched environment promoting the differentiation of Th1 cells, the possibility that HP-NAP might be able to elicit an anti-tumor response, was worth investigating.

The first study, carried out in an orthotopic model of bladder cancer, revealed that the local administration of HP-NAP, by eliciting a potent Th1/Tc1 response, counteracted tumor growth and reduced vascularization of the mass due to the anti-angiogenic activity of IFN-γ (40). Notably, while the administration of Bacillus Calmette-Guérin (BCG), gold standard treatment for non-muscle-invasive bladder cancer, resulted in a strong hematuria, a condition often associated with the therapy, none of the HP-NAP-treated animals showed a macroscopic alteration of the urine aspect. Similar results were obtained in mouse models of hepatoma and sarcoma in which the protein was administered as chimera, fused with the maltose binding protein (rMBP-NAP) (41). The evidence that IFN-γ^+ T cells were not produced, and tumor growth was not inhibited in TLR-2-knock-out mice following administration of HP-NAP (40) or by co-administrating rMBP-NAP and a TLR-2 blocking antibody (41), confirmed the *in vitro* finding suggesting the essential role of the immune receptor for the HP-NAP activity (18).

In a work by Mohabati Mobarez et al. (42), HP-NAP was loaded in chitosan nanoparticles (Chi-rNAP) and applied in a mouse model of breast cancer. The Chi-rNAP formulation strongly affected tumor growth, with an efficacy superior to that of the recombinant protein alone, in accordance to the fact that chitosan nanoparticles, by activating the antigen presenting cells, act as adjuvants (43).

Due to the ability to link the innate with the adaptive immune response, TLR agonists are highly promising as adjuvants in vaccines against life-threatening and complex diseases such as cancer. The possibility of using HP-NAP as adjuvant for cancer treatment was explored by some studies in which the protein was expressed in oncolytic viruses (OVs). The capacity of OVs to selectively replicate in tumor cells leading to cell death makes OVs promising agents for cancer therapy (44). In a neuroendocrine cancer mouse model, the intratumoral injection of OVs expressing HP-NAP improved the animal survival and increased the plasma level of the p40 subunit of IL-12 (45). Using an adenoviral vector encoding HP-NAP, it was demonstrated that the protein promotes the maturation of dendritic cells, both *in vitro* and *in vivo*. Dendritic cells matured by vector-encoded HP-NAP secrete high level of IL-12, and in accordance have the capacity to induce antigen-specific T cell expansion with a predominant Th1 profile. In the same line of evidence it was shown that HP-NAP *per se* promotes the maturation of dendritic cells and the activation and proliferation of cytotoxic T cells towards melanoma cells (46, 47).

An attenuated measles virus strain and vaccinia virus were engineered to express HP-NAP and both were effective in counteracting tumor growth and in improving the survival of animals with breast cancer and neuroblastoma, respectively (48, 49). CAR T cells engineering to produce HP-NAP turned out to be a very promising approach for treating solid tumors that are difficult to completely eradicate with conventional CAR T cells, due to heterogeneity in antigen expression. In mouse models of cancer, injection of CAR(NAP) T cells slowed tumor growth and increased survival rates compared to standard mice CAR T cells, regardless of target antigen or tumor type. The evidence on the safety of this approach in mice bode well for its clinical application (50).

All these studies have converged on the notion that the anti-tumor potential of HP-NAP relies on the activation and shaping of the adaptive immune response, but the possibility that HP-NAP might counteract tumor growth due to the modulation of

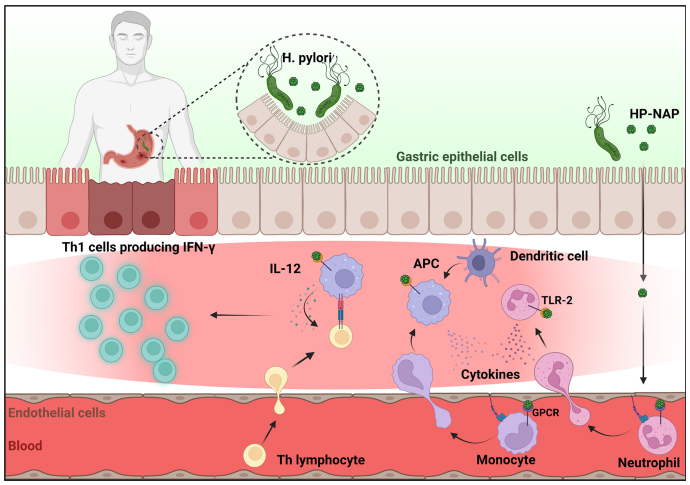

FIGURE 1 | HP-NAP activity in the context of *H. pylori* infection. Once released by *H. pylori* in the stomach lumen, HP-NAP crosses the gastric epithelial cell layer and the endothelium. Bound to the luminal face of the latter, it directly stimulates leukocytes to adhere and extravasate. In addition, HP-NAP activates recruited neutrophils and monocytes to secrete cytokines that further promote inflammation, and stimulates monocytes/macrophages and dendritic cells (antigen presenting cells, APC) to release of IL-12 which drives the differentiation of T helper cells towards the IFN-γ producing Th1 phenotype. Figure created with BioRender.com.

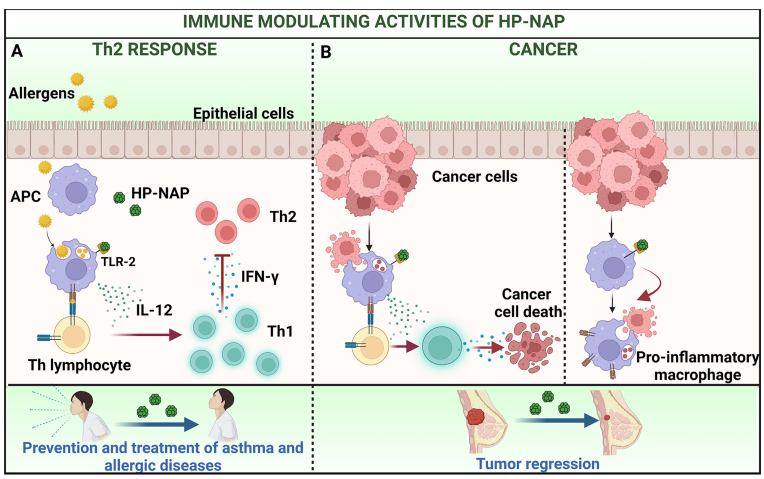

FIGURE 2 | Immune modulating activities of HP-NAP applied to the treatment of allergy and cancer. **(A)** The delivery of pollen allergens to sub-epithelial APC that initiates the priming of T helper 2 (Th2) cells is a key step in the immunopathology of allergy. Treatment with HP-NAP stimulates APC to secrete IL-12 which mediate the skewing of Th2 lymphocytes towards a Th1 profile. This impacts on the allergic cascade and ameliorates the subsequent symptoms. **(B)** HP-NAP can potentiate weak natural Th1 responses, that *per se* are unable to exert protection against tumors (left) and shift the profile of macrophages from pro-oncogenic to pro-inflammatory and anti-tumoral (right). This results in a regression of tumor mass. Figure created with BioRender.com.

mononuclear cells, regardless of the participation of the adaptive immunity, remained unexplored. Codolo and colleagues, taking advantage of the zebrafish model, examined the therapeutic efficacy of HP-NAP against metastatic human melanoma, limiting the observational window to 9 days post-fertilization, well before the maturation of the adaptive immunity. The study disclosed a new property of the miniferritin, namely the capacity of reverting the immune suppressive profile of macrophages, so as to counteract the tumor growth even in the absence of the acquired immune system (51).

CONCLUDING REMARKS

Since its discovery in 1995, HP-NAP, the miniferritin produced by *H. pylori* has been under intense focus because of its

remarkable ability to modulate the human immune response. *H. pylori* infection leads to an intense inflammatory response in the gastric mucosa, characterized by the infiltration of polymorphonuclear and mononuclear cells. It is assumed that HP-NAP, by cooperating to the recruitment of inflammatory cells but especially by generating a pro-inflammatory Th1 skewing environment (**Figure 1**) can make a substantial contribution to the gastric damage caused by *H. pylori* infection. In accordance, HP-NAP is one of the antigens included in the vaccine formulations currently under investigation (52).

On the other hand, the immune modulating activity of HP-NAP makes it an excellent candidate for developing new therapeutic strategies aimed at preventing and treating allergic disorders, such as bronchial asthma, rhinitis, conjunctivitis and, most importantly, at fighting malignant tumors (**Figures 2A, B**).

Whether the iron-binding ability of HP-NAP is related to the pathogenesis of *H. pylori* infection or to the immune modulating properties of the miniferritin is not clear. The bacterial protein is constitutively expressed under iron-depletion, and its expression is not regulated by the presence or absence of iron and it has no part in the metal resistance of *H. pylori* (53). Probably HP-NAP protects the bacterium from the oxidative stress produced in ferrous ion-mediated Fenton reactions, since the degree of DNA damage is much higher in the *napA* knock-out mutant strain than that in the wild-type strain (54). Moreover, iron plays an important role in generation of the quaternary structure of HP-NAP by promoting stable dimers that are crucial for the ensuing dodecamer structure (55), that is likely to be essential for the immune modulatory properties.

Although more pre-clinical studies are mandatory, the evidence of the clinical potential of HP-NAP are promising and strongly support the possibility of adopting HP-NAP as immunomodulatory agent. The immunostimulatory activity of the bacterial protein could also enhance the immunogenicity of poor immunogens, thus HP-NAP could be used as an adjuvant to be included in vaccines formulations.

AUTHOR CONTRIBUTIONS

MdB and MMDE conceived the article content. GC prepared the first draft. SC provided a critical review and prepared the figures. All authors contributed to the article and approved the submitted version.

ACKNOWLEDGMENTS

We thank the Italian Ministry of University and Research, the University of Padua, the University of Florence, and the Associazione Piccoli Punti, for supporting our studies.

REFERENCES

1. Andrews SC. "Iron Storage in Bacteria". In: *Advances in Microbial Physiology*. (Amsterdam: Elsevier) (1998). p. 281–351. doi: 10.1016/S0065-2911(08)60134-4
2. Smith JL. The Physiological Role of Ferritin-Like Compounds in Bacteria. *Crit Rev Microbiol* (2004) 30:173–85. doi: 10.1080/10408410490435151
3. Almiron M, Link AJ, Furlong D, Kolter R. A Novel DNA-Binding Protein With Regulatory and Protective Roles in Starved Escherichia Coli. *Genes Dev* (1992) 6:2646–54. doi: 10.1101/gad.6.12b.2646
4. Martinez A, Kolter R. Protection of DNA During Oxidative Stress by the Nonspecific DNA-Binding Protein Dps. *J Bacteriol* (1997) 179:5188–94. doi: 10.1128/jb.179.16.5188-5194.1997
5. Davis MM, Brock AM, DeHart TG, Boribong BP, Lee K, McClune ME, et al. The Peptidoglycan-Associated Protein NapA Plays an Important Role in the Envelope Integrity and in the Pathogenesis of the Lyme Disease Spirochete. *PloS Pathog* (2021) 17:e1009546. doi: 10.1371/journal.ppat.1009546
6. Guerra JPL, Jacinto JP, Tavares P. Miniferritins: Small Multifunctional Protein Cages. *Coordination Chem Rev* (2021) 449:214187. doi: 10.1016/j.ccr.2021.214187
7. Evans DJ, Evans DG, Lampert HC, Nakano H. Identification of Four New Prokaryotic Bacterioferritins, From Helicobacter pylori, Anabaena variabilis, Bacillus subtilis and Treponema pallidum by Analysis of Gene Sequences. *Gene* (1995) 153:123–7. doi: 10.1016/0378-1119(94)00774-M
8. Grant RA, Filman DJ, Finkel SE, Kolter R, Hogle JM. The Crystal Structure of Dps, a Ferritin Homolog That Binds and Protects DNA. *Nat Struct Mol Biol* (1998) 5:294–303. doi: 10.1038/nsb0498-294
9. Ilari A, Stefanini S, Chiancone E, et al. The Dodecameric Ferritin from Listeria innocua Contains a Novel Intersubunit Iron-Binding Site. *Nat Struct Mol Biol* (2000) 7:38–43. doi: 10.1038/71236
10. Evans DJ, Evans DG, Takemura T, Nakano H, Lampert HC, Graham DY, et al. Characterization of a Helicobacter Pylori Neutrophil-Activating Protein. *Infect Immun* (1995) 63:2213–20. doi: 10.1128/iai.63.6.2213-2220.1995
11. Codolo G, Bossi F, Durigutto P, Bella CD, Fischetti F, Amedei A, et al. Orchestration of Inflammation and Adaptive Immunity in *Borrelia Burgdorferi* -Induced Arthritis by Neutrophil-Activating Protein a. *Arthritis Rheumatism* (2013) 65:1232–42. doi: 10.1002/art.37875
12. Babolin C, Amedei A, Ozoliņš D, Žileviča A, D'Elios MM, de Bernard M. TpF1 From *Treponema Pallidum* Activates Inflammasome and Promotes the Development of Regulatory T Cells. *JI* (2011) 187:1377–84. doi: 10.4049/jimmunol.1100615
13. Pozzobon T, Facchinello N, Bossi F, Capitani N, Benagiano M, Di Benedetto G, et al. Treponema Pallidum (Syphilis) Antigen TpF1 Induces Angiogenesis Through the Activation of the IL-8 Pathway. *Sci Rep* (2016) 6:18785. doi: 10.1038/srep18785
14. D'Elios MM, Vallese F, Capitani N, Benagiano M, Bernardini ML, Rossi M, et al. The Helicobacter Cinaedi Antigen CAIP Participates in Atherosclerotic Inflammation by Promoting the Differentiation of Macrophages in Foam Cells. *Sci Rep* (2017) 7:40515. doi: 10.1038/srep40515
15. Hooi JKY, Lai WY, Ng WK, Suen MMY, Underwood FE, Tanyingoh D, et al. Global Prevalence of Helicobacter Pylori Infection: Systematic Review and Meta-Analysis. *Gastroenterology* (2017) 153:420–9. doi: 10.1053/j.gastro.2017.04.022
16. Martin-Nuñez GM, Cornejo-Pareja I, Clemente-Postigo M, Tinahones FJ. Gut Microbiota: The Missing Link Between Helicobacter Pylori Infection and Metabolic Disorders? *Front Endocrinol* (2021) 12:639856. doi: 10.3389/fendo.2021.639856
17. Montemurro P, Nishioka H, Dundon WG, de Bernard M, Del Giudice G, Rappuoli R, et al. The Neutrophil-Activating Protein (HP-NAP) of Helicobacter Pylori is a Potent Stimulant of Mast Cells. *Eur J Immunol* (2002) 32:671. doi: 10.1002/1521-4141(200203)32:3<671::AID-IMMU671>3.3.CO;2-X
18. Amedei A, Cappon A, Codolo G, Cabrelle A, Polenghi A, Benagiano M, et al. The Neutrophil-Activating Protein of Helicobacter Pylori Promotes Th1 Immune Responses. *J Clin Invest* (2006) 116:1092–101. doi: 10.1172/JCI27177
19. Montemurro P, Barbuti G, Dundon WG, Del Giudice G, Rappuoli R, Colucci M, et al. *Helicobacter pylori* Neutrophil-Activating Protein Stimulates Tissue Factor and Plasminogen Activator Inhibitor–2 Production by Human Blood Mononuclear Cells. *J Infect Dis* (2001) 183:1055–62. doi: 10.1086/319280

20. Middleton J, Neil S, Wintle J, Clark-Lewis I, Moore H, Lam C, et al. Transcytosis and Surface Presentation of IL-8 by Venular Endothelial Cells. *Cell* (1997) 91:385–95. doi: 10.1016/S0092-8674(00)80422-5
21. Polenghi A, Bossi F, Fischetti F, Durigutto P, Cabrelle A, Tamassia N, et al. The Neutrophil-Activating Protein of Helicobacter Pylori Crosses Endothelia to Promote Neutrophil Adhesion. *vivo. J Immunol* (2007) 178:1312–20. doi: 10.4049/jimmunol.178.3.1312
22. Satin B, Del Giudice G, Della Bianca V, Dusi S, Laudanna C, Tonello F, et al. The Neutrophil-Activating Protein (Hp-Nap) of Helicobacter Pylori Is a Protective Antigen and a Major Virulence Factor. *J Exp Med* (2000) 191:1467–76. doi: 10.1084/jem.191.9.1467
23. de Bernard M, D'Elios MM. The Immune Modulating Activity of the Helicobacter Pylori HP-NAP: Friend or Foe? *Toxicon* (2010) 56:1186–92. doi: 10.1016/j.toxicon.2009.09.020
24. Nishioka H, Baesso I, Semenzato G, Trentin L, Rappuoli R, Del Giudice G, et al. The Neutrophil-Activating Protein of Helicobacter Pylori (HP-NAP) Activates the MAPK Pathway in Human Neutrophils. *Eur J Immunol* (2003) 33:840–9. doi: 10.1002/eji.200323726
25. D'Elios MM, Manghetti M, De Carli M, Costa F, Baldari CT, Burroni D, et al. T Helper 1 Effector Cells Specific for Helicobacter Pylori in the Gastric Antrum of Patients With Peptic Ulcer Disease. *J Immunol* (1997) 158:962–7.
26. Bamford KB, Fan X, Crowe SE, Leary JF, Gourley WK, Luthra GK, et al. Lymphocytes in the Human Gastric Mucosa During Helicobacter Pylori Have a T Helper Cell 1 Phenotype. *Gastroenterology* (1998) 114:482–92. doi: 10.1016/S0016-5085(98)70531-1
27. Luzza F, Parrello T, Monteleone G, Sebkova L, Romano M, Zarrilli R, et al. Up-Regulation of IL-17 Is Associated With Bioactive IL-8 Expression in *Helicobacter Pylori* -Infected Human Gastric Mucosa. *J Immunol* (2000) 165:5332–7. doi: 10.4049/jimmunol.165.9.5332
28. Tomita T, Jackson AM, Hida N, Hayat M, Dixon MF, Shimoyama T, et al. Expression of Interleukin-18, a Th1 Cytokine, in Human Gastric Mucosa Is Increased in *Helicobacter Pylori* Infection. *J Infect Dis* (2001) 183:620–7. doi: 10.1086/318541
29. Walker JA, McKenzie ANJ. TH2 Cell Development and Function. *Nat Rev Immunol* (2018) 18:121–33. doi: 10.1038/nri.2017.118
30. León B, Ballesteros-Tato A. Modulating Th2 Cell Immunity for the Treatment of Asthma. *Front Immunol* (2021) 12:637948. doi: 10.3389/fimmu.2021.637948
31. Codolo G, Mazzi P, Amedei A, Del Prete G, Berton G, D'Elios MM, et al. The Neutrophil-Activating Protein of *Helicobacter Pylori* Down-Modulates Th2 Inflammation in Ovalbumin-Induced Allergic Asthma. *Cell Microbiol* (2008) 10:2355–63. doi: 10.1111/j.1462-5822.2008.01217.x
32. Liu X, Fu G, Ji Z, Huang X, Ding C, Jiang H, et al. A Recombinant DNA Plasmid Encoding the sIL-4r-NAP Fusion Protein Suppress Airway Inflammation in an OVA-Induced Mouse Model of Asthma. *Inflammation* (2016) 39:1434–40. doi: 10.1007/s10753-016-0375-6
33. Dong H, Huang Y, Yao S, Liang B, Long Y, Xie Y, et al. The Recombinant Fusion Protein of Cholera Toxin B and Neutrophil-Activating Protein Expressed on Bacillus Subtilis Spore Surface Suppresses Allergic Inflammation in Mice. *Appl Microbiol Biotechnol* (2017) 101:5819–29. doi: 10.1007/s00253-017-8370-x
34. Guo X, Ding C, Lu J, Zhou T, Liang T, Ji Z, et al. HP-NAP Ameliorates OXA-Induced Atopic Dermatitis Symptoms in Mice. *Immunopharmacol Immunotoxicology* (2020) 42:416–22. doi: 10.1080/08923973.2020.1806869
35. Thangam EB, Jemima EA, Singh H, Baig MS, Khan M, Mathias CB, et al. The Role of Histamine and Histamine Receptors in Mast Cell-Mediated Allergy and Inflammation: The Hunt for New Therapeutic Targets. *Front Immunol* (2018) 9:1873. doi: 10.3389/fimmu.2018.01873
36. Harris NL, Loke P. Recent Advances in Type-2-Cell-Mediated Immunity: Insights From Helminth Infection. *Immunity* (2017) 47:1024–36. doi: 10.1016/j.immuni.2017.11.015
37. Del Prete G, Chiumiento L, Amedei A, Piazza M, D'Elios MM, Codolo G, et al. Immunosuppression of TH2 Responses in Trichinella Spiralis Infection by Helicobacter Pylori Neutrophil-Activating Protein. *J Allergy Clin Immunol* (2008) 122:908–913.e5. doi: 10.1016/j.jaci.2008.08.016
38. Waldman AD, Fritz JM. Lenardo Mj. *A guide to Cancer immunotherapy: T Cell basic Sci to Clin practice. Nat Rev Immunol* (2020) 20:651–68. doi: 10.1038/s41577-020-0306-5
39. Velcheti V, Schalper K. Basic Overview of Current Immunotherapy Approaches in Cancer. *Am Soc Clin Oncol Educ Book* (2016) 35:298–308. doi: 10.1200/EDBK_156572
40. Codolo G, Fassan M, Munari F, Volpe A, Bassi P, Rugge M, et al. HP-NAP Inhibits the Growth of Bladder Cancer in Mice by Activating a Cytotoxic Th1 Response. *Cancer Immunol Immunother* (2012) 61:31–40. doi: 10.1007/s00262-011-1087-2
41. Wang T, Liu X, Ji Z, Men Y, Du M, Ding C, et al. Antitumor and Immunomodulatory Effects of Recombinant Fusion Protein rMBP-NAP Through TLR-2 Dependent Mechanism in Tumor Bearing Mice. *Int Immunopharmacol* (2015) 29:876–83. doi: 10.1016/j.intimp.2015.08.027
42. Mohabati Mobarez A, Soleimani N, Esmaeili S-A, Farhangi B. Nanoparticle-Based Immunotherapy of Breast Cancer Using Recombinant Helicobacter Pylori Proteins. *Eur J Pharmaceutics Biopharmaceutics* (2020) 155:69–76. doi: 10.1016/j.ejpb.2020.08.013
43. Ruenraroengsak P, Cook JM, Florence AT. Nanosystem Drug Targeting: Facing Up to Complex Realities. *J Control Release* (2010) 141:265–76. doi: 10.1016/j.jconrel.2009.10.032
44. Kaufman HL, Kohlhapp FJ, Zloza A. Oncolytic Viruses: A New Class of Immunotherapy Drugs. *Nat Rev Drug Discovery* (2015) 14:642–62. doi: 10.1038/nrd4663
45. Ramachandran M, Yu D, Wanders A, Essand M, Eriksson F. An Infection-Enhanced Oncolytic Adenovirus Secreting H. pylori Neutrophil-activating Protein with Therapeutic Effects on Neuroendocrine Tumors. *Mol Ther* (2013) 21:2008–18. doi: 10.1038/mt.2013.153
46. Ramachandran M, Jin C, Yu D, Eriksson F, Essand M. Vector-Encoded *Helicobacter Pylori* Neutrophil-Activating Protein Promotes Maturation of Dendritic Cells With Th1 Polarization and Improved Migration. *JI* (2014) 193:2287–96. doi: 10.4049/jimmunol.1400339
47. Hou M, Wang X, Lu J, Guo X, Ding C, Liang T, et al. TLR Agonist rHP-NAP as an Adjuvant of Dendritic Cell-Based Vaccine to Enhance Anti-Melanoma Response. *IranJImmunol* (2020) 17:14–25. doi: 10.22034/iji.2020.80291
48. Iankov ID, Allen C, Federspiel MJ, Myers RM, Peng KW, Ingle JN, et al. Expression of Immunomodulatory Neutrophil-Activating Protein of Helicobacter Pylori Enhances the Antitumor Activity of Oncolytic Measles Virus. *Mol Ther* (2012) 20:1139–47. doi: 10.1038/mt.2012.4
49. Ma J, Jin C, Čančer M, Wang H, Ramachandran M, Yu D. Concurrent Expression of HP-NAP Enhances Antitumor Efficacy of Oncolytic Vaccinia Virus But Not for Semliki Forest Virus. *Mol Ther - Oncolytics* (2021) 21:356–66. doi: 10.1016/j.omto.2021.04.016
50. Jin C, Ma J, Ramachandran M, Yu D, Essand M. CAR T Cells Expressing a Bacterial Virulence Factor Trigger Potent Bystander Antitumour Responses in Solid Cancers. *Nat BioMed Eng* (2022). doi: 10.1038/s41551-022-00875-5
51. Codolo G, Facchinello N, Papa N, Bertocco A, Coletta S, Benna C, et al. Macrophage-Mediated Melanoma Reduction After HP-NAP Treatment in a Zebrafish Xenograft Model. *IJMS* (2022) 23:1644. doi: 10.3390/ijms23031644
52. Guo L, Yang H, Tang F, Yin R, Liu H, Gong X, et al. Oral Immunization With a Multivalent Epitope-Based Vaccine, Based on NAP, Urease, HSP60, and HpaA, Provides Therapeutic Effect on H. *pylori Infection Mongolian gerbils. Front Cell Infect Microbiol* (2017) 7:349. doi: 10.3389/fcimb.2017.00349
53. Dundon WG, Nishioka H, Polenghi A, Papinutto E, Zanotti G, Montemurro P, et al. The Neutrophil-Activating Protein of Helicobacter Pylori. *Int J Med Microbiol* (2001) 291:545–50. doi: 10.1078/1438-4221-00165
54. Wang G, Hong Y, Olczak A, Maier SE, Maier RJ. Dual Roles of Helicobacter Pylori NapA in Inducing and Combating Oxidative Stress. *Infect Immun* (2006) 74:6839–46. doi: 10.1128/IAI.00991-06
55. Kottakis F, Papadopoulos G, Pappa EV, Cordopatis P, Pentas S, Choli-Papadopoulou T. Helicobacter Pylori Neutrophil-Activating Protein Activates Neutrophils by its C-Terminal Region Even Without Dodecamer Formation,

Which Is a Prerequisite for DNA Protection - Novel Approaches Against Helicobacter Pylori Inflammation: DNA Protection and Neutrophil Activation by HP-NAP. *FEBS J* (2008) 275:302–17. doi: 10.1111/j.1742-4658.2007.06201.x

Conflict of Interest: The authors declare that the research was conducted in the absence of any commercial or financial relationships that could be construed as a potential conflict of interest.

Publisher's Note: All claims expressed in this article are solely those of the authors and do not necessarily represent those of their affiliated organizations, or those of the publisher, the editors and the reviewers. Any product that may be evaluated in this article, or claim that may be made by its manufacturer, is not guaranteed or endorsed by the publisher.

Copyright © 2022 Codolo, Coletta, D'Elios and de Bernard. This is an open-access article distributed under the terms of the Creative Commons Attribution License (CC BY). The use, distribution or reproduction in other forums is permitted, provided the original author(s) and the copyright owner(s) are credited and that the original publication in this journal is cited, in accordance with accepted academic practice. No use, distribution or reproduction is permitted which does not comply with these terms.

frontiers | Frontiers in Immunology

REVIEW
published: 01 July 2022
doi: 10.3389/fimmu.2022.921272

Phylogenetic Classification and Functional Review of Autotransporters

Kaitlin R. Clarke[1], Lilian Hor[1], Akila Pilapitiya[1], Joen Luirink[2], Jason J. Paxman[1] and Begoña Heras[1*]*

[1] Department of Biochemistry and Chemistry, La Trobe Institute for Molecular Science, La Trobe University, Melbourne, VIC, Australia, [2] Department of Molecular Microbiology, Amsterdam Institute of Molecular and Life Sciences (AIMMS), Vrije Universiteit, Amsterdam, Netherlands

Autotransporters are the core component of a molecular nano-machine that delivers cargo proteins across the outer membrane of Gram-negative bacteria. Part of the type V secretion system, this large family of proteins play a central role in controlling bacterial interactions with their environment by promoting adhesion to surfaces, biofilm formation, host colonization and invasion as well as cytotoxicity and immunomodulation. As such, autotransporters are key facilitators of fitness and pathogenesis and enable co-operation or competition with other bacteria. Recent years have witnessed a dramatic increase in the number of autotransporter sequences reported and a steady rise in functional studies, which further link these proteins to multiple virulence phenotypes. In this review we provide an overview of our current knowledge on classical autotransporter proteins, the archetype of this protein superfamily. We also carry out a phylogenetic analysis of their functional domains and present a new classification system for this exquisitely diverse group of bacterial proteins. The sixteen phylogenetic divisions identified establish sensible relationships between well characterized autotransporters and inform structural and functional predictions of uncharacterized proteins, which may guide future research aimed at addressing multiple unanswered aspects in this group of therapeutically important bacterial factors.

Keywords: type V secretion system, virulence, bacterial pathogenesis, toxins, adhesins, secreted proteins

OPEN ACCESS

Edited by:
Mario M. D'Elios, University of Florence, Italy

Reviewed by:
Arsenio M. Fialho, Universidade de Lisboa, Portugal
Jack Christopher Leo, Nottingham Trent University, United Kingdom

***Correspondence:**
Begoña Heras
b.heras@latrobe.edu.au
Jason J. Paxman
j.paxman@latrobe.edu.au

Specialty section:
This article was submitted to Microbial Immunology, a section of the journal Frontiers in Immunology

Received: *15 April 2022*
Accepted: *06 June 2022*
Published: *01 July 2022*

Citation:
Clarke KR, Hor L, Pilapitiya A, Luirink J, Paxman JJ and Heras B (2022) Phylogenetic Classification and Functional Review of Autotransporters. Front. Immunol. 13:921272. doi: 10.3389/fimmu.2022.921272

1 INTRODUCTION

Many processes essential for bacterial survival require proteins located extracellularly or at the bacterial surface (1, 2). To facilitate their transport across the cell envelope, bacteria have evolved a diverse range of secretion systems. This includes the secretion of virulence factors that promote bacterial pathogenesis *via* functions such as invasion, adherence, dissemination, and immune evasion (3, 4). Accordingly, these secretion systems are fundamental for bacterial pathogenesis. The most ubiquitous are the Sec and Tat systems, which transport a large variety of proteins across the phospholipid biolayer of the inner membrane (IM) (5). In Gram-negative bacteria, the outer membrane (OM), with phospholipid and lipopolysaccharide leaflets, presents a second barrier to secretion. To overcome the multilayered cell envelope, Gram-negative bacteria possess additional

secretion machineries including the chaperone usher system and those classified as type 1 to type 9 secretion systems (T1SS to T9SS) (1, 6). In addition to these established secretion systems, other secretory systems are likely present in Gram-negative bacteria and this list is expected to grow to include further members (7, 8). These systems may directly secrete proteins outside the cell (T1SS and T7SS), traverse multiple membranes and deliver them into the cytoplasm of recipient cells (T3SS, T4SS, T6SS), or transport them across the OM in two steps assisted by the Sec or Tat IM transportation systems (T2SS, T5SS, T8SS, T9SS) (9). Because the periplasm lacks ATP, most of these machineries are large complexes including IM components to access cytoplasmic ATP (10). By comparison, the T5SS does not require ATP and is remarkably simple, typically involving a single dedicated protein (2, 11, 12). This review focuses on the T5SS, alternatively called the autotransporter system reflecting its uniquely simple and energy-efficient transport mechanism.

1.1 The T5SS: Autotransporters (ATs)

The type 5 secretion system (T5SS) is the largest group of secreted proteins in Gram-negative bacteria (13–15). While it encompasses functionally diverse proteins, their journey from cytoplasm to OM is similar (**Figure 1A**) (16, 17). T5SS proteins are termed autotransporters (ATs) because each contains both, secretion machinery (translocator) and functional cargo (passenger) (17). In the cytoplasm, ATs carry an N-terminal signal peptide (SP) for Sec-mediated transport across the IM where the SP is cleaved (23, 24). Periplasmic chaperones keep ATs unfolded until reaching the OM (25–28). The translocator forms a pore in the OM to facilitate the transport of the passenger to the cell surface (29). The passengers are frequently comprised of repetitive secondary structure elements, the sequential folding of which on the bacterial surface may provide a driving force for AT translocation (30–33). The first model of an autotransport mechanism was proposed in 1987 (29) and this has remained an active area of research with several recent reviews on the topic (19, 34, 35). While these basic transport steps are largely consistent with the initial model, later studies revealed the process is not entirely autonomous. Most notably, the barrel assembly machinery (BAM) complex, which catalyzes folding of many OM proteins, is required for insertion of the translocator into the OM and may also facilitate passenger translocation directly (25, 36–39). Significant advances have also been made in our understanding of passenger functions, and these are reviewed in the current work.

While all T5SS members contain both a passenger and translocator, there are variations in their domain arrangement dividing them into subtypes Va to Vf (**Figure 1B**). The Va ATs include, from the N- to C-terminus, a signal peptide, passenger and translocator. The Vc ATs, that include YadA from *Yersinia ssp*. are similar except that their passenger and translocator form trimers, with three ATs forming a single passenger-translocator in the bacterial outer membrane (40, 41). By comparison the Ve ATs represented by intimin from enteropathogenic and enterohaemorrhagic *Escherichia coli* are similar to that of the Va subtype except that their passenger and translocator are switched in position (42). In contrast, the passenger and translocator of Vb ATs such as *Bordetella pertussis* FHA, are expressed as separate proteins. Their translocators include two periplasmic polypeptide-transport-associated (POTRA) domains (20, 43). Similarly, the Vd ATs such as PlpD from *Pseudomonas aeruginosa* and FplA from *Fusobacterium nucleatum* also include a POTRA domain, but only a single POTRA domain exists between the passenger and translocator which are expressed as a single protein (44, 45). Lastly, the type Vf ATs represented by BapA from *Helicobacter pylori* are the most distant subtype, whereby its inclusion into the T5SS is still unclear (18). The likely passenger of the Vf ATs derives from a loop that is part of its putative β-barrel translocator. The Va ATs are the focus of this study, where for clarity, the term 'AT' will hereafter refer to this group.

1.2 Type Va ATs

ATs are highly diverse outer membrane proteins that are distributed widely throughout Gram-negative bacteria, including the phylum Fusobacteria, the order Chlamydiales and all classes of Proteobacteria (14). However, each AT exhibits a similar domain organization consisting of an N-terminal SP followed by a passenger, linker, and C-terminal translocator (**Figure 1A**) (29, 46, 47).

1.2.1 Translocator: Conserved Sequence, Structure, and Function

Translocators exhibit sequence conservation corresponding to the Pfam entry PF03797 (48) and form β-barrel structures that span the OM and facilitate passenger translocation (14, 47, 49–53). The first translocator crystal structure, NalP from *Neisseria meningitidis*, revealed a monomeric, 12-stranded β-barrel forming a 10 Å by 12.5 Å pore (47). Homologous structures have since been determined for distantly related ATs AIDA-I, Hbp/Tsh, EspP, EstA, NalP, and BrkA (50–54). Along with the observation that chaperones are required for proper secretion, the narrow pore size suggests passengers are unfolded during translocation (19, 27, 36, 47). However, folded passengers may be secreted through a larger pore formed by the translocator together with the BamA insertase (19, 25, 55). Despite this, there are limitations on the complexity of folded regions tolerated (31, 56, 57).

1.2.2 The Linker Domain, Cleavage, and Release

The linker connects the passenger and translocator, where after transport of the passenger to the bacterial surface, the linker forms an α-helix spanning the translocator pore (54). In many cases, the passenger is cleaved from the translocator either within the linker or at a nearby site. Cleavage is catalyzed by separate proteases or by the AT itself *via* its own protease subdomain contained within the passenger, or through an autoproteolytic mechanism within the β-barrel (58–64). Many ATs remain at the bacterial surface, either covalently attached to the translocator or through non-covalent interactions after cleavage (65–68). These ATs influence the surface properties of bacteria such as AIDA-I promoting bacterial aggregation through self-adhesion (65). Other ATs are released into the external milieu to act on targets away from the bacterial surface, for example the

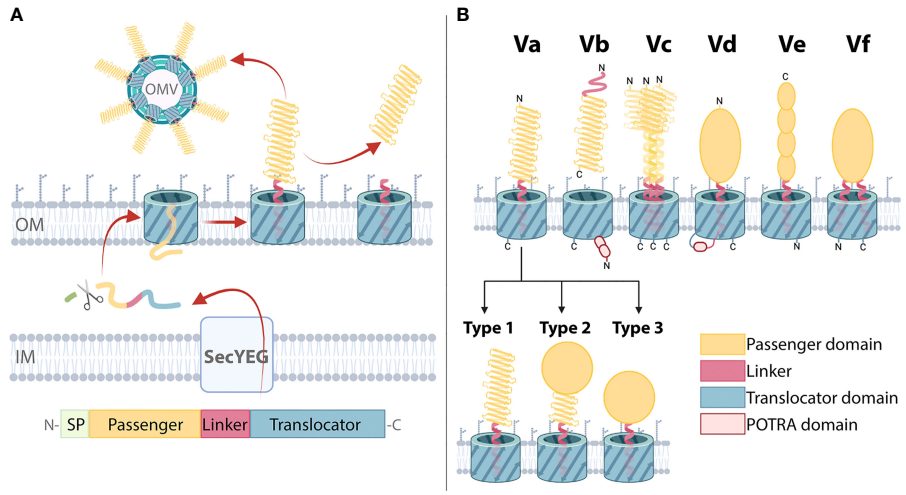

FIGURE 1 | Biogenesis and domain architecture of the type 5 secretion system (T5SS). **(A)** AT secretion mechanism modelled on classical ATs with the following domain organization: The N-terminal signal peptide (SP) is followed by the passenger, linker, and translocator. The SP targets the ATs for inner membrane (IM) secretion via the SecYEG translocon which is subsequently cleaved by a periplasmic peptidase. The translocator inserts into the outer membrane (OM), forming a β-barrel with the α-helical linker spanning its pore. The passenger is translocated to the OM surface where it folds into its tertiary structure. In some ATs, the passenger is cleaved and secreted into the external milieu. Release can also occur through outer membrane vesicles (OMVs). **(B)** T5SS subtypes Va-Vf. Three basic domains (the passenger, linker, and translocator) are present in all T5SS subtypes with variations in topology, domain order, and oligomeric states producing six different subtypes (16–18). These AT classes include: the classical ATs (Va), where the translocator that forms a 12-stranded β-barrel in the outer membrane, and a mostly β-helical passenger, are part of one polypeptide; the two-partner secretion systems (Vb), which are unique because the β-helical passenger is encoded by a separate gene from the translocator, which forms a 16-stranded β-barrel that harbors two polypeptide-transport-associated (POTRA) domains that facilitate the interaction of the passenger and translocators; trimeric ATs (Vc), which require three polypeptides to constitute a full 12-stranded β-barrel translocator to secrete the passengers which includes a coiled-coil stalk and β-helical head regions; patatin-like ATs (Vd), with similar domain architecture to Va but where the translocator is a 16-stranded β-barrel that contains a POTRA domain; inverse ATs (Ve), which comprise an inverted domain organization with an N-terminal signal sequence followed by the translocator, then the linker and a C-terminal passenger; and Hop-family ATs (Vf) possessing an interrupted β-barrel translocator where the passenger is inserted in the loop joining the 1st and second β-strands, and therefore resembling a prolonged loop protruding from the 8-stranded β-barrel. Outer membrane (OM) is indicated. Within classical Va ATs, passengers can adopt various structural configurations: Type 1 passenger structures consist of a β-helix, which may be decorated with functional loops and are connected to the translocator *via* the α-helical linker; in Type 2 structures a catalytic domain is present at the β-helix N-terminus; Type 3 structures lack a β-helix, instead a catalytic domain is directly connected to the translocator *via* the linker. This visual representation of T5SS subtype domain organization is consistent with other reviews (16, 17, 19–22).

passenger of IgA1 protease is proteolytically released and moves away to cleave host immunoglobulins (29). ATs can also be released *via* outer membrane vesicles (OMVs) that pinch off from the OM, for example Vag8 released in OMVs activates and depletes host immune factors away from the bacterial surface (68, 69).

1.2.3 Passenger: Common Structural Themes

Passengers execute the specific function of each AT, and thus show more sequence variation compared to the translocators (49). Despite their sequence and functional diversity, passenger structures are strikingly similar. Most are predicted to include β-solenoid content, with over 90% of published passenger structures comprising a right-handed three-stranded β-helix (70–81). Although the β-helix structure predominates, variations include β-helices with curved or extended sections and the addition of subdomains and loops that protrude out from the β-helix (70–78, 80, 81). The passenger β-helix facilitates multifunctionality as it may directly function as a binding domain specialized to interact with specific host or bacterial factors (70, 71) and can act as a scaffold for catalytic subdomains (72–75, 77, 81). Notably, some ATs lack β-helical structure entirely, for instance, EstA from *P. aeruginosa* is the only published passenger structure comprised of a globular catalytic domain attached directly to the linker (54). Taken together, published AT passenger structures can be divided into three broad types: Type 1, β-helix only; Type 2, globular enzymatic domain supported by a β-helix stalk; Type 3, enzymatic domain without a β-helix (**Figure 1B**). However, given the small proportion of AT structures available the full extent of structural variation within this family remains to be fully uncovered.

1.3 Functional Properties of AT Proteins

ATs are multifunctional proteins that contribute to supporting bacterial survival and growth in different environments. Of significance is that many of these functions are virulence traits that enhance bacterial pathogenic potential (14, 82–87). AT passengers exhibit highly varied sequences, consistent with the variety of functions they perform (88). Some examples of the roles executed by ATs include host adhesion, auto-aggregation, biofilm formation, hemagglutination, invasion, intracellular

motility, toxicity, and immune evasion, along with enzymatic functions such as protease, lipase, and sialidase activities (16). In many cases, these ATs are expressed by bacterial pathogens where these activities promote disease.

Based on functional properties, some classical AT proteins are classified into four broad groups. These are the serine protease ATs of *Enterobacteriaceae* (SPATEs) (87), subtilisin-like ATs (17), self-associating ATs (SAATs) (89), and GDSL-lipases (90).

SPATEs are a family of secreted AT toxins that cleave a variety of host substrates including fodrin, hemoglobin, mucin and Factor V, among others (91). SPATEs are probably the best-studied group of ATs where several reviews have covered current knowledge about SPATE functions (87, 91–94). The passenger of these ATs incorporates a β-helical scaffold with an N-terminal chymotrypsin-like subdomain corresponding to the S6 serine protease family in the MEROPS database (49, 95). Detailed phylogenetic analysis performed on SPATEs have divided these proteins into Class-1 cytotoxins that degrade intracellular substrates and Class-2 immunomodulators that degrade extracellular substrates (87).

Another group of AT proteases are the subtilisin-like ATs, which may be anchored to the bacterial surface or released into the extracellular environment (96–98). These ATs are predicted to contain a β-helical stalk with an N-terminal subtilisin-like subdomain corresponding to the S8A serine protease family in the MEROPS database (17, 95). Overall, subtilisin-like AT functions are poorly understood, but have been associated with surface maturation of other virulence factors to promote virulence functions like cytotoxicity, aggregation, and hemagglutination (17).

Self-associating ATs (SAATs) are a prominent functional subgroup in the AT superfamily (89). These diverse OM-anchored adhesins are predicted to share β-helix architecture in their passenger, as shown for two canonical SAATs, Ag43 and TibA (71, 80). Although ATs in this group can have different functions, all promote bacterial aggregation and biofilm formation through self-association between passengers on neighboring bacteria (71, 89).

Another class of ATs with catalytic activity are the GDSL-lipase ATs. These ATs lack the archetypal β-helix scaffold found in the majority of ATs (54, 90) and are primarily membrane anchored where they hydrolyze ester bonds in host or bacterial lipids (90). Although their natural substrates are unknown, it is assumed they hydrolyze membrane lipids, where they have been shown to affect host cell lysis, lipid and phosphate metabolism, adhesion, and motility (90).

While the identification and definition of these functional groups has provided an important framework for understanding AT proteins, many ATs have been characterized that do not belong to these established functional group.

2 PHYLOGENETIC CLASSIFICATION OF AT PROTEINS

Over the past decades, different groups have devoted considerable effort to the phylogenetic characterization of AT proteins. Henderson, et al. (17) published a landmark phylogenetic analysis of ATs with described phenotypes. This analysis used the sequences of the more conserved AT translocator resulting in the division into 11 subgroups. This enabled comparison and description of the functions within each phylogenetic group and has provided a guiding principle for AT research for the last 18 years. Since this time Celik, et al. (14) using a bioinformatics strategy, presented a large-scale phylogenetic analysis with hundreds of predicted AT passenger sequences, which highlighted the anticipated diversity and widespread distribution of these proteins. Additionally, other phylogenetic analyses have been reported focused on specific AT subgroups (21, 87, 88, 99). With the advent of genome sequencing techniques, the past years have seen a substantial increase in the number of AT sequences reported in public databases along with a steady rise in AT functional characterization, to the point where there is now sufficient data for functional phylogenetic classification studies.

2.1 Sequence Alignment of Characterized ATs

In this work we sought to carry out a comprehensive analysis of functionally characterized ATs. Given the passenger of ATs is the region primarily responsible for facilitating the associated bacterial phenotype through its interactions with the host and/or environment, our analysis concentrated on AT passengers alone to gain insights into the functional relationships between ATs.

Functionally characterized ATs were identified from the literature, particularly focusing on previous reviews (16, 17, 19, 94) and by searching published databases (PubMed and Web of Science) using the keywords "autotransporter" and "T5SS". After eliminating those lacking experimental characterization, 112 ATs were identified from 32 species across 24 genera of Gram-negative bacteria. Proteobacteria accounted for 97 ATs including classes α-proteobacteria (8 ATs), β-proteobacteria (16 ATs), ϵ-proteobacteria (7 ATs), and γ-proteobacteria (66 ATs, including 31 from *E. coli*). Twelve ATs from Chlamydiae and 3 ATs from Fusobacteria are also represented. Full-length amino acid sequences were retrieved from the National Centre of Biotechnology (NCBI) for prediction of the SP, α-helical linker, and translocators using SignalP 4.1 (100), PSIPRED (101), and InterPro (102), respectively. **Table S1** details the accession numbers for all 112 ATs analyzed. Passenger sequences were identified and recorded as the region flanked by the SP and α-helical linker. PSIPRED secondary structure predictions were also used to predict the secondary structure of the passengers. Clustal Omega (103) was used to generate a multiple sequence alignment of the passengers, which demonstrated high diversity within the AT family. Consistent with previous reports (14), we found that passenger lengths were highly varied, ranging from 193 to 3,374 aa with an average of 945 aa (**Supplementary Figure S1**). This diversity of sequence lengths between ATs may have skewed some of the phylogenetic relationships, particularly for very short and very long sequences. A heatmap of pairwise identities (**Supplementary Figure S2**) from the alignment

identified 15 high-identity groups, with low identities between the groups, indicating that each group is highly unique.

2.2 Functional Phylogenetic Classification of ATs

To obtain a phylogenetic classification that reflects AT function, following sequence alignment of the 112 curated passengers, an unrooted consensus tree was generated using PhyML (104) with 100 bootstrap iterations and visualized using the interactive tree of life (iTOL) (105). The consensus PhyML tree found the 112 AT passengers formed 16 homologous groupings (**Figure 2**) with 15 of these corresponding to the high-identity groups seen in the multiple sequence alignment pairwise identity heatmap (**Supplementary Figure S2**). The rationale for grouping ATs together took into consideration strong phylogenetic relationships on the tree (cladding together, short branch lengths, and strong bootstrapping support values) as well as similar reported functions and structural features. More distant similarities between nearby groups that share functional themes are considered together as larger clusters. The 16 phylogenetic groups are organized into broad AT functional themes, and importantly show that previously established functional groups

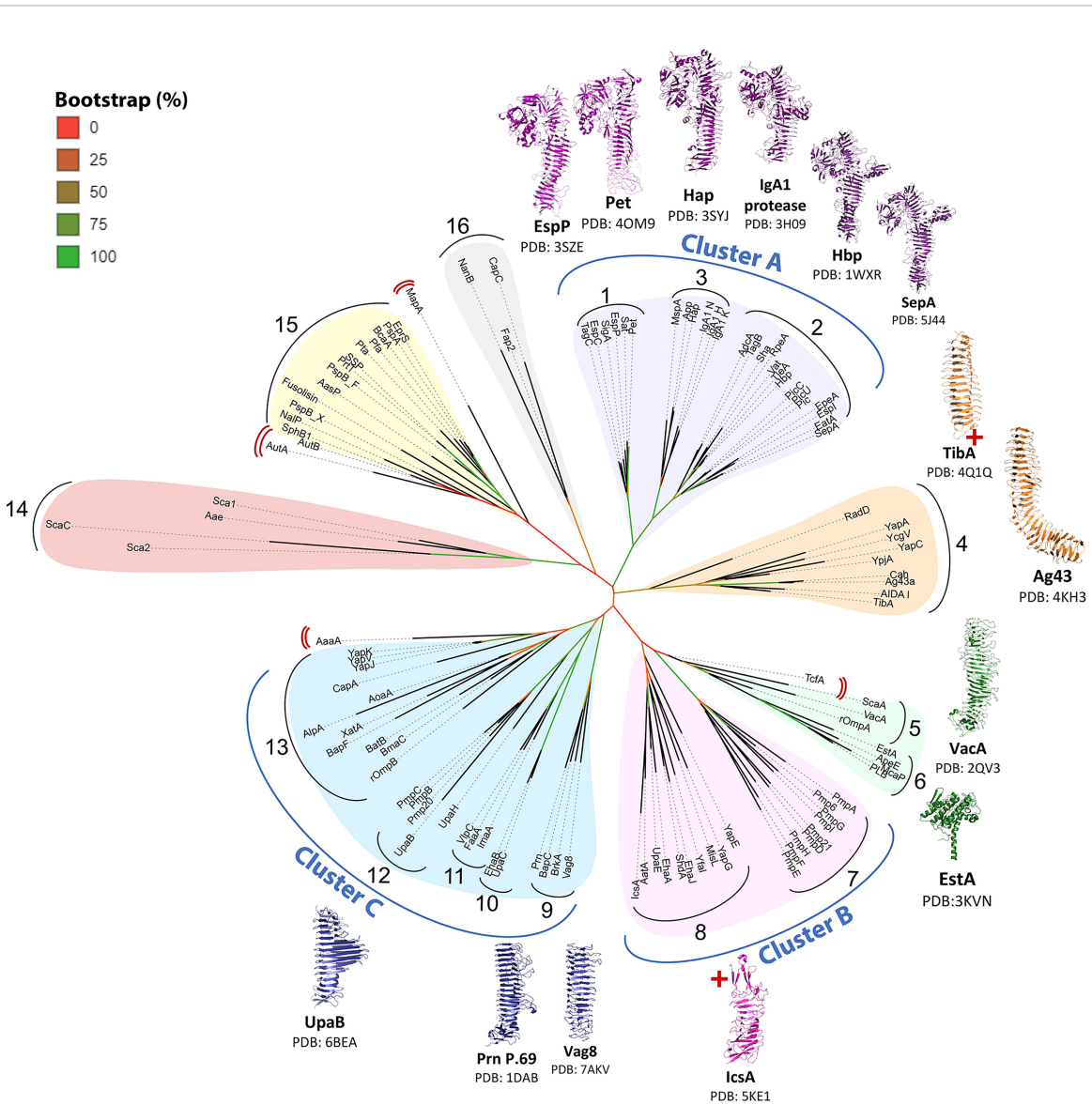

FIGURE 2 | Phylogenetic tree of AT passengers. Unrooted maximum-likelihood phylogenetic tree using Clustal Omega MSA and PhyML with 100 bootstrap iterations and visualized using the interactive tree of life (iTOL). Branch color (red to green) indicates branch support values of 0–90%. Phylogenetic groups are numbered 1—16 with major functional categories indicated by colored shading. 14 published passenger structures are mapped onto the consensus tree, highlighting gaps in structural knowledge. AT structures (54, 70–77, 79–81, 106, 107) were visualized with PyMOL Molecular Graphics System (Schrödinger, LLC) (108). Red cross (+) indicates incomplete passenger structure. Red double brackets indicate ungrouped ATs.

form distinct clades: SPATEs (Group 1-2), SAATs (Group 4), GDSL-lipases (Group 6), and subtilisin-like ATs (Group 15). Furthermore, several of these individual clades form part of larger functionally related clusters (Clusters A-C).

Successful identification of these established groups validates the ability of this phylogenetics strategy to distinguish AT groups that share functional and structural similarities. This in turn supports the interpretation of novel groups identified here as functionally related AT classes. The groupings are discussed below, with overall functional themes assigned to each group. **Table S1** provides a comprehensive list of the ATs and their experimentally defined functions.

2.2.1 Cluster A (Groups 1–3): Chymotrypsin-Like Serine Proteases

Cluster A contains Groups 1–3 totaling 26 ATs belonging to the chymotrypsin-like serine protease family (95). This includes Class-1 SPATEs (Group 1) and Class-2 SPATEs (Group 2) as defined by Ruiz–Perez and Nataro (87). These are now brought together with SPATE-like ATs (SLATs) from outside of the Enterobacteriaceae (Group 3). This is the first time to our knowledge that the close relationship between the SPATEs and SLATs has been shown. This relationship can be interpreted with confidence considering the high branch support values connecting Groups 1–3 (88–95%) and the conservation of well-defined structures among all Cluster A proteases. These are probably the best characterized ATs including six passenger structures (Pet, EspP, IgA1, Hap, SepA, and Hbp) exhibiting similar Type 2 architecture (**Figure 1B**) with a β-helix supporting an N-terminal serine protease subdomain (d1) (72–75, 77, 81). Extended loops arising from the β-helical stalk give rise to further smaller subdomains d2–d4 where d2 resembles a chitin-binding domain, d3 forms an α-helix, and d4 forms a β-hairpin (**Figure 3B**) (87). Recent work revealed that subdomain

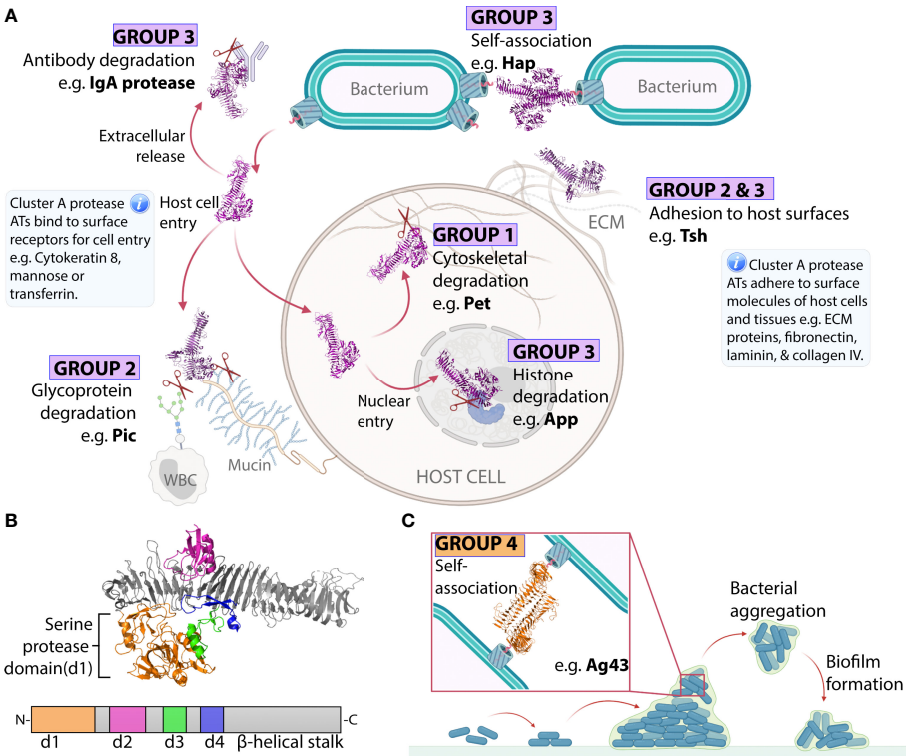

FIGURE 3 | Virulence functions of ATs from Groups 1-4. **(A)** Cluster A chymotrypsin-like protease AT mechanisms. Cluster A protease ATs (Groups 1–3) are released into the extracellular space and move away from the bacterial surface to degrade host proteins. Group 1 proteases then enter host cells and degrade intracellular cytoskeletal components, triggering cytotoxicity. Group 2 proteases remain in the extracellular space where they degrade large host glycoproteins. Group 3 proteases degrade extracellular immunoglobulins or enter host nuclei to degrade nuclear proteins, triggering cell death. Some Cluster A proteases can execute additional functions if they remain at the bacterial surface where they contribute to adhesion to host and bacterial molecules. This includes some members of Group 2 and Group 3, which can promote bacteria-bacteria or bacteria-host adhesion interactions. **(B)** Subdomain organization of a representative Cluster A protease AT. Structure of the Hbp (Group 2) passenger showing the structural elements that are conserved across Cluster A proteases including the β-helical stalk (grey) which acts as a scaffold supporting the globular d1 protease subdomain (orange), the d2 subdomain which resembles a chitin-binding domain (pink), the α-helical loop of the d3 subdomain (green), and the β-hairpin loop of the d4 subdomain (blue). These subdomains are highly conserved, except d2, which is absent from Group 1 proteases. **(C)** Group 4 Self-associating ATs (SAATs) adhesion mechanism. The SAAT Ag43 on adjacent bacterial surfaces self-associate in a molecular Velcro-like manner. This bacteria-bacteria contact contributes to aggregation and biofilm formation. The structures of Hbp (PDB: 1WXR) (75) and Ag43 (PDB: 4KH3) (71) were visualized with PyMOL Molecular Graphics System (Schrödinger, LLC) (108).

d3 mediates host cell internalization of Pet from Group 1 by binding cytokeratin-8 to initiate receptor-mediated endocytosis, an essential step in Pet-mediated virulence (109). Currently, no functions have been associated with d2 and d4 subdomains. The finding that the β-helix extended loop that forms d3 is involved in cell binding interactions is consistent with research on the AT adhesins, where their β-helices directly participate in binding interactions (70, 71, 106).

While their clustering together reflects structural conservation, the division of Cluster A proteases into Groups 1–3 reflects their differences.

Group 1 contains six ATs (SigA, EspP, EspC, Pet, Sat, TagC) and encompasses the Class-1 SPATEs described by Ruiz–Perez and Nataro (87). These ATs enter host cells and degrade a vast range of large intracellular host proteins, including cytoskeletal components, which causes cytotoxicity and tissue damage at the site of infection (**Figure 3A**) (110–115). Most originate from diarrheagenic pathogens of the Enterobacteriaceae family where cytotoxicity contributes to cell exfoliation that is characteristic of diarrheal disease. This includes SigA from *Shigella flexneri* (112) alongside EspP, EspC, and Pet from enterohemorrhagic *E. coli* (EHEC), enteropathogenic *E. coli* (EPEC), and enteroaggregative *E. coli* (EAEC) strains, respectively (115–117). Meanwhile, Sat and TagC are expressed by *E. coli* strains associated with urinary tract infections (Sat is also expressed in other pathogens such as enteroaggregative *E. coli* (EAEC) and *Shigella flexneri*) (114, 118).

Group 2 contains 14 ATs (TagB, AdcA, RpeA, Sha, Vat, Hbp/Tsh, TleA, PicC, Pic, PicU, EspI, EpeA, SepA, EatA) and encompasses the Class-2 SPATEs described by Ruiz–Perez and Nataro (87). These ATs primarily cleave extracellular targets including mucin and immune glycoproteins (**Figure 3A**) (91, 119–123). Most originate from enteric pathogens responsible for intestinal infections where mucin degradation increases penetration into the protective mucous layer covering intestinal tissue. This includes PicC and AdcA from *Citrobacter rodentium* (119, 124), SepA from *Shigella flexneri* (125), alongside ATs from *E. coli* strains including EpeA from EHEC (122), TleA and EatA from enterotoxigenic *E. coli* (ETEC) (120, 126), EspI from Shiga toxin-producing *E. coli* (STEC) (127), Pic from *Shigella flexneri* and EAEC (128), and RpeA from rabbit-specific EPEC (REPEC) (129). Meanwhile, ATs such as Sha, TagB, PicC, Hbp, and Vat derive from extraintestinal pathogenic *E. coli* strains (114, 124, 130, 131), that cause urinary tract infections and wound formation (132). Hbp (haemoglobin protease), first found in a human *E. coli* pathogen (EB1) isolated from a peritoneal would infection, shares 99.8% identity with Tsh (temperature-sensitive hemagglutinin), which originates from the avian pathogenic *E. coli* which causes severe respiratory disease in avian populations (75, 130).

Group 3 contains five ATs and encompasses the SPATE-like ATs (SLATs) (MspA, Hap, App, IgA1 proteases). SLATs have properties found in both Class-1 and Class-2 SPATEs (**Figure 3A**). These ATs are expressed by pathogens that infect mucosal epithelia and may become invasive to cause severe disease. For example, App and MspA derive from *Neisseria meningitidis*, while IgA protease and Hap derive from *Haemophilus influenzae* (133–135). These are respiratory pathogens that can disseminate to cause meningitis (136–138). IgA protease is also expressed by *Neisseria gonorrhoeae*, a urogenital pathogen that can spread to cause septic arthritis and endocarditis (139, 140). SLAT functions are well-suited to such pathogens including immune evasion and adhesion to host and bacterial surfaces, which promotes mucosal colonization, as well as tissue damage, which is often required for dissemination.

Specifically, Hap has been shown to adhere to host surfaces and increase aggregation, while App and MspA bind to and enter host cells, degrade histone proteins in the nucleus, and trigger cell death which likely causes tissue damage (81, 141–145). Meanwhile, the IgA1 proteases degrade IgA, which is the most abundant immunoglobulin and an important line of defense at mucosal surfaces (141, 146, 147).

2.2.2 Group 4: Biofilm Forming AT Adhesins

Perhaps the most striking feature of AT adhesins is their sequence diversity despite overall conservation of Type 1 β-helical passenger architecture (**Figure 1B**) in all published structures (**Figure 2**) (70, 71, 76, 79, 80, 106). This diversity underlies their dispersal into 11 phylogenetic groups. Of these, the best studied adhesins are the SAATs encompassed by Group 4. SAATs Ag43, Cah, TibA, and AIDA-I are expressed by *E. coli* where they self-associate with other SAATs on adjacent bacterial surfaces to promote aggregation and biofilm formation (**Figure 3C**) (65, 89, 148–150). These prototypical SAATs are close together within Group 4, which reflects their functional and structural similarities (71, 80, 150–153). Group 4 includes four additional ATs YapC, YpjA, YcgV, YapA, and RadD, all of which are associated with biofilm formation except YapA for which no biofilm studies have been published (154–158). These proteins may be novel members of the SAAT class given their proximity to prototypical SAATs and functional role in biofilm formation. However, the mechanism used to promote biofilm formation remains unknown and structural studies have not been published for YpjA, YcgV, YapA, or RadD. Using PSIPRED (101) we predict a β-helix structure along the full length of the passenger for each of these proteins, which is consistent with the Type 1 AT structure observed in SAATs.

Most Group 4 ATs derive from pathogenic *E. coli* including diarrheagenic strains. This includes YpjA from EHEC (155), TibA from ETEC (159), and AIDA-I from EPEC (160). Meanwhile, Ag43 is one of the most prevalent AT adhesins across many *E. coli* subtypes (21) and YcgV was first identified in the *E. coli* K-12 laboratory strain (156). Conversely, YapC and YapA are expressed by *Yersinia pestis*, the causative agent of pneumonic, septicemic, and bubonic plague (154, 157). Finally, RadD is the only member of Group 4 originating outside the Proteobacteria phylum, being expressed by *Fusobacterium nucleatum*, which contributes to periodontal disease (158). Notably, the SAAT mechanism has only been characterized for ATs from *E. coli* (71, 161, 162). Future studies should determine if YapC, YapA, and RadD use an Ag43-like dimerization mechanism to expand our understanding of ATs adhesins in important pathogens other than *E. coli* (70, 76, 106).

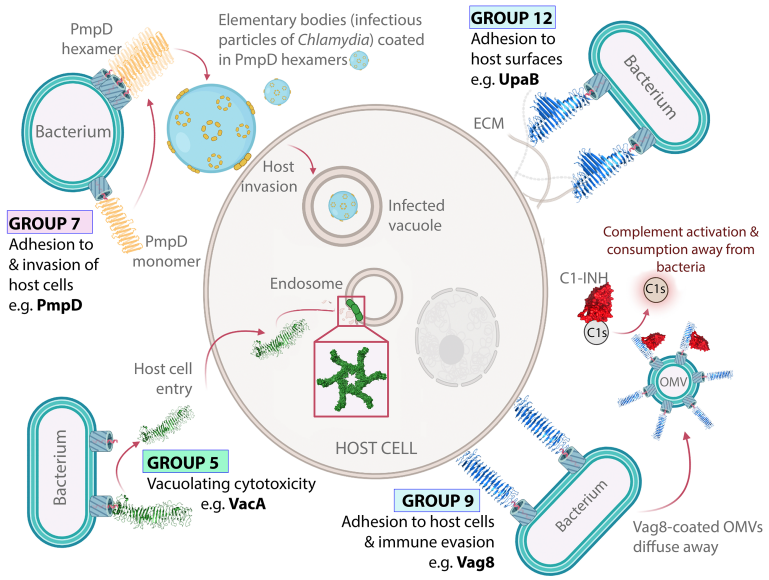

FIGURE 4 | Virulence functions of ATs from Groups 5–12. VacA forms oligomeric pores in intracellular host membranes. VacA (Group 5) forms oligomeric pores in host intracellular membranes including endosomes through horizontal interactions in the lipid bilayer. PmpD is an oligomeric host adhesin. PmpD (Group 7) forms oligomeric rings within the bacterial OM and facilitates host cell invasion. Oligomeric ring structures based on electron microscopy images published by Swanson, et al. (168). Vag8 displays dual immunomodulation and adhesion activities. Vag8 (Group 9) binds to and inhibits the host immune regulator C1-inhibitor (C1-INH), which perturbs the host immune response. Vag8 also promotes adhesion to host cells through an unknown binding interaction. UpaB allows uropathogenic *E. coli* to bind directly to the urogenital epithelia. UpaB (Group 12) binds to ECM proteins on the surface of epithelial cells, which allows bacteria to bind directly to host surfaces within the urogenital tract, thus promoting disease (70). The structures of VacA (PDB: 6NYF) (107), Vag8 (PDB: 7AKV) (106), and UpaB (PDB: 7AKV) (70) were visualized with PyMOL Molecular Graphics System (Schrödinger, LLC) (108).

Ag43 is possibly one of the best studied AT in Group 4 and the AT family more broadly. A high-resolution structure of the Ag43a passenger from uropathogenic *E. coli* revealed an L-shaped β-helix forming head-to-tail homodimers through 'Velcro-like' non-covalent interactions along the β-helix (71). Ag43 homologues from other *E. coli* pathogens are now known to follow a similar mechanism of interaction to that of Ag43a (161, 162). It is expected that similar modes of action exist for the other ATs in this group such as TibA and AIDA-1 (89). Apart from self-interactions, some of the ATs in this group can also promote binding to host surfaces (152, 153, 159). How the self-interaction binding is coordinated with binding to host surfaces is unknown. Nevertheless, the Ag43a self-interaction mechanism was one of the first clear indications that the β-helix can directly participate in AT function, and since this time AT β-helices from other groups have been shown to participate in diverse binding interactions (70, 106).

2.2.3 Group 5 VacA and Homologs

The best characterized protein in Group 5 is VacA, owing to its important role as a pore-forming toxin during *Helicobacter pylori* gastric infection (163–165). The VacA mechanism of action has been reviewed extensively elsewhere (166). Briefly, after being released from the OM, VacA enters host cells to form oligomeric pores in intracellular host membranes, thereby causing vacuolating cytotoxicity (166). A crystal structure of a VacA fragment (residues 388–844), revealed a β-helical passenger structure (78). This was validated by a cryo-EM structure of full-length VacA, which showed that the remainder of the passenger continued into a right-handed β-helix. Importantly, cryo-EM showed that the VacA membrane pore is formed by homo-hexameric rings through interactions between the N-terminal region of each β-helix, with this region also responsible for making contact with the host membrane (107, 167) (**Figure 4**). Other Group 5 ATs include, ScaA from *Orientia tsutsugamushi*, which causes scrub typhus, and rOmpA from *Rickettsia rickettsii*, which causes rocky mountain spotted fever (169, 170). Although less is known about these proteins, both mediate adhesion to host epithelial cells (169–171) and PSIPRED (101) predictions indicate β-helix structure along both passengers, suggesting structural similarity to the β-helical VacA.

2.2.4 Group 6 GDSL-Lipases

Group 6 encompasses the GDSL-lipases EstA, ApeE, PLB, and McaP, all of which exhibit esterase activity catalyzing the hydrolysis of generic lipid substrates (172–175). Although their biological substrates remain unknown, Group 6 ATs may have a broad role in damaging the phospholipids of host cell membranes (90). Given their small size (<300 aa) and that they largely remain tethered to the outer membrane, the activities of these lipases are likely restricted to the immediate bacterial surface (172–176). The lipolytic activity of EstA has been associated with lipid biosynthesis, bacterial motility, and biofilm regulation (172). Meanwhile, McaP in addition to

lipolytic activity also promotes bacterial adhesion to host cells (175, 176). The EstA crystal structure revealed the first non-β-helical AT passenger, whereby the protein is predominantly α-helical due to the GDSL-lipase domain which is directly connected to the α-helical AT linker domain (54). Among published structures, EstA is the only example of Type 3 passenger architecture comprising a catalytic domain without a β-helical stalk (**Figure 1B**). InterPro (102) predicted the lipase domain occupies the entire length of the passenger for ApeE, PLB, and McaP while PSIPRED (101) did not predict β-solenoid structure in this region, suggesting a non-β-helix structure similar to that of EstA. Although this is the only structural evidence of classical ATs lacking a β-helix, this is not uncommon in the wider T5SS. However, outside of the Va group, α-helical ATs tend to form much larger overall structures (17). All Group 6 ATs derive from γ-proteobacteria including EstA from *Pseudomonas aeruginosa*, an opportunistic pathogen associated with nosocomial infections (172), ApeE from *Salmonella enterica* Typhimurium, which causes the diarrheal disease salmonellosis (173), PLB from *Moraxella bovis*, which causes infectious bovine conjunctivitis (174), and McaP from *Moraxella catarrhalis*, which causes otitis media and upper respiratory tract infections (175, 176).

Notably, the clades for Groups 5 and 6 are close together, linked with strong branch supports in the phylogenetic tree (**Figure 2**) and can share up to 20% local amino acid identity. However, they are not known to share structural or functional similarities. The proximity of these distinct groups is therefore striking, and their sequence similarities are not confined to local regions or motifs, but rather spread throughout the sequences, possibly inferring a distant evolutionary relationship (data not shown).

Not shown within the tree but included within this group is the GDSL-lipase BatA from *Burkholderia* (177). BatA with only up to 28% sequence identity to members of this group, positions at its margins. Notably, BatA also shares significant sequence identity to the Group 13 adhesins.

2.2.5 Cluster B (Groups 7–8): Adhesins

Cluster B encompasses Groups 7 and 8 containing ATs that function as adhesins. Host binding is common to all Cluster B ATs while many Group 8 ATs also contribute to bacterial aggregation and/or biofilm formation (155, 156, 178–195). Furthermore, PSIPRED (101) predicted β-helix structure for all Cluster B passengers, which is consistent with the β-helical structure observed in the partial structure of IcsA (79).

Group 7 contains nine ATs designated 'polymorphic membrane proteins' (Pmps) including Pmp6 and Pmp21 from *Chlamydia pneumoniae* along with PmpA, PmpD, PmpE, PmpF, PmpG, PmpH, and PmpI from *Chlamydia trachomatis*. These are typically OM-anchored ATs that promote host cell adhesion and invasion, consistent with the intracellular lifestyle of the *Chlamydia* spp. from which they are derived (178, 179, 181, 196). Beyond this broad function, most Pmps are poorly characterized with no published structures. However, PmpD and Pmp21 have been observed to form higher-order oligomers (168, 197, 198). For PmpD, these oligomers appear as flower-like rings in the bacterial OM (168) (**Figure 4**). Notably, VacA, which is placed nearby in Group 5, is also known to form flower-like oligomers within lipid bilayers (199). This oligomerization may be important in the Pmp binding mechanism, however, the functional significance of PmpD and Pmp21 oligomerization has not been well established. Pmp21 is the only Group 7 AT where the binding partner required for host cell entry is known as it has been shown to promote invasion of host cells by binding to epidermal growth factor receptor (EGFR) (180).

Group 8 consists of ten proteins, YapE, MisL, YapG, Yfal, ShdA, EhaJ, UpaE, EhaA, IcsA and AatA, most of which derive from Enterobacteriaceae that cause diarrheal disease. This includes EhaA and EhaJ from diarrheagenic *E. coli* (155, 194), ShdA and MisL from *Salmonella enterica* Typhimurium (184, 193), and IcsA from *Shigella flexneri* (200). Others including AatA, YfaL, and UpaE derive from extraintestinal *E. coli* (156, 183, 195). Group 8 ATs that are found outside the Enterobacteriaceae family, include YapE from *Yersinia pestis* and YapG from *Yersinia pseudotuberculosis*, the latter causing Far East scarlet-like fever (157, 188).

Group 8 proteins are outer membrane anchored and primarily act as adhesins, with many having dual binding abilities to both host and bacterial targets. Specifically, most, including YapE, MisL, ShdA, EhaJ, UpaE, EhaA, IcsA and AatA mediate host adhesion (155, 183, 184, 186–189, 191–195, 201). For ShdA, MisL, EhaJ, and UpaE, this involves binding to extracellular matrix (ECM) proteins (184, 186, 187, 193–195). Whether ECM binding is a common host binding mechanism across Group 8 remains unknown as binding partners on host epithelial surfaces have not been published for YapE, EhaA, IcsA, and AatA. However, a host intracellular target of IcsA is known, Neural Wiskott–Aldrich syndrome protein (N-WASP), which contributes to the regulation of actin polymerisation as part of the cell cytoskeleton (202). IcsA activates N-WASP to promote intracellular actin-based spread of *S. flexneri* through the colonic epithelial layer. Regarding bacterial aggregation and/or biofilm formation, all but ShdA are associated with this phenotype (155, 156, 182, 188, 190, 192, 194, 195). However, the mechanism by which these ATs promote bacterial aggregation/biofilm formation has not been determined. IcsA promotes both biofilm formation and forms homodimers, which has raised the possibility of self-association similar to that of Ag43a (190, 203). However, a link between IcsA dimerisation and biofilm formation has not been established and dimerisation has not been demonstrated for other group members. Furthermore, the only passenger structure for Group 8 is a small IcsA fragment (residues 419–758) in the monomeric form, providing no insight into self-association (79).

2.2.6 Cluster C (Groups 9–13): Adhesins

Cluster C (Groups 9–13) contain a separate cluster of adhesin ATs that are primarily anchored to the outer membrane where their predominant function is adhesion to host cells and/or surfaces. Currently, Groups 10, 11, and 13 lack published structures.

Group 9 contains four ATs (Vag8, BrkA, Prn, and BapC), all of which derive from *Bordetella* spp. and exhibit high conservation in sequence, structure, and function. The

reported crystal structure of Prn (76) and the cryo-EM structure of Vag8 (106) both reveal Type 1 AT β-helices. Meanwhile, PSIPRED (101) predicts β-helical passengers for BrkA and BapC, which is also consistent with Type 1 AT β-helices.

Group 9 ATs exhibit dual host adhesion and immune evasion activities (69, 204–206). For Prn, host binding involves its RGD integrin-binding motif (205). BrkA, BapC, and Vag8 also contain RGD motifs, suggesting a possible common host binding mechanism (206–208). To date, the host factors recognized by Group 9 ATs to promote cell adhesion are unknown. Furthermore, while evasion of the innate immune response is also common among Group 9 ATs, each is unique in its approach. Prn affords protection from the inflammatory response and neutrophil-mediated clearance (209, 210). Meanwhile, BapC, Vag8, and BrkA promote serum resistance by reducing complement-mediated killing (68, 208, 211, 212). The Vag8 immune evasion mechanism is the best understood. Vag8 enhances serum resistance by inhibiting the serpin C1-inhibitor (C1-INH) (106, 212), which regulates the complement system (68, 212). Structural studies have shown that Vag8 binds C1-INH using extended loops lining one face of its β-helix (106), thus providing further evidence that β-helix structures can directly participate in AT functions.

Although Group 9 ATs are present at the outer membrane, growing evidence suggests *Bordetella* may deploy ATs (i.e., Prn, BrkA, and Vag8) in OMVs, disseminating AT function away from the bacterial surface (68, 213, 214). This finding has been crucial for understanding Vag8 function. Hovingh, et al. (68) proposed that OMVs coated with Vag8 block C1-INH and enable unregulated complement activation away from the bacterial surface, thus protecting bacteria by depleting complement factors before they can be deposited on the bacterial surface (**Figure 4**).

Group 10 contains two ATs derived from pathogenic *E. coli*, UpaC and EhaB, both of which promote biofilm formation (215, 216). In addition, EhaB also mediates host adhesion by binding to ECM proteins (155). Group 11 contains three ATs (FaaA, VlpC, ImaA) that increase murine gastric colonization by *H. pylori* (217). Their placement in Cluster C suggests their contribution to colonization may involve host adhesion, aggregation, or biofilm formation. Unfortunately, to date, little is known about the mechanism of action of Group 10 and 11 ATs.

Group 12 comprises five ATs that promote host adhesion, UpaB, UpaH, PmpB, PmpC and Pmp20 (178, 179, 215, 218, 219). For UpaB and UpaH, both of which derive from uropathogenic *E. coli*, this involves binding to host ECM proteins (215, 218, 219). Meanwhile, the less-defined members PmpB, PmpC, and Pmp20 promote adhesion and entry of Chlamydia into host cells (178, 179). However, ECM binding or biofilm formation studies have not been conducted for the Pmps. The best-studied member of Group 12 is UpaB, which promotes bladder colonization through direct adhesion to urogenital epithelia (215). The crystal structure of the UpaB passenger is consistent with a Type 1 AT β-helix (70). However, its structure reveals unique features, in particular long loops and β-strand extensions projecting out from the β-helix, which form a long hydrophilic groove (70). UpaB was found to bind polysaccharides at this site, and in silico modelling and the resemblance of this groove to the active site of glycosaminoglycan (GAG) lyases, suggests that UpaB binds GAGs lining the human uroepithelium using this binding groove (70). In addition, on the opposite side of UpaB's β-helix is a second binding site which was shown to bind human fibronectin. Altogether, this demonstrates that residues within the UpaB β-helix contribute to two host binding sites that promote urinary tract colonization. UpaB is therefore an excellent example of an AT β-helix exhibiting multiple direct contributions to the virulence phenotype.

Group 13 contains 11 ATs (CapA, YapJ, YapK, YapV, rOmpB, BatB, BmaC, XatA, BapF, AoaA, AlpA), most of which are anchored to the bacterial surface and function as adhesins. Notably, this is the largest adhesin group in the present study and the most diverse in sequence identity (ranging from 0–81%), passenger length (ranging from 280–3333 aa), and taxonomically with ATs deriving from ten Genera: *Yersinia*, *Campylobacter*, *Pseudomonas*, *Brucella*, *Bordetella*, *Rickettsia*, *Helicobacter*, *Azorhizobium*, *Burkholderia*, and *Xylella* (83, 177, 220–227). This covers a wide range of bacteria, from *H. pylori*, among the most widespread and oldest human pathogens and a major cause of stomach cancer worldwide (227), to *Xylella fastidiosa*, a genus of plant pathogens that is rapidly spreading across the globe and destroying important agricultural crops with huge economic impacts (225). This diversity is reflected by the bootstrapping values with Group 13 showing the lowest within-group bootstrapping among the Cluster C adhesins (**Figure 2**).

Consistent with the rest of Cluster C, PSIPRED (101) predictions indicate β-helical passenger structure for the majority of Group 13 ATs. However, notable exceptions include AlpA which has been predicted to be α-helical. Another unusual feature only shared by AlpA and CapA in this group includes the lipidation at the N-terminus of their mature passengers (220, 227). Lipidation is thought to allow the passengers to remain associated with the bacterial surface (98), a characteristic which would be favorable for an adhesin.

Overall, the reported functions for Group 13 ATs broadly resemble those of other Cluster C adhesins. Specifically, BapF and XatA promote bacterial aggregation and/or biofilm formation (225, 226). Meanwhile, YapJ, YapK, YapV, CapA, BmaC, rOmpA, and AlpA promote host adhesion, including ECM binding for the Yaps and BmaC (220–222, 224, 226–228). Additionally, BatB binds immunoglobulins to perturb the human immune response (223), while AoaA promotes the symbiotic relationship between legume root nodules and rhizobia by dampening plant defenses (83). While these immunomodulatory activities are somewhat reminiscent of the dual action adhesins and immunomodulators of Group 10, the adhesive properties of BatB and AoaA have not been reported.

Collectively, although Group 13 ATs display related functional properties, these proteins are very diverse and their phylogenetic relationships with well characterized ATs are uncertain, which warrants further studies on this AT grouping.

2.2.7 Group 14: α-Helical Adhesins

Our phylogenetic analysis identified a separate clade containing four surface-bound ATs that contribute to host adhesion

including Aae from *Acintobacillus actinomycetemcomitans* (96) alongside Sca1, Sca2, and ScaC from Rickettsiaceae (229–231). Other functions associated with Group 14 include biofilm formation for Aae and intracellular invasion and motility for Sca2 (232, 233). Mechanistically, ATs in this group are poorly characterized and no structures are currently available in the PDB. Interestingly, PSIPRED (101) analysis predicts α-helical passenger structures for all Group 14 ATs, distinguishing this group as a type Va AT subfamily composed only of α-helical adhesins.

2.2.8 Group 15: Subtilisin-Like Serine Proteases

Group 15 contains 13 subtilisin-like protease ATs with remarkably diverse taxonomic backgrounds primarily deriving from β- and γ-proteobacteria. This includes PspB_F, Pfa, BcaA, EprS, and PspA from *Pseudomonas* spp. (234–238), SSP and PrtT from *Serratia marcescens* (239, 240), NalP from *N. meningitidis* (59), SphB1 from *B. pertussis* (241), AasP from *Actinobacillus pleuropneumoniae* (242), PspB_X from *X. fastidiosa* (243), along with Pta from *P. mirabilis* (97). These subtilisin-like ATs are also present in bacteria outside the Proteobacteria phylum as evidenced by the presence of Fusolisin from *Fusobacterium nucleatum* (61). In stark contrast to the Cluster A proteases, the subtilisin-like proteases of Group 15 are among the least understood ATs. Based on secondary structure and conserved domains predicted with PSIPRED (101) and InterPro (102), these ATs are thought to comprise of an ~400 aa N-terminal protease domain followed by an ~200 aa β-helix structure, thus following a Type 2 AT organization similar to the Cluster A proteases. Subtilisin-like ATs are known to have dual roles in bacteria, both at the bacterial surface and when released into the host environment. At the bacterial surface, protease activities of Pfa1, EprS, SphB1, AasP, and NalP are used to process other extracytoplasmic proteins including virulence factors (59, 235, 241, 242, 244–246). For example, NalP is responsible for proteolytic maturation of Cluster A protease ATs App, MspA, and IgA1 protease (59, 246). Meanwhile, SphB1 indirectly modifies host adhesion by modifying filamentous hemagglutinin adhesion molecules (241, 245). The capacity of NalP and SphB1 to process these virulence factors, is thought to rely on their abilities to remain temporarily associated with the bacterial surface *via* their lipidation at their N-terminus similar to members of Group 13 (98, 245). After their release from the bacterial surface, subtilisin-like protease activity appears responsible altering host processes. For example, Pta and Pfa promote host cell cytotoxicity (97, 235) and Fusolisin, EprS, PspB_F, Pfa, and NalP contribute to immunomodulation (234, 235, 237, 247, 248). This likely results from degradation of host proteins as Fusolisin degrades IgA whereas NalP cleaves C3 of the complement system (247, 248). Meanwhile, NalP can also enter a range of host cell types where it alters cellular metabolism (249). Notably, cytotoxicity, host cell internalization, and immunomodulation are also features of the Cluster A chymotrypsin-like proteases.

2.2.9 Group 16: Adhesins and a Sialidase

Group 16 contains three bacterial surface associated ATs including CapC from *Campylobacter jejuni* and Fap2 from *Fusobacterium nucleatum*, which promote host adhesion and mediate bacterial aggregation (250, 251). This group also includes NanB from *Pasteurella multocida*, the only AT with defined sialidase activity, thought to benefit in nutrient acquisition (252). PSIPRED (101) analysis predicted β-helix passenger structure for all members, however, this group is poorly characterized in terms of both structure and function. Accordingly, future research may further define the functional classification of the Group 16 ATs. Importantly, unlike all other phylogenetic groups reviewed here, Group 16 did not form a high-identity cluster on the multiple sequence alignment heatmap (**Supplementary Figure S2**). This suggests that Group 16 may be an outgroup of proteins lacking strong homologs in the current pool of functionally investigated ATs.

2.2.10 Ungrouped ATs

Our phylogenetic analysis also uncovered several ATs without strong relationships to any clade, as evidenced by low sequence identity across the AT pool in the sequence alignment heatmap (**Supplementary Figure S2**) and low bootstrap values within the phylogenetic tree (**Figure 2**). For example, the passenger of TcfA, an adhesin from *B. pertussis*, does not share significant identity with any other passenger included in this study. PSIPRED (101) analysis predicted a predominantly unstructured passenger for TcfA, which is consistent with its unusually high proline content (17%). TcfA has been shown to promote *B. pertussis* adhesion to the respiratory tract (69).

The adhesins AutA and AutB share homology with one another but showed no similarity to other AT adhesin groups in either the sequence alignment heatmap (**Supplementary Figure S2**) or the phylogenetic tree (**Figure 2**). These proteins are positioned within the subtilisin-like protease clade (Group 15) but with extremely low branch support values (13%). As such, AutA and AutB remain ungrouped. Functionally, AutA and AutB promote aggregation and biofilm formation in *N. meningitidis* (84, 253, 254). PSIPRED (101) analysis of both AutA and AutB predicts substantial β-helical passenger structure. This is typical of AT adhesins, however their distinction from other adhesins at the sequence level suggests unique structural and functional features.

In addition to the ungrouped adhesins, we found three enzyme classes on the tree with a single AT representative that did not therefore form a large functional group. This includes two enzymes that remain ungrouped: AaaA, a surface-bound arginine-specific aminopeptidase (255), and MapA, an acid phosphatase (256). These enzymes encompass two of the five enzyme classes observed in the phylogenetic analysis with the others being proteases, esterases, and the lone sialidase, NanB (252). NanB is part of Group 16, a probable outgroup of mostly unrelated proteins. Catalytic domain and secondary structure predictions using InterPro (102) and PSIPRED (101), respectively, indicate MapA may adopt a Type 2 AT architecture encompassing an N-terminal catalytic domain with a β-helix C-terminus, while AaaA appears to take on Type 3 AT architecture wherein the catalytic domain spans the full length of the passenger (**Supplementary Figure S3**).

Future structure-function studies on additional proteins in the Type Va AT family may shed some light as to whether these

to date unrelated ATs proteins form part of other functional phylogenetic groups yet to be identified.

3 DISCUSSION

The T5SS, which involves self-mediated transport of autotransporter (AT) proteins outside the cell, is the simplest system for extracellular secretion in Gram-negative bacteria (13–15). Transport relies on a modular architecture wherein each AT contains a signal peptide, translocator module and a functional passenger. Passenger functions vary widely, conferring functional diversity to this large family of bacterial secreted proteins. Comparatively, translocators are highly conserved where each promotes translocation of a passenger that may possess various structural elements and catalytic domains. This combination of variation and uniformity underlies the robustness of this secretion system: by leveraging both the passenger's functional flexibility and the translocator's simple and energetically economical secretion capacity, ATs have evolved into highly specialized molecular tools that promote many aspects of bacterial fitness and pathogenesis.

Steadily increasing numbers of publicly available ATs sequences and publications describing their functional properties prompted us to re-evaluate the classification of this protein family, focusing on their diverse passengers. In this study we show that 112 functionally characterized ATs can be divided into 16 phylogenetic groups. By using the passenger sequences alone, the divisions best reflect common passenger functions, many of which contribute to bacterial virulence. Overall, we found AT enzymes form three main divisions: chymotrypsin-like proteases (Cluster A), subtilisin-like proteases (Group 15), and GDSL-lipase esterases (Group 6). In addition to different enymatic actions, these AT enzymes also exhibited diverse structural compositions. Protease ATs adopt Type 2 passenger structures (**Figure 1B**) wherein an N-terminal protease subdomain responsible for cleaving target proteins sits atop a β-helix for which the functional role is less clear (94). Meanwhile, GDSL-lipases represent Type 3 structure (**Figure 1B**) which includes an esterase domain responsible for hydrolyzing target lipids without any β-helical content (54). Beyond these three main divisions, we observed a further three enzyme classes with a single representative in the pool of characterized ATs, including the aminopeptidase AaaA (ungrouped), the acid phosphatase MapA (ungrouped), and the sialidase NanB (Group 16). Future phylogenetic studies may reveal additional groups that capture these enzyme functions. Most of the remaining ATs are adhesins distributed into 11 groups reflecting a wide range of specialized functions. Based on limited published structural studies, AT adhesins typically exhibit Type 1 structure (**Figure 1B**) with long β-helical passengers (70, 71, 76, 79, 80, 106). Where adhesion mechanisms have been studied at the molecular level, the long β-helix forms an extended binding interface with specific host or bacterial targets, achieving high affinity through the additive effect of many non-covalent interactions (70, 71, 106). In some cases, the β-helix forms a groove along the binding interface to further facilitate specific binding (70, 106). Furthermore, ATs may bind multiple targets using different faces of the β-helix (70). Through these interactions adhesins promote adherence to host surfaces, biofilm formation, or bacterial aggregation. Biofilm formation is most strongly associated with the Group 4 SAATs but is also observed in some Group 8 and Group 10 ATs. Meanwhile, most Cluster B adhesins (Groups 7–8) promote adhesion to host surfaces yet some, including the Group 7 Pmps and IcsA from Group 8, also self-associate to form homo-oligomers. Furthermore, Cluster C adhesins (Groups 9–13) that are not known to oligomerize, include an array of ATs that promote adhesion to host surfaces and less frequently bacterial surfaces. A handful of poorly characterized adhesins are also present in Groups 5 and 16. Meanwhile, Group 14 is predicted to encompass adhesins with α-helical passengers, which has not been described previously for Type Va ATs and requires experimental verification. Importantly, Group 1 and 2 (SPATEs), Group 4 (SAATs), Group 15 (subtilisin-like proteases) and Group 6 (GDSL-lipases) represent previously established classes, which authenticated the phylogeny along with the 11 new groups.

4 CONCLUSION AND FUTURE PERSPECTIVES

Our work through providing a better understanding into the relationships of AT structure and function has revealed insights into the mechanisms and diversity of ATs, that, importantly, sheds light on the lesser-known ATs. We anticipate that this will aid in the characterization of further ATs and has also identified groups of ATs that require further research attention. This is particularly true of the six functional groups that entirely lack published structures and detailed mechanisms of action (Groups 7, 11, 13, 14, 15, and 16). Following the trend observed for other groups, we would expect these six groups to reveal new types of AT structures and modes of action. Although our pool of 112 sequences only represents a fraction of the >1500 ATs that have already been identified (14), our use of only ATs with some functional characterization performed should increase the reliability of our findings. This in itself also highlights the overall lack of knowledge regarding ATs, with most still uncharacterized especially outside of *E. coli*. Unfortunately, this may have also created some bias in our study and also contributed to the findings such as the lack of characterized homologs for functional outliers such as NanB (sialidase), MapA (acid phosphatase) and AaaA (aminopeptidase), which are likely representatives of separate functional groups. Apart from an increased awareness surrounding ATs, our work has also shed further light on bacterial pathogenesis and could be used to develop new technologies including antimicrobials and vaccines. Currently, the classical AT Prn is used in pertussis vaccines including Boostrix®, Infantrix®, and Adacel® (257–259), and the trimeric AT NadA is included in the meningococcal vaccine Bexsero® (260). ATs have also been identified as useful targets for anti-virulence antimicrobials (261). However, efforts to target ATs have been perhaps hampered by the scarcity of molecular-level knowledge. This can be observed in the biotechnological applications of ATs,

which primarily exploit the relatively well-defined translocation mechanism for secretion or surface display of recombinant proteins such as β-lactamase (262) and DNA polymerase (263) amongst others (264–266). Further, the ATs have been used to engineer live bacteria that secrete a peptide therapeutic (267). The detailed protein structure for Hbp also allowed engineering of the passenger for multivalent antigen display on OMV-based vaccines (268–270). Overall, this work has provided an updated perspective of AT classification, that informs on AT functional relationships, which could benefit antimicrobial and vaccine research, but above all hopefully inspire further research into this area of widespread and abundant bacterial proteins.

AUTHOR CONTRIBUTIONS

BH and JP contributed to conception of the study. KC, JP, and BH contributed to the design of the study. KC compiled the database of protein sequences and functions and performed the bioinformatics and phylogenetic analyses. KC wrote the first draft of the manuscript. JP, BH, and LH wrote sections of the manuscript. All authors contributed to manuscript revision, read, and approved the submitted version.

FUNDING

This work was supported by the Australian Research Council (ARC) project grants (DP180102987, DP210100673), a National Health and Medical Research Council (NHMRC) Project Grant (GNT1143638) and an La Trobe Strategic Innovation Fund project.

ACKNOWLEDGMENTS

We acknowledge the support of the Australian Research Council, the National Health and Medical Research Council, The Amsterdam Institute of Molecular and Life Sciences (Vrije Universiteit), and the La Trobe Institute for Molecular Science (La Trobe University).

SUPPLEMENTARY MATERIAL

The Supplementary Material for this article can be found online at: https://www.frontiersin.org/articles/10.3389/fimmu.2022.921272/full#supplementary-material

REFERENCES

1. Green ER, Mecsas J. Bacterial Secretion Systems: An Overview. *Microbiol Spectr* (2016) 4(1):10.1128/microbiolspec.VMBF-0012-2015. doi: 10.1128/microbiolspec.VMBF-0012-2015
2. Costa TR, Felisberto-Rodrigues C, Meir A, Prevost MS, Redzej A, Trokter M, et al. Secretion Systems in Gram-Negative Bacteria: Structural and Mechanistic Insights. *Nat Rev Microbiol* (2015) 13(6):343–59. doi: 10.1038/nrmicro3456
3. Subashchandrabose S, Mobley HLT. Virulence and Fitness Determinants of Uropathogenic. *Escherichia coli. Microbiol Spectr* (2015) 3(4). doi: 10.1128/microbiolspec.UTI-0015-2012
4. Beceiro A, Tomas M, Bou G. Antimicrobial Resistance and Virulence: A Successful or Deleterious Association in the Bacterial World? *Clin Microbiol Rev* (2013) 26(2):185–230. doi: 10.1128/CMR.00059-12
5. Natale P, Bruser T, Driessen AJ. Sec- and Tat-Mediated Protein Secretion Across the Bacterial Cytoplasmic Membrane—Distinct Translocases and Mechanisms. *Biochim Biophys Acta* (2008) 1778(9):1735–56. doi: 10.1016/j.bbamem.2007.07.015
6. Lasica AM, Ksiazek M, Madej M, Potempa J. The Type IX Secretion System (T9SS): Highlights and Recent Insights Into its Structure and Function. *Front Cell Infect Microbiol* (2017) 7:215. doi: 10.3389/fcimb.2017.00215
7. Palmer T, Finney AJ, Saha CK, Atkinson GC. Sargent F. *A holin/peptidoglycan hydrolase-dependent Protein secretion system. Mol Microbiol* (2021) 115(3):345–55. doi: 10.1111/mmi.14599
8. Grossman AS, Mauer TJ, Forest KT. Goodrich-Blair H. *A Widespread Bacterial Secretion System Diverse Substrates. mBio* (2021) 12(4):e0195621. doi: 10.1128/mBio.01956-21
9. Rapisarda C, Tassinari M, Gubellini F, Fronzes R. Using Cryo-EM to Investigate Bacterial Secretion Systems. *Annu Rev Microbiol* (2018) 72:231–54. doi: 10.1146/annurev-micro-090817-062702
10. Thanassi DG, Stathopoulos C, Karkal A, Li H. Protein Secretion in the Absence of ATP: The Autotransporter, Two-Partner Secretion and Chaperone/Usher Pathways of Gram-Negative Bacteria. *Mol Membr Biol* (2005) 22(1-2):63–72. doi: 10.1080/09687860500063290
11. Christie PJ. The Rich Tapestry of Bacterial Protein Translocation Systems. *Protein J* (2019) 38(4):389–408. doi: 10.1007/s10930-019-09862-3
12. Leo JC, Grin I, Linke D. Type V Secretion: Mechanism(s) of Autotransport Through the Bacterial Outer Membrane. *Philos Trans R Soc Lond B Biol Sci* (2012) 367(1592):1088–101. doi: 10.1098/rstb.2011.0208
13. Pallen MJ, Chaudhuri RR, Henderson IR. Genomic Analysis of Secretion Systems. *Curr Opin Microbiol* (2003) 6(5):519–27. doi: 10.1016/j.mib.2003.09.005
14. Celik N, Webb CT, Leyton DL, Holt KE, Heinz E, Gorrell R, et al. A Bioinformatic Strategy for the Detection, Classification and Analysis of Bacterial Autotransporters. *PloS One* (2012) 7(8):e43245. doi: 10.1371/journal.pone.0043245
15. Abby SS, Cury J, Guglielmini J, Neron B, Touchon M, Rocha EP. Identification of Protein Secretion Systems in Bacterial Genomes. *Sci Rep* (2016) 6:23080. doi: 10.1038/srep23080
16. Meuskens I, Saragliadis A, Leo JC, Linke D. Type V Secretion Systems: An Overview of Passenger Domain Functions. *Front Microbiol* (2019) 10:1163. doi: 10.3389/fmicb.2019.01163
17. Henderson IR, Navarro-Garcia F, Desvaux M, Fernandez RC, Ala'Aldeen D. Type V Protein Secretion Pathway: The Autotransporter Story. *Microbiol Mol Biol Rev* (2004) 68(4):692–744. doi: 10.1128/MMBR.68.4.692-744.2004
18. Coppens F, Castaldo G, Debraekeleer A, Subedi S, Moonens K, Lo A, et al. Hop-Family *Helicobacter* Outer Membrane Adhesins Form a Novel Class of Type 5-Like Secretion Proteins With an Interrupted Beta-Barrel Domain. *Mol Microbiol* (2018) 110(1):33–46. doi: 10.1111/mmi.14075
19. Bernstein HD. Type V Secretion in Gram-Negative Bacteria. *EcoSal Plus* (2019) 8(2). doi: 10.1128/ecosalplus.ESP-0031-2018
20. Guerin J, Bigot S, Schneider R, Buchanan SK, Jacob-Dubuisson F. Two-Partner Secretion: Combining Efficiency and Simplicity in the Secretion of Large Proteins for Bacteria-Host and Bacteria-Bacteria Interactions. *Front Cell Infect Microbiol* (2017) 7:148. doi: 10.3389/fcimb.2017.00148
21. Vo JL, Martinez Ortiz GC, Subedi P, Keerthikumar S, Mathivanan S, Paxman JJ, et al. Autotransporter Adhesins in Escherichia Coli Pathogenesis. *Proteomics* (2017) 17(23-24):1600431. doi: 10.1002/pmic.201600431
22. Wells TJ, Henderson IR. Type 1 and 5 Secretion Systems and Associated Toxin. Escherichia Coli: Pathotypes and Principles of Pathogenesis, *2nd Edition*. (2013), 499–532. doi: 10.1016/B978-0-12-397048-0.00016-4
23. Sijbrandi R, Urbanus ML, ten Hagen-Jongman CM, Bernstein HD, Oudega B, Otto BR, et al. Signal Recognition Particle (SRP)-Mediated Targeting and

Sec-Dependent Translocation of an Extracellular *Escherichia Coli* Protein. *J Biol Chem* (2003) 278(7):4654–9. doi: 10.1074/jbc.M211630200
24. Leyton DL, Rossiter AE, Henderson IR. From Self Sufficiency to Dependence: Mechanisms and Factors Important for Autotransporter Biogenesis. *Nat Rev Microbiol* (2012) 10(3):213–25. doi: 10.1038/nrmicro2733
25. Ieva R, Bernstein HD. Interaction of an Autotransporter Passenger Domain With BamA During its Translocation Across the Bacterial Outer Membrane. *Proc Natl Acad Sci U.S.A.* (2009) 106(45):19120–5. doi: 10.1073/pnas.0907912106
26. Ieva R, Tian P, Peterson JH, Bernstein HD. Sequential and Spatially Restricted Interactions of Assembly Factors With an Autotransporter β Domain. *Proc Natl Acad Sci U.S.A.* (2011) 108(31):E383–91. doi: 10.1073/pnas.1103827108
27. Ruiz-Perez F, Henderson IR, Leyton DL, Rossiter AE, Zhang Y, Nataro JP. Roles of Periplasmic Chaperone Proteins in the Biogenesis of Serine Protease Autotransporters of Enterobacteriaceae. *J Bacteriol* (2009) 191(21):6571–83. doi: 10.1128/JB.00754-09
28. Ruiz-Perez F, Henderson IR, Nataro JP. Interaction of FkpA, A Peptidyl-Prolyl Cis/Trans Isomerase With EspP Autotransporter Protein. *Gut Microbes* (2010) 1(5):339–44. doi: 10.4161/gmic.1.5.13436
29. Pohlner J, Halter R, Beyreuther K, Meyer TF. Gene Structure and Extracellular Secretion of *Neisseria Gonorrhoeae* IgA Protease. *Nature* (1987) 325(6103):458–62. doi: 10.1038/325458a0
30. Junker M, Schuster CC, McDonnell AV, Sorg KA, Finn MC, Berger B, et al. Pertactin Beta-Helix Folding Mechanism Suggests Common Themes for the Secretion and Folding of Autotransporter Proteins. *Proc Natl Acad Sci U.S.A.* (2006) 103(13):4918–23. doi: 10.1073/pnas.0507923103
31. Junker M, Besingi RN, Clark PL. Vectorial Transport and Folding of an Autotransporter Virulence Protein During Outer Membrane Secretion. *Mol Microbiol* (2009) 71(5):1323–32. doi: 10.1111/j.1365-2958.2009.06607.x
32. Sikdar R, Bernstein HD. Sequential Translocation of Polypeptides Across the Bacterial Outer Membrane Through the Trimeric Autotransporter Pathway. *mBio* (2019) 10(5):e01973–19. doi: 10.1128/mBio.01973-19
33. Leo JC, Oberhettinger P, Yoshimoto S, Udatha DB, Morth JP, Schutz M, et al. Secretion of the Intimin Passenger Domain Is Driven by Protein Folding. *J Biol Chem* (2016) 291(38):20096–112. doi: 10.1074/jbc.M116.731497
34. van Ulsen P, Zinner KM, Jong WSP, Luirink J. On Display: Autotransporter Secretion and Application. *FEMS Microbiol Lett* (2018) 365(18). doi: 10.1093/femsle/fny165
35. Albenne C, Ieva R. Job Contenders: Roles of the β-Barrel Assembly Machinery and the Translocation and Assembly Module in Autotransporter Secretion. *Mol Microbiol* (2017) 106(4):505–17. doi: 10.1111/mmi.13832
36. Pavlova O, Peterson JH, Ieva R, Bernstein HD. Mechanistic Link Between β Barrel Assembly and the Initiation of Autotransporter Secretion. *Proc Natl Acad Sci U.S.A.* (2013) 110(10):E938–47. doi: 10.1073/pnas.1219076110
37. Sauri A, Soprova Z, Wickstrom D, de Gier JW, van der Schors RC, Smit AB, et al. The Bam (Omp85) Complex is Involved in Secretion of the Autotransporter Haemoglobin Protease. *Microbiol (Reading)* (2009) 155(Pt 12):3982–91. doi: 10.1099/mic.0.034991-0
38. Roman-Hernandez G, Peterson JH, Bernstein HD. Reconstitution of Bacterial Autotransporter Assembly Using Purified Components. *Elife* (2014) 3:e04234. doi: 10.7554/eLife.04234
39. Soprova Z, Sauri A, van Ulsen P, Tame JR, den Blaauwen T, Jong WS, et al. A Conserved Aromatic Residue in the Autochaperone Domain of the Autotransporter Hbp is Critical for Initiation of Outer Membrane Translocation. *J Biol Chem* (2010) 285(49):38224–33. doi: 10.1074/jbc.M110.180505
40. Linke D, Riess T, Autenrieth IB, Lupas A, Kempf VA. Trimeric Autotransporter Adhesins: Variable Structure, Common Function. *Trends Microbiol* (2006) 14(6):264–70. doi: 10.1016/j.tim.2006.04.005
41. Kiessling AR, Malik A, Goldman A. Recent Advances in the Understanding of Trimeric Autotransporter Adhesins. *Med Microbiol Immunol* (2020) 209 (3):233–42. doi: 10.1007/s00430-019-00652-3
42. Leo JC, Oberhettinger P, Schutz M, Linke D. The Inverse Autotransporter Family: Intimin, Invasin and Related Proteins. *Int J Med Microbiol* (2015) 305(2):276–82. doi: 10.1016/j.ijmm.2014.12.011
43. Jacob-Dubuisson F, Locht C, Antoine R. Two-Partner Secretion in Gram-Negative Bacteria: A Thrifty, Specific Pathway for Large Virulence Proteins. *Mol Microbiol* (2001) 40(2):306–13. doi: 10.1046/j.1365-2958.2001.02278.x
44. Casasanta MA, Yoo CC, Smith HB, Duncan AJ, Cochrane K, Varano AC, et al. A Chemical and Biological Toolbox for Type Vd Secretion: Characterization of the Phospholipase A1 Autotransporter FplA From Fusobacterium Nucleatum. *J Biol Chem* (2017) 292(49):20240–54. doi: 10.1074/jbc.M117.819144
45. Salacha R, Kovacic F, Brochier-Armanet C, Wilhelm S, Tommassen J, Filloux A, et al. The Pseudomonas Aeruginosa Patatin-Like Protein PlpD is the Archetype of a Novel Type V Secretion System. *Environ Microbiol* (2010) 12(6):1498–512. doi: 10.1111/j.1462-2920.2010.02174.x
46. Jose J, Jahnig F, Meyer TF. Common Structural Features of IgA1 Protease-Like Outer Membrane Protein Autotransporters. *Mol Microbiol* (1995) 18 (2):378–80. doi: 10.1111/j.1365-2958.1995.mmi_18020378.x
47. Oomen CJ, Van Ulsen P, Van Gelder P, Feijen M, Tommassen J, Gros P. Structure of the Translocator Domain of a Bacterial Autotransporter. *EMBO J* (2004) 23(6):1257–66. doi: 10.1038/sj.emboj.7600148
48. Mistry J, Chuguransky S, Williams L, Qureshi M, Salazar GA, Sonnhammer ELL, et al. Pfam: The Protein Families Database in 2021. *Nucleic Acids Res* (2021) 49(D1):D412–D9. doi: 10.1093/nar/gkaa913
49. Henderson IR, Navarro-Garcia F, Nataro JP. The Great Escape: Structure and Function of the Autotransporter Proteins. *Trends Microbiol* (1998) 6 (9):370–8. doi: 10.1016/S0966-842X(98)01318-3
50. Gawarzewski I, DiMaio F, Winterer E, Tschapek B, Smits SHJ, Jose J, et al. Crystal Structure of the Transport Unit of the Autotransporter Adhesin Involved in Diffuse Adherence From. *Escherichia coli. J Struct Biol* (2014) 187(1):20–9. doi: 10.1016/j.jsb.2014.05.003
51. Tajima N, Kawai F, Park SY, Tame JR. A Novel Intein-Like Autoproteolytic Mechanism in Autotransporter Proteins. *J Mol Biol* (2010) 402(4):645–56. doi: 10.1016/j.jmb.2010.06.068
52. Barnard TJ, Dautin N, Lukacik P, Bernstein HD, Buchanan SK. Autotransporter Structure Reveals Intra-Barrel Cleavage Followed by Conformational Changes. *Nat Struct Mol Biol* (2007) 14(12):1214–20. doi: 10.1038/nsmb1322
53. Zhai Y, Zhang K, Huo Y, Zhu Y, Zhou Q, Lu J, et al. Autotransporter Passenger Domain Secretion Requires a Hydrophobic Cavity at the Extracellular Entrance of the β-Domain Pore. *Biochem J* (2011) 435 (3):577–87. doi: 10.1042/BJ20101548
54. van den Berg B. Crystal Structure of a Full-Length Autotransporter. *J Mol Biol* (2010) 396(3):627–33. doi: 10.1016/j.jmb.2009.12.061
55. Veiga E, de Lorenzo V, Fernandez LA. Structural Tolerance of Bacterial Autotransporters for Folded Passenger Protein Domains. *Mol Microbiol* (2004) 52(4):1069–80. doi: 10.1111/j.1365-2958.2004.04014.x
56. Jong WS, ten Hagen-Jongman CM, den Blaauwen T, Slotboom DJ, Tame JR, Wickstrom D, et al. Limited Tolerance Towards Folded Elements During Secretion of the Autotransporter Hbp. *Mol Microbiol* (2007) 63(5):1524–36. doi: 10.1111/j.1365-2958.2007.05605.x
57. Skillman KM, Barnard TJ, Peterson JH, Ghirlando R, Bernstein HD. Efficient Secretion of a Folded Protein Domain by a Monomeric Bacterial Autotransporter. *Mol Microbiol* (2005) 58(4):945–58. doi: 10.1111/j.1365-2958.2005.04885.x
58. van Ulsen P, Tommassen J. Protein Secretion and Secreted Proteins in Pathogenic. *Neisseriaceae. FEMS Microbiol Rev* (2006) 30(2):292–319. doi: 10.1111/j.1574-6976.2006.00013.x
59. van Ulsen P, van Alphen L, ten Hove J, Fransen F, van der Ley P, Tommassen JA. Neisserial Autotransporter NalP Modulating the Processing of Other Autotransporters. *Mol Microbiol* (2003) 50(3):1017–30. doi: 10.1046/j.1365-2958.2003.03773.x
60. Dautin N, Barnard TJ, Anderson DE, Bernstein HD. Cleavage of a Bacterial Autotransporter by an Evolutionarily Convergent Autocatalytic Mechanism. *EMBO J* (2007) 26(7):1942–52. doi: 10.1038/sj.emboj.7601638
61. Doron L, Coppenhagen-Glazer S, Ibrahim Y, Eini A, Naor R, Rosen G, et al. Identification and Characterization of Fusolisin, the *Fusobacterium Nucleatum* Autotransporter Serine Protease. *PloS One* (2014) 9(10): e111329. doi: 10.1371/journal.pone.0111329
62. Roussel-Jazede V, Arenas J, Langereis JD, Tommassen J, van Ulsen P. Variable Processing of the IgA Protease Autotransporter at the Cell

Surface of Neisseria Meningitidis. *Microbiology* (2014) 160(Pt 11):2421–31. doi: 10.1099/mic.0.082511-0
63. Charbonneau ME, Janvore J, Mourez M. Autoprocessing of the *Escherichia Coli* AIDA-I Autotransporter: A New Mechanism Involving Acidic Residues in the Junction Region. *J Biol Chem* (2009) 284(25):17340–51. doi: 10.1074/jbc.M109.010108
64. Noriea NF, Clark TR, Mead D, Hackstadt T. Proteolytic Cleavage of the Immunodominant Outer Membrane Protein Rompa in *Rickettsia Rickettsii*. *J Bacteriol* (2017) 199(6):e00826–16. doi: 10.1128/JB.00826-16
65. Sherlock O, Schembri MA, Reisner A, Klemm P. Novel Roles for the AIDA Adhesin From Diarrheagenic *Escherichia Coli*: Cell Aggregation and Biofilm Formation. *J Bacteriol* (2004) 186(23):8058–65. doi: 10.1128/JB.186.23.8058-8065.2004
66. Hendrixson DR, St Geme JW3rd. The Haemophilus Influenzae Hap Serine Protease Promotes Adherence and Microcolony Formation, Potentiated by a Soluble Host Protein. *Mol Cell* (1998) 2(6):841–50. doi: 10.1016/s1097-2765(00)80298-1
67. Caffrey P, Owen P. Purification and N-Terminal Sequence of the Alpha Subunit of Antigen 43, a Unique Protein Complex Associated With the Outer Membrane of. *Escherichia coli. J Bacteriol* (1989) 171(7):3634–40. doi: 10.1128/jb.171.7.3634-3640.1989
68. Hovingh ES, van den Broek B, Kuipers B, Pinelli E, Rooijakkers SHM, Jongerius I. Acquisition of C1 Inhibitor by *Bordetella Pertussis* Virulence Associated Gene 8 Results in C2 and C4 Consumption Away From the Bacterial Surface. *PloS Pathog* (2017) 13(7):e1006531. doi: 10.1371/journal.ppat.1006531
69. Gasperini G, Biagini M, Arato V, Gianfaldoni C, Vadi A, Norais N, et al. Outer Membrane Vesicles (OMV)-Based and Proteomics-Driven Antigen Selection Identifies Novel Factors Contributing to *Bordetella Pertussis* Adhesion to Epithelial Cells. *Mol Cell Proteomics* (2018) 17(2):205–15. doi: 10.1074/mcp.RA117.000045
70. Paxman JJ, Lo AW, Sullivan MJ, Panjikar S, Kuiper M, Whitten AE, et al. Unique Structural Features of a Bacterial Autotransporter Adhesin Suggest Mechanisms for Interaction With Host Macromolecules. *Nat Commun* (2019) 10(1):1967. doi: 10.1038/s41467-019-09814-6
71. Heras B, Totsika M, Peters KM, Paxman JJ, Gee CL, Jarrott RJ, et al. The Antigen 43 Structure Reveals a Molecular Velcro-Like Mechanism of Autotransporter-Mediated Bacterial Clumping. *Proc Natl Acad Sci USA* (2014) 111(1):457–62. doi: 10.1073/pnas.1311592111
72. Khan S, Mian HS, Sandercock LE, Chirgadze NY, Pai EF. Crystal Structure of the Passenger Domain of the *Escherichia Coli* Autotransporter EspP. *J Mol Biol* (2011) 413(5):985–1000. doi: 10.1016/j.jmb.2011.09.028
73. Domingo Meza-Aguilar J, Fromme P, Torres-Larios A, Mendoza-Hernandez G, Hernandez-Chinas U, Arreguin-Espinosa de Los Monteros RA, et al. X-Ray Crystal Structure of the Passenger Domain of Plasmid Encoded Toxin(Pet), an Autotransporter Enterotoxin From Enteroaggregative Escherichia Coli (EAEC). *Biochem Biophys Res Commun* (2014) 445(2):439–44. doi: 10.1016/j.bbrc.2014.02.016
74. Maldonado-Contreras A, Birtley JR, Boll E, Zhao Y, Mumy KL, Toscano J, et al. Shigella Depends on SepA to Destabilize the Intestinal Epithelial Integrity *via* Cofilin Activation. *Gut Microbes* (2017) 8(6):544–60. doi: 10.1080/19490976.2017.1339006
75. Otto BR, Sijbrandi R, Luirink J, Oudega B, Heddle JG, Mizutani K, et al. Crystal Structure of Hemoglobin Protease, a Heme Binding Autotransporter Protein From Pathogenic. *Escherichia coli. J Biol Chem* (2005) 280(17):17339–45. doi: 10.1074/jbc.M412885200
76. Emsley P, Charles IG, Fairweather NF, Isaacs NW. Structure of *Bordetella Pertussis* Virulence Factor P.69 Pertactin. *Nature* (1996) 381(6577):90–2. doi: 10.1038/381090a0
77. Johnson TA, Qiu J, Plaut AG, Holyoak T. Active-Site Gating Regulates Substrate Selectivity in a Chymotrypsin-Like Serine Protease the Structure of *Haemophilus Influenzae* Immunoglobulin A1 Protease. *J Mol Biol* (2009) 389(3):559–74. doi: 10.1016/j.jmb.2009.04.041
78. Gangwer KA, Mushrush DJ, Stauff DL, Spiller B, McClain MS, Cover TL, et al. Crystal Structure of the *Helicobacter Pylori* Vacuolating Toxin P55 Domain. *Proc Natl Acad Sci U.S.A.* (2007) 104(41):16293–8. doi: 10.1073/pnas.0707447104
79. Leupold S, Busing P, Mas PJ, Hart DJ, Scrima A. Structural Insights Into the Architecture of the *Shigella Flexneri* Virulence Factor IcsA/VirG and Motifs Involved in Polar Distribution and Secretion. *J Struct Biol* (2017) 198(1):19–27. doi: 10.1016/j.jsb.2017.03.003
80. Lu Q, Yao Q, Xu Y, Li L, Li S, Liu Y, et al. An Iron-Containing Dodecameric Heptosyltransferase Family Modifies Bacterial Autotransporters in Pathogenesis. *Cell Host Microbe* (2014) 16(3):351–63. doi: 10.1016/j.chom.2014.08.008
81. Meng G, Spahich N, Kenjale R, Waksman G, St Geme JW3rd. Crystal Structure of the *Haemophilus Influenzae* Hap Adhesin Reveals an Intercellular Oligomerization Mechanism for Bacterial Aggregation. *EMBO J* (2011) 30(18):3864–74. doi: 10.1038/emboj.2011.279
82. Shimoda Y, Nishigaya Y, Yamaya-Ito H, Inagaki N, Umehara Y, Hirakawa H, et al. The Rhizobial Autotransporter Determines the Symbiotic Nitrogen Fixation Activity of Lotus Japonicus in a Host-Specific Manner. *Proc Natl Acad Sci U.S.A.* (2020) 117(3):1806–15. doi: 10.1073/pnas.1913349117
83. Suzuki T, Aono T, Liu CT, Suzuki S, Iki T, Yokota K, et al. An Outer Membrane Autotransporter, AoaA, of Azorhizobium Caulinodans is Required for Sustaining High N2-Fixing Activity of Stem Nodules. *FEMS Microbiol Lett* (2008) 285(1):16–24. doi: 10.1111/j.1574-6968.2008.01215.x
84. Arenas J, Cano S, Nijland R, van Dongen V, Rutten L, van der Ende A, et al. The Meningococcal Autotransporter AutA Is Implicated in Autoaggregation and Biofilm Formation. *Environ Microbiol* (2015) 17(4):1321–37. doi: 10.1111/1462-2920.12581
85. Beatson SA, Ben Zakour NL, Totsika M, Forde BM, Watts RE, Mabbett AN, et al. Molecular Analysis of Asymptomatic Bacteriuria *Escherichia Coli* Strain VR50 Reveals Adaptation to the Urinary Tract by Gene Acquisition. *Infect Immun* (2015) 83(5):1749–64. doi: 10.1128/IAI.02810-14
86. Sandt CH, Hill CW. Four Different Genes Responsible for Nonimmune Immunoglobulin-Binding Activities Within a Single Strain of *Escherichia Coli*. *Infect Immun* (2000) 68(4):2205–14. doi: 10.1128/IAI.68.4.2205-2214.2000
87. Ruiz-Perez F, Nataro JP. Bacterial Serine Proteases Secreted by the Autotransporter Pathway: Classification, Specificity, and Role in Virulence. *Cell Mol Life Sci* (2014) 71(5):745–70. doi: 10.1007/s00018-013-1355-8
88. Wells TJ, Totsika M, Schembri MA. Autotransporters of Escherichia Coli: A Sequence-Based Characterization. *Microbiol (Reading)* (2010) 156(Pt 8):2459–69. doi: 10.1099/mic.0.039024-0
89. Klemm P, Vejborg RM, Sherlock O. Self-Associating Autotransporters, SAATs: Functional and Structural Similarities. *Int J Med Microbiol* (2006) 296(4-5):187–95. doi: 10.1016/j.ijmm.2005.10.002
90. Wilhelm S, Rosenau F, Kolmar H, Jaeger KE. Autotransporters With GDSL Passenger Domains: Molecular Physiology and Biotechnological Applications. *Chembiochem* (2011) 12(10):1476–85. doi: 10.1002/cbic.201100013
91. Dutta PR, Cappello R, Navarro-Garcia F, Nataro JP. Functional Comparison of Serine Protease Autotransporters of Enterobacteriaceae. *Infect Immun* (2002) 70(12):7105–13. doi: 10.1128/iai.70.12.7105-7113.2002
92. Pokharel P, Habouria H, Bessaiah H, Dozois CM. Serine Protease Autotransporters of the Enterobacteriaceae (SPATEs): Out and About and Chopping It Up. *Microorganisms* (2019) 7(12):594. doi: 10.3390/microorganisms7120594
93. Dautin N. Serine Protease Autotransporters of *Enterobacteriaceae* (SPATEs): Biogenesis and Function. *Toxins (Basel)* (2010) 2(6):1179–206. doi: 10.3390/toxins2061179
94. Yen YT, Kostakioti M, Henderson IR, Stathopoulos C. Common Themes and Variations in Serine Protease Autotransporters. *Trends Microbiol* (2008) 16(8):370–9. doi: 10.1016/j.tim.2008.05.003
95. Rawlings ND, Waller M, Barrett AJ, Bateman A. MEROPS: The Database of Proteolytic Enzymes, Their Substrates and Inhibitors. *Nucleic Acids Res* (2014) 42(Database issue):D503–9. doi: 10.1093/nar/gkt953
96. Rose JE, Meyer DH, Fives-Taylor PM. Aae, an Autotransporter Involved in Adhesion of *Actinobacillus Actinomycetemcomitans* to Epithelial Cells. *Infect Immun* (2003) 71(5):2384–93. doi: 10.1128/iai.71.5.2384-2393.2003
97. Alamuri P, Mobley HL. A Novel Autotransporter of Uropathogenic *Proteus Mirabilis* is Both a Cytotoxin and an Agglutinin. *Mol Microbiol* (2008) 68(4):997–1017. doi: 10.1111/j.1365-2958.2008.06199.x
98. Roussel-Jazede V, Grijpstra J, van Dam V, Tommassen J, van Ulsen P. Lipidation of the Autotransporter NalP of Neisseria Meningitidis is Required

for its Function in the Release of Cell-Surface-Exposed Proteins. *Microbiol (Reading)* (2013) 159(Pt 2):286–95. doi: 10.1099/mic.0.063982-0
99. Zude I, Leimbach A, Dobrindt U. Prevalence of Autotransporters in Escherichia Coli: What is the Impact of Phylogeny and Pathotype? *Int J Med Microbiol* (2014) 304(3-4):243–56. doi: 10.1016/j.ijmm.2013.10.006
100. Petersen TN, Brunak S, von Heijne G, Nielsen H. SignalP 4.0: Discriminating Signal Peptides From Transmembrane Regions. *Nat Methods* (2011) 8 (10):785–6. doi: 10.1038/nmeth.1701
101. Jones DT. Protein Secondary Structure Prediction Based on Position-Specific Scoring Matrices. *J Mol Biol* (1999) 292(2):195–202. doi: 10.1006/jmbi.1999.3091
102. Mitchell AL, Attwood TK, Babbitt PC, Blum M, Bork P, Bridge A, et al. InterPro in 2019: Improving Coverage, Classification and Access to Protein Sequence Annotations. *Nucleic Acids Res* (2019) 47(D1):D351–D60. doi: 10.1093/nar/gky1100
103. Sievers F, Wilm A, Dineen D, Gibson TJ, Karplus K, Li W, et al. Fast, Scalable Generation of High-Quality Protein Multiple Sequence Alignments Using Clustal Omega. *Mol Syst Biol* (2011) 7:539. doi: 10.1038/msb.2011.75
104. Guindon S, Dufayard JF, Lefort V, Anisimova M, Hordijk W, Gascuel O. New Algorithms and Methods to Estimate Maximum-Likelihood Phylogenies: Assessing the Performance of PhyML 3.0. *Syst Biol* (2010) 59 (3):307–21. doi: 10.1093/sysbio/syq010
105. Letunic I, Bork P. Interactive Tree Of Life (iTOL) V4: Recent Updates and New Developments. *Nucleic Acids Res* (2019) 47(W1):W256–W9. doi: 10.1093/nar/gkz239
106. Dhillon A, Deme JC, Furlong E, Roem D, Jongerius I, Johnson S, et al. Molecular Basis for Bordetella Pertussis Interference With Complement, Coagulation, Fibrinolytic, and Contact Activation Systems: The Cryo-EM Structure of the Vag8-C1 Inhibitor Complex. *mBio* (2021) 12(2): e02823–20. doi: 10.1128/mBio.02823-20
107. Zhang K, Zhang H, Li S, Pintilie GD, Mou TC, Gao Y, et al. Cryo-EM Structures of Helicobacter Pylori Vacuolating Cytotoxin A Oligomeric Assemblies at Near-Atomic Resolution. *Proc Natl Acad Sci U.S.A.* (2019) 116(14):6800–5. doi: 10.1073/pnas.1821959116
108. Schrodinger LLC, DeLano W. *PyMOL*. Available at: http://www.pymol.org/pymol. (2020).
109. Chavez-Duenas L, Serapio-Palacios A, Nava-Acosta R, Navarro-Garcia F. Subdomain 2 of the Autotransporter Pet is the Ligand Site for Recognizing the Pet Receptor on the Epithelial Cell Surface. *Infect Immun* (2016) 84 (7):2012–21. doi: 10.1128/IAI.01528-15
110. Cappello RE, Estrada-Gutierrez G, Irles C, Giono-Cerezo S, Bloch RJ, Nataro JP. Effects of the Plasmid-Encoded Toxin of Enteroaggregative Escherichia Coli on Focal Adhesion Complexes. *FEMS Immunol Med Microbiol* (2011) 61(3):301–14. doi: 10.1111/j.1574-695X.2010.00776.x
111. Navarro-Garcia F, Serapio-Palacios A, Vidal JE, Salazar MI, Tapia-Pastrana G. EspC Promotes Epithelial Cell Detachment by Enteropathogenic Escherichia Coli *via* Sequential Cleavages of a Cytoskeletal Protein and Then Focal Adhesion Proteins. *Infect Immun* (2014) 82(6):2255–65. doi: 10.1128/IAI.01386-13
112. Al-Hasani K, Navarro-Garcia F, Huerta J, Sakellaris H, Adler B. The Immunogenic SigA Enterotoxin of Shigella Flexneri 2a Binds to HEp-2 Cells and Induces Fodrin Redistribution in Intoxicated Epithelial Cells. *PloS One* (2009) 4(12):e8223. doi: 10.1371/journal.pone.0008223
113. Maroncle NM, Sivick KE, Brady R, Stokes FE, Mobley HL. Protease Activity, Secretion, Cell Entry, Cytotoxicity, and Cellular Targets of Secreted Autotransporter Toxin of Uropathogenic Escherichia Coli. *Infect Immun* (2006) 74(11):6124–34. doi: 10.1128/IAI.01086-06
114. Habouria H, Pokharel P, Maris S, Garenaux A, Bessaiah H, Houle S, et al. Three New Serine-Protease Autotransporters of Enterobacteriaceae (SPATEs) From Extra-Intestinal Pathogenic Escherichia Coli and Combined Role of SPATEs for Cytotoxicity and Colonization of the Mouse Kidney. *Virulence* (2019) 10 (1):568–87. doi: 10.1080/21505594.2019.1624102
115. Djafari S, Ebel F, Deibel C, Kramer S, Hudel M, Chakraborty T. Characterization of an Exported Protease From Shiga Toxin-Producing Escherichia Coli. *Mol Microbiol* (1997) 25(4):771–84. doi: 10.1046/j.1365-2958.1997.5141874.x
116. Drago-Serrano ME, Parra SG, Manjarrez-Hernandez HA. EspC, an Autotransporter Protein Secreted by Enteropathogenic Escherichia Coli (EPEC), Displays Protease Activity on Human Hemoglobin. *FEMS Microbiol Lett* (2006) 265(1):35–40. doi: 10.1111/j.1574-6968.2006.00463.x
117. Navarro-Garcia F, Sears C, Eslava C, Cravioto A, Nataro JP. Cytoskeletal Effects Induced by Pet, the Serine Protease Enterotoxin of Enteroaggregative. *Escherichia coli*. *Infect Immun* (1999) 67(5):2184–92. doi: 10.1128/IAI.67.5.2184-2192.1999
118. Guyer DM, Radulovic S, Jones FE, Mobley HL. Sat, the Secreted Autotransporter Toxin of Uropathogenic Escherichia Coli, is a Vacuolating Cytotoxin for Bladder and Kidney Epithelial Cells. *Infect Immun* (2002) 70(8):4539–46. doi: 10.1128/iai.70.8.4539-4546.2002
119. Ayala-Lujan JL, Vijayakumar V, Gong M, Smith R, Santiago AE, Ruiz-Perez F. Broad Spectrum Activity of a Lectin-Like Bacterial Serine Protease Family on Human Leukocytes. *PloS One* (2014) 9(9):e107920. doi: 10.1371/journal.pone.0107920
120. Gutierrez D, Pardo M, Montero D, Onate A, Farfan MJ, Ruiz-Perez F, et al. TleA, a Tsh-Like Autotransporter Identified in a Human Enterotoxigenic Escherichia Coli Strain. *Infect Immun* (2015) 83(5):1893–903. doi: 10.1128/IAI.02976-14
121. Pokharel P, Díaz JM, Bessaiah H, Houle S, Guerrero-Barrera AL, Dozois CM. The Serine Protease Autotransporters TagB, TagC, and Sha From Extraintestinal Pathogenic Escherichia Coli Are Internalized by Human Bladder Epithelial Cells and Cause Actin Cytoskeletal Disruption. *Int J Mol Sci* (2020) 21(9):3047. doi: 10.3390/ijms21093047
122. Leyton DL, Sloan J, Hill RE, Doughty S, Hartland EL. Transfer Region of Po113 From Enterohemorrhagic Escherichia Coli: Similarity With R64 and Identification of a Novel Plasmid-Encoded Autotransporter, EpeA. *Infect Immun* (2003) 71(11):6307–19. doi: 10.1128/iai.71.11.6307-6319.2003
123. Kumar P, Luo Q, Vickers TJ, Sheikh A, Lewis WG, Fleckenstein JM. EatA, an Immunogenic Protective Antigen of Enterotoxigenic Escherichia Coli, Degrades Intestinal Mucin. *Infect Immun* (2014) 82(2):500–8. doi: 10.1128/IAI.01078-13
124. Bhullar K, Zarepour M, Yu H, Yang H, Croxen M, Stahl M, et al. The Serine Protease Autotransporter Pic Modulates Citrobacter Rodentium Pathogenesis and Its Innate Recognition by the Host. *Infect Immun* (2015) 83(7):2636–50. doi: 10.1128/IAI.00025-15
125. Benjelloun-Touimi Z, Sansonetti PJ, Parsot C. SepA, the Major Extracellular Protein of Shigella Flexneri: Autonomous Secretion and Involvement in Tissue Invasion. *Mol Microbiol* (1995) 17(1):123–35. doi: 10.1111/j.1365-2958.1995.mmi_17010123.x
126. Patel SK, Dotson J, Allen KP, Fleckenstein JM. Identification and Molecular Characterization of EatA, an Autotransporter Protein of Enterotoxigenic Escherichia Coli. *Infect Immun* (2004) 72(3):1786–94. doi: 10.1128/iai.72.3.1786-1794.2004
127. Schmidt H, Zhang WL, Hemmrich U, Jelacic S, Brunder W, Tarr PI, et al. Identification and Characterization of a Novel Genomic Island Integrated at selC in Locus of Enterocyte Effacement-Negative, Shiga Toxin-Producing Escherichia Coli. *Infect Immun* (2001) 69(11):6863–73. doi: 10.1128/IAI.69.11.6863-6873.2001
128. Henderson IR, Czeczulin J, Eslava C, Noriega F, Nataro JP. Characterization of Pic, a Secreted Protease of Shigella Flexneri and Enteroaggregative Escherichia Coli. *Infect Immun* (1999) 67(11):5587–96. doi: 10.1128/IAI.67.11.5587-5596.1999
129. Leyton DL, Adams LM, Kelly M, Sloan J, Tauschek M, Robins-Browne RM, et al. Contribution of a Novel Gene, Rpea, Encoding a Putative Autotransporter Adhesin to Intestinal Colonization by Rabbit-Specific Enteropathogenic Escherichia Coli. *Infect Immun* (2007) 75(9):4664–9. doi: 10.1128/IAI.00972-06
130. Otto BR, van Dooren SJ, Nuijens JH, Luirink J, Oudega B. Characterization of a Hemoglobin Protease Secreted by the Pathogenic Escherichia Coli Strain EB1. *J Exp Med* (1998) 188(6):1091–103. doi: 10.1084/jem.188.6.1091
131. Parreira VR, Gyles CL. A Novel Pathogenicity Island Integrated Adjacent to the thrW tRNA Gene of Avian Pathogenic Escherichia Coli Encodes a Vacuolating Autotransporter Toxin. *Infect Immun* (2003) 71(9):5087–96. doi: 10.1128/iai.71.9.5087-5096.2003
132. Gutiérrez-Lucas LR, Mendoza-Hernández G, González-Pedrajo B, Eslava-Campos C, Bustos-Martínez J, Sainz-Espuñes T. Identification of the Autotransporter Pet Toxin in *Proteus Mirabilis* Strain Isolated From Patients With Urinary Tract Infections. *Adv Biol Chem* (2012) 02(03):283–90. doi: 10.4236/abc.2012.23036

133. Dutta S, Oldfield N, Wooldridge K. Investigating the Nuclear Localisation and Proteolytic Activity of the Meningococcal App and MspA Autotransporters (2019). doi: 10.1099/acmi.ac2019.po0383
134. Beck SC, Meyer TF. IgA1 Protease From Neisseria Gonorrhoeae Inhibits TNFalpha-Mediated Apoptosis of Human Monocytic Cells. *FEBS Lett* (2000) 472(2-3):287–92. doi: 10.1016/s0014-5793(00)01478-2
135. Fink DL, Cope LD, Hansen EJ, Geme JW3rd. The Hemophilus Influenzae Hap Autotransporter Is a Chymotrypsin Clan Serine Protease and Undergoes Autoproteolysis *via* an Intermolecular Mechanism. *J Biol Chem* (2001) 276(42):39492–500. doi: 10.1074/jbc.M106913200
136. Devakanthan B, Liyanapathirana V, Dissanayake N, Harasgama P, Punchihewa J. Identification of Bacterial Aetiology in Acute Meningitis. *Ceylon Med J* (2021) 66(2):65–72. doi: 10.4038/cmj.v66i2.9465
137. van Deuren M, Brandtzaeg P, van der Meer JW. Update on Meningococcal Disease With Emphasis on Pathogenesis and Clinical Management. *Clin Microbiol Rev* (2000) 13(1):144–66. doi: 10.1128/CMR.13.1.144
138. Ulanova M, Tsang RSW. *Haemophilus Influenzae* Serotype a as a Cause of Serious Invasive Infections. *Lancet Infect Dis* (2014) 14(1):70–82. doi: 10.1016/S1473-3099(13)70170-1
139. Humbert MV, Christodoulides M. Atypical, Yet Not Infrequent, Infections With Neisseria Species. *Pathogens* (2019) 9(1):10. doi: 10.3390/pathogens9010010
140. Mathew R, Chahin M, Isache C. Neisseria Gonorrhoeae: An Unexpected Cause of Polyarthritis and Meningitis. *J Investig Med High Impact Case Rep* (2021) 9:23247096211012194. doi: 10.1177/23247096211012194
141. Khairalla AS, Omer SA, Mahdavi J, Aslam A, Dufailu OA, Self T, et al. Nuclear Trafficking, Histone Cleavage and Induction of Apoptosis by the Meningococcal App and MspA Autotransporters. *Cell Microbiol* (2015) 17 (7):1008–20. doi: 10.1111/cmi.12417
142. Serruto D, Adu-Bobie J, Scarselli M, Veggi D, Pizza M, Rappuoli R, et al. Neisseria Meningitidis App, a New Adhesin With Autocatalytic Serine Protease Activity. *Mol Microbiol* (2003) 48(2):323–34. doi: 10.1046/j.1365-2958.2003.03420.x
143. Turner DP, Marietou AG, Johnston L, Ho KK, Rogers AJ, Wooldridge KG, et al. Characterization of MspA, an Immunogenic Autotransporter Protein That Mediates Adhesion to Epithelial and Endothelial Cells in Neisseria Meningitidis. *Infect Immun* (2006) 74(5):2957–64. doi: 10.1128/IAI.74.5.2957-2964.2006
144. St Geme JW3rd, de la Morena ML, Falkow S. A Haemophilus influenzae IgA protease-like Protein promotes intimate interaction Hum epithelial Cells. *Mol Microbiol* (1994) 14(2):217–33. doi: 10.1111/j.1365-2958.1994.tb01283.x
145. Fink DL, Buscher AZ, Green B, Fernsten P, St Geme JW3rd. The Haemophilus Influenzae Hap Autotransporter Mediates Microcolony Formation and Adherence to Epithelial Cells and Extracellular Matrix *via* Binding Regions in the C-Terminal End of the Passenger Domain. *Cell Microbiol* (2003) 5(3):175–86. doi: 10.1046/j.1462-5822.2003.00266.x
146. Kilian M, Thomsen B, Petersen TE, Bleeg H. Molecular Biology of Haemophilus Influenzae IgA1 Proteases. *Mol Immunol* (1983) 20(9):1051–8. doi: 10.1016/0161-5890(83)90046-9
147. Plaut AG, Gilbert JV, Artenstein MS, Capra JD. Neisseria Gonorrhoeae and Neisseria Meningitidis: Extracellular Enzyme Cleaves Human Immunoglobulin a. *Science* (1975) 190(4219):1103–5. doi: 10.1126/science.810892
148. Danese PN, Pratt LA, Dove SL, Kolter R. The Outer Membrane Protein, Antigen 43, Mediates Cell-to-Cell Interactions Within *Escherichia Coli* Biofilms. *Mol Microbiol* (2000) 37(2):424–32. doi: 10.1046/j.1365-2958.2000.02008.x
149. Torres AG, Perna NT, Burland V, Ruknudin A, Blattner FR, Kaper JB. Characterization of Cah, a Calcium-Binding and Heat-Extractable Autotransporter Protein of Enterohaemorrhagic. *Escherichia coli. Mol Microbiol* (2002) 45(4):951–66. doi: 10.1046/j.1365-2958.2002.03094.x
150. Sherlock O, Vejborg RM, Klemm P. The TibA Adhesin/Invasin From Enterotoxigenic *Escherichia Coli* Is Self Recognizing and Induces Bacterial Aggregation and Biofilm Formation. *Infect Immun* (2005) 73(4):1954–63. doi: 10.1128/IAI.73.4.1954-1963.2005
151. Knudsen SK, Stensballe A, Franzmann M, Westergaard UB, Otzen DE. Effect of Glycosylation on the Extracellular Domain of the Ag43 Bacterial Autotransporter: Enhanced Stability and Reduced Cellular Aggregation. *Biochem J* (2008) 412(3):563–77. doi: 10.1042/BJ20071497
152. Sherlock O, Dobrindt U, Jensen JB, Munk Vejborg R, Klemm P. Glycosylation of the Self-Recognizing *Escherichia Coli* Ag43 Autotransporter Protein. *J Bacteriol* (2006) 188(5):1798–807. doi: 10.1128/JB.188.5.1798-1807.2006
153. Laarmann S, Schmidt MA. The *Escherichia Coli* AIDA Autotransporter Adhesin Recognizes an Integral Membrane Glycoprotein as Receptor. *Microbiol (Reading)* (2003) 149(Pt 7):1871–82. doi: 10.1099/mic.0.26264-0
154. Felek S, Lawrenz MB, Krukonis ES. The Yersinia Pestis Autotransporter YapC Mediates Host Cell Binding, Autoaggregation and Biofilm Formation. *Microbiol (Reading)* (2008) 154(Pt 6):1802–12. doi: 10.1099/mic.0.2007/010918-0
155. Wells TJ, Sherlock O, Rivas L, Mahajan A, Beatson SA, Torpdahl M, et al. EhaA is a Novel Autotransporter Protein of Enterohemorrhagic *Escherichia Coli* O157:H7 That Contributes to Adhesion and Biofilm Formation. *Environ Microbiol* (2008) 10(3):589–604. doi: 10.1111/j.1462-2920.2007.01479.x
156. Roux A, Beloin C, Ghigo JM. Combined Inactivation and Expression Strategy to Study Gene Function Under Physiological Conditions: Application to Identification of New *Escherichia Coli* Adhesins. *J Bacteriol* (2005) 187(3):1001–13. doi: 10.1128/JB.187.3.1001-1013.2005
157. Yen YT, Karkal A, Bhattacharya M, Fernandez RC, Stathopoulos C. Identification and Characterization of Autotransporter Proteins of *Yersinia Pestis* KIM. *Mol Membr Biol* (2007) 24(1):28–40. doi: 10.1080/09687860600927626
158. Kaplan CW, Lux R, Haake SK, Shi W. The Fusobacterium Nucleatum Outer Membrane Protein RadD Is an Arginine-Inhibitable Adhesin Required for Inter-Species Adherence and the Structured Architecture of Multispecies Biofilm. *Mol Microbiol* (2009) 71(1):35–47. doi: 10.1111/j.1365-2958.2008.06503.x
159. Elsinghorst EA, Weitz JA. Epithelial Cell Invasion and Adherence Directed by the Enterotoxigenic *Escherichia Coli* Tib Locus is Associated With a 104-Kilodalton Outer Membrane Protein. *Infect Immun* (1994) 62(8):3463–71. doi: 10.1128/iai.62.8.3463-3471.1994
160. Benz I, Schmidt MA. Cloning and Expression of an Adhesin (AIDA-I) Involved in Diffuse Adherence of Enteropathogenic. *Escherichia coli. Infect Immun* (1989) 57(5):1506–11. doi: 10.1128/iai.57.5.1506-1511.1989
161. Ageorges V, Schiavone M, Jubelin G, Caccia N, Ruiz P, Chafsey I, et al. Differential Homotypic and Heterotypic Interactions of Antigen 43 (Ag43) Variants in Autotransporter-Mediated Bacterial Autoaggregation. *Sci Rep* (2019) 9(1):11100. doi: 10.1038/s41598-019-47608-4
162. Vo JL, Ortiz GCM, Totsika M, Lo AW, Hancock SJ, Whitten AE, et al. Variation of Antigen 43 Self-Association Modulates Bacterial Compacting Within Aggregates and Biofilms. *NPJ Biofilms Microbiomes* (2022) 8(1):20. doi: 10.1038/s41522-022-00284-1
163. Cover TL, Blaser MJ. Purification and Characterization of the Vacuolating Toxin From Helicobacter Pylori. *J Biol Chem* (1992) 267(15):10570–5. doi: 10.1016/S0021-9258(19)50054-0
164. Papini E, de Bernard M, Milia E, Bugnoli M, Zerial M, Rappuoli R, et al. Cellular Vacuoles Induced by Helicobacter Pylori Originate From Late Endosomal Compartments. *Proc Natl Acad Sci U.S.A.* (1994) 91(21):9720–4. doi: 10.1073/pnas.91.21.9720
165. Kimura M, Goto S, Wada A, Yahiro K, Niidome T, Hatakeyama T, et al. Vacuolating Cytotoxin Purified From Helicobacter Pylori Causes Mitochondrial Damage in Human Gastric Cells. *Microb Pathog* (1999) 26 (1):45–52. doi: 10.1006/mpat.1998.0241
166. Foegeding NJ, Caston RR, McClain MS, Ohi MD, Cover TL. An Overview of Helicobacter Pylori VacA Toxin Biology. *Toxins (Basel)* (2016) 8(6):173. doi: 10.3390/toxins8060173
167. Su M, Erwin AL, Campbell AM, Pyburn TM, Salay LE, Hanks JL, et al. Cryo-EM Analysis Reveals Structural Basis of Helicobacter Pylori VacA Toxin Oligomerization. *J Mol Biol* (2019) 431(10):1956–65. doi: 10.1016/j.jmb.2019.03.029
168. Swanson KA, Taylor LD, Frank SD, Sturdevant GL, Fischer ER, Carlson JH, et al. *Chlamydia Trachomatis* Polymorphic Membrane Protein D Is an Oligomeric Autotransporter With a Higher-Order Structure. *Infect Immun* (2009) 77(1):508–16. doi: 10.1128/IAI.01173-08
169. Ha NY, Sharma P, Kim G, Kim Y, Min CK, Choi MS, et al. Immunization With an Autotransporter Protein of Orientia Tsutsugamushi Provides Protective Immunity Against Scrub Typhus. *PloS Negl Trop Dis* (2015) 9 (3):e0003585. doi: 10.1371/journal.pntd.0003585

170. Li H, Walker DH. Rompa Is a Critical Protein for the Adhesion of *Rickettsia Rickettsii* to Host Cells. *Microb Pathog* (1998) 24(5):289–98. doi: 10.1006/mpat.1997.0197
171. Hillman RDJr., Baktash YM, Martinez JJ. OmpA-Mediated Rickettsial Adherence to and Invasion of Human Endothelial Cells is Dependent Upon Interaction With α2β1 Integrin. *Cell Microbiol* (2013) 15(5):727–41. doi: 10.1111/cmi.12068
172. Wilhelm S, Gdynia A, Tielen P, Rosenau F, Jaeger KE. The Autotransporter Esterase EstA of Pseudomonas Aeruginosa is Required for Rhamnolipid Production, Cell Motility, and Biofilm Formation. *J Bacteriol* (2007) 189 (18):6695–703. doi: 10.1128/JB.00023-07
173. Carinato ME, Collin-Osdoby P, Yang X, Knox TM, Conlin CA, Miller CG. The apeE Gene of *Salmonella Typhimurium* Encodes an Outer Membrane Esterase Not Present in *Escherichia Coli*. . *J Bacteriol* (1998) 180(14):3517–21. doi: 10.1128/JB.180.14.3517-3521.1998
174. Farn JL, Strugnell RA, Hoyne PA, Michalski WP, Tennent JM. Molecular Characterization of a Secreted Enzyme With Phospholipase B Activity From Moraxella Bovis. *J Bacteriol* (2001) 183(22):6717–20. doi: 10.1128/JB.183.22.6717-6720.2001
175. Timpe JM, Holm MM, Vanlerberg SL, Basrur V, Lafontaine ER. Identification of a *Moraxella Catarrhalis* Outer Membrane Protein Exhibiting Both Adhesin and Lipolytic Activities. *Infect Immun* (2003) 71 (8):4341–50. doi: 10.1128/iai.71.8.4341-4350.2003
176. Lipski SL, Akimana C, Timpe JM, Wooten RM, Lafontaine ER. The *Moraxella Catarrhalis* Autotransporter McaP Is a Conserved Surface Protein That Mediates Adherence to Human Epithelial Cells Through its N-Terminal Passenger Domain. *Infect Immun* (2007) 75(1):314–24. doi: 10.1128/IAI.01330-06
177. Lafontaine ER, Chen Z, Huertas-Diaz MC, Dyke JS, Jelesijevic TP, Michel F, et al. The Autotransporter Protein BatA Is a Protective Antigen Against Lethal Aerosol Infection With Burkholderia Mallei and Burkholderia Pseudomallei. *Vaccine: X* (2019) 1:100002. doi: 10.1016/j.jvacx.2018.100002
178. Molleken K, Schmidt E, Hegemann JH. Members of the Pmp Protein Family of *Chlamydia Pneumoniae* Mediate Adhesion to Human Cells *via* Short Repetitive Peptide Motifs. *Mol Microbiol* (2010) 78(4):1004–17. doi: 10.1111/j.1365-2958.2010.07386.x
179. Becker E, Hegemann JH. All Subtypes of the Pmp Adhesin Family are Implicated in Chlamydial Virulence and Show Species-Specific Function. *Microbiologyopen* (2014) 3(4):544–56. doi: 10.1002/mbo3.186
180. Molleken K, Becker E, Hegemann JH. The *Chlamydia Pneumoniae* Invasin Protein Pmp21 Recruits the EGF Receptor for Host Cell Entry. *PloS Pathog* (2013) 9(4):e1003325. doi: 10.1371/journal.ppat.1003325
181. Wehrl W, Brinkmann V, Jungblut PR, Meyer TF, Szczepek AJ. From the Inside Out–Processing of the Chlamydial Autotransporter PmpD and its Role in Bacterial Adhesion and Activation of Human Host Cells. *Mol Microbiol* (2004) 51(2):319–34. doi: 10.1046/j.1365-2958.2003.03838.x
182. Wang S, Xia Y, Dai J, Shi Z, Kou Y, Li H, et al. Novel Roles for Autotransporter Adhesin AatA of Avian Pathogenic *Escherichia Coli*: Colonization During Infection and Cell Aggregation. *FEMS Immunol Med Microbiol* (2011) 63(3):328–38. doi: 10.1111/j.1574-695X.2011.00862.x
183. Li G, Feng Y, Kariyawasam S, Tivendale KA, Wannemuehler Y, Zhou F, et al. AatA is a Novel Autotransporter and Virulence Factor of Avian Pathogenic. *Escherichia coli*. *Infect Immun* (2010) 78(3):898–906. doi: 10.1128/IAI.00513-09
184. Kingsley RA, Santos RL, Keestra AM, Adams LG, Baumler AJ. Salmonella Enterica Serotype Typhimurium ShdA Is an Outer Membrane Fibronectin-Binding Protein That Is Expressed in the Intestine. *Mol Microbiol* (2002) 43 (4):895–905. doi: 10.1046/j.1365-2958.2002.02805.x
185. Kingsley RA, Humphries AD, Weening EH, De Zoete MR, Winter S, Papaconstantinopoulou A, et al. Molecular and Phenotypic Analysis of the CS54 Island of Salmonella Enterica Serotype Typhimurium: Identification of Intestinal Colonization and Persistence Determinants. *Infect Immun* (2003) 71(2):629–40. doi: 10.1128/iai.71.2.629-640.2003
186. Kingsley RA, Abi Ghanem D, Puebla-Osorio N, Keestra AM, Berghman L, Baumler AJ. Fibronectin Binding to the *Salmonella Enterica* Serotype Typhimurium ShdA Autotransporter Protein Is Inhibited by a Monoclonal Antibody Recognizing the A3 Repeat. *J Bacteriol* (2004) 186(15):4931–9. doi: 10.1128/JB.186.15.4931-4939.2004
187. Kingsley RA, Keestra AM, de Zoete MR, Baumler AJ. The ShdA Adhesin Binds to the Cationic Cradle of the Fibronectin 13fniii Repeat Module: Evidence for Molecular Mimicry of Heparin Binding. *Mol Microbiol* (2004) 52(2):345–55. doi: 10.1111/j.1365-2958.2004.03995.x
188. Lawrenz MB, Lenz JD, Miller VL. A Novel Autotransporter Adhesin is Required for Efficient Colonization During Bubonic Plague. *Infect Immun* (2009) 77(1):317–26. doi: 10.1128/IAI.01206-08
189. Lawrenz MB, Pennington J, Miller VL. Acquisition of Omptin Reveals Cryptic Virulence Function of Autotransporter YapE in *Yersinia Pestis*. *Mol Microbiol* (2013) 89(2):276–87. doi: 10.1111/mmi.12273
190. Koseoglu VK, Hall CP, Rodriguez-Lopez EM, Agaisse H. The Autotransporter IcsA Promotes *Shigella Flexneri* Biofilm Formation in the Presence of Bile Salts. *Infect Immun* (2019) 87(7): e00861–18. doi: 10.1128/IAI.00861-18
191. Brotcke Zumsteg A, Goosmann C, Brinkmann V, Morona R, Zychlinsky A. IcsA Is a *Shigella Flexneri* Adhesin Regulated by the Type III Secretion System and Required for Pathogenesis. *Cell Host Microbe* (2014) 15(4):435–45. doi: 10.1016/j.chom.2014.03.001
192. Wang S, Yang D, Wu X, Wang Y, Wang D, Tian M, et al. Autotransporter MisL of *Salmonella Enterica* Serotype Typhimurium Facilitates Bacterial Aggregation and Biofilm Formation. *FEMS Microbiol Lett* (2018) 365(17): fny142. doi: 10.1093/femsle/fny142
193. Dorsey CW, Laarakker MC, Humphries AD, Weening EH, Baumler AJ. *Salmonella Enterica* Serotype Typhimurium MisL is an Intestinal Colonization Factor That Binds Fibronectin. *Mol Microbiol* (2005) 57 (1):196–211. doi: 10.1111/j.1365-2958.2005.04666.x
194. Easton DM, Totsika M, Allsopp LP, Phan MD, Idris A, Wurpel DJ, et al. Characterization of EhaJ, a New Autotransporter Protein From Enterohemorrhagic and Enteropathogenic. *Escherichia coli*. *Front Microbiol* (2011) 2:120. doi: 10.3389/fmicb.2011.00120
195. Battaglioli EJ, Goh KGK, Atruktsang TS, Schwartz K, Schembri MA, Welch RA. Identification and Characterization of a Phase-Variable Element That Regulates the Autotransporter UpaE in Uropathogenic. *Escherichia coli*. *mBio* (2018) 9(4):e01360–18. doi: 10.1128/mBio.01360-18
196. Crane DD, Carlson JH, Fischer ER, Bavoil P, Hsia RC, Tan C, et al. *Chlamydia Trachomatis* Polymorphic Membrane Protein D is a Species-Common Pan-Neutralizing Antigen. *Proc Natl Acad Sci U.S.A.* (2006) 103 (6):1894–9. doi: 10.1073/pnas.0508983103
197. Paes W, Dowle A, Coldwell J, Leech A, Ganderton T, Brzozowski A. The *Chlamydia Trachomatis* PmpD Adhesin Forms Higher Order Structures Through Disulphide-Mediated Covalent Interactions. *PloS One* (2018) 13(6): e0198662. doi: 10.1371/journal.pone.0198662
198. Luczak SE, Smits SH, Decker C, Nagel-Steger L, Schmitt L, Hegemann JH. The *Chlamydia Pneumoniae* Adhesin Pmp21 Forms Oligomers With Adhesive Properties. *J Biol Chem* (2016) 291(43):22806–18. doi: 10.1074/jbc.M116.728915
199. Palframan SL, Kwok T, Gabriel K. Vacuolating Cytotoxin A (VacA), a Key Toxin for Helicobacter Pylori Pathogenesis. *Front Cell Infect Microbiol* (2012) 2:92. doi: 10.3389/fcimb.2012.00092
200. Goldberg MB, Theriot JA. *Shigella Flexneri* Surface Protein IcsA is Sufficient to Direct Actin-Based Motility. *Proc Natl Acad Sci U.S.A.* (1995) 92 (14):6572–6. doi: 10.1073/pnas.92.14.6572
201. Dai J, Wang S, Guerlebeck D, Laturnus C, Guenther S, Shi Z, et al. Suppression Subtractive Hybridization Identifies an Autotransporter Adhesin Gene of E. Coli IMT5155 Specifically Associated With Avian Pathogenic *Escherichia Coli* (APEC). *BMC Microbiol* (2010) 10:236. doi: 10.1186/1471-2180-10-236
202. Egile C, Loisel TP, Laurent V, Li R, Pantaloni D, Sansonetti PJ, et al. Activation of the CDC42 Effector N-WASP by the Shigella Flexneri IcsA Protein Promotes Actin Nucleation by Arp2/3 Complex and Bacterial Actin-Based Motility. *J Cell Biol* (1999) 146(6):1319–32. doi: 10.1083/jcb.146.6.1319
203. May KL, Grabowicz M, Polyak SW, Morona R. Self-Association of the *Shigella Flexneri* IcsA Autotransporter Protein. *Microbiol (Reading)* (2012) 158(Pt 7):1874–83. doi: 10.1099/mic.0.056465-0
204. Bokhari H, Bilal I, Zafar S. BapC Autotransporter Protein of *Bordetella Pertussis* Is an Adhesion Factor. *J Basic Microbiol* (2012) 52(4):390–6. doi: 10.1002/jobm.201100188
205. Leininger E, Roberts M, Kenimer JG, Charles IG, Fairweather N, Novotny P, et al. Pertactin, an Arg-Gly-Asp-Containing Bordetella Pertussis Surface

Protein That Promotes Adherence of Mammalian Cells. *Proc Natl Acad Sci U.S.A.* (1991) 88(2):345–9. doi: 10.1073/pnas.88.2.345
206. Fernandez RC, Weiss AA. Cloning and Sequencing of a *Bordetella Pertussis* Serum Resistance Locus. *Infect Immun* (1994) 62(11):4727–38. doi: 10.1128/iai.62.11.4727-4738.1994
207. Finn TM, Amsbaugh DF. Vag8, a *Bordetella Pertussis* Bvg-Regulated Protein. *Infect Immun* (1998) 66(8):3985–9. doi: 10.1128/IAI.66.8.3985-3989.1998
208. Noofeli M, Bokhari H, Blackburn P, Roberts M, Coote JG, Parton R. BapC Autotransporter Protein is a Virulence Determinant of Bordetella Pertussis. *Microb Pathog* (2011) 51(3):169–77. doi: 10.1016/j.micpath.2011.04.004
209. Inatsuka CS, Xu Q, Vujkovic-Cvijin I, Wong S, Stibitz S, Miller JF, et al. Pertactin is Required for Bordetella Species to Resist Neutrophil-Mediated Clearance. *Infect Immun* (2010) 78(7):2901–9. doi: 10.1128/IAI.00188-10
210. Hovingh ES, Mariman R, Solans L, Hijdra D, Hamstra HJ, Jongerius I, et al. Bordetella Pertussis Pertactin Knock-Out Strains Reveal Immunomodulatory Properties of This Virulence Factor. *Emerg Microbes Infect* (2018) 7(1):39. doi: 10.1038/s41426-018-0039-8
211. Barnes MG, Weiss AA. BrkA Protein of *Bordetella Pertussis* Inhibits the Classical Pathway of Complement After C1 Deposition. *Infect Immun* (2001) 69(5):3067–72. doi: 10.1128/IAI.69.5.3067-3072.2001
212. Hovingh ES, de Maat S, Cloherty APM, Johnson S, Pinelli E, Maas C, et al. Virulence Associated Gene 8 of *Bordetella Pertussis* Enhances Contact System Activity by Inhibiting the Regulatory Function of Complement Regulator C1 Inhibitor. *Front Immunol* (2018) 9:1172. doi: 10.3389/fimmu.2018.01172
213. Raeven RH, van der Maas L, Tilstra W, Uittenbogaard JP, Bindels TH, Kuipers B, et al. Immunoproteomic Profiling of *Bordetella Pertussis* Outer Membrane Vesicle Vaccine Reveals Broad and Balanced Humoral Immunogenicity. *J Proteome Res* (2015) 14(7):2929–42. doi: 10.1021/acs.jproteome.5b00258
214. Raeven RHM, van Vlies N, Salverda MLM, van der Maas L, Uittenbogaard JP, Bindels THE, et al. The Role of Virulence Proteins in Protection Conferred by Bordetella Pertussis Outer Membrane Vesicle Vaccines. *Vaccines (Basel)* (2020) 8(3):429. doi: 10.3390/vaccines8030429
215. Allsopp LP, Beloin C, Ulett GC, Valle J, Totsika M, Sherlock O, et al. Molecular Characterization of UpaB and UpaC, Two New Autotransporter Proteins of Uropathogenic *Escherichia Coli* CFT073. *Infect Immun* (2012) 80(1):321–32. doi: 10.1128/IAI.05322-11
216. Wells TJ, McNeilly TN, Totsika M, Mahajan A, Gally DL, Schembri MA. The *Escherichia Coli* O157:H7 EhaB Autotransporter Protein Binds to Laminin and Collagen I and Induces a Serum IgA Response in O157:H7 Challenged Cattle. *Environ Microbiol* (2009) 11(7):1803–14. doi: 10.1111/j.1462-2920.2009.01905.x
217. Radin JN, Gaddy JA, Gonzalez-Rivera C, Loh JT, Algood HM, Cover TL. Flagellar Localization of a Helicobacter Pylori Autotransporter Protein. *mBio* (2013) 4(2):e00613–12. doi: 10.1128/mBio.00613-12
218. Allsopp LP, Beloin C, Moriel DG, Totsika M, Ghigo JM, Schembri MA. Functional Heterogeneity of the UpaH Autotransporter Protein From Uropathogenic. *Escherichia coli. J Bacteriol* (2012) 194(21):5769–82. doi: 10.1128/JB.01264-12
219. Allsopp LP, Totsika M, Tree JJ, Ulett GC, Mabbett AN, Wells TJ, et al. UpaH is a Newly Identified Autotransporter Protein That Contributes to Biofilm Formation and Bladder Colonization by Uropathogenic *Escherichia Coli* CFT073. *Infect Immun* (2010) 78(4):1659–69. doi: 10.1128/IAI.01010-09
220. Ashgar SS, Oldfield NJ, Wooldridge KG, Jones MA, Irving GJ, Turner DP, et al. CapA, an Autotransporter Protein of Campylobacter Jejuni, Mediates Association With Human Epithelial Cells and Colonization of the Chicken Gut. *J Bacteriol* (2007) 189(5):1856–65. doi: 10.1128/JB.01427-06
221. Nair MK, De Masi L, Yue M, Galvan EM, Chen H, Wang F, et al. Adhesive Properties of YapV and Paralogous Autotransporter Proteins of. *Yersinia pestis. Infect Immun* (2015) 83(5):1809–19. doi: 10.1128/IAI.00094-15
222. Uchiyama T, Kawano H, Kusuhara Y. The Major Outer Membrane Protein Rompb of Spotted Fever Group Rickettsiae Functions in the Rickettsial Adherence to and Invasion of Vero Cells. *Microbes Infect* (2006) 8(3):801–9. doi: 10.1016/j.micinf.2005.10.003
223. Williams CL, Haines R, Cotter PA. Serendipitous Discovery of an Immunoglobulin-Binding Autotransporter in Bordetella Species. *Infect Immun* (2008) 76(7):2966–77. doi: 10.1128/IAI.00323-08
224. Posadas DM, Ruiz-Ranwez V, Bonomi HR, Martin FA, Zorreguieta A. BmaC, a Novel Autotransporter of Brucella Suis, is Involved in Bacterial Adhesion to Host Cells. *Cell Microbiol* (2012) 14(6):965–82. doi: 10.1111/j.1462-5822.2012.01771.x
225. Matsumoto A, Huston SL, Killiny N, Igo MM. XatA, an AT-1 Autotransporter Important for the Virulence of *Xylella Fastidiosa* Temecula1. *Microbiologyopen* (2012) 1(1):33–45. doi: 10.1002/mbo3.6
226. Feitosa-Junior OR, Stefanello E, Zaini PA, Nascimento R, Pierry PM, Dandekar AM. Proteomic and Metabolomic Analyses of Xylella fastidiosa OMV-Enriched Fractions Reveal Association with Virulence Factors and Signaling Molecules of the DSF Family. *Phytopathology* (2019). 109(8):1344–1353. doi: 10.1094/PHYTO-03-19-0083-R.
227. Odenbreit S, Till M, Hofreuter D, Faller G, Haas R. Genetic and Functional Characterization of the alpAB Gene Locus Essential for the Adhesion of *Helicobacter Pylori* to Human Gastric Tissue. *Mol Microbiol* (1999) 31(5):1537–48. doi: 10.1046/j.1365-2958.1999.01300.x
228. Chan YG, Cardwell MM, Hermanas TM, Uchiyama T, Martinez JJ. Rickettsial Outer-Membrane Protein B (Rompb) Mediates Bacterial Invasion Through Ku70 in an Actin, C-Cbl, Clathrin and Caveolin 2-Dependent Manner. *Cell Microbiol* (2009) 11(4):629–44. doi: 10.1111/j.1462-5822.2008.01279.x
229. Riley SP, Goh KC, Hermanas TM, Cardwell MM, Chan YG, Martinez JJ. The *Rickettsia Conorii* Autotransporter Protein Sca1 Promotes Adherence to Nonphagocytic Mammalian Cells. *Infect Immun* (2010) 78(5):1895–904. doi: 10.1128/IAI.01165-09
230. Cardwell MM, Martinez JJ. The Sca2 Autotransporter Protein From *Rickettsia Conorii* is Sufficient to Mediate Adherence to and Invasion of Cultured Mammalian Cells. *Infect Immun* (2009) 77(12):5272–80. doi: 10.1128/IAI.00201-09
231. Ha NY, Cho NH, Kim YS, Choi MS, Kim IS. An Autotransporter Protein From *Orientia Tsutsugamushi* Mediates Adherence to Nonphagocytic Host Cells. *Infect Immun* (2011) 79(4):1718–27. doi: 10.1128/IAI.01239-10
232. Nunes AC, Longo PL, Mayer MP. Influence of Aae Autotransporter Protein on Adhesion and Biofilm Formation by Aggregatibacter Actinomycetemcomitans. *Braz Dent J* (2016) 27(3):255–60. doi: 10.1590/0103-6440201600260
233. Haglund CM, Choe JE, Skau CT, Kovar DR, Welch MD. Rickettsia Sca2 is a Bacterial Formin-Like Mediator of Actin-Based Motility. *Nat Cell Biol* (2010) 12(11):1057–63. doi: 10.1038/ncb2109
234. Sun YY, Sun L. Pseudomonas Fluorescens: Iron-Responsive Proteins and Their Involvement in Host Infection. *Vet Microbiol* (2015) 176(3-4):309–20. doi: 10.1016/j.vetmic.2015.01.020
235. Hu YH, Liu CS, Hou JH, Sun L. Identification, Characterization, and Molecular Application of a Virulence-Associated Autotransporter From a Pathogenic *Pseudomonas Fluorescens* Strain. *Appl Environ Microbiol* (2009) 75(13):4333–40. doi: 10.1128/AEM.00159-09
236. Campos CG, Borst L, Cotter PA. Characterization of BcaA, a Putative Classical Autotransporter Protein in Burkholderia Pseudomallei. *Infect Immun* (2013) 81(4):1121–8. doi: 10.1128/IAI.01453-12
237. Kida Y, Taira J, Yamamoto T, Higashimoto Y, Kuwano K. EprS, an Autotransporter Protein of *Pseudomonas Aeruginosa*, Possessing Serine Protease Activity Induces Inflammatory Responses Through Protease-Activated Receptors. *Cell Microbiol* (2013) 15(7):1168–81. doi: 10.1111/cmi.12106
238. Liu L, Chi H, Sun L. Pseudomonas Fluorescens: Identification of Fur-Regulated Proteins and Evaluation of Their Contribution to Pathogenesis. *Dis Aquat Organ* (2015) 115(1):67–80. doi: 10.3354/dao02874
239. Ohnishi Y, Horinouchi S. Extracellular Production of a *Serratia Marcescens* Serine Protease in *Escherichia Coli. Biosci Biotechnol Biochem* (1996) 60(10):1551–8. doi: 10.1271/bbb.60.1551
240. Miyazaki H, Yanagida N, Horinouchi S, Beppu T. Characterization of the Precursor of *Serratia Marcescens* Serine Protease and COOH-Terminal Processing of the Precursor During its Excretion Through the Outer Membrane of *Escherichia Coli. J Bacteriol* (1989) 171(12):6566–72. doi: 10.1128/jb.171.12.6566-6572.1989
241. Coutte L, Antoine R, Drobecq H, Locht C, Jacob-Dubuisson F. Subtilisin-Like Autotransporter Serves as Maturation Protease in a Bacterial Secretion Pathway. *EMBO J* (2001) 20(18):5040–8. doi: 10.1093/emboj/20.18.5040

242. Ali T, Oldfield NJ, Wooldridge KG, Turner DP, Ala'Aldeen DA. Functional Characterization of AasP, a Maturation Protease Autotransporter Protein of Actinobacillus Pleuropneumoniae. *Infect Immun* (2008) 76(12):5608–14. doi: 10.1128/IAI.00085-08
243. Chen J, Civerolo E, Tubajika K, Livingston S, Higbee B. Hypervariations of a Protease-Encoding Gene, PD0218 (Pspb), in *Xylella Fastidiosa* Strains Causing Almond Leaf Scorch and Pierce's Disease in California. *Appl Environ Microbiol* (2008) 74(12):3652–7. doi: 10.1128/AEM.02386-07
244. Kida Y, Taira J, Kuwano K. EprS, an Autotransporter Serine Protease, Plays an Important Role in Various Pathogenic Phenotypes of Pseudomonas Aeruginosa. *Microbiol (Reading)* (2016) 162(2):318–29. doi: 10.1099/mic.0.000228
245. Coutte L, Willery E, Antoine R, Drobecq H, Locht C, Jacob-Dubuisson F. Surface Anchoring of Bacterial Subtilisin Important for Maturation Function. *Mol Microbiol* (2003) 49(2):529–39. doi: 10.1046/j.1365-2958.2003.03573.x
246. van Ulsen P, Adler B, Fassler P, Gilbert M, van Schilfgaarde M, van der Ley P, et al. A Novel Phase-Variable Autotransporter Serine Protease, AusI, of Neisseria Meningitidis. *Microbes Infect* (2006) 8(8):2088–97. doi: 10.1016/j.micinf.2006.03.007
247. Bachrach G, Rosen G, Bellalou M, Naor R, Sela MN. Identification of a Fusobacterium Nucleatum 65 kDa Serine Protease. *Oral Microbiol Immunol* (2004) 19(3):155–9. doi: 10.1111/j.0902-0055.2004.00132.x
248. Del Tordello E, Vacca I, Ram S, Rappuoli R, Serruto D. *Neisseria Meningitidis* NalP Cleaves Human Complement C3, Facilitating Degradation of C3b and Survival in Human Serum. *Proc Natl Acad Sci U.S.A.* (2014) 111(1):427–32. doi: 10.1073/pnas.1321556111
249. Dufailu OA, Mahdavi J, Ala'Aldeen DAA, Wooldridge KG, Oldfield NJ. Uptake of Neisserial Autotransporter Lipoprotein (NalP) Promotes an Increase in Human Brain Microvascular Endothelial Cell Metabolic Activity. *Microb Pathog* (2018) 124:70–5. doi: 10.1016/j.micpath.2018.08.001
250. Mehat JW, Park SF, van Vliet AHM, La Ragione RM. CapC, a Novel Autotransporter and Virulence Factor of Campylobacter Jejuni. *Appl Environ Microbiol* (2018) 84(16):e01032–18. doi: 10.1128/AEM.01032-18
251. Coppenhagen-Glazer S, Sol A, Abed J, Naor R, Zhang X, Han YW, et al. Fap2 of Fusobacterium Nucleatum is a Galactose-Inhibitable Adhesin Involved in Coaggregation, Cell Adhesion, and Preterm Birth. *Infect Immun* (2015) 83(3):1104–13. doi: 10.1128/IAI.02838-14
252. Mizan S, Henk A, Stallings A, Maier M, Lee MD. Cloning and Characterization of Sialidases With 2-6' and 2-3' Sialyl Lactose Specificity From. *Pasteurella multocida. J Bacteriol* (2000) 182(24):6874–83. doi: 10.1128/jb.182.24.6874-6883.2000
253. Arenas J, Paganelli FL, Rodriguez-Castano P, Cano-Crespo S, van der Ende A, van Putten JP, et al. Expression of the Gene for Autotransporter AutB of *Neisseria Meningitidis* Affects Biofilm Formation and Epithelial Transmigration. *Front Cell Infect Microbiol* (2016) 6:162. doi: 10.3389/fcimb.2016.00162
254. Perez-Ortega J, Rodriguez A, Ribes E, Tommassen J, Arenas J. Interstrain Cooperation in Meningococcal Biofilms: Role of Autotransporters NalP and AutA. *Front Microbiol* (2017) 8:434. doi: 10.3389/fmicb.2017.00434
255. Luckett JC, Darch O, Watters C, Abuoun M, Wright V, Paredes-Osses E, et al. A Novel Virulence Strategy for Pseudomonas Aeruginosa Mediated by an Autotransporter With Arginine-Specific Aminopeptidase Activity. *PloS Pathog* (2012) 8(8):e1002854. doi: 10.1371/journal.ppat.1002854
256. Hoopman TC, Wang W, Brautigam CA, Sedillo JL, Reilly TJ, Hansen EJ. *Moraxella Catarrhalis* Synthesizes an Autotransporter That is an Acid Phosphatase. *J Bacteriol* (2008) 190(4):1459–72. doi: 10.1128/JB.01688-07
257. Chapman TM, Goa KL. Reduced-Antigen Combined Diphtheria-Tetanus-Acellular Pertussis Vaccine (Boostrix). *Drugs* (2003) 63(13):1407–13. doi: 10.2165/00003495-200363130-00005
258. Curran MP, Goa KL. DTPa-HBV-IPV/Hib Vaccine (Infanrix Hexa). *Drugs* (2003) 63(7):673–82. doi: 10.2165/00003495-200363070-00004
259. Pichichero ME, DeTora LM, Johnson DR. An Adolescent and Adult Formulation Combined Tetanus, Diphtheria and Five-Component Pertussis Vaccine. *Expert Rev Vaccines* (2006) 5(2):175–87. doi: 10.1586/14760584.5.2.175
260. Gorringe AR, Pajon R. Bexsero: A Multicomponent Vaccine for Prevention of Meningococcal Disease. *Hum Vaccin Immunother* (2012) 8(2):174–83. doi: 10.4161/hv.18500
261. Heras B, Scanlon MJ, Martin JL. Targeting Virulence Not Viability in the Search for Future Antibacterials. *Br J Clin Pharmacol* (2015) 79(2):208–15. doi: 10.1111/bcp.12356
262. Lattemann CT, Maurer J, Gerland E, Meyer TF. Autodisplay: Functional Display of Active Beta-Lactamase on the Surface of *Escherichia Coli* by the AIDA-I Autotransporter. *J Bacteriol* (2000) 182(13):3726–33. doi: 10.1128/jb.182.13.3726-3733.2000
263. Chung ME, Goroncy K, Kolesnikova A, Schonauer D, Schwaneberg U. Display of Functional Nucleic Acid Polymerase on *Escherichia Coli* Surface and its Application in Directed Polymerase Evolution. *Biotechnol Bioeng* (2020) 117(12):3699–711. doi: 10.1002/bit.27542
264. Ko HJ, Park E, Song J, Yang TH, Lee HJ, Kim KH, et al. Functional Cell Surface Display and Controlled Secretion of Diverse Agarolytic Enzymes by *Escherichia Coli* With a Novel Ligation-Independent Cloning Vector Based on the Autotransporter YfaL. *Appl Environ Microbiol* (2012) 78(9):3051–8. doi: 10.1128/AEM.07004-11
265. Dvorak P, Bayer EA, de Lorenzo V. Surface Display of Designer Protein Scaffolds on Genome-Reduced Strains of *Pseudomonas Putida*. *ACS Synth Biol* (2020) 9(10):2749–64. doi: 10.1021/acssynbio.0c00276
266. Stratker K, Haidar S, Dubiel M, Estevez-Braun A, Jose J. Autodisplay of Human PIP5K1alpha Lipid Kinase on *Escherichia Coli* and Inhibitor Testing. *Enzyme Microb Technol* (2021) 143:109717. doi: 10.1016/j.enzmictec.2020.109717
267. Mateos-Chavez AA, Munoz-Lopez P, Becerra-Baez EI, Flores-Martinez LF, Prada-Gracia D, Moreno-Vargas LM, et al. Live Attenuated Salmonella Enterica Expressing and Releasing Cell-Permeable Bax BH3 Peptide Through the MisL Autotransporter System Elicits Antitumor Activity in a Murine Xenograft Model of Human B Non-Hodgkin's Lymphoma. *Front Immunol* (2019) 10:2562. doi: 10.3389/fimmu.2019.02562
268. Jong WS, Soprova Z, de Punder K, ten Hagen-Jongman CM, Wagner S, Wickstrom D, et al. A Structurally Informed Autotransporter Platform for Efficient Heterologous Protein Secretion and Display. *Microb Cell Fact* (2012) 11:85. doi: 10.1186/1475-2859-11-85
269. van den Berg van Saparoea HB, Houben D, Kuijl C, Luirink J, Jong WSP. Combining Protein Ligation Systems to Expand the Functionality of Semi-Synthetic Outer Membrane Vesicle Nanoparticles. *Front Microbiol* (2020) 11:890. doi: 10.3389/fmicb.2020.00890
270. van den Berg van Saparoea HB, Houben D, de Jonge MI, Jong WSP, Luirink J. Display of Recombinant Proteins on Bacterial Outer Membrane Vesicles by Using Protein Ligation. *Appl Environ Microbiol* (2018) 84(8): e02567–17. doi: 10.1128/AEM.02567-17

Conflict of Interest: The authors declare that the research was conducted in the absence of any commercial or financial relationships that could be construed as a potential conflict of interest.

Publisher's Note: All claims expressed in this article are solely those of the authors and do not necessarily represent those of their affiliated organizations, or those of the publisher, the editors and the reviewers. Any product that may be evaluated in this article, or claim that may be made by its manufacturer, is not guaranteed or endorsed by the publisher.

Copyright © 2022 Clarke, Hor, Pilapitiya, Luirink, Paxman and Heras. This is an open-access article distributed under the terms of the Creative Commons Attribution License (CC BY). The use, distribution or reproduction in other forums is permitted, provided the original author(s) and the copyright owner(s) are credited and that the original publication in this journal is cited, in accordance with accepted academic practice. No use, distribution or reproduction is permitted which does not comply with these terms.

frontiers | Frontiers in Immunology

REVIEW
published: 13 July 2022
doi: 10.3389/fimmu.2022.943344

The Immunological Synapse: An Emerging Target for Immune Evasion by Bacterial Pathogens

Nagaja Capitani * *and Cosima T. Baldari* *

Department of Life Sciences, University of Siena, Siena, Italy

Similar to other pathogens, bacteria have developed during their evolution a variety of mechanisms to overcome both innate and acquired immunity, accounting for their ability to cause disease or chronic infections. The mechanisms exploited for this critical function act by targeting conserved structures or pathways that regulate the host immune response. A strategic potential target is the immunological synapse (IS), a highly specialized structure that forms at the interface between antigen presenting cells (APC) and T lymphocytes and is required for the establishment of an effective T cell response to the infectious agent and for the development of long-lasting T cell memory. While a variety of bacterial pathogens are known to impair or subvert cellular processes essential for antigen processing and presentation, on which IS assembly depends, it is only recently that the possibility that IS may be a direct target of bacterial virulence factors has been considered. Emerging evidence strongly supports this notion, highlighting IS targeting as a powerful, novel means of immune evasion by bacterial pathogens. In this review we will present a brief overview of the mechanisms used by bacteria to affect IS assembly by targeting APCs. We will then summarize what has emerged from the current handful of studies that have addressed the direct impact of bacterial virulence factors on IS assembly in T cells and, based on the strategic cellular processes targeted by these factors in other cell types, highlight potential IS-related vulnerabilities that could be exploited by these pathogens to evade T cell mediated immunity.

Keywords: pathogens, immunological synapse, Antigen Presenting Cell (APC), major histocompatibility complex class II (MHCII), T cell receptor (TCR), actin cytoskeleton

OPEN ACCESS

Edited by:
Marina De Bernard,
University of Padua, Italy

Reviewed by:
Yung-Fu Chang,
Cornell University, United States
Baoxue Ge,
Tongji University, China
Haiying Liu,
China Academy of Chinese Medical Sciences, China

***Correspondence:**
Nagaja Capitani
capitani2@unisi.it
Cosima T. Baldari
cosima.baldari@unisi.it

Specialty section:
This article was submitted to Microbial Immunology, a section of the journal Frontiers in Immunology

Received: *13 May 2022*
Accepted: *20 June 2022*
Published: *13 July 2022*

Citation:
Capitani N and Baldari CT (2022) The Immunological Synapse: An Emerging Target for Immune Evasion by Bacterial Pathogens. Front. Immunol. 13:943344. doi: 10.3389/fimmu.2022.943344

1 INTRODUCTION

Successful microbial pathogens, such as bacteria, have evolved complex and efficient strategies to evade the host immune response. To establish chronic infection bacteria have to overcome the two powerful arms of the host immune defenses, innate and adaptive immunity. Innate immunity is evolutionarily conserved among higher eukaryotes and represents the first line of defense against infections, with the key role to recognize pathogen components and start the process of microbial clearance. Additionally, innate immune cells are central for the development of adaptive immunity. Hence, not surprisingly, pathogens have evolved a

variety of mechanisms to elude this first line of the host immune defenses, from building a protective capsule (e.g. *Streptococcus pneumoniae*, *Haemophilus influenzae*, *Escherichia coli*, *Neisseria meningitidis*) (1), to interfering with recognition of Pathogen-Associated Molecular Patterns (PAMPs) by host Pattern Recognition Receptors (PRRs) such as Toll-like receptors (TLRs) and C-type lectin receptors (e.g. *Helicobacter pylori*) (2), to inhibiting phagocytic activity (e.g. *H. pylori*, *Yersinia pestis*) (3). Remarkably, evasion of innate immunity is often accompanied by the exploitation of innate immune cells such as macrophages, which have been incapacitated to kill internalized bacteria by specific virulence factors, as a protected niche for replication.

Another strategy deployed by several bacterial pathogens to escape the host immune system is to prevent the development of the exquisitely specific and highly effective adaptive response. Adaptive immunity involves a tightly regulated interplay among B lymphocytes, T lymphocytes and antigen presenting cells (APCs) to activate pathogen-specific and lifelong immunological effector pathways. The development of T cell mediated immunity relies on the assembly of a highly specialized signaling and secretory platform formed by T cells at the interface with cognate APCs, known as the immunological synapse (IS). In this minireview we will briefly review the strategies evolved by bacterial pathogens to suppress T cell activation and discuss emerging evidence that highlights the IS as a key target for pathogens to evade the T cell-mediated host immune response.

2 THE IMMUNOLOGICAL SYNAPSE

T cell activation is initiated in response to the interaction of the T cell antigen receptor (TCR) with antigenic peptides bound to major histocompatibility complex (MHC) molecules (pMHC) expressed on the surface of APCs, which participate in the cellular immune response by processing and presenting antigens for recognition by T lymphocytes. Antigen presentation is a complex multistep process, involving the processing of endogenous or exogenous pathogen-associated antigens, peptide loading on MHC, and localization at the cell surface of pMHC complexes which can interact with T cells expressing a cognate TCR. Bacterial antigen presentation is mainly mediated by MHC class II (MHCII) molecules found on the surface of professional APCs that present antigen-derived peptides to be recognized by $CD4^+$ T cells.

Following TCR interaction with cognate pMHC, a specialized supramolecular structure, defined as immunological synapse (IS), forms at the T cell interface with the APC. IS formation requires not only TCR:pMHC interaction but also the accumulation of coreceptors, adhesion molecules, and signaling and cytoskeletal components at the T cell-APC contact area (4). In its mature configuration the IS features a peculiar "bull's eye" architecture characterized by concentric domains, known as supramolecular activation clusters (SMAC), that differ in molecular composition and function (5). The central SMAC (cSMAC), mainly enriched in TCRs and TCR-associated proteins, is surrounded by the peripheral (pSMAC), enriched in integrins, such as lymphocyte function-associated antigen (LFA-1), and cytoskeleton-associated proteins. The pSMAC is in turn surrounded by the distal SMAC (dSMAC), which is enriched in F-actin as well as in molecules that are excluded from the IS centre due either to steric hindrance (e.g. CD43) or to their ability to negatively regulate signaling (e.g. CD45) (4). The dSMAC is also the IS domain where signaling starts with the assembly of TCR-CD28 microclusters that move centripetally towards the IS to eventually segregate to the cSMAC (6), where exhausted TCR are internalized to make room to new TCRs microclusters that continuously form at the periphery.

TCRs are associated not only with the plasma membrane, but also with recycling endosomes (7). Delivery to the synaptic membrane of this intracellular TCR pool is essential to replenish the plasma membrane pool as TCRs are internalized at the cSMAC, allowing for the steady inward flow of actively signaling TCR microclusters to sustain signaling for the extended timeframe required for T cell activation (7). This process is dependent on the polarization of the centrosome together with the secretory apparatus to the region beneath the T cell-APC contact (8), which sets the stage for polarized exocytosis. Polarized recycling from an intracellular vesicular pool is a strategy co-opted by a number of molecules that participate in IS architecture and function. These include surface receptors, such as the co-inhibitory receptor cytotoxic T lymphocyte antigen-4 (CTLA-4) (9), and intracellular signaling molecules, such as the lymphocyte-specific protein tyrosine kinase (Lck), the adaptor molecule LAT (10–12), and the small GTPase Rac1 (13).

IS assembly is coordinated by the cytoskeleton (14–16), which plays a key role at different step of IS assembly, from integrin activation (16), to TCR microcluster movement from the periphery to the center of the IS (6), to centrosome translocation toward the IS (14), to the directional vesicular trafficking that ensures the continuous availability of receptors and signaling molecules at the IS (17–19) (**Figure 1**).

TCR interaction with pMHC at the IS triggers an intracellular tyrosine phosphorylation cascade, resulting in the activation of multiple signaling pathways. Briefly, the activated TCR recruits the initiating kinases Lck and ζ-associated kinase of 70 kDa (ZAP-70) which phosphorylates LAT, a multifunctional transmembrane adaptor that orchestrates the activation of phospholipase Cγ (PLCγ). By producing key second messengers, PLCγ promotes the activation of the PKC, Ras and Ca^{2+} pathways which couple TCR triggering to gene expression through the activation of transcription factors such as nuclear factor of activated T cells (NF-AT), nuclear factor-κB (NF-κB) and activating protein 1 (AP-1) (20).

As IS assembly is a key event for the development of T cell-mediated immunity, it is not surprising that many pathogens have developed virulence mechanisms to target IS formation, either indirectly by impairing the ability of APCs to present antigen to the T cell, or, as supported by emerging evidence, by directly inhibiting IS assembly within the T cell.

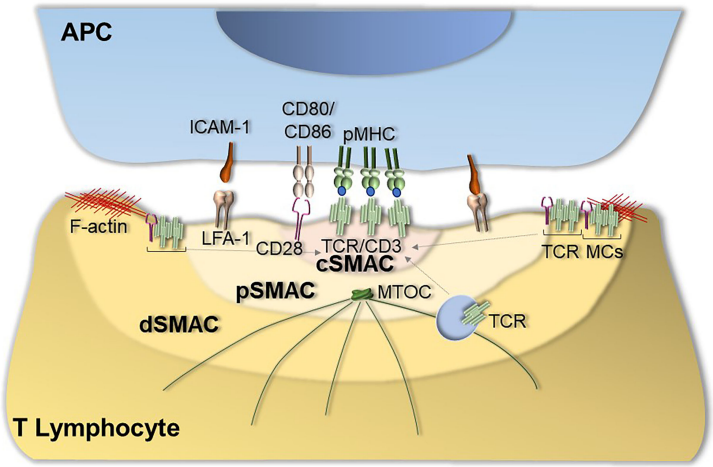

FIGURE 1 | Immunological synapse assembly. The canonical IS shows a well-organized bull's eye architecture that features the central supramolecular activation cluster (cSMAC) characterized by the presence of TCRs and TCR-associated proteins such as the co-stimulatory receptor CD28, the peripheral SMAC (pSMAC) enriched in the integrin LFA-1 and the distal SMAC (dSMAC) enriched in TCR-CD28 microclusters (TCR MCs) that move centripetally towards the cSMAC driven by F-actin. IS assembly is also coordinated by cytoskeletal dynamics that allow for centrosome translocation toward the IS as well as for the directional vesicular trafficking of receptors and signaling mediators to sustain signaling at the IS.

3 HOW BACTERIAL INFECTION AFFECTS IS ASSEMBLY

3.1 Indirect Modulation of IS Assembly by Bacterial Pathogens Through APC Targeting

To initiate adaptive immunity to pathogens, T cells must interact with cognate APCs that have previously taken up antigen at the site of infection and have migrated to the draining lymph node. This role is subserved by dendritic cells (DCs) which are specialized for antigen presentation to naïve T cells, but in the context of bacterial infections it can also be taken over by macrophages. Several steps are required before an APC can acquire the appropriate functional status and be in the appropriate location to form an IS with a cognate T cell. These steps are orchestrated by innate immune receptors, which on recognition of bacterial PAMPs trigger the maturation of DCs, the phagocytic uptake and destruction of the pathogen, and the migration of the phagocyte to the closest lymph node station. As largely documented for viruses (1), also bacterial pathogens have evolved a variety of strategies to interfere with each of these steps, including camouflaging as host components (e.g. GAG proteins of *Streptococcus*), modifying PAMPs to decrease their potency in innate immune receptor activation (e.g. modified LPS core component lipid A of *Salmonella*) (21), inhibiting PRR signaling (e.g. *Salmonella* TIR domain-like TIpA to disrupt TLR4 signaling (22); *Yersinia* acetyltransferase YopJ to inhibit NF-kB signaling (23); *Mycobacterium tuberculosis* (*M. tubercolosis*) ubiquitin ligase PnkG to degrade components of the NF-kB-activating signalosome (24), or exploiting mimicry to activate inhibitory circuits (e.g. sialylated capsular polysaccharides of group B Streptococcus) (25, 26). For details on these upstream steps we refer the reader to excellent reviews (1, 27). Here we will focus on the process that is directly implicated in IS assembly -antigen presentation-, limiting the discussion to MHCII.

Antigen presentation to T cells by APCs plays an essential role in the initiation of adaptive immunity. As such, disruption of the process of antigen presentation is a mechanism co-opted by a number of bacterial pathogens to prevent the generation of specific effector T cells. Bacteria can modulate the MHCII pathway acting at different levels: by inhibiting MHCII gene transcription, by interfering with MHCII loading and trafficking, or by impairing antigen processing. The resulting defects in IS assembly translate into defects in T cell activation and differentiation to pathogen-specific helper T cell effectors. The intracellular pathogen *M. tubercolosis* is a remarkable example of how an individual pathogen can target the process of antigen presentation at every single level and we will use it as paradigm in the following sections.

3.1.1 Inhibition of MHCII Expression

M. tubercolosis has the ability to potently downregulate MHCII expression, which occurs as part of the APC activation program triggered by PRR engagement. A well characterized *M. tubercolosis* factor implicated in this function is the 19-kDa lipoprotein (LpqH) which acts a potent TLR2 agonist. The resulting excessive or prolonged TLR2 activation leads to the expression of isoforms of the transcriptional transactivator C/EBP that inhibit the IFNγ-dependent induction of class II transactivator (CIITA), on which MHCII gene expression crucially depends (28, 29). Preventing MHCII upregulation to disrupt antigen presentation is shared by other *M. tubercolosis* virulence factors such as the cell envelope-associated serine protease Hip1 (30), and co-opted by a number of pathogenic bacteria (e.g. 31). One such example is *H. pylori*, which uses ADP183 heptose, an intermediate metabolite in LPS

biosynthesis, to promote miR146b expression in macrophages, leading to downmodulation of CIITA expression (32).

Whether the protease activity of Hip1 influences directly CIITA expression is not known. However, this mechanism has been documented for *Chlamydia trachomatis*, which secretes proteases that promote the degradation of the transcription factor USF-1 that regulates IFN-γ induction of CIITA expression (33). A different mechanism to lower MHCII expression is exploited by *Salmonella*, which induces surface MHCII internalization by promoting the expression of the E3 ubiquitin ligase MARCH1 and K63-linked MHCII ubiquitination. Internalized ubiquitylated MHCII molecules are subsequently degraded following routing to the endolysosomal system (34) (**Figure 2**, **Table 1**).

3.1.2 Inhibition of Antigen Processing

Pathogenic bacteria can modulate the MHCII pathway by inhibiting the fusion of the phagosome containing internalized bacteria with the lysosome, which not only allows escape from killing but leads to impaired antigen processing. Again, using *M. tuberculosis* as paradigm, inhibition of phagolysosomal fusion has been shown to involve retention of the early endosome marker Rab5 at the phagosomal membrane, with concomitant exclusion of the lysosome marker Rab7 (83), which results in a delay in phagosome maturation and defective antigen processing. ***M. tuberculosis*** targets this process by using its lipid phosphatase SapM to hydrolyze the phospholipid PI3P, which is essential for phagosome-late endosome fusion (35). Similarly, *Salmonella* blocks phagosome maturation by modulating the phosphoinositide composition of the *Salmonella*-containing vacuole through its lipid phosphatase SopB (45). Hence inhibition of phagosome maturation is co-opted by many pathogenic bacteria to prevent antigen processing while escaping killing.

An alternative strategy used by *M.* tubercolosis for disrupting antigen processing is inhibition of phagosome function. One of the underlying mechanisms involves a M. tubercolosis-derived lipid, the mannose-capped form of lipoarabinomannan (manLAM). manLAM blocks phagosome acidification by reducing the local recruitment of the tethering molecule EEA1, which is essential for delivery of lysosomal hydrolases to the phagosome (36). The failure of EEA1 to associate with the phagosome in M. tubercolosis-infected cells is caused by defective production of PI3P at the phagosome membrane due to defective Ca^{2+}-dependent activation of the PI3K component VPS34 (35, 37, 84). Additionally, the transport of vacuolar ATPase (v-ATPase), which is essential for phagosome acidification and activation of lysosomal hydrolases, is impaired in *M. tuberculosis*-infected cells due to dephosphorylation of the VPS33B component of the v-ATPase sorting complex by the *M. tuberculosis* phosphatase PtpA (38) (**Figure 2**, **Table 1**).

3.1.3 Inhibition of MHCII Loading and Trafficking

An alternative strategy exploited by a variety of pathogens to inhibit antigen presentation is to interfere with MHCII loading

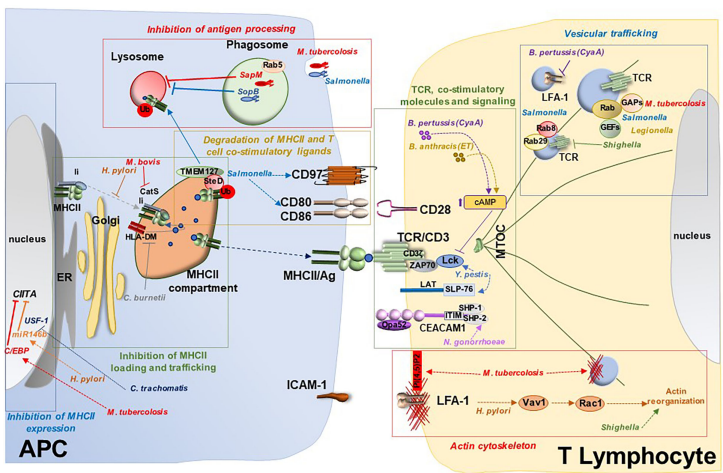

FIGURE 2 | Bacterial targeting of the immunological synapse. Model for suppression of IS assembly by bacterial pathogens. Bacterial pathogens exploit a variety of virulence factors to interfere with IS assembly at different steps, both at the APC side and at the T cell side. Bacteria target APCs and hence indirectly IS assembly by interfering with different mechanisms: i) MHCII inhibition through modulation of transcription factors responsible for its expression (e.g. CIITA regulation by *M. tuberculosis, Helicobacter pylori* and *Chlamydia trachomatis*); ii) inhibition of antigen processing through suppression of phagolysosomal fusion (e.g. *M. tuberculosis* and *Salmonella)*; iii) defective antigen processing and loading onto MHCII in the MHCII compartment (e.g. inhibition of the Ii-dependent pathway by *Helicobacter pylori* or targeting CatS and HLA-DM by *M. tuberculosis* and *Coxiella burnetii*, respectively); iv) degradation of MHCII and T cell co-stimulatory ligands such as CD80/CD86 and CD97 (e.g. *Salmonella*). Bacteria interfere directly with IS assembly at the T lymphocyte side by i) targeting expression and function of the TCR and co-stimulatory molecules (e.g. CD3ζ degradation by *M. tuberculosis*, CEACAM1 disabling by *Neisseria gonorrhoeae* or impairment of TCR signaling by *Yersinia pestis, Bordetella pertussis* and *Bacillus anthracis*); ii) subverting the actin cytoskeleton (e.g. *Shigella flexneri*, *Yersinia pestis* and *Salmonella enterica* serovar *Typhimurium)*; and iii) interfering with vesicular trafficking by modulating Rab GTPases (e.g. *Salmonella enterica*, *Legionella pneumophila*, *Shigella*, *M. tuberculosis*) or by targeting receptor trafficking (e.g the TCR by *Shigella* or LFA-1 by *Bordetella pertussis*).

TABLE 1 | Bacterial virulence factors that target directly or indirectly IS as.

Pathogens	IS targeting site	Vitulence factors	IS inhibition mechanisms	Ref.
Mycobacterium tuberculosis	**APC**	LpqH, Hip1	MHCII expression (C/EBP, CIITA)	28–
	T cell	SapM	Antigen processing (inhibition of phagolysosomal fusion)	30
		manLAM	Antigen processing (inhibition of phagosome acidification)	35
		miR-106b-5p	MHCII loading and trafficking (inhibition of CatS activity and expression)	35–
		manLAM	TCR and co-stimulatory molecules (CD3ζ degradation)	38
		mycolactone	Signaling at the IS (degradation of Lck, ZAP-70, LAT)	39
		SerB2	Signaling at the IS (inhibition of TCR signaling)	40
		SapM	Actin cytoskeleton (modulation of F-actin filament assembly)	41
		NdK	Actin cytoskeleton (modulation of phosphoinositide signaling)	42
			Vesicular trafficking (recruitment of Rab proteins)	35
			Vesicular trafficking (Rab GAP)	43
Mycobacterium bovis	**APC**	IL-10	MHCII loading and trafficking (inhibition of CatS activity and expression)	44
Chlamydia trachomatis	**APC**	proteases	MHCII expression (INF-γ, USF1, CIITA)	33
Salmonella enterica	**APC**	pH regulation	MHCII surface expression (E3 ubiquitin ligase, MARCH1, K63-linked MHCII ubiquitination)	34
	T cell	SopB	Antigen processing (inhibition of phagosome maturation)	45
		SteD	Degradation of MHCII (ubiquitylation)	46
		SopB, SopE, SptP	Inhibition of T cell co-stimulatory ligands (CD86/B7-2, CD97)	47,
		SopB	Actin cytoskeleton (Rho GEF mimics, GAP mimics)	48
		SopD2	Vesicular trafficking (SopB recruitment of Rab proteins)	49–
		GtgE	Vesicular trafficking (Rab GAP)	51
			Vesicular trafficking (inhibition of polarized TCR recycling)	52
				53
				54
Helicobacter pylori	**APC**	ADP-heptose	MHCII expression (miR146b, CIITA)	32
	T cell	VacA	MHCII loading and trafficking (inhibition of the Ii-dependent pathway)	55,
		VacA	TCR and co-stimulatory molecules (suppression of TCR signaling, Ca^{2+}-calcineurin pathway, dysfunctional MAP kinase network)	56
				57,
			Actin cytoskeleton perturbation	58
				57,
				59
Coxiella burnetii	**APC**		MHCII loading and trafficking (alteration of MHCII/HLA-DM interaction)	60
Pneumococcus pneumonia	**T cell**		TCR and co-stimulatory molecules (downregulation of CD28, ICOS, CD40L)	61
Staphylococcus aureus	**T cell**	SEA, SEB, SEE toxins	TCR and co-stimulatory molecules (massive T cell activation)	62
Neisseria gonorrhoeae	**T cell**	Opa52	TCR and co-stimulatory molecules (CEACAM1 suppression by phosphatases)	63
Yersinia pestis	**T cell**	YopH	TCR and co-stimulatory molecules (dephosphorylation of TCR signalosome)	64–
		YopE, YopT	Actin cytoskeleton (GAP mimics, modulation of GTP- GDP-bound forms of Rho GTPases)	67
				68,
				69
Bordetella pertussis	**T cell**	CyaA	TCR and co-stimulatory molecules (suppression of TCR signaling, cAMP)	70–
				72
Bacillus anthracis	**T cell**	edema toxin	TCR and co-stimulatory molecules (suppression of TCR signaling, cAMP)	73
Clostridium botulinum	**T cell**	C3 toxin	Actin cytoskeleton (modulation of GTP- GDP-bound forms of Rho GTPases)	74
Shigella flexneri	**T cell**	IcsA	Actin cytoskeleton (modulation of F-actin filament assembly)	75
		IpgD	Actin cytoskeleton (inhibition of cell chemotaxis)	76
		unidentified T3SS	Actin cytoskeleton (inhibition of IS assembly)	77
		effector	Vesicular trafficking (Rab GAP, inhibition of the polarized recycling of TCR-containing endosomes)	77,
		VirA, IpaJ		78
Listeria	**T cell**	ActA	Actin cytoskeleton (modulation of F-actin filament assembly)	79
Legionella pneumophila	**T cell**	LepB	Vesicular trafficking (Rab GAP)	80
		Lgp0393, DrrA/ SidM	Vesicular trafficking (Rab GEF)	81,
				82

and trafficking. Macrophage infection with *M. bovis* leads to the inhibition of both activity and expression of the cystein protease cathepsin S (Cat S) (44), which mediates the late cleavage steps of the invariant chain (Ii) cleavage (85) required for the generation of MHCII molecules that can be efficiently loaded with peptide antigens and delivered to the cell surface. The defect in CatS expression has been ascribed to the *M. bovis*-dependent induction of the suppressive cytokine IL-10 which blocks Cat S gene expression (44) as well as of *M. tubercolosis* microRNA miR-106b-5p which downregulates its transcript (39).

Other bacterial pathogens target the key steps of MHC loading and trafficking to suppress the initiation of T cell response. This is the case of *H. pylori* which, through its major virulence factor Vacuolating cytotoxin A (VacA), interferes with the proteolytic generation of T cell epitopes that are loaded onto newly synthesized MHCII molecules, specifically inhibiting the Ii-dependent pathway (55). In addition, MHCII molecules are retained in the *H. pylori*-containing vacuoles in *H. pylori*-infected DCs, such that their trafficking to the cell surface is prevented (56). *Coxiella burnetii* impairs antigen presentation at a different step -loading of peptide antigen- by altering the interaction of MHCII with HLA-DM, a key step required for displacing from MHCII the Ii CLIP peptide to allow for loading of pathogen-derived peptides and transport to the plasma membrane of functional pMHC complexes. In *C. burnetii*-infected cells MHCII molecules fail to dissociate form HLA-DM and accumulate in enlarged intracellular compartments (60) (**Figure 2**, **Table 1**).

3.1.4 Degradation of MHCII and T Cell Co-Stimulatory Ligands

An alternative mechanism for reducing the levels of pMHC complexes at the APC surface has been reported for *Salmonella*. This function is mediated by the type 3 secretion system effector SteD. This transmembrane protein forms a complex with mature endosome-associated MHCII molecules and the transmembrane host tumor suppressor TMEM127, a Nedd4 family E3 ubiquitin ligase adaptor. TMEM127 recruits the E3 ligase Wwp2 to the complex, inducing ubiquitylation of MHCII for subsequent lysosomal degradation (46). Interestingly, SteD exploits this degradation-promoting activity to reduce the expression of important T cell activating ligands expressed on APCs, including CD86/B7-2 which activated the key co-stimulatory receptor CD28 (47), and the plasma membrane protein CD97 that is required to stabilize the IS formed with T cells (48) (**Figure 2**, **Table 1**).

3.2 Direct Targeting of the T Cell IS by Bacterial Pathogens

Since the seminal discovery that lymphotropic viruses such as HIV-1 and HTLV-1 not only exploit the IS to evade the T cell response but apply the same building principles to form the virological synapse, a platform for cell-to-cell transmission, the IS has attracted major interest as a target for immune evasion by viral pathogens (86, 87). Whether and how bacterial pathogens can subvert IS assembly to avoid T cell immunity not indirectly by modulating DC activation and function, but directly, are questions that are only beginning to be formulated. DCs are present at the sites of infection where they can readily recognize pathogens through their wide array of PRRs, orchestrating a sophisticated response that not only optimizes their antigen presentation capacity but also provides all the signals that T cells require to differentiate to the most appropriate type of effector. At variance, T cells continuously cycle between blood and lymph and are activated in secondary lymphoid organs, where DCs migrate following pathogen recognition. However, a number of bacterial virulence factors are released as soluble factors that can be transported through the lymph to the closest lymph node station, where they can interact with naïve T cells and even enter them while not establishing a productive infection, as exemplified by the T cell delivery of Shigella T3SS effectors (88). Importantly, following their differentiation, effector T cells, whether CTLs or Th cells, are recruited to the site of infection to coordinate a combined attack with innate immune cells against the invading pathogen. There, effector T cells become a very relevant target for immune evasion.

Examples of IS targeting by bacterial pathogens are as yet very few. However, the substantial body of information acquired on how bacteria subvert pivotal cellular processes in host cells, such as cytoskeletal dynamics and vesicular trafficking, which are essential for IS assembly, suggests that we are looking at the tip of the iceberg. In this section we will present arguments to support this notion, discussing specific instances that provide experimental evidence that the IS is exploited not only by viruses, but also by bacteria, to evade T cell-mediated immunity.

3.2.1 Targeting the TCR and Co-Stimulatory Molecules

A strategy that mirrors at the T cell side what we described above on the APC side is downregulation of TCR expression, as exemplified in Pneumococcus-related sepsis. Of note, T cells from these patients also coordinately downregulated the expression of the major co-stimulatory receptors CD28, essential for T cell activation, and ICOS and CD40L, required for T cell-dependent B cell maturation (61). A different mechanism to modulate CD3 expression is exploited by *M. tubercolosis*, involving degradation of its key component CD3ζ. This is achieved through upregulation of the E3 ubiquitin ligase Grail by manLAM (40). Although not tested directly, downregulation of surface TCR is expected to impact on IS assembly and local signaling, as witnessed by primary immunodeficiency disorders with CD3 deficiency (89).

Staphylococcus aureus uses the amply characterized mechanism of forced, antigen-independent TCR binding to MHCII mediated by its toxins SEA, SEB and SEE to promote massive T cell activation and inflammatory cytokine production associated with defective anti-bacterial T cell response. These toxins are able to elicit IS assembly with high efficiency and are in fact used as surrogate antigens to study IS assembly in polyclonal T cells. Interestingly, a different mechanism involving the *Staphylococcus* superantigens SEA, SEB and TSST-1, has been recently reported, based on cross-linking the co-stimulatory receptor CD28 with its ligand B7.2 on APCs (62). Since CD28 co-localizes with the TCR at the cSMAC, this double locking action is expected to lead to the generation of hyperstable and hyperactive immune synapses.

Another example of co-inhibitory receptor targeting for T cell suppression is CEACAM1 disabling by *Neisseria gonorrhoeae*. CEACAM1 is expressed as two isoforms differing in the length of its intracellular domain, with the long isoform endowed of two immunoreceptor tyrosine-based inhibitory motifs (ITIM). The gonococcal protein Opa52 interacts with CEACAM1 on $CD4^+$ T

cells, leading to phosphorylation of its ITIM motifs and recruitment of the tyrosine phosphatases SHP-1 and SHP-2, which dampen TCR signaling (63). A similar strategy to suppress $CD4^+$ T cell activation is exploited by *Fusobacterium nucleatum*, *Neisseria meningitidis*, *Moraxella catarrhalis*, and *Haemophilus influenzae*, which also trigger CEACAM1 activation through specific adhesins (90–92). At variance, CEACAM1 has been recently reported to also act as a co-stimulatory receptor essential for the activation and proliferation of $CD8^+$ T cells, preventing their exhaustion and promoting their antiviral activity (93). Interestingly, CEACAM1 engagement leads to the recruitment of Lck to the TCR and stabilizes this key initiating kinase at the IS (93). This finding underscores the IS as a potential important target of bacterial pathogens that produce CEACAM1 ligands (**Figure 2**, **Table 1**).

3.2.2 Targeting Signaling at the IS

Major bacterial pathogens have the potential to target signaling downstream of the TCR, thereby affecting IS assembly and stability. *M. tubercolosis* exploits the manLAM-dependent upregulation of Grail mentioned above for CD3ζ downregulation to coordinately promote the degradation of essential mediators of the TCR signaling cascade, including the initiating tyrosine kinases Lck and ZAP-70, and the adaptor LAT required for signal amplification and diversification (40). Again, deficiency of these signaling mediators in experimental systems or primary immunodeficiencies supports the potential negative impact of *M. tubercolosis* in IS assembly. Another *M. tubercolosis*-derived molecule, mycolactone, interferes with T cell activation by inhibiting TCR signaling through an as yet unknown mechanism (41), underscoring T cell activation -and by inference IS assembly- as a relevant target for T cell disabling by *M. tubercolosis*.

Other pathogens have been reported to disrupt specific steps in TCR signaling. One such example is *Yersinia pestis*, which terminates TCR signaling using one of its outer membrane proteins, the protein tyrosine phosphatase YopH, that dephosphorylates key TCR signalosome components, including Lck, LAT and SLP-76 (64–67). *Bordetella pertussis* and *Bacillus anthracis* also suppress TCR signaling from its earliest step -activation of Lck- by elevating the cellular concentration of cAMP through their adenylate cyclase toxins, CyaA and edema toxin, respectively (70, 71). At variance, the *H. pylori* vacuolating cytotoxin (VacA) inhibits the Ca^{2+}-calcineurin pathway that is responsible for the activation of the key transcription factor NF-AT by inducing plasma membrane depolarization through its anion channel activity (57, 58). Additionally, VacA perturbs TCR signaling through an independent pathway triggered by its receptor-binding moiety, which selectively enhances the activity of the MAP kinase p38 but not Erk, leading to a dysfunctional MAP kinase network (57). That these effects have the potential to target the IS is witnessed by the ability of *Bordetella pertussis* CyaA to impair IS assembly through local cAMP production (71, 72) (**Figure 2**, **Table 1**).

3.2.3 Targeting the Actin Cytoskeleton

IS assembly is coordinated by the interplay of the actin and tubulin cytoskeletons. F-actin reorganization regulates multiple steps of IS formation, from integrin-mediated T cell adhesion to its cognate APC, to the recruitment of TCR microclusters to the cSMAC, to centrosome polarization beneath the synaptic membrane, to the process of sorting of cargoes, including TCRs, from early endosomes for their recycling to the IS to sustain signaling (94). Bacterial pathogens are masters at exploiting the host cell actin cytoskeleton for engulfment by host cells and intercellular dissemination, as exemplified by *Shigella flexneri*, *Yersinia pestis* and *Salmonella enterica* serovar *Typhimurium*. This is achieved by a remarkable array of T3SS effectors that promote actin remodeling by targeting directly or indirectly the Rho GTPases. The strategies evolved to modulate the activity of these small GTPases are multifarious, ranging from Rho GEF mimics (e.g. *Salmonella* SopB and SopE), to GAP mimics (e.g. *Salmonella* SptP, *Yersinia* YopE), to direct modulators of the active (GTP-bound) or inactive (GDP-bound) forms of Rho GTPases (e.g. the ADP-ribolysating *Clostridium* C3 toxin; the *Yersinia* protease YopT), to the process of F-actin filament assembly (e.g. *Shigella* IcsA and *Listeria* ActA mimicking activators of the actin nucleator N-WASP and of the actin adaptor Arp2/3, respectively; *M. tubercolosis* MtSerB2-mediated dephosphorylation and activation of cofilin) (95, 96). By acting on F-actin remodeling, these bacterial pathogens have the potential to interfere with the highly regulated process of IS assembly.

Direct experimental evidence in support of this hypothesis has been recently generated. *Shigella* had been previously shown to directly impair T cell chemotaxis through its T3SS effector IpgD, a lipid phosphatase that hydrolyses PI(4,5)P2, thus preventing leading edge formation in which actin dynamics plays a pivotal role (76). Recently Samassa and colleagues demonstrated that *Shigella* promotes actin polymerization in $CD4^+$ T cell through an as yet unidentified T3SS effector which leads to an increase in cell stiffness, thereby impairing the ability of T cells to scan APCs for the presence of specific pMHC and hence affecting the efficiency of T cell:APC conjugate formation, which is sets the stage for IS assembly (77). Since other bacterial pathogens may exploit their T3SS system to invade, albeit not productively infect, T cells, they might exploit the actin-subverting effectors to similarly affect IS formation. A similar scenario can be hypothesized for the *H. pylori* vacuolating cytotoxin VacA, which binds T cells by interacting with the integrin LFA-1 (59) and triggers the activation of the Rho family guanine nucleotide exchanger Vav1 and the downstream activation of Rac1, leading to perturbations in the actin cytoskeleton (57).

F-actin reorganization during IS assembly is critically controlled by the dynamic redistribution of lipid kinases and phosphatases that generate local pools of specific phosphoinositides. Actin clearance from the IS center is required to generate the secretory domain where exocytic and endocytic events occur. This is regulated by depletion from the IS center of the lipid kinase PIP5K, which is required to replenish PI(4,5)P2 at the synaptic membrane, thus sustaining actin polymerization (97). Remarkably, modulation of phosphoinositide signaling is a major target shared by a variety of bacterial pathogens (98). An interesting example is the *M.*

tubercolosis lipid phosphatase SapM, which dephosphorylates PI (4,5)P2 and PI3P to regulate the early stages of microbial phagocytosis and phagosome formation (35). Of note, while PI (4,5)P2 is implicated in F-actin polymerization during IS assembly, PI3P plays a crucial role in endosome trafficking, which is also centrally implicated in IS assembly, as detailed in the following section (**Figure 2**, **Table 1**).

3.2.4 Targeting Vesicular Trafficking

T cell activation requires TCR signaling to be sustained for several hours (99). This is achieved through the sequential mobilization of two TCR pools associated with the plasma membrane and recycling endosomes, respectively (17–19). Translocation of the centrosome towards the T cell:APC contact sets the stage for the polarized delivery of endosomal TCRs through their dynein-dependent transport along the microtubules. This strategy is co-exploited by a number of other receptors as well as membrane-associated signaling mediators that modulate the TCR signaling cascade (11, 12).

Vesicular trafficking is widely highjacked by bacterial pathogens for infection as well as to disable the bactericidal mechanisms of phagocytes. Major targets in this process are the Rab GTPases, largely through the modulation of their activity by a variety of virulence factors that act as GAPs or GEFs on specific Rab family members (100). Examples of bacterial Rab GAPs are *M. tubercolosis* Ndk (43), *Salmonella enterica* SopD2 (53), *Legionella pneumophila* LepB (80) and *Shigella* VirA (78), while examples of bacterial Rab GEFs are *Legionella pneumophila* Lgp0393 (82) and DrrA/SidM (81). Additionally, as mentioned in the previous paragraph, phosphoinositide signaling, which is essential for endosome maturation through recruitment of Rab proteins or their regulators or effectors, is disrupted by phosphoinositide-specific virulence factors, such as the phosphoinositide phosphatases *M. tubercolosis* SapM and *Salmonella* enterica SopB (98). Hence, similar to phagocytes, these factors may be expected to interfere with vesicular trafficking in T cells, thereby impacting on IS assembly and function.

Strong support to this hypothesis has been provided by the finding that *Shigella* impairs IS assembly by disrupting the polarized recycling of TCR-containing endosomes to the IS through two T3SS effectors, the Rab1 GAP VirA and the Arf/Arl targeting cysteine protease IpaJ (77). Additionally, we have shown that forced expression of the *Salmonella* protease GtgE, which cleaves and inactivates Rab29 and Rab8 (101, 102), similarly impairs IS assembly by inhibiting two sequential steps in the vesicular transport pathway that regulates polarized TCR recycling to the IS (54). Of note, the activity of Rab32 is also modulated by *Salmonella* SopD2 acting as a GAP (53), highlighting a combined targeting of Rab29 by distinct virulence factors of this pathogen. A different strategy is exploited by *Bordetella pertussis*, which uses its adenylate cyclase toxin CyaA to impair recycling of the integrin LFA-1, leading to premature IS disassembly (71) (**Figure 2**, **Table 1**).

4 CONCLUSIONS AND OUTLOOK

Pathogens are masters in the art of spotting the vulnerabilities of target cells and evolve strategies to either neutralize or subvert these to their own advantage to infect target cells and evade immune mediated destruction. As the platform where the T cell response to antigen recognition is coordinated, the IS represents one of such vulnerabilities. This is witnessed by evidence accumulated over the past several years showing that the processes that regulate IS assembly, from TCR signaling, to cytoskeleton dynamics, to vesicular trafficking, are targeted by lymphotropic viruses to thwart the antiviral T cell response and infect neighboring cells while remaining undetectable (86, 87). Interesting, IS targeting is exploited also by tumor cells to suppress antitumor immunity through both contact-dependent and -independent mechanisms, as amply documented in chronic lymphocytic leukemia (103). Hence, it is not surprising that bacterial pathogens have co-opted this strategy to evade T cell mediated immunity. While the evidence supporting this notion is as yet scant, it is likely to represent only the tip of the iceberg since the cellular processes known to be disrupted or subverted by bacterial virulence factors that coordinate infection of target cells, such as cytoskeletal dynamics, membrane trafficking or phosphoinositide signaling, are also centrally implicated in the process of IS assembly. Hence studies focusing on the IS as target of bacterial virulence factors are expected to provide major insights into the mechanisms of immune evasion by bacterial pathogens. Of note, bacterial pathogens that infect cells that are transported to peripheral lymphoid tissues, such as DCs or macrophages, can interfere with priming pathogen-specific T cells. While pathogens that remain confined in infected tissues may influence T cell priming through soluble factors that can be transported by the lymph, their physical separation prevents them from directly deploying the full array of virulence factors, targeting rather APCs for targeting this process. However, naive T cells differentiated to helper or cytotoxic effectors are recruited to the site of infection to coordinate the fight against the pathogens in concert with the innate immune cells. Since effector T cells assemble immune synapses with target cells for the selective delivery of cytokines and cytotoxic molecules, the potential IS-modulating functions of bacterial virulence factors may be highly effective to evade the effector mechanisms of these cells.

AUTHOR CONTRIBUTIONS

NC and CB wrote the paper. NC prepared the artwork.

FUNDING

CB is supported by grants from EU (ERC Synergy Grant 951329), AIRC (IG-2017 - ID 20148) and 464 Ministero dell'Istruzione, dell'Università e della Ricerca (Grant PRIN bando 2017 - 2017FS5SHL).

REFERENCES

1. Finlay BB, McFadden G. Anti-Immunology: Evasion of the Host Immune System by Bacterial and Viral Pathogens. *Cell* (2006) 124:767–82. doi: 10.1016/j.cell.2006.01.034
2. Karkhah A, Ebrahimpour S, Rostamtabar M, Koppolu V, Darvish S, Vasigala VKR, et al. Helicobacter Pylori Evasion Strategies of the Host Innate and Adaptive Immune Responses to Survive and Develop Gastrointestinal Diseases. *Microbiol Res* (2019) 218:49–57. doi: 10.1016/j.micres.2018.09.011
3. Celli J, Finlay BB. Bacterial Avoidance of Phagocytosis. *Trends Microbiol* (2002) 10:232–7. doi: 10.1016/s0966-842x(02)02343-0
4. Dustin ML. The Immunological Synapse. *Cancer Immunol Res* (2014) 2:1023–33. doi: 10.1158/2326-6066.CIR-14-0161
5. Monks CRF, Freiberg BA, Kupfer H, Sciaky N, Kupfer A. Three-Dimensional Segregation of Supramolecular Activation Clusters in T Cells. *Nature* (1998) 395:82–6. doi: 10.1038/25764
6. Yokosuka T, Saito T. The Immunological Synapse, TCR Microclusters, and T Cell Activation. *Curr Top Microbiol Immunol* (2010) 340:81–107. doi: 10.1007/978-3-642-03858-7_5
7. Das V, Nal B, Dujeancourt A, Thoulouze MI, Galli T, Roux P, et al. Activation-Induced Polarized Recycling Targets T Cell Antigen Receptors to the Immunological Synapse; Involvement of SNARE Complexes. *Immunity* (2004) 20:577–88. doi: 10.1016/s1074-7613(04)00106-2
8. Martín-Cófreces NB, Baixauli F, Sánchez-Madrid F. Immune Synapse: Conductor of Orchestrated Organelle Movement. *Trends Cell Biol* (2014) 24:61–72. doi: 10.1016/j.tcb.2013.09.005
9. Egen JG, Allison JP. Cytotoxic T Lymphocyte Antigen-4 Accumulation in the Immunological Synapse is Regulated by TCR Signal Strength. *Immunity* (2002) 16:23–35. doi: 10.1016/s1074-7613(01)00259-x
10. Bunnell SC, Hong DI, Kardon JR, Yamazaki T, McGlade CJ, Barr VA, et al. T Cell Receptor Ligation Induces the Formation of Dynamically Regulated Signaling Assemblies. *J Cell Biol* (2002) 158:1263–75. doi: 10.1083/jcb.200203043
11. Ehrlich LIR, Ebert PJR, Krummel MF, Weiss A, Davis MM. Dynamics of P56lck Translocation to the T Cell Immunological Synapse Following Agonist and Antagonist Stimulation. *Immunity* (2002) 17:809–22. doi: 10.1016/s1074-7613(02)00481-8
12. Bonello G, Blanchard N, Montoya MC, Aguado E, Langlet C, He HT, et al. Dynamic Recruitment of the Adaptor Protein LAT: LAT Exists in Two Distinct Intracellular Pools and Controls its Own Recruitment. *J Cell Sci* (2004) 117:1009–16. doi: 10.1242/jcs.00968
13. Bouchet J, Del Río-Iñiguez I, Lasserre R, Agüera-Gonzalez S, Cuche C, Danckaert A, et al. Rac1-Rab11-FIP3 Regulatory Hub Coordinates Vesicle Traffic With Actin Remodeling and T-Cell Activation. *EMBO J* (2016) 35:1160–74. doi: 10.15252/embj.201593274
14. Ritter AT, Angus KL, Griffiths GM. The Role of the Cytoskeleton at the Immunological Synapse. *Immunol Rev* (2013) 256:107–17. doi: 10.1111/imr.12117
15. Martín-Cófreces NB, Sánchez-Madrid F. Sailing to and Docking at the Immune Synapse: Role of Tubulin Dynamics and Molecular Motors. *Front Immunol* (2018) 9:1174. doi: 10.3389/fimmu.2018.01174
16. Hammer JA, Wang JC, Saeed M, Pedrosa AT. Origin, Organization, Dynamics, and Function of Actin and Actomyosin Networks at the T Cell Immunological Synapse. *Annu Rev Immunol* (2019) 37:201–24. doi: 10.1146/annurev-immunol-042718-04134
17. Soares H, Lasserre R, Alcover A. Orchestrating Cytoskeleton and Intracellular Vesicle Traffic to Build Functional Immunological Synapses. *Immunol Rev* (2013) 256:118–32. doi: 10.1111/imr.12110
18. Onnis A, Finetti F, Baldari CT. Vesicular Trafficking to the Immune Synapse: How to Assemble Receptor-Tailored Pathways From a Basic Building Set. *Front Immunol* (2016) 7:50. doi: 10.3389/fimmu.2016.00050
19. Finetti F, Cassioli C, Baldari CT. Transcellular Communication at the Immunological Synapse: A Vesicular Traffic-Mediated Mutual Exchange. *F1000Res* (20171880) 6. doi: 10.12688/f1000research.11944.1
20. Dustin ML, Chan AC. Signaling Takes Shape in Review the Immune System. *Cell* (2000) 103:283–94. doi: 10.1016/s0092-8674(00)00120-3
21. Kawasaki K, Ernst RK, Miller SI. 3-O-Deacylation of Lipid A by PagL, a PhoP/PhoQ-Regulated Deacylase of Salmonella Typhimurium, Modulates Signaling Through Toll-Like Receptor 4. *J Biol Chem* (2004) 279:20044–8. doi: 10.1074/jbc.M401275200
22. Newman RM, Salunkhe P, Godzik A, Reed JC. Identification and Characterization of a Novel Bacterial Virulence Factor That Shares Homology With Mammalian Toll/interleukin-1 Receptor Family Proteins. *Infect Immun* (2006) 74:594–601. doi: 10.1128/IAI.74.1.594-601.2006
23. Schesser K, Spiik AK, Dukuzumuremyi JM, Neurath MF, Pettersson S, Wolf-Watz H. The yopJ Locus is Required for Yersinia-Mediated Inhibition of NF-kappaB Activation and Cytokine Expression: YopJ Contains a Eukaryotic SH2-Like Domain That is Essential for its Repressive Activity. *Mol Microbiol* (1998) 28:1067–79. doi: 10.1046/j.1365-2958.1998.00851.x
24. Wang J, Ge P, Lei Z, Lu Z, Qiang L, Chai Q, et al. Mycobacterium Tuberculosis Protein Kinase G Acts as an Unusual Ubiquitinating Enzyme to Impair Host Immunity. *EMBO Rep* (2021) 22:e52175. doi: 10.15252/embr.202052175
25. Carlin AF, Lewis AL, Varki A, Nizet V. Group B Streptococcal Capsular Sialic Acids Interact With Siglecs (Immunoglobulin-Like Lectins) on Human Leukocytes. *J Bacteriol* (2007) 189:1231–7. doi: 10.1128/JB.01155-06
26. Carlin AF, Uchiyama S, Chang YC, Lewis AL, Nizet V, Varki A. Molecular Mimicry of Host Sialylated Glycans Allows a Bacterial Pathogen to Engage Neutrophil Siglec-9 and Dampen the Innate Immune Response. *Blood* (2009) 113:3333–6. doi: 10.1182/blood-2008-11-187302
27. Zhou D, Galán J. Salmonella Entry Into Host Cells: The Work in Concert of Type III Secreted Effector Proteins. *Microbes Infect* (2001) 3:1293–8. doi: 10.1016/s1286-4579(01)01489-7
28. Pai RK, Convery M, Hamilton TA, Boom WH, Harding CV. Inhibition of IFN-Gamma-Induced Class II Transactivator Expression by a 19-kDa Lipoprotein From Mycobacterium Tuberculosis: A Potential Mechanism for Immune Evasion. *J Immunol* (2003) 171:175–84. doi: 10.4049/jimmunol.171.1.175
29. Pennini ME, Pai RK, Schultz DC, Boom WH, Harding CV. Mycobacterium Tuberculosis 19-kDa Lipoprotein Inhibits IFN-Gamma-Induced Chromatin Remodeling of MHC2TA by TLR2 and MAPK Signaling. *J Immunol* (2006) 176:4323–30. doi: 10.4049/jimmunol.176.7.4323
30. Madan-Lala R, Sia JK, King R, Adekambi T, Monin L, Khader SA, et al. Mycobacterium Tuberculosis Impairs Dendritic Cell Functions Through the Serine Hydrolase Hip1. *J Immunol* (2014) 192:4263–72. doi: 10.4049/jimmunol.1303185
31. Barbaro Ade L, Tosi G, Frumento G, Bruschi E, D'Agostino A, Valle MT, et al. Block of Stat-1 Activation in Macrophages Phagocytosing Bacteria Causes Reduced Transcription of CIITA and Consequent Impaired Antigen Presentation. *Eur J Immunol* (2002) 32:1309–18. doi: 10.1002/1521-4141(200205)32:5<1309::aid-immu1309>3.0.co;2-4
32. Coletta S, Battaggia G, Della Bella C, Furlani M, Hauke M, Faass L, et al. ADP-Heptose Enables Helicobacter Pylori to Exploit Macrophages as a Survival Niche by Suppressing Antigen-Presenting HLA-II Expression. *FEBS Lett* (2021) 595:2160–8. doi: 10.1002/1873-3468.14156
33. Zhong G, Fan T, Liu L. Chlamydia Inhibits Interferon Gamma-Inducible Major Histocompatibility Complex Class II Expression by Degradation of Upstream Stimulatory Factor 1. *J Exp Med* (1999) 189:1931–8. doi: 10.1084/jem.189.12.1931
34. Gogoi M, Ravikumar V, Dixit NM, Chakravortty D. Salmonella Escapes Antigen Presentation Through K63 Ubiquitination Mediated Endosomal Proteolysis of*via* Modulation of Endosomal Acidification in Dendritic Cells. *Pathog Dis* (2018) 76. doi: 10.1093/femspd/ftx125
35. Vergne I, Chua J, Lee HH, Lucas M, Belisle J, Deretic V. Mechanism of Phagolysosome Biogenesis Block by Viable Mycobacterium Tuberculosis. *Proc Natl Acad Sci USA* (2005) 102:4033–8. doi: 10.1073/pnas.0409716102
36. Fratti RA, Chua J, Vergne I, Deretic V. Mycobacterium Tuberculosis Glycosylated Phosphatidylinositol Causes Phagosome Maturation Arrest. *Proc Natl Acad Sci USA* (2003) 100:5437–42. doi: 10.1073/pnas.0737613100
37. Vergne I, Chua J, Deretic V. Mycobacterium Tuberculosis Phagosome Maturation Arrest: Selective Targeting of PI3P-Dependent Membrane Trafficking. *Traffic* (2003) 4:600–6. doi: 10.1034/j.1600-0854.2003.00120.x
38. Wong D, Bach H, Sun J, Hmama Z, Av-Gay Y. Mycobacterium Tuberculosis Protein Tyrosine Phosphatase (PtpA) Excludes Host Vacuolar-H+-ATPase

to Inhibit Phagosome Acidification. *Proc Natl Acad Sci USA* (2011) 108:19371–6. doi: 10.1073/pnas.1109201108
39. Pires D, Bernard EM, Pombo JP, Carmo N, Fialho C, Gutierrez MG, et al. Mycobacterium Tuberculosis Modulates miR-106b-5p to Control Cathepsin S Expression Resulting in Higher Pathogen Survival and Poor T-Cell Activation. *Front Immunol* (2017) 8:1819. doi: 10.3389/fimmu.2017.01819
40. Sande OJ, Karim AF, Li. Q, Ding X, Harding CV, Rojas RE, et al. Mannose-Capped Lipoarabinomannan From Mycobacterium Tuberculosis Induces CD4+ T Cell Anergy *via* GRAIL. *J Immunol* (2016) 196:691–702. doi: 10.4049/jimmunol.1500710
41. Boulkroun S, Guenin-Macé L, Thoulouze MI, Monot M, Merckx A, Langsley G, et al. Mycolactone Suppresses T Cell Responsiveness by Altering Both Early Signaling and Posttranslational Events. *J Immunol* (2010) 184:1436–44. doi: 10.4049/jimmunol.0902854
42. Grant GA. Regulatory Mechanism of Mycobacterium Tuberculosis Phosphoserine Phosphatase Serb2. *Biochemistry* (2017) 56:6481–90. doi: 10.1021/acs.biochem.7b01082
43. Sun J, Wang X, Lau A, Liao TY, Bucci C, Hmama Z. Mycobacterial Nucleoside Diphosphate Kinase Blocks Phagosome Maturation in Murine RAW 264.7 Macrophages. *PloS One* (2010) 5:e8769. doi: 10.1371/journal.pone.0008769
44. Sendide K, Deghmane A, Pechkovsky D, Av-Gay Y, Talal A, Hmama Z. Mycobacterium Bovis BCG Attenuates Surface Expression of Mature Class II Molecules Through IL-10-Dependent Inhibition of Cathepsin S. *J Immunol* (2005) 175:5324–32. doi: 10.4049/jimmunol.175.8.5324
45. Norris FA, Wilson MP, Wallis TS, Galyov EE, Majerus PW. SopB, a Protein Required for Virulence of Salmonella Dublin, is an Inositol Phosphate Phosphatase. *Proc Natl Acad Sci USA* (1998) 95:14057–9. doi: 10.1073/pnas.95.24.14057
46. Alix E, Godlee C, Cerny O, Blundell S, Tocci R, Matthews S, et al. The Tumour Suppressor TMEM127 is a Nedd4-Family E3 Ligase Adaptor Required by Salmonella SteD to Ubiquitinate and Degrade MHC Class II Molecules. *Cell Host Microbe* (2020) 28:54–68.e7. doi: 10.1016/j.chom.2020.04.024
47. Bayer-Santos E, Durkin CH, Rigano LA, Kupz A, Alix E, Cerny O, et al. The Salmonella Effector SteD Mediates MARCH8-Dependent Ubiquitination of MHC II Molecules and Inhibits T Cell Activation. *Cell Host Microbe* (2016) 20:584–95. doi: 10.1016/j.chom.2016.10.007
48. Cerny O, Godlee C, Tocci R, Cross NE, Shi H, Williamson JC, et al. CD97 Stabilises the Immunological Synapse Between Dendritic Cells and T Cells and is Targeted for Degradation by the Salmonella Effector SteD. *PloS Pathog* (2021) 17:e1009771. doi: 10.1371/journal.ppat.1009771
49. Hardt WD, Chen LM, Schuebel KE, Bustelo XR, Galán JE. S. Typhimurium Encodes an Activator of Rho GTPases That Induces Membrane Ruffling and Nuclear Responses in Host Cells. *Cell* (1998) 93:815–26. doi: 10.1016/s0092-8674(00)81442-7
50. Fu Y, Galán JE. A Salmonella Protein Antagonizes Rac-1 and Cdc42 to Mediate Host-Cell Recovery After Bacterial Invasion. *Nature* (1999) 401:293–7. doi: 10.1038/45829
51. Truong D, Boddy KC, Canadien V, Brabant D, Fairn GD, D'Costa VM, et al. Salmonella Exploits Host Rho GTPase Signalling Pathways Through the Phosphatase Activity of SopB. *Cell Microbiol* (2018) 20:e12938. doi: 10.1111/cmi.12938
52. Hernandez LD, Hueffer K, Wenk MR, Galán JE. Salmonella Modulates Vesicular Traffic by Altering Phosphoinositide Metabolism. *Science* (2004) 304:1805–7. doi: 10.1126/science.1098188
53. Spanò S, Gao X, Hannemann S, Lara-Tejero M, Galán JE. A Bacterial Pathogen Targets a Host Rab-Family GTPase Defense Pathway With a GAP. *Cell Host Microbe* (2016) 19:216–26. doi: 10.1016/j.chom.2016.01.004
54. Onnis A, Finetti F, Patrussi L, Gottardo M, Cassioli C, Spanò S, et al. The Small GTPase Rab29 is a Common Regulator of Immune Synapse Assembly and Ciliogenesis. *Cell Death Differ* (2015) 22:1687–99. doi: 10.1038/cdd.2015.17
55. Molinari M, Salio M, Galli C, Norais N, Rappuoli R, Lanzavecchia A, et al. Selective Inhibition of Ii-Dependent Antigen Presentation by Helicobacter Pylori Toxin VacA. *J Exp Med* (1998) 187:135–40. doi: 10.1084/jem.187.1.135
56. Wang YH, Gorvel JP, Chu YT, Wu JJ, Lei HY. Helicobacter Pylori Impairs Murine Dendritic Cell Responses to Infection. *PloS One* (2010) 5:e10844. doi: 10.1371/journal.pone.0010844
57. Boncristiano M, Paccani SR, Barone S, Ulivieri C, Patrussi L, Ilver D, et al. The Helicobacter Pylori Vacuolating Toxin Inhibits T Cell Activation by Two Independent Mechanisms. *J Exp Med* (2003) 198:1887–97. doi: 10.1084/jem.20030621
58. Gebert B, Fischer W, Weiss E, Hoffmann R, Haas R. Helicobacter Pylori Vacuolating Cytotoxin Inhibits T Lymphocyte Activation. *Science* (2003) 301:1099–102. doi: 10.1126/science.1086871
59. Sewald X, Gebert-Vogl B, Prassl S, Barwig I, Weiss E, Fabbri M, et al. Integrin Subunit CD18 Is the T-Lymphocyte Receptor for the Helicobacter Pylori Vacuolating Cytotoxin. *Cell Host Microbe* (2008) 3:20–9. doi: 10.1016/j.chom.2007.11.003
60. Lem L, Riethof DA, Scidmore-Carlson M, Griffiths GM, Hackstadt T, Brodsky FM. Enhanced Interaction of HLA-DM With HLA-DR in Enlarged Vacuoles of Hereditary and Infectious Lysosomal Diseases. *J Immunol* (1999) 162:523–32.
61. Davenport EE, Burnham KL, Radhakrishnan J, Humburg P, Hutton P, Mills TC, et al. Genomic Landscape of the Individual Host Response and Outcomes in Sepsis: A Prospective Cohort Study. *Lancet Respir Med* (2016) 4:259–71. doi: 10.1016/S2213-2600(16)00046-1
62. Popugailo A, Rotfogel Z, Supper E, Hillman D, Kaempfer R. Staphylococcal and Streptococcal Superantigens Trigger B7/CD28 Costimulatory Receptor Engagement to Hyperinduce Inflammatory Cytokines. *Front Immunol* (2019) 10:942. doi: 10.3389/fimmu.2019.00942
63. Boulton IC, Gray-Owen SD. Neisserial Binding to CEACAM1 Arrests the Activation and Proliferation of CD4+ T Lymphocytes. *Nat Immunol* (2002) 3:229–36. doi: 10.1038/ni769
64. Yao T, Mecsas J, Healy JI, Falkow S, Chien Y. Suppression of T and B Lymphocyte Activation by a Yersinia Pseudotuberculosis Virulence Factor, yopH. *J Exp Med* (1999) 190:1343–50. doi: 10.1084/jem.190.9.1343
65. Alonso A, Bottini N, Bruckner S, Rahmouni S, Williams S, Schoenberger SP, et al. Lck Dephosphorylation at Tyr-394 and Inhibition of T Cell Antigen Receptor Signaling by Yersinia Phosphatase YopH. *J Biol Chem* (2004) 279:4922–8. doi: 10.1074/jbc.M308978200
66. Gerke C, Falkow S, Chien YH. The Adaptor Molecules LAT and SLP-76 are Specifically Targeted by Yersinia to Inhibit T Cell Activation. *J Exp Med* (2005) 201:361–71. doi: 10.1084/jem.20041120
67. de la Puerta ML, Trinidad AG, del Carmen Rodríguez M, Bogetz J, Sánchez Crespo M, Mustelin M, et al. Characterization of New Substrates Targeted by Yersinia Tyrosine Phosphatase YopH. *PloS One* (2009) 4:e4431. doi: 10.1371/journal.pone.000443
68. Von Pawel-Rammingen U, Telepnev MV, Schmidt G, Aktories K, Wolf-Watz H, Rosqvist R. GAP Activity of the Yersinia YopE Cytotoxin Specifically Targets the Rho Pathway: A Mechanism for Disruption of Actin Microfilament Structure. *Mol Microbiol* (2000) 36:737–48. doi: 10.1046/j.1365-2958.2000.01898.x
69. Shao F, Vacratsis PO, Bao Z, Bowers KE, Fierke CA, Dixon JE. Biochemical Characterization of the Yersinia YopT Protease: Cleavage Site and Recognition Elements in Rho GTPases. *Proc Natl Acad Sci USA* (2003) 100:904–9. doi: 10.1073/pnas.252770599
70. Paccani SR, Dal Molin F, Benagiano M, Ladant D, D'Elios MM, Montecucco C, et al. Suppression of T-Lymphocyte Activation and Chemotaxis by the Adenylate Cyclase Toxin of Bordetella Pertussis. *Infect Immun* (2008) 76:2822–32. doi: 10.1128/IAI.00200-08
71. Paccani SR, Finetti F, Davi M, Patrussi L, D'Elios MM, Ladant D, et al. The Bordetella Pertussis Adenylate Cyclase Toxin Binds to T Cells *via* LFA-1 and Induces its Disengagement From the Immune Synapse. *J Exp Med* (2011) 208:1317–30. doi: 10.1084/jem.20101558
72. Arumugham VB, Ulivieri C, Onnis A, Finetti F, Tonello F, Ladant D, et al. Compartmentalized Cyclic AMP Production by the Bordetella Pertussis and Bacillus Anthracis Adenylate Cyclase Toxins Differentially Affects the Immune Synapse in T Lymphocytes. *Front Immunol* (2018) 9:919. doi: 10.3389/fimmu.2018.00919
73. Paccani SR, Tonello F, Ghittoni R, Natale M, Muraro L, D'Elios MM, et al. Anthrax Toxins Suppress T Lymphocyte Activation by Disrupting Antigen

Receptor Signaling. *J Exp Med* (2005) 201:325–31. doi: 10.1084/jem.20041557
74. Chardin P, Bouquet P, Madaule P, Popoff MR, Rubin EJ, Gill DM. The Mammalian G Protein rhoC is ADP-Ribosylated by Clostridium Botulinum Exoenzyme C3 and Affects Actin Microfilaments in Vero Cells. *EMBO J* (1989) 8:1087–92. doi: 10.1002/j.1460-2075.1989.tb03477.x
75. Goldberg MB, Theriot JA. Shigella Flexneri Surface Protein IcsA is Sufficient to Direct Actin-Based Motility. *Proc Natl Acad Sci USA* (1995) 92:6572–6. doi: 10.1073/pnas.92.14.6572
76. Konradt C, Frigimelica E, Nothelfer K, Puhar A, Salgado-Pabon W, di Bartolo V, et al. The Shigella Flexneri Type Three Secretion System Effector IpgD Inhibits T Cell Migration by Manipulating Host Phosphoinositide Metabolism. *Cell Host Microbe* (2011) 9:263–72. doi: 10.1016/j.chom.2011.03.010
77. Samassa F, Ferrari ML, Husson J, Mikhailova A, Porat Z, Sidaner F, et al. Shigella Impairs Human T Lymphocyte Responsiveness by Hijacking Actin Cytoskeleton Dynamics and T Cell Receptor Vesicular Trafficking. *Cell Microbiol* (2020) 22:e13166. doi: 10.1111/cmi.13166
78. Ferrari ML, Malardé V, Grassart A, Salavessa L, Nigro G, Descorps-Declere S, et al. Shigella Promotes Major Alteration of Gut Epithelial Physiology and Tissue Invasion by Shutting Off Host Intracellular Transport. *Proc Natl Acad Sci USA* (2019) 116:13582–91. doi: 10.1073/pnas.1902922116
79. Kocks C, Hellio R, Gounon. P, Ohayon H, Cossart P. Polarized Distribution of Listeria Monocytogenes Surface Protein ActA at the Site of Directional Actin Assembly. *J Cell Sci* (1993) 105:699–710. doi: 10.1242/jcs.105.3.699
80. Ingmundson A, Delprato A, Lambright DG, Roy CR. Legionella Pneumophila Proteins That Regulate Rab1 Membrane Cycling. *Nature* (2007) 450:365–9. doi: 10.1038/nature06336
81. Machner MP, Isberg RR. Targeting of Host Rab GTPase Function by the Intravacuolar Pathogen Legionella Pneumophila. *Dev Cell* (2006) 11:47–56. doi: 10.1016/j.devcel.2006.05.013
82. Sohn YS, Shin HC, Park WS, Ge J, Kim CH, Lee BL, et al. Lpg0393 of Legionella Pneumophila is a Guanine-Nucleotide Exchange Factor for Rab5, Rab21 and Rab22. *PloS One* (2015) 10:e0118683. doi: 10.1371/journal.pone.0118683
83. Via LE, Deretic D, Ulmer RJ, Hibler NS, Huber LA, Deretic V. Arrest of Mycobacterial Phagosome Maturation is Caused by a Block in Vesicle Fusion Between Stages Controlled by Rab5 and Rab7. *J Biol Chem* (1997) 272:13326–31. doi: 10.1074/jbc.272.20.13326
84. Vergne I, Chua J, Deretic V. Tuberculosis Toxin Blocking Phagosome Maturation Inhibits a Novel Ca2+/Calmodulin-PI3K Hvps34 Cascade. *J Exp Med* (2003) 198:653–9. doi: 10.1084/jem.20030527
85. Bania J, Gatti E, Lelouard H, David A, Cappello F, Weber E, et al. Human Cathepsin S, But Not Cathepsin L, Degrades Efficiently MHC Class II-Associated Invariant Chain in Nonprofessional APCs. *Proc Natl Acad Sci USA* (2003) 10:6664–9. doi: 10.1073/pnas.1131604100
86. Fackler OT, Alcover A, Schwartz O. Modulation of the Immunological Synapse: A Key to HIV-1 Pathogenesis? *Nat Rev Immunol* (2007) 7:310–7. doi: 10.1038/nri2041
87. Bayliss RJ, Piguet V. Masters of Manipulation: Viral Modulation of the Immunological Synapse. *Cell Microbiol* (2018) 20:e12944. doi: 10.1111/cmi.12944
88. Brunner K, Samassa F, Sansonetti PJ, Phalipon A. Shigella-Mediated Immunosuppression in the Human Gut: Subversion Extends From Innate to Adaptive Immune Responses. *Hum Vaccin. Immunother.* (2019) 15:1317–25. doi: 10.1080/21645515.2019.1594132
89. Capitani N, Patrussi L, D'Elios MM, Baldari CT. "Dysfunctional Immune Synapses in T Cell Immunodeficiencies". In: MN D'Elios, CT Baldari and F Annunziato, editors. *Cellular Primary Immunodeficiencies*. Springer Cham: Springer (2021). p. 43–63.
90. Voges M, Bachmann V, Kammerer R, Gophna U, Hauck CR. CEACAM1 Recognition by Bacterial Pathogens is Species-Specific. *BMC Microbiol* (2010) 10:117. doi: 10.1186/1471-2180-10-117
91. Brewer ML, Dymock D, Brady RL, Singer BB, Virji M, Hill DJ. Fusobacterium Spp. Target Human CEACAM1 *via* the Trimeric Autotransporter Adhesin CbpF. *J Oral. Microbiol* (2019) 11:1565043. doi: 10.1080/20002297.2018.1565043
92. Galaski J, Shhadeh A, Umaña A, Yoo CC, Arpinati L, Isaacson B, et al. Fusobacterium Nucleatum CbpF Mediates Inhibition of T Cell Function Through CEACAM1 Activation. Front. *Cell Infect Microbiol* (2021) 11:69254. doi: 10.3389/fcimb.2021.69254
93. Khairnar V, Duhan V, Patil AM, Zhou F, Bhat H, Thoens C, et al. CEACAM1 Promotes CD8(+) T Cell Responses and Improves Control of a Chronic Viral Infection. *Nat Commun* (2018) 9:2561. doi: 10.1038/s41467-018-04832-2
94. Onnis A, Baldari CT. Orchestration of Immunological Synapse Assembly by Vesicular Trafficking. *Front Cell Dev Biol* (2019) 7:110. doi: 10.3389/fcell.2019.00110
95. Lemichez E, Aktories K. Hijacking of Rho GTPases During Bacterial Infection. *Exp Cell Res* (2013) 319:2329–36. doi: 10.1016/j.yexcr.2013.04.021
96. Stradal TEB, Schelhaas M. Actin Dynamics in Host-Pathogen Interaction. *FEBS Lett* (2018) 592:3658–69. doi: 10.1002/1873-3468.13173
97. Gawden-Bone CM, Frazer GL, Richard AC, Ma CY, Strege K, Griffiths GM. PIP5 Kinases Regulate Membrane Phosphoinositide and Actin Composition for Targeted Granule Secretion by Cytotoxic Lymphocytes. *Immunity* (2018) 49:427–437.e4. doi: 10.1016/j.immuni.2018.08.017
98. Pizarro-Cerdá J, Kühbacher A, Cossart P. Phosphoinositides and Host-Pathogen Interactions. *Biochim Biophys Acta* (2015) 1851:911–8. doi: 10.1016/j.bbalip.2014.09.011
99. Iezzi G, Karjalainen K, Lanzavecchia A. The Duration of Antigenic Stimulation Determines the Fate of Naive and Effector T Cells. *Immunity* (1998) 8:89–95. doi: 10.1016/s1074-7613(00)80461-6
100. Spanò S, Galán JE. Taking Control: Hijacking of Rab GTPases by Intracellular Bacterial Pathogens. *Small GTPases*. (2018) 9:182–91. doi: 10.1080/21541248.2017.1336192
101. Spanò S, Liu X, Galán JE. Proteolytic Targeting of Rab29 by an Effector Protein Distinguishes the Intracellular Compartments of Human-Adapted and Broad-Host Salmonella. *Proc Natl Acad Sci USA* (2011) 108:18418–23. doi: 10.1073/pnas.1111959108
102. Savitskiy S, Itzen A. SopD From Salmonella Specifically Inactivates Rab8. *Biochim Biophys Acta Proteins Proteom.* (2021) 186:140661. doi: 10.1016/j.bbapap.2021.140661
103. Ramsay AG, Clear AJ, Fatah R, Gribben JG. Multiple Inhibitory Ligands Induce Impaired T-Cell Immunologic Synapse Function in Chronic Lymphocytic Leukemia That can be Blocked With Lenalidomide: Establishing a Reversible Immune Evasion Mechanism in Human Cancer. *Blood* (2012) 120:1412–21. doi: 10.1182/blood-2012-02-411678

Conflict of Interest: The authors declare that the research was conducted in the absence of any commercial or financial relationships that could be construed as a potential conflict of interest.

Publisher's Note: All claims expressed in this article are solely those of the authors and do not necessarily represent those of their affiliated organizations, or those of the publisher, the editors and the reviewers. Any product that may be evaluated in this article, or claim that may be made by its manufacturer, is not guaranteed or endorsed by the publisher.

Copyright © 2022 Capitani and Baldari. This is an open-access article distributed under the terms of the Creative Commons Attribution License (CC BY). The use, distribution or reproduction in other forums is permitted, provided the original author(s) and the copyright owner(s) are credited and that the original publication in this journal is cited, in accordance with accepted academic practice. No use, distribution or reproduction is permitted which does not comply with these terms.

frontiers | Frontiers in Immunology

TYPE Original Research
PUBLISHED 15 July 2022
DOI 10.3389/fimmu.2022.874922

Check for updates

OPEN ACCESS

EDITED BY
Marina De Bernard,
University of Padua, Italy

REVIEWED BY
Yong Yang,
China Pharmaceutical University, China
Chao Jiang,
Zhejiang University, China
Jingxin Li,
Shandong University, China
Ning-Ning Liu,
Shanghai Jiao Tong University, China

*CORRESPONDENCE
Yiming Yin
yinyiming@xbiome.com
Wenjing Zhao
zhaowj29@ms.sysu.edu.cn

†These authors have contributed equally to this work

SPECIALTY SECTION
This article was submitted to Microbial Immunology, a section of the journal Frontiers in Immunology

RECEIVED 13 February 2022
ACCEPTED 27 June 2022
PUBLISHED 15 July 2022

CITATION
Huang J, Zheng X, Kang W, Hao H, Mao Y, Zhang H, Chen Y, Tan Y, He Y, Zhao W and Yin Y (2022) Metagenomic and metabolomic analyses reveal synergistic effects of fecal microbiota transplantation and anti-PD-1 therapy on treating colorectal cancer.
Front. Immunol. 13:874922.
doi: 10.3389/fimmu.2022.874922

COPYRIGHT
Copyright © 2022 Huang, Zheng, Kang, Hao, Mao, Zhang, Chen, Tan, He, Zhao and Yin. This is an open-access article distributed under the terms of the Creative Commons Attribution License (CC BY). The use, distribution or reproduction in other forums is permitted, provided the original author (s) and the copyright owner(s) are credited and that the original publication in this journal is cited, in accordance with accepted academic practice. No use, distribution or reproduction is permitted which does not comply with these terms.

Metagenomic and metabolomic analyses reveal synergistic effects of fecal microbiota transplantation and anti-PD-1 therapy on treating colorectal cancer

Jiayuan Huang[1†], Xing Zheng[2†], Wanying Kang[1†], Huaijie Hao[2], Yudan Mao[1], Hua Zhang[3], Yuan Chen[1], Yan Tan[2], Yulong He[1,3], Wenjing Zhao[1*] and Yiming Yin[2*]

[1]School of Medicine, Shenzhen Campus of Sun Yat-Sen University, Shenzhen, China, [2]Department of Research and Development, Shenzhen Xbiome Biotech Co. Ltd., Shenzhen, China, [3]Guangdong Provincial Key Laboratory of Digestive Cancer Research, Digestive Diseases Center, The Seventh Affiliated Hospital, Sun Yat-Sen University, Shenzhen, China

Anti-PD-1 immunotherapy has saved numerous lives of cancer patients; however, it only exerts efficacy in 10-15% of patients with colorectal cancer. Fecal microbiota transplantation (FMT) is a potential approach to improving the efficacy of anti-PD-1 therapy, whereas the detailed mechanisms and the applicability of this combination therapy remain unclear. In this study, we evaluated the synergistic effect of FMT with anti-PD-1 in curing colorectal tumor-bearing mice using a multi-omics approach. Mice treated with the combination therapy showed superior survival rate and tumor control, compared to the mice received anti-PD-1 therapy or FMT alone. Metagenomic analysis showed that composition of gut microbiota in tumor-bearing mice treated with anti-PD-1 therapy was remarkably altered through receiving FMT. Particularly, *Bacteroides* genus, including FMT-increased *B. thetaiotaomicron*, *B. fragilis*, and FMT-decreased *B. ovatus* might contribute to the enhanced efficacy of anti-PD-1 therapy. Furthermore, metabolomic analysis upon mouse plasma revealed several potential metabolites that upregulated after FMT, including punicic acid and aspirin, might promote the response to anti-PD-1 therapy *via* their immunomodulatory functions. This work broadens our understanding of the mechanism by which FMT improves the efficacy of anti-PD-1 therapy, which may contribute to the development of novel microbiota-based anti-cancer therapies.

KEYWORDS

fecal microbiota transplantation, anti-PD-1 therapy, immunotherapy, colorectal cancer, *Bacteroides*

Introduction

The application of immune checkpoint inhibitors (ICIs) has led to remarkable advances in the treatment of a wide range of cancers, including melanoma, non-small-cell lung cancer (NSCLC), gastric cancer, and breast cancer (1). Antibodies targeting the programmed cell death protein 1 (PD-1) are the most widely used ICIs, which work by blocking the binding between PD-1 receptor of T cells and PD-L1 ligand of tumor cells, and restoring the function of T cells that recognizes and eliminates tumor cells (2). ICI therapy has saved numerous lives since its approval in 2014 and could maintain long-term disease control in ICI responders. However, in terms of curing colorectal cancer (CRC), the majority of patients would present non-response to anti-PD-1 treatment due to the insufficient tumor-infiltrating lymphocytes (TILs) in the tumor microenvironment (TME) (3, 4). Only approximately 10% of patients with CRC, which are mismatch repair deficient (dMMR) or microsatellite instability high (MSI-H) subtypes, could benefit from anti-PD-1 therapy (5, 6). Therefore, it is important to develop novel strategies to optimize our current ICI therapy.

Human intestine harbors more than 10^{13} microorganisms, which play a key role in mediating human health and disease *via* shaping systemic and local immune functions (7). Since 2015, multiple studies have elucidated that the composition of gut microbiota was associated with the efficacy of anti-PD-1 therapy (8, 9). Notably, three groups (10–12) reported their work in 2018 observing highly diversified bacterial features (i.e. high abundance of *Akkermansia, Ruminococcus*, and *Bifidobacterium*) were individually related to the favorable clinical outcomes. The mechanisms by which gut microbiota improves anti-PD-1 efficacy involve the increased abundance of beneficial bacteria, enhancement of dendritic cell (DC) maturation, increased activity of anti-tumor $CD8^+$ T cells, and the promotion of T cell tumor infiltration (13). These findings suggest the potential approach to enhancing the effect of immunotherapy *via* regulating gut microbes (14).

Fecal microbiota transplantation (FMT) is a biomedical technology of transplanting functional microbiota into patients, to cure diseases *via* restoration of gut microbiota with normal composition and functions (12). FMT has been employed clinically as a main or adjunctive approach in treating a number of diseases, including *Clostridium difficile* infection, inflammatory bowel diseases, and irritable bowel syndrome (15). In 2021, two independent clinical studies demonstrated that FMT could promote the efficacy of anti-PD-1 therapy in 3/10 and 6/15 patients with PD-1-refractory melanoma, respectively (16, 17). Genes associated with peptides presentation by antigen-presenting cells (APCs) through MHC class I and IL-1 mediated signal transduction were upregulated in melanoma patients after FMT treatment (16). Another study demonstrated that patients with epithelial tumors who responded to the combinational treatment of FMT and ICI exerted increased compositions of $CD8^+$ T cells, T helper 1 (Th1) cells, and APCs in the tumor microenvironment, while a reduction of myeloid-derived suppressor cells infiltration was observed (10). Animal experiments elucidated that fecal transplantation into mouse models for lung cancer led to superior tumor suppression (18). However, the detailed mechanism and the applicability of this combination therapy in other cancer types require to be further illustrated.

In this study, we evaluated the antitumor efficacy of FMT from healthy human in combination with anti-PD-1 immunotherapy using CRC tumor-bearing mouse models and investigated the underlying mechanisms through multi-omics approaches. Our results provide a potential mechanistic basis of the synergistic effects of FMT and anti-PD-1 therapy on treating colorectal cancer, which will expand our knowledge on the mechanism of immunotherapy and assist with the development of novel anticancer therapy through modulating microbiota.

Methods

Animals

All animal experiments were conducted at Crown Biosciences Co. Ltd. (Taicang, China) and approved by its Institutional Animal Care and Use Committee (approval number: E4756-B1901). Female BALB/c mice were purchased from Shanghai Lingchang Biological Technology Co. Ltd. (animal certificate number: 20180003003129). All mice were housed under specific-pathogen-free conditions with ingested pellet food (radio-sterilized with cobalt 60) and autoclaved water provided ad libitum.

FMT production

Stool samples from healthy human donors with informed consent (volunteer number: 20190382) were collected using sterile boxes and processed within 2 h, as previously described (19). In a sterile anaerobic environment, the samples were thoroughly mixed with sterile normal saline (mass: volume = 1:5). Subsequently, filter bags with apertures of 1 mm, 0.25 mm, and 0.05 mm were used to remove solid particles and impurities in the stool samples. The filtered liquid was centrifuged at 5500 g at 4°C for 5 min, and the precipitation was collected. Bacterial viable counting was conducted *via* flow cytometry and anaerobic plate counting. The bacterial solution was adjusted to 0.83×10^{11} colony forming units per mL (CFU/mL), and mixed with autoclaved glycerol, frozen at −80°C until next use.

Cell culture

CT26 mouse colon carcinoma cells (one of the most commonly used murine tumor models) were obtained from

the Shanghai Institute of Life Sciences (CAT#: TCM37). Cells were cultured in RPMI 1640 culture medium (Gibco) supplemented with 10% fetal bovine serum (FBS) (Excell) and were cultured in a humidified incubator at 37°C, 5% CO_2. CT26 cells at the exponential growth stage were suspended in PBS for subcutaneous tumor inoculation in mice.

Tumor-bearing mouse model

Mice (7-8 weeks old) were inoculated with 5×10^5 CT26 cells per mouse by subcutaneous injection at Day 0 (Figure 1A). A total of 40 mice were randomly divided into four groups: Saline plus Rat IgG2a (designated as Control), FMT plus Rat IgG2a (FMT), Saline plus PD-1 antibody (aPD-1), and FMT in combination with PD-1 antibody (Combo). Sterile normal saline (200 µL per dose) or FMT (5×10^9 CFU/mouse) was administered by oral gavage on Days 9, 12, 15, and 18; Rat IgG2a (200 µg/mouse, Lenico) and PD-1 antibody (200 µg/mouse, RMP1-14, Lenico) was given by intraperitoneal injection on Days 8, 11, 14, and 17. On Day 24, the endpoint of the experiment, feces, blood, and tumors of tumor-bearing mice were collected, and tumor volume was determined as length × width^2 × 0.5. Survival rate was defined as the percentage of mice with a tumor volume of less than 2,000 mm^3 in each group.

Antibiotic treatment

From eight days before the tumor inoculation (Day -8) to Day -4, antibiotics were added to the drinking water in proportion, including ampicillin 1 (mg/mL), neomycin (1 mg/mL), metronidazole (1 mg/mL), vancomycin (0.5 mg/mL). From Day -3 to Day 7, ampicillin 1 mg/mL was added to the drinking water, and the mixture of metronidazole 10 mg/mL, neomycin 10 mg/mL, vancomycin 5 mg/mL, and amphotericin B 0.1 mg/mL was orally gavaged into each mouse twice a day, 200 µL each time.

Fecal DNA extraction and metagenomic analysis

Total genomic DNA of mouse fecal samples was extracted using QIAamp PowerFecal Pro DNA Kit (Qiagen, CAT#: 51804), according to the manufacturer's instructions. The concentration was measured by Qubit and the integrity of DNA bands was detected by agarose gel electrophoresis. Library construction and sequencing (Illumina NovaSeq 6000 platform) were performed at Novogene. Following data analyses were performed using KneadData, MetaPhlAn 2.0 and HUMAnN 2.0 with default settings (20).

Untargeted metabolomic analysis

Mice blood samples were mixed with ice-cold methanol (3:1, v:v), and centrifuged with 12,000 rpm at 4°C for 10 min. The supernatant was collected and centrifuged at 12,000 pm at 4°C for 5 min. The sample extractions were analyzed using an LC-ESI-MS/MS system (UPLC, Shim-pack UFLC Shimadzu CBM A system; MS, QTRAP® system). Chromatographic separation

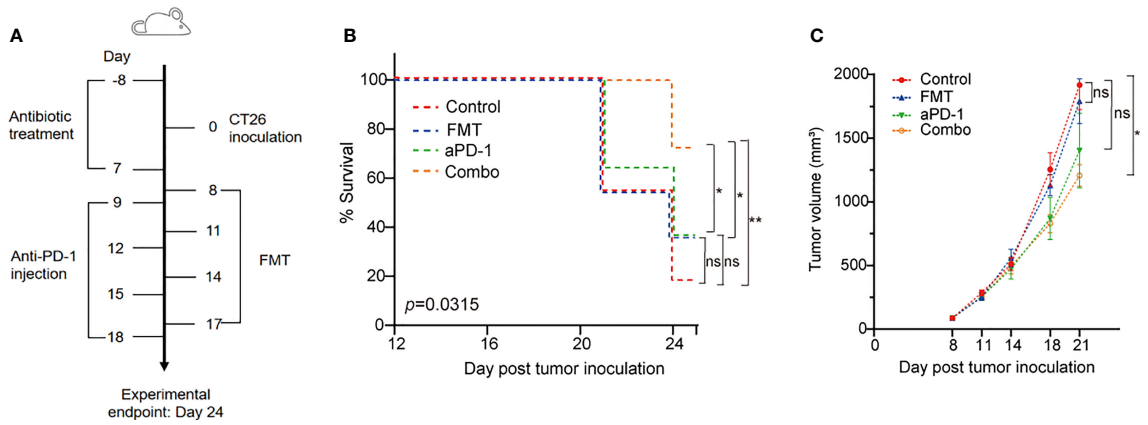

FIGURE 1
FMT and PD-1 antibody exerted synergistic anti-tumor effect in the CT26 tumor-bearing mice. **(A)** Schematic diagram of this study. **(B)** Survival curve of the CT26 tumor-bearing mice treated with FMT, aPD-1 or the combination. Statistical differences among four groups were examined using log-rank (Mantel-Cox) tests. *Post hoc* pair-wise comparisons were performed; *, p-value < 0.05; **, p-value < 0.01. **(C)** Tumor growth curves of the CT26 tumor-bearing mice treated with FMT, aPD-1 or the combination. Data are represented as mean ± SD (n = 10). Statistical differences were examined using Dunnett's test; *, p-value < 0.05.

was carried out on a Waters ACQUITY UPLC HSS T3 C18 (1.8 μm, 2.1 mm*100 mm) column. Subsequently, the mass spectrometry separation was carried out using electrospray ionization (ESI) in the positive and negative mode (21). Following untargeted metabolomic data analysis was performed using MetaboAnalyst 4.0 with default settings (22).

Statistical analysis

Statistical analyses were performed using R programming (version 4.0.3) and GraphPad Prism (version 8.0.2). Linear discriminant analysis effect size (LEfSe) was applied to identify differential species based on relative abundance using the Galaxy platform (http://huttenhower.sph.harvard.edu/galaxy). One-way analysis of variance (ANOVA) was performed to illustrate differential bacterial species and blood metabolites among multiple groups. False positive rate (FDR) method was employed to adjust the *p*-values when multiple comparisons were undertaken. Spearman's correlation analysis was used to illustrate the relationship between bacterial species and metabolites.

Results

FMT improved the efficacy of aPD-1 in tumor-bearing mouse model

We evaluated tumor volume and survival rate in CT26 tumor-bearing mice treated with FMT or aPD-1 either alone or in combination (Figure 1A). The Combo group showed the highest animal survival rate (70% vs. 10%, 30%, and 30% in control, FMT, and aPD-1 groups, respectively) on Day 24 after tumor incubation (Figure 1B). Log-rank (Mantel-Cox) tests showed a superior survival rate of mice treated with the combination compared to those treated with FMT or aPD-1 alone (Figure 1B). Consistently, compared with the Control group (tumor volume 1916.9 ± 193.0 on Day 21), the Combo group exhibited a significant tumor suppression (tumor volume 1206. 6 ± 86.4, *p*-value = 0.045), while the FMT and aPD-1 groups showed the tumor volumes of 1790.4 ± 176.3 (*p*-value = 0.945) and 1402.6 ± 293.2 (*p*-value = 0.188), respectively (Figure 1C). These results showed that the combinational therapy had a superior effect than either monotherapy alone in treating CT26-bearing mice in terms of both survival rate and tumor control.

FMT altered the composition of gut microbiota in tumor-bearing mice treated with aPD-1.

To investigate whether FMT improved the effects of aPD-1 by refining the gut microbiome, we next performed metagenomic analysis to examine FMT-induced changes of gut microbial composition and gene function. The PCA plot showed an obvious group-based clustering pattern among groups with or without FMT treatment, indicating that FMT significantly changed the composition of gut microbiota (Adonis R^2 = 0.58, *p*-value=0.000167), while the change caused by aPD-1 was less remarkable (Figure 2A). FMT were associated with, at the family level, the decrease of the relative abundance of *Bifidobacteriaceae*, *Porphyromonadaceae*, *Verrucomicrobiaceae*, and the increase of *Desulfovibrionaceae* and *Bacteroidaceae* (Figure 2B).

Nineteen significantly differential abundant species between the Combo group and aPD-1 group were identified using linear discriminant analysis. The relative abundance of multiple *Bacteroides* species (*B. thetaiotaomicron, B. stercoris, B. salyersiae, B. fragilis, B. cellulosilyticus, B. uniformis*, and *B. massiliensis*) and *Parabacteroides* species (*P. distasonis* and *P.* unclassified) were significantly increased in the mice treated with the combination of FMT and aPD-1, compared to those treated with aPD-1 alone. We also observed the decreased abundance of the abundance of *Clostridium* sp HGF2, *Enterococcus hirae, Dorea* 52, *Lactobacillus murinus*, and *Bacteroides ovatus* were observed (Figures 2C, E, S1A, B). In addition, we observed the abundance of specific bacteria, including *Alistipes indistinctus, Faecalibacterium prausnitzii, Bacteroides vulgatus*, and *Oscillibacter* unclassified were enriched, while *Bifidobacterium pseudolongum* were decreased by FMT treatment(p<0.05), and opposite trends were observed in aPD-1 group (Figure S1B).

The abundance of the aforementioned *Bacteroides* species showed a strong positive correlation with each other (|coefficient value|>0.6, p<0.05), as well as a negative correlation with *Enterococcus hirae, Dorea* 52, and *Lactobacillus murinus* (Figure 2D). Interestingly, the abundance of *Bacteroides ovatus* correlated negatively with the abundance of most of the FMT-upregulated species (Figure 2D). In a nutshell, our results showed that FMT altered the composition of gut microbiota, particularly *Bacteroides* (the increased *B. thetaiotaomicron, B. fragilis*, and *B. cellulosilyticus* and the decreased *B. ovatus*).

FMT upregulated microbial biosynthetic pathways of nucleotides and amino acids

Other than microbial composition, we also examined microbial gene functional changes upon treatments, which may influence gastrointestinal and systemic physiology. Compared to those of aPD-1 group, 27 differently abundant pathways out of 491 were identified in the combination group (|log2FC|>1, *p*-adjusted<0.05), indicating the potential microbial contribution towards better anti-PD-1 efficacy induced by FMT (Figure 3A). We observed that the anabolic pathways of several amino acids, including ornithine, histidine, lysine, citrulline, and isoleucine were significantly enriched by

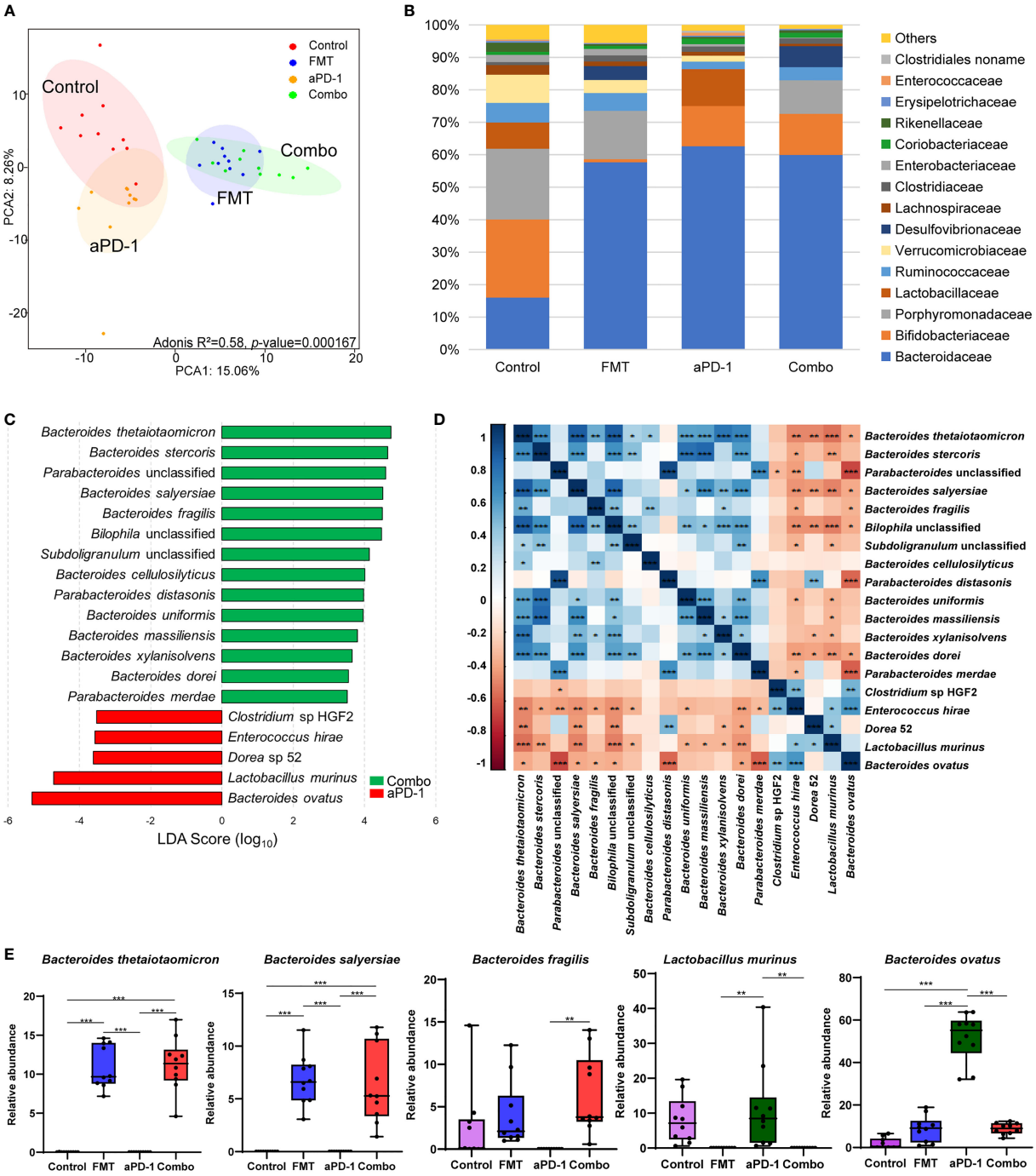

FIGURE 2
FMT altered the composition of gut microbiota in CT-26 tumor-bearing mice receiving anti-PD-1 therapy. **(A)** Principal components analysis (PCA) plot of the gut microbiota from mice. **(B)** Relative abundance of top 15 bacterial families in different groups. **(C)** LEfSe analysis showing differentially abundant bacterial species between FMT and Combo groups. **(D)** Heatmap showing the correlations of species significantly different between FMT and Combo groups. **(E)** Abundance of specific species in different groups. Data are represented as mean ± SD. *, p-value < 0.05; **, p-value < 0.01; ***, p-value < 0.001.

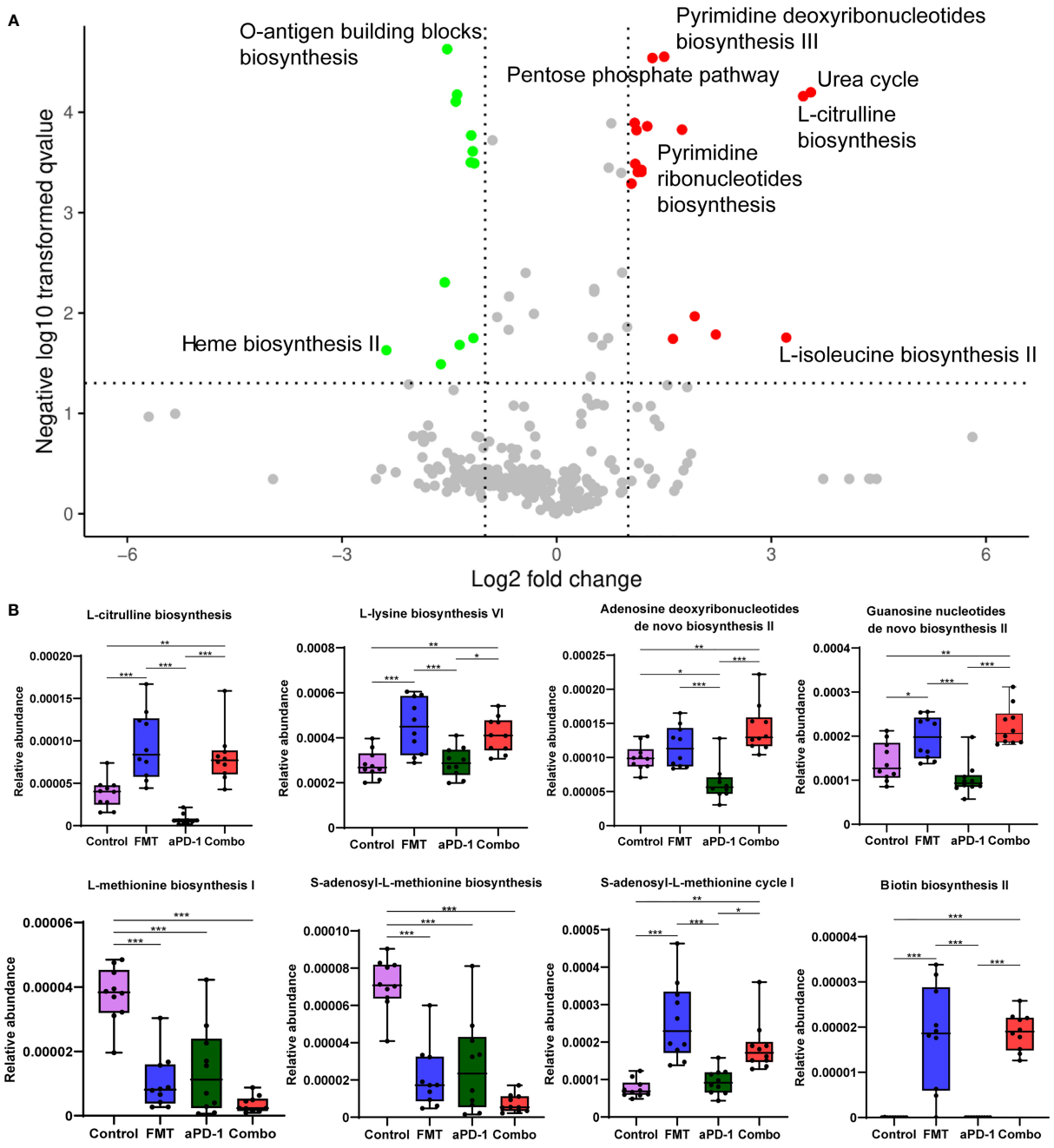

FIGURE 3
The effect of FMT and PD-1 antibody administration on gut metagenomic gene pathways. **(A)** Volcano plot showing differentially expressed microbial gene pathways between Combo and aPD-1 groups. **(B)** Abundance of specific gene pathways in different groups. Data are represented as mean ± SD. *, p-value < 0.05; **, p-value < 0.01; ***, p-value < 0.001.

FMT treatment. And the pathways of nucleotides *de novo* biosynthesis, including pyrimidine deoxyribonucleotides, guanosine nucleotides, and adenosine nucleotides were significantly up-regulated in FMT and Combo group. Notably, the pathways of methionine and S-adenosyl-L-methionine (SAM) biosynthesis were significantly decreased, and pathways of S-adenosyl-L-methionine cycle I was increased by FMT treatment. Moreover, the pathways of coenzyme A biosynthesis I, O-antigen building blocks biosynthesis, and heme biosynthesis II were enriched in the

aPD-1 group, while down-regulated in the Combo group. Furthermore, the pathway of biotin biosynthesis was significantly up-regulated by FMT treatment (Figure 3B, Figure S2).

FMT and aPD-1 synergistically remodeled mouse plasma metabolome

Metabolomic analyses were performed to examine the systemic change caused by FMT in tumor-bearing mice. Among a total number of 369 metabolites detected, the abundance of 8, 9, 34 metabolites were altered (p-adjusted < 0.05) following aPD-1, FMT, and Combo treatment, respectively, suggesting the synergistic effect of the combinational treatment (Figure 4A, Table S1). Abundance of 24 metabolites were altered upon the combinational treatment but not upon the treatment of FMT or aPD-1 alone, including the up-regulated kynurenic acid, estrone 3-sulfate and N -acetyl-D-glucosamine, and down-regulated glycine, nicotinamide and salicyluric acid (Table S1). The PCA plot also showed the distinct mouse plasma metabolome after different treatments (Figure 4B) (Adonis R^2 = 0.29, p-value = 0.000167).

Top 30 most differentially abundant metabolites among the four groups were identified based on the FDR values from one-way ANOVA analysis (Figure 4C). Compared with the PD-1 group, dethiobiotin, punicic acid, aspirin, L-arabitol, N-acetyl-D-glucosamine, L-dihydroorotic acid, dimethyl fumarate, trans-citridic acid, 1-Phenylethanol were significantly increased in the Combo group ($p<0.01$). While lysoPE (16:0), triethylamine, glycine, L-lysine, mandelic acid, L-glutamic acid, L-phenylalanine were significantly decreased ($p<0.01$) (Figures 4C, E, S3). The results indicated that combinational treatment of FMT and aPD-1 significantly altered plasma metabolic profiles. Furthermore, amino acids, including N-(2-Methylbenzoyl) glycine, N-phenyl acetyl glycine, glycine, L-proline, L-cysteine, L-serine and L-lysine were significantly down-regulated in the Combo group ($p<0.05$). Notably, the abundance of dethiobiotin, propyl hexanoate, and N-acetyl-D-glucosamine were significantly up-regulated in the Combo group (Figures 4C, E, S3).

To better understand the involvement of specific bacteria species in the alteration of host metabolism, correlation between plasma metabolites and the abundance of specific bacteria species were investigated. High abundance of *Bacteroides* species, such as *B. thetaiotaomicron, B. stercoris, B. salyersiae, B. cellulosilyticus*, was positively correlated with the low abundance of lysoPE (18:0), lysoPE (18:1), N-phenyl acetyl glycine, N-(2-Methylbenzoyl) glycine in plasma, and opposite trends were observed in *B. ovatus* and *Lactobacillus murinus* (Figure 4D). This result suggests a potential link among commensal microorganisms, differentially abundant metabolites, and treatment outcomes of anti-PD-1 therapeutic efficacy.

Discussion

Fecal microbiota transplantation from patients who responded to ICIs combined with ICIs exerts as a promising approach to treating melanoma (17). However, the detailed mechanisms and the applicability of this therapy are required to be further evaluated in multiple cancer types, such as colorectal cancer and lung cancer. Moreover, FMT using feces of cancer patients might carry safety risks such as detrimental pathogens or pathobionts; therefore, it's necessary to examine the effect of FMT using feces from healthy donors. In this study, our multi-omics investigation shows the potential synergistic effects of FMT using feces from healthy screened donors and anti-PD-1 therapy, in the treatment of mice bearing colorectal tumor.

A wide range of commensal bacterial species have been reported to be associated with the enhanced efficacy of ICIs, including *B. thetaiotaomicron* (23), *B. fragilis* (24), *B. cellulosilyticus* (25), *Parabacteroides distasonis* (26), *B. salyersiae* (27), and *B. uniformis* (13). In this study, our metagenomic analysis showed that FMT significantly upregulated the abundance of those potentially beneficial species, particularly those species from *Bacteroides* genus (Figures 2C, E). The reshaped microbiota caused by FMT might be associated with the refinement of tumor immune microenvironment (TIME) (28). Previous literature shows that *B. thetaiotaomicron*, which is most significantly upregulated by FMT in our data, has been reported to induce immune responses in dendritic cells (e.g. the expression of IL-10) and mediate intestinal homeostasis (29). *B. thetaiotaomicron* is also able to inhibit the growth of CRC cells *via* its metabolite propionate (23). Another *Bacteroides* species *B. fragilis* is associated with the favorable clinical outcome of CTLA-4 inhibitors (24) *via* inducing regulatory T cells to secrete IL-10 through the immunomodulatory molecule polysaccharide A (PSA) of *B. fragilis* (30). Additional immunomodulatory function of *B. fragilis* includes producing unique alpha-galactose ceramides (BfaGC) and subsequently activating NKT cells (e.g. upregulating IL-2 expression) (31). More recently, *B. cellulosilyticus* has been reported to be enriched in humanized microbiome mouse model of glioma and is a potential contributor to the enhanced efficacy of anti-PD-1 therapy (25). *B. cellulosilyticus* might modulate host immunity *via* its specific zwitterionic capsular polysaccharides (ZPSs) which can activate IL-10^+ regulatory T cells to secrete IL-10 (25). Notably, the abundance of upregulated *Bacteroides* species showed a strong positive correlation with each other (Figure 2D), suggesting their potential symbiotic link. Furthermore, several bacterial species which showed an up-regulation in the Combo group, *Bilophila wadsworthia* and *Lachnospiraceae bacterium* have not been reported previously. Their roles in anti-PD-1 treatment would be very interesting to investigate.

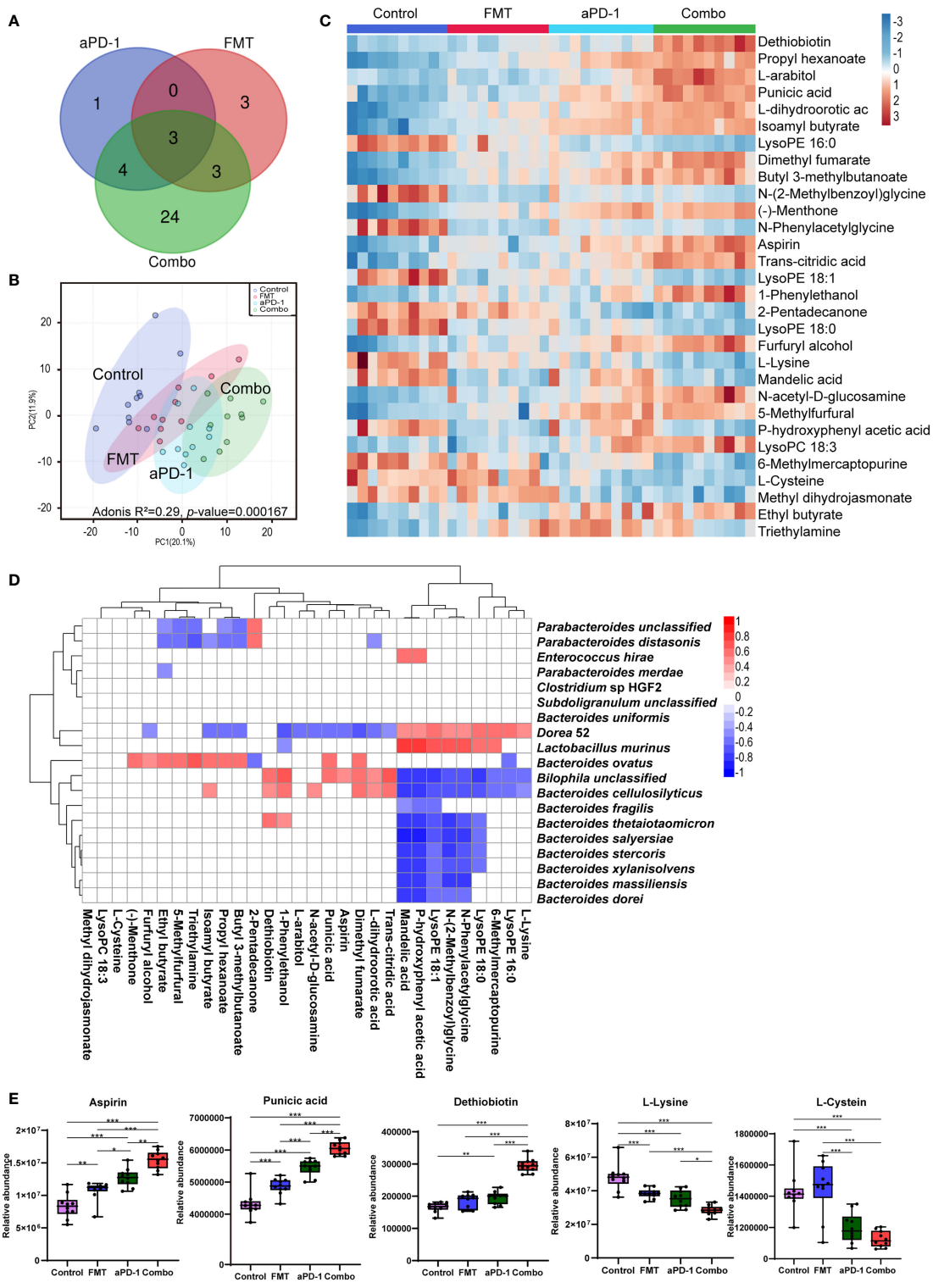

FIGURE 4
FMT altered plasma metabolites in CT-26 tumor-bearing mice receiving anti-PD-1 therapy. **(A)** Venn diagrams showing number of significantly changed metabolites in each group after treatment. **(B)** PCA plot of metabolomic results. **(C)** Heatmap of differentially abundant metabolites using one-way analysis of variance. **(D)** The correlations between metabolites and microorganism. **(E)** Abundance of specific metabolites in different groups. Data are represented as mean ± SD. *, p-value < 0.05; **, p-value < 0.01; ***, p-value < 0.001.

The abundance of two potentially detrimental species, *B. ovatus* and *Lactobacillus murinus*, were significantly decreased by FMT (Figures 2C, E). It was previously reported that the abundance of *B. ovatus* was associated with shorter progression-free survival (PFS) in melanoma patients receiving immunotherapy (32). *B. ovatus* might affect host immunity *via* inducing IgA and other approaches (33). In addition, the outgrowth of *L. murinus* is considered to impair gut metabolic function and exacerbate intestinal dysbiosis (34), therefore the depletion of *L. murinus* led by FMT may attenuate the microbial dysbiosis. Our metagenomic results are in line with the previously published studies that FMT could reshape the composition of both beneficial and harmful bacteria in the gut microbiome upon the anti-PD-1 treatment, which might result in the enhanced therapeutic efficacy.

Microbial gene functions and host metabolome were also reshaped by FMT in this study, which might benefit the efficacy of immunotherapy. Microbial gene pathways including nucleotides and amino acid biosynthesis pathways (e.g., pyrimidine deoxyribonucleotides, guanosine nucleotides, ornithine, isoleucine) were enriched after FMT, whereas methionine and SAM biosynthesis pathways were significantly downregulated (Figure 3A, B). Methionine is involved in the pathogenesis of cancer (35), and negatively related to the efficacy of radiotherapy (36). SAM, a universal methyl donor, is formed from methionine and has been reported to be associated with metastasis and recurrence in colorectal cancer patients (37). Inhibition of the production of methionine and SAM might contribute to the tumor regression. Furthermore, our metabolomics analysis showed higher abundance of aspirin which can inhibit the growth of *Fusobacterium nucleatum* (a detrimental bacteria species which aggravates colorectal cancer) after FMT treatment (38). Likewise, punicic acid was regulated upon FMT. The potent anti-tumor effect of punicic acid might play a role in tumor control (39, 40). Lastly, the abundance of several amino acids was also decreased in the plasma, including glycine, serine, and cysteine (Figure 4C, E, Figure S3). Previous research reported that the growth and proliferation of cancer cells require serine and glycine, and limiting exogenous serine and glycine could inhibit tumor growth in mouse models of colon cancer (41, 42). Moreover, the combinational treatment up-regulated the abundance of blood metabolite kynurenic acid, which has been reported to inhibit proliferation of colon cancer and renal cancer cells (43). To summarize, the enhanced efficacy of anti-PD-1 therapy led by FMT might be mediated by the altered microbial genome and blood metabolome.

The limitations of this study include the lack of experimental validation of the aforementioned bacterial species, metabolic pathways and changes of immune cells. Also, the synergistic effect exerted in mouse model may vary from that in the clinic. Further clinical investigation is being conducted in our laboratory and is anticipated to shed light on the detailed mechanisms of the promising combined use of FMT and anti-PD-1 therapy.

Conclusion

In summary, our study provides novel insight into the synergetic effects of microbiota transplantation and anti-PD-1 therapy in treating colorectal cancer, including the remodeling of gut microbiota and plasma metabolome. Our results suggest that *Bacteroides*, including the FMT-increased *B. thetaiotaomicron, B. fragilis*, and *B. cellulosilyticus* and decreased *B. ovatus* might contribute to the improved the efficacy of anti-PD-1 therapy. This work provides a potential mechanistic basis to further understand the role of FMT combined with anti-PD-1 therapy in treating various cancer types including colorectal cancer.

Data availability statement

The original contributions presented in the study are publicly available. This data can be found here: https://www.ncbi.nlm.nih.gov/bioproject/PRJNA799796.

Ethics statement

The animal study was reviewed and approved by Crown Biosciences Co. Ltd. (Taicang, China).

Author contributions

HH, YT, YY and WZ conceived the study. JH, XZ, WK and HH conducted the experiments. JH, XZ, HH, WK, YM and HZ performed data analysis and interpretation. YC, YH, YT, WZ and YY supervised and financially supported the study. JH, XZ, WK, WZ and YY wrote the manuscript with extensive input from all authors. All authors contributed to the article and approved the submitted version.

Funding

This study received funding from National Key Research and Development Program of China (2020YFA0907800) and Shenzhen Science and Technology Innovation Program (KQTD20200820145822023). The funders were not involved in the study design, collection, analysis, interpretation of data, the writing of this article or the decision to submit it for publication.

Acknowledgments

We thank Yan Kou, Xiaomin Xu, Bangzhuo Tong, Zhaoyan Lin (Xbiome) for their kind help with data analysis.

Conflict of interest

Authors XZ, HH, YT and YY are employed by Xbiome Biotech Co. Ltd.

The remaining authors declare that the research was conducted in the absence of any commercial or financial relationships that could be construed as a potential conflict of interest.

Publisher's note

All claims expressed in this article are solely those of the authors and do not necessarily represent those of their affiliated organizations, or those of the publisher, the editors and the reviewers. Any product that may be evaluated in this article, or claim that may be made by its manufacturer, is not guaranteed or endorsed by the publisher.

Supplementary material

The Supplementary Material for this article can be found online at: https://www.frontiersin.org/articles/10.3389/fimmu.2022.874922/full#supplementary-material.

SUPPLEMENTARY TABLE 1
Differentially abundant blood metabolites of the CT26 tumor-bearing mice upon different types of treatment. *p*-adjusted value < 0.05 is considered as statistically significant.

References

1. Schoenfeld AJ, Hellmann MD. Acquired resistance to immune checkpoint inhibitors. *Cancer Cell* (2020) 37(4):443–55. doi: 10.1016/j.ccell.2020.03.017

2. Alsaab HO, Sau S, Alzhrani R, Tatiparti K, Bhise K, Kashaw SK, et al. PD-1 and PD-L1 checkpoint signaling inhibition for cancer immunotherapy: mechanism, combinations, and clinical outcome. *Front Pharmacol* (2017) 8:561. doi: 10.3389/fphar.2017.00561

3. Zhang Y, Chen L. Classification of advanced human cancers based on tumor immunity in the microenvironment (time) for cancer immunotherapy. *JAMA Oncol* (2016) 2(11):1403–4. doi: 10.1001/jamaoncol.2016.2450

4. Kim TK, Herbst RS, Chen L. Defining and understanding adaptive resistance in cancer immunotherapy. *Trends Immunol* (2018) 39(8):624–31. doi: 10.1016/j.it.2018.05.001

5. Puccini A, Lenz HJ. Colorectal cancer in 2017: Practice-changing updates in the adjuvant and metastatic setting. *Nat Rev Clin Oncol* (2018) 15(2):77–8. doi: 10.1038/nrclinonc.2017.185

6. Ganesh K, Stadler ZK, Cercek A, Mendelsohn RB, Shia J, Segal NH, et al. Immunotherapy in colorectal cancer: rationale, challenges and potential. *Nat Rev Gastroenterol Hepatol* (2019) 16(6):361–75. doi: 10.1038/s41575-019-0126-x

7. Cox LM, Yamanishi S, Sohn J, Alekseyenko AV, Leung JM, Cho I, et al. Altering the intestinal microbiota during a critical developmental window has lasting metabolic consequences. *Cell* (2014) 158(4):705–21. doi: 10.1016/j.cell.2014.05.052

8. Gao Y, Bi D, Xie R, Li M, Guo J, Liu H, et al. *Fusobacterium nucleatum* enhances the efficacy of pd-l1 blockade in colorectal cancer. *Signal Transduct Targeted Ther* (2021) 6(1):398. doi: 10.1038/s41392-021-00795-x

9. Huang Y, Zhu N, Zheng X, Liu Y, Lu H, Yin X, et al. Intratumor microbiome analysis identifies positive association between *megasphaera* and survival of chinese patients with pancreatic ductal adenocarcinomas. *Front Immunol* (2022) 13:785422. doi: 10.3389/fimmu.2022.785422

10. Routy B, Le Chatelier E, Derosa L, Duong CPM, Alou MT, Daillère R, et al. Gut microbiome influences efficacy of pd-1-based immunotherapy against epithelial tumors. *Sci (New York NY)* (2018) 359(6371):91–7. doi: 10.1126/science.aan3706

11. Gopalakrishnan V, Spencer CN, Nezi L, Reuben A, Andrews MC, Karpinets TV, et al. Gut microbiome modulates response to anti-pd-1 immunotherapy in melanoma patients. *Sci (New York NY)* (2018) 359(6371):97–103. doi: 10.1126/science.aan4236

12. Matson V, Fessler J, Bao R, Chongsuwat T, Zha Y, Alegre ML, et al. The commensal microbiome is associated with anti-pd-1 efficacy in metastatic melanoma patients. *Sci (New York NY)* (2018) 359(6371):104–8. doi: 10.1126/science.aao3290

13. Si W, Liang H, Bugno J, Xu Q, Ding X, Yang K, et al. *Lactobacillus rhamnosus* GG induces cGAS/STING-dependent type I interferon and improves response to immune checkpoint blockade. *Gut* (2021) 71:521–533. doi: 10.1136/gutjnl-2020-323426

14. Toker J, Arora R, Wargo JA. The microbiome in immuno-oncology. *Adv Exp Med Biol* (2020) 1244:325–34. doi: 10.1007/978-3-030-41008-7_19

15. Borody TJ, Eslick GD, Clancy RL. Fecal microbiota transplantation as a new therapy: from *Clostridioides difficile* infection to inflammatory bowel disease, irritable bowel syndrome, and colon cancer. *Curr Opin Pharmacol* (2019) 49:43–51. doi: 10.1016/j.coph.2019.04.017

16. Baruch EN, Youngster I, Ben-Betzalel G, Ortenberg R, Lahat A, Katz L, et al. Fecal microbiota transplant promotes response in immunotherapy-refractory melanoma patients. *Sci (New York NY)* (2021) 371(6529):602–9. doi: 10.1126/science.abb5920

17. Davar D, Dzutsev AK, McCulloch JA, Rodrigues RR, Chauvin JM, Morrison RM, et al. Fecal microbiota transplant overcomes resistance to anti-pd-1 therapy in melanoma patients. *Sci (New York NY)* (2021) 371(6529):595–602. doi: 10.1126/science.abf3363

18. Huang J, Liu D, Wang Y, Liu L, Li J, Yuan J, et al. Ginseng polysaccharides alter the gut microbiota and kynurenine/tryptophan ratio, potentiating the antitumour effect of antiprogrammed cell death 1/programmed cell death ligand 1 (anti-PD-1/PD-L1) immunotherapy. *Gut* (2021), 71:1–12. doi: 10.1136/gutjnl-2020-321031

19. Wang Y, Tang J, Lv Q, Tan Y, Dong X, Liu H, et al. Establishment and resilience of transplanted gut microbiota in aged mice. *iScience* (2022) 25 (1):103654. doi: 10.1016/j.isci.2021.103654

20. Beghini F, McIver LJ, Blanco-Míguez A, Dubois L, Asnicar F, Maharjan S, et al. Integrating taxonomic, functional, and strain-level profiling of diverse microbial communities with biobakery 3. *eLife* (2021) 10:e65088. doi: 10.7554/eLife.65088

21. Chen W, Gong L, Guo Z, Wang W, Zhang H, Liu X, et al. A novel integrated method for large-scale detection, identification, and quantification of widely targeted metabolites: application in the study of rice metabolomics. *Mol Plant* (2013) 6(6):1769–80. doi: 10.1093/mp/sst080

22. Chong J, Wishart DS, Xia J. Using metaboanalyst 4.0 for comprehensive and integrative metabolomics data analysis. *Curr Protoc Bioinf* (2019) 68(1):e86. doi: 10.1002/cpbi.86

23. Ryu TY, Kim K, Han TS, Lee MO, Lee J, Choi J, et al. Human gut-microbiome-derived propionate coordinates proteasomal degradation *via* hectd2 upregulation to target EHMT2 in colorectal cancer. *ISME J* (2022), 16:1–17. doi: 10.1038/s41396-021-01119-1

24. Vétizou M, Pitt JM, Daillère R, Lepage P, Waldschmitt N, Flament C, et al. Anticancer immunotherapy by CTLA-4 blockade relies on the gut microbiota. *Sci (New York NY)* (2015) 350(6264):1079–84. doi: 10.1126/science.aad1329

25. Neff CP, Rhodes ME, Arnolds KL, Collins CB, Donnelly J, Nusbacher N, et al. Diverse intestinal bacteria contain putative zwitterionic capsular polysaccharides with anti-inflammatory properties. *Cell Host Microbe* (2016) 20 (4):535–47. doi: 10.1016/j.chom.2016.09.002

26. Gao G, Ma T, Zhang T, Jin H, Li Y, Kwok LY, et al. Adjunctive probiotic *Lactobacillus rhamnosus* probio-M9 administration enhances the effect of anti-pd-1 antitumor therapy *via* restoring antibiotic-disrupted gut microbiota. *Front Immunol* (2021) 12:772532. doi: 10.3389/fimmu.2021.772532

27. Derosa L, Routy B, Fidelle M, Iebba V, Alla L, Pasolli E, et al. Gut bacteria composition drives primary resistance to cancer immunotherapy in renal cell carcinoma patients. *Eur Urol* (2020) 78(2):195–206. doi: 10.1016/j.eururo.2020.04.044

28. Wong-Rolle A, Wei HK, Zhao C, Jin C. Unexpected guests in the tumor microenvironment: microbiome in cancer. *Protein Cell* (2021) 12(5):426–35. doi: 10.1007/s13238-020-00813-8

29. Durant L, Stentz R, Noble A, Brooks J, Gicheva N, Reddi D, et al. *Bacteroides thetaiotaomicron*-derived outer membrane vesicles promote regulatory dendritic cell responses in health but not in inflammatory bowel disease. *Microbiome* (2020) 8(1):88. doi: 10.1186/s40168-020-00868-z

30. Dasgupta S, Erturk-Hasdemir D, Ochoa-Reparaz J, Reinecker HC, Kasper DL. Plasmacytoid dendritic cells mediate anti-inflammatory responses to a gut commensal molecule *via* both innate and adaptive mechanisms. *Cell Host Microbe* (2014) 15(4):413–23. doi: 10.1016/j.chom.2014.03.006

31. Oh SF, Praveena T, Song H, Yoo JS, Jung DJ, Erturk-Hasdemir D, et al. Host immunomodulatory lipids created by symbionts from dietary amino acids. *Nature* (2021) 600(7888):302–7. doi: 10.1038/s41586-021-04083-0

32. Peters BA, Wilson M, Moran U, Pavlick A, Izsak A, Wechter T, et al. Relating the gut metagenome and metatranscriptome to immunotherapy responses in melanoma patients. *Genome Med* (2019) 11(1):61. doi: 10.1186/s13073-019-0672-4

33. Yang C, Mogno I, Contijoch EJ, Borgerding JN, Aggarwala V, Li Z, et al. Fecal IgA levels are determined by strain-level differences in bacteroides ovatus and are modifiable by gut microbiota manipulation. *Cell Host Microbe* (2020) 27 (3):467–75.e6. doi: 10.1016/j.chom.2020.01.016

34. Hayashi A, Mikami Y, Miyamoto K, Kamada N, Sato T, Mizuno S, et al. Intestinal dysbiosis and biotin deprivation induce alopecia through overgrowth of *Lactobacillus murinus* in mice. *Cell Rep* (2017) 20(7):1513–24. doi: 10.1016/j.celrep.2017.07.057

35. Sanderson SM, Gao X, Dai Z, Locasale JW. Methionine metabolism in health and cancer: a nexus of diet and precision medicine. *Nat Rev Cancer* (2019) 19(11):625–37. doi: 10.1038/s41568-019-0187-8

36. Gao X, Sanderson SM, Dai Z, Reid MA, Cooper DE, Lu M, et al. Dietary methionine influences therapy in mouse cancer models and alters human metabolism. *Nature* (2019) 572(7769):397–401. doi: 10.1038/s41586-019-1437-3

37. Zhang Y, Yu H, Zhang J, Gao H, Wang S, Li S, et al. Cul4A-DDB1-mediated monoubiquitination of phosphoglycerate dehydrogenase promotes colorectal cancer metastasis *via* increased s-adenosylmethionine. *J Clin Invest* (2021) 131 (21):1–18. doi: 10.1172/jci146187

38. Brennan CA, Nakatsu G, Gallini Comeau CA, Drew DA, Glickman JN, Schoen RE, et al. Aspirin modulation of the colorectal cancer-associated microbe *Fusobacterium nucleatum*. *mBio* (2021) 12(2):1–16. doi: 10.1128/mBio.00547-21

39. Mete M, Ünsal Ü, Aydemir I, Sönmez PK, Tuglu MI. Punicic acid inhibits glioblastoma migration and proliferation v*ia* the PI3k/AKT1/mTOR signaling pathway. *Anti-Cancer Agents Medicinal Chem* (2019) 19(9):1120–31. doi: 10.2174/1871520619666190405112507

40. Yuan G, Tan M, Chen X. Punicic acid ameliorates obesity and liver steatosis by regulating gut microbiota composition in mice. *Food Funct* (2021) 12(17):7897–908. doi: 10.1039/d1fo01152a

41. Maddocks ODK, Athineos D, Cheung EC, Lee P, Zhang T, van den Broek NJF, et al. Modulating the therapeutic response of tumours to dietary serine and glycine starvation. *Nature* (2017) 544(7650):372–6. doi: 10.1038/nature22056

42. Muthusamy T, Cordes T, Handzlik MK, You L, Lim EW, Gengatharan J, et al. Serine restriction alters sphingolipid diversity to constrain tumour growth. *Nature* (2020) 586(7831):790–5. doi: 10.1038/s41586-020-2609-x

43. Walczak K, Turski WA, Rajtar G. Kynurenic acid inhibits colon cancer proliferation in vitro: Effects on signaling pathways. *Amino Acids* (2020) 46 (10):2393–401. doi: 10.1007/s00726-014-1790-3

frontiers | Frontiers in Immunology

CASE REPORT
published: 22 July 2022
doi: 10.3389/fimmu.2022.923341

Case Report: Suspected Case of *Brucella*-Associated Immune Reconstitution Inflammatory Syndrome

Chunmei Qu[1†], *Nannan Xu*[1†], *Dehong Niu*[2], *Sai Wen*[1], *Hui Yang*[1], *Shanshan Wang*[1] *and Gang Wang*[1*]

[1] Department of Infectious Disease, Qilu Hospital, Cheeloo College of Medicine, Shandong University, Jinan, China, [2] Department of Oncology, the Fifth People's Hospital of Jinan, Jinan, China

Human brucellosis is one of the most prevalent zoonoses. There are many similarities between the pathogenesis of *Mycobacterium tuberculosis* (MTB) infection and that of brucellosis. Immune reconstitution inflammatory syndrome (IRIS) may occur during the treatment of MTB infection, but it has not been reported in brucellosis cases thus far. We report the case of a 40-year-old male whose condition initially improved after adequate anti-*Brucella* therapy. However, 3 weeks later, the patient presented with exacerbation of symptoms and development of a paravertebral abscess. After exclusion of other possible causes of clinical deterioration, immune reconstitution inflammatory syndrome (IRIS) with brucellosis was presumed. After supplementation with anti-*Brucella* treatment with corticosteroids, the abscess disappeared, and the symptoms completely resolved. Our case suggests that it is necessary to be aware of the possible occurrence of IRIS in patients with brucellosis in clinical practice.

Keywords: human brucellosis, IRIS, immune reconstitution, infection, case report

OPEN ACCESS

Edited by:
Maria Kaparakis-Liaskos, La Trobe University, Australia

Reviewed by:
Wondwossen Amogne Degu, Addis Ababa University, Ethiopia
Maryam Dadar, Razi Vaccine and Serum Research Institute, Iran

***Correspondence:**
Gang Wang
wangg1975@hotmail.com

[†]These authors have contributed equally to this work

Specialty section:
This article was submitted to Microbial Immunology, a section of the journal Frontiers in Immunology

Received: *19 April 2022*
Accepted: *24 June 2022*
Published: *22 July 2022*

Citation:
Qu C, Xu N, Niu D, Wen S, Yang H, Wang S and Wang G (2022) Case Report: Suspected Case of Brucella-Associated Immune Reconstitution Inflammatory Syndrome. Front. Immunol. 13:923341. doi: 10.3389/fimmu.2022.923341

CASE REPORT

A 40-year-old male farmer without any underlying condition was admitted to the hospital because of fever, night sweats, and pain in the lower back. The patient had reportedly been well until 3 weeks earlier, when back pain developed. He reported no associated trauma or injury, and no treatment was administered. On the 10th day of illness, he began to have fever with a temperature as high as 38.3°C, along with night sweats, fatigue, and weakness. He took antipyretics, but the fever and back pain persisted. The patient was sent to this hospital for further evaluation. The patient had occupational exposure to livestock. He was married and lived with his wife and children, who were well. There was no history of tuberculosis (TB), recent travel, transfusions, alcohol consumption, smoking, or intravenous drug use. The patient took no medications and had no history of drug allergy. There was no family history of disease.

Upon admission to the hospital, his core body temperature was 39°C, and he had severe pain in the L4–L5 area. Other vital signs and the remainder of the physical examination were normal. The erythrocyte sedimentation rate (ESR) was 70 mm/h. The levels of C-reactive protein (CRP) and interleukin-6 (IL-6) were slightly elevated to 28.93 mg/L and 10.88 pg/ml, respectively (**Figure 1A**).

A human immunodeficiency virus (HIV) test was negative, and other blood parameters, including routine blood parameters, liver enzyme concentrations, procalcitonin and creatinine levels, and antinuclear antibody concentrations, were normal. Blood culture was negative. Magnetic resonance imaging (MRI) showed abnormalities suggesting inflammation in the L4 region (**Figure 1B**). An enzyme-linked immunosorbent assay (ELISA) for the detection of *Brucella* antibodies was performed on plasma, and the results were positive, with an IgM concentration of 12.88 U/ml and an IgG concentration of 89.15 U/ml. To confirm the diagnosis, vertebral tissue aspiration was performed on the second day after admission. The aspirate was sent for bacterial culture and molecular TB detection. An automated blood culture system was used for bacterial culture. Five days later, the bacterial culture result was positive for *Brucella*, which is a very small, faintly stained Gram-negative coccobacillus that microscopically looks like "fine sand". Polymerase chain reaction (PCR) was negative for *Mycobacterium tuberculosis* (MTB) DNA. With a confirmed diagnosis of *Brucella*-related complicated infection, triple therapy including intravenous ceftriaxone (2.0 g qd) and oral rifampin (0.6 g qd) and doxycycline (0.1 g q12 h) was administered. After 2 weeks of treatment, the patient's body temperature returned to normal. The pain in the lower back was also relieved. However, 1 week later (3 weeks from the beginning of anti-*Brucella* therapy), the patient's symptoms recurred; he had a moderate to low fever (top temperature up to 38.5°C) accompanied by lower back pain. On physical examination, the pain in the L4–L5 area was significantly worse than before. The results of laboratory re-examination showed a normal white blood cell count (8.11×10^9/L), with 62.1% neutrophils, and a highly elevated ESR (86 mm/h) and CRP level (79.75 mg/L). The level of IL-6 increased to 53.91 pg/ml. Liver enzymes, creatinine levels, and antinuclear antibodies were within normal ranges. The second MRI (**Figure 1C**) scan of the spinal cord showed lesion expansion involving the lower posterior part of L4 and focal abscess formation. Due to the recurrent clinical symptoms and imaging findings, abscess puncture and drainage were performed. Cytology showed inflammatory infiltration (of which 65% were neutrophils) without neoplastic cells. Abscess fluid culture results were negative. Despite drainage for 5 days, the symptoms of fever and lower back pain persisted.

Because the patient had been hospitalized since the beginning of treatment, poor treatment adherence could be excluded. Other

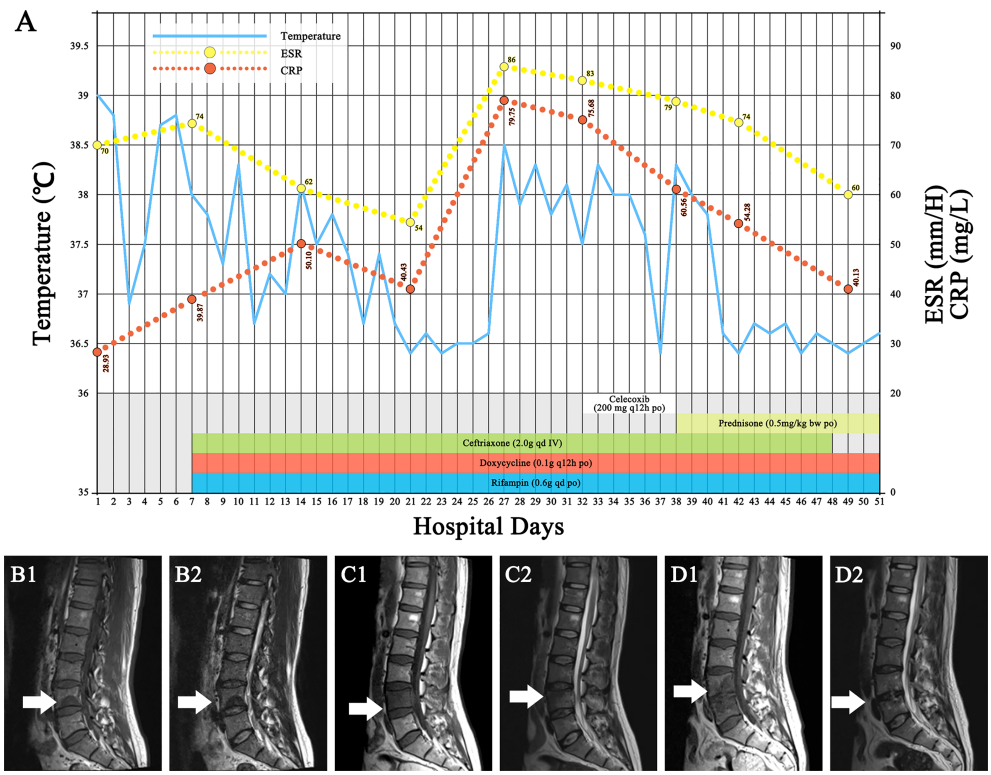

FIGURE 1 | Clinical data. **(A)** The hospitalization course, with the timeline of antibiotic treatment and the changes in body temperature and inflammatory markers. **(B1, B2)** The first MRI scan of the patient showed a lesion on the lower $^1/_2$ part of the fourth lumbar vertebra (white arrow), with low intensity on T1WI and high intensity on T2WI. **(C1, C2)** The second MRI scan, which occurred on follow-up day 27, showed that the lesion had expanded (white arrow), involving the posterior lower part of the fourth lumbar vertebra and with fusiform abscess formation behind the fourth vertebral body and lumbosacral soft tissue edema. **(D1, D2)** The last MRI scan (white arrow) after 3 months showed that the lower edge endplate of the fourth lumbar vertebra was damaged, the L4/L5 intervertebral disc was turbid, the retrovertebral abscess had disappeared, and the lumbosacral soft tissue edema was significantly improved. ESR, erythrocyte sedimentation rate; CRP, C-reactive protein.

infections and drug side effects were also ruled out. Accordingly, brucellosis-associated IRIS was suspected. There is no clinical consensus on the definition of infection-associated IRIS, and there is no treatment standard. With reference to the regimen for TB-IRIS treatment (1), the triple-agent anti-*Brucella* regimen was continued, and 200 mg of celecoxib twice a day was initiated. However, the patient's symptoms remained after 1 week of treatment. Anti-inflammatory treatment was changed to 0.5 mg of prednisone per kilogram bodyweight (35 mg). Within 3 days, the patient's body temperature returned to normal, and the back pain significantly improved. Both the ESR and CRP level also gradually returned to within normal ranges. Steroid therapy was tapered over a 2-month period. The triple-agent anti-*Brucella* therapy was continued for 2 weeks, followed by sequential treatment with oral doxycycline (0.1 g q12 h) and rifampin (0.6 g qd). After the overall 14-week treatment course, the third MRI scan (**Figure 1D**) showed that the lower edge endplate of L4 had been damaged, the paravertebral abscess had disappeared, and the lumbosacral soft tissue edema had significantly improved. At the last follow-up visit 2 months after completing the anti-*Brucella* therapy, the patient had no complaints, and the physical examination was normal.

DISCUSSION

IRIS is an excessive inflammatory response to infectious or noninfectious antigens after the reversal of underlying immunosuppression (2). The most common presentation is HIV-associated TB-IRIS (3), where patients' symptoms worsen following the initiation of anti-retroviral therapy. It also occurs among HIV-uninfected patients (4–6). IRIS has also been observed in infections by other pathogens, such as *Mycobacterium leprae* (7), *Mycobacterium ulcerans* (8), the *Mycobacterium avium* complex, and *Cryptococcus* (9). There are two forms of IRIS: paradoxical and unmasking (1).

There are currently no definitive diagnostic criteria for IRIS, especially in HIV-uninfected patients. IRIS is a diagnosis of exclusion (1). In our case, this patient's symptoms initially improved after adequate anti-*Brucella* treatment, but he subsequently presented with the paradoxical exacerbation of brucellosis-related symptoms and abnormal radiologic findings at the primary or new locations during treatment. Poor drug compliance, drug side effects, and other infections were excluded. ESR, IL-6, and CRP levels were markedly elevated. In addition, this patient showed a rapid and remarkable response to steroids. All of the above suggested a diagnosis of brucellosis-IRIS.

There are many similarities between the pathogenesis of MTB infection and that of brucellosis (10, 11). During MTB infection, multiple MTB components interfere with host cellular functions, inciting specific host immunodeficiency and helping the pathogen evade host innate immunity (12). A similar phenomenon also occurs in *Brucella* infection. For example, the outer membrane protein of *Brucella* can inhibit the production of TNF (13), IL-12 (14), and IFN-β (15); depress T-cell responses; and compromise monocyte/macrophage function, causing temporal immunosuppression (16). Therefore, it can invade multiple organs and often induce chronic infection (17). It is speculated that the mechanism of brucellosis-related IRIS is similar to that of TB-IRIS in HIV-uninfected individuals.

On the basis of previous studies, paradoxical reactions to TB-IRIS in immunocompetent patients have been attributed to immunological causes (6, 18). Antibiotic therapy leads to an apparent reversal of the immunosuppressive state, with phagocytosis of mycobacteria and a rapid onset of local cellular immune responses (5). An overwhelming and exaggerated immune recovery may lead to excessive immunopathological damage at the tissue level.

It is believed that patients with a high bacterial load have a high degree of immunosuppression at the foci of infection. We feel that, in the patient with effective antimicrobial therapy, the bacterial load is reduced, and host immunosuppression is restored, leading to an excessive inflammatory response. In addition, this patient was a young male, and according to TB-IRIS data, young age and male sex are high-risk factors for IRIS (19).

There is no standard treatment for IRIS; some patients experience spontaneous resolution, whereas others require the use of anti-inflammatory drugs, depending on the site and severity (20).

There are no previously reported cases of *Brucella*-related IRIS. This may be because IRIS might be misdiagnosed as superimposed infections, inadequate anti-*Brucella* treatment, or relapse. It is necessary to be aware of the possible occurrence of IRIS in brucellosis patients in clinical practice. Clinical deterioration during antibiotic treatment may be interpreted as treatment failure, leading to the change of antibiotic regimens or the prolongation of their use.

However, our study has some limitations. First, the high level of bacteriological hazard of live *Brucella* did not allow us to perform a drug susceptibility test for isolated *Brucella*. Additionally, we did not further screen the patient for potential immunodeficiency.

In summary, this is the first suspected case report describing paradoxical reactions during the treatment of *Brucella*. The case that we report here demonstrates that IRIS may occur during the treatment of *Brucella* infection. It is urgent to develop a definition of *Brucella*-associated IRIS for accurate diagnosis. The epidemiology, pathophysiology, and risk factors for *Brucella*-associated IRIS need further study.

DATA AVAILABILITY STATEMENT

The original contributions presented in the study are included in the article/supplementary material. Further inquiries can be directed to the corresponding author.

ETHICS STATEMENT

The studies involving human participants were reviewed and approved by the Shandong University Qilu Hospital human research protection committee. The patients/participants provided their written informed consent to participate in this study.

AUTHOR CONTRIBUTIONS

GW conceived of and coordinated the study. Material preparation, data collection and analysis were performed by CQ, DN, SaW, HY and ShW. The first draft of the manuscript was written by CQ. NX and GW edited and revised the manuscript. All authors read and approved the final manuscript.

REFERENCES

1. Lanzafame M, Vento S. Tuberculosis-Immune Reconstitution Inflammatory Syndrome. *J Clin Tuberc Other Mycobact Dis* (2016) 3:6–9. doi: 10.1016/j.jctube.2016.03.002
2. Armstrong WS. The Immune Reconstitution Inflammatory Syndrome: A Clinical Update. *Curr Infect Dis Rep* (2013) 15(1):39–45. doi: 10.1007/s11908-012-0308-y
3. Muller M, Wandel S, Colebunders R, Attia S, Furrer H, Egger M, et al. Immune Reconstitution Inflammatory Syndrome in Patients Starting Antiretroviral Therapy for HIV Infection: A Systematic Review and Meta-Analysis. *Lancet Infect Dis* (2010) 10(4):251–61. doi: 10.1016/S1473-3099(10)70026-8
4. Cheng VC, Ho PL, Lee RA, Chan KS, Chan KK, Woo PC, et al. Clinical Spectrum of Paradoxical Deterioration During Antituberculosis Therapy in non-HIV-Infected Patients. *Eur J Clin Microbiol Infect Dis* (2002) 21(11):803–9. doi: 10.1007/s10096-002-0821-2
5. Breen RA, Smith CJ, Bettinson H, Dart S, Bannister B, Johnson MA, et al. Paradoxical Reactions During Tuberculosis Treatment in Patients With and Without HIV Co-Infection. *Thorax* (2004) 59(8):704–7. doi: 10.1136/thx.2003.019224
6. Geri G, Passeron A, Heym B, Arlet JB, Pouchot J, Capron L, et al. Paradoxical Reactions During Treatment of Tuberculosis With Extrapulmonary Manifestations in HIV-Negative Patients. *Infection* (2013) 41(2):537–43. doi: 10.1007/s15010-012-0376-9
7. Ranque B, Nguyen VT, Vu HT, Nguyen TH, Nguyen NB, Pham XK, et al. Age is an Important Risk Factor for Onset and Sequelae of Reversal Reactions in Vietnamese Patients With Leprosy. *Clin Infect Dis* (2007) 44(1):33–40. doi: 10.1086/509923
8. O'Brien DP, Robson ME, Callan PP, McDonald AH. "Paradoxical" Immune-Mediated Reactions to Mycobacterium Ulcerans During Antibiotic Treatment: A Result of Treatment Success, Not Failure. *Med J Aust* (2009) 191(10):564–6. doi: 10.5694/j.1326-5377.2009.tb03313.x
9. Aggarwal D, Bhardwaj M, Kumar A, Saini V, Sawal N. Immune Reconstitution Inflammatory Syndrome in non-HIV Patients With Tuberculosis. *A Case Series Indian J Tuberc* (2020) 67(1):143–7. doi: 10.1016/j.ijtb.2019.02.018
10. Liu CH, Liu H, Ge B. Innate Immunity in Tuberculosis: Host Defense vs Pathogen Evasion. *Cell Mol Immunol* (2017) 14(12):963–75. doi: 10.1038/cmi.2017.88
11. Elfaki MG, Alaidan AA, Al-Hokail AA. Host Response to Brucella Infection: Review and Future Perspective. *J Infect Dev Ctries* (2015) 9(7):697–701. doi: 10.3855/jidc.6625
12. Tufariello JM, Chan J, Flynn JL. Latent Tuberculosis: Mechanisms of Host and Bacillus That Contribute to Persistent Infection. *Lancet Infect Dis* (2003) 3(9):578–90. doi: 10.1016/S1473-3099(03)00741-2
13. Jubier-Maurin V, Boigegrain RA, Cloeckaert A, Gross A, Alvarez-Martinez MT, Terraza A, et al. Major Outer Membrane Protein Omp25 of Brucella Suis is Involved in Inhibition of Tumor Necrosis Factor Alpha Production During Infection of Human Macrophages. *Infect Immun* (2001) 69(8):4823–30. doi: 10.1128/IAI.69.8.4823-4830.2001
14. Cui B, Liu W, Wang X, Chen Y, Du Q, Zhao X, et al. Brucella Omp25 Upregulates miR-155, miR-21-5p, and miR-23b to Inhibit Interleukin-12 Production *via* Modulation of Programmed Death-1 Signaling in Human Monocyte/Macrophages. *Front Immunol* (2017) 8:708. doi: 10.3389/fimmu.2017.00708
15. Li R, Liu W, Yin X, Zheng F, Wang Z, Wu X, et al. Brucella Spp. Omp25 Promotes Proteasome-Mediated cGAS Degradation to Attenuate IFN-Beta Production. *Front Microbiol* (2021) 12:702881. doi: 10.3389/fmicb.2021.702881
16. Elfaki MG, Al-Hokail AA. Transforming Growth Factor Beta Production Correlates With Depressed Lymphocytes Function in Humans With Chronic Brucellosis. *Microbes Infect* (2009) 11(14-15):1089–96. doi: 10.1016/j.micinf.2009.08.001
17. Roop RM2nd, Gaines JM, Anderson ES, Caswell CC, Martin DW. Survival of the Fittest: How Brucella Strains Adapt to Their Intracellular Niche in the Host. *Med Microbiol Immunol* (2009) 198(4):221–38. doi: 10.1007/s00430-009-0123-8
18. Cheng SL, Wang HC, Yang PC. Paradoxical Response During Anti-Tuberculosis Treatment in HIV-Negative Patients With Pulmonary Tuberculosis. *Int J Tuberc Lung Dis* (2007) 11(12):1290–5.
19. Weber MR, Fehr JS, Kuhn FP, Kaelin MB. Approach for Tuberculosis-Associated Immune Reconstitution Inflammatory Syndrome in an HIV-Negative Patient. *BMJ Case Rep* (2021) 14(8):e232639. doi: 10.1136/bcr-2019-232639
20. Friedland G. Tuberculosis Immune Reconstitution Inflammatory Syndrome: Drug Resistance and the Critical Need for Better Diagnostics. *Clin Infect Dis* (2009) 48(5):677–9. doi: 10.1086/596765

Conflict of Interest: The authors declare that the research was conducted in the absence of any commercial or financial relationships that could be construed as a potential conflict of interest.

Publisher's Note: All claims expressed in this article are solely those of the authors and do not necessarily represent those of their affiliated organizations, or those of the publisher, the editors and the reviewers. Any product that may be evaluated in this article, or claim that may be made by its manufacturer, is not guaranteed or endorsed by the publisher.

Copyright © 2022 Qu, Xu, Niu, Wen, Yang, Wang and Wang. This is an open-access article distributed under the terms of the Creative Commons Attribution License (CC BY). The use, distribution or reproduction in other forums is permitted, provided the original author(s) and the copyright owner(s) are credited and that the original publication in this journal is cited, in accordance with accepted academic practice. No use, distribution or reproduction is permitted which does not comply with these terms.

frontiers | Frontiers in Immunology

TYPE Review
PUBLISHED 28 July 2022
DOI 10.3389/fimmu.2022.930882

Check for updates

OPEN ACCESS

EDITED BY
Joseph Alex Duncan,
University of North Carolina at Chapel Hill, United States

REVIEWED BY
Shraddha Tuladhar,
St. Jude Children's Research Hospital, United States
Irving Coy Allen,
Virginia Tech, United States
Catherine Grimes,
University of Delaware, United States

*CORRESPONDENCE
Thomas A. Kufer
thomas.kufer@uni-hohenheim.de

SPECIALTY SECTION
This article was submitted to Microbial Immunology, a section of the journal Frontiers in Immunology

RECEIVED 28 April 2022
ACCEPTED 04 July 2022
PUBLISHED 28 July 2022

CITATION
Kienes I, Johnston EL, Bitto NJ, Kaparakis-Liaskos M and Kufer TA (2022) Bacterial subversion of NLR-mediated immune responses. *Front. Immunol.* 13:930882. doi: 10.3389/fimmu.2022.930882

COPYRIGHT
© 2022 Kienes, Johnston, Bitto, Kaparakis-Liaskos and Kufer. This is an open-access article distributed under the terms of the Creative Commons Attribution License (CC BY). The use, distribution or reproduction in other forums is permitted, provided the original author(s) and the copyright owner(s) are credited and that the original publication in this journal is cited, in accordance with accepted academic practice. No use, distribution or reproduction is permitted which does not comply with these terms.

Bacterial subversion of NLR-mediated immune responses

Ioannis Kienes[1], Ella L. Johnston[2,3], Natalie J. Bitto[2,3], Maria Kaparakis-Liaskos[2,3] and Thomas A. Kufer[1]*

[1]Department of Immunology, University of Hohenheim, Stuttgart, Germany, [2]Department of Microbiology, Anatomy, Physiology and Pharmacology, La Trobe University, Melbourne, VIC, Australia, [3]Research Centre for Extracellular Vesicles, La Trobe University, Melbourne, VIC, Australia

Members of the mammalian Nod-like receptor (NLR) protein family are important intracellular sensors for bacteria. Bacteria have evolved under the pressure of detection by host immune sensing systems, leading to adaptive subversion strategies to dampen immune responses for their benefits. These include modification of microbe-associated molecular patterns (MAMPs), interception of innate immune pathways by secreted effector proteins and sophisticated instruction of anti-inflammatory adaptive immune responses. Here, we summarise our current understanding of subversion strategies used by bacterial pathogens to manipulate NLR-mediated responses, focusing on the well-studied members NOD1/2, and the inflammasome forming NLRs NLRC4, and NLRP3. We discuss how bacterial pathogens and their products activate these NLRs to promote inflammation and disease and the range of mechanisms used by bacterial pathogens to evade detection by NLRs and to block or dampen NLR activation to ultimately interfere with the generation of host immunity. Moreover, we discuss how bacteria utilise NLRs to facilitate immunotolerance and persistence in the host and outline how various mechanisms used to attenuate innate immune responses towards bacterial pathogens can also aid the host by reducing immunopathologies. Finally, we describe the therapeutic potential of harnessing immune subversion strategies used by bacteria to treat chronic inflammatory conditions.

KEYWORDS

PAMP, DAMP, infection, tolerance, pathogens, NLRs, inflammation, inflammasome

1 Introduction

Bacteria have evolved complex interactions with mammals, resulting in both beneficial and detrimental effects for the host. On the host side, molecular sensing systems of the innate immune system detect non-host components and products, typically conserved structural components of microbes, such as peptidoglycan (PGN), lipopolysaccharides, and lipoteichoic acids. These microbe-associated molecular patterns (MAMPs) activate receptors on and within host cells, referred to as pattern-recognition

receptors (PRRs), to trigger signal transduction events ultimately leading to the production of immune mediators and anti-microbial peptides (reviewed in (1)).

While overwhelming colonisation of the host with bacteria must be avoided and most organs are regarded as sterile, the host also depends on bacteria, their MAMPs and metabolites for proper function of its immune system and the development and homeostasis of its protective barrier surfaces. This is probably best exemplified by the well-studied intestinal barrier, where a wealth of recent studies show that the gut microbiota provides essential signals that also affect the regulation of systemic immune responses (2). Besides providing such beneficial effects, overwhelming replication of bacteria in the host would impair its survival. Moreover, some pathogenic bacteria can actively invade the host *via* the expression and use of virulence factors that enable them to overcome physical and immunological barriers (3). In addition, some pathogenic bacteria can also promote their uptake by host cells and live and replicate in cellular compartments such as endosomes, or in some cases replicate and move freely in the cytosol of the host cell. As such, these organisms present a threat to the host and their replication needs to be timely and tightly controlled by the host's immune response.

On the other side, pathogens try to subvert immune responses for their replicative benefit. This system is highly dynamic and driven by the rapid evolution of pathogens and the adaptation of the host. This can be illustrated by the paradigm of the "Red-Queen" from Lewis Carrol's fairy tale that is often used to describe the arms race between pathogens and their hosts (4). However, such an immuno-centric view lacks consideration of the fact that an uncontrolled, and overwhelming immune response focused on completely eradicating pathogens could come at the cost of significant collateral damage of host tissue, eventually leading to severe pathologies. Thus, this arms-race between host and pathogens needs to be controlled and tightly regulated.

Indeed, the host and its surrounding microbes have evolved for fine-tuning of the immune response, in order to guarantee sufficient restriction of the invading pathogen and assure integrity and functionality of the host, while at the same time limiting harmful tissue damage and immunopathology. This is described by the concept of resistance and tolerance, where resistance refers to the capacity of elimination of the pathogen by the immune response, and tolerance to a state of acceptance of some colonisation and increased tissue homeostasis to avoid immunopathology (5).

Historically, the field of infection biology research has focussed on examining the beneficial roles of the immune system to defend against microbes and to understand how pathogens can use subversion strategies to overcome host immune responses. However, within the past decade, our understanding of immunomodulation of innate immune responses and its importance in promoting tolerance to infection and host fitness is emerging. Recent data suggests that during the evolution of humans, attenuation of cytokine responses towards intracellular pathogens might have been a key event to guarantee survival and fitness of the host (6).

Charles Janeway's idea that the host detects pathogens using germline encoded receptors of the innate immune system to trigger inflammation and to introduce adaptive immunity (7) paved the way for the identification of a wealth of PRRs and deciphering their cellular signalling pathways (8). In humans we have several classes of PRRs that represent both membrane anchored receptors, such as the Toll-like receptors (TLRs) (9) or C-type lectin receptors (CLRs) (10) and intracellular receptors such as the NOD-like receptors (NLRs) (11), RIG-I like receptors (RLRs), and cyclic GMP-AMP synthase (cGAS) (12). All these PRRs have different specificities that collectively cover the detection of a broad range of MAMPs derived from bacterial, fungal and metazoan pathogens. Activation of PRRs leads to the induction of cellular signalling events that ultimately triggers the release of anti-microbial substances such as antibacterial peptides, the production of cytokines, recruitment of immune cells and the induction of adaptive immune responses.

Amongst the PRR families, Nod-like receptor (NLR) proteins gained interest due to the fact that this family of 22 proteins in humans serve diverse functions in innate immunity (13). NLRs show a typical tripartite structure hallmarked by a central oligomerization domain with nucleotide binding capacity, a C-terminal leucine rich repeat (LRRs) domain that is also found in other PRRs such as TLRs, and different N-terminal domains that define their signalling function. NOD1 and NOD2 were the first NLRs to be described as PRRs and to serve as intercellular receptors for invasive bacteria (14). They induce transcriptional reprogramming by their CARD domains that interact with the Receptor Interacting Serine/Threonine Kinase 2 (RIP2) to induce Mitogen-activated protein kinase (MAPK) and I kappa-B Kinase (IKK) activation (14). In contrast, many PYD domain containing NLRs form inflammasomes that act as a scaffold for the activation of caspase-1, which subsequently can process pro-IL-1β, pro-IL-18 and gasdermin D to induce release of the potent pro-inflammatory mediators IL-1β and IL-18 (15). Of note, inflammasomes not only respond to MAMPs but are also activated by perturbance of cellular membrane integrity and danger-associated molecular patterns (DAMPs) which are factors that are released upon tissue and cell disintegration. The innate immune system thus can detect pathogen-induced damage of tissues and cells, and also the perturbation of cellular pathways (16, 17). This indirect recognition of pathogens as a result of changes in cellular signalling and induction of cellular stress is also referred to as effector-triggered-immunity (ETI) in relation to the immune response triggered by pathogen effector proteins in plants (18, 19).

Here we focus on well-studied members of the NLR-family, a class of host PRRs that are expressed in the cytosol. We will discuss our current understanding of their roles as PRRs for bacteria, but also take a closer look at the mechanisms used by

bacterial pathogens to overcome NLR-mediated responses. In view of the need of a well-adapted immune response towards pathogens to avoid immunopathologies, we hypothesise that such adaptations of bacteria did not evolve solely to assure better colonisation and survival in the host, but also to support fitness of the host for the benefit of the bacteria.

2 Non inflammasome NLRs

2.1 NOD1 and NOD2 detect bacterial peptidoglycan resulting in a proinflammatory immune response

Among the non-inflammasome forming NLRs that regulate inflammation, NOD1 and NOD2 are the most well characterised receptors. NOD1 and NOD2 detect bacterial PGN, specifically the synthetic minimal PGN moieties γ-D-Glu-*meso* diaminopimelic acid (iE-DAP) and muramyl dipeptide (MDP) respectively (20, 21). Although NOD1 and NOD2 are closely related receptors that both detect specific components of bacterial PGN, NOD1 is typically expressed broadly throughout tissues at varying levels, however NOD2 expression is mostly restricted to monocytes (22–24). NOD1 and NOD2 are expressed by non-vertebrate and vertebrate species, and several amino acids are conserved in NOD1 and NOD2 which are especially notable in the LRR domains, which may be indicative of evolutionarily conserved ligand binding or recognition regions (25). Murine and human NOD1 differ in their ability to detect some PGN moieties, whereby human NOD1 requires a tripeptide for activation, and murine NOD1 requires a tetrapeptide (26). Interestingly, some bacteria such as commensal *Enterococcus* species have been shown to modify their release of PGN fragments which resulted in increased activation of murine NOD2 (27). Delivery of NOD1 and NOD2 PGN ligands into the host cell cytosol is required for their activation. As such, PGN ligands have been shown to enter host cells using a variety of mechanisms, either *via* endosomal peptide transporters of the SLC15 family (28, 29), by injection of PGN by bacterial type 4 secretion systems (T4SS) (20, 30), and by the entry of bacterial membrane vesicles (BMVs) into host cells (Figure 1) (31, 32). After PGN detection, NOD1 and NOD2 have been shown to associate with endosomal membranes (33, 34), which are hypothesised to be the site for NOD complex formation, coined the "nodosome" (35, 36). Before activation, NOD1 and NOD2 are thought to exist as monomers in an autoinhibited state when inactive in the cytosol, however upon ligand recognition, NOD1 and NOD2 self-oligomerise *via* their central NACHT domain (23, 37). Once activated, NOD1 and NOD2 recruit the kinase RIP2, that acts as a scaffolding protein for downstream signalling mediators and the formation of the nodosome (37). This results in downstream activation of NF-κB and MAPK signalling pathways, which ultimately leads to the production of inflammatory cytokines and chemokines (Figure 1) (23, 37–39). RIP2-mediated signalling is dependent on the recruitment of inhibitor of apoptosis protein (IAP) E3-ligase family members including X-linked IAP (XIAP), cellular IAP-1 (cIAP1) and cIAP2, and tumour necrosis factor (TNF) receptor associated factors such as TRAF2, TRAF5 and TRAF6 (40, 41).

NOD1 and NOD2 specifically require the action of the ubiquitin ligase XIAP for RIP2-induced activation of downstream kinases, which was confirmed in several independent studies (40, 42–44). XIAP itself is inhibited by the mitochondrial effector SMAC to control apoptosis and inflammation (45, 46). However, the enteroinvasive pathogen *Shigella flexneri*, for which NOD1 is a critical sensor, uses a sophisticated system to target XIAP by inducing a selective permeability of the mitochondria that leads to the release of SMAC but not of the apoptosis inducing cytochrome c in a BID-dependent manner (Figure 1) (47). It remains to be seen if this strategy to dampen NOD1 signalling is also used by other pathogens. Of note, targeting of the RIP2-XIAP interaction to block NOD1/2 induced inflammatory signals is emerging as a therapeutical option, as small compound XIAP- and RIP2-inhibitors limit inflammation by blocking XIAP-RIP2 interactions (48). Such drugs could be useful to dampen excessive or chronic inflammation resulting from inflammatory and infectious diseases. Overall, the most efficient strategy to subvert NOD1/2 detection is the targeting of signalling downstream of NOD1/2. Inhibition of NF-κB and MAPK signalling for example are a common theme of many bacterial pathogens that evolved secreted effectors to target these pathways. In this review, we will focus our discussion on bacterial mechanisms of NOD1/2 specific subversion. For further details summarising the general inhibition of inflammatory pathways by bacteria, we refer the reader to the following detailed reviews (49, 50).

2.2 Stress sensing, disruption of the actin cytoskeleton and S1P sensing affect NOD1 and NOD2 signalling

In addition to the detection of bacterial PGN by NODs, NOD1 and NOD2 have also been shown to be important for the clearance of bacteria by autophagy in several studies (51, 52). Furthermore, NOD1 and NOD2 activation is also linked to endoplasmic reticulum (ER) stress and inflammatory diseases, and therefore NOD1 and NOD2 are thought to have complex roles in inflammatory signalling (38, 53–58). Specifically, bacterial induction of ER stress and cytoskeletal perturbations are linked to modulation of NOD1 and NOD2 signalling and are also the target of bacterial subversion mechanisms of NOD1/2 activation. NOD2 was initially discovered due to its involvement in Crohn's disease (CD) through genetic linkage studies (59),

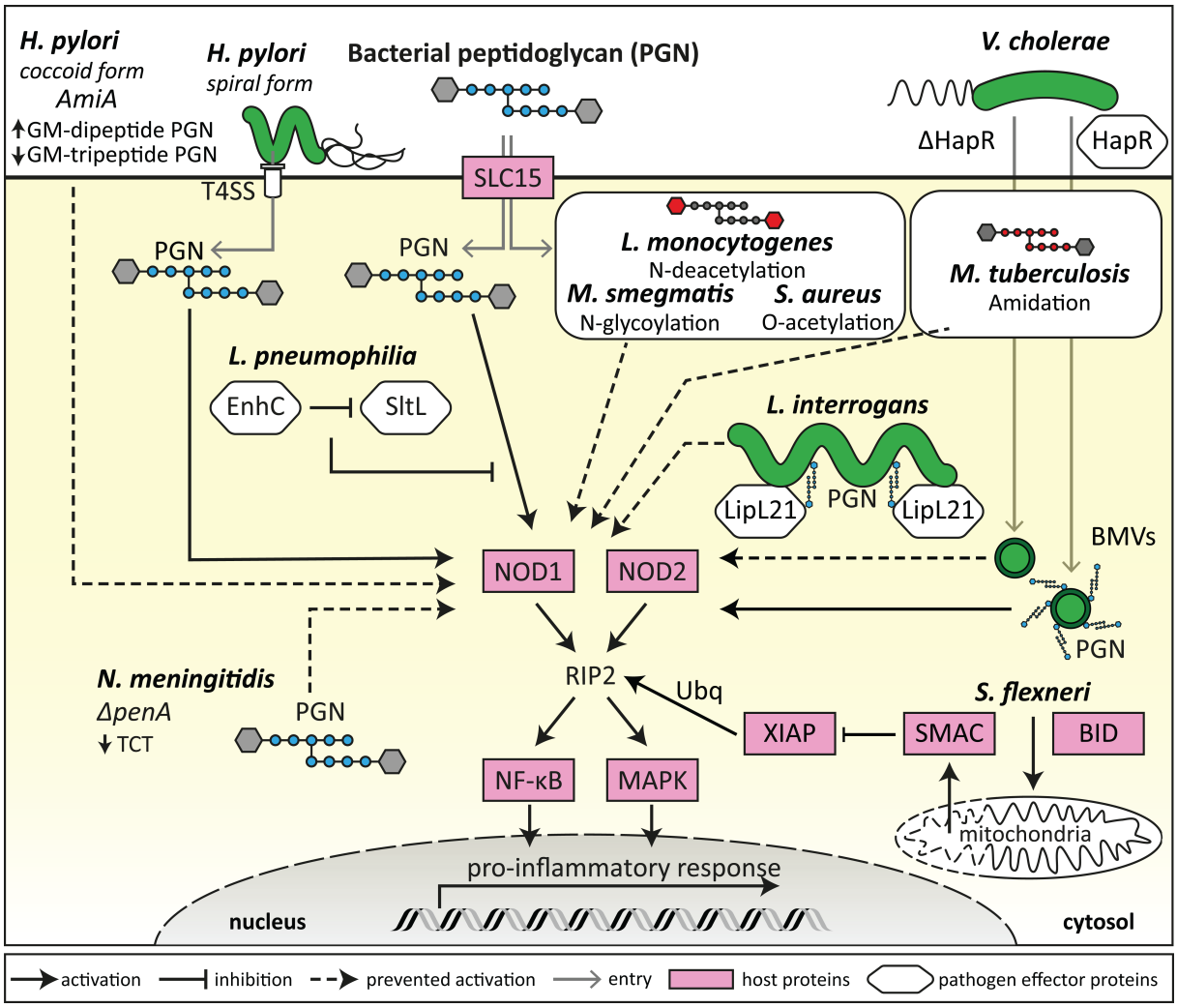

FIGURE 1
Bacterial evasion of NOD1 and NOD2 detection. Bacteria can modify their morphology and metabolism to evade detection by NODs by a range of mechanisms. This includes *H. pylori* transitioning from spiral to coccoid morphology, which results in decreased GM-tripeptide accumulation, and deletion of *penA* by *N. meningitidis* which results in decreased TCT tetrapeptide peptidoglycan (PGN) moieties, ultimately reducing the availability of NOD ligands to prevent NOD1 activation. Some bacteria express proteins that can block the enzymatic release of specific NOD-activating PGN moieties (*L. pneumophila*) or can sequester NOD ligands to the bacterial surface (*L. interrogans*), thus preventing NOD1 and NOD2 activation. Several bacterial strains, such as *S. aureus, M. tuberculosis, M. smegmatis* and *L. monocytogenes*, have processes to modify their PGN in order to evade NOD1/2 detection and activation, resulting in an attenuated proinflammatory response. Bacteria also release bacterial membrane vesicles (BMVs) containing PGN that can activate NODs, and bacterial expression of proteins such as HapR (*V. cholerae*) can alter the PGN content of BMVs and therefore modulate NOD1 and NOD2 activation. Bacteria such as *S. flexneri* can induce BID-dependent selective permeability of the mitochondria, resulting in the release of SMAC, which blocks XIAP ubiquitination of RIP2 downstream of NOD1 and NOD2 activation.

with a loss-of-function mutation being the most common mutation associated with CD (60). More recently, further evidence has demonstrated that NOD1 and NOD2 are also linked to several inflammatory diseases in addition to CD, including Type 2 Diabetes (T2D), and asthma (20, 21, 38, 53–55). ER stress has more recently been identified as a major contributor to the pathology of inflammatory diseases including CD and T2D (56, 61–63), with NOD1 and NOD2 activation also being shown to be linked to ER stress (56). Thus, NOD1 and NOD2 not only act as sensors for PGN but are also activated indirectly by cellular stress responses that can be induced by pathogens. Cells respond to cellular stress with a complex program that involves the generation of the lipid sphingosine-1-phosphate (S1P) (57). S1P is a bioactive metabolite that has been shown to target TRAF2 and cIAP (64) but can also interact directly with NOD1 and NOD2 to induce IL-6 and IL-8

expression in a NOD1/2-dependent manner (57). Additionally, ER stress induced by thapsigargin and dithiothreitol were found to trigger the production of IL-6 in a NOD1/2 dependent manner (56). This suggests that S1P might be a common factor that links cellular stress to NOD1/2-induced inflammation. Furthermore, different signalling components downstream of the unfolded protein response (UPR) during ER stress might also contribute to NOD1 activation. For example, treatment of HeLa cells that expressed an NF-κB reporter with tunicamycin, a chemical that interferes with *N*-linked glycosylation to induce ER stress, did not affect the ability of NOD1 to induce NF-κB activation (58). However, treatment of HeLa cells with thapsigargin, which depletes ER calcium stores to induce ER stress, resulted in NOD1 activation when cells were stimulated with the NOD1 agonist C12-iE-DAP in combination with the *Salmonella enterica* serovar Typhimurium effector protein SopE (58). It should be noted that this sensing mechanism can also lead to adverse effects, as it was shown that ER stress can increase the susceptibility of HeLa cells to infection with *S.* Typhimurium, likely due to NOD1 hyperresponsiveness (58). Therefore, the indirect activation of NOD1 and NOD2 by cellular stress signalling may be another potential target for bacterial subversion mechanisms.

In addition to the direct activation of NOD1 and NOD2 during stress signalling, NOD1 and NOD2 have also been shown to be activated as a result of actin cytoskeleton perturbations (44, 65, 66). For example, it was demonstrated that NOD1 is recruited to the cell membrane at the site of bacterial entry, and that NOD1 and NOD2 recruit the autophagy protein ATG16L1 to direct autophagy of invading bacteria (52, 66). NOD1 also interacts with the cofilin phosphatase SSH1, that regulates the actin severing activity of cofilin, which contributes to NOD1 activation upon infection with *S. flexneri* (44). NOD1 was also found to be linked to activation of the small GTPases Rac1 and CDC42 by bacterial virulence factors, such as SopE from the enteric pathogen *S.* Typhimurium (67). In monocytes treated with MDP, NOD2 was shown to be recruited to the plasma membrane by a mechanism which required the RhoGTPase Rac1 and Rho guanine nucleotide exchange factor 7 (Rho GEF7) (68). Additionally, NOD2 was also reported to interact with a cytoskeletal protein, vimentin, to regulate NF-κB activation and autophagy (69). In this study, it was demonstrated that some NOD2 variants with mutations in the LRR domain, responsible for detection of PGN (20), were unable to bind vimentin which correlated with the inability of NOD2 to localise to the plasma membrane and initiate the cellular degradation pathway of autophagy (69). Furthermore, a recent study demonstrated that NOD2-MDP binding is enhanced the action of the small GTPase ADP-ribosylation factor 6 (Arf6) which contributes to membrane anchoring during activation of NOD2 (70). These indirect pathogen sensing mechanisms of NOD1/2, by monitoring actin and small GTPase activity in host cells, might also be subject for bacterial subversion and adaption to the host. *Klebsiella pneumoniae*, for example, has been found to dampen the inflammatory immune response in an indirect NOD1-dependent manner, by inhibiting Rac1 activation. This triggers NOD1-mediated upregulation of CYLD and mitogen-activated protein kinase 1 (MKP-1) expression, in turn attenuating IL-1β induced IL-8 production (71). In this way, *K. pneumoniae* utilises NOD1 to reduce the production of proinflammatory cytokines and chemokines to prevent bacterial clearance (71). Bacteria may also use several direct mechanisms to modulate NOD1 and NOD2 signalling, such as the release of PGN-containing bacterial membrane vesicles (BMVs).

2.3 Bacterial membrane vesicles affect NOD1 and NOD2 signalling

BMVs have been shown to package PGN cargo and can enter host cells to modulate NOD1 and NOD2 signalling (31–33, 72–75). Specifically, deletion of the quorum sensing regulator HapR, involved in *Vibrio cholerae* virulence, can reduce the packaging of PGN cargo within BMVs (72). Furthermore, stimulation of host cells using BMVs produced by HapR deletion mutants resulted in attenuated NOD1 and NOD2 responses compared to stimulation with wild-type *V. cholerae* BMVs, further pinpointing the effects of PGN packaging within BMVs and their ability to activate NOD1 and NOD2 (Figure 1) (72). Interestingly, HapR deletion did not affect the bacterial membrane of *V. cholerae*, despite the influence of HapR deletion on the PGN content of BMVs, which may indicate selective PGN packaging within *V. cholerae* BMVs as a mechanism to modulate NOD1/2 activation (72). *Porphyromonas gingivalis*, a periodontal pathogen, was also shown to produce BMVs that induce NOD1 and NOD2 activation (75). However, BMVs produced by other periodontal pathogens, *Tannerella forsythia* and *Treponema denticola*, induced a weak or no NOD1/2 response respectively, highlighting the different abilities of BMVs to activate NOD1 and NOD2 in the context of periodontitis (75). In contrast to pathogen derived BMVs, commensal derived BMVs produced by the commensal gut bacterium *Bacteroides fragilis*, downregulated the production of the anti-inflammatory cytokine IL-10 by NOD2 knockout murine bone marrow-derived dendritic cells (BMDCs) (76). This indicated that commensal BMVs may be involved in the regulation of anti-inflammatory immune responses in a NOD-dependent manner. Overall, in addition to PGN-containing BMVs entering host cells to initiate NOD1 or NOD2 dependent pro- or anti-inflammatory immune responses (reviewed by 77, 78), several studies have also demonstrated that bacteria can modify their PGN to subvert detection by NOD1 and NOD2, in order to increase bacterial survival and persistence in the host.

2.4 Subversion of NOD1 and NOD2 detection by PGN adaption

To establish an infection within the host and to limit inflammation, several bacteria have adapted mechanisms to subvert detection by NOD1 and NOD2. For example, *Listeria monocytogenes* undergoes PGN N-deacetylation to prevent NOD agonist presentation during intracellular infection to limit inflammation and clearance from the host (Figure 1) (79). Deletion of the N-deacetylase gene *pgdA* in *L. monocytogenes* resulted in loss of infectivity of such mutants in mice, and *L. monocytogenes pgdA* mutants were efficiently killed by murine macrophages resulting in the generation of a TLR2 and NOD1-dependent IFN-β response (79). This indicates that PGN modification by N-deacetylation is an effective mechanism used by *L. monocytogenes* to evade NOD detection and clearance from the host (79). Other bacterial species including *Mycobacterium tuberculosis, Mycobacterium smegmatis, Staphylococcus aureus* and *Neisseria meningitidis* have also developed mechanisms of PGN modification, including N-glycosylation, O-acetylation and amidation of muramic acid residues resulting in resistance to host lysozyme (Figure 1) (80–83). For example, *M. tuberculosis* reduces NOD1 activation by peptide-amidation of PGN fragments, which may be a mechanism to reduce the host inflammatory response in a NOD1-dependent manner in order to establish an effective infection in the host (83).

In addition to post-translational modifications such as O-acetylation which may contribute to NOD1 and NOD2 immune evasion (82), *N. meningitidis* penicillin-binding protein 2 (PBP2) is also thought to contribute to evasion of NOD1 activation (84). PBP2 is involved in PGN biosynthesis, cell elongation and increased resistance to penicillin G, and *N. meningitidis* strains with alterations to *penA* had decreased tetrapeptide-containing muropeptides, resulting in reduced NOD1 activation compared to wild-type *N. meningitidis* (Figure 1) (84). These strains also contained a decreased amount of the monomeric muropeptide anhydrous disaccharide-tetrapeptide, known as tracheal cytotoxin (TCT), which is known to have cytopathologic and proinflammatory properties (84) and is the key ligand of the murine NOD1 protein (26). Interestingly, *N. meningitidis* with *penA* mutations were less virulent despite their resistance to penicillin G (84). Therefore, it has been proposed that reduced TCT production, and reduced NOD1 and NOD2 activation by *N. meningitidis* strains is a disadvantage during infection, whereby cytotoxicity and inflammation are associated with the effective establishment of infection (84). Other bacteria also have inherent differences in their PGN composition which can differentially affect the activation of NOD1 and NOD2, for example the periodontal pathogen *P. gingivalis* demonstrated weaker activation of NOD1 and NOD2 compared to *Escherichia coli* and *Fusobacterium nucleatum* (85), despite *P. gingivalis* BMVs being shown to activate NOD1 and NOD2 (75). Similarly to *N. meningitidis*, it is thought that different *P. gingivalis* strains are variable in their dipeptide and tripeptide PGN content, and therefore their ability to activate NOD1 and NOD2 (85). The weak activation of NOD1 and NOD2 by *P. gingivalis* bacteria may be a mechanism to modulate host inflammatory immune responses, and therefore promote survival of pathogenic bacteria in the periodontal environment (85, 86).

Helicobacter pylori has also been shown to evade detection by NOD1 and NOD2, which occurs during its transition from spiral to coccoid forms (87). Spiral *H. pylori* expresses a T4SS that can inject PGN into host cells and initiate a NOD1-dependent inflammatory response but are sensitive to antibiotics and host inflammatory molecules (Figure 1) (30). However, coccoid forms of *H. pylori* are more resistant to antibiotics and host inflammatory assaults (reviewed by 88). The putative PGN hydrolase encoded by the *amiA* gene in *H. pylori* is thought to contribute to the accumulation of GM-dipeptide, a NOD2 agonist, during the transformation from spiral to coccoid forms (Figure 1) (87). Conversely, as GM-dipeptide accumulates in coccoid *H. pylori*, the NOD1 agonist GM-tripeptide is decreased (87). This suggests that switching of *H. pylori* from the spiral form to coccoid results in evasion from detection by NOD1 in human epithelial cells and escape from the host proinflammatory immune response (Figure 1) (87). The invasive bacterium *Legionella pneumophila* has also been shown to have mechanisms to subvert NOD1 activation (89). *L. pneumophila* infects macrophages intracellularly and has been shown to subvert NOD1 detection by expressing the protein EnhC which interferes with the bacterial protein SltL, a PGN degradative enzyme responsible for the generation of NOD1 ligand (89). By blocking the generation of NOD1 ligand, *L. pneumophila* prevents its detection by NOD1 and the generation of a proinflammatory immune response, thus contributing to bacterial viability (Figure 1) (89).

In addition to inherent PGN modifications that result in evasion of NOD1 and NOD2 detection, the Gram-negative pathogen *Leptospira interrogans* has been shown to express a protein that enables evasion of NOD1 and NOD2 activation (90). *L. interrogans* escapes recognition by NOD1 and NOD2 by producing a lipoprotein, LipL21, that binds to *L. interrogans* PGN and prevents the action of PGN hydrolases, resulting in sequestration of NOD agonists on the bacterial surface (Figure 1) (90). As NOD1 and NOD2 agonists are not released from the surface of *L. interrogans* due to the action of LipL21, *L. interrogans* is able to also escape recognition by NOD1 and NOD2 to establish an infection in the host (90). Further molecular mechanisms of NOD1 and NOD2 modulation and specific PGN biochemical modifications that affect NOD1/2 signalling are reviewed in detail elsewhere (91).

Taken together, recent advances show that NOD1 and NOD2 are much more complex than being exclusively MAMP sensors. Both NLRs can be activated by cellular stress, modulation of cellular small GTPase activity and F-actin

perturbations. Bacterial pathogens have evolved multiple measures to counteract NOD activation and to adopt the inflammatory response in the host for their benefit. This includes the modification of PGN, PGN packaging by BMVs, interception of NOD1/2 signalling and targeting of small GTPases by effector proteins. It is clear that NLRs have several roles not only in the detection of bacterial PGN, but also in regulation of immunity in concert with other NLR proteins (92). In particular, bacteria can indirectly affect NLR signalling in several ways, including the inactivation of GTPases which have been shown to be important for both NOD1/2 and pyrin inflammasome signalling (92, 93). In this way, bacteria may modify their PGN in order to alter their activation of several NLRs to ultimately activate or subvert host immunity.

3 Inflammasome forming NLRs

The formation of multiprotein signalling complexes termed inflammasomes that consists of an NLR protein, the adaptor protein apoptosis-associated speck-like protein containing a CARD (ASC) and caspase-1, was first described by the group of Jürg Tschopp for NLRP1 (94). Inflammasome oligomerisation induces the production of active caspase-1, triggering the processing of pro-IL-1β, pro-IL-18 (95, 96) and gasdermin D, leading to pore formation, release of IL-1β and IL-18 and eventually pyroptosis (97–100).

Inflammasome formation of NLRP1, NLRP3 and NLRC4 (101–103) as well as for the non-NLR proteins AIM2 (104–106) and Pyrin (107) has been well characterised. The formation of inflammasomes was further reported for NLRP6, NLRP7, NLRP12 and NLRC5 (108–111). Recruitment of ASC by NLRP proteins is mediated through homotypic PYD-PYD interactions. ASC then recruits pro-Caspase-1 *via* homotypic CARD-CARD interactions. In this section we will focus on two of the best described inflammasome-forming NLRs: NLRP3 and NLRC4 and describe how different bacterial pathogens evade their activation.

3.1 The NLRC4/NAIP inflammasome

A unique NLR-NLR interaction exists between the intracellular receptor neuronal apoptosis inhibitory proteins (NAIP) and inflammasome adaptor protein NOD-LRR-and CARD-containing 4 (NLRC4) that form the NLRC4/NAIP inflammasome (112, 113). The NAIP thereby serve as sensors to detect specific bacterial-derived MAMPs, namely the inner rod proteins of the bacterial type III secretion system (T3SS), and flagellin [reviewed in (102)]. NAIP/NLRC4 activation occurs in response to the delivery of their specific ligands *via* the bacterial T3SS or T4SS (114), flagella-containing bacterial membrane vesicles (115), or the presence of intracellular pathogens (116). NAIP receptors were first observed as being critical in the defence against infection by the intracellular pathogen *L. pneumophila*, whereby it was observed that murine macrophages harbouring a mutation in the Lgn1 locus, which encodes the *Naip5* gene, were susceptible to *L. pneumophila* infection (117–119). Furthermore, expression of NLRC4 has been shown to be critical in defence against enteric pathogens including *S.* Typhimurium (120), *E. coli* (121) and *S. flexneri* (122), as well as systemic pathogens such as *L. pneumophila* (123), *Pseudomonas aeruginosa* and *K. pneumoniae* (124, 125). Mice express four NAIP receptors, namely NAIP1 and NAIP2 that detect T3SS inner rod proteins, and NAIP5 and NAIP6 that detect flagellin; while humans express a single NAIP with splice variants that detect both T3SS proteins and flagellin [reviewed in (126)]. The NLRC4 inflammasome is especially important during infection of intestinal epithelial cells (127), and its expression can be upregulated by pro-inflammatory stimuli, such as TNFα (128). Following an initial priming signal generally involving the activation of TLRs, the ligand-triggered activation of NAIP initiates co-oligomerization with the NLRC4 adaptor to form a multiprotein inflammasome complex, culminating in a potent inflammasome response hallmarked by production of active caspase-1, IL-1β and IL-18, as well as pyroptosis [reviewed in (102)]. NLRC4 is different to other NLRPs as it can recruit caspase-1 independently of ASC through CARD-CARD interaction, however ASC is nucleated by NLRC4 and can greatly enhance caspase-1 activation (15). Pathogenic bacteria have co-evolved counter mechanisms to either avoid detection by NAIP, prevent NLRC4 signalling, exploit the NLRC4 pathway to the benefit of the pathogen, or dampen the inflammasome response (Figures 2A, C). In addition, dampening of NAIP-NLRC4 activation is thought to be critical for promoting immunotolerance to enteric commensal bacteria.

3.1.1 Evasion of detection by NAIP

Several pathogens evade NAIP detection by reducing the accessibility of ligands. When intracellular, *S.* Typhimurium represses expression of the flagellin protein FliC through the expression of the protease ClpXP, allowing the pathogen to transverse the epithelial barrier undetected (129). *S.* Typhimurium also impedes clearance from macrophages by reducing expression of the immunogenic T3SS rod protein PrgJ, in favour of the poorly immunogenic SsaI rod proteins (Figure 2A) (130). In addition, *L. monocytogenes* evades detection by expressing flagellin that is a poor activator of NLRC4 (Figure 2A) (131), while *P. aeruginosa* secretes proteases that degrade extracellular flagellin (Figure 2A) to limit TLR5 activation, however whether this mechanism also leads to evasion of NLRC4 inflammasome sensing is unknown. These evasion mechanisms enable pathogens to remain undetected by the NAIP, and thereby facilitate host colonisation.

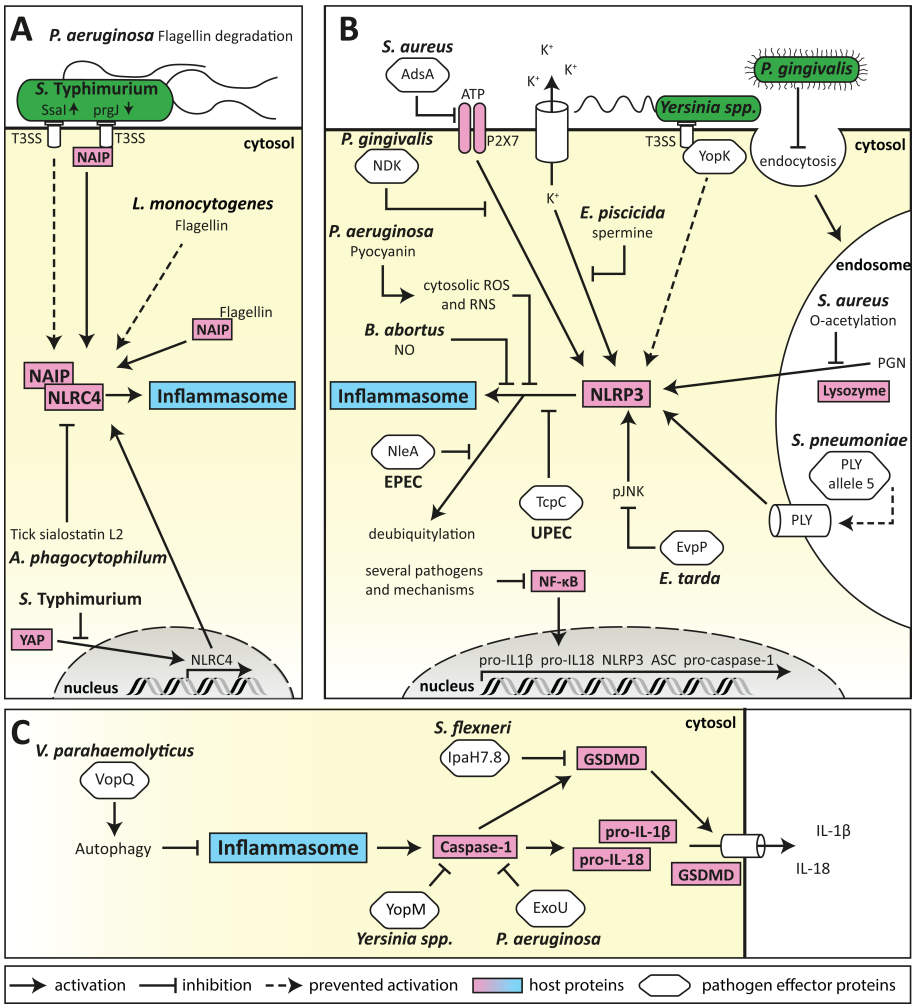

FIGURE 2
Mechanism of bacterial evasion of inflammasome activation and signalling. **(A)** Bacterial evasion of the NLRC4 inflammasome. Evasion of NAIP detection is one of the major subversion strategies for bacteria recognised by the NLRC4 inflammasome. This can be performed by the expression of poorly immunogenic *S.* Typhimurium T3SS rod proteins, or *L. monocytogenes* flagellin, as well as by proteasomal degradation of *P. aeruginosa* flagellin. Furthermore, expression of NLRC4 can be suppressed by *S.* Typhimurium through inhibition of host transcription factors, and by *A. phagocytophilum* by exploitation of vector-mediated release of anti-inflammatory compounds. **(B)** Bacterial evasion of the NLRP3 inflammasome. Subversion of the NLRP3 inflammasome can be conferred by several different mechanisms (shown in clockwise order). First, several pathogens can prevent transcription of inflammasome components by inhibiting NF-κB signalling. Second, pathogenic bacteria can inhibit activation of the NLRP3 inflammasome by DAMPs, such as *via* the degradation of extracellular ATP by AdsA from *S. aureus*, inhibition of the ATP-receptor P2X7 signalling by *P. gingivalis* NDK, or accumulation of cytosolic spermine by *E. piscicida*. Third, pathogens can evade recognition by preventing the detection of their ligands such as masking of *Yersinia* spp. T3SS effector YopK, suppression of endocytosis by *P. gingivalis*, modification of *S. aureus* PGN by O-acetylation, or expression of mutant virulence factors that lack NLRP3-activating properties, such as *S. pneumoniae* PLY. Finally, NLRP3 inflammasome formation can be targeted directly by bacterial effector proteins such as *E. tarda* EvpP or UPEC TcpC, and by EPEC NleA-mediated deubiquitylation as well as by *P. aeruginosa* pyocyanin or *B. abortus*-derived nitric oxide (NO). **(C)** Targeting mechanisms common to NLRP3 and NLRC4 inflammasome formation allow pathogens to efficiently prevent secretion of IL-1β and IL-18. ASC-speck formation can be prevented by induction of autophagy by *V. parahaemolyticus* VopQ. Caspase-1 can be directly targeted by bacterial effector proteins such as *Yersinia* spp. YopM, or *P. aeruginosa* ExoU, to prevent proteolytic processing of pro-IL-1β, pro-IL-18 and gasdermin D (GSDMD). GSDMD is further targeted by *S. flexneri* IpaH7.8 for degradation, preventing NLRC4-mediated pore-formation.

3.1.2 Blocking NLRC4 signalling

Several pathogens block NLRC4 signalling to prevent inflammasome-mediated cytokine production or pyroptosis. *S.* Typhimurium can directly modulate the host response by downregulating NLRC4 expression in infected B-cells (132). This is mediated by phosphorylation of the host transcriptional activator Yap, thereby preventing its nuclear translocation and transcriptional activation of NLRC4 (Figure 2A) in a process depended on the *Salmonella* pathogenicity island 1 (SPI1) T3SS (132). Furthermore, a

unique subversion mechanism is utilised by the tick-borne pathogen *Anaplasma phagocytophilum* which profits from the anti-inflammatory tick salivary protein sialostatin L2. Sialostatin L2 blocks NLRC4 oligomerisation and prevents caspase-1 activation, thereby preventing an inflammasome response to *A. phagocytophilum* (Figure 2A) (133). This represents a unique cross-kingdom mechanism that allows the bacterial pathogen to establish colonisation of the human host (133). Collectively, these studies reveal the sophisticated mechanisms employed by pathogens to block NLRC4 signalling at different points in the inflammasome pathway.

3.1.3 Exploitation of NLRC4 activation

An alternative method of subverting the host response is to exploit it for the benefit of the pathogen. The gastric pathogen *H. pylori* induces NLRC4 activation in gastric epithelial cells mediated by its type IV secretion system, which results in the inhibition of the Th17/IL-17 response and downregulation of beta defensin-1 (BD-1), leading to reduced killing of *H. pylori* (134). NLRC4-deficient mice were found to be more adept at clearing *H. pylori* infection, highlighting the importance of this subversion mechanism in *H. pylori* colonisation and persistence (134). Similarly, activation of NLRC4 by *S. aureus* in murine lung epithelial cells was shown to impair IL-17A-dependent neutrophil recruitment (135), preventing bacterial clearance from the lungs. In contrast, NLRC4-deficient mice displayed increased bacterial clearance and improved host survival, highlighting the vital role this subversion mechanism plays in *S. aureus* colonisation (135).

During *S.* Typhimurium infection in mice, NLRC4 is activated by flagellin of the bacteria (136). An elegant study showed that NLRC4 activation can affect adaptive immunity by reducing $CD4^+$ T-cell-mediated immune memory (136). In NLRC4-deficient animals as well as in animals infected with an *S.* Typhimurium strain that expressed a form of flagellin that cannot activate NLRC4, higher levels of IFN-γ secreting Th1 cells and memory $CD4^+$ T-cells were observed (136). The exact mechanism remains elusive but involves activation of NLRP3 (136).

These studies illustrate that PRR activation can have consequences beyond the direct innate response that can be detrimental to the host. Understanding of these complex interactions between the innate and adaptive immune system will be essential to gaining insight into their role in immunopathology and infectious disease towards specific pathogens.

3.1.4 Dampening of the NLRC4 response to facilitate immunotolerance

Dampening of the NLRC4 response has also been linked to facilitating immunotolerance to commensal bacteria (137). Studies have shown that the uptake of free flagellin by intestinal phagocytes leads to an adaptive immune response that inhibits the NLRC4 response, which is thought to promote immunotolerance to commensals. Similarly, a study showed that uptake of commensal bacteria by intestinal phagocytes did not lead to activation of NLRC4, yet uptake of the pathogens *S.* Typhimurium or *P. aeruginosa* triggered NLRC4-mediated production of mature IL-1β, suggesting the NAIP-NLRC4 system can discriminate between pathogenic and non-pathogenic bacteria (137). More studies are required to determine the mechanisms involved in regulating NAIP-NLRC4 activation and signalling that tailors the host response to commensals or pathogens and the bacterial factors involved.

3.2 The NLRP3 inflammasome

Canonical formation of the NLRP3 inflammasome requires two distinct signals. First, a priming signal leads to NF-κB-induced transcription of the inflammasome components, as well as pro-IL-1β and pro-IL-18. A second activation step then induces the formation of the inflammasome and activation of caspase-1. The second signal can be conferred by a broad range of stimuli which induce extensive changes in cellular homeostasis. These stimuli include extracellular ATP, lysosomal rupture by crystalline structures, mitochondrial ROS, pore formation and changes in the K^+ or Ca^{2+} homeostasis, (reviewed in (101)). Interestingly, flagellin can also activate the NLRP3 inflammasome indirectly in a ROS- and cathepsin-dependent manner (138), suggesting that ROS is a central activator linking NLRP3 to bacterial detection.

NLRP3 is found predominantly in myeloid cells and its activation is a tightly regulated mechanism (reviewed in (101)). Excessive inflammasome activity is associated with systemic auto-inflammatory syndromes, termed cryopyrin-associated periodic-syndromes (CAPS) (139). Regulation of NLRP3 is orchestrated by several post translational modifications including deubiquitylation, selective phosphorylation and dephosphorylation as well as degradation of small ubiquitin-related modifier (SUMO) known as deSUMOylation (101). Furthermore, interaction partners that are critical for NLRP3 inflammasome activation have been identified, such as the kinase NEK7 (140, 141) and the RNA-helicase DDX3X (142).

The NLRP3 inflammasome can additionally be activated by non-canonical mechanisms involving caspase-11 in mice and caspase-4/5 in humans (143–146). Direct sensing of LPS by those caspases (147, 148) results in caspase activation and subsequent cleavage of gasdermin D, releasing its N-terminal fragment which forms pores in the cell membrane and induces a form of lytic cell death, termed pyroptosis (98). The cleaved p30 gasdermin D fragment then leads to cell-intrinsic activation of NLRP3 (143).

Gasdermin D is also cleaved upon caspase-1 activation by classical NLRP3 activation to allow for the release of IL-1β and

IL-18. This also leads to induction of pyroptosis, a highly pro-inflammatory form of cell death, as the cellular contents of pyroptotic are released and can act as DAMPs. Additionally, IL-1β and IL-18 are among the most potent pro-inflammatory cytokines with multiple functions, including the induction of fever, and available data suggests that in most cells the NLRP3 inflammasome is the main platform for caspase-1 activation. It is hence not surprising that several pathogens have evolved subversion mechanisms to evade NLRP3-induced immune responses. As bacterial subversion mechanisms of NLR- and TLR-induced NF-κB signalling have been extensively reviewed in the literature (49, 50), we will focus on strategies directly targeting the activation and function of the NLRP3 inflammasome (Figures 2B, C).

3.3 Evasion of NLRP3-mediated recognition

Although NLRP3 is activated by a broad range of DAMPs, several bacterial pathogens have evolved mechanisms to evade detection by reducing the generation of NLRP3 activating stimuli. Phagocytic internalisation and lysozymal degradation of particulate *S. aureus* PGN is known to induce NLRP3-dependent IL-1β secretion from murine bone marrow-derived macrophages (BMDMs) independently of NOD2, yet the cell wall of pathogenic *S. aureus* strains has been shown to be highly resistant to lysozyme (149), due to O-acetylation of PGN. This modification prevents NLRP3 activation, IL-1β secretion and ultimately reduces macrophage-mediated killing of *S. aureus* (81) (Figure 2B). Additionally, *S. aureus* surface enzyme adenosine synthase A (AdsA) degrades ATP, ADP, and AMP to adenosine, thereby preventing NLRP3 activation by extracellular ATP (150) (Figure 2B). These subversion strategies allow *S. aureus* to remain undetected by the NLRP3 inflammasome, facilitating colonisation of the host and preventing bacterial killing.

Similarly, the emerging *S. pneumoniae* serotype 1 MLST306 and serotype 8 MLST53 strains have been described to evade NLRP3 inflammasome detection (151) by expression of an altered version of the endotoxin pneumolysin (PLY) (152). While retaining other virulence-related functions (153–157), this PLY lacks pore-forming ability (158) which strongly reduces IL-1β induction, thereby reducing bacterial killing (159) (Figure 2B). Furthermore, while the *Y. pseudotuberculosis* T3SS effectors YopB and YopD induce NLRP3 inflammasome activation by a poorly understood mechanism, translocation of these bacterial proteins is tightly controlled by YopK during infection, which inhibits exessive translocation of these effectors (160, 161) and therefore limits NLRP3 activation (162) (Figure 2B). This exemplifies the co-evolution of pathogen and host, resulting in elegant mechanisms of the pathogen to fine-tune inflammasome regulation for the benefit of host fitness and bacterial replication.

3.4 Metabolic interference with NLRP3 inflammasome formation

Recently, the role of several metabolites and secondary messenger molecules in modulation of innate immune receptors has been identified. For example, nitric oxide (NO) (163) and the Krebs cycle derived metabolite itaconate (164) have been described as inhibitors of the NLRP3 inflammasome. It is hence not surprising that several bacterial pathogens alter cellular metabolism for their benefit.

Nitrate reduction to di-nitrogen by *Brucella abortus* has been demonstrated to result in the presence of intermediate NO in iNOS-deficient cells and thus inhibition of the NLRP3 inflammasome (165) (Figure 2B). Furthermore, upon macrophage engulfment, the fish pathogen *Edwardsiella piscicida* delivers spermine to the cytosol in a T3SS-dependent manner, mediated by recruitment of arginine importer cationic acid transporter 1 (mCAT-1) and putrescin exporter organic cation transporter 2 (Oct-2) to the bacteria-containing vacuole (166). Cytosolic accumulation of spermine then inhibits the K^+ efflux-dependent activation of the NLRP3 inflammasome (166, 167) (Figure 2B). These studies demonstrate how the interplay between bacterial and host metabolism can regulate innate immune responses.

3.5 Direct targeting of NLRP3 by bacterial effector proteins

Suppression of NLRP3 activation is a common subversion strategy among several pathogens. This occurs by either the interference with the second signal of NLRP3 inflammasome activation, or by direct targeting of NLRP3 itself. Inhibition of the second signal is often conferred by preventing alterations of cellular homeostasis that are necessary for NLRP3 activation. This is seen for example in *P. gingivalis* infection where secreted nucleoside diphosphate kinase homologue (NDK) supresses NLRP3 inflammasome formation upon recognition of ATP through the P2X purinoceptor 7 (P2X7). Here, NDK seems to establish an anti-oxidative environment, limiting ATP-induced mitochondrial ROS production (168) (Figure 2B). Similarly, the *Edwardsiella tarda* T6SS effector protein EvpP inhibits activation of the NLRP3 inflammasome by counteracting the cytoplasmic Ca^{2+} increase, necessary for c-Jun NH2-terminal protein kinase (Jnk) activation, however the exact mechanism by which EvpP confers its effect is still unclear (169) (Figure 2B).

Direct interaction with NLRP3, or alteration of its post transcriptional modification (PTM) have also been described as subversion mechanisms for several pathogens. The enteropathogenic *E. coli* (EPEC) effector protein NleA interacts with NLRP3 and prevents its de-ubiquitination, resulting in reduced caspase-1 recruitment to the NLRP3 foci (170) (Figure 2B). Similarly, direct interaction of Toll/IL-1

receptor containing protein C (TcpC) from uropathogenic *E. coli* (UPEC) with NLRP3 and caspase-1 in BMDMs inhibits NLRP3-inflammasome induced IL-1β secretion (171) (Figure 2B). Furthermore, the pigment phenazine pyocyanin (PCN) produced by *P. aeruginosa* acts as a virulence factor that generates superoxide by the transfer of electrons from NADH and NADPH to oxygen. It was shown that PCN-derived ROS and RNS can lead to specific inhibition of the NLRP3 inflammasome by post-translationally blocking both ASC speck formation in BMDMs (172) and subsequent IL-1β secretion (169). In this manner, *P. aeruginosa* evades immune recognition and escapes macrophage-mediated killing (172). These studies highlight the broad yet highly effective range of effector functions through which bacterial pathogens prevent NLRP3 inflammasome formation.

Inhibition of the NLRP3 response is beneficial for bacterial fitness, as mutant strains lacking NLRP3 subversion mechanisms, in general show reduced survival *in vivo* (149, 173, 174). However, while activation of the NLRP3 inflammasome benefits the host by facilitating bacterial clearance, it can also lead to detrimental effects for the host. It has been shown that the increased clearance of *S. aureus* mutants, incapable of NLRP3 subversion, can lead to the appearance of skin lesions at the site of subcutaneous infection, indicating enhanced host-response-mediated tissue damage (149). Furthermore, activation of the NLRP3-inflammasome has been shown to drive immunopathology in *Bacillus cereus* infection, where NLRP3-induced inflammation strongly enhances the mortality of infected mice (175) and in pneumococcal meningitis, driven by IL-18 and IFN-γ (176, 177). Thus, while NLRP3-suppression generally is beneficial for pathogen survival, it can also be beneficial to limit tissue damage in the host. Overall, the importance of the NLRP3-inflammasome in the antibacterial immune response is highlighted by the broad range of pathogens which subvert its activation and effects for better survival in the host. However, although the general mechanisms of inflammasome activation appear to be highly conserved between mice and humans, there are differences in the relative importance of singular components of the multifaceted immune response (178). Overall, the translation from findings regarding NLR activation in mouse models into the human setting must be evaluated critically.

3.6 Subversion of inflammasome effector mechanisms

In the response against pathogens, co-operation of several inflammasomes will happen in the host and is often necessary to facilitate bacterial clearance (179). Yet to counter the host's multi-faceted response, many pathogens have evolved subversion strategies to target general mechanisms that prevent the assembly, activation, or signalling of several inflammasomes.

Suppression of inflammasome assembly is utilised by several pathogens. The *P. aeruginosa* quorum sensing-regulated virulence factor PCN and autoinducer 3-oxo-C12-homoserine lactone suppress the assembly and activation of both the NLRP3 and NLRC4 inflammasomes (180). Similarly, *S.* Typhimurium can suppress the activation of the NLRP3 and NLRC4 inflammasomes in human macrophages by a hitherto unknown SPI2 T3SS secreted effector to prevent IL-1β production and cell death, allowing bacterial persistence in macrophages (181).

Inhibition of the inflammatory caspases is another central mechanism employed by several bacterial species for immune evasion. For example, *Yersinia pestis* expresses a broad range of effector proteins that can target caspase-1 activation through different mechanisms, such as sequestration and inhibition of auto-proteolytic processing by YopM (182) or through inactivation of Rho GTPases by YopE and YopT (183, 184) (Figure 2C). *P. aeruginosa* secretes a phospholipase enzyme exoenzyme U (ExoU) that inhibits caspase-1 activity to block NLRP3 and NLRC4 inflammasome signalling (124) (Figure 2C). *S. flexneri* for example can block the non-canonical inflammasome by posttranslational modification of caspase-4 by its T3SS effector OspC3 using the uncommon ADP riboxanation to prevent cell death and inflammatory cytokine production upon intracellular LPS sensing (185, 186).

Pathogens can also block cell death to allow them to persist in host cells. For example, *S. flexneri* secretes the ubiquitin ligase IpaH7.8 *via* its T3SS, which cleaves gasdermin D to prevent NLRC4-mediated pyroptosis (Figure 2C). This allows the bacteria to persist in human epithelial cells, while also preventing the release of danger signals to limit the activation and recruitment of immune molecules (187). While IpaH7.8 has only been shown to block NLRC4-mediated pyroptosis, it remains to be seen whether it can block broader activation of pyroptosis.

To reduce inflammasome signalling, pathogens can also exploit the host cellular degradation process of autophagy to degrade effector molecules released upon inflammasome activation, a mechanism recently termed "inflammophagy" that is also used by the host cell to control innate immune responses (188). The *Vibrio parahaemolyticus* T3SS effector protein VopQ induces autophagy in infected macrophages, which interferes with ASC speck formation to suppress NLRC4 and partially suppress NLRP3 signalling (189) (Figure 2C). Furthermore, the phosphothreonin lyase SpvC of *S.* Typhimurium was suggested to dampen xenophagy and induce autophagy-dependent degradation of NLRP3 and NLRC4, albeit the exact mechanism remains elusive (190).

Furthermore, a given pathogen will likely activate multiple PRRs in the host, and therefore, to facilitate host colonisation, pathogens have evolved mechanisms to subvert a broad range of PRRs in addition to inflammasomes. For example, infection of

macrophages with *B. abortus* that are deficient in NO production, which is known to inhibit NLRP3, resulted in higher secretion of IL-1β, but no differences in bacterial load were observed, indicating that *B. abortus* employs additional mechanisms to ensure survival in macrophages (165). Similarly, although recognition of *Y. pestis* T3SS by the NLRP3 inflammasome was important for the caspase-1 response observed in cultured BMDMs, bacterial colonisation levels of *Y. pestis* were unaltered between WT and *Nlrp3*$^{-/-}$ mice (162). These studies suggest that although inflammasome activation is central to the response against several pathogens, a multifaceted response is required to successfully prevent host colonisation. Taken together, pathogens have evolved multiple mechanisms to avoid inflammasome detection and signalling, to facilitate colonisation, and to promote persistence in the host.

3.7 Therapeutic exploitation of inflammasome subversion

It is interesting to speculate whether bacterial subversion of inflammasome activation and signalling could be harnessed for the alleviation of inflammasome-driven diseases. *Lactobacillus paracasei*, a strain of the lactic acid bacteria commonly used as a probiotic, has been shown to dampen the activation of the NLRP3, as well as the NLRC4 and AIM2 inflammasomes, by induction of IL-10 *via* NOD2 in BMDMs (191). In initial studies, oral administration of *L. paracasei* strain KW3110 has been used *in vivo* to reduce NLRP3-dependent neutrophil recruitment in monosodium urate (MSU)-induced peritonitis of C56BL/6 mice and improve insulin sensitivity in high fat diet (HFD) fed, obese mice (191). Additionally, oral administration of KW3110 reduced T-cell infiltration of visceral adipose tissue in HFD fed mice (191), an NLRP3-dependent mechanism which contributes to insulin resistance (192). General evasion of inflammasome activation by *P. gingivalis* through suppression of endocytosis can also prevent inflammasome activation by *E. coli, F. nucleatum*, or DAMPs and PAMPs delivered by endocytosis (193), further indicating a potentially complex regulatory network which has developed within the microbiota that may be harnessed for therapeutic applications.

4 Conclusion

NLR proteins are host sensors for bacterial pathogens and recent advances have shown that NOD1/2, NLRC4/NAIP and NLRP3 are physiological relevant PRRs in mammals. Bacterial pathogens co-evolved with these proteins in order to establish a fruitful balance of the immune response to support both fitness of the host and replication of the pathogen. Subversion strategies used by bacteria to avoid NLR activation include the use of modification and reduced release of their PAMPs, targeting of the receptors and their pathway components as well as sophisticated use of the immune response of the host to dampen adaptive immune functions. Here we discussed the most prominent examples of bacterial subversion of the key NLR protein pathways. Albeit most studies concentrated on individual NLRs or bacterial components and effector proteins, bacteria can activate a multitude of PRRs, produce several MAMPs, and can release a large range of effector proteins that can result in a much more complex scenario of immune activation and inhibition in the host. Therefore, future studies using novel holistic technological approaches to delineate the molecular details of host-pathogen interactions both in complex models and at the single cell level will allow us to gain insights regarding systemic and adaptive immune responses and metabolic alternations related to the activation of host PRRs by bacterial pathogens. Ultimately, this will be helpful for defining new therapeutic strategies and treatments for infectious disease and their prevention by vaccination.

Author contributions

TAK and MK-L conceived and edited the manuscript and assured funding. IK wrote the first draft, edited the manuscript and generated the figures. EJ and NB wrote the first draft and edited the manuscript. All authors contributed to the article and approved the submitted version.

Funding

MK-L is funded by the Australian Research Council (Discovery Project DP190101655) and a veski Inspiring Women Fellowship. This work was supported by a mobility grant from the German Academic Exchange Service (DAAD), grant PPP 57445802 to TAK and MK-L.

Acknowledgments

We apologize to all colleagues whose excellent work could not be included due to space limitations.

Conflict of interest

The authors declare that the research was conducted in the absence of any commercial or financial relationships that could be construed as a potential conflict of interest.

Publisher's note

All claims expressed in this article are solely those of the authors and do not necessarily represent those of their affiliated organizations, or those of the publisher, the editors and the reviewers. Any product that may be evaluated in this article, or claim that may be made by its manufacturer, is not guaranteed or endorsed by the publisher.

References

1. Brubaker SW, Bonham KS, Zanoni I, Kagan JC. Innate immune pattern recognition: A cell biological perspective. *Annu Rev Immunol* (2015) 33:257–90. doi: 10.1146/annurev-immunol-032414-112240

2. Thaiss CA, Zmora N, Levy M, Elinav E. The microbiome and innate immunity. *Nature* (2016) 535(7610):65–74. doi: 10.1038/nature18847

3. Diard M, Hardt WD. Evolution of bacterial virulence. *FEMS Microbiol Rev* (2017) 41(5):679–97. doi: 10.1093/femsre/fux023

4. Lacey CA, Miao EA. Programmed cell death in the evolutionary race against bacterial virulence factors. *Cold Spring Harb Perspect Biol* (2020) 12(2). doi: 10.1101/cshperspect.a036459

5. Soares MP, Teixeira L, Moita LF. Disease tolerance and immunity in host protection against infection. *Nat Rev Immunol* (2017) 17(2):83–96. doi: 10.1038/nri.2016.136

6. Dominguez-Andres J, Kuijpers Y, Bakker OB, Jaeger M, Xu CJ, van der Meer JW, et al. Evolution of cytokine production capacity in ancient and modern European populations. *Elife* (2021) 10. doi: 10.7554/eLife.64971

7. Janeway CAJr. Approaching the asymptote? evolution and revolution in immunology. *Cold Spring Harb Symp Quant Biol* (1989) 54 Pt 1:1–13. doi: 10.1101/SQB.1989.054.01.003

8. Medzhitov R. Approaching the asymptote: 20 years later. *Immunity* (2009) 30 (6):766–75. doi: 10.1016/j.immuni.2009.06.004

9. Kawai T, Akira S. The role of pattern-recognition receptors in innate immunity: Update on toll-like receptors. *Nat Immunol* (2010) 11(5):373–84. doi: 10.1038/ni.1863

10. Nikolakopoulou C, Willment JA, Brown GD. C-type lectin receptors in antifungal immunity. *Adv Exp Med Biol* (2020) 1204:1–30. doi: 10.1007/978-981-15-1580-4_1

11. Kanneganti TD, Lamkanfi M, Nunez G. Intracellular nod-like receptors in host defense and disease. *Immunity* (2007) 27(4):549–59. doi: 10.1016/j.immuni.2007.10.002

12. Lee JH, Chiang C, Gack MU. Endogenous nucleic acid recognition by rig-I-Like receptors and cgas. *J Interferon Cytokine Res* (2019) 39(8):450–8. doi: 10.1089/jir.2019.0015

13. Kufer TA, Sansonetti PJ. Nlr functions beyond pathogen recognition. *Nat Immunol* (2011) 12(2):121–8. doi: 10.1038/ni.1985

14. Kufer TA, Fritz JH, Philpott DJ. Nacht-lrr proteins (Nlrs) in bacterial infection and immunity. *Trends Microbiol* (2005) 13(8):381–8. doi: 10.1016/j.tim.2005.06.004

15. Broz P, Dixit VM. Inflammasomes: Mechanism of assembly, regulation and signalling. *Nat Rev Immunol* (2016) 16(7):407–20. doi: 10.1038/nri.2016.58

16. Bianchi ME. Damps, pamps and alarmins: All we need to know about danger. *J Leukoc Biol* (2007) 81(1):1–5. doi: 10.1189/jlb.0306164

17. Matzinger P. Tolerance, danger, and the extended family. *Annu Rev Immunol* (1994) 12:991–1045. doi: 10.1146/annurev.iy.12.040194.005015

18. Stuart LM, Paquette N, Boyer L. Effector-triggered versus pattern-triggered immunity: How animals sense pathogens. *Nat Rev Immunol* (2013) 13(3):199–206. doi: 10.1038/nri3398

19. Kufer TA, Creagh EM, Bryant CE. Guardians of the cell: Effector-triggered immunity steers mammalian immune defense. *Trends Immunol* (2019) 40 (10):939–51. doi: 10.1016/j.it.2019.08.001

20. Girardin SE, Boneca IG, Carneiro LA, Antignac A, Jehanno M, Viala J, et al. Nod1 detects a unique muropeptide from gram-negative bacterial peptidoglycan. *Science* (2003) 300(5625):1584–7. doi: 10.1126/science.1084677

21. Girardin SE, Boneca IG, Viala J, Chamaillard M, Labigne A, Thomas G, et al. Nod2 is a general sensor of peptidoglycan through muramyl dipeptide (Mdp) detection. *J Biol Chem* (2003) 278(11):8869–72. doi: 10.1074/jbc.C200651200

22. Bertin J, Nir WJ, Fischer CM, Tayber OV, Errada PR, Grant JR, et al. Human Card4 protein is a novel ced-4/Apaf-1 cell death family member that activates nf-kappab. *J Biol Chem* (1999) 274(19):12955–8. doi: 10.1074/jbc.274.19.12955

23. Inohara N, Koseki T, del Peso L, Hu Y, Yee C, Chen S, et al. Nod1, an apaf-1-Like activator of caspase-9 and nuclear factor-kappab. *J Biol Chem* (1999) 274 (21):14560–7. doi: 10.1074/jbc.274.21.14560

24. Ogura Y, Inohara N, Benito A, Chen FF, Yamaoka S, Nunez G. Nod2, a Nod1/Apaf-1 family member that is restricted to monocytes and activates nf-kappab. *J Biol Chem* (2001) 276(7):4812–8. doi: 10.1074/jbc.M008072200

25. Boyle JP, Mayle S, Parkhouse R, Monie TP. Comparative genomic and sequence analysis provides insight into the molecular functionality of Nod1 and Nod2. *Front Immunol* (2013) 4:317. doi: 10.3389/fimmu.2013.00317

26. Magalhaes JG, Philpott DJ, Nahori MA, Jehanno M, Fritz J, Le Bourhis L, et al. Murine Nod1 but not its human orthologue mediates innate immune detection of tracheal cytotoxin. *EMBO Rep* (2005) 6(12):1201–7. doi: 10.1038/sj.embor.7400552

27. Griffin ME, Espinosa J, Becker JL, Luo JD, Carroll TS, Jha JK, et al. Enterococcus peptidoglycan remodeling promotes checkpoint inhibitor cancer immunotherapy. *Science* (2021) 373(6558):1040–6. doi: 10.1126/science.abc9113

28. Lee J, Tattoli I, Wojtal KA, Vavricka SR, Philpott DJ, Girardin SE. Ph-dependent internalization of muramyl peptides from early endosomes enables Nod1 and Nod2 signaling. *J Biol Chem* (2009) 284(35):23818–29. doi: 10.1074/jbc.M109.033670

29. Marina-Garcia N, Franchi L, Kim YG, Hu Y, Smith DE, Boons GJ, et al. Clathrin- and dynamin-dependent endocytic pathway regulates muramyl dipeptide internalization and Nod2 activation. *J Immunol* (2009) 182(7):4321–7. doi: 10.4049/jimmunol.0802197

30. Viala J, Chaput C, Boneca IG, Cardona A, Girardin SE, Moran AP, et al. Nod1 responds to peptidoglycan delivered by the helicobacter pylori cag pathogenicity island. *Nat Immunol* (2004) 5(11):1166–74. doi: 10.1038/ni1131

31. Kaparakis M, Turnbull L, Carneiro L, Firth S, Coleman HA, Parkington HC, et al. Bacterial membrane vesicles deliver peptidoglycan to Nod1 in epithelial cells. *Cell Microbiol* (2010) 12(3):372–85. doi: 10.1111/j.1462-5822.2009.01404.x

32. Bitto NJ, Cheng L, Johnston EL, Pathirana R, Phan TK, Poon IKH, et al. Staphylococcus aureus membrane vesicles contain immunostimulatory DNA, rna and peptidoglycan that activate innate immune receptors and induce autophagy. *J Extracell Vesicles* (2021) 10(6):e12080. doi: 10.1002/jev2.12080

33. Irving AT, Mimuro H, Kufer TA, Lo C, Wheeler R, Turner LJ, et al. The immune receptor Nod1 and kinase Rip2 interact with bacterial peptidoglycan on early endosomes to promote autophagy and inflammatory signaling. *Cell Host Microbe* (2014) 15(5):623–35. doi: 10.1016/j.chom.2014.04.001

34. Nakamura N, Lill JR, Phung Q, Jiang Z, Bakalarski C, de Maziere A, et al. Endosomes are specialized platforms for bacterial sensing and Nod2 signalling. *Nature* (2014) 509(7499):240–4. doi: 10.1038/nature13133

35. Keestra AM, Baumler AJ. Detection of enteric pathogens by the nodosome. *Trends Immunol* (2014) 35(3):123–30. doi: 10.1016/j.it.2013.10.009

36. Tattoli I, Travassos LH, Carneiro LA, Magalhaes JG, Girardin SE. The nodosome: Nod1 and Nod2 control bacterial infections and inflammation. *Semin Immunopathol* (2007) 29(3):289–301. doi: 10.1007/s00281-007-0083-2

37. Inohara N, Koseki T, Lin J, del Peso L, Lucas PC, Chen FF, et al. An induced proximity model for nf-kappa b activation in the Nod1/Rick and rip signaling pathways. *J Biol Chem* (2000) 275(36):27823–31. doi: 10.1074/jbc.M003415200

38. Hugot JP, Chamaillard M, Zouali H, Lesage S, Cezard JP, Belaiche J, et al. Association of Nod2 leucine-rich repeat variants with susceptibility to crohn's disease. *Nature* (2001) 411(6837):599–603. doi: 10.1038/35079107

39. Girardin SE, Tournebize R, Mavris M, Page AL, Li X, Stark GR, et al. Card4/Nod1 mediates nf-kappab and jnk activation by invasive shigella flexneri. *EMBO Rep* (2001) 2(8):736–42. doi: 10.1093/embo-reports/kve155

40. Krieg A, Correa RG, Garrison JB, Le Negrate G, Welsh K, Huang Z, et al. Xiap mediates nod signaling *Via* interaction with Rip2. *Proc Natl Acad Sci United States America* (2009) 106(34):14524–9. doi: 10.1073/pnas.0907131106

41. Ellwanger K, Briese S, Arnold C, Kienes I, Heim V, Nachbur U, et al. Xiap controls Ripk2 signaling by preventing its deposition in speck-like structures. *Life Sci Alliance* (2019) 2(4):e201900346. doi: 10.26508/lsa.201900346

42. Damgaard RB, Fiil BK, Speckmann C, Yabal M, zur Stadt U, Bekker-Jensen S, et al. Disease-causing mutations in the xiap Bir2 domain impair Nod2-

dependent immune signalling. *EMBO Mol Med* (2013) 5(8):1278–95. doi: 10.1002/emmm.201303090

43. Lipinski S, Grabe N, Jacobs G, Billmann-Born S, Till A, Hasler R, et al. Rnai screening identifies mediators of Nod2 signaling: Implications for spatial specificity of mdp recognition. *Proc Natl Acad Sci United States America* (2012) 109 (52):21426–31. doi: 10.1073/pnas.1209673109

44. Bielig H, Lautz K, Braun PR, Menning M, Machuy N, Bruegmann C, et al. The cofilin phosphatase slingshot homolog 1 (Ssh1) links Nod1 signaling to actin remodeling. *PloS Pathog* (2014) 10(9):e1004351. doi: 10.1371/journal.ppat.1004351

45. Jost PJ, Vucic D. Regulation of cell death and immunity by xiap. *Cold Spring Harb Perspect Biol* (2020) 12(8):a036426. doi: 10.1101/cshperspect.a036426

46. Damgaard RB, Gyrd-Hansen M. Inhibitor of apoptosis (Iap) proteins in regulation of inflammation and innate immunity. *Discovery Med* (2011) 11 (58):221–31.

47. Andree M, Seeger JM, Schuell S, Coutelle O, Wagner-Stippich D, Wiegmann K, et al. Bid-dependent release of mitochondrial smac dampens xiap-mediated immunity against shigella. *EMBO (European Mol Biol Organization) J* (2014) 33 (19):2171–87. doi: 10.15252/embj.201387244

48. Goncharov T, Hedayati S, Mulvihill MM, Izrael-Tomasevic A, Zobel K, Jeet S, et al. Disruption of xiap-Rip2 association blocks Nod2-mediated inflammatory signaling. *Mol Cell* (2018) 69(4):551–65.e7. doi: 10.1016/j.molcel.2018.01.016

49. Le Negrate G. Subversion of innate immune responses by bacterial hindrance of nf-kappab pathway. *Cell Microbiol* (2012) 14(2):155–67. doi: 10.1111/j.1462-5822.2011.01719.x

50. Rahman MM, McFadden G. Modulation of nf-kappab signalling by microbial pathogens. *Nat Rev Microbiol* (2011) 9(4):291–306. doi: 10.1038/nrmicro2539

51. Ogawa M, Yoshikawa Y, Mimuro H, Hain T, Chakraborty T, Sasakawa C. Autophagy targeting of listeria monocytogenes and the bacterial countermeasure. *Autophagy* (2011) 7(3):310–4. doi: 10.4161/auto.7.3.14581

52. Travassos LH, Carneiro LA, Ramjeet M, Hussey S, Kim YG, Magalhaes JG, et al. Nod1 and Nod2 direct autophagy by recruiting Atg16l1 to the plasma membrane at the site of bacterial entry. *Nat Immunol* (2010) 11(1):55–62. doi: 10.1038/ni.1823

53. Hysi P, Kabesch M, Moffatt MF, Schedel M, Carr D, Zhang Y, et al. Nod1 variation, immunoglobulin e and asthma. *Hum Mol Genet* (2005) 14(7):935–41. doi: 10.1093/hmg/ddi087

54. Weidinger S, Klopp N, Rummler L, Wagenpfeil S, Novak N, Baurecht HJ, et al. Association of Nod1 polymorphisms with atopic eczema and related phenotypes. *J Allergy Clin Immunol* (2005) 116(1):177–84. doi: 10.1016/j.jaci.2005.02.034

55. Schertzer JD, Tamrakar AK, Magalhaes JG, Pereira S, Bilan PJ, Fullerton MD, et al. Nod1 activators link innate immunity to insulin resistance. *Diabetes* (2011) 60(9):2206–15. doi: 10.2337/db11-0004

56. Keestra-Gounder AM, Byndloss MX, Seyffert N, Young BM, Chavez-Arroyo A, Tsai AY, et al. Nod1 and Nod2 signalling links er stress with inflammation. *Nature* (2016) 532(7599):394–7. doi: 10.1038/nature17631

57. Pei G, Zyla J, He L, Moura-Alves P, Steinle H, Saikali P, et al. Cellular stress promotes Nod1/2-dependent inflammation *Via* the endogenous metabolite sphingosine-1-Phosphate. *EMBO J* (2021) 40(13):e106272. doi: 10.15252/embj.2020106272

58. Mendez JM, Kolora LD, Lemon JS, Dupree SL, Keestra-Gounder AM. Activation of the endoplasmic reticulum stress response impacts the Nod1 signaling pathway. *Infection Immun* (2019) 87(8):e00826–18. doi: 10.1128/IAI.00826-18

59. Hugot JP, Laurent-Puig P, Gower-Rousseau C, Olson JM, Lee JC, Beaugerie L, et al. Mapping of a susceptibility locus for crohn's disease on chromosome 16. *Nature* (1996) 379(6568):821–3. doi: 10.1038/379821a0

60. Kufer TA, Banks DJ, Philpott DJ. Innate immune sensing of microbes by nod proteins. *Ann N Y Acad Sci* (2006) 1072:19–27. doi: 10.1196/annals.1326.020

61. Kaser A, Lee AH, Franke A, Glickman JN, Zeissig S, Tilg H, et al. Xbp1 links er stress to intestinal inflammation and confers genetic risk for human inflammatory bowel disease. *Cell* (2008) 134(5):743–56. doi: 10.1016/j.cell.2008.07.021

62. Montane J, Cadavez L, Novials A. Stress and the inflammatory process: A major cause of pancreatic cell death in type 2 diabetes. *Diabetes Metab Syndr Obes* (2014) 7:25–34. doi: 10.2147/dmso.S37649

63. Cao P, Chen Y, Guo X, Chen Y, Su W, Zhan N, et al. Fusobacterium nucleatum activates endoplasmic reticulum stress to promote crohn's disease development *Via* the upregulation of Card3 expression. *Front Pharmacol* (2020) 11:106. doi: 10.3389/fphar.2020.00106

64. Alvarez SE, Harikumar KB, Hait NC, Allegood J, Strub GM, Kim EY, et al. Sphingosine-1-Phosphate is a missing cofactor for the E3 ubiquitin ligase Traf2. *Nature* (2010) 465(7301):1084–8. doi: 10.1038/nature09128

65. Legrand-Poels S, Kustermans G, Bex F, Kremmer E, Kufer TA, Piette J. Modulation of Nod2-dependent nf-kappab signaling by the actin cytoskeleton. *J Cell Sci* (2007) 120(Pt 7):1299–310. doi: 10.1242/jcs.03424

66. Kufer TA, Kremmer E, Adam AC, Philpott DJ, Sansonetti PJ. The pattern-recognition molecule Nod1 is localized at the plasma membrane at sites of bacterial interaction. *Cell Microbiol* (2008) 10(2):477–86. doi: 10.1111/j.1462-5822.2007.01062.x

67. Keestra AM, Winter MG, Auburger JJ, Frassle SP, Xavier MN, Winter SE, et al. Manipulation of small rho gtpases is a pathogen-induced process detected by Nod1. *Nature* (2013) 496(7444):233–7. doi: 10.1038/nature12025

68. Eitel J, Krull M, Hocke AC, N'Guessan PD, Zahlten J, Schmeck B, et al. Beta-pix and Rac1 gtpase mediate trafficking and negative regulation of Nod2. *J Immunol* (2008) 181(4):2664–71. doi: 10.4049/jimmunol.181.4.2664

69. Stevens C, Henderson P, Nimmo ER, Soares DC, Dogan B, Simpson KW, et al. The intermediate filament protein, vimentin, is a regulator of Nod2 activity. *Gut* (2013) 62(5):695–707. doi: 10.1136/gutjnl-2011-301775

70. Hespen CW, Zhao X, Hang HC. Membrane targeting enhances muramyl dipeptide binding to Nod2 and Arf6-gtpase in mammalian cells. *Chem Commun (Camb)* (2022) 58(46):6598–601. doi: 10.1039/d2cc01903e

71. Regueiro V, Moranta D, Frank CG, Larrarte E, Margareto J, March C, et al. Klebsiella pneumoniae subverts the activation of inflammatory responses in a Nod1-dependent manner. *Cell Microbiol* (2011) 13(1):135–53. doi: 10.1111/j.1462-5822.2010.01526.x

72. Bielig H, Rompikuntal PK, Dongre M, Zurek B, Lindmark B, Ramstedt M, et al. Nod-like receptor activation by outer membrane vesicles from vibrio cholerae non-O1 non-O139 strains is modulated by the quorum-sensing regulator hapr. *Infect Immun* (2011) 79(4):1418–27. doi: 10.1128/iai.00754-10

73. Chatterjee D, Chaudhuri K. Vibrio cholerae O395 outer membrane vesicles modulate intestinal epithelial cells in a Nod1 protein-dependent manner and induce dendritic cell-mediated Th2/Th17 cell responses. *J Biol Chem* (2013) 288 (6):4299–309. doi: 10.1074/jbc.M112.408302

74. Thay B, Damm A, Kufer TA, Wai SN, Oscarsson J. Aggregatibacter actinomycetemcomitans outer membrane vesicles are internalized in human host cells and trigger Nod1- and Nod2-dependent nf-kappab activation. *Infect Immun* (2014) 82(10):4034–46. doi: 10.1128/iai.01980-14

75. Cecil JD, O'Brien-Simpson NM, Lenzo JC, Holden JA, Chen YY, Singleton W, et al. Differential responses of pattern recognition receptors to outer membrane vesicles of three periodontal pathogens. *PLoS One* (2016) 11(4):e0151967. doi: 10.1371/journal.pone.0151967

76. Chu H, Khosravi A, Kusumawardhani IP, Kwon AH, Vasconcelos AC, Cunha LD, et al. Gene-microbiota interactions contribute to the pathogenesis of inflammatory bowel disease. *Science* (2016) 352(6289):1116–20. doi: 10.1126/science.aad9948

77. Johnston EL, Kufer TA, Kaparakis-Liaskos M. Immunodetection and pathogenesis mediated by bacterial membrane vesicles. In: M Kaparakis-Liaskos and TA Kufer, editors. *Bacterial membrane vesicles biogenesis, functions and applications*. Switzerland: Springer International Publishing, Springer Nature (2020). p. 159–88.

78. Johnston EL, Heras B, Kufer TA, Kaparakis-Liaskos M. Detection of bacterial membrane vesicles by nod-like receptors. *Int J Mol Sci* (2021) 22 (3):1005. doi: 10.3390/ijms22031005

79. Boneca IG, Dussurget O, Cabanes D, Nahori MA, Sousa S, Lecuit M, et al. A critical role for peptidoglycan n-deacetylation in listeria evasion from the host innate immune system. *Proc Natl Acad Sci United States America* (2007) 104 (3):997–1002. doi: 10.1073/pnas.0609672104

80. Raymond JB, Mahapatra S, Crick DC, Pavelka MSJr. Identification of the namh gene, encoding the hydroxylase responsible for the n-glycolylation of the mycobacterial peptidoglycan. *J Biol Chem* (2005) 280(1):326–33. doi: 10.1074/jbc.M411006200

81. Bera A, Herbert S, Jakob A, Vollmer W, Götz F. Why are pathogenic staphylococci so lysozyme resistant? the peptidoglycan O-acetyltransferase oata is the major determinant for lysozyme resistance of staphylococcus aureus. *Mol Microbiol* (2005) 55(3):778–87. doi: 10.1111/j.1365-2958.2004.04446.x

82. Antignac A, Rousselle JC, Namane A, Labigne A, Taha MK, Boneca IG. Detailed structural analysis of the peptidoglycan of the human pathogen neisseria meningitidis. *J Biol Chem* (2003) 278(34):31521–8. doi: 10.1074/jbc.M304749200

83. Wang Q, Matsuo Y, Pradipta AR, Inohara N, Fujimoto Y, Fukase K. Synthesis of characteristic mycobacterium peptidoglycan (Pgn) fragments utilizing with chemoenzymatic preparation of meso-diaminopimelic acid (Dap), and their modulation of innate immune responses. *Org Biomol Chem* (2016) 14 (3):1013–23. doi: 10.1039/c5ob02145f

84. Zarantonelli ML, Skoczynska A, Antignac A, El Ghachi M, Deghmane AE, Szatanik M, et al. Penicillin resistance compromises Nod1-dependent proinflammatory activity and virulence fitness of neisseria meningitidis. *Cell Host Microbe* (2013) 13(6):735–45. doi: 10.1016/j.chom.2013.04.016

85. Okugawa T, Kaneko T, Yoshimura A, Silverman N, Hara Y. Nod1 and Nod2 mediate sensing of periodontal pathogens. *J Dent Res* (2010) 89(2):186–91. doi: 10.1177/0022034509354843

86. Darveau RP, Belton CM, Reife RA, Lamont RJ. Local chemokine paralysis, a novel pathogenic mechanism for porphyromonas gingivalis. *Infect Immun* (1998) 66(4):1660–5. doi: 10.1128/iai.66.4.1660-1665.1998

87. Chaput C, Ecobichon C, Cayet N, Girardin SE, Werts C, Guadagnini S, et al. Role of amia in the morphological transition of helicobacter pylori and in immune escape. *PloS Pathog* (2006) 2(9):e97. doi: 10.1371/journal.ppat.0020097

88. Gladyshev N, Taame M, Kravtsov V. Clinical and laboratory importance of detecting helicobacter pylori coccoid forms for the selection of treatment. *Prz Gastroenterol* (2020) 15(4):294–300. doi: 10.5114/pg.2020.101557

89. Liu M, Haenssler E, Uehara T, Losick VP, Park JT, Isberg RR. The legionella pneumophila enhc protein interferes with immunostimulatory muramyl peptide production to evade innate immunity. *Cell Host Microbe* (2012) 12(2):166–76. doi: 10.1016/j.chom.2012.06.004

90. Ratet G, Santecchia I, Fanton d'Andon M, Vernel-Pauillac F, Wheeler R, Lenormand P, et al. Lipl21 lipoprotein binding to peptidoglycan enables leptospira interrogans to escape Nod1 and Nod2 recognition. *PloS Pathog* (2017) 13(12): e1006725. doi: 10.1371/journal.ppat.1006725

91. D'Ambrosio EA, Drake WR, Mashayekh S, Ukaegbu OI, Brown AR, Grimes CL. Modulation of the nod-like receptors Nod1 and Nod2: A chemist's perspective. *Bioorg Med Chem Lett* (2019) 29(10):1153–61. doi: 10.1016/j.bmcl.2019.03.010

92. Keestra-Gounder AM, Tsolis RM. Nod1 and Nod2: Beyond peptidoglycan sensing. *Trends Immunol* (2017) 38(10):758–67. doi: 10.1016/j.it.2017.07.004

93. Xu H, Yang J, Gao W, Li L, Li P, Zhang L, et al. Innate immune sensing of bacterial modifications of rho gtpases by the pyrin inflammasome. *Nature* (2014) 513(7517):237–41. doi: 10.1038/nature13449

94. Martinon F, Burns K, Tschopp J. The inflammasome: A molecular platform triggering activation of inflammatory caspases and processing of proil-beta. *Mol Cell* (2002) 10(2):417–26. doi: 10.1016/s1097-2765(02)00599-3

95. Howard AD, Kostura MJ, Thornberry N, Ding GJ, Limjuco G, Weidner J, et al. Il-1-Converting enzyme requires aspartic acid residues for processing of the il-1 beta precursor at two distinct sites and does not cleave 31-kda il-1 alpha. *J Immunol* (1991) 147(9):2964–9.

96. Fantuzzi G, Puren AJ, Harding MW, Livingston DJ, Dinarello CA. Interleukin-18 regulation of interferon gamma production and cell proliferation as shown in interleukin-1beta-Converting enzyme (Caspase-1)-Deficient mice. *Blood* (1998) 91(6):2118–25. doi: 10.1182/blood.V91.6.2118

97. Ding J, Wang K, Liu W, She Y, Sun Q, Shi J, et al. Pore-forming activity and structural autoinhibition of the gasdermin family. *Nature* (2016) 535(7610):111–6. doi: 10.1038/nature18590

98. Liu X, Zhang Z, Ruan J, Pan Y, Magupalli VG, Wu H, et al. Inflammasome-activated gasdermin d causes pyroptosis by forming membrane pores. *Nature* (2016) 535(7610):153–8. doi: 10.1038/nature18629

99. Sborgi L, Ruhl S, Mulvihill E, Pipercevic J, Heilig R, Stahlberg H, et al. Gsdmd membrane pore formation constitutes the mechanism of pyroptotic cell death. *EMBO J* (2016) 35(16):1766–78. doi: 10.15252/embj.201694696

100. Aglietti RA, Estevez A, Gupta A, Ramirez MG, Liu PS, Kayagaki N, et al. Gsdmd P30 elicited by caspase-11 during pyroptosis forms pores in membranes. *Proc Natl Acad Sci* (2016) 113(28):7858–63. doi: 10.1073/pnas.1607769113

101. Swanson KV, Deng M, Ting JP. The Nlrp3 inflammasome: Molecular activation and regulation to therapeutics. *Nat Rev Immunol* (2019) 19(8):477–89. doi: 10.1038/s41577-019-0165-0

102. Duncan JA, Canna SW. The Nlrc4 inflammasome. *Immunol Rev* (2018) 281(1):115–23. doi: 10.1111/imr.12607

103. Chavarria-Smith J, Vance RE. The Nlrp1 inflammasomes. *Immunol Rev* (2015) 265(1):22–34. doi: 10.1111/imr.12283

104. Bürckstümmer T, Baumann C, Blüml S, Dixit E, Dürnberger G, Jahn H, et al. An orthogonal proteomic-genomic screen identifies Aim2 as a cytoplasmic DNA sensor for the inflammasome. *Nat Immunol* (2009) 10(3):266–72. doi: 10.1038/ni.1702

105. Fernandes-Alnemri T, Yu JW, Datta P, Wu J, Alnemri ES. Aim2 activates the inflammasome and cell death in response to cytoplasmic DNA. *Nature* (2009) 458(7237):509–13. doi: 10.1038/nature07710

106. Hornung V, Ablasser A, Charrel-Dennis M, Bauernfeind F, Horvath G, Caffrey DR, et al. Aim2 recognizes cytosolic dsdna and forms a caspase-1-Activating inflammasome with asc. *Nature* (2009) 458(7237):514–8. doi: 10.1038/nature07725

107. Jamilloux Y, Magnotti F, Belot A, Henry T. The pyrin inflammasome: From sensing rhoa gtpases-inhibiting toxins to triggering autoinflammatory syndromes. *Pathog Dis* (2018) 76(3). doi: 10.1093/femspd/fty020

108. Grenier JM, Wang L, Manji GA, Huang WJ, Al-Garawi A, Kelly R, et al. Functional screening of five pypaf family members identifies Pypaf5 as a novel regulator of nf-kappab and caspase-1. *FEBS Lett* (2002) 530(1-3):73–8. doi: 10.1016/S0014-5793(02)03416-6

109. Wang L, Manji GA, Grenier JM, Al-Garawi A, Merriam S, Lora JM, et al. Pypaf7, a novel pyrin-containing Apaf1-like protein that regulates activation of nf-kappa b and caspase-1-Dependent cytokine processing. *J Biol Chem* (2002) 277 (33):29874–80. doi: 10.1074/jbc.M203915200

110. Davis BK, Roberts RA, Huang MT, Willingham SB, Conti BJ, Brickey WJ, et al. Cutting edge: Nlrc5-dependent activation of the inflammasome. *J Immunol* (2011) 186(3):1333–7. doi: 10.4049/jimmunol.1003111

111. Khare S, Dorfleutner A, Bryan NB, Yun C, Radian AD, de Almeida L, et al. An Nlrp7-containing inflammasome mediates recognition of microbial lipopeptides in human macrophages. *Immunity* (2012) 36(3):464–76. doi: 10.1016/j.immuni.2012.02.001

112. Lightfield KL, Persson J, Brubaker SW, Witte CE, von Moltke J, Dunipace EA, et al. Critical function for Naip5 in inflammasome activation by a conserved carboxy-terminal domain of flagellin. *Nat Immunol* (2008) 9(10):1171–8. doi: 10.1038/ni.1646

113. Lightfield KL, Persson J, Trinidad Norver J, Brubaker Sky W, Kofoed Eric M, Sauer J-D, et al. Differential requirements for Naip5 in activation of the Nlrc4 inflammasome. *Infect Immun* (2011) 79(4):1606–14. doi: 10.1128/iai.01187-10

114. Franchi L, Amer A, Body-Malapel M, Kanneganti T-D, Özören N, Jagirdar R, et al. Cytosolic flagellin requires ipaf for activation of caspase-1 and interleukin 1β in salmonella-infected macrophages. *Nat Immunol* (2006) 7(6):576–82. doi: 10.1038/ni1346

115. Yang J, Hwang I, Lee E, Shin SJ, Lee E-J, Rhee JH, et al. Bacterial outer membrane vesicle-mediated cytosolic delivery of flagellin triggers host Nlrc4 canonical inflammasome signaling. *Front Immunol* (2020) 11:581165(2857). doi: 10.3389/fimmu.2020.581165

116. Mariathasan S, Newton K, Monack DM, Vucic D, French DM, Lee WP, et al. Differential activation of the inflammasome by caspase-1 adaptors asc and ipaf. *Nature* (2004) 430(6996):213–8. doi: 10.1038/nature02664

117. Diez E, Lee S-H, Gauthier S, Yaraghi Z, Tremblay M, Vidal S, et al. Birc1e is the gene within the Lgn1 locus associated with resistance to legionella pneumophila. *Nat Genet* (2003) 33(1):55–60. doi: 10.1038/ng1065

118. Wright EK, Goodart SA, Growney JD, Hadinoto V, Endrizzi MG, Long EM, et al. Naip5 affects host susceptibility to the intracellular pathogen legionella pneumophila. *Curr Biol* (2003) 13(1):27–36. doi: 10.1016/S0960-9822(02)01359-3

119. Zamboni DS, Kobayashi KS, Kohlsdorf T, Ogura Y, Long EM, Vance RE, et al. The Birc1e cytosolic pattern-recognition receptor contributes to the detection and control of legionella pneumophila infection. *Nat Immunol* (2006) 7(3):318–25. doi: 10.1038/ni1305

120. Hausmann A, Böck D, Geiser P, Berthold DL, Fattinger SA, Furter M, et al. Intestinal epithelial Naip/Nlrc4 restricts systemic dissemination of the adapted pathogen salmonella typhimurium due to site-specific bacterial pamp expression. *Mucosal Immunol* (2020) 13(3):530–44. doi: 10.1038/s41385-019-0247-0

121. Nordlander S, Pott J, Maloy KJ. Nlrc4 expression in intestinal epithelial cells mediates protection against an enteric pathogen. *Mucosal Immunol* (2014) 7 (4):775–85. doi: 10.1038/mi.2013.95

122. Mitchell PS, Roncaioli JL, Turcotte EA, Goers L, Chavez RA, Lee AY, et al. Naip-Nlrc4-Deficient mice are susceptible to shigellosis. *Elife* (2020) 9:e59022. doi: 10.7554/eLife.59022

123. Amer A, Franchi L, Kanneganti TD, Body-Malapel M, Ozören N, Brady G, et al. Regulation of legionella phagosome maturation and infection through flagellin and host ipaf. *J Biol Chem* (2006) 281(46):35217–23. doi: 10.1074/jbc.M604933200

124. Sutterwala FS, Mijares LA, Li L, Ogura Y, Kazmierczak BI, Flavell RA. Immune recognition of pseudomonas aeruginosa mediated by the Ipaf/Nlrc4 inflammasome. *J Exp Med* (2007) 204(13):3235–45. doi: 10.1084/jem.20071239

125. Cai S, Batra S, Wakamatsu N, Pacher P, Jeyaseelan S. Nlrc4 inflammasome-mediated production of il-1β modulates mucosal immunity in the lung against gram-negative bacterial infection. *J Immunol* (2012) 188(11):5623–35. doi: 10.4049/jimmunol.1200195

126. Vance RE. The Naip/Nlrc4 inflammasomes. *Curr Opin Immunol* (2015) 32:84–9. doi: 10.1016/j.coi.2015.01.010

127. Sellin ME, Muller AA, Felmy B, Dolowschiak T, Diard M, Tardivel A, et al. Epithelium-intrinsic Naip/Nlrc4 inflammasome drives infected enterocyte expulsion to restrict salmonella replication in the intestinal mucosa. *Cell Host Microbe* (2014) 16(2):237–48. doi: 10.1016/j.chom.2014.07.001

128. Gutierrez O, Pipaon C, Fernandez-Luna JL. Ipaf is upregulated by tumor necrosis factor-alpha in human leukemia cells. *FEBS Lett* (2004) 568(1-3):79–82. doi: 10.1016/j.febslet.2004.04.095

129. Cummings LA, Wilkerson WD, Bergsbaken T, Cookson BT. *In vivo*, flic expression by salmonella enterica serovar typhimurium is heterogeneous, regulated

by clpx, and anatomically restricted. *Mol Microbiol* (2006) 61(3):795–809. doi: 10.1111/j.1365-2958.2006.05271.x

130. Miao EA, Mao DP, Yudkovsky N, Bonneau R, Lorang CG, Warren SE, et al. Innate immune detection of the type iii secretion apparatus through the Nlrc4 inflammasome. *PNAS* (2010) 107(7):3076–80. doi: 10.1073/pnas.0913087107

131. Sauer J-D, Pereyre S, Archer KA, Burke TP, Hanson B, Lauer P, et al. Listeria monocytogenes engineered to activate the Nlrc4 inflammasome are severely attenuated and are poor inducers of protective immunity. *PNAS* (2011) 108(30):12419. doi: 10.1073/pnas.1019041108

132. Perez-Lopez A, Rosales-Reyes R, Alpuche-Aranda CM, Ortiz-Navarrete V. Salmonella downregulates nod-like receptor family card domain containing protein 4 expression to promote its survival in b cells by preventing inflammasome activation and cell death. *J Immunol* (2013) 190(3):1201. doi: 10.4049/jimmunol.1200415

133. Wang X, Shaw DK, Sakhon OS, Snyder GA, Sundberg EJ, Santambrogio L, et al. The tick protein sialostatin L2 binds to annexin A2 and inhibits Nlrc4-mediated inflammasome activation. *Infection Immun* (2016) 84(6):1796–805. doi: 10.1128/IAI.01526-15

134. Semper RP, Vieth M, Gerhard M, Mejias-Luque R. Helicobacter pylori exploits the Nlrc4 inflammasome to dampen host defenses. *J Immunol* (2019) 203 (8):2183–93. doi: 10.4049/jimmunol.1900351

135. Paudel S, Ghimire L, Jin L, Baral P, Cai S, Jeyaseelan S. Nlrc4 suppresses il-17a-Mediated neutrophil-dependent host defense through upregulation of il-18 and induction of necroptosis during gram-positive pneumonia. *Mucosal Immunol* (2019) 12(1):247–57. doi: 10.1038/s41385-018-0088-2

136. Tourlomousis P, Wright JA, Bittante AS, Hopkins LJ, Webster SJ, Bryant OJ, et al. Modifying bacterial flagellin to evade nod-like receptor card 4 recognition enhances protective immunity against salmonella. *Nat Microbiol* (2020) 5 (12):1588–97. doi: 10.1038/s41564-020-00801-y

137. Franchi L, Kamada N, Nakamura Y, Burberry A, Kuffa P, Suzuki S, et al. Nlrc4-driven production of il-1β discriminates between pathogenic and commensal bacteria and promotes host intestinal defense. *Nat Immunol* (2012) 13(5):449–56. doi: 10.1038/ni.2263

138. Gram AM, Wright JA, Pickering RJ, Lam NL, Booty LM, Webster SJ, et al. Salmonella flagellin activates Naip/Nlrc4 and canonical Nlrp3 inflammasomes in human macrophages. *J Immunol* (2021) 206(3):631–40. doi: 10.4049/jimmunol.2000382

139. Broderick L, De Nardo D, Franklin BS, Hoffman HM, Latz E. The inflammasomes and autoinflammatory syndromes. *Annu Rev Pathol* (2015) 10:395–424. doi: 10.1146/annurev-pathol-012414-040431

140. He Y, Zeng MY, Yang D, Motro B, Núñez G. Nek7 is an essential mediator of Nlrp3 activation downstream of potassium efflux. *Nature* (2016) 530(7590):354–7. doi: 10.1038/nature16959

141. Shi H, Wang Y, Li X, Zhan X, Tang M, Fina M, et al. Nlrp3 activation and mitosis are mutually exclusive events coordinated by Nek7, a new inflammasome component. *Nat Immunol* (2016) 17(3):250–8. doi: 10.1038/ni.3333

142. Samir P, Kesavardhana S, Patmore DM, Gingras S, Malireddi RKS, Karki R, et al. Ddx3x acts as a live-or-Die checkpoint in stressed cells by regulating Nlrp3 inflammasome. *Nature* (2019) 573(7775):590–4. doi: 10.1038/s41586-019-1551-2

143. Kayagaki N, Stowe IB, Lee BL, O'Rourke K, Anderson K, Warming S, et al. Caspase-11 cleaves gasdermin d for non-canonical inflammasome signaling. *Nature* (2015) 526(7575):666–71. doi: 10.1038/nature15541

144. Knodler LA, Crowley SM, Sham HP, Yang H, Wrande M, Ma C, et al. Noncanonical inflammasome activation of caspase-4/Caspase-11 mediates epithelial defenses against enteric bacterial pathogens. *Cell Host Microbe* (2014) 16(2):249–56. doi: 10.1016/j.chom.2014.07.002

145. Schmid-Burgk JL, Gaidt MM, Schmidt T, Ebert TS, Bartok E, Hornung V. Caspase-4 mediates non-canonical activation of the Nlrp3 inflammasome in human myeloid cells. *Eur J Immunol* (2015) 45(10):2911–7. doi: 10.1002/eji.201545523

146. Casson CN, Yu J, Reyes VM, Taschuk FO, Yadav A, Copenhaver AM, et al. Human caspase-4 mediates noncanonical inflammasome activation against gram-negative bacterial pathogens. *Proc Natl Acad Sci United States America* (2015) 112 (21):6688–93. doi: 10.1073/pnas.1421699112

147. Hagar JA, Powell DA, Aachoui Y, Ernst RK, Miao EA. Cytoplasmic lps activates caspase-11: Implications in Tlr4-independent endotoxic shock. *Science* (2013) 341(6151):1250–3. doi: 10.1126/science.1240988

148. Shi J, Zhao Y, Wang Y, Gao W, Ding J, Li P, et al. Inflammatory caspases are innate immune receptors for intracellular lps. *Nature* (2014) 514(7521):187–92. doi: 10.1038/nature13683

149. Shimada T, Park BG, Wolf AJ, Brikos C, Goodridge HS, Becker CA, et al. Staphylococcus aureus evades lysozyme-based peptidoglycan digestion that links phagocytosis, inflammasome activation, and il-1beta secretion. *Cell Host Microbe* (2010) 7(1):38–49. doi: 10.1016/j.chom.2009.12.008

150. Thammavongsa V, Kern JW, Missiakas DM, Schneewind O. Staphylococcus aureus synthesizes adenosine to escape host immune responses. *J Exp Med* (2009) 206(11):2417–27. doi: 10.1084/jem.20090097

151. Fatykhova D, Rabes A, Machnik C, Guruprasad K, Pache F, Berg J, et al. Serotype 1 and 8 pneumococci evade sensing by inflammasomes in human lung tissue. *PloS One* (2015) 10(8):e0137108. doi: 10.1371/journal.pone.0137108

152. Jefferies JMC, Johnston CHG, Kirkham L-AS, Cowan GJM, Ross KS, Smith A, et al. Presence of nonhemolytic pneumolysin in serotypes of streptococcus pneumoniae associated with disease outbreaks. *J Infect Dis* (2007) 196(6):936–44. doi: 10.1086/520091

153. Karmakar M, Katsnelson M, Malak HA, Greene NG, Howell SJ, Hise AG, et al. Neutrophil il-1β processing induced by pneumolysin is mediated by the Nlrp3/Asc inflammasome and caspase-1 activation and is dependent on k+ efflux. *J Immunol* (2015) 194(4):1763–75. doi: 10.4049/jimmunol.1401624

154. Fang R, Tsuchiya K, Kawamura I, Shen Y, Hara H, Sakai S, et al. Critical roles of asc inflammasomes in caspase-1 activation and host innate resistance to streptococcus pneumoniae infection. *J Immunol* (2011) 187(9):4890–9. doi: 10.4049/jimmunol.1100381

155. Hoegen T, Tremel N, Klein M, Angele B, Wagner H, Kirschning C, et al. The Nlrp3 inflammasome contributes to brain injury in pneumococcal meningitis and is activated through atp-dependent lysosomal cathepsin b release. *J Immunol* (2011) 187(10):5440–51. doi: 10.4049/jimmunol.1100790

156. Witzenrath M, Pache F, Lorenz D, Koppe U, Gutbier B, Tabeling C, et al. The Nlrp3 inflammasome is differentially activated by pneumolysin variants and contributes to host defense in pneumococcal pneumonia. *J Immunol* (2011) 187 (1):434–40. doi: 10.4049/jimmunol.1003143

157. McNeela EA, Burke A, Neill DR, Baxter C, Fernandes VE, Ferreira D, et al. Pneumolysin activates the Nlrp3 inflammasome and promotes proinflammatory cytokines independently of Tlr4. *PloS Pathog* (2010) 6(11):e1001191. doi: 10.1371/journal.ppat.1001191

158. Kirkham LA, Jefferies JM, Kerr AR, Jing Y, Clarke SC, Smith A, et al. Identification of invasive serotype 1 pneumococcal isolates that express nonhemolytic pneumolysin. *J Clin Microbiol* (2006) 44(1):151–9. doi: 10.1128/jcm.44.1.151-159.2006

159. Harvey RM, Hughes CE, Paton AW, Trappetti C, Tweten RK, Paton JC. The impact of pneumolysin on the macrophage response to streptococcus pneumoniae is strain-dependent. *PloS One* (2014) 9(8):e103625. doi: 10.1371/journal.pone.0103625

160. Zwack EE, Snyder AG, Wynosky-Dolfi MA, Ruthel G, Philip NH, Marketon MM, et al. Inflammasome activation in response to the yersinia type iii secretion system requires hyperinjection of translocon proteins yopb and yopd. *mBio* (2015) 6(1):e02095–14. doi: 10.1128/mBio.02095-14

161. Dewoody R, Merritt PM, Marketon MM. Yopk controls both rate and fidelity of yop translocation. *Mol Microbiol* (2013) 87(2):301–17. doi: 10.1111/mmi.12099

162. Brodsky IE, Palm NW, Sadanand S, Ryndak MB, Sutterwala FS, Flavell RA, et al. A yersinia effector protein promotes virulence by preventing inflammasome recognition of the type iii secretion system. *Cell Host Microbe* (2010) 7(5):376–87. doi: 10.1016/j.chom.2010.04.009

163. Hernandez-Cuellar E, Tsuchiya K, Hara H, Fang R, Sakai S, Kawamura I, et al. Cutting edge: Nitric oxide inhibits the Nlrp3 inflammasome. *J Immunol* (2012) 189(11):5113–7. doi: 10.4049/jimmunol.1202479

164. Hooftman A, Angiari S, Hester S, Corcoran SE, Runtsch MC, Ling C, et al. The immunomodulatory metabolite itaconate modifies Nlrp3 and inhibits inflammasome activation. *Cell Metab* (2020) 32(3):468–78.e7. doi: 10.1016/j.cmet.2020.07.016

165. Campos PC, Gomes MTR, Marinho FAV, Guimarães ES, de Moura Lodi Cruz MGF, Oliveira SC. Brucella abortus nitric oxide metabolite regulates inflammasome activation and il-1β secretion in murine macrophages. *Eur J Immunol* (2019) 49(7):1023–37. doi: 10.1002/eji.201848016

166. Jiang J, Wang W, Sun F, Zhang Y, Liu Q, Yang D. Bacterial infection reinforces host metabolic flux from arginine to spermine for Nlrp3 inflammasome evasion. *Cell Rep* (2021) 34(10):108832. doi: 10.1016/j.celrep.2021.108832

167. Williams K. Modulation and block of ion channels: A new biology of polyamines. *Cell Signalling* (1997) 9(1):1–13. doi: 10.1016/S0898-6568(96)00089-7

168. Johnson L, Atanasova KR, Bui PQ, Lee J, Hung SC, Yilmaz Ö, et al. Porphyromonas gingivalis attenuates atp-mediated inflammasome activation and Hmgb1 release through expression of a nucleoside-diphosphate kinase. *Microbes Infect* (2015) 17(5):369–77. doi: 10.1016/j.micinf.2015.03.010

169. Chen H, Yang D, Han F, Tan J, Zhang L, Xiao J, et al. The bacterial T6ss effector evpp prevents Nlrp3 inflammasome activation by inhibiting the Ca(2+)-dependent mapk-jnk pathway. *Cell Host Microbe* (2017) 21(1):47–58. doi: 10.1016/j.chom.2016.12.004

170. Yen H, Sugimoto N, Tobe T. Enteropathogenic escherichia coli uses nlea to inhibit Nlrp3 inflammasome activation. *PloS Pathog* (2015) 11(9):e1005121. doi: 10.1371/journal.ppat.1005121

171. Waldhuber A, Puthia M, Wieser A, Cirl C, Durr S, Neumann-Pfeifer S, et al. Uropathogenic escherichia coli strain Cft073 disrupts Nlrp3 inflammasome activation. *J Clin Invest* (2016) 126(7):2425–36. doi: 10.1172/JCI81916

172. Virreira Winter S, Zychlinsky A. The bacterial pigment pyocyanin inhibits the Nlrp3 inflammasome through intracellular reactive oxygen and nitrogen species. *J Biol Chem* (2018) 293(13):4893–900. doi: 10.1074/jbc.RA117.001105

173. Wynosky-Dolfi MA, Snyder AG, Philip NH, Doonan PJ, Poffenberger MC, Avizonis D, et al. Oxidative metabolism enables salmonella evasion of the Nlrp3 inflammasome. *J Exp Med* (2014) 211(4):653–68. doi: 10.1084/jem.20130627

174. Yadav M, Zhang J, Fischer H, Huang W, Lutay N, Cirl C, et al. Inhibition of tir domain signaling by tcpc: Myd88-dependent and independent effects on escherichia coli virulence. *PloS Pathog* (2010) 6(9):e1001120. doi: 10.1371/journal.ppat.1001120

175. Mathur A, Feng S, Hayward JA, Ngo C, Fox D, Atmosukarto II, et al. A multicomponent toxin from bacillus cereus incites inflammation and shapes host outcome *Via* the Nlrp3 inflammasome. *Nat Microbiol* (2019) 4(2):362–74. doi: 10.1038/s41564-018-0318-0

176. Mitchell AJ, Yau B, McQuillan JA, Ball HJ, Too LK, Abtin A, et al. Inflammasome-dependent ifn-Γ drives pathogenesis in streptococcus pneumoniae meningitis. *J Immunol* (2012) 189(10):4970–80. doi: 10.4049/jimmunol.1201687

177. Zwijnenburg PJ, van der Poll T, Florquin S, Akira S, Takeda K, Roord JJ, et al. Interleukin-18 gene-deficient mice show enhanced defense and reduced inflammation during pneumococcal meningitis. *J Neuroimmunol* (2003) 138(1-2):31–7. doi: 10.1016/s0165-5728(03)00088-2

178. Atianand MK, Duffy EB, Shah A, Kar S, Malik M, Harton JA. Francisella tularensis reveals a disparity between human and mouse Nlrp3 inflammasome activation. *J Biol Chem* (2011) 286(45):39033–42. doi: 10.1074/jbc.M111.244079

179. Vladimer GI, Marty-Roix R, Ghosh S, Weng D, Lien E. Inflammasomes and host defenses against bacterial infections. *Curr Opin Microbiol* (2013) 16 (1):23–31. doi: 10.1016/j.mib.2012.11.008

180. Yang J, Lee KM, Park S, Cho Y, Lee E, Park JH, et al. Bacterial secretant from pseudomonas aeruginosa dampens inflammasome activation in a quorum sensing-dependent manner. *Front Immunol* (2017) 8:333. doi: 10.3389/fimmu.2017.00333

181. Bierschenk D, Monteleone M, Moghaddas F, Baker PJ, Masters SL, Boucher D, et al. The salmonella pathogenicity island-2 subverts human Nlrp3 and Nlrc4 inflammasome responses. *J Leukoc Biol* (2019) 105(2):401–10. doi: 10.1002/jlb.Ma0318-112rr

182. LaRock CN, Cookson BT. The yersinia virulence effector yopm binds caspase-1 to arrest inflammasome assembly and processing. *Cell Host Microbe* (2012) 12(6):799–805. doi: 10.1016/j.chom.2012.10.020

183. Schotte P, Denecker G, Van Den Broeke A, Vandenabeele P, Cornelis GR, Beyaert R. Targeting Rac1 by the yersinia effector protein yope inhibits caspase-1-Mediated maturation and release of interleukin-1beta. *J Biol Chem* (2004) 279 (24):25134–42. doi: 10.1074/jbc.M401245200

184. Shao F, Merritt PM, Bao Z, Innes RW, Dixon JE. A yersinia effector and a pseudomonas avirulence protein define a family of cysteine proteases functioning in bacterial pathogenesis. *Cell* (2002) 109(5):575–88. doi: 10.1016/s0092-8674(02) 00766-3

185. Kobayashi T, Ogawa M, Sanada T, Mimuro H, Kim M, Ashida H, et al. The shigella Ospc3 effector inhibits caspase-4, antagonizes inflammatory cell death, and promotes epithelial infection. *Cell Host Microbe* (2013) 13(5):570–83. doi: 10.1016/j.chom.2013.04.012

186. Li Z, Liu W, Fu J, Cheng S, Xu Y, Wang Z, et al. Shigella evades pyroptosis by arginine adp-riboxanation of caspase-11. *Nature* (2021) 599(7884):290–5. doi: 10.1038/s41586-021-04020-1

187. Luchetti G, Roncaioli JL, Chavez RA, Schubert AF, Kofoed EM, Reja R, et al. Shigella ubiquitin ligase Ipah7.8 targets gasdermin d for degradation to prevent pyroptosis and enable infection. *Cell Host Microbe* (2021) 29(10):1521–30.e10. doi: 10.1016/j.chom.2021.08.010

188. Chauhan S, Jena KK, Mehto S, Chauhan NR, Sahu R, Dhar K, et al. Innate immunity and inflammophagy: Balancing the defence and immune homeostasis. *FEBS J* (2021). doi: 10.1111/febs.16298

189. Higa N, Toma C, Koizumi Y, Nakasone N, Nohara T, Masumoto J, et al. Vibrio parahaemolyticus effector proteins suppress inflammasome activation by interfering with host autophagy signaling. *PloS Pathog* (2013) 9(1):e1003142. doi: 10.1371/journal.ppat.1003142

190. Zhou L, Li Y, Gao S, Yuan H, Zuo L, Wu C, et al. Salmonella spvc gene inhibits autophagy of host cells and suppresses Nlrp3 as well as Nlrc4. *Front Immunol* (2021) 12:639019. doi: 10.3389/fimmu.2021.639019

191. Suzuki H, Yamazaki T, Ohshio K, Sugamata M, Yoshikawa M, Kanauchi O, et al. A specific strain of lactic acid bacteria, lactobacillus paracasei, inhibits inflammasome activation in vitro and prevents inflammation-related disorders. *J Immunol* (2020) 205(3):811–21. doi: 10.4049/jimmunol.1900657

192. Vandanmagsar B, Youm YH, Ravussin A, Galgani JE, Stadler K, Mynatt RL, et al. The Nlrp3 inflammasome instigates obesity-induced inflammation and insulin resistance. *Nat Med* (2011) 17(2):179–88. doi: 10.1038/nm.2279

193. Taxman DJ, Swanson KV, Broglie PM, Wen H, Holley-Guthrie E, Huang MT, et al. Porphyromonas gingivalis mediates inflammasome repression in polymicrobial cultures through a novel mechanism involving reduced endocytosis. *J Biol Chem* (2012) 287(39):32791–9. doi: 10.1074/jbc.M112.401737

frontiers | Frontiers in Immunology

TYPE Review
PUBLISHED 28 July 2022
DOI 10.3389/fimmu.2022.923477

Check for updates

OPEN ACCESS

EDITED BY
Maria Kaparakis-Liaskos,
La Trobe University, Australia

REVIEWED BY
Elba Mónica Vermeulen,
Instituto de Biología y Medicina Experimental, Argentina
Chiara Della Bella,
University of Florence, Italy

*CORRESPONDENCE
Yanyan Shi
shiyanyan@bjmu.edu.cn
Shigang Ding
dingshigang222@163.com

†These authors share first authorship

SPECIALTY SECTION
This article was submitted to Microbial Immunology, a section of the journal Frontiers in Immunology

RECEIVED 19 April 2022
ACCEPTED 04 July 2022
PUBLISHED 28 July 2022

CITATION
Deng R, Zheng H, Cai H, Li M, Shi Y and Ding S (2022) Effects of *helicobacter pylori* on tumor microenvironment and immunotherapy responses. *Front. Immunol.* 13:923477. doi: 10.3389/fimmu.2022.923477

COPYRIGHT
© 2022 Deng, Zheng, Cai, Li, Shi and Ding. This is an open-access article distributed under the terms of the Creative Commons Attribution License (CC BY). The use, distribution or reproduction in other forums is permitted, provided the original author(s) and the copyright owner(s) are credited and that the original publication in this journal is cited, in accordance with accepted academic practice. No use, distribution or reproduction is permitted which does not comply with these terms.

Effects of *helicobacter pylori* on tumor microenvironment and immunotherapy responses

Ruiyi Deng[1,2†], Huiling Zheng[3†], Hongzhen Cai[1,2], Man Li[1,4], Yanyan Shi[1*] and Shigang Ding[3*]

[1]Peking University Third Hospital, Research Center of Clinical Epidemiology, Beijing, China, [2]Peking University Health Science Center, Peking University First Medical School, Beijing, China, [3]Peking University Third Hospital, Department of Gastroenterology, Beijing, China, [4]Peking University Health Science Center, Peking University Third Medical School, Beijing, China

Helicobacter pylori is closely associated with gastric cancer. During persistent infection, *Helicobacter pylori* can form a microenvironment in gastric mucosa which facilitates the survival and colony formation of *Helicobacter pylori*. Tumor stromal cells are involved in this process, including tumor-associated macrophages, mesenchymal stem cells, cancer-associated fibroblasts, and myeloid-derived suppressor cells, and so on. The immune checkpoints are also regulated by *Helicobacter pylori* infection. *Helicobacter pylori* virulence factors can also act as immunogens or adjuvants to elicit or enhance immune responses, indicating their potential applications in vaccine development and tumor immunotherapy. This review highlights the effects of *Helicobacter pylori* on the immune microenvironment and its potential roles in tumor immunotherapy responses.

KEYWORDS

***Helicobacter pylori*, immune evasion, gastric cancer, microenvironment, immunotherapy**

Introduction

Helicobacter pylori is a gram-negative, helical, microaerophilic, and flagellated bacteria that colonizes the gastric mucosa in approximately 50% of the world population (1, 2). *Helicobacter pylori* infection is the main cause of gastric mucosal diseases such as gastric cancer (GC), chronic non-atrophic gastritis, atrophic gastritis, intestinal metaplasia, and dysplasia (3). GC is the fifth most common cancer and the fourth leading cause of cancer-related deaths worldwide (4). *H. pylori* is classified by the WHO as a class I carcinogen associated with the onset of GC, as chronic *H. pylori* infection leads to at least 75% of GC cases (5–8). 2% of *H. pylori* infected patients will develop GC (7).

Tumor growth is supported by oncogene-driven metabolic activities as well as by the microenvironment. Infection with *H. pylori* promotes gastric tumorigenesis, mainly by influencing the microenvironment (9). Virulence factors such as cytotoxin-associated gene A (CagA), vacuolating cytotoxin A (VacA), urease (Ure), arginase (Arg),

lipopolysaccharide (LPS), and neutrophil-activating protein (NAP), enable *H. pylori* to survive and colonize the gastric mucosa, maintain chronic inflammation, and induce malignant changes within the gastric mucosa (1, 10–12). The immune system plays a pivotal role in eliminating *H. pylori* infection and controlling inflammation. Throughout a long-term co-existence with human hosts, *H. pylori* has developed several strategies to maintain a balance between the immune response and immune escape (13, 14). Through regulating tumor stromal cells, immune checkpoints, and other regulatory factors, *H. pylori* constructs a microenvironment that favors persistent colonization and facilitates tumorigenesis.

However, the influence of *H. pylori* on responses to immunotherapies and the prognosis of GC remains controversial (15–18). Recent studies have presented that *H. pylori* infection might affect the curative effect of tumor therapy by the induced immuno-regulation (19, 20). Besides, *H. pylori* virulence factors such as NAP, VacA, and Ure might elicit or enhance immune responses, which indicates the potential application in vaccine development and tumor immunotherapy (21, 22). These virulence factors are immunodominant antigens of *H. pylori* and might improve patient prognosis as immunogens or adjuvants in immunotherapy (23). Here, this review describes the mechanisms and effects of *H. pylori* on the immune microenvironment of GC and tumor immunotherapy responses.

Effects of *H. pylori* on tumor stromal cells in gastric tumor immune microenvironment

The tumor microenvironment (TME) consists of a continuously evolving complex of tumor cells and stroma. Stroma comprises surrounding non-cancerous fibroblasts, epithelial, immune and blood cells, and extracellular components such as cytokines, growth factors, hormones, and extracellular matrix (ECM) (24, 25). Stroma plays a key role during tumor initiation, progression, and metastasis, meanwhile it significantly influences therapeutic responses and clinical outcomes (26). *Helicobacter pylori* and its virulence factors can form a microenvironment that facilitates its survival and colony formation by regulating the constituents and functions of the TME. This section summarizes the interactions between *H. pylori* and tumor stromal cells during GC initiation, progression, and metastasis and describes potential strategies to improve the prognosis (Figure 1; Table 1).

Effects of *H. pylori* on tumor-associated macrophages in gastric tumor immune microenvironment

Changes in immune responses and the immune escape of *H. pylori* are closely associated with tumor-associated macrophages (TAMs), which are emerging key players in the TME. Macrophages play crucial roles in host defense against bacterial infections and in the regulation of immune responses during *H. pylori* infection (68). However, macrophages can also induce angiogenesis and suppress the host immune response during cancer development (37, 69). Generally, TAMs comprise M1 and M2 subtypes (27). Proinflammatory activated M1 macrophages promote the type I T helper (Th1) immune response by producing type I proinflammatory cytokines such as IL-1β, IL-1α, and IL-6 to clear pathogens and inhibit tumor progression, while simultaneously suppressing Th2-type responses (27, 70, 71). Activated M2 macrophages contribute to production of ECM and anti-inflammatory effectors such as IL-4 and IL-10 that are involved in the Th2 immune response, promotion of wound healing, and suppression of Th1 responses (72–75). Additionally, a third type called regulatory macrophages (Mregs) secrete abundant IL-10 that limits inflammation but do not secrete ECM (72). *Helicobacter pylori* and other pathogens might impair M1 macrophage differentiation while inducing M2 macrophage differentiation or M1 transdifferentiation into M2 macrophages, which can promote tumor progression and invasion by inducing angiogenesis and mediating immunosuppressive signals in solid tumors (27).

Furthermore, *H. pylori* infection might regulate specific microRNAs (miRNAs) to control macrophage function and affect the TME (28, 76). Infection with *H. pylori* leads to the downregulated expression of miR-4270 by human monocyte-derived macrophages. This favors upregulation of expression of CD300E immune receptors that enhance the proinflammatory potential of macrophages. However, the expression and exposure of major histocompatibility complex class II (MHC-II) molecules on the plasma membrane are simultaneously compromised. Hence, antigen presentation ability is decreased, leading to persistent *H. pylori* infection (28). The upregulation of let-7i-5p, miR-146b-5p and miR-185-5p, and miR146b expression in macrophages caused by *H. pylori* infection can similarly decrease HLA-II expression on the plasma membrane, which ultimately compromises bacterial antigen presentation to Th lymphocytes and impairs immune responses against *H. pylori* (29, 30). Collectively, *H. pylori* infection mainly downregulates surface recognition factors at the transcriptional level by rendering macrophages fail to degrade the bacteria. Thus, macrophages become a protective niche for *H. pylori*.

Helicobacter pylori can induce the production of specific enzymes that regulate macrophage function and affect TME. The production of arginase II (Arg2) in macrophages induced by *H. pylori* infection results in cell apoptosis and restrained proinflammatory cytokine responses, thus promotes *H. pylori* immune evasion (31, 32). Matrix metalloproteinase 7 (MMP7) plays a pivotal role in *H. pylori*-mediated immune escape (33). Heme oxygenase-1 (HO-1) expression in macrophages also be induced, resulting in a polarization switch towards a reduction

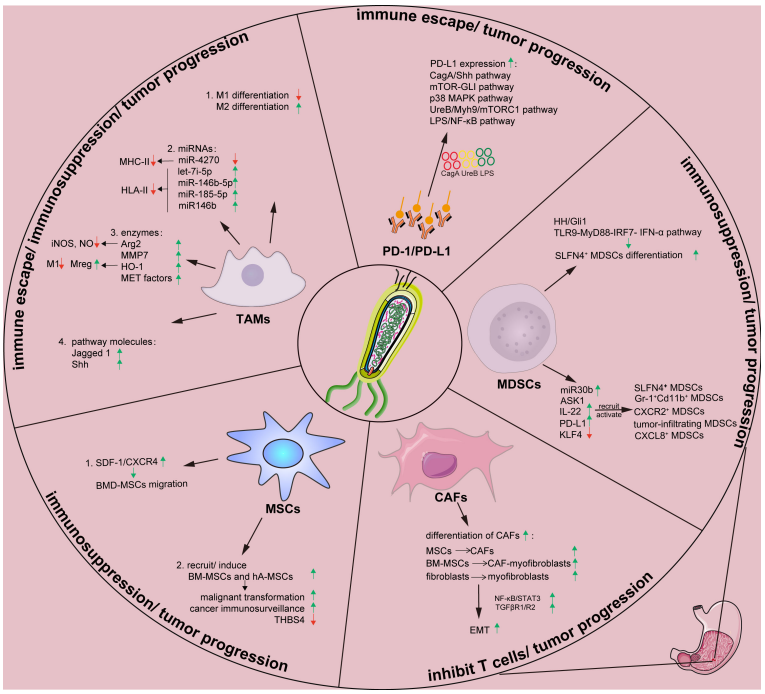

FIGURE 1
Effects of *H. pylori* on tumor stromal cells and tumor-related proteins in gastric tumor immune microenvironment. Arg, arginase; ASK1, apoptosis signal-regulating kinase 1; BM-MSC, Bone marrow-derived mesenchymal stem cells; CAF, cancer-associated fibroblast; Cag A, cytotoxin-associated gene A; CXCL8, chemokine (C-X-C motif) ligand 8; EMT, epithelial-mesenchymal transition; hA-MSC, human adipose-derived mesenchymal stem cells; HH, Hedgehog; HO-1, heme oxygenase-1; *H.pylori*, *Helicobacter pylori*; IL-22, Interleukin-22; IRF, interferon regulatory factor; IFN, interferon; KLF4, Krüppel-like factor 4; LPS, lipopolysaccharide; MAPK, mitogen-activated protein kinases; MDSCs, myeloid-derived suppressor cells; MET, mesenchymal-epithelial transition; MHC-II, major histocompatibility complex class II; MMP, matrix metalloproteinase; mTOR, mammalian target of rapamycin; Myh9, myosin heavy chain 9; NF-κB, nuclear factor kappa B; miR, microRNA; MSCs, mesenchymal stem cells; PD-1, programmed death 1; PD-L1, programmed death-ligand 1; PI3K-AKT, phosphatidylinositol 3 kinase-protein kinase B; ROS, reactive oxygen species; SDF, stromal-derived factor; Shh, Sonic hedgehog; SLFN4, Schlafen 4; STAT3, signal transducer and activator of transcription 3; TAMs, tumor-associated macrophages; TGFβ, transforming growth factor β; TLR, Toll-like receptor; Ure, urease; Vac A, vacuolating cytotoxin A.

in the M1 population and an increase in the Mreg profile, causing innate and adaptive immune responses failure (34). Transfer exosomes expressing mesenchymal–epithelial transition (MET) factor, a cell-surface receptor tyrosine kinase from *H. pylori*-infected GC cells, can elicit uncontrolled macrophage activation and downstream inflammation and might be associated with tumorigenesis and cancer development (35). These findings shed light on how *H. pylori* influences the gastric microenvironment by inducing the expression of macrophage-associated enzymes in TAMs.

Moreover, *H. pylori* upregulates the expression of Jagged 1, a ligand of Notch signaling that plays an important role in M1 macrophage activation and bactericidal activity to prevent *H. pylori* infection. Upregulated Jagged 1 expression induces an increase in the expression of proinflammatory mediators and phagocytosis and a decrease in the bacterial load, which together impart antibacterial activity in macrophages (36). The hedgehog (HH) signaling pathway also plays an important role in the gastric TME. Sonic hedgehog (SHH) induced by *H. pylori* infection acts as a macrophage chemoattractant, which is a prerequisite in the gastric immune response (37).

In conclusion, *H. pylori* infection at the early stage can induce the infiltration of polymorphonuclear leukocytes and mononuclear phagocytes in the gastric mucosa as an innate immune response (77). During the advanced stages of GC, *H. pylori* can escape immune surveillance by impairing the antigen presentation of TAMs or by disrupting the M1/M2 (or Mreg) balance in favor of an M2 (or Mreg) phenotype (34, 72). Immunosuppressive status eventually promotes tumorigenesis and cancer development (78). These mechanisms also provide the potential for investigating novel targeted drugs (79). Specific miRNAs such as let-7i-5p, miR-146b-5p, and miR-185-5p can be targeted to reduce adverse effects on macrophage antigen presentation (29). Targeting specific enzymes including MMP7 and HO-1 or signaling pathways, such as Notch and HH, to regulate the M1/M2 (or Mreg) balance might also warrant investigation (33, 34).

TABLE 1 Effects of *H. pylori* on tumor cells in gastric tumor immune microenvironment.

Tumor cells affected by *H. pylori*	Roles of *H. pylori*		Results
TAMs	Simultaneous impairment and induction of M1 macrophage and M2 macrophage differentiation, respectively, or transdifferentiation to M2 macrophages (27)		Promotes tumor progression and invasion by inducing angiogenesis and mediating immunosuppressive signals in solid tumors
	Regulation of specific miRNAs	Downregulates miR-4270 expression (28)	Impairs MHC-II expression and exposure, decreases antigen presentation ability, favors persistent *H. pylori* infection
		Upregulates let-7i-5p, miR-146b-5p, miR-185-5p, and miR146b expression (29, 30)	Inhibits HLA-II expression, compromises bacterial antigen presentation to Th lymphocytes, impairs immune responses to *H. pylori*
	Induces production of specific enzymes	Arg2 (31, 32)	Promotes immune escape of *H. pylori*, mediates macrophage apoptosis, restrains inflammatory responses
		MMP7 (33)	Promotes immune escape of *H. pylori*
		HO-1 (34)	Reduces M1 population, increases the number of Mregs, promotes immune escape of *H. pylori*
		MET factor (35)	Elicits uncontrolled activation of macrophages and inflammation involved in tumorigenesis and cancer development
	Regulation of some signaling pathway molecules	Upregulation of Jagged 1 expression (36)	Increases secretion of proinflammatory mediators and phagocytosis, decreases bacterial load, confers anti-bacterial activity on macrophages
		Induces SHH release from the stomach (37)	Induces macrophage migration during early *H. pylori* infection, involved in gastric immune response
MSCs	Upregulates CXCR4 expression and enhances MSCs migration toward SDF-1 (38)		Enhances BM-MSC migration into gastric tissues
	Recruits or induces BM-MSCs and hA-MSCs	Promotes malignant transformation (39–42)	Promotes *H. pylori*-mediated gastric tumorigenesis and development
		Mediates local and systemic immunosuppression (43, 44)	
		Alters THBS expression (45, 46)	
CAFs	Induces MSC differentiation into CAFs	Enhances expression of fibroblast markers, CAF activation, and levels of aggression/invasion markers (47, 48)	Promotes survival, proliferation, and migration of GC cell lines, inhibits antitumor functions of T cells in GC TME
	Stimulates BM-MSC differentiation into CAF myofibroblasts	Increases HDGF expression (49)	Enhances tumor cell ability to proliferate, invade, and metastasize (49, 50)
	Induces fibroblast transdifferentiation into myofibroblasts	Upregulates and downregulates HIF-1α and Bax expression, respectively (51)	Promotes gastric tumorigenesis
	Propels EMT *via* signal pathways and TGF-β secretion	Induces activation or differentiation of rat gastric fibroblasts by NF-κB and STAT3 signaling (52)	Induces Snail1 expression and propels EMT leading to GC progression
		Secretes TGFβ1 and regulates TGFβR1/R2-dependent signaling in *H. pylori*-activated gastric fibroblasts (53–55)	Prompts reprogramming normal gastric epithelial cells towards a precancerous phenotype and promotes EMT in normal epithelial cells
MDSCs	Induces differentiation of $SLFN4^+$ MDSCs	HH/Gli1 (56, 57)	Inhibits gastric inflammatory response by *H. pylori*, suppresses T cell function, immune dysregulation, and tumor progression
		TLR9-MyD88-IRF7- IFN-α pathway (58)	
	Interaction between *H. pylori* and MDSCs is regulated by several factors	MiR130b (59)	Activates $SLFN4^+$ MDSCs and promotes *H. pylori*-induced metaplasia
		ASK1 (25, 60)	Suppresses inflammation induced by infiltrating immature MDSCs
		IL-22 (61)	Induces expression of proinflammatory proteins, suppresses Th1 cell responses, promotes development of *H. pylori*-associated gastritis
		PD-L1 (62–64)	Promotes tumor infiltration of MDSCs, mediates resistance to anti-PD-1/PD-L1 therapy

(Continued)

TABLE 1 Continued

Tumor cells affected by *H. pylori*	Roles of *H. pylori*	Results
	KLF-4 (65–67)	Promotes recruitment of MDSCs to tumors, creates immunosuppressive microenvironment, promotes tumor growth

Effects of *H. pylori* on recruiting and inducing bone marrow-derived mesenchymal stem cells in gastric tumor immune microenvironment

Multipotent mesenchymal stem cells (MSCs) can self-renew and differentiate into various cell types that play key roles in tissue healing, regeneration, and immune regulation (80). Bone marrow-derived mesenchymal stem cells (BM-MSCs) might play important roles in *H. pylori*-associated gastric tumorigenesis and immunosuppression. Upon sensing signals indicating gastric mucosa damage, BM-MSCs migrate from bone marrow to stomach *via* the peripheral circulation. BM-MSCs heal damaged mucosa through a paracrine mechanism and directed differentiation (81, 82). *H. pylori*-induced persistent inflammation is required for BM-MSC migration and tumorigenesis (43, 83). Upregulated C-X-C chemokine receptor type 4 (CXCR4) interacts with its ligand, stromal-derived factor (SDF-1) and then promote BM-MSC migration to the gastric tissues (38).

Gastric epithelial glands become repopulated with BM-MSCs in mice model one year after *H. pylori* infection (39). After recruitment to stomach, BM-MSCs can become entrapped in a microenvironment containing *H. pylori* and malignant cells, 25% of which originate from BM-MSCs. Fusion with epithelial cells might render BM-MSCs more susceptible to malignant transformation or lead to the promotion of cancerous processes (40). BM-MSCs gradually acquire a clonal advantage and undergo stepwise transformation to malignant cells (39). During malignant progression, gastric epithelial glandular units undergo monoclonal transformation, resulting in emerging cancer stem cell (CSC) clones and adenocarcinomas (39, 41). Human adipose-derived mesenchymal stem cells (hA-MSCs) also participate in gastric tumorigenesis by increasing tumor cells invasion and metastasis during *H. pylori* infection (42).

In addition to malignant transformation, MSCs can promote tumorigenesis locally and systemically by compromising cancer immune surveillance or altering tumor stroma. When transplanting BM-MSCs in *H. pylori* infected mice model, IL-10 and transforming growth factor-β1 (TGF-β1) can be increased, as well as T cells secreting IL-10 and $CD4^+$ $CD25^+$ $Foxp3^+$ regulatory T (Treg) cells in splenic mononuclear cells (43, 44). BM-MSCs can reduce the fraction of T cells that produce IFN-γ, thus inhibiting $CD4^+$ and $CD8^+$ T cell proliferation. Local and systemic immunosuppression mediated by BM-MSCs contributes to GC development induced by *H. pylori* (43).

MSCs can also promote tumorigenesis by altering tumor stromal components. Thrombospondin (THBS) promotes tumorigenesis through crosstalk with BM-MSCs. Infection with *H. pylori* significantly upregulates the expression of THBS4 in BM-MSCs. Overexpressed THBS4 then mediates BM-MSC-induced angiogenesis in GC by activating the THBS4/integrin α2/PI3K/AKT pathway (45). Moreover, BM-MSCs can differentiate into pan-cytokeratin-positive (pan-CK^+) epithelial cells and alpha-smooth muscle actin (α-SMA^+) cancer-associated fibroblasts (CAFs) by secreting THBS2, thus promoting the development of *H. pylori*-associated GC (46).

BM-MSCs play pivotal roles in *H. pylori*-associated GC. The immune regulatory functions of MSCs remain obscure. Shedding light on these functions and their mechanisms will provide clues on therapeutic targets for preventing GC development.

Effects of *H. pylori* on induction of cancer-associated fibroblasts in gastric tumor immune microenvironment

CAFs are activated myofibroblasts that accompany solid tumors and are principal constituents of tumor stroma (84, 85). They play important roles in the TME. They can create a niche for cancer cells and promote cancer progression by stimulating cancer cell proliferation, migration, invasion, and angiogenesis (85–87). Proinflammatory and tumor-associated factors secreted by CAFs might induce persistent inflammation or intervene in tumor immunity, thus mediate tumor immune escape (52, 88). Mainly derived from MSCs, CAFs could induce epithelial-mesenchymal transition (EMT), which enhances the invasive properties of malignant cells (89, 90) that detach from primary tumor site to surrounding tissues (91).

Helicobacter pylori infection can induce MSCs differentiating into CAFs, and upregulate the expression of fibroblast markers, fibroblast activation protein (FAP), CAF activation markers, and aggressive/invasive markers (47). FAP-positive CAFs enhance the survival, proliferation, and migration of GC cell lines and inhibit T cells function (48). *H. pylori* infection also increases the

expression of hepatoma-derived growth factor (HDGF) (49, 50). Exposure to HDGF promotes the recruitment of BM-MSCs, stimulates their differentiation into CAF-myofibroblasts, and enhances tumor cell proliferation, invasiveness, and metastasis (49). Moreover, *H. pylori* infection can induce fibroblasts transdifferentiating into myofibroblasts, which upregulating the early carcinogenic marker hypoxia-inducible factor 1-alpha (HIF-1α) and downregulating proapoptotic bcl-2-like protein 4 (Bax) expression (51).

CAFs induced by *H. pylori* propel EMT by nuclear factor kappa B (NF-κB), signal transducer and activator of transcription 3 (STAT3), and TGF-β. *Helicobacter pylori* might induce the activation or differentiation of rat gastric fibroblasts *in vitro*, which then activate NF-κB and STAT3 signaling, and upregulate Snail1. This is an EMT-inducing transcription factor (EMT-TF) (52). As a major propeller of EMT in cancer progression and metastasis (53, 54), TGF-β can initiate tumorigenesis by activating EMT-type III initiation in epithelial cell compartments at the early stage of cancer development (55, 92). Gastric fibroblasts activated by *H. pylori* promote normal gastric epithelial cells to precancerous phenotype, and promote EMT by regulating TGFβ R1/R2-dependent signaling (55). The HH, Wnt, and Notch signaling pathways can interact with TGF-β pathway and induce EMT progression (93–97).

Collectively, persistent *H. pylori* infection increases the differentiation of CAFs, which propel EMT through NF-κB, STAT3, and TGF-β. As CAFs play key roles in the gastric microenvironment, targeting CAFs might be a potential strategy to improve the prognosis of patients (98, 99).

Effects of *H. pylori* on myeloid-derived suppressor cells in gastric tumor immune microenvironment

Immature myeloid (progenitor) cells (IMCs) do not mediate immunosuppression in healthy individuals. However, chronic inflammation, infections, and autoimmune diseases impair IMC differentiation and decrease peripheral myeloid cells numbers, resulting in more myelopoiesis (100–103). This eventually results in myeloid-derived suppressor cells (MDSCs) accumulation and immunosuppression (102, 104). MDSCs mediate immune suppression by inducing immunosuppressive cells (105), blocking lymphocyte homing (106), producing reactive oxygen and nitrogen species (107, 108), exhausting critical metabolites for T cell function (109), expressing negative immune checkpoint molecules (110).

Interactions between *H. pylori* and MDSCs are important in gastric immune microenvironment. On one hand, *H. pylori* can induce the differentiation of myeloid cell differentiation factor Schlafen 4 (SLFN4$^+$) MDSCs (56, 58). This factor marks a subset of MDSCs in the stomach during *H. pylori*-induced spasmolytic polypeptide-expressing metaplasia (SPEM) (57). During chronic *H. pylori* infection in mice model, a subset of HH-Gli1-dependent immune cells is recruited to the gastric epithelium, and polarizes into SLFN4$^+$ MDSCs. Overexpression of the SHH ligand in infected WT mice accelerates SLFN4$^+$ MDSCs differentiataion in gastric corpus (57). Furthermore, *H. pylori* can stimulate plasmacytoid dendritic cells to secrete IFN-α through toll-like receptor 9-myeloid differentiation factor 88-interferon regulatory factor 7 (TLR9-MyD88-IRF7 pathway) (58). Differentiated SLFN4$^+$ MDSCs inhibit gastric inflammatory response induced by *H. pylori* and suppress T cell function (56–59). Persistent immune dysregulation then favors intestinal metaplasia and neoplastic transformation, which leads to immune disorders and tumor progression.

Several markers, such as MiR130b, apoptosis signal-regulating kinase 1 (ASK1), interleukin 22 (IL-22), programmed death-ligand 1 (PD-L1), and Krüppel-like factor 4 (KLF4) play regulatory roles in the interactions between *H. pylori* and MDSCs. MiR130b produced by SLFN4$^+$ MDSCs suppress T cells function and promote *H. pylori*-induced metaplasia (59). ASK1 deficiency promotes a Th1-dependent immune response and recruits immature Gr-1$^+$Cd11b$^+$ MDSCs with *H. pylori* infection. This could lead to the development of gastric atrophy and metaplasia (25, 60). Moreover, IL-22 secreted by polarized Th22 cells induced by *H. pylori* can stimulate CXCL2 production from gastric epithelial cells. This causes CXCR2$^+$ MDSCs migration to gastric mucosa, where they produce proinflammatory proteins and suppress Th1 cell responses, contributing to the development of *H. pylori*-associated gastritis (61). PD-L1 upregulation on the surface of gastric epithelial cells at the early stage of *H. pylori* infection (62) promotes tumor infiltration of MDSCs (63) and then lead to anti-PD-1/PD-L1 treatment resistance (64). KLF4 is an evolutionarily conserved zinc finger transcription factor and key regulator of diverse cellular processes (111–113). *Helicobacter pylori* and its virulence factor CagA can influence KLF4 expression. The transduction of CagA or infection with *H. pylori* downregulates KLF4 expression by inducing CXCL8 expression, and low KLF4 expression further upregulates CXCL8 expression (65). Increased CXCL8 expression promotes MDSCs recruitment to tumors as well as tumor growth, and creates an immunosuppressive microenvironment conducive to resistance against immune response (65–67).

A high abundance of MDSCs in patients correlate with more advanced GC and a poor prognosis (114, 115). MDSCs infiltration induced by *H. pylori* mediates immunosuppression, immune dysfunction, gastric tumorigenesis, and reduces the effect of chemotherapy and immunotherapy (63). The possibility that combining immunotherapy or chemotherapy with MDSC-targeting therapy might overcome drug resistance and improve prognosis warrants investigation (116–118).

Effects of *H. pylori* on PD-1/PD-L1 in gastric tumor immune microenvironment

In addition to cells in TME, immune checkpoints are involved in regulating *H. pylori*-associated TME. (Table 2).

The 55 kDa transmembrane protein programmed death 1 (PD-1) is expressed in activated T cells, natural killer (NK) cells, B lymphocytes, macrophages, dendritic cells (DCs), and monocytes. It is abundantly expressed in tumor-specific T cells (126–128). PD-L1 (also known as CD274 or B7-H1) is a 33 kDa type 1 transmembrane glycoprotein that is widely expressed in macrophages, activated T lymphocytes, B cells, DCs, and also expressed in tumor cells (129). Binding of PD-1 and PD-L1 enhances T cell tolerance, inhibits T cell activation and proliferation, increases Th cell transformation to Foxp3$^+$ Treg cell, and prevents T cell cytolysis in tumor cells (130). Thus, interaction between PD-1 and PD-L1 is a double-edged sword. It can inhibit immune responses and promote self-tolerance, while it can also lead to immune escape and tumor progression.

Helicobacter pylori infection could upregulate PD-1/PD-L1 expression in gastric ulcers and GC patients (119), which might be related with poor prognosis (131, 132). Chronic *H. pylori* infection could cause excessive damage to gastric mucosa. Upregulated PD-1/PD-L1 is launched to avoid such damage, meanwhile this also reduces T cell-mediated cytotoxicity and promotes GC progression (119–121). SHH pathway is involved in PD-L1 upregulating (62). As an HH transcriptional effector, zinc finger protein GL1, mediates mammalian target of rapamycin (mTOR)-induced PD-L1 expression in GC organoids (64). Kinds of *H. pylori* virulence factors are reported in this process. *H. pylori* T4SS components activate p38 MAPK pathway and upregulate PD-L1 expression, thus inhibiting T cell proliferation and inducing Treg differentiation from naïve T cells, which lead to immune escape (122, 123). *Helicobacter pylori* urease B subunit mediates PD-L1 upregulation *via* myosin heavy chain 9 (Myh9) or mTORC1 signaling in bone marrow-derived macrophages (BMDMs) and, and regulates CD8$^+$ T cells infiltration and activation (124). *Helicobacter pylori* LPS induces PD-L1 expression *via* NF-κB pathway in GC cells and eventually promotes GC progression (125).

Overall, PD-1/PD-L1 play vital roles in *H. pylori*-infected GC, which presents an opportunity and challenge for treatment. However, numerous unknown mechanisms of PD-1/PD-L1 expression might be the basis for overcoming drug resistance and developing novel immunotherapies (133). The mechanisms and functions of PD1/PD-L1 with *H. pylori* infection requires further investigation (132, 134–136).

Effects of *H. pylori* on tumor immunotherapy responses

Immunotherapy stimulates the immune system against neoplasms and harnesses the specificity of innate immune to fight cancer, particularly by activating T-cell mediated immunity (137, 138). With the wide application of immune therapy, the immune checkpoint inhibitors (ICIs) targeting immune checkpoint molecules such as PD-1 and CTLA-4, and other immune therapies such as cancer vaccine, the immune cells input, antigen vaccine, oncolytic viruses, and recombinant cytokines, have been receiving worldwide attention and have made a certain progress (139–147). However, as lack of optimal criteria selecting suitable patients until now, the objective response rate of immunotherapy remains low (148, 149). Hence, factors that influence the effectiveness of tumor immunotherapy need to be identified. In this section, we focused on the effects and potential applications of *H. pylori* infection on tumor immunotherapies (Figure 2; Table 3).

TABLE 2 Effects of *H. pylori* on tumor-related proteins in gastric tumor immune microenvironment.

Tumor-related proteins affected by *H. pylori*	Roles of *H. pylori*	Results
PD-1/PD-L1	Upregulates PD-1/PD-L1 expression (119–121)	Reduces excessive damage induced by *H. pylori*, reduces T cell-mediated cytotoxicity, promotes GC progression
	Upregulates PD-L1 expression by *H. pylori* CagA through the SHH pathway (62)	Inhibits T cell proliferation and Treg cell induction from naïve T cells, increases immune escape, promotes GC progression
	Upregulates PD-L1 expression by mTOR-GLI signaling (64)	
	Upregulates PD-L1 expression by the p38 MAPK pathway (122, 123)	
	Upregulates PD-L1 expression by *H. pylori* urease subunit through the Myh9/mTORC1 pathway (124)	
	Upregulates PD-L1 expression by *H. pylori* LPS through the NF-κB pathway (125)	

Effects and applications of *H. pylori* and its factors on GC immunotherapy

The 5-year survival rate of advanced GC patients is <30%. Although platinum-fluoropyrimidine combination chemotherapy is the standard first-line treatment for advanced GC, its low complete response rate and severe adverse reactions have limited its application (63, 166). Novel effective therapies are urgently required. For example, PD-1 inhibitor pembrolizumab received accelerated approval from the US Food and Drug Administration (FDA) in 2017 to treat recurrent advanced or metastatic gastric or gastroesophageal junction adenocarcinomas expressing PD-L1 (63, 167–169).

Helicobacter pylori is a class I carcinogen associated with GC (170–172). The overall survival of GC diagnosis is reported to be higher for patients with *H. pylori* infection (17). *Helicobacter pylori* infection induces PD-L1 expression and MDSC infiltration that mediate immune escape. HH signaling activated by *H. pylori* infection induces PD-L1 expression and tumor cell proliferation in GC, resulting in cancer cell resistance to immunotherapy (150). In addition, *Helicobacter pylori* and its virulence factors can act as antigens or adjuvants to enhance tumor immunity.

Helicobacter pylori virulence factors, such as CagA, VacA, blood-group antigen-binding adhesin gene (BabA), and *H. pylori* neutrophil-activating protein (HP-NAP), can act as antigens or adjuvants to enhance tumor immunity. The stimulation of autoantibodies during antigen processing and presentation and subsequent T-cell activation and proliferation improves the host immune status, which can kill cancer cells and even suppress metastasis (151). Moreover, *H. pylori* DNA vaccines encoding fragments of CagA, VacA, and BabA can induce Th1 shift to Th2 response in immunized BALB/c mice, which mimics the immune status of GC patients with chronic *H. pylori* infection. Stimulated $CD3^+$ T cells inhibit the proliferation of human GC cells *in vitro*, and the adoptive infusion of $CD3^+$ T cells inhibits the growth of GC xenografts *in vivo* (152).

HP-NAP is a major virulence factor in *H. pylori* infection and colony formation, and it can also act as a protective factor (173, 174). As a Toll-like receptor-2 (TLR2) agonist, HP-NAP can bind to TLR2 of neutrophils (161, 175). Furthermore, HP-NAP promotes the maturation of DCs with Th1 polarization and improves migration of mature DCs. Stimulating neutrophils and monocytes by HP-NAP induces IL-12 and IL-23 expression, thus shifting antigen-specific T cell responses from the Th2 to the Th1 phenotype which characterized by abundant IFN-γ and TNF-α expression (153). Vaccination with HP-NAP A subunit (NapA) promotes Th17 and Th1 polarization. Such vaccines have potential effects as an anti-*H. pylori* oral vaccine candidate and a mucosal immunomodulatory agent, which could be used in antitumor strategies (154).

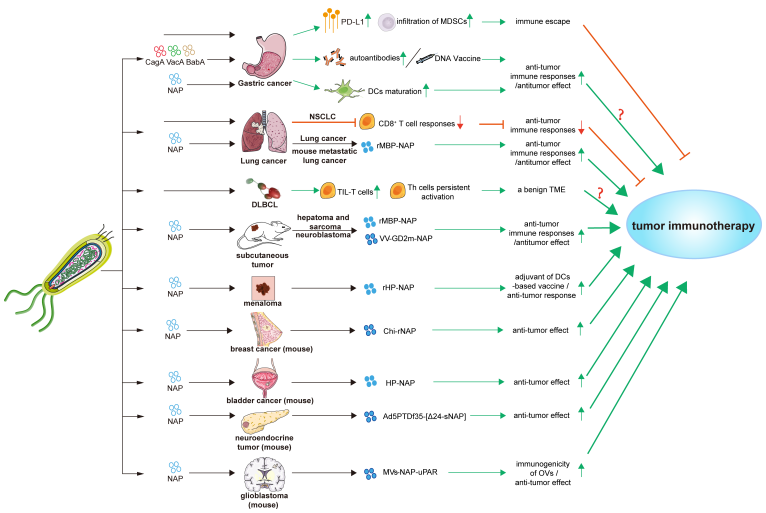

FIGURE 2
Effects and applications of *H. pylori* and its factors in tumor immunotherapies. Bab A, blood-group antigen-binding adhesin gene A; Cag A, cytotoxin-associated gene A; Chi-rNap, rNAP coated chitosan nanoparticles; DCs, dendritic cells; DLBCL, diffuse large B-cell lymphoma; HP-NAP, *H. pylori* neutrophil-activating protein; MDSCs, myeloid-derived suppressor cells; MV-NAP-uPAR, recombinant measles virus-NAP-urokinase-type plasminogen activator receptor; NSCLC, non-small cell lung cancer; OVs, oncolytic viruses; PD-L1, programmed death-ligand 1; rHP-NAP, recombinant *H. pylori* neutrophil-activating protein; rMBP-NAP, recombinant HP-NAP with the maltose-binding protein of Escherichia coli; Th cells, T helper cells; TIL-T cells, tumor-infiltrating T lymphocytes; TME, tumor microenvironment; Vac A, vacuolating cytotoxin A; VV-GD2m-NAP, vaccinia virus - neuroblastoma-associated antigen disialoganglioside mimotope.

TABLE 3 Effects of *H. pylori* on tumor immunotherapy responses.

Cancer targeted by immunotherapy affected by *H. pylori*	Roles of *H. pylori*		Effects and applications
Gastric cancer	Induces PD-L1 expression and MDSC infiltration (62–64, 150)		Mediates immune escape by cancer cells, causing resistance to immunotherapy
	Enhances tumor immunity by virulence factors	CagA, VacA and BabA	Increases levels of CagA, VacA, and BabA autoantibodies, enhances antigen processing and presentation and T-cell activation and proliferation, and improves host immune status (151)
			DNA vaccine from CagA, VacA and BabA induces a shift from Th1 to Th2 response and activates $CD3^+$ T cells to inhibit GC xenograft growth *in vivo* (152)
		HP-NAP	HP-NAP promotes maturation of DCs and stimulates neutrophils and monocytes to enhance antigen-specific T cell responses (153)
			Oral NapA vaccination promotes Th17 and Th1 polarization, exerts anti-*H. pylori* and antitumor effects, enhances immune responses (154)
Non-small cell lung carcinoma	Decreases immune responses, inhibits antitumoral $CD8^+$ T cell responses (19)		Partially blocks the activity of ICIs and vaccine-based cancer immunotherapy
DLBCL	Causes increased numbers of tumor-infiltrating T lymphocytes and persistent activation of autoimmune Th cells (155)		Results in a benign tumor immune microenvironment
Mouse subcutaneous hepatoma and sarcoma	rMBP-NAP promotes Th1 differentiation and increases the number of $CD4^+$ IFN-γ-secreting cells (156)		rMBP-NAP has antitumor potential
Lung cancer	rMBP-NAP increases the number of IFN–γ-secreting cells and CTL activity of PBMCs (157)		
Mouse metastatic lung cancer	rMBP-NAP restricts tumor progression by triggering antitumor immunity (158)		
Mouse breast and bladder cancers	HP-NAP enhances immune response and inhibits tumor growth (137, 159)		HP-NAP has antitumor potential
Melanoma	rHP-NAP promotes the maturation of dendritic cells in dendritic cell-based vaccines (160)		rHP-NAP has potential as an adjuvant
Mouse neuroendocrine tumor	HP-NAP improves median survival (161)		HP-NAP is a powerful source of immune-stimulatory agonists that can boost OV immunogenicity and enhance ICI effects (162, 163)
Mouse subcutaneous neuroblastoma	HP-NAP enhances antitumor efficacy of oncolytic vaccinia virus (164, 165)		
Glioblastoma	MVs-NAP-uPAR improves tumor immunotherapy efficacy (163)		

Effects and applications of *H. pylori* and its factors in other tumor immunotherapies

In addition to GC, the influence of *H. pylori* on other tumor immunotherapies is also paid much attention recently. *Helicobacter pylori* infection might disrupt the immune system and exert detrimental effects on the outcomes of cancer immunotherapies (19).

Helicobacter pylori seropositivity could reduce anti-PD-1 immunotherapy effect in non-small cell lung cancer (NSCLC) patients. *Helicobacter pylori* infection partially blocks the activities of ICIs and vaccine-based cancer immunotherapies. *Helicobacter pylori* suppresses the innate and adaptive immune responses of infected hosts and inhibits antitumor $CD8^+$ T cell responses by altering the cross-presentation activity of DCs (19). In contrast, a significantly high proportion of tumor-infiltrating T lymphocytes in *H. pylori*-positive *de novo* diffuse large B-cell lymphoma (DLBCL) patients preliminarily indicates a benign TME. Inflammation induced by *H. pylori* confers persistent activation of autoimmune Th cells, which would explain the benign TME (155). More researches are necessary to elucidate how *H. pylori* infection status influences the effects of tumor immunotherapies.

The immunomodulatory activity and potential applications of NAP in tumor immunotherapy have been investigated. Recombinant HP-NAP with the maltose-binding protein of *Escherichia coli* (rMBP-NAP) can mediate T helper lymphocytes differentiation into the Th1 phenotype and significantly increase the number of $CD4^+$ IFN-γ-secreting T cells. This induces antitumor effects through a TLR-2-dependent mechanism in subcutaneous hepatoma and sarcoma mice model (156). rMBP-NAP can significantly increase peripheral blood mononuclear cells (PBMCs) that secrete IFN-γ, and prominently increases the cytotoxic activity of PBMCs derived from lung cancer patients (157). Treatment with rMBP-NAP restricts the progression of metastatic lung cancer in mice model by triggering antitumor immunity (158). A therapeutic nanocomplex of HP-NAP altered the production rate of cytokines and increase tumoricidal activities of the immune system, leading to decreased breast tumor growth in mice (137). Local administration of HP-NAP inhibits tumor growth by triggering tumor cell necrosis in bladder cancer mice model (159). Recombinant HP-NAP has potential effects as an adjuvant in DC-based vaccines for treating melanoma (160).

Because of its ideal immunogenicity, NAP has recently been applied as an immune adjuvant to enhance the antitumor immune response. When combined with oncolytic viruses (OVs), HP-NAP can activate the immune response. The intratumoral administration of adenovirus armed with secretory HP-NAP can improve the median survival rate of nude mice xenografted with neuroendocrine tumors (161). A recombinant vaccinia virus (VV) neuroblastoma-associated antigen disialoganglioside mimotope (GD2m)-NAP significantly improved therapeutic efficacy. *Helicobacter pylori*-NAP might help to overcome virus-mediated suppressive immune responses, resulting in improved anti-GD2 antibody production and a better therapeutic outcome (164, 165). Moreover, recombinant measles virus (MV)-NAP-urokinase-type plasminogen activator receptor (uPAR) can improve immunotherapeutic effects on glioblastoma with a better tumor prognosis and increased susceptibility to $CD8^+$ T cell-mediated lysis. Overall, HP-NAP represents a potential immunostimulatory agonists which can boost the immunogenicity of OVs and enhance ICIs effects (162, 163).

In conclusion, *H. pylori* and its virulence factors could be closely related with personalized treatment strategies during tumor immunotherapies. The mechanisms of *H. pylori* infection in tumor immunotherapies requires further elucidation, and the translation of research findings to clinical applications should be accelerated.

Summary

This review summarized current knowledge of the effects of *H. pylori* on the immune microenvironment of GC and tumor immunotherapy responses. *Helicobacter pylori* elicits powerful immune responses during surviving and colonizing gastric mucosa. *Helicobacter pylori* has also developed several strategies to evade recognition and disrupt immune function. The constituents and functions of stroma are regulated by *H. pylori* and its virulence factors to facilitate its survival and colony. Persistent *H. pylori* infection can induce immune evasion and tumorigenesis.

The stroma provides TME for tumor initiation and development after *H. pylori* persistent infection. Immunotherapy targeting tumor-associated immune cells is more mature and improved, particularly immunotherapy targeting T cells, such as ICIs. PD-1 inhibitor pembrolizumab has received approval from the US FDA in 2017 to treat recurrent advanced or metastatic gastric or gastroesophageal junction adenocarcinomas (167). While some clinical trials targeting non-immune cells in TME such as CAFs, MSCs, have failed to show promising efficacy in cancer patients (176–178). The main reason might be a lack of deep understanding of the fundamental mechanisms of stromal cells and elements as well as a lack of reliable biomarkers to guide stroma-targeted therapies (176). Of course, because of the important roles of regulating the immune response in TME, targeting TAMs is getting more and more attraction. For example, targeting colony-stimulating factor 1 receptor (CSF1R) signaling and the CCL2-CCR2 axis are developing drugs (179, 180). And there are some developing drugs to reprogram TAMs from a pro-tumor phenotype to an anti-tumor phenotype and interrupt the bad cycle between TAMs and tumor cells (176, 177), such as agonistic anti-CD40 antibodies (181), PI3Kγ inhibitors (182). These ongoing researches show good prospects in immunotherapy. Based on these, it seems that immunotherapy intervening tumor-associated immune cells may be more appropriate currently. However, we should also pay attention to the study of non-immune cells in TME. Further research on these cells may provide clues for developing new therapies in the future.

H. pylori infection might affect the tumor immunotherapy. Although *H. pylori* infection has been reported as a protective factor in GC immunotherapy while in NSCLC as a negative factor, the mechanisms and effect of *H. pylori* on GC immunotherapy still remains unclear (19, 183). *Helicobacter pylori* virulence factors can act as immunogens or adjuvants to elicit or enhance immune responses. Some *H. pylori* virulence factors such as HP-NAP, have been applied as adjuvants or combined with drugs in pan-tumor treatment to improve immunotherapeutic efficiency. The effects of *H. pylori* in TME should be further explored, and clinical applications should be performed to select the proper features of population for better immunotherapy benefits.

Author contributions

RD and HZ searched the literature and wrote the manuscript. HC and ML re-checked the literature. YS and SD

designed this study and revised the manuscript. All authors contributed to the article and approved the submitted version.

Funding

This study was funded by the National Natural Science Foundation of China (Grant No. 81700496 and 81870386), Peking University Medicine Fund of Fostering Young Scholars' Scientific and Technological Innovation (BMU2021PY002), and Key laboratory for Helicobacter pylori infection and upper gastrointestinal diseases, Beijing Key Laboratory (No.BZ0371).

Conflict of interest

The authors declare that the research was conducted in the absence of any commercial or financial relationships that could be construed as a potential conflict of interest.

Publisher's note

All claims expressed in this article are solely those of the authors and do not necessarily represent those of their affiliated organizations, or those of the publisher, the editors and the reviewers. Any product that may be evaluated in this article, or claim that may be made by its manufacturer, is not guaranteed or endorsed by the publisher.

References

1. Baj J, Forma A, Sitarz M, Portincasa P, Garruti G, Krasowska D, et al. Helicobacter pylori virulence factors-mechanisms bacterial pathogenicity gastric microenvironment. *Cells* (2020) 10(1):27. doi: 10.3390/cells10010027

2. Mentis A, Lehours P, Megraud F. Epidemiology and diagnosis of helicobacter pylori infection. *Helicobacter.* (2015) 20(Suppl 1):1–7. doi: 10.1111/hel.12250

3. Machlowska J, Baj J, Sitarz M, Maciejewski R, Sitarz R. Gastric cancer: Epidemiology, risk factors, classification, genomic characteristics and treatment strategies. *Int J Mol Sci* (2020) 21(11):4012. doi: 10.3390/ijms21114012

4. Sung H, Ferlay J, Siegel RL, Laversanne M, Soerjomataram I, Jemal A, et al. Global cancer statistics 2020: GLOBOCAN estimates of incidence and mortality worldwide for 36 cancers in 185 countries. *CA Cancer J Clin* (2021) 71(3):209–49. doi: 10.3322/caac.21660

5. Plummer M, Franceschi S, Vignat J, Forman D, de Martel C. Global burden of gastric cancer attributable to helicobacter pylori. *Int J Cancer* (2015) 136(2):487–90. doi: 10.1002/ijc.28999

6. McColl KE. Clinical practice. *Helicobacter pylori Infect N Engl J Med* (2010) 362(17):1597–604. doi: 10.1056/NEJMcp1001110

7. Ishaq S, Nunn L. Helicobacter pylori and gastric cancer: a state of the art review. *Gastroenterol Hepatol Bed Bench.* (2015) 8(Suppl 1):S6–S14. doi: 10.22037/ghfbb.v8iSupplement.653

8. Anwar W, Armstrong BK, Correa P, Forman D, Gentile JM, Haswell-Elkins M, et al. Schistosomes, liver flukes and helicobacter pylori. In: *IARC working group on the evaluation of carcinogenic risks to humans*, vol. 61. . Lyon: IARC Monogr Eval Carcinog Risks Hum. p. 1–241.

9. Seeneevassen L, Bessede E, Megraud F, Lehours P, Dubus P, Varon C. Gastric cancer: Advances in carcinogenesis research and new therapeutic strategies. *Int J Mol Sci* (2021) 22(7):3418. doi: 10.3390/ijms22073418

10. Liccardi G, Pentimalli F. Cancer, immunity and inflammation. report from the CDD Cambridge conferences 2018 and 2019. *Cell Death Dis* (2019) 10(11):798. doi: 10.1038/s41419-019-2032-0

11. Grivennikov SI, Greten FR, Karin M. Immunity, inflammation, and cancer. *Cell.* (2010) 140(6):883–99. doi: 10.1016/j.cell.2010.01.025

12. Yolanda LV, Sergio PD, Hugo ES, Isabel AF, Rafael BZ, Aldo TD, et al. Gastric cancer progression associated with local humoral immune responses. *BMC Cancer* (2015) 15:924. doi: 10.1186/s12885-015-1858-9

13. Mejias-Luque R, Gerhard M. Immune evasion strategies and persistence of helicobacter pylori. *Curr Top Microbiol Immunol* (2017) 400:53–71. doi: 10.1007/978-3-319-50520-6_3

14. Song L, Song M, Rabkin CS, Williams S, Chung Y, Van Duine J, et al. Helicobacter pylori immunoproteomic profiles in gastric cancer. *J Proteome Res* (2021) 20(1):409–19. doi: 10.1021/acs.jproteome.0c00466

15. Alexander SM, Retnakumar RJ, Chouhan D, Devi TNB, Dharmaseelan S, Devadas K, et al. Helicobacter pylori in human stomach: The inconsistencies in clinical outcomes and the probable causes. *Front Microbiol* (2021) 12:713955. doi: 10.3389/fmicb.2021.713955

16. Zhang MJ, Chen DS, Li S, Chen L, Qi YX, Zhang CJ. Helicobacter pylori infection as a potential favorable factor for immune checkpoint inhibitor therapy for gastric cancer. *Invest New Drugs* (2021) 39(5):1436–8. doi: 10.1007/s10637-021-01122-5

17. Fang X, Liu K, Cai J, Luo F, Yuan F, Chen P. Positive helicobacter pylori status is associated with better overall survival for gastric cancer patients: evidence from case-cohort studies. *Oncotarget.* (2017) 8(45):79604–17. doi: 10.18632/oncotarget.18758

18. Li G, Yu S, Xu J, Zhang X, Ye J, Wang Z, et al. The prognostic role of helicobacter pylori in gastric cancer patients: A meta-analysis. *Clin Res Hepatol Gastroenterol* (2019) 43(2):216–24. doi: 10.1016/j.clinre.2018.08.012

19. Oster P, Vaillant L, Riva E, McMillan B, Begka C, Truntzer C, et al. Helicobacter pylori infection has a detrimental impact on the efficacy of cancer immunotherapies. *Gut.* (2021) 71(3):457–66. doi: 10.1136/gutjnl-2020-323392

20. Shi Y, Zheng H, Wang M, Ding S. Influence of helicobacter pylori infection on PD-1/PD-L1 blockade therapy needs more attention. *Helicobacter.* (2022) 27(2): e12878. doi: 10.1111/hel.12878

21. Mohammadzadeh R, Soleimanpour S, Pishdadian A, Farsiani H. Designing and development of epitope-based vaccines against helicobacter pylori. *Crit Rev Microbiol* (2021), 1–24. doi: 10.1080/1040841X.2021.1979934

22. Del Giudice G, Malfertheiner P, Rappuoli R. Development of vaccines against helicobacter pylori. *Expert Rev Vaccines* (2009) 8(8):1037–49. doi: 10.1586/erv.09.62

23. Fu HW. Helicobacter pylori neutrophil-activating protein: from molecular pathogenesis to clinical applications. *World J Gastroenterol* (2014) 20(18):5294–301. doi: 10.3748/wjg.v20.i18.5294

24. Hinshaw DC, Shevde LA. The tumor microenvironment innately modulates cancer progression. *Cancer Res* (2019) 79(18):4557–66. doi: 10.1158/0008-5472.CAN-18-3962

25. Navashenaq JG, Shabgah AG, Banach M, Jamialahmadi T, Penson PE, Johnston TP, et al. The interaction of helicobacter pylori with cancer immunomodulatory stromal cells: New insight into gastric cancer pathogenesis. *Semin Cancer Biol* (2021) S1044-579X(21):00248–0. doi: 10.1016/j.semcancer.2021.09.014

26. Wu T, Dai Y. Tumor microenvironment and therapeutic response. *Cancer Lett* (2017) 387:61–8. doi: 10.1016/j.canlet.2016.01.043

27. Gambardella V, Castillo J, Tarazona N, Gimeno-Valiente F, Martinez-Ciarpaglini C, Cabeza-Segura M, et al. The role of tumor-associated macrophages in gastric cancer development and their potential as a therapeutic target. *Cancer Treat Rev* (2020) 86:102015. doi: 10.1016/j.ctrv.2020.102015

28. Pagliari M, Munari F, Toffoletto M, Lonardi S, Chemello F, Codolo G, et al. Helicobacter pylori affects the antigen presentation activity of macrophages modulating the expression of the immune receptor CD300E through miR-4270. *Front Immunol* (2017) 8:1288. doi: 10.3389/fimmu.2017.01288

29. Codolo G, Toffoletto M, Chemello F, Coletta S, Soler Teixidor G, Battaggia G, et al. Helicobacter pylori dampens HLA-II expression on macrophages *via* the up-regulation of miRNAs targeting CIITA. *Front Immunol* (2019) 10:2923. doi: 10.3389/fimmu.2019.02923

30. Coletta S, Battaggia G, Della Bella C, Furlani M, Hauke M, Faass L, et al. ADP-heptose enables helicobacter pylori to exploit macrophages as a survival niche

by suppressing antigen-presenting HLA-II expression. *FEBS Lett* (2021) 595 (16):2160–8. doi: 10.1002/1873-3468.14156

31. Lewis ND, Asim M, Barry DP, de Sablet T, Singh K, Piazuelo MB, et al. Immune evasion by helicobacter pylori is mediated by induction of macrophage arginase II. *J Immunol* (2011) 186(6):3632–41. doi: 10.4049/jimmunol.1003431

32. Hardbower DM, Asim M, Murray-Stewart T, Casero RAJr., Verriere T, Lewis ND, et al. Arginase 2 deletion leads to enhanced M1 macrophage activation and upregulated polyamine metabolism in response to helicobacter pylori infection. *Amino Acids* (2016) 48(10):2375–88. doi: 10.1007/s00726-016-2231-2

33. Krakowiak MS, Noto JM, Piazuelo MB, Hardbower DM, Romero-Gallo J, Delgado A, et al. Matrix metalloproteinase 7 restrains helicobacter pylori-induced gastric inflammation and premalignant lesions in the stomach by altering macrophage polarization. *Oncogene.* (2015) 34(14):1865–71. doi: 10.1038/onc.2014.135

34. Gobert AP, Verriere T, Asim M, Barry DP, Piazuelo MB, de Sablet T, et al. Heme oxygenase-1 dysregulates macrophage polarization and the immune response to helicobacter pylori. *J Immunol* (2014) 193(6):3013–22. doi: 10.4049/jimmunol.1401075

35. Che Y, Geng B, Xu Y, Miao X, Chen L, Mu X, et al. Helicobacter pylori-induced exosomal MET educates tumour-associated macrophages to promote gastric cancer progression. *J Cell Mol Med* (2018) 22(11):5708–19. doi: 10.1111/jcmm.13847

36. Wen J, Chen C, Luo M, Liu X, Guo J, Wei T, et al. Notch signaling ligand Jagged1 enhances macrophage-mediated response to helicobacter pylori. *Front Microbiol* (2021) 12:692832. doi: 10.3389/fmicb.2021.692832

37. Schumacher MA, Donnelly JM, Engevik AC, Xiao C, Yang L, Kenny S, et al. Gastric sonic hedgehog acts as a macrophage chemoattractant during the immune response to helicobacter pylori. *Gastroenterology.* (2012) 142(5):1150–9.e6. doi: 10.1053/j.gastro.2012.01.029

38. Fakhari S, Kalantar E, Nikzaban M, Hakhamneshi MS, Fathi F, Nikkhoo B, et al. Effect of helicobacter pylori infection on stromal-derived factor-1/CXCR4 axis in bone marrow-derived mesenchymal stem cells. *Adv BioMed Res* (2014) 3:19. doi: 10.4103/2277-9175.124650

39. Varon C, Dubus P, Mazurier F, Asencio C, Chambonnier L, Ferrand J, et al. Helicobacter pylori infection recruits bone marrow-derived cells that participate in gastric preneoplasia in mice. *Gastroenterology.* (2012) 142(2):281–91. doi: 10.1053/j.gastro.2011.10.036

40. Ferrand J, Lehours P, Schmid-Alliana A, Megraud F, Varon C. Helicobacter pylori infection of gastrointestinal epithelial cells *in vitro* induces mesenchymal stem cell migration through an NF-kappaB-dependent pathway. *PLoS One* (2011) 6 (12):e29007. doi: 10.1371/journal.pone.0029007

41. Alison MR, Islam S, Wright NA. Stem cells in cancer: instigators and propagators? *J Cell Sci* (2010) 123(Pt 14):2357–68. doi: 10.1242/jcs.054296

42. Moradi SL, Eslami G, Goudarzi H, Hajishafieeha Z, Soleimani M, Mohammadzadeh A, et al. Role of helicobacter pylori on cancer of human adipose-derived mesenchymal stem cells and metastasis of tumor cells-an *in vitro* study. *Tumou Biol* (2016) 37(3):3371–8. doi: 10.1007/s13277-015-4137-0

43. Lin R, Ma H, Ding Z, Shi W, Qian W, Song J, et al. Bone marrow-derived mesenchymal stem cells favor the immunosuppressive T cells skewing in a helicobacter pylori model of gastric cancer. *Stem Cells Dev* (2013) 22(21):2836–48. doi: 10.1089/scd.2013.0166

44. Yaghoobi M. Bone marrow-derived stem cells in pathogenesis of helicobacter pylori-associated gastric cancer. *Clin Transl Gastroenterol* (2015) 6: e110. doi: 10.1038/ctg.2015.35

45. He L, Wang W, Shi H, Jiang C, Yao H, Zhang Y, et al. THBS4/integrin alpha2 axis mediates BM-MSCs to promote angiogenesis in gastric cancer associated with chronic helicobacter pylori infection. *Aging (Albany NY)* (2021) 13(15):19375–96. doi: 10.18632/aging.203334

46. Shi H, Qi C, Meng L, Yao H, Jiang C, Fan M, et al. Bone marrow-derived mesenchymal stem cells promote helicobacter pylori-associated gastric cancer progression by secreting thrombospondin-2. *Cell Prolif* (2021) 54(10):e13114. doi: 10.1111/cpr.13114

47. Zhang Q, Wang M, Huang F, Yang T, Cai J, Zhang X, et al. H. pylori infection-induced MSC differentiation into CAFs promotes epithelial-mesenchymal transition in gastric epithelial cells. *Int J Mol Med* (2013) 32 (6):1465–73. doi: 10.3892/ijmm.2013.1532

48. Wen X, He X, Jiao F, Wang C, Sun Y, Ren X, et al. Fibroblast activation protein-alpha-Positive fibroblasts promote gastric cancer progression and resistance to immune checkpoint blockade. *Oncol Res* (2017) 25(4):629–40. doi: 10.3727/096504016X14768383625385

49. Liu CJ, Wang YK, Kuo FC, Hsu WH, Yu FJ, Hsieh S, et al. Helicobacter pylori infection-induced hepatoma-derived growth factor regulates the differentiation of human mesenchymal stem cells to myofibroblast-like cells. *Cancers (Basel)* (2018) 10(12):479. doi: 10.3390/cancers10120479

50. Lee KH, Choi EY, Kim MK, Lee SH, Jang BI, Kim TN, et al. Hepatoma-derived growth factor regulates the bad-mediated apoptotic pathway and induction of vascular endothelial growth factor in stomach cancer cells. *Oncol Res* (2010) 19 (2):67–76. doi: 10.3727/096504010X12864748215043

51. Krzysiek-Maczka G, Targosz A, Ptak-Belowska A, Korbut E, Szczyrk U, Strzalka M, et al. Molecular alterations in fibroblasts exposed to helicobacter pylori: a missing link in bacterial inflammation progressing into gastric carcinogenesis? *J Physiol Pharmacol* (2013) 64(1):77–87.

52. Krzysiek-Maczka G, Targosz A, Szczyrk U, Strzalka M, Brzozowski T, Ptak-Belowska A. Involvement of epithelial-mesenchymal transition-inducing transcription factors in the mechanism of helicobacter pylori-induced fibroblasts activation. *J Physiol Pharmacol* (2019) 70(5):727–36. doi: 10.26402/jpp.2019.5.08

53. Krzysiek-Maczka G, Wrobel T, Targosz A, Szczyrk U, Strzalka M, Ptak-Belowska A, et al. Helicobacter pylori-activated gastric fibroblasts induce epithelial-mesenchymal transition of gastric epithelial cells *in vitro* in a TGF-beta-dependent manner. *Helicobacter.* (2019) 24(5):e12653. doi: 10.1111/hel.12653

54. Katsuno Y, Lamouille S, Derynck R. TGF-beta signaling and epithelial-mesenchymal transition in cancer progression. *Curr Opin Oncol* (2013) 25(1):76–84. doi: 10.1097/CCO.0b013e32835b6371

55. Krzysiek-Maczka G, Targosz A, Szczyrk U, Wrobel T, Strzalka M, Brzozowski T, et al. Long-term helicobacter pylori Infect switches gastric epithelium reprogram towards cancer stem cell-related differ program Hp-activated gastric fibroblast-TGFbeta dependent manner. *Microorganisms* (2020) 8(10):1519. doi: 10.3390/microorganisms8101519

56. El-Zaatari M, Kao JY, Tessier A, Bai L, Hayes MM, Fontaine C, et al. Gli1 deletion prevents helicobacter-induced gastric metaplasia and expansion of myeloid cell subsets. *PLoS One* (2013) 8(3):e58935. doi: 10.1371/journal.pone.0058935

57. Ding L, Hayes MM, Photenhauer A, Eaton KA, Li Q, Ocadiz-Ruiz R, et al. Schlafen 4-expressing myeloid-derived suppressor cells are induced during murine gastric metaplasia. *J Clin Invest* (2016) 126(8):2867–80. doi: 10.1172/JCI82529

58. Xiang X, Wu Y, Li H, Li C, Yan L, Li Q. Plasmacytoid dendritic cell-derived type I interferon is involved in helicobacter pylori infection-induced differentiation of schlafen 4-expressing myeloid-derived suppressor cells. *Infect Immun* (2021) 89 (11):e0040721. doi: 10.1128/IAI.00407-21

59. Ding L, Li Q, Chakrabarti J, Munoz A, Faure-Kumar E, Ocadiz-Ruiz R, et al. MiR130b from Schlafen4(+) MDSCs stimulates epithelial proliferation and correlates with preneoplastic changes prior to gastric cancer. *Gut.* (2020) 69 (10):1750–61. doi: 10.1136/gutjnl-2019-318817

60. Hayakawa Y, Hirata Y, Hata M, Tsuboi M, Oya Y, Kurokawa K, et al. Dysregulated immune responses by ASK1 deficiency alter epithelial progenitor cell fate and accelerate metaplasia development during h. pylori infection. *Microorganisms* (2020) 8(12):1995. doi: 10.3390/microorganisms8121995

61. Zhuang Y, Cheng P, Liu XF, Peng LS, Li BS, Wang TT, et al. A pro-inflammatory role for Th22 cells in helicobacter pylori-associated gastritis. *Gut.* (2015) 64(9):1368–78. doi: 10.1136/gutjnl-2014-307020

62. Holokai L, Chakrabarti J, Broda T, Chang J, Hawkins JA, Sundaram N, et al. Increased programmed death-ligand 1 is an early epithelial cell response to helicobacter pylori infection. *PLoS Pathog* (2019) 15(1):e1007468. doi: 10.1371/journal.ppat.1007468

63. Kim W, Chu TH, Nienhuser H, Jiang Z, Del Portillo A, Remotti HE, et al. PD-1 signaling promotes tumor-infiltrating myeloid-derived suppressor cells and gastric tumorigenesis in mice. *Gastroenterology.* (2021) 160(3):781–96. doi: 10.1053/j.gastro.2020.10.036

64. Koh V, Chakrabarti J, Torvund M, Steele N, Hawkins JA, Ito Y, et al. Hedgehog transcriptional effector GLI mediates mTOR-induced PD-L1 expression in gastric cancer organoids. *Cancer Lett* (2021) 518:59–71. doi: 10.1016/j.canlet.2021.06.007

65. Liu Z, Wu X, Tian Y, Zhang W, Qiao S, Xu W, et al. H. pylori infection induces CXCL8 expression and promotes gastric cancer progress through downregulating KLF4. *Mol Carcinog* (2021) 60(8):524–37. doi: 10.1002/mc.23309

66. Li BH, Garstka MA, Li ZF. Chemokines and their receptors promoting the recruitment of myeloid-derived suppressor cells into the tumor. *Mol Immunol* (2020) 117:201–15. doi: 10.1016/j.molimm.2019.11.014

67. Alfaro C, Teijeira A, Onate C, Perez G, Sanmamed MF, Andueza MP, et al. Tumor-produced interleukin-8 attracts human myeloid-derived suppressor cells and elicits extrusion of neutrophil extracellular traps (NETs). *Clin Cancer Res* (2016) 22(15):3924–36. doi: 10.1158/1078-0432.CCR-15-2463

68. Zhang X, Arnold IC, Muller A. Mechanisms of persistence, innate immune activation and immunomodulation by the gastric pathogen helicobacter pylori. *Curr Opin Microbiol* (2020) 54:1–10. doi: 10.1016/j.mib.2020.01.003

69. Kaparakis M, Walduck AK, Price JD, Pedersen JS, van Rooijen N, Pearse MJ, et al. Macrophages are mediators of gastritis in acute helicobacter pylori infection in C57BL/6 mice. *Infect Immun* (2008) 76(5):2235–9. doi: 10.1128/IAI.01481-07

70. Mosser DM, Edwards JP. Exploring the full spectrum of macrophage activation. *Nat Rev Immunol* (2008) 8(12):958–69. doi: 10.1038/nri2448

71. Wynn TA. Type 2 cytokines: mechanisms and therapeutic strategies. *Nat Rev Immunol* (2015) 15(5):271–82. doi: 10.1038/nri3831

72. Cassetta L, Cassol E, Poli G. Macrophage polarization in health and disease. *ScientificWorldJournal.* (2011) 11:2391–402. doi: 10.1100/2011/213962

73. Biswas SK, Chittezhath M, Shalova IN, Lim JY. Macrophage polarization and plasticity in health and disease. *Immunol Res* (2012) 53(1-3):11–24. doi: 10.1007/s12026-012-8291-9

74. Qian BZ, Pollard JW. Macrophage diversity enhances tumor progression and metastasis. *Cell.* (2010) 141(1):39–51. doi: 10.1016/j.cell.2010.03.014

75. Gordon S. Alternative activation of macrophages. *Nat Rev Immunol* (2003) 3(1):23–35. doi: 10.1038/nri978

76. Fabian MR, Sonenberg N. The mechanics of miRNA-mediated gene silencing: a look under the hood of miRISC. *Nat Struct Mol Biol* (2012) 19 (6):586–93. doi: 10.1038/nsmb.2296

77. Wilson KT, Crabtree JE. Immunology of helicobacter pylori: insights into the failure of the immune response and perspectives on vaccine studies. *Gastroenterology.* (2007) 133(1):288–308. doi: 10.1053/j.gastro.2007.05.008

78. Huber V, Camisaschi C, Berzi A, Ferro S, Lugini L, Triulzi T, et al. Cancer acidity: An ultimate frontier of tumor immune escape and a novel target of immunomodulation. *Semin Cancer Biol* (2017) 43:74–89. doi: 10.1016/j.semcancer.2017.03.001

79. Pulendran B, Davis MM. The science and medicine of human immunology. *Science.* (2020) 369(6511):eaay4014. doi: 10.1126/science.aay4014

80. Baj J, Korona-Glowniak I, Forma A, Maani A, Sitarz E, Rahnama-Hezavah M, et al. Mechanisms of the epithelial-mesenchymal transition and tumor microenvironment in helicobacter pylori-induced gastric cancer. *Cells* (2020) 9 (4):1055. doi: 10.3390/cells9041055

81. Fu X, Liu G, Halim A, Ju Y, Luo Q, Song AG. Mesenchymal stem cell migration and tissue repair. *Cells.* (2019) 8(8):784. doi: 10.3390/cells8080784

82. Baker N, Boyette LB, Tuan RS. Characterization of bone marrow-derived mesenchymal stem cells in aging. *Bone.* (2015) 70:37–47. doi: 10.1016/j.bone.2014.10.014

83. Houghton J, Stoicov C, Nomura S, Rogers AB, Carlson J, Li H, et al. Gastric cancer originating from bone marrow-derived cells. *Science.* (2004) 306 (5701):1568–71. doi: 10.1126/science.1099513

84. Arcucci A, Ruocco MR, Granato G, Sacco AM, Montagnani S. Cancer: An oxidative crosstalk between solid tumor cells and cancer associated fibroblasts. *BioMed Res Int* (2016) 2016:4502846. doi: 10.1155/2016/4502846

85. Karagiannis GS, Poutahidis T, Erdman SE, Kirsch R, Riddell RH, Diamandis EP. Cancer-associated fibroblasts drive the progression of metastasis through both paracrine and mechanical pressure on cancer tissue. *Mol Cancer Res* (2012) 10 (11):1403–18. doi: 10.1158/1541-7786.MCR-12-0307

86. Yamaguchi H, Sakai R. Direct interaction between carcinoma cells and cancer associated fibroblasts for the regulation of cancer invasion. *Cancers (Basel)* (2015) 7(4):2054–62. doi: 10.3390/cancers7040876

87. Kalluri R, Zeisberg M. Fibroblasts in cancer. *Nat Rev Cancer* (2006) 6 (5):392–401. doi: 10.1038/nrc1877

88. Lim H, Moon A. Inflammatory fibroblasts in cancer. *Arch Pharm Res* (2016) 39(8):1021–31. doi: 10.1007/s12272-016-0787-8

89. Giannoni E, Bianchini F, Masieri L, Serni S, Torre E, Calorini L, et al. Reciprocal activation of prostate cancer cells and cancer-associated fibroblasts stimulates epithelial-mesenchymal transition and cancer stemness. *Cancer Res* (2010) 70(17):6945–56. doi: 10.1158/0008-5472.CAN-10-0785

90. Spaeth EL, Dembinski JL, Sasser AK, Watson K, Klopp A, Hall B, et al. Mesenchymal stem cell transition to tumor-associated fibroblasts contributes to fibrovascular network expansion and tumor progression. *PLoS One* (2009) 4(4): e4992. doi: 10.1371/journal.pone.0004992

91. Krzysiek-Maczka G, Targosz A, Szczyrk U, Strzalka M, Sliwowski Z, Brzozowski T, et al. Role of helicobacter pylori infection in cancer-associated fibroblast-induced epithelial-mesenchymal transition in vitro. *Helicobacter* (2018) 23(6):e12538. doi: 10.1111/hel.12538

92. Yoshida K, Murata M, Yamaguchi T, Matsuzaki K, Okazaki K. Reversible human TGF-beta signal shifting between tumor suppression and fibro-carcinogenesis: Implications of smad phospho-isoforms for hepatic epithelial-mesenchymal transitions. *J Clin Med* (2016) 5(1):7. doi: 10.3390/jcm5010007

93. Nantajit D, Lin D, Li JJ. The network of epithelial-mesenchymal transition: potential new targets for tumor resistance. *J Cancer Res Clin Oncol* (2015) 141 (10):1697–713. doi: 10.1007/s00432-014-1840-y

94. Zhang J, Thorikay M, van der Zon G, van Dinther M, Ten Dijke P. Studying TGF-beta signaling and TGF-beta-induced epithelial-to-mesenchymal transition in breast cancer and normal cells. *J Vis Exp* (2020) 164:e61830. doi: 10.3791/61830

95. Yoo JY, Ku BJ, Kim TH, Il Ahn J, Ahn JY, Yang WS, et al. Beta-catenin activates TGF-beta-induced epithelial-mesenchymal transition in adenomyosis. *Exp Mol Med* (2020) 52(10):1754–65. doi: 10.1038/s12276-020-00514-6

96. Zhang J, Fan J, Zeng X, Nie M, Luan J, Wang Y, et al. Hedgehog signaling in gastrointestinal carcinogenesis and the gastrointestinal tumor microenvironment. *Acta Pharm Sin B* (2021) 11(3):609–20. doi: 10.1016/j.apsb.2020.10.022

97. von Ahrens D, Bhagat TD, Nagrath D, Maitra A, Verma A. The role of stromal cancer-associated fibroblasts in pancreatic cancer. *J Hematol Oncol* (2017) 10(1):76. doi: 10.1186/s13045-017-0448-5

98. Fujii S, Fujihara A, Natori K, Abe A, Kuboki Y, Higuchi Y, et al. TEM1 expression in cancer-associated fibroblasts is correlated with a poor prognosis in patients with gastric cancer. *Cancer Med* (2015) 4(11):1667–78. doi: 10.1002/cam4.515

99. Zhai J, Shen J, Xie G, Wu J, He M, Gao L, et al. Cancer-associated fibroblasts-derived IL-8 mediates resistance to cisplatin in human gastric cancer. *Cancer Lett* (2019) 454:37–43. doi: 10.1016/j.canlet.2019.04.002

100. Meyer C, Sevko A, Ramacher M, Bazhin AV, Falk CS, Osen W, et al. Chronic inflammation promotes myeloid-derived suppressor cell activation blocking antitumor immunity in transgenic mouse melanoma model. *Proc Natl Acad Sci U S A* (2011) 108(41):17111–6. doi: 10.1073/pnas.1108121108

101. Dorhoi A, Du Plessis N. Monocytic myeloid-derived suppressor cells in chronic infections. *Front Immunol* (2017) 8:1895. doi: 10.3389/fimmu.2017.01895

102. Groth C, Hu X, Weber R, Fleming V, Altevogt P, Utikal J, et al. Immunosuppression mediated by myeloid-derived suppressor cells (MDSCs) during tumour progression. *Br J Cancer* (2019) 120(1):16–25. doi: 10.1038/s41416-018-0333-1

103. Gabrilovich DI, Ostrand-Rosenberg S, Bronte V. Coordinated regulation of myeloid cells by tumours. *Nat Rev Immunol* (2012) 12(4):253–68. doi: 10.1038/nri3175

104. Gabrilovich DI, Bronte V, Chen SH, Colombo MP, Ochoa A, Ostrand-Rosenberg S, et al. The terminology issue for myeloid-derived suppressor cells. *Cancer Res* (2007) 67(1):425; author reply 6. doi: 10.1158/0008-5472.CAN-06-3037

105. Lee CR, Lee W, Cho SK, Park SG. Characterization of multiple cytokine combinations and TGF-beta on differentiation and functions of myeloid-derived suppressor cells. *Int J Mol Sci* (2018) 19(3):869. doi: 10.3390/ijms19030869

106. Ku AW, Muhitch JB, Powers CA, Diehl M, Kim M, Fisher DT, et al. Tumor-induced MDSC act via remote control to inhibit l-selectin-dependent adaptive immunity in lymph nodes. *Elife.* (2016) 5:e17375. doi: 10.7554/eLife.17375

107. Corzo CA, Cotter MJ, Cheng P, Cheng F, Kusmartsev S, Sotomayor E, et al. Mechanism regulating reactive oxygen species in tumor-induced myeloid-derived suppressor cells. *J Immunol* (2009) 182(9):5693–701. doi: 10.4049/jimmunol.0900092

108. Jayaraman P, Parikh F, Lopez-Rivera E, Hailemichael Y, Clark A, Ma G, et al. Tumor-expressed inducible nitric oxide synthase controls induction of functional myeloid-derived suppressor cells through modulation of vascular endothelial growth factor release. *J Immunol* (2012) 188(11):5365–76. doi: 10.4049/jimmunol.1103553

109. Rodriguez PC, Ochoa AC. Arginine regulation by myeloid derived suppressor cells and tolerance in cancer: mechanisms and therapeutic perspectives. *Immunol Rev* (2008) 222:180–91. doi: 10.1111/j.1600-065X.2008.00608.x

110. Lu C, Redd PS, Lee JR, Savage N, Liu K. The expression profiles and regulation of PD-L1 in tumor-induced myeloid-derived suppressor cells. *Oncoimmunology.* (2016) 5(12):e1247135. doi: 10.1080/2162402X.2016.1247135

111. Ghaleb AM, Yang VW. Kruppel-like factor 4 (KLF4): What we currently know. *Gene.* (2017) 611:27–37. doi: 10.1016/j.gene.2017.02.025

112. Zhang J, Zhu Z, Wu H, Yu Z, Rong Z, Luo Z, et al. PODXL, negatively regulated by KLF4, promotes the EMT and metastasis and serves as a novel prognostic indicator of gastric cancer. *Gastric Cancer* (2019) 22(1):48–59. doi: 10.1007/s10120-018-0833-y

113. Ghaleb AM, Nandan MO, Chanchevalap S, Dalton WB, Hisamuddin IM, Yang VW. Kruppel-like factors 4 and 5: the yin and yang regulators of cellular proliferation. *Cell Res* (2005) 15(2):92–6. doi: 10.1038/sj.cr.7290271

114. Wang L, Chang EW, Wong SC, Ong SM, Chong DQ, Ling KL. Increased myeloid-derived suppressor cells in gastric cancer correlate with cancer stage and plasma S100A8/A9 proinflammatory proteins. *J Immunol* (2013) 190(2):794–804. doi: 10.4049/jimmunol.1202088

115. Wang PF, Song SY, Wang TJ, Ji WJ, Li SW, Liu N, et al. Prognostic role of pretreatment circulating MDSCs in patients with solid malignancies: A meta-analysis of 40 studies. *Oncoimmunology.* (2018) 7(10):e1494113. doi: 10.1080/2162402X.2018.1494113

116. Lu X, Horner JW, Paul E, Shang X, Troncoso P, Deng P, et al. Effective combinatorial immunotherapy for castration-resistant prostate cancer. *Nature.* (2017) 543(7647):728–32. doi: 10.1038/nature21676

117. Highfill SL, Cui Y, Giles AJ, Smith JP, Zhang H, Morse E, et al. Disruption of CXCR2-mediated MDSC tumor trafficking enhances anti-PD1 efficacy. *Sci Transl Med* (2014) 6(237):237ra67. doi: 10.1126/scitranslmed.3007974

118. Wesolowski R, Markowitz J, Carson WE3rd. Myeloid derived suppressor cells - a new therapeutic target in the treatment of cancer. *J Immunother Cancer* (2013) 1:10. doi: 10.1186/2051-1426-1-10

119. Aydin EM, Demir TD, Seymen N, Said SS, Oktem-Okullu S, Tiftikci A, et al. The crosstalk between h. pylori virulence factors and the PD1:PD-L1 immune checkpoint inhibitors in progression to gastric cancer. *Immunol Lett* (2021) 239:1–11. doi: 10.1016/j.imlet.2021.06.009

120. Shen B, Qian A, Lao W, Li W, Chen X, Zhang B, et al. Relationship between helicobacter pylori and expression of programmed death-1 and its ligand in gastric intraepithelial neoplasia and early-stage gastric cancer. *Cancer Manag Res* (2019) 11:3909–19. doi: 10.2147/CMAR.S203035

121. Go DM, Lee SH, Lee SH, Woo SH, Kim K, Kim K, et al. Programmed death ligand 1-expressing classical dendritic cells MitigateHelicobacter-induced gastritis. *Cell Mol Gastroenterol Hepatol* (2021) 12(2):715–39. doi: 10.1016/j.jcmgh.2021.04.007

122. Lina TT, Alzahrani S, House J, Yamaoka Y, Sharpe AH, Rampy BA, et al. Helicobacter pylori cag pathogenicity island's role in B7-H1 induction and immune evasion. *PLoS One* (2015) 10(3):e0121841. doi: 10.1371/journal.pone.0121841

123. Beswick EJ, Pinchuk IV, Das S, Powell DW, Reyes VE. Expression of the programmed death ligand 1, B7-H1, on gastric epithelial cells after helicobacter pylori exposure promotes development of CD4+ CD25+ FoxP3+ regulatory T cells. *Infect Immun* (2007) 75(9):4334–41. doi: 10.1128/IAI.00553-07

124. Wu J, Zhu X, Guo X, Yang Z, Cai Q, Gu D, et al. Helicobacter urease suppresses cytotoxic CD8+ T-cell responses through activating Myh9-dependent induction of PD-L1. *Int Immunol* (2021) 33(9):491–504. doi: 10.1093/intimm/dxab044

125. Li H, Xia JQ, Zhu FS, Xi ZH, Pan CY, Gu LM, et al. LPS promotes the expression of PD-L1 in gastric cancer cells through NF-kappaB activation. *J Cell Biochem* (2018) 119(12):9997–10004. doi: 10.1002/jcb.27329

126. Han Y, Liu D, Li L. PD-1/PD-L1 pathway: current researches in cancer. *Am J Cancer Res* (2020) 10(3):727–42.

127. Baumeister SH, Freeman GJ, Dranoff G, Sharpe AH. Coinhibitory pathways in immunotherapy for cancer. *Annu Rev Immunol* (2016) 34:539–73. doi: 10.1146/annurev-immunol-032414-112049

128. Ribas A, Wolchok JD. Cancer immunotherapy using checkpoint blockade. *Science.* (2018) 359(6382):1350–5. doi: 10.1126/science.aar4060

129. Taube JM, Anders RA, Young GD, Xu H, Sharma R, McMiller TL, et al. Colocalization of inflammatory response with B7-h1 expression in human melanocytic lesions supports an adaptive resistance mechanism of immune escape. *Sci Transl Med* (2012) 4(127):127ra37. doi: 10.1126/scitranslmed.3003689

130. Dong P, Xiong Y, Yue J, Hanley SJB, Watari H. Tumor-intrinsic PD-L1 signaling in cancer initiation, development and treatment: Beyond immune evasion. *Front Oncol* (2018) 8:386. doi: 10.3389/fonc.2018.00386

131. Wang X, Teng F, Kong L, Yu J. PD-L1 expression in human cancers and its association with clinical outcomes. *Onco Targets Ther* (2016) 9:5023–39. doi: 10.2147/OTT.S105862

132. Liu X, Choi MG, Kim K, Kim KM, Kim ST, Park SH, et al. High PD-L1 expression in gastric cancer (GC) patients and correlation with molecular features. *Pathol Res Pract* (2020) 216(4):152881. doi: 10.1016/j.prp.2020.152881

133. Wu L, Cai S, Deng Y, Zhang Z, Zhou X, Su Y, et al. PD-1/PD-L1 enhanced cisplatin resistance in gastric cancer through PI3K/AKT mediated p-gp expression. *Int Immunopharmacol* (2021) 94:107443. doi: 10.1016/j.intimp.2021.107443

134. Kawazoe A, Shitara K, Boku N, Yoshikawa T, Terashima M. Current status of immunotherapy for advanced gastric cancer. *Jpn J Clin Oncol* (2021) 51(1):20–7. doi: 10.1093/jjco/hyaa202

135. Kim ST, Cristescu R, Bass AJ, Kim KM, Odegaard JI, Kim K, et al. Comprehensive molecular characterization of clinical responses to PD-1 inhibition in metastatic gastric cancer. *Nat Med* (2018) 24(9):1449–58. doi: 10.1038/s41591-018-0101-z

136. Kono K, Nakajima S, Mimura K. Current status of immune checkpoint inhibitors for gastric cancer. *Gastric Cancer* (2020) 23(4):565–78. doi: 10.1007/s10120-020-01090-4

137. Mohabati Mobarez A, Soleimani N, Esmaeili SA, Farhangi B. Nanoparticle-based immunotherapy of breast cancer using recombinant helicobacter pylori proteins. *Eur J Pharm Biopharm* (2020) 155:69–76. doi: 10.1016/j.ejpb.2020.08.013

138. Solbrig CM, Saucier-Sawyer JK, Cody V, Saltzman WM, Hanlon DJ. Polymer nanoparticles for immunotherapy from encapsulated tumor-associated antigens and whole tumor cells. *Mol Pharm* (2007) 4(1):47–57. doi: 10.1021/mp060107e

139. Topalian SL, Hodi FS, Brahmer JR, Gettinger SN, Smith DC, McDermott DF, et al. Safety, activity, and immune correlates of anti-PD-1 antibody in cancer. *N Engl J Med* (2012) 366(26):2443–54. doi: 10.1056/NEJMoa1200690

140. Darvin P, Toor SM, Sasidharan Nair V, Elkord E. Immune checkpoint inhibitors: recent progress and potential biomarkers. *Exp Mol Med* (2018) 50(12):1–11. doi: 10.1038/s12276-018-0191-1

141. Li B, Chan HL, Chen P. Immune checkpoint inhibitors: Basics and challenges. *Curr Med Chem* (2019) 26(17):3009–25. doi: 10.2174/0929867324666170804143706

142. Taefehshokr S, Parhizkar A, Hayati S, Mousapour M, Mahmoudpour A, Eleid L, et al. Cancer immunotherapy: Challenges and limitations. *Pathol Res Pract* (2022) 229:153723. doi: 10.1016/j.prp.2021.153723

143. Hegde PS, Chen DS. Top 10 challenges in cancer immunotherapy. *Immunity.* (2020) 52(1):17–35. doi: 10.1016/j.immuni.2019.12.011

144. Odunsi K. Immunotherapy in ovarian cancer. *Ann Oncol* (2017) 28(suppl_8):viii1–7. doi: 10.1093/annonc/mdx444

145. Rowshanravan B, Halliday N, Sansom DM. CTLA-4: a moving target in immunotherapy. *Blood.* (2018) 131(1):58–67. doi: 10.1182/blood-2017-06-741033

146. Keir ME, Butte MJ, Freeman GJ, Sharpe AH. PD-1 and its ligands in tolerance and immunity. *Annu Rev Immunol* (2008) 26:677–704. doi: 10.1146/annurev.immunol.26.021607.090331

147. Dyck L, Mills KHG. Immune checkpoints and their inhibition in cancer and infectious diseases. *Eur J Immunol* (2017) 47(5):765–79. doi: 10.1002/eji.201646875

148. Kang YK, Boku N, Satoh T, Ryu MH, Chao Y, Kato K, et al. Nivolumab in patients with advanced gastric or gastro-oesophageal junction cancer refractory to, or intolerant of, at least two previous chemotherapy regimens (ONO-4538-12, ATTRACTION-2): a randomised, double-blind, placebo-controlled, phase 3 trial. *Lancet.* (2017) 390(10111):2461–71. doi: 10.1016/S0140-6736(17)31827-5

149. Fuchs CS, Doi T, Jang RW, Muro K, Satoh T, Machado M, et al. Safety and efficacy of pembrolizumab monotherapy in patients with previously treated advanced gastric and gastroesophageal junction cancer: Phase 2 clinical KEYNOTE-059 trial. *JAMA Oncol* (2018) 4(5):e180013. doi: 10.1001/jamaoncol.2018.0013

150. Chakrabarti J, Holokai L, Syu L, Steele NG, Chang J, Wang J, et al. Hedgehog signaling induces PD-L1 expression and tumor cell proliferation in gastric cancer. *Oncotarget.* (2018) 9(100):37439–57. doi: 10.18632/oncotarget.26473

151. Xue LJ, Su QS, Yang JH, Lin Y. Autoimmune responses induced by helicobacter pylori improve the prognosis of gastric carcinoma. *Med Hypotheses* (2008) 70(2):273–6. doi: 10.1016/j.mehy.2007.05.045

152. Xue LJ, Mao XB, Liu XB, Gao H, Chen YN, Dai TT, et al. Activation of CD3(+) T cells by helicobacter pylori DNA vaccines in potential immunotherapy of gastric carcinoma. *Cancer Biol Ther* (2019) 20(6):866–76. doi: 10.1080/15384047.2019.1579957

153. Ramachandran M, Jin C, Yu D, Eriksson F, Essand M. Vector-encoded helicobacter pylori neutrophil-activating protein promotes maturation of dendritic cells with Th1 polarization and improved migration. *J Immunol* (2014) 193(5):2287–96. doi: 10.4049/jimmunol.1400339

154. Peng X, Zhang R, Duan G, Wang C, Sun N, Zhang L, et al. Production and delivery of helicobacter pylori NapA in lactococcus lactis and its protective efficacy and immune modulatory activity. *Sci Rep* (2018) 8(1):6435. doi: 10.1038/s41598-018-24879-x

155. Deng Y, Su W, Zhu J, Ji H, Zhou X, Geng J, et al. Helicobacter pylori infection disturbs the tumor immune microenvironment and is associated with a discrepant prognosis in gastric de novo diffuse large b-cell lymphoma. *J Immunother Cancer* (2021) 9(10):e002947. doi: 10.1136/jitc-2021-002947

156. Wang T, Liu X, Ji Z, Men Y, Du M, Ding C, et al. Antitumor and immunomodulatory effects of recombinant fusion protein rMBP-NAP through TLR-2 dependent mechanism in tumor bearing mice. *Int Immunopharmacol* (2015) 29(2):876–83. doi: 10.1016/j.intimp.2015.08.027

157. Ding C, Li L, Zhang Y, Ji Z, Zhang C, Liang T, et al. Toll-like receptor agonist rMBP-NAP enhances antitumor cytokines production and CTL activity of peripheral blood mononuclear cells from patients with lung cancer. *Oncol Lett* (2018) 16(4):4707–12. doi: 10.3892/ol.2018.9182

158. Wang T, Du M, Ji Z, Ding C, Wang C, Men Y, et al. Recombinant protein rMBP-NAP restricts tumor progression by triggering antitumor immunity in mouse metastatic lung cancer. *Can J Physiol Pharmacol* (2018) 96(2):113–9. doi: 10.1139/cjpp-2017-0186

159. Codolo G, Fassan M, Munari F, Volpe A, Bassi P, Rugge M, et al. HP-NAP inhibits the growth of bladder cancer in mice by activating a cytotoxic Th1 response. *Cancer Immunol Immunother* (2012) 61(1):31–40. doi: 10.1007/s00262-011-1087-2

160. Hou M, Wang X, Lu J, Guo X, Ding C, Liang T, et al. TLR agonist rHP-NAP as an adjuvant of dendritic cell-based vaccine to enhance anti-melanoma response. *Iran J Immunol* (2020) 17(1):14–25. doi: 10.22034/iji.2020.80291

161. Ramachandran M, Yu D, Wanders A, Essand M, Eriksson F. An infection-enhanced oncolytic adenovirus secreting h. pylori neutrophil-activating protein with therapeutic effects on neuroendocrine tumors. *Mol Ther* (2013) 21(11):2008–18. doi: 10.1038/mt.2013.153

162. Yang W, Li Y, Gao R, Xiu Z, Sun T. MHC class I dysfunction of glioma stem cells escapes from CTL-mediated immune response *via* activation of wnt/beta-catenin signaling pathway. *Oncogene.* (2020) 39(5):1098–111. doi: 10.1038/s41388-019-1045-6

163. Panagioti E, Kurokawa C, Viker K, Ammayappan A, Anderson SK, Sotiriou S, et al. Immunostimulatory bacterial antigen-armed oncolytic measles virotherapy significantly increases the potency of anti-PD1 checkpoint therapy. *J Clin Invest* (2021) 131(13):e141614. doi: 10.1172/JCI141614

164. Ma J, Jin C, Cancer M, Wang H, Ramachandran M, Yu D. Concurrent expression of HP-NAP enhances antitumor efficacy of oncolytic vaccinia virus but not for semliki forest virus. *Mol Ther Oncolytics* (2021) 21:356–66. doi: 10.1016/j.omto.2021.04.016

165. Ma J, Ramachandran M, Jin C, Quijano-Rubio C, Martikainen M, Yu D, et al. Characterization of virus-mediated immunogenic cancer cell death and the consequences for oncolytic virus-based immunotherapy of cancer. *Cell Death Dis* (2020) 11(1):48. doi: 10.1038/s41419-020-2236-3

166. Smyth EC, Verheij M, Allum W, Cunningham D, Cervantes A, Arnold D, et al. Gastric cancer: ESMO clinical practice guidelines for diagnosis, treatment and follow-up. *Ann Oncol* (2016) 27(suppl 5):v38–49. doi: 10.1093/annonc/mdw350

167. Fashoyin-Aje L, Donoghue M, Chen H, He K, Veeraraghavan J, Goldberg KB, et al. FDA Approval summary: Pembrolizumab for recurrent locally advanced or metastatic gastric or gastroesophageal junction adenocarcinoma expressing PD-L1. *Oncologist.* (2019) 24(1):103–9. doi: 10.1634/theoncologist.2018-0221

168. Fuchs CS, Doi T, Jang RW-J, Muro K, Satoh T, Machado M, et al. KEYNOTE-059 cohort 1: Efficacy and safety of pembrolizumab (pembro) monotherapy in patients with previously treated advanced gastric cancer. *J Clin Oncol* (2017) 35(15_suppl):4003. doi: 10.1200/JCO.2017.35.15_suppl.4003

169. Muro K, Chung HC, Shankaran V, Geva R, Catenacci D, Gupta S, et al. Pembrolizumab for patients with PD-L1-positive advanced gastric cancer (KEYNOTE-012): a multicentre, open-label, phase 1b trial. *Lancet Oncol* (2016) 17(6):717–26. doi: 10.1016/S1470-2045(16)00175-3

170. Senchukova MA, Tomchuk O, Shurygina EI. Helicobacter pylori in gastric cancer: Features of infection and their correlations with long-term results of treatment. *World J Gastroenterol* (2021) 27(37):6290–305. doi: 10.3748/wjg.v27.i37.6290

171. Kayapinar AK, Solakoglu D, Bas K, Oymaci E, Isbilen B, Calik B, et al. Relationship of prognostic factors in stomach cancer with helicobacter pylori: A retrospective study. *Acta Gastroenterol Belg* (2021) 84(4):607–17. doi: 10.51821/84.4.012

172. Tsai KF, Liou JM, Chen MJ, Chen CC, Kuo SH, Lai IR, et al. Distinct clinicopathological features and prognosis of helicobacter pylori negative gastric cancer. *PLoS One* (2017) 12(2):e0170942. doi: 10.1371/journal.pone.0170942

173. Tsuruta O, Yokoyama H, Fujii S. A new crystal lattice structure of helicobacter pylori neutrophil-activating protein (HP-NAP). *Acta Crystallogr Sect F Struct Biol Cryst Commun* (2012) 68(Pt 2):134–40. doi: 10.1107/S1744309111052675

174. Zanotti G, Papinutto E, Dundon W, Battistutta R, Seveso M, Giudice G, et al. Structure of the neutrophil-activating protein from helicobacter pylori. *J Mol Biol* (2002) 323(1):125–30. doi: 10.1016/S0022-2836(02)00879-3

175. Kottakis F, Papadopoulos G, Pappa EV, Cordopatis P, Pentas S, Choli-Papadopoulou T. Helicobacter pylori neutrophil-activating protein activates neutrophils by its c-terminal region even without dodecamer formation, which is a prerequisite for DNA protection–novel approaches against helicobacter pylori inflammation. *FEBS J* (2008) 275(2):302–17. doi: 10.1111/j.1742-4658.2007.06201.x

176. Xiao Y, Yu D. Tumor microenvironment as a therapeutic target in cancer. *Pharmacol Ther* (2021) 221:107753. doi: 10.1016/j.pharmthera.2020.107753

177. Kozlova N, Grossman JE, Iwanicki MP, Muranen T. The interplay of the extracellular matrix and stromal cells as a drug target in stroma-rich cancers. *Trends Pharmacol Sci* (2020) 41(3):183–98. doi: 10.1016/j.tips.2020.01.001

178. Ridge SM, Sullivan FJ, Glynn SA. Mesenchymal stem cells: key players in cancer progression. *Mol Cancer* (2017) 16(1):31. doi: 10.1186/s12943-017-0597-8

179. Poh AR, Ernst M. Targeting macrophages in cancer: From bench to bedside. *Front Oncol* (2018) 8:49. doi: 10.3389/fonc.2018.00049

180. Peranzoni E, Lemoine J, Vimeux L, Feuillet V, Barrin S, Kantari-Mimoun C, et al. Macrophages impede CD8 T cells from reaching tumor cells and limit the efficacy of anti-PD-1 treatment. *Proc Natl Acad Sci U S A* (2018) 115(17):E4041–E50. doi: 10.1073/pnas.1720948115

181. Li DK, Wang W. Characteristics and clinical trial results of agonistic anti-CD40 antibodies in the treatment of malignancies. *Oncol Lett* (2020) 20(5):176. doi: 10.3892/ol.2020.12037

182. Sullivan RJ, Hong DS, Tolcher AW, Patnaik A, Shapiro G, Chmielowski B, et al. Initial results from first-in-human study of IPI-549, a tumor macrophage-targeting agent, combined with nivolumab in advanced solid tumors. *J Clin Oncol* (2018) 36(15):3013. doi: 10.1200/JCO.2018.36.15_suppl.3013

183. Jia Z, Zheng M, Jiang J, Cao D, Wu Y, Zhang Y, et al. Positive h. pylori status predicts better prognosis of non-cardiac gastric cancer patients: results from cohort study and meta-analysis. *BMC Cancer* (2022) 22(1):155. doi: 10.1186/s12885-022-09222-y

frontiers | Frontiers in Immunology

TYPE Original Research
PUBLISHED 01 August 2022
DOI 10.3389/fimmu.2022.951232

Check for updates

OPEN ACCESS

EDITED BY
Mario M. D'Elios,
University of Florence, Italy

REVIEWED BY
Nagaja Capitani,
University of Siena, Italy
Ursula Rossi,
Conicet, Argentina
Gaia Codolo,
University of Padua, Italy
Ricardo Mora-Cartin,
University of Chicago Medicine,
United States

*CORRESPONDENCE
Panagiotis Skendros
pskendro@med.duth.gr

†These authors have contributed equally to this work

SPECIALTY SECTION
This article was submitted to Microbial Immunology, a section of the journal Frontiers in Immunology

RECEIVED 23 May 2022
ACCEPTED 13 July 2022
PUBLISHED 01 August 2022

CITATION
Mitroulis I, Chrysanthopoulou A, Divolis G, Ioannidis C, Ntinopoulou M, Tasis A, Konstantinidis T, Antoniadou C, Soteriou N, Lallas G, Mitka S, Lesche M, Dahl A, Gembardt S, Panopoulou M, Sideras P, Wielockx B, Coskun Ü, Ritis K and Skendros P (2022) A gene expression map of host immune response in human brucellosis.
Front. Immunol. 13:951232.
doi: 10.3389/fimmu.2022.951232

A gene expression map of host immune response in human brucellosis

Ioannis Mitroulis[1,2], Akrivi Chrysanthopoulou[1,3†], Georgios Divolis[4†], Charalampos Ioannidis[5], Maria Ntinopoulou[1], Athanasios Tasis[1], Theocharis Konstantinidis[1,6], Christina Antoniadou[1,2], Natalia Soteriou[7], George Lallas[7], Stella Mitka[8], Mathias Lesche[9], Andreas Dahl[9], Stephanie Gembardt[5], Maria Panopoulou[6], Paschalis Sideras[4], Ben Wielockx[5], Ünal Coskun[5], Konstantinos Ritis[1,2] and Panagiotis Skendros[1,2*]

[1]Laboratory of Molecular Hematology, Democritus University of Thrace, University Hospital of Alexandroupolis, Alexandroupolis, Greece, [2]First Department of Internal Medicine, Democritus University of Thrace, University Hospital of Alexandroupolis, Alexandroupolis, Greece, [3]Department of Biological Applications and Technology, University of Ioannina, Ioannina, Greece, [4]Biomedical Research Foundation Academy of Athens, Center for Clinical, Experimental Surgery and Translational Research, Athens, Greece, [5]Institute for Clinical Chemistry and Laboratory Medicine, Faculty of Medicine, Technische Universität Dresden, Dresden, Germany, [6]Laboratory of Microbiology, Democritus University of Thrace, University Hospital of Alexandroupolis, Alexandroupolis, Greece, [7]R&D Department, P. Zafiropoulos S.A., Athens, Greece, [8]School of Biomedical Sciences, International Hellenic University, Thessaloniki, Greece, [9]DRESDEN-concept Genome Center, Center for Molecular and Cellular Bioengineering, Technische Universität Dresden, Dresden, Germany

Brucellosis is a common zoonotic disease caused by intracellular pathogens of the genus *Brucella*. *Brucella* infects macrophages and evades clearance mechanisms, thus resulting in chronic parasitism. Herein, we studied the molecular changes that take place in human brucellosis both *in vitro* and *ex vivo*. RNA sequencing was performed in primary human macrophages (Mφ) and polymorphonuclear neutrophils (PMNs) infected with a clinical strain of *Brucella* spp. We observed a downregulation in the expression of genes involved in host response, such as TNF signaling, IL-1β production, and phagosome formation in Mφ, and phosphatidylinositol signaling and TNF signaling in PMNs, being in line with the ability of the pathogen to survive within phagocytes. Further transcriptomic analysis of isolated peripheral blood mononuclear cells (PBMCs) and PMNs from patients with acute brucellosis before treatment initiation and after successful treatment revealed a positive correlation of the molecular signature of active disease with pathways associated with response to interferons (IFN). We identified 24 common genes that were significantly altered in both PMNs and PBMCs, including genes involved in IFN signaling that were downregulated after treatment in both cell populations, and *IL1R1* that was upregulated. The concentration of several inflammatory mediators was measured in the serum of these patients,

and levels of IFN-γ, IL-1β and IL-6 were found significantly increased before the treatment of acute brucellosis. An independent cohort of patients with chronic brucellosis also revealed increased levels of IFN-γ during relapse compared to remissions. Taken together, this study provides for the first time an in-depth analysis of the transcriptomic alterations that take place in human phagocytes upon infection, and in peripheral blood immune populations during active disease.

KEYWORDS

brucellosis, immunity, transcriptomics, macrophages, polymorphonuclear neutrophils, peripheral blood mononuclear cells

Introduction

Brucellosis is a common bacterial zoonotic disease worldwide and an emerging zoonosis in several developed countries (1, 2). Despite its importance in public health brucellosis remains widespread and neglected in many areas, including southeastern Europe, Asia, Central and Latin America, and Africa (2, 3). It is caused by various species of the bacterial genus *Brucella*, which mainly infect domestic animals, especially goats, sheep, and cows, and use them as natural reservoirs. The disease is transmitted to humans by consumption of unpasteurized milk and dairy products or by occupational contact with infected animals. Additionally, *Brucella* is highly infectious through the aerosol route, thus is considered as one of the most common laboratory-acquired pathogens and is also classified as a category B agent on the biodefense list (4).

Human brucellosis causes high morbidity and protean clinical manifestations, mimicking many infectious and non-infectious diseases since it can affect multiple organs. Despite early diagnosis and prolonged therapy with antibiotics is associated with substantial residual disability (4). Up to 30% of patients develop chronic disease, which is characterized by atypical clinical manifestations, high frequency of focal complications such as spondylitis, chronic fatigue syndrome, and relapses (4, 5).

Host protection against *Brucella* and prevention of its intracellular parasitism in macrophages depends on cell-mediated immunity, involving adequate Th1 immune response, with significant production of interferon-gamma (IFN-γ) (5). Previous data support also a key role of innate immunity and neutrophils in early proinflammatory responses against *Brucella* that may affect T-cell dynamics during infection (5–7). On the other hand, *Brucella* has developed various stealthy strategies to evade innate and adaptive immune responses, in order to establish intracellular long-term survival and replication (8, 9). Several studies have demonstrated that patients with chronic brucellosis display defective cell-mediated immunity (brucellosis-acquired cellular anergy) probably due to modulation of host cellular immunity by *Brucella* (5). However, immunopathogenesis of human brucellosis remains incompletely understood and integrated molecular data that characterize complex interactions between *Brucella* and host immunity are missing today.

Here, we shed light on the transcriptomic alterations that macrophages (Mφ) and polymorphonuclear neutrophils (PMNs) undergo during the crucial early events of *Brucella* infection. Moreover, we analyze the transcriptomic alterations that take place concomitantly in peripheral blood mononuclear cells (PBMCs) and PMNs of patients upon treatment, uncovering candidate molecular targets and pathways that may characterize active infection and disease eradication.

Materials and methods

Patients

Ten adult patients with acute brucellosis were recruited. EDTA anticoagulated blood and serum were collected from patients with active brucellosis before the initiation of antibiotic treatment and three months after the completion of treatment, when all patients were successfully treated. The diagnosis was based on compatible clinical manifestations in combination with high serum titers of anti-*Brucella* antibodies (Wright's agglutination test ≥160) or a four-fold increase of the initial titers in two-paired samples drawn 2 weeks apart, or/and Brucella isolation, according to Centers for Disease Control and Prevention (CDC)/Council of State and Territorial Epidemiologists (CSTE) Laboratory Criteria for Diagnosis (10). None of these patients suffered any relapse during a six-month post-treatment follow-up period. Patient characteristics and treatment are described in Table 1. PBMCs and PMNs were

10.3389/fimmu.2022.951232

TABLE 1 Characteristics of patients with acute brucellosis (AB).

Patient#	Sex	Age (years)	Symptoms/Findings	Route of transmission	Wright SAT	Bloodculture	Antibiotictreatment
AB1	F	40	Fatigue, malaise myalgias, arthralgias	Consumption	1/640	N/A	Rifampicin Doxycycline
AB2	F	53	Fever, sweating, arthralgias, peripheral arthritis	Consumption	1/320	Negative	Rifampicin Doxycycline Amikacin
AB3	M	31	Fever, sweating, fatigue	Consumption/ contact	1/320	Negative	Rifampicin Doxycycline Amikacin
AB4	M	36	Fever, sweating, malaise, fatigue	Consumption	1/5120	Negative	Rifampicin Doxycycline Amikacin
AB5	M	55	Fever, sweating, lumbar spondylitis	Contact	1/160	*Brucella spp*	Rifampicin Doxycycline Amikacin
AB6	M	39	Fever, myalgia	Contact	1/320	*Brucella spp*	Rifampicin Doxycycline Amikacin
AB7	M	64	Sweating, fatigue, low back pain	Consumption	1/320	*Brucella spp*	Rifampicin Doxycycline Amikacin
AB8	F	45	Fatigue, lumbar spondylitis	Consumption	1/640	N/A	Rifampicin Doxycycline Amikacin
AB9	M	18	Fever, sweating, malaise, fatigue myalgias, arthralgias	Consumption/ contact	1/160	*Brucella spp*	Rifampicin Doxycycline Amikacin
AB10	M	52	Fatigue, myalgias, arthralgias, peripheral arthritis	Contact/REV1 vaccine	1/160	Negative	Rifampicin Doxycycline
Age (years, mean ± SD)		43.3 ± 13.4					

F, female; M, male; N/A, not available; SAT, serum agglutination test; SD, standard deviation.
Duration of antibiotic treatment was 8-12 weeks for rifampicin (600 mg/daily) and doxycycline (200 mg/daily), and 2-3 weeks for Amikacin (1 gr/daily).

simultaneously isolated from patients. PBMCs and PMNs were also isolated from ten healthy, sex and age-matched, subjects who served as controls (Table 2). Sera from a second cohort of 25 chronic relapsing brucellosis patients at clinical relapse and remission, were also used. These patients had a disease duration of ≥12 months in combination with positive serum agglutination tests (SATs) or/and complement fixation test, or/ and Brucella isolation (Supplementary Table S1).

Exclusion criteria were co-existence of other infectious, neoplastic or autoimmune disease, administration of immunomodulating agents or vaccination for at least 4 weeks before the entry to study, and pregnancy. The study was approved by the Local Scientific and Ethics Committee of the University Hospital of Alexandroupolis, Greece (Approval Number #1195/19-12-2017). All subjects provided written informed consent in accordance with the principles expressed in the Declaration of Helsinki.

TABLE 2 Demographic characteristics of healthy subjects (controls).

Control#	Sex	Age (years)
C1*	F	38
C2*	M	47
C3*	M	35
C4*	M	34
C5^	M	55
C6^	M	40
C7^	F	51
C8^	F	44
C9^	M	23
C10^	M	52
Age (years, mean ± SD)		41.9 ± 9.8

F, female; M, male; SD, standard deviation. All controls had no previous history of brucellosis and yielded a negative Wright serum agglutination test (<1/80). *Isolation of PBMCs that were used for macrophage differentiation and *in vitro* infection with *Brucella spp*, ^isolation of PMNs that were used for *in vitro* infection with *Brucella spp*.

PBMCs and PMNs isolation

PBMCs and PMNs were isolated from EDTA blood by Histopaque (Sigma-Aldrich, 1077 and 1119) double-gradient density centrifugation (30 minutes, 700g, at 20°C-25°C) according to the manufacturer's recommendations. Then, cells were washed once with phosphate buffered saline (PBS-1x, ThermoFisher Scientific) and cultured. Cell purity was ≥ 98% as assessed by microscopy (May Grunwald-Giemsa staining) and/or flow cytometry.

For RNA experiments, cell pellet was resuspended in 1mL TRIzol reagent (ThermoFisher Scientific) and the extraction procedure was performed immediately after cell isolation, according to the manufacturer's instructions.

Mφ differentiation

Human Mφ were differentiated from isolated PBMCs from four controls (Table 2). To promote Mφ differentiation, monocytes were isolated in RPMI-1640 (ThermoFisher Scientific) using plastic adherence. Non-adherent cells were removed after 6h (day 0). Adherent cells were cultured in RPMI-1640 culture medium supplemented with 10% autologous serum for 6 additional days (day 1-6) and penicillin/streptomycin solution (ThermoFisher Scientific) (11). Cell cultures were washed with prewarmed PBS-1x and culture medium was changed every other day, to ensure the removal of remaining contaminating lymphocytes. On day 7, cell culture medium was removed and *in vitro* infection with *Brucella* was performed.

Phenotypic characterization of Mφ

To assess the differentiation status of human macrophages, fixation and permeabilization were performed with 4% paraformaldehyde and Triton-X (Sigma-Aldrich), respectively. Then, cells were stained using a mouse monoclonal anti-CD68 antibody (Clone: KP1, ThermoFisher Scientific) for 1 hour. A rabbit-anti mouse IgG Alexa Fluor 594 (ThermoFisher Scientific) was used as secondary antibody. DAPI solution (Ibidi) was used as nuclear counterstain. Samples were visualized with a fluorescence microscope (OLYMPUS BX51) with a fixed Nikon camera (model DS-Fi1, lens 100x) (Supplementary Figure S1A).

In vitro infection

A clinical strain of *Brucella* spp., isolated from peripheral blood from a patient with acute brucellosis, was used for *in vitro* experiments. Isolate was presumptively identified as *B. melitensis* by automated system VITEK 2 (bioMérieux), based on the biochemical characteristics of isolate. The isolate was aliquoted, and stored at −70°C until used. Bacterial inoculum for cell infection was cultured on blood agar for 3 days under aerobic conditions, at 37°C and 5% CO_2 according to the literature and American Society for Microbiology (ASM) guidelines (12, 13). Bacterial suspension with 0.5 McFarland was opsonized for 30 minutes using human serum and then diluted in RPMI and ~ 10^7 bacteria in 0.5 ml of RPMI were added to each well (20 MOI) of PMNs or Mφ. Subsequently, cells were cultured for 0.5h for PMNs and 2h and 24h for Mφ. After a washing step with PBS, cells were resuspended in TRIzol reagent (ThermoFisher Scientific) and the RNA extraction procedure was performed immediately, according to the manufacturer's instructions. Untreated PMNs and untreated Mφ, cultured for 0.5h or 2h respectively, served as control. The experimental procedure with *Brucella* spp. was performed at biosafety level 3. The above time points and concentrations were optimal for Mφ or PMNs stimulation, and established in preliminary experiments.

Assessment of phagocytosis in Mφ and PMNs

To evaluate phagocytosis in Mφ and PMNs, cells were fixed with 4% paraformaldehyde (Sigma-Aldrich), permed with Triton-X (Sigma-Aldrich) and then stained using a mouse monoclonal anti-Brucella antibody (LSBio) for 1 hour. After thorough washes with PBS-1x, a rabbit-anti mouse IgG Alexa Fluor 594 (ThermoFisher Scientific) was used as secondary antibody. DAPI solution (Ibidi) was used as nuclear counterstain. Samples were visualized with either a fluorescence microscope (OLYMPUS BX51) with a fixed Nikon camera (model DS-Fi1, lens 40x or 60x) or a confocal microscope (Spinning Disk Andor Revolution Confocal System, Ireland) with PLAPON 606O/TIRFM-SP, NA 1.45 and UPLSAPO 100XO, NA 1.4 objectives (Olympus) (Supplementary Figures S1B, C).

To further evaluate phagocytosis in PMNs, cells were analyzed by flow cytometry, using the neutrophil-specific marker CD66b (PerCP-Cyanine5.5 conjugated CD66b, Biolegend). Bacteria were stained using a mouse monoclonal anti-Brucella antibody (LSBio), detected with a rabbit anti-mouse Alexa Fluor 647 (ThermoFisher Scientific) (Supplementary Figure S1D).

RNA sequencing

RNA sequencing for Mφ and PBMCs was performed as previously described (14). To analyze RNA sequencing data, fragments were aligned with GSNAP (2020–12–16) to the Homo sapiens (human) genome assembly GRCh38 (hg38) from

Genome Reference Consortium, and Ensembl annotation version 98 was used for the splice site support. Uniquely aligned fragments were counted with featureCounts (subread v2.0.1), again with the support of the Ensembl annotation. The exploratory analysis was performed with the DESeq 2 (v1.24.0) package within R (v3.6.3). Bias for patients was assessed using an exploratory correction with the variance stabilized transformation data of DESeq2 and the removeBatchEffect function of edgeR (3.26.8). Differential expression between before and after treatment was performed with a correction for patient.

For PMNs, 1000 ng of total RNA were used for the preparation of cDNA libraries, using the TruSeq RNA Library Preparation Kit v2 (Illumina), according to the manufacturer's instructions. Library quality was evaluated using the Agilent DNA 1000 Kit (Agilent) with an Agilent 2100 Bioanalyzer. Quantification was performed by amplifying a set of six pre-diluted DNA standards (KAPA Biosystems) and diluted cDNA libraries by RT-qPCR. Isomolar quantities of up to 20 cDNA libraries, barcoded with different adaptors, were multiplexed. Sequencing was performed in a single-end manner at the Greek Genome Center, using a NextSeq 500/550 75c kit (Illumina) for the *in vitro* samples and a NovaSeq 6000 SP 100c kit (Illumina) for the *ex vivo* samples, generating 75 bp and 100 bp long reads, respectively, and an average of 25 million reads per library. Raw sequence data in FastQ format were uploaded to the Galaxy web platform, and standard tools of the public server "usegalaxy.org" were used for subsequent analysis (15). Briefly, quality control of raw reads was performed with FastQC (v072+galaxy1), followed by the removal of adapter sequences and low-quality bases using Trim Galore! (v0.6.3). Next, HISAT2 (v2.2.1+galaxy0) was applied for the alignment of trimmed reads to the Homo sapiens genome assembly GRCh37 (hg19) from Genome Reference Consortium. Assessment of uniform read coverage for exclusion of 5'/3' bias and evaluation of RNA integrity at the transcript level were performed using Gene Body Coverage (v2.6.4.3) and Transcript Integrity Number (v2.6.4.1) tools, respectively. Differential gene expression was determined with DESeq2 (v2.11.40.6+galaxy1), using the count tables generated from HTSeq-count (v0.9.1) as input. The variability within and between individuals in this paired-data study was incorporated in the analysis, considering the treatment as the primary factor and the individual/patient as the secondary factor affecting gene expression. RNA sequencing data are provided in Supplementary File S1.

Pathway and biological processes analysis was performed using the Enrichr analysis tool (14, 16). Heat maps were generated using the Morpheus software, https://software.broadinstitute.org/morpheus (Broad Institute). Gene set enrichment (GSEA) pre-ranked analysis (1000 permutations, minimum term size of 15, maximum term size of 500) was performed using the GSEA software (Broad Institute). Gene sets were ranked by taking the -log10 transform of the p-value and signed as positive or negative based on the direction of fold change. Annotated gene sets from Molecular Signatures Database (MSigDB) were used as input (16).

Cytokine measurement

The levels of cytokines were measured using the LEGENDplex™ Multi-Analyte Flow Assay Kit (Biolegend) in a CyFlow Cube 8 flow cytometer (Sysmex Partec, Germany), according to the manufacturer's instructions. For comparisons between the groups the Wilcoxon signed-rank test for paired samples was used. Statistical analysis was performed using GraphPad Prism (version 9.0, GraphPad Inc., La Jolla, CA). Significance was set at $p < 0.05$.

Results

Analysis of the molecular signature of human macrophages infected *in vitro* with *Brucella* spp.

To provide a time-course analysis of the molecular alterations of human Mφ during infection with *Brucella* spp., we performed *in vitro* infection of human Mφ, derived from the differentiation of peripheral blood monocytes from control subjects, and compared the transcriptomic signature of untreated Mφ compared to that of infected cells at 2h and 24h post-infection. Principal component analysis (PCA) revealed that there was a prominent change in the transcriptomic profile of Mφ at 24h after infection compared to untreated cells and cells at 2h after infection (Figure 1A). Pathway analysis, using the Kyoto Encyclopedia of Genes and Genomes (KEGG) database, of the significantly upregulated differentially expressed genes (DEG) (False Discovery Rate/FDR <0.01) between untreated Mφ and Mφ at 2h post-infection revealed an overrepresentation of circadian rhythm and ribosome biogenesis pathways, whereas downregulated DEGs were enriched in pathways associated with viral infection and infection from intracellular pathogens processes, including herpes simplex virus 1 infection, hepatitis C, and *Salmonella* infection and TNF signaling (Figures 1B, C). Interestingly, we observed a decreased expression of genes encoding proteins critical in pathogen recognition, such as *NOD1, TLR5, TLR6* and *NLRC4* (Figure 1C).

We next assessed the molecular changes that take place at 24h post-infection. Pathway analysis of the downregulated DEGs with the highest variance (log2 fold change > 2 and < -2, FDR<0.01) showed overrepresentation of pathways associated with infection with *S. aureus* and infection with intracellular pathogens, such as leishmaniasis and tuberculosis, as well as the pathways associated with phagosome and lysosome

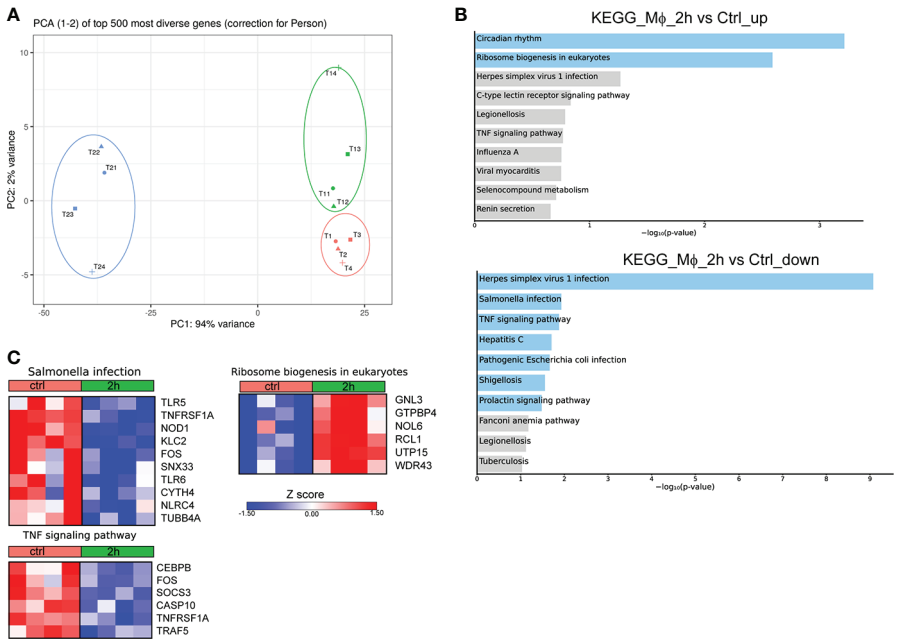

FIGURE 1
Alterations in the transcriptomic profile of human Mφ infected *in vitro* for 2h with *Brucella* spp.**(A)** Principal component analysis (PCA) of the transcriptome of all 12 Mφ samples. T1-T4 represent untreated control Mφ, T11-T14 represent samples from Mφ at 2h post-infection and T21-T24 represent samples at the 24h time point. **(B)** Pathway analysis of the DEGs at 2h post-infection compared to control, using the KEGG database as reference. Light blue color represents statistical significance **(C)** Heatmaps depicting the DEGs of the respective pathways.

(Figure 2A). No statistically significant pathway was observed in the respective analysis of upregulated genes. Further, analysis of the DEGs that were downregulated at 24h after infection revealed that they are involved in biological processes associated with inflammation, and more specifically with the production of IL-1 and Mφ function (Figure 2B). Regarding the genes involved in the aforementioned pathways, there was a downregulation of several genes involved in the phagosome formation and function at 24h after infection, including those encoding for several Fcγ receptors (*FCGR1A, FCGR2A, FCGR2B, FCGR2C, FCGR3A, FCGR3B*), toll-like receptors (*TLR2, TLR4, TLR6*), other sensors of pathogen-associated molecular patterns (*CLEC7A, CD14*), integrins and other receptors involved in phagocytosis (*ITGB3, ITGAM, ITGB2, CD36*) (Figure 2C). We also observed a downregulation in the expression of genes encoding cytokines and cytokine receptors of the IL-1 family (*IL18*, *IL1RN, IL36RN*), chemokines (*CCL1, CCL2, CCL7, CCL8, CCL13, CXCL9*) and chemokine receptors (*CCR1, CCR2, CCR3, CCR5*), formyl peptide receptors (*FPR1, FPR2, FPR3*), and complement anaphylatoxin receptors (*C3AR1, C5AR1, C5AR2*) (Figure 2C). Regarding the regulation of IL-1 production, we observed the downregulation of several genes encoding inflammasome sensors (*NLRC4*, *NLRP12*, *MEFV*, *AIM2)*, the adaptor *PYCARD*, and the gene that encodes the effector *CASP1* (Figure 2C). Taken together, infection of Mφ with *Brucella* spp. drives major changes in the transcriptomic profile of infected Mφ, downregulating a plethora of genes involved in the formation of phagosomes and the recognition of pathogens, in an effort to preserve pathogen survival within Mφ.

Analysis of the molecular signature of human PMNs infected *in vitro* with *Brucella* spp.

Even though Mφ are the major cell population infected by *Brucella* spp, it has been previously shown that this pathogen can also infect neutrophils (7, 17). To characterize the molecular signature of infected PMNs with *Brucella spp*, we performed *in vitro* infection of human PMNs for 0.5h, derived from control subjects, and compared the transcriptomic signature of untreated PMNs to that of infected cells. Pathway analysis of the significantly overexpressed DEGs (FDR<0.01), using the KEGG database, highlighted Ribosome as the top upregulated pathway in *Brucella*-infected PMNs (Figure 3A). Notably, almost all genes (75 out of the 79) encoding for structural proteins of both small and large subunits of cytoplasmic ribosomes were found significantly upregulated (Figure 3B). Respective analysis of the downregulated DEGs demonstrated modulation of several pathways, some of which were also

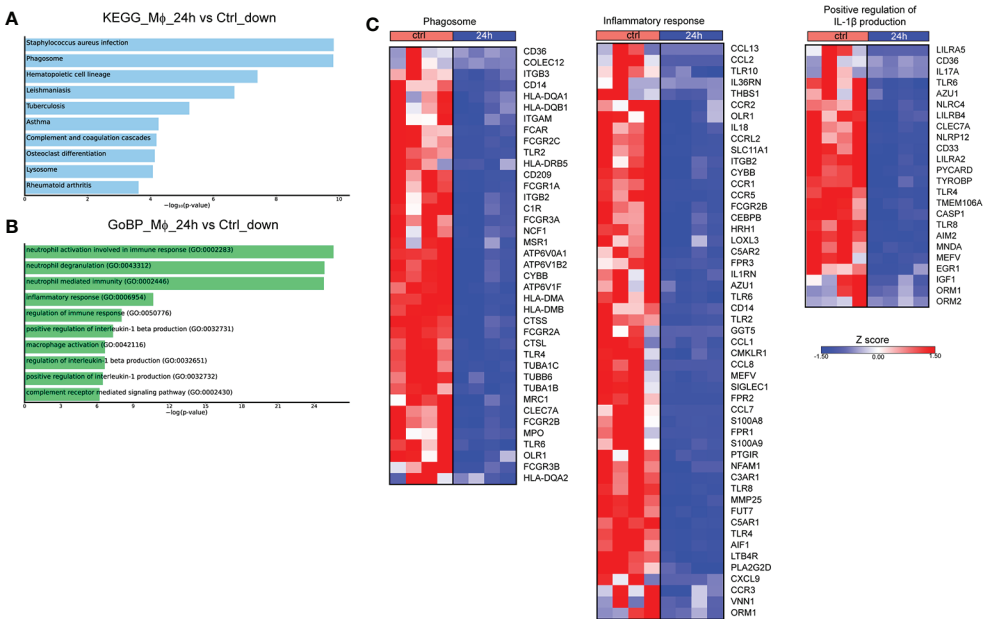

FIGURE 2
Transcriptomic profiling of human Mφ infected *in vitro* with *Brucella spp* at 24h post-infection. **(A)** Pathway analysis of the DEGs with the highest variance at 24h post infection compared to control, using the KEGG database as reference. **(B)** Enriched biological processes in which the downregulated genes are involved. **(C)** Heatmaps depicting the DEGs of the phagosome pathway, the inflammatory response and positive regulation of IL-1β production biological processes.

downregulated in *Brucella*-infected Mφ at 2h post-infection, such as TNF signaling and herpes simplex virus 1 infection (Figures 1B, 3C). However, various inflammation-related biological processes were significantly downregulated selectively in PMNs, namely the phosphatidylinositol signaling, NF-kappa B signaling, and cellular senescence pathways (Figure 3C). Amongst the downregulated transcripts in *Brucella*-infected PMNs, we identified several modulators of apoptosis (*BIRC3, FOXO3, DNM1L, ITPR1, TRAF1, TRAF5*) and inflammation, as exemplified by decreased mRNA expression of cytokines and corresponding receptors of the IL-1 family (*IL1A*, *IL1B, IL18R1*), chemokines (eg. *CCL20*), and various signaling mediators, such as kinases (*AKT3, ATM, ATR, CDK6, DGKD, DGKE, IPMK, IPPK, MAPK13, MAPK14, RPK1*) (Figure 3C).

Transcriptomic profiling of active human brucellosis

We further investigated the transcriptomic signature of active human brucellosis. To do so, PMNs were isolated from eight patients with active brucellosis before the initiation of antibiotic treatment (active disease) and three months after completion of the antibiotic treatment, when patients were free of symptoms (remission). Transcriptomic analysis identified 318 DEGs (FDR<0.1). DEGs that were upregulated after treatment are involved in RNA transport and autophagy pathways, whereas downregulated DEGs after treatment are involved in NOD-like receptor signaling pathway and cytokine-cytokine receptor interaction pathways, as well as several pathways associated with infectious diseases (Figure 4A). The upregulated genes that encode proteins involved in RNA transport were the members of the eukaryotic initiator factors (EIF) family *EIF1, EIF3I, EIF4A3, EIF5*, and the genes of the autophagy pathway were *ATG2A, GABARAPL1, TP53INP2, DDIT4* and *IRS2* (Figure 4B). On the other hand, we observed a downregulation of critical genes in immune regulation, such as *IL1B, CX3CR1, CCR2, CCR5, CXCR6, STAT1, AIM2*, and *CD40*, as well as genes associated with interferon signaling, such as *OAS1, OAS2, GBP1* and *GPB3* (Figure 4B). We further performed gene set enrichment analysis (GSEA) using the Hallmark Gene Set collection of the Molecular Signatures Database. We observed a positive correlation of the transcriptomic signature of PMNs during active brucellosis with IFN-γ and IFN-α response and with inflammatory response (Figure 4C). Moreover, comparing the transcriptomic profiling of *ex vivo* PMNs after successful completion of treatment versus that of *in vitro Brucella*-infected PMNs, we found that 188 genes (59% of the *ex vivo* identified DEGS) were commonly regulated in both datasets (Supplementary Figure S2A). Furthermore, the majority of commonly regulated genes (111 out of 188) followed

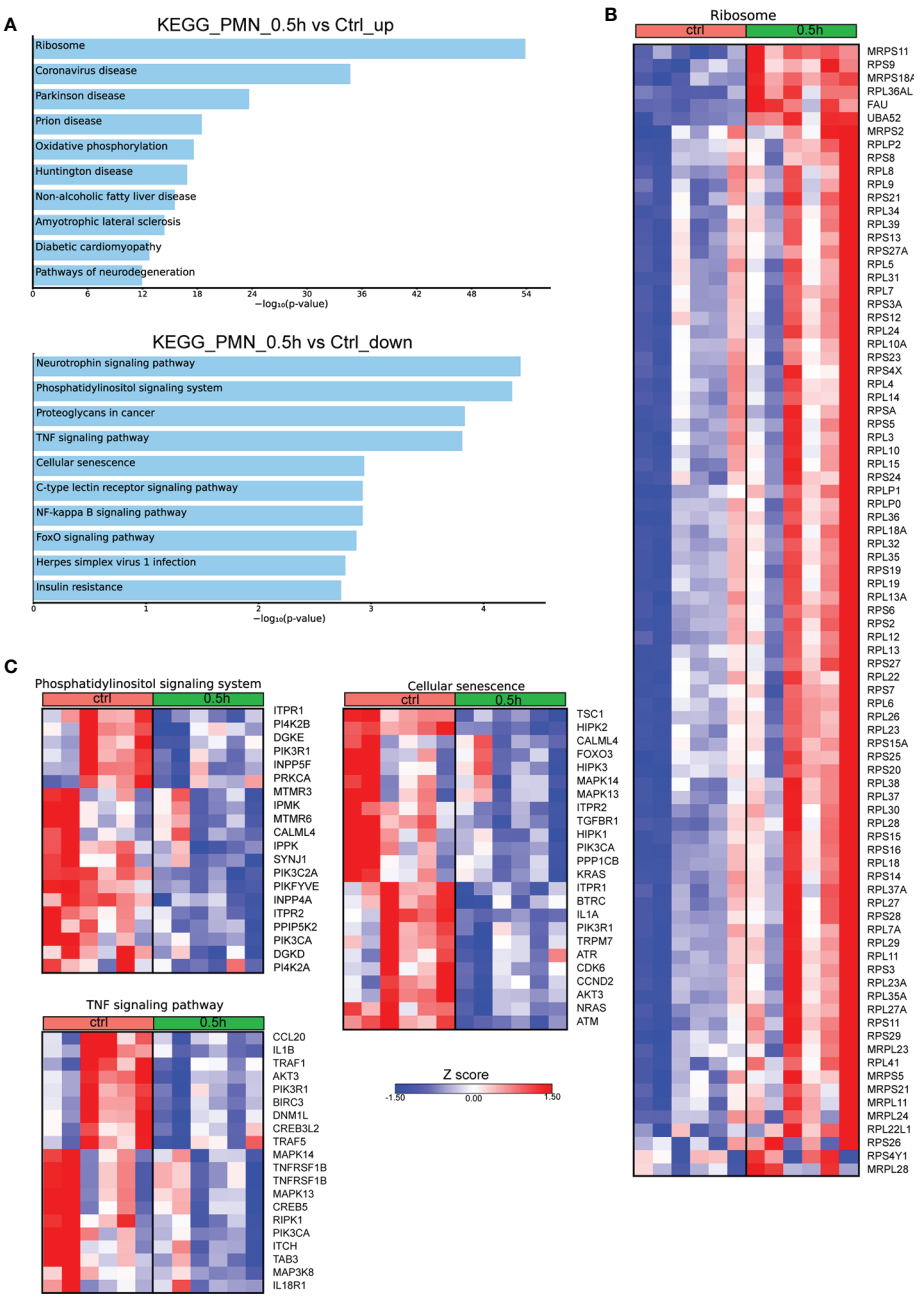

FIGURE 3
Alterations in the transcriptomic profile of human PMNs infected *in vitro* with *Brucella* spp. **(A)** Pathway analysis of the DEGs from PMNs at 0.5h post infection with *Brucella spp* compared to control, using the KEGG database as reference. **(B)** Heatmap depicting the DEGs of the ribosome pathway. **(C)** Heatmaps depicting the DEGs of the pathways enriched for downregulated genes.

a reverse pattern of differential expression (eg. upregulated upon *in vitro Brucella* infection and downregulated *ex vivo*, upon successful completion of treatment, Supplementary Figures S2B, C).

In parallel, we performed transcriptomic analysis of PBMCs isolated from six patients with active brucellosis before and after antibiotic treatment. Transcriptomic analysis identified 62 genes with significantly altered expression (FDR<0.1) after treatment (Figure 5A). We observed that successful treatment resulted in the increased expression of *HIF1A*, a critical regulator of inflammation, and of the genes that encode IL-1 receptor *IL1R1*, and its accessory protein *IL1RAP*, which form a complex that

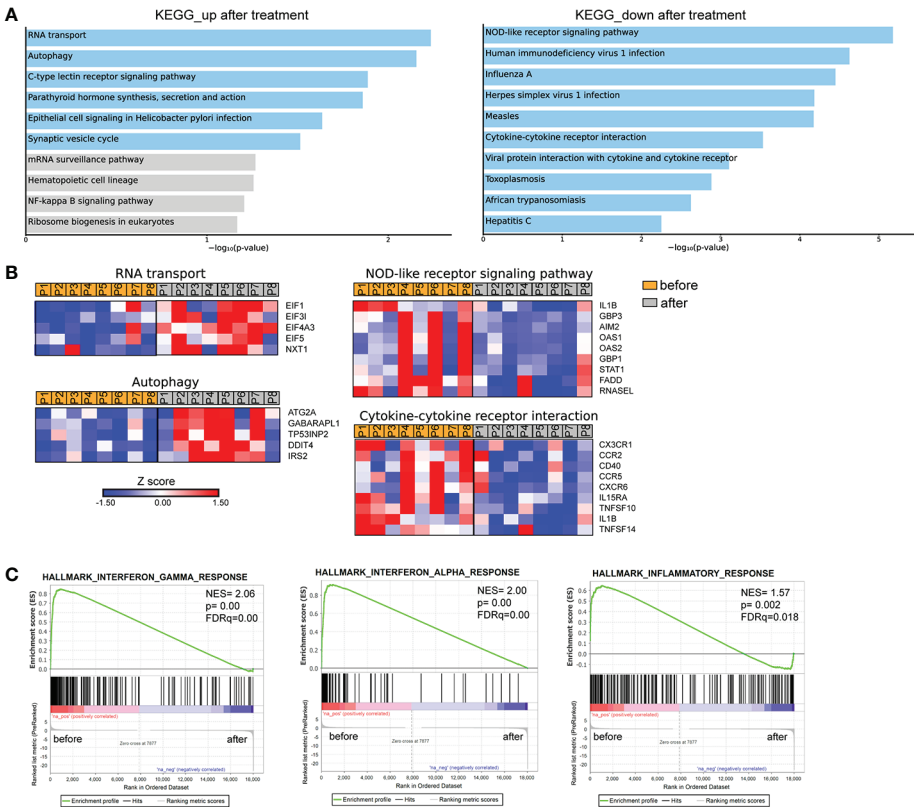

FIGURE 4
Transcriptomic analysis of PMNs from patients with brucellosis before treatment initiation and after successful completion of treatment. **(A)** Pathway analysis of the DEGs from PMNs after treatment compared to PMNs isolated from the same patients (paired-data analysis) during active brucellosis, using the KEGG database as reference. Light blue color represents statistical significance **(B)** Heatmaps depicting the DEGs of the respective pathways. P1-P8 refer to different patients. **(C)** GSEA for genes related to response to interferons, and inflammation.

mediates IL-1 signal transduction (Figure 5A). On the other hand, there was a downregulation in the expression of genes that play a major role in immune function, such as *CD274*, which encodes PD-L1, *STAT1*, *CD3G*, the intracellular immunoglobulin receptor *TRIM21*, *CXCR6*, the lymphocytic activation molecules *SLMF6*, *SLAMF7* and genes that encode proteins important in effector cell cytolytic processes, such as *CD160*, *GZMA*, *GZMH* (Figure 5A). Moreover, several identified genes are involved in interferon-related activation pathways, such as *GPB3*, *GPB4*, *OAS1*, *OAS2*, *OASL*, *IFI16*, and *XAF1* (Figure 5A). In the same line, GSEA analysis revealed that the gene sets with the most significant positive association with active disease were IFN signaling and OXPHOS, whereas the one with the most significant negative association was the hypoxia gene set (Figure 5B). Notably, we further identified 24 genes that were differentially expressed both in PMNs and PBMCs (Figure 5C). Among these common genes, *CXCR6*, *TRIM21*, *SLAM7*, *CD274* and the genes associated with IFN signaling *OASL*, *OAS1*, *OAS2*, *GBP3*, and *STAT1* were downregulated in both datasets, whereas *IL1R1* was commonly upregulated (Figure 5D).

Cytokine levels in acute brucellosis

To this point, we observed that the molecular signature that characterizes acute brucellosis is positively correlated with those of IFN-α and IFN-γ responses. For this reason, we measured the levels of several cytokines in the sera of patients during acute brucellosis and after successful treatment. We observed a significant downregulation in the levels of IFN-γ, IL-1β and IL-6 post-treatment, whereas there was no statistically significant difference in the levels of IFN-α, IL-18, TNF, MCP-1 and IL-17A (Figures 6A–H). We further confirmed that the levels of IFN-γ are increased in active disease in a cohort of patients with chronic relapsing brucellosis. In this cohort, the levels of IFN-γ were increased during relapse compared to remission (Figure 6I).

Discussion

The interaction between *Brucella* and the host immune system is critical for the development of persistent infection or infection

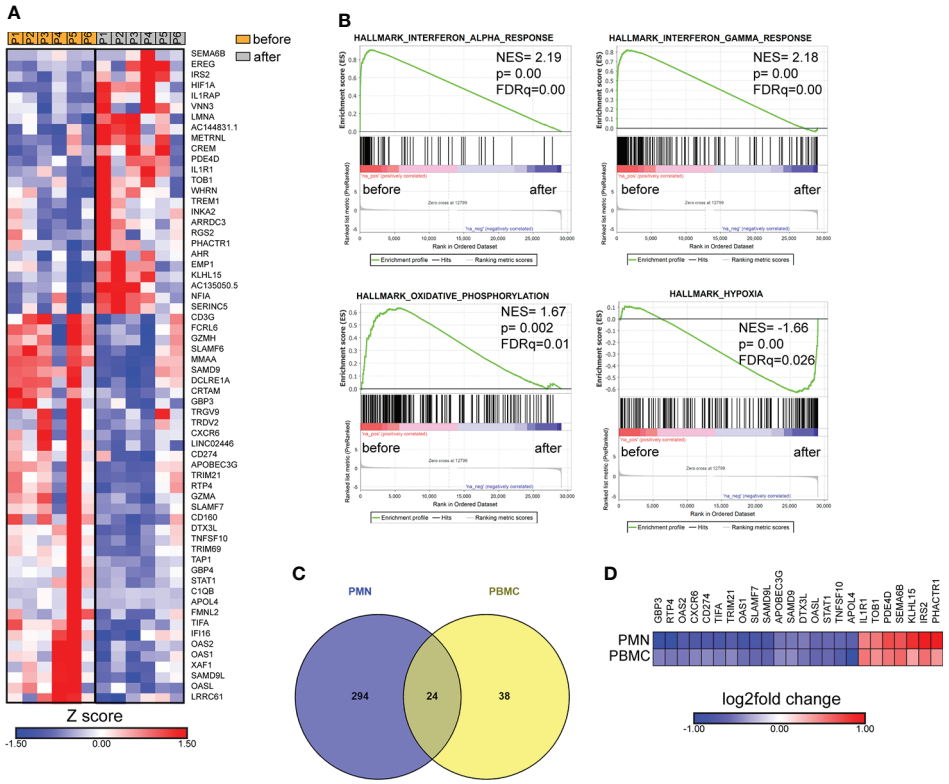

FIGURE 5
Transcriptomic analysis of PBMCs from patients with brucellosis before treatment initiation and after successful completion of treatment. **(A)** Heatmap depicting the DEGs from PBMCs from patients with acute brucellosis before treatment initiation and from the same patients (paired analysis) after successful treatment. P1-P6 refer to different patients. **(B)** GSEA for genes related to response to interferons, oxidative phosphorylation and hypoxia. **(C)** Venn diagram and **(D)** heatmap depicting the common genes that were significantly differentially expressed in PMNs and PBMCs from patients with brucellosis after treatment.

clearance (5, 9). To date, transcriptomic data were derived from *Brucella*-infected mouse macrophages or mouse cell lines, domestic ruminants or *Brucella*-vaccinated animals (18–24). This study analyses, for the first time, the transcriptome profile, both *in vitro*, in *Brucella*-infected primary Mφ and PMNs, and *ex vivo*, in PBMCs and PMNs derived from patients with acute brucellosis before and after treatment. This provides the molecular signature that characterizes the main host cellular immune populations during their initial interplay with invading *Brucella*, and the molecular signature of different stages of the disease.

Macrophages differentiated *in vitro* from purified peripheral blood monocytes are widely used in the literature to simulate human macrophages for *in vitro* studies (11). Different isolation strategies may affect the purity and cell yield of resulting monocytes and/or monocyte-derived macrophages, as well as the monocyte subtype and the polarization status of subsequently differentiated cells. To address the transcriptomic changes that take place during Mφ infection, we engaged cell cultures of monocytes isolated with plastic adhesion, a setup that results in the generation of Mφ with inflammatory characteristics and M1 skewing (11). Although, plastic adhesion is a straightforward, uncomplicated, and low-cost isolation method, it results in lower monocyte yield compared to other immune-based methods (11). Whilst all our samples were handled similarly, we should always take into consideration the described limitations of these *in vitro* systems when forming conclusions.

Early molecular events following phagocytosis of *Brucella* by macrophages are crucial for the activation of innate immunity leading to the induction of a favorable Th1 response (5, 8, 9). Several lines of evidence indicated that *Brucella* manipulates multiple effector mechanisms in macrophages to its benefit (5, 9). In line with this, we identified that in Mφ infected *in vitro* by a clinical strain of *Brucella spp*, the expression of several genes encoding key proteins involved in the recognition of *Brucella* and in the proinflammatory response against the pathogen were markedly suppressed. These alterations may initiate as soon as 2h post-infection being more prominent at 24h post-infection. Interestingly, most downregulated DEGs related to phagosome, TNFα signaling and IL-1β production. Indeed, previous studies reported that various *Brucella* virulence factors and pathogen-associated molecular patterns (PAMPs), such as Type IV

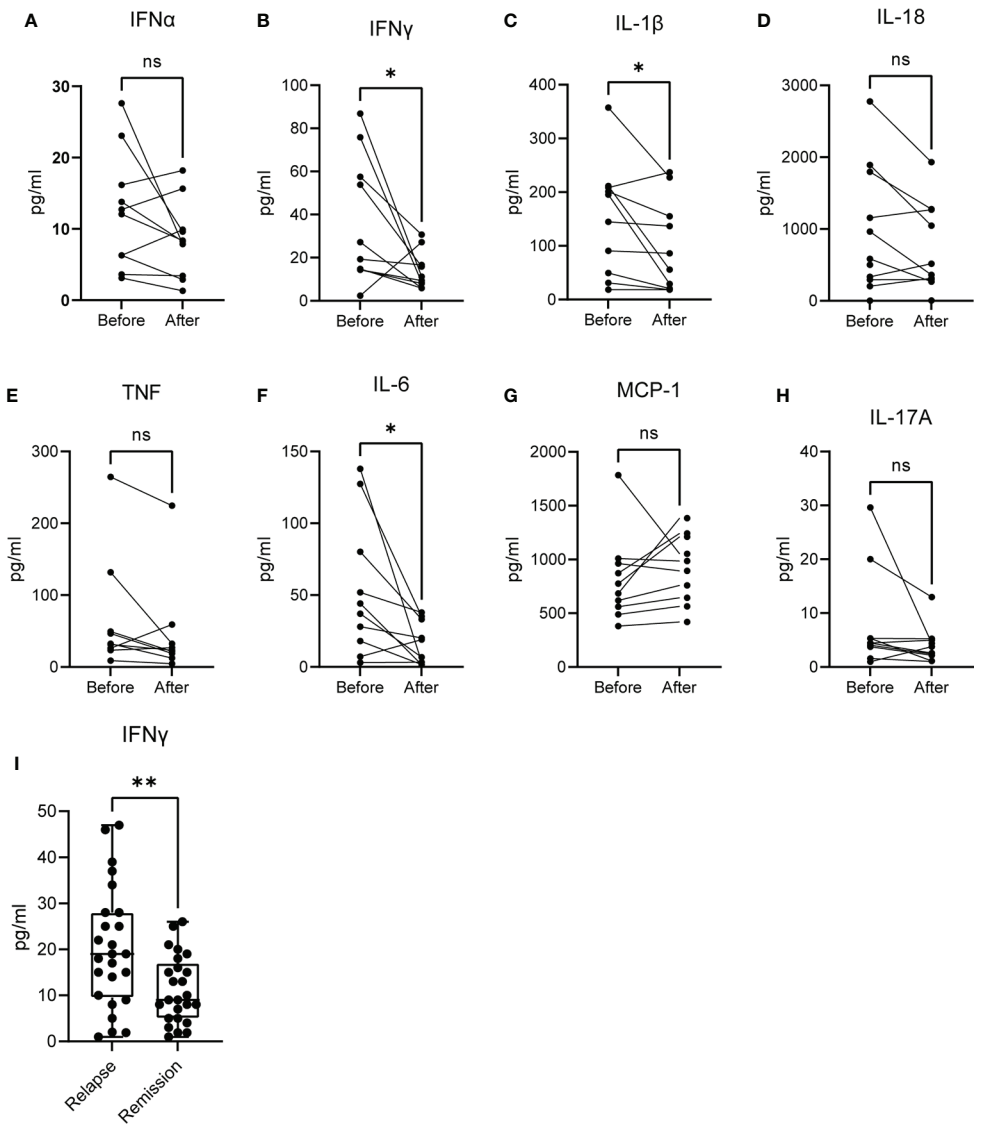

FIGURE 6
Levels of cytokines in the serum of patients with active brucellosis. **(A–H)** Levels of IFN-α, IFN-γ, IL-1β, IL-18, TNF, IL-6, MCP-1 and IL-17A in the serum of patients with acute brucellosis before treatment initiation and after successful treatment. **(I)** Levels of IFN-γ in an independent cohort of patients with chronic relapsing brucellosis during relapse and remission. *p<0.05, **p<0.01. Wilcoxon signed rank test. ns, non significant.

secretory system (T4SS), lipopolysaccharide (LPS) and outer membrane lipoproteins (OMPs) modify phagosome biogenesis and trafficking in macrophages to inhibit phagolysosome fusion, and develop suitable vacuolar compartments to enable intracellular replication of the microbe (5, 9). Moreover, the current study comes in agreement with previous data demonstrated that *Brucella* Omp25 protein inhibits *in vitro* the production of TNF in human Mφ and dendritic cells preventing cell maturation and antigen presentation (25–27). Furthermore, several genes encoding members of the IL-1 family (*IL18*, *IL1RN*, *IL36RN*) and inflammasome complexes (*NLRC4*, *NLRP12*, *MEFV*, *AIM2*, *PYCARD*, *CASP1)* are significantly downregulated in *Brucella*-infected Mφ. Experimental studies indicated that inflammasomes and their effectors are essential for an initial effective immune response against *Brucella* infection (28–30). On the other hand, *Brucella* can regulate canonical and non-canonical inflammasome signaling and pyroptosis in macrophages by impairing caspase-1 and caspase-4/11 activation, and IL-1β secretion (31, 32). It is intriguing that *Brucella* downregulates macrophage *MEFV* expression, the gene responsible for familial Mediterranean fever, the prototype IL-1β-mediated autoinflammatory disease (33). Mutations in the *MEFV* gene are highly prevalent in the Middle East and Mediterranean countries where brucellosis is endemic (33). Our data further support the hypothesis that *MEFV* mutations

may provide an evolutionary selective advantage to confer protection against brucellosis (34).

Recently, PMNs emerge as novel players during the initial stages of innate immune response against *Brucella* infection (7). *Brucella* resists the killing mechanisms of human PMNs and induces the early death of these cells promoting their phagocytosis by Mφ, which become vehicles for bacterial dispersion within the host (35). Studies in murine brucellosis proposed that infected PMNs attenuate cellular adaptive immunity, given that depletion of PMNs favored bacterial elimination (36). Based on these, this study examined the early transcriptome alterations of *in vitro Brucella*-infected neutrophils, before their premature death. *Brucella spp*-infected PMNs were characterized by increased expression of genes associated with ribosome biogenesis, probably in an effort to arm their bactericidal mechanisms and survive. Of interest and in a similar way to Mφ, *in vitro* infection of PMNs with *Brucella* led to downregulated gene expression in key molecular pathways for PMNs physiology and function including phosphatidylinositol signaling, TNF signaling, and cellular senescence. Phosphatidylinositol signaling pathway plays an important role in membrane dynamics and trafficking, including proteins implicated in endosomal membranes and autophagosome assembly and activity (37, 38). Autophagy is closely related to the intracellular lifestyle of many pathogens, including *Brucella* (39). We hypothesize that the downregulation of several autophagy sensors and regulators belonging to phosphatidylinositol pathway further modulates the autophagic capacity of PMNs against *Brucella*. This may also explain the inability of *Brucella*-infected PMNs to form neutrophil extracellular traps (NETs) (17), an effector mechanism positively associated with the autophagy machinery (40). Downregulation of the cellular senescence pathway is in agreement with the reported premature death of *Brucella*-infected PMNs (17). Additionally, senescence has been associated with resistance to cell death (41). Moreover, it appears that perturbation of TNF signaling represents a common stealth strategy of *Brucella* to avoid both Mφ- and PMNs-induced inflammation further restricting cellular immunity (8).

Human brucellosis causes high clinical morbidity and protean clinical manifestations, mimicking many infectious and non-infectious diseases, as any organ can be affected. The definition and diagnosis of different disease types of human brucellosis, such as acute, chronic/relapsing, asymptomatic/subclinical, and cured, continues to be challenging making the therapeutic decision difficult in many cases. This is due to various factors including the non-specific and atypical clinical features, the slow growth rate of *Brucella* in blood cultures and the reduced sensitivity of the method for detecting chronic cases. Furthermore, laboratory diagnosis in people living in endemic regions, high-risk occupational groups and previously infected individuals, as well as cross-reactivity in some serological assays renders challenging the serodiagnosis of brucellosis (3, 4, 10, 12).

To investigate the impact of human brucellosis on host immunity and identify possible candidate markers of active disease and response to treatment, we next assessed the transcriptome profiling of PBMCs and PMNs isolated from newly diagnosed patients with acute brucellosis, before and three months after their successful treatment. We observed, both in PBMCs and PMNs, transcriptomic alterations related to major pathways of inflammation, supporting its role in infection overcome. PBMCs from patients successfully treated were characterized by the overexpression of genes critically involved in hypoxia (*HIF1A*) and IL-1 signaling, and the downregulation of genes implicated in oxidative phosphorylation, lymphocyte activation, and cytotoxicity. In line with these data, a recent experimental study has demonstrated that absence of HIF-1α renders mice susceptible to *Brucella* infection, while HIF-1α reduces oxidative phosphorylation and increases glycolysis leading to inflammasome activation and IL-1β release in infected macrophages (42).

Treatment of brucellosis led to increased expression of several genes related to autophagy machinery in PMNs, including *DDIT4/REDD1* encoding a key regulator of autophagy-mediated NET formation (43). It seems that after clearance of infection, PMNs restored critical functions impaired by *Brucella*, such as autophagy. However, they did not acquire a proinflammatory phenotype as indicated by the downregulated expression in genes related NOD-like receptor signaling and cytokine-cytokine interaction pathways.

Comparison of the transcriptomic profiling of *ex vivo* PMNs after successful completion of treatment versus that of *in vitro Brucella*-infected PMNs, showed a substantial overlap, as 59% of the *ex vivo* identified DEGs were commonly regulated in both datasets. However, data derived from *in vitro* infected cells under "controlled" laboratory conditions cannot simulate completely the complex cellular interactions that occur upon human infection, or the possible differences in the kinetics by which certain processes unfold *in vitro* versus *ex vivo*.

Of note, this study identified a common set of 24 genes that were differentially expressed both in PMNs and PBMCs suggesting candidate molecular diagnostic/prognostic targets for human brucellosis. Among them, type II IFN pathway, which is the major driver of Th1 immunity against *Brucella* (5), appears to be induced in active disease and attenuated after treatment. Indeed, using patients' sera, we confirmed at the protein level, that IFN-γ and other Th1 cytokines, such as IL-1β and IL-6, were increased during active disease and significantly diminished in cured, non-relapsed patients, whereas the levels of IFN-α, which belongs to type I IFN family, did not show significant changes. Collectively, these results confirmed past studies highlighting the significant role of a robust Th1 response to tackle acute infection and brucellosis-acquired cellular anergy of chronic disease (44–46).

In conclusion, this study provides an integrated transcriptome landscape of immune cells signature in human brucellosis suggesting candidate molecular pathways and targets for active disease and response to treatment. Based on these data, future validation and mechanistic studies may further decipher the pathogenesis of this ancient and continuously re-emerging zoonotic disease (1, 2, 47).

Data availability statement

The datasets presented in this study can be found in online repositories. The name of the repository and accession numbers can be found below: NCBI Sequence Read Archive; PRJNA812759 and PRJNA812762.

Ethics statement

The studies involving human participants were reviewed and approved by Local Scientific and Ethics Committee of the University Hospital of Alexandroupolis, Greece (Approval Number #1195/19-12-2017). The patients/participants provided their written informed consent to participate in this study.

Author contributions

IM: Conceptualization, Funding acquisition, Visualization, Writing - original draft, Writing – review and editing. AC: Formal analysis, Investigation, Writing - review and editing. GD: Investigation, Data curation, Formal analysis, Writing - review and editing. CI: Data curation, Investigation. MN: Investigation, Validation. AT: Data curation. TK, CA, NS, SG and MP: Investigation. GL: Methodology, Validation. SM: Validation. ML, AD: Formal analysis. PS: Formal analysis, Methodology. UC: Methodology, Writing - review and editing. BW, KR: Writing - review and editing. PSk: Conceptualization, Funding acquisition, Project administration, Supervision, Writing - original draft, Writing - review and editing. All authors contributed to manuscript revision, read, and approved the submitted version.

Funding

This study was supported by the German Federal Ministry for Education and Research (BMBF) and Greek General Secretariat for Research and Technology (GSRT), Greek-German Bilateral Research & Innovation Programme BRIDGING, grants MIS 5030062, 01EI1703A and 01EI1703B, and by the GSRT, Research & Innovation Programme CYTONET, grant MIS 5048548.

Acknowledgments

We thank Prof. Triantafyllos Chavakis for his support and advice, and Dr. Apostolos Vasileiou for his technical and administrative assistance.

Conflict of interest

Authors NS and GL were employed by the company P. Zafiropoulos S.A.

The remaining authors declare that the research was conducted in the absence of any commercial or financial relationships that could be construed as a potential conflict of interest.

Publisher's note

All claims expressed in this article are solely those of the authors and do not necessarily represent those of their affiliated organizations, or those of the publisher, the editors and the reviewers. Any product that may be evaluated in this article, or claim that may be made by its manufacturer, is not guaranteed or endorsed by the publisher.

Supplementary material

The Supplementary Material for this article can be found online at: https://www.frontiersin.org/articles/10.3389/fimmu.2022.951232/full#supplementary-material

References

1. Dean AS, Crump L, Greter H, Schelling E, Zinsstag J. Global burden of human brucellosis: a systematic review of disease frequency. *PLoS Negl Trop Dis* (2012) 6:e1865. doi: 10.1371/journal.pntd.0001865

2. European Food Safety Authority and European Centre for Disease Prevention and Control (EFSA and ECDC). The European union summary report on trends and sources of zoonoses, zoonotic agents and food-borne outbreaks in 2017. *EFSA J* (2018) 16:e05500. doi: 10.2903/j.efsa.2018.5500

3. Franc KA, Krecek RC, Häsler BN, Arenas-Gamboa AM. Brucellosis remains a neglected disease in the developing world: a call for interdisciplinary action. *BMC Public Health* (2018) 18:125. doi: 10.1186/s12889-017-5016-y

4. Pappas G, Akritidis N, Bosilkovski M, Tsianos E. Brucellosis. *N Engl J Med* (2005) 352:2325–36. doi: 10.1056/NEJMra050570

5. Skendros P, Boura P. Immunity to brucellosis. *Rev Sci Tech* (2013) 32:137–47. doi: 10.20506/rst.32.1.2190

6. Garry Adams L J, Schutta C. Natural resistance against brucellosis: A review. *Open Vet Sci J* (2010) 4, 61–71. doi: 10.2174/1874318801004010061

7. Moreno E, Barquero-Calvo E. The role of neutrophils in brucellosis. *Microbiol Mol Biol Rev* (2020) 84:e00048–20. doi: 10.1128/MMBR.00048-20

8. Martirosyan A, Moreno E, Gorvel J-P. An evolutionary strategy for a stealthy intracellular brucella pathogen. *Immunol Rev* (2011) 240:211–34. doi: 10.1111/j.1600-065X.2010.00982.x

9. Jiao H, Zhou Z, Li B, Xiao Y, Li M, Zeng H, et al. The mechanism of facultative intracellular parasitism of brucella. *Int J Mol Sci* (2021) 22:3673. doi: 10.3390/ijms22073673

10. *Clinicians | brucellosis | CDC* (2021). Available at: https://www.cdc.gov/brucellosis/clinicians/index.html (Accessed July 5, 2022).

11. Nielsen MC, Andersen MN, Møller HJ. Monocyte isolation techniques significantly impact the phenotype of both isolated monocytes and derived

macrophages *in vitro*. *Immunology* (2020) 159:63–74. doi: 10.1111/imm.13125

12. Laboratory response network (LRN) sentinel level clinical laboratory protocols, in: *ASM.org* . Available at: https://asm.org/Articles/CPHMC/Laboratory-Response-Network-LRN-Sentinel-Level-C (Accessed July 7, 2022).

13. Yagupsky P, Morata P, Colmenero JD. Laboratory diagnosis of human brucellosis. *Clin Microbiol Rev* (2019) 33:e00073–19. doi: 10.1128/CMR.00073-19

14. Mitroulis I, Ruppova K, Wang B, Chen L-S, Grzybek M, Grinenko T, et al. Modulation of myelopoiesis progenitors is an integral component of trained immunity. *Cell* (2018) 172:147–61.e12. doi: 10.1016/j.cell.2017.11.034

15. Afgan E, Baker D, Batut B, van den Beek M, Bouvier D, Cech M, et al. The galaxy platform for accessible, reproducible and collaborative biomedical analyses: 2018 update. *Nucleic Acids Res* (2018) 46:W537–44. doi: 10.1093/nar/gky379

16. Lamprianidou E, Kordella C, Kazachenka A, Zoulia E, Bernard E, Filia A, et al. Modulation of IL-6/STAT3 signaling axis in CD4+FOXP3- T cells represents a potential antitumor mechanism of azacitidine. *Blood Adv* (2021) 5:129–42. doi: 10.1182/bloodadvances.2020002351

17. Barquero-Calvo E, Mora-Cartín R, Arce-Gorvel V, de Diego JL, Chacón-Díaz C, Chaves-Olarte E, et al. Brucella abortus induces the premature death of human neutrophils through the action of its lipopolysaccharide. *PLoS Pathog* (2015) 11:e1004853. doi: 10.1371/journal.ppat.1004853

18. Zhou Z, Gu G, Luo Y, Li W, Li B, Zhao Y, et al. Immunological pathways of macrophage response to brucella ovis infection. *Innate Immun* (2020) 26:635–48. doi: 10.1177/1753425920958179

19. Zhou D, Zhi F, Fang J, Zheng W, Li J, Zhang G, et al. RNA-Seq analysis reveals the role of Omp16 in brucella-infected RAW264.7 cells. *Front Vet Sci* (2021) 8:646839. doi: 10.3389/fvets.2021.646839

20. Solanki KS, Gandham RK, Thomas P, Chaudhuri P. Transcriptome analysis of brucella abortus S19Δper immunized mouse spleen revealed activation of MHC-I and MHC-II pathways. *Access Microbiol* (2020) 2:acmi000082. doi: 10.1099/acmi.0.000082

21. Hop HT, Arayan LT, Reyes AWB, Huy TXN, Min W, Lee HJ, et al. Simultaneous RNA-seq based transcriptional profiling of intracellular brucella abortus and b. abortus-infected murine macrophages. *Microb Pathog* (2017) 113:57–67. doi: 10.1016/j.micpath.2017.10.029

22. Liu Q, Han W, Sun C, Zhou L, Ma L, Lei L, et al. Deep sequencing-based expression transcriptional profiling changes during brucella infection. *Microb Pathog* (2012) 52:267–77. doi: 10.1016/j.micpath.2012.02.001

23. Rossetti CA, Galindo CL, Everts RE, Lewin HA, Garner HR, Adams LG. Comparative analysis of the early transcriptome of brucella abortus–infected monocyte-derived macrophages from cattle naturally resistant or susceptible to brucellosis. *Res Vet Sci* (2011) 91:40–51. doi: 10.1016/j.rvsc.2010.09.002

24. Wang F, Hu S, Liu W, Qiao Z, Gao Y, Bu Z. Deep-sequencing analysis of the mouse transcriptome response to infection with brucella melitensis strains of differing virulence. *PLoS One* (2011) 6:e28485. doi: 10.1371/journal.pone.0028485

25. Jubier-Maurin V, Boigegrain RA, Cloeckaert A, Gross A, Alvarez-Martinez MT, Terraza A, et al. Major outer membrane protein Omp25 of brucella suis is involved in inhibition of tumor necrosis factor alpha production during infection of human macrophages. *Infect Immun* (2001) 69:4823–30. doi: 10.1128/IAI.69.8.4823-4830.2001

26. Caron E, Gross A, Liautard JP, Dornand J. Brucella species release a specific, protease-sensitive, inhibitor of TNF-alpha expression, active on human macrophage-like cells. *J Immunol* (1996) 156:2885–93.

27. Billard E, Dornand J, Gross A. Brucella suis prevents human dendritic cell maturation and antigen presentation through regulation of tumor necrosis factor alpha secretion. *Infect Immun* (2007) 75:4980–9. doi: 10.1128/IAI.00637-07

28. Costa Franco MMS, Marim FM, Alves-Silva J, Cerqueira D, Rungue M, Tavares IP, et al. AIM2 senses brucella abortus DNA in dendritic cells to induce IL-1β secretion, pyroptosis and resistance to bacterial infection in mice. *Microbes Infect* (2019) 21:85–93. doi: 10.1016/j.micinf.2018.09.001

29. Lacey CA, Mitchell WJ, Dadelahi AS, Skyberg JA. Caspase-1 and caspase-11 mediate pyroptosis, inflammation, and control of brucella joint infection. *Infect Immun* (2018) 86:e00361–18. doi: 10.1128/IAI.00361-18

30. Gomes MTR, Campos PC, Oliveira FS, Corsetti PP, Bortoluci KR, Cunha LD, et al. Critical role of ASC inflammasomes and bacterial type IV secretion system in caspase-1 activation and host innate resistance to brucella abortus infection. *J Immunol* (2013) 190:3629–38. doi: 10.4049/jimmunol.1202817

31. Jakka P, Namani S, Murugan S, Rai N, Radhakrishnan G. The brucella effector protein TcpB induces degradation of inflammatory caspases and thereby subverts non-canonical inflammasome activation in macrophages. *J Biol Chem* (2017) 292:20613–27. doi: 10.1074/jbc.M117.815878

32. Campos PC, Gomes MTR, Marinho FAV, Guimarães ES, de Moura Lodi Cruz MGF, Oliveira SC. Brucella abortus nitric oxide metabolite regulates inflammasome activation and IL-1β secretion in murine macrophages. *Eur J Immunol* (2019) 49:1023–37. doi: 10.1002/eji.201848016

33. Özen S. Update on the epidemiology and disease outcome of familial Mediterranean fever. *Best Pract Res Clin Rheumatol* (2018) 32:254–60. doi: 10.1016/j.berh.2018.09.003

34. Ross JJ. Goats, germs, and fever: Are the pyrin mutations responsible for familial Mediterranean fever protective against brucellosis? *Med Hypotheses* (2007) 68:499–501. doi: 10.1016/j.mehy.2006.07.027

35. Gutiérrez-Jiménez C, Mora-Cartín R, Altamirano-Silva P, Chacón-Díaz C, Chaves-Olarte E, Moreno E, et al. Neutrophils as Trojan horse vehicles for brucella abortus macrophage infection. *Front Immunol* (2019) 10:1012. doi: 10.3389/fimmu.2019.01012

36. Mora-Cartín R, Gutiérrez-Jiménez C, Alfaro-Alarcón A, Chaves-Olarte E, Chacón-Díaz C, Barquero-Calvo E, et al. Neutrophils dampen adaptive immunity in brucellosis. *Infect Immun* (2019) 87:e00118–19. doi: 10.1128/IAI.00118-19

37. Baba T, Balla T. Emerging roles of phosphatidylinositol 4-phosphate and phosphatidylinositol 4,5-bisphosphate as regulators of multiple steps in autophagy. *J Biochem* (2020) 168:329–36. doi: 10.1093/jb/mvaa089

38. Claude-Taupin A, Morel E. Phosphoinositides: Functions in autophagy-related stress responses. *Biochim Biophys Acta Mol Cell Biol Lipids* (2021) 1866:158903. doi: 10.1016/j.bbalip.2021.158903

39. Starr T, Child R, Wehrly TD, Hansen B, Hwang S, López-Otin C, et al. Selective subversion of autophagy complexes facilitates completion of the brucella intracellular cycle. *Cell Host Microbe* (2012) 11:33–45. doi: 10.1016/j.chom.2011.12.002

40. Skendros P, Mitroulis I, Ritis K. Autophagy in neutrophils: From granulopoiesis to neutrophil extracellular traps. *Front Cell Dev Biol* (2018) 6:109. doi: 10.3389/fcell.2018.00109

41. Sasaki M, Kumazaki T, Takano H, Nishiyama M, Mitsui Y. Senescent cells are resistant to death despite low bcl-2 level. *Mech Ageing Dev* (2001) 122:1695–706. doi: 10.1016/s0047-6374(01)00281-0

42. Gomes MTR, Guimarães ES, Marinho FV, Macedo I, Aguiar ERGR, Barber GN, et al. STING regulates metabolic reprogramming in macrophages *via* HIF-1α during brucella infection. *PLoS Pathog* (2021) 17:e1009597. doi: 10.1371/journal.ppat.1009597

43. Skendros P, Chrysanthopoulou A, Rousset F, Kambas K, Arampatzioglou A, Mitsios A, et al. Regulated in development and DNA damage responses 1 (REDD1) links stress with IL-1β–mediated familial Mediterranean fever attack through autophagy-driven neutrophil extracellular traps. *J Allergy Clin Immunol* (2017) 140:1378–87.e13. doi: 10.1016/j.jaci.2017.02.021

44. Skendros P, Sarantopoulos A, Tselios K, Boura P. Chronic brucellosis patients retain low frequency of CD4+ T-lymphocytes expressing CD25 and CD28 after escherichia coli LPS stimulation of PHA-cultured PBMCs. *Clin Dev Immunol* (2008) 2008:327346. doi: 10.1155/2008/327346

45. Giambartolomei GH, Delpino MV, Cahanovich ME, Wallach JC, Baldi PC, Velikovsky CA, et al. Diminished production of T helper 1 cytokines correlates with T cell unresponsiveness to brucella cytoplasmic proteins in chronic human brucellosis. *J Infect Dis* (2002) 186:252–9. doi: 10.1086/341449

46. Rafiei A, Ardestani SK, Kariminia A, Keyhani A, Mohraz M, Amirkhani A. Dominant Th1 cytokine production in early onset of human brucellosis followed by switching towards Th2 along prolongation of disease. *J Infect* (2006) 53:315–24. doi: 10.1016/j.jinf.2005.11.024

47. Godfroid J, Cloeckaert A, Liautard J-P, Kohler S, Fretin D, Walravens K, et al. From the discovery of the Malta fever's agent to the discovery of a marine mammal reservoir, brucellosis has continuously been a re-emerging zoonosis. *Vet Res* (2005) 36:313–26. doi: 10.1051/vetres:2005003

COPYRIGHT

© 2022 Mitroulis, Chrysanthopoulou, Divolis, Ioannidis, Ntinopoulou, Tasis, Konstantinidis, Antoniadou, Soteriou, Lallas, Mitka, Lesche, Dahl, Gembardt, Panopoulou, Sideras, Wielockx, Coskun, Ritis and Skendros. This is an open-access article distributed under the terms of the Creative Commons Attribution License (CC BY). The use, distribution or reproduction in other forums is permitted, provided the original author(s) and the copyright owner(s) are credited and that the original publication in this journal is cited, in accordance with accepted academic practice. No use, distribution or reproduction is permitted which does not comply with these terms.

frontiers | Frontiers in Immunology

TYPE Review
PUBLISHED 23 August 2022
DOI 10.3389/fimmu.2022.953354

Check for updates

OPEN ACCESS

EDITED BY
Maria Kaparakis-Liaskos,
La Trobe University, Australia

REVIEWED BY
Razvan-Cosmin Petca,
Carol Davila University of Medicine and Pharmacy, Romania
Wondwossen Amogne Degu,
Addis Ababa University, Ethiopia

*CORRESPONDENCE
Xiang Xie
xiangxie@swmu.edu.cn
Huan Chen
huanchen@swmu.edu.cn

†These authors have contributed equally to this work

SPECIALTY SECTION
This article was submitted to Microbial Immunology, a section of the journal Frontiers in Immunology

RECEIVED 26 May 2022
ACCEPTED 05 August 2022
PUBLISHED 23 August 2022

CITATION
Li L, Li Y, Yang J, Xie X and Chen H (2022) The immune responses to different *Uropathogens* call individual interventions for bladder infection. *Front. Immunol.* 13:953354. doi: 10.3389/fimmu.2022.953354

COPYRIGHT
© 2022 Li, Li, Yang, Xie and Chen. This is an open-access article distributed under the terms of the Creative Commons Attribution License (CC BY). The use, distribution or reproduction in other forums is permitted, provided the original author(s) and the copyright owner(s) are credited and that the original publication in this journal is cited, in accordance with accepted academic practice. No use, distribution or reproduction is permitted which does not comply with these terms.

The immune responses to different *Uropathogens* call individual interventions for bladder infection

Linlong Li[1†], Yangyang Li[1†], Jiali Yang[1], Xiang Xie[1,2*] and Huan Chen[1,3*]

[1]The School of Basic Medical Sciences, Southwest Medical University, Luzhou, China, [2]Public Center of Experimental Technology, Model Animal and Human Disease Research of Luzhou Key Laboratory, Southwest Medical University, Luzhou, China, [3]Nucleic Acid Medicine of Luzhou Key Laboratory, Southwest Medical University, Luzhou, China

Urinary tract infection (UTI) caused by uropathogens is the most common infectious disease and significantly affects all aspects of the quality of life of the patients. However, uropathogens are increasingly becoming antibiotic-resistant, which threatens the only effective treatment option available-antibiotic, resulting in higher medical costs, prolonged hospital stays, and increased mortality. Currently, people are turning their attention to the immune responses, hoping to find effective immunotherapeutic interventions which can be alternatives to the overuse of antibiotic drugs. Bladder infections are caused by the main nine uropathogens and the bladder executes different immune responses depending on the type of uropathogens. It is essential to understand the immune responses to diverse uropathogens in bladder infection for guiding the design and development of immunotherapeutic interventions. This review firstly sorts out and comparatively analyzes the immune responses to the main nine uropathogens in bladder infection, and summarizes their similarities and differences. Based on these immune responses, we innovatively propose that different microbial bladder infections should adopt corresponding immunomodulatory interventions, and the same immunomodulatory intervention can also be applied to diverse microbial infections if they share the same effective therapeutic targets.

KEYWORDS

bladder infection, uropathogens, immune responses, individual intervention, uropathogen escherichia coli

Introduction

Urinary tract infection (UTI) is the most common infectious disease of the urinary system caused by diverse uropathogens, affecting females and males of all ages (1). In 2019, the overall global incident cases of UTI were 4046.12×10^5, with 871.90×10^5 for males and 3174.22×10^5 for females (2). Notably, the incident cases of UTI increased by 60.40% in the past thirty decades. UTI results in dysuria, frequency, urgency, suprapubic pain, hematuria, and serious sequelae including frequent recurrences, pyelonephritis with sepsis, renal damage, and preterm birth and significantly affects all aspects of the quality of life of the patients (3, 4). In addition, UTI ranges in severity from mild self-limitation to severe sepsis, with 20-40% mortality (2). UTI has been causing a huge burden on human health, medical resources, and financial expenditure (2). In the United States alone, UTI results in >10 million outpatient visits and $3.5 billion in societal costs per year (2, 5).

UTI is caused by main nine pathogens, epidemiologically covering almost 100% of UTI confirmed cases (1). These pathogens include *uropathogen escherichia coli* (UPEC), *Klebsiella pneumoniae* (*K. pneumoniae*), *Staphylococcus saprophyticus* (*S. saprophyticus*), *Enterococcus faecalis* (*E. faecalis*), *Group B Streptococcus* (GBS), *Proteus mirabilis* (*P. mirabilis*), *Pseudomonas aeruginosa* (*P. aeruginosa*), *Staphylococcus aureus* (*S. aureus*), and *Candida* spp. (*Candida.*) (1). Antibiotics are the first-line treatment options for UTI but the effectiveness is being increasingly limited due to the rise of bacterial resistance (6, 7) (Table 1). More than 80% resistance of *Escherichia coli* (*E. coli*) isolated from UTI to amoxicillin-clavulanic acid, ciprofloxacin, and trimethoprim-sulfamethoxazole has been observed in developing countries (39). In developed countries such as the United States, the resistance of Enterobacteria to some antibiotics for UTI has exceeded 30% (39, 40). Both the World Health Organization (WHO) and the Infectious Disease Society of America (IDSA) claimed the lack of antibiotics for the main pathogens of UTI and urged countries around the world to develop new drugs and therapies that can replace the overuse of antibiotics (41, 42). Thus, people move their sights on the immune responses hoping to find some effective therapeutic targets to combat the infection (4, 43–45).

The bladder possesses a wide range of immune responses against diverse uropathogens, including inhibitors of adhesion and antimicrobial protein production (4, 43–45). The bladder immune responses to invading uropathogens have some in common but also show differences depending on the type of uropathogens. For example, both UPEC and GBS stimulate bladder epithelial cells (BECs) to produce the antimicrobial peptide LL-37, and it is surprising that LL-37 has antibacterial effects on UPEC, but promotes GBS infection in the bladder (46–48). As such, individual immunomodulatory intervention options for UTI should be taken based on immune responses to the specific uropathogen in the bladder. Improved understanding of the bladder immune responses to diverse uropathogens is crucial for our ability to design immunomodulatory interventions and target them properly.

In this Review, we comparatively analyzed the similar and different immune responses triggered by the main nine uropathogens in the bladder. Based on the immune responses, we discussed the immune therapeutic targets with great prospects in-depth and innovatively proposed that when the bladder infection is treated through the modulation of immune responses, different uropathogens should adopt corresponding modulation options to improve the therapeutic effects.

The bladder immune responses to the main nine uropathogens

Since the differences in virulence factors of the nine uropathogens (Table 1), the immune responses against the nine uropathogens are diverse in the bladder. In this section, we summarize the characteristics and research status of immune responses to the major nine uropathogens in bladder infection.

UPEC

UPEC is the most common uropathogen of bladder infection (49). When UPEC ascends to the bladder along the urinary tract, it adheres to the mannose receptors of BECs through type I fimbriae (50). Tamm-Horsfall glycoprotein (THP), the most abundant urine protein, plays a key role to prevent the adhesion of UPEC to the BECs (51, 52). THP has a high-mannose structure among its disaccharides, which binds to the type I fimbriae and competes with the mannose receptors of BECs, thereby reducing the adhesion and colonization of UPEC to the bladder, and leading to the elimination of UPEC through urination (53, 54). In addition, the THP can prevent excessive inflammation in bladder infection *via* inhibition of the chemotaxis and reactive oxygen species (ROS) production by binding to sialic acid-binding Ig-like lectin-9 (Siglec-9) receptor of the neutrophils (55). Once UPEC successfully adheres to BECs, extracellular immune responses will be activated by lipopolysaccharide (LPS) and type I fimbriae of UPEC *via* binding to toll-like receptor 4 (TLR4) on BECs (56). The activation of TLR4 stimulates BECs to secrete stromal-cell derived factor 1 (SDF-1), and interleukin- 6 (IL-6) (57, 58). SDF-1 can bind to the CXC-motif chemokine receptor 4 (CXCR4) on neutrophils and recruit them to accumulate to the infection site (57). The aggregated neutrophils have the ability to engulf UPEC and can be significantly enhanced by BECs-secreted pentraxins (PTX3) (59). Cytokine IL-6 upon activation of TLR4 promotes the expression of C-X3-C motif chemokine 1 (CX3CL1) and recruits macrophages to the

TABLE 1 Drug resistance and virulence factors of the main nine uropathogens.

	Drug resistance	Main virulence factors					Refs
		Adherence	Toxin	Immune evasion	Iron acquisition	Others	
UPEC	Penicillin, tetracycline, vancomycin resistance is 100%, ampicillin resistance is 90%, and cefazolin, ceftriaxone, cefepime, levofloxacin, and ciprofloxacin resistance reaches 70% in China.	Type 1 pili Type 2 pili P pili Dr adhesion S pili F1C pili	HlyA Cnf1	Capsule	Aerobactin Enterobactin Salmochelin Yersiniabactin	Flagella	(8–10)
K.m	Ampicillin penicillin, tetracycline, vancomycin resistance is close to 100%, nitrofurantoin resistance exceeds 90%, and Cefpidoxime is close to 80% in China.	Type 1 pili Type 3 pili	Lps	Capsule	Aerobactin Enterobactin		(8, 9, 11–13)
S.s	Cefuroxime resistance is 81%, Ceftazidime resistance is 76%, Amoxicillin-Clavulanic Acid, Gentamicin resistance is more than 65% in Nigeria.	Aas adhesin Ssp adhesin SdrI adhesin Uaf adhesin	Aas			Urease	(9, 14–17)
E.f	The resistance to amikacin, gentamicin, cefuroxime, ciprofloxacin, and cotrimoxazole is close to 100% in Poland.	Ebp pili Esp pili Ace adhesin	Protease			SigV	(9, 18–21)
GBS	Tetracycline resistance is over 74%, erythromycin resistance is 63%, and the resistance to clindamycin and fluoroquinolones is over 40% in China.		βH/C	Capsule			(22–24)
P.m	Amoxicillin-clavulanat resistance is 100%, ampicillin and nitrofurantoin resistances are 75% in Nepal.	MR/P pili	HpmA HlyA Pta	Capsule ZapA	Proteobactin Yersiniabactin	Flagella Urease	(25–31)
P.a	Topiperacillin-tazobactam and ceftazidime resistances are 100%, cefepime resistance is 75% in Saudi Arabia.	Extracellular DNA Exopolysaccharides	ExoU ExoT Elastase Phospholipase Rhamnolipids	ExoS	Pyochelin Pyoverdi	QS	(32–35)
Candida.	Posaconazole resistance is 92% in Iran.	Als proteins	Phospholipase B				(36, 37)
S.s	Nitrofurantoin resistance is 100% in Poland.	ClfA and ClfB					(18, 38)

Aas: a hemagglutinin-autolysinadhesin, Als: agglutinin-like sequence, βH/C: β-hemolysin/cytolysin, *Candida.: Candida spp*, ClfA/B: Clumping Factors A and B, Cnf1: cytotoxic necrotizing factor 1, Ebp: endocarditis- and biofilm-associated, *E.f, Enterococcus faecalis*, Esp: enterococcal surface protein, ExoU/T/S: exoenzyme U/T/S, F1C pili: type 1-like immunological group C pili, *GBS, Group B streptococcus*, HlyA: α-hemolysin, Lps: lipopolysaccharide, HpmA: haemolysin, *K.p, Klebsiella pneumoniae*, MR/P pili: mannose-resistant Proteus-like, *P.a, Pseudomonas aeruginosa*, Pta: Proteus toxic agglutinin, *P.m, Proteus mirabilis*, P pili: pyelonephritis-associated pili, QS: Quorum sensing, *S.a, Staphylococcus aureus*, SdrI: a surface-associated collagen-binding protein, SigV: extracytoplasmic function sigma factor, *S.s, Staphylococcus saprophyticus*, SssF, S. saprophyticus surface protein F; Ssp: a surface-associated lipase, UafB: a cell wall-anchored protein, ZapA: an extracellular metalloprotease.

10.3389/fimmu.2022.953354

epithelium, which kill UPEC by phagocytosis and lipocalin-2 (LCN2) (60). LCN2 can restrict access of UPEC to iron, one of the key nutrients for the growth of UPEC, and starve them to death (61). Besides, IL-6 can enhance the expression of antimicrobial peptides (AMPs), such as ribonuclease 7 (RNase 7) and LL-37, which exert antibacterial effects by disrupting the microbial membrane (47, 58, 62–64). In the bladder of mice lacking RNase 7 and LL-37, the UPEC communities are significantly increased (47, 63). (Figure 1)

Some UPEC survives from the extracellular immune responses and invades BECs, which then initiate the intracellular efflux immune responses (65, 66). Once BECs are invaded, two waves of UPEC expulsion in an innate immune signaling-orchestrated process occur (67). The first wave is mediated by the activation of TLR4 between 4 and 6h after infection followed by the second mucolipin transient receptor potential 3 (TRPML3)-activated wave occurring around 8h after infection (67). In the first wave of UPEC expulsion, UPEC is encapsulated within RAB27b$^+$ vesicle and activates TLR4 by type I fimbriae (67, 68). Activation of TLR4 signaling advances the K33-linked polyubiquitination of TNF receptor associated factors (TRAF3), which is then sensed by the RalGDS-activating exocyst complex to locate and tether vesicles (68). After that, Sec 6 and Sec 15, two submit of the activated exocyst complex, stimulate collaboration between Rab11a/Rab11FIP3/Dynein and Rab27b/MyRIP/MyosinVIIa to transport UPEC-containing vesicles (67, 69). In addition, the activation of TLR4 can lead to the increase of cyclic adenosine monophosphate (cAMP) which subsequently stimulates the caveolin-1/Rab27b/PKA/MyRIP complex formation, and as a consequence, expels UPEC from infected BECs (70). Once UPEC escapes the first wave of efflux immune response by destroying the RAB27b$^+$ vesicle, the second wave is initiated by lysosomal autophagy (71). After the lysosome engulfed UPEC, the pH of the lysosome will change from acid to neutral, and TRPML3 is able to sense the UPEC-mediated lysosome neutralization of pH and release calcium ions, which leads to the efflux of UPEC (71). (Figure 2)

BECs can adopt more intense immune responses against UPEC by secretion of IL-6, IL-17, tumor necrosis factor-α (TNF-α), C-X-C motif chemokine ligand 1 (CXCL1), CXCL2, and CXCL5, which result in extensive neutrophil recruitment to induction of BECs' death and exfoliation (72–75). BECs' death and exfoliation carry a large amount of UPEC into the urine and then excretes UPEC by urination (72–75). In addition, in response to α-hemolysin, which is a virulence factor expressed by UPEC, human BECs induce the production of IL-1β and IL-18 through p38/ERK/ROS/NLRP3/caspase-1 signaling to recruit mast cells, which can produce tryptase to promote the exfoliation of BECs (76, 77). A point worthy of attention is that ROS and inflammation associated with NOD-like receptor thermal protein domain associated protein 3 (NLRP3) or cyclooxygenase-2 (COX-2) also contribute to BECs' exfoliation (76–79). However, excessive ROS and inflammation are believed to do more harm than good to the host, since the bladder infection gradually intensifies with the increase of ROS and inflammation (80, 81). Although the exfoliation of BECs promotes the excretion of UPEC into the urine, it also exposes deep immature epithelium, thus allowing UPEC to invade them

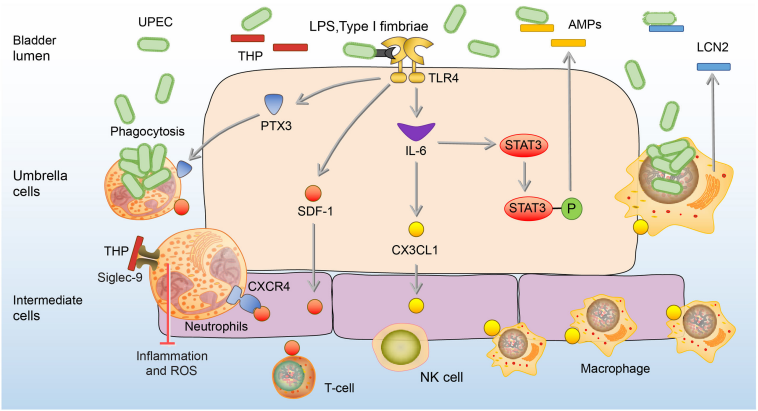

FIGURE 1
Extracellular immune responses to UPEC in the bladder. At the beginning of infection, THP reduces the adhesion of UPEC to the BECs. In addition, the THP can prevent excessive inflammation and ROS production of neutrophils. Once adhesion, BECs secrete SDF-1, PTX3, and IL-6. SDF-1 recruit neutrophils, T-cells, and NK cells to the site of infection. PTX3 promotes neutrophils to engulf UPEC, and IL-6 promotes the expression of CX3CL1 to recruit macrophages which kill UPEC by phagocytosis and LCN2. IL-6 also enhances the release of AMPs through phosphorylation of Stat3.AMPs, antimicrobial peptides; BEC, bladder epithelial cells; CXCR4, CXC-motif chemokine receptor 4; CX3CL1, C-X3-C motif chemokine 1; LCN2, lipocalin-2; IL-6, interleukin 6; NK cells, natural killer cells; PTX3, Pentraxins; SDF-1, stromal cell-derived factor1; Siglec-9, sialic acid-binding Ig-like lectin-9; Stat3, signal transducers and activators of transcription 3; THP, Tamm-Horsfall protein; UPEC, *Uropathogenic Escherichia coli*.

and form quiescent intracellular reservoirs (QIRs), which can avoid immune responses and antibiotics (82). In order to prevent the formation of QIRs caused by shedding, the proliferation ability of the epithelial layer after shedding is enhanced (83). This ability is mainly related to Th2 cells, as Th2 cells have an ability to secret epidermal growth factor (EGF), transforming growth factor-α (TGFα), and insulin-like growth factors-1 (IGF-1), which contribute to epithelial regeneration (84). The differentiation of Th2 cells in the bladder mainly depends on dendritic cells (DCs) presenting UPEC antigen to CD4+ T cells after infection (84). In addition, sonic hedgehog (SHH) expressed by basal stem cells and peroxisome proliferator-activated receptor-γ (Pparg) expressed by BECs also contribute to the regeneration and proliferation of BECs (85–87). (Figure 3)

K.pneumoniae

K. pneumoniae, one of the most common pathogens of intensive care unit infections, is the second leading cause of UTI from community or hospital sources (1, 88–90). Similar to the effects of THP on UPEC, THP exerts anti-adhesion and anti-inflammation effects on *K. pneumoniae* (91). In the THP-deficient mouse models, *K. pneumoniae* load in the urine and bladder significantly increased, as well as the number of inflammatory cells (91, 92). Once *K.pneumoniae* adheres to and invades BECs, intracellular immune defense mechanisms are initiated to inhibit the internalization of *K.pneumoniae* and promote its efflux. The first mechanism is initiated by TLR4, which down-regulates Rho through the expression of cAMP, and ultimately achieves the goal of inhibiting the invasion of *K.pneumoniae* (92). The second mechanism is mediated by high-mobility group protein N2 (HMGN2), which plays a key role in the inhibition of *K.pneumoniae* internalization by reduction of bacteria-induced activation of extracellular signal-regulated kinase (ERK1/2) and the polymerization of actin (93, 94). The last mechanism is that the invasion of *K.pneumoniae* promotes the synthesis of dual oxidase 2, which has the ability to inhibit bacterial internalization by the production of intracellular ROS (95, 96). The proper concentration of ROS has antibacterial against invading pathogenic bacteria (95, 97–99). (Figure 4A)

The type I fimbriae of *K.pneumoniae* is involved in the triggering of multiple immune responses in the bladder, which are very similar to UPEC type I fimbriae-induced immune responses (91, 92). Both UPEC and *K.pneumoniae* can be inhibited by the effect of THP against type I fimbriae, and they can both increase cAMP through type I fimbriae to regulate actin and ultimately promote bacterial efflux (53, 70, 91, 92). In addition, the UPEC and *K. pneumoniae* type I fimbriae play similar roles in the pathogenic process of bladder infection, as both of them rely on

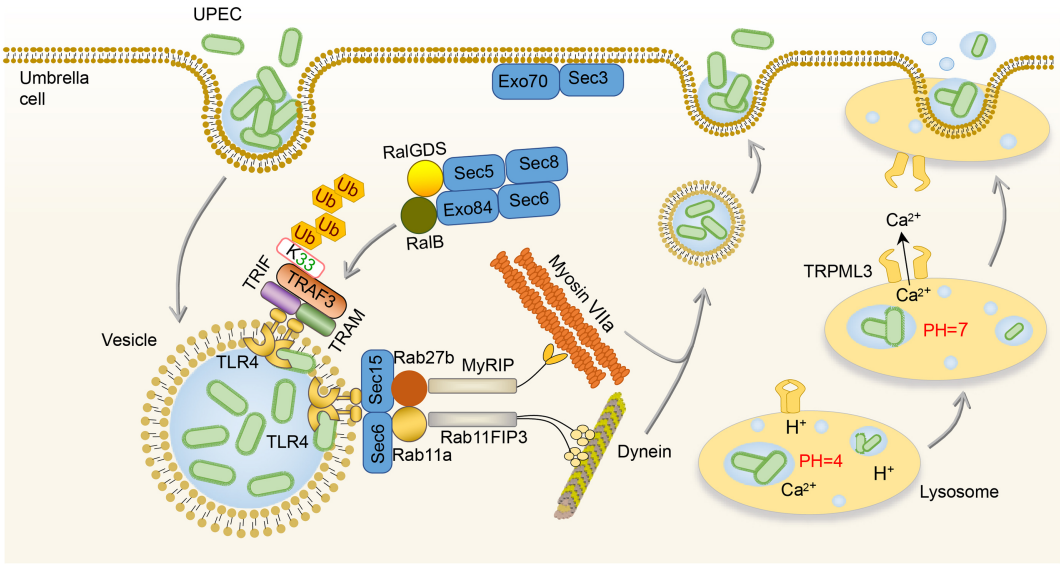

FIGURE 2
Intracellular immune responses to UPEC in the bladder. After invading BECs, TLR4 is activated by UPEC to promote the K33-linked polyubiquitination of TRAF3, which is sensed by the RalGDS-activating exocyst complex to locate and tether vesicles. Then, the Sec 6 and Sec 15 of the exocyst complex stimulate collaboration between Rab11a/Rab11FIP3/Dynein and Rab27b/MyRIP/MyosinVIIa to transport UPEC-containing vesicles. Once the lysosome engulfs UPEC, TRPML3 senses the pH neutralization and then releases calcium ions, leading to the efflux of UPEC. BEC, bladder epithelial cells; TLR4, toll-like receptor 4; TRPML3, transient receptor potential 3; UPEC, *uropathogenic Escherichia coli*.

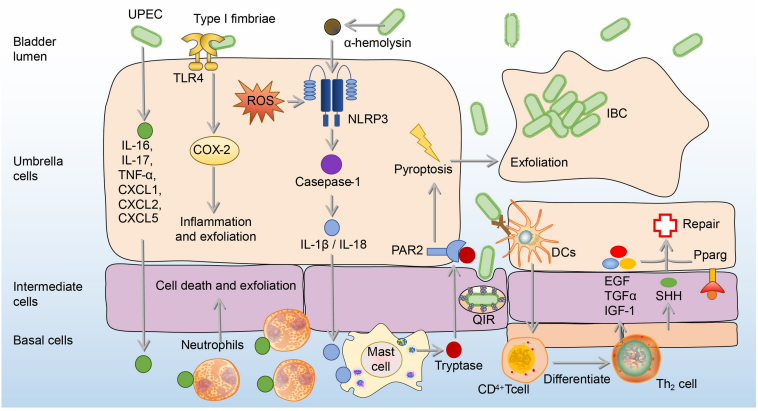

FIGURE 3
The exfoliation and regeneration of BECs in UPEC bladder infection. Cytokines from BECs are released to recruit neutrophils to induce cell death and exfoliation. Besides, Type 1 fimbriated UPEC activates TLR4 and causes the expression of COX-2, which promotes inflammation and exfoliation of BECs. Moreover, α-hemolysin produced by UPEC recruits mast cells through the ROS/NLRP3/caspase-1/IL-1β, which produces tryptase to mediate the BECs exfoliation. To repair shed BECs, transitional BECs will regenerate under the influence of EGF, TGF-α, IGF-1, SHH, and Pparg. BECs, bladder epithelial cells; EGF, epidermal growth factor; ERK, extracellular signal-related kinase; IGF-1, insulin-like growth factors-1; IL-1β, interleukin 1β; JNK, c-Jun-NH2-terminal kinase; NLRP3, NOD-like receptor thermal protein domain associated protein 3; PAR2, Protease-activated receptor 2; Pparg, peroxisome proliferator-activated receptor-γ; ROS, reactive oxygen species; SHH, sonic hedgehog; TGF-α, transforming growth factor-α; UPEC, *uropathogenic Escherichia coli*.

type I fimbriae to attach, invade, and form intracellular bacterial communities (1). By comparing the nucleic acid sequences of UPEC and *K.pneumoniae* type I fimbriae, they are highly homologous, which can explain why UPEC and *K. pneumoniae* type I fimbriae play similar roles in the pathogenicity and stimulate resembling immune responses of bladder infection (100, 101). However, *K.pneumoniae* carries the gene fimK but lacks the gene fimX, leading to reduce expression of type I fimbriae, which may explain *K. pneumoniae* form fewer intracellular bacterial communities (IBCs) and have lower titers in the bladder than UPEC and are more easily cleared by host defense response during infection (102).

S.saprophyticus

Bladder infection caused by *S.saprophyticus* is most likely to occur in sexually active, non-pregnant women (103). Generally speaking, when *S.saprophyticus* contaminates the vaginal area, it ascends through the urinary tract (103). In the ascending process, *S.saprophyticus* uses citrate in urine to synthesize carboxylate siderophores and obtain iron ions in urine to supply its nutrition and growth (104). In order to limit the growth of *S.saprophyticus*, the bladder maintains a weakly acidic urine environment to reduce the activity of citrate synthase and thereby reduce the synthesis of citrate, ultimately achieving the goal of limiting *S.saprophyticus* from obtaining iron and starving them to death (104, 105). In addition, THP in urine has the ability to inhibit the adhesion of *S.saprophyticus* to BECs, which is similar to the effects on UPEC (53, 91). However, the antibacterial ability of urine is limited, as some *S.saprophyticus* still survive from THP and the acidic environment and adhere to BECs, stimulating BECs to increase the expression of AMPs including regenerating islet-derived 3γ (RegIIIγ) and RNase 7 (106, 107). RegIIIγ is able to promote the proliferation and repair of the injury epithelial cells (108, 109). RNase 7 mainly binds to the negatively charged bacterial cell membrane through cationic residues on its surface, destroys the physical and physiological functions of the bacteria, and ultimately kills the bacteria (62). In addition to AMPs, BECs mediate the production of cytokines, such as TNF-α, macrophage inflammatory protein-1 (MIP-1), IL-1, IL-6, and IL-12, to recruit the macrophages (14). Macrophages depend on genes associated with retinoid-IFN-induced mortality-19 (GRIM-19), a component of the mitochondrial respiratory chain, to phagocytize *S.saprophyticus* (110, 111). In GRIM-19-deficient macrophages, the expression of IL-1, IL-6, IL-12, interferon-γ (INF-γ) cytokines, and phagocytic ability are significantly reduced (110). (Figure 4B)

The immune responses to *S.saprophyticus* in bladder infection have differences from these to other uropathogens, as the urine pH and GRIM-19 have abilities to inhibit the growth of *S.saprophyticus* (104, 110). Acidic urine reduces the synthesis of citrate, consequently resulting in inhibition of *S.saprophyticus* growth, and GRIM-19 molecule exerts immune defense effects by regulating the phagocytic ability of macrophages in bladder infection (104, 110). Therefore, modulating urine pH and GRIM-19 is a promising target for *S.saprophyticus* UTI.

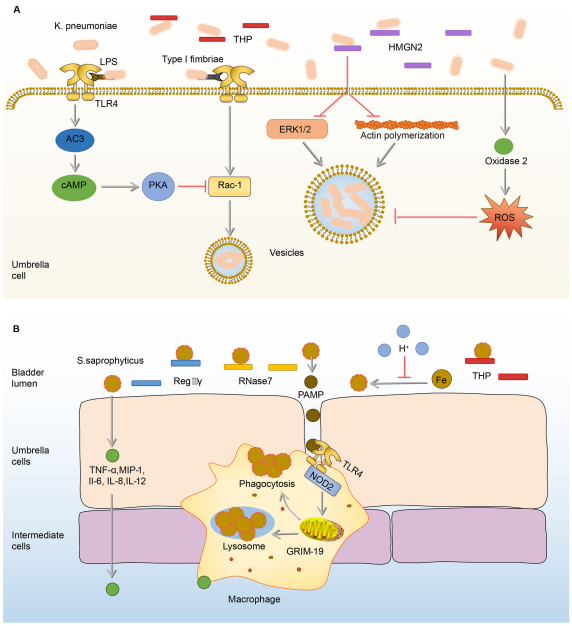

FIGURE 4
Immune responses to K. *pneumoniae* and *S.saprophyticus* in the bladder. **(A)** In the urine, THP exerts anti-adhesion and anti-inflammation effects on K. *pneumoniae*. Once adhered, K. *pneumoniae* lipopolysaccharide activates TLR4 to initiate AC-3/cAMP/PKA signaling pathway, then down-regulates Rac-1 and abrogates the endocytic lipid raft. HMGN2 also can inhibit K. *pneumoniae* internalization by inhibiting the attachment of bacteria and reducing bacterial-induced ERK1/2 activation and actin polymerization. In addition, the ROS promoted by oxidase 2 can inhibit endocytosis. **(B)** Before adhesion, RegIIIγ, RNase 7, and THP have anti-adhesion and sterilization abilities to *S. saprophyticus*. The acidic urine environment suppresses *S. saprophyticu* uptake and utilization of iron thus limiting its growth. After the adhesion, BECs produce TNF-α, MIP-1, IL-1, IL-6, and IL-12 to recruit macrophages. Upon the activation of TLR4 by PAMP, macrophages phagocytize *S.saprophyticus* depending on genes associated with GRIM-19. AC-3, adenylyl cyclase-3; cAMP, cyclic adenosine monophosphate; ERK1/2, extracellular-regulated kinase 1/2; GRIM-19, genes associated with retinoid-IFN-induced mortality-19; HMGN2, high-mobility group protein N2; IL-1, interleukin-1; INF-γ, interferon-γ; *K.pneumoniae*, *Klebsiella pneumoniae*; MIP-1, macrophage inflammatory protein-1; PAMP, pathogen-associated molecular pattern; PKA, protein kinase A; RegIIIγ, regenerating islet-derived 3γ; RNase 7, ribonuclease 7; ROS, reactive oxygen species; *S.saprophyticus*, *Staphylococcus saprophytes*; THP, Tamm-Horsfall protein; TLR4, toll-like receptor 4; TNF-α, tumor necrosis factor-α.

E.faecalis

E.faecalis is one of the most resistant gram-positive bacteria in UTI, which has caused great trouble for clinical treatment (112). Current research on the immune responses to *E.faecalis* bladder infection are more about the responses of macrophages, DCs, and Natural killer (NK) cells (113, 114).

Under normal circumstances, activation of TLR2-Toll/interleukin-1 receptor (TIR) on macrophages can trigger the production of chemokines dependent on the NF-κB signaling pathway, and recruit immune cells in the bladder (115, 116). However, *E.faecalis* has a TIR domain-containing protein structure, which is similar to the TIR domain of TLR2 on macrophages (113, 117). Hence, the TIR domain-containing protein of *E.faecalis* (TcpF) has an ability to compete with the TIR domain of human TLR2 to form TLR dimers, thereby further eliminating downstream signals and ultimately inhibiting the immune responses of macrophages in the bladder (113, 117). Therefore, immune responses of macrophages to *E.faecalis* and UPEC co-infected in the bladder are significantly inhibited compared to the infection of UPEC alone, consequently promoting UPEC virulence during a mixed-species bladder infection (113, 118).

Different from immunosuppressive effects on macrophages, *E.faecalis* has the ability to intensify the proliferation and activation of NK cells, which in turn promote the maturation and differentiation of DCs (114). In addition, NK cells also can be activated by *E.faecalis*-induced DC-derived effectors signals. *E. faecalis* specific DC/NK interaction is necessary for the killing of transformed or infected cells in *E.faecalis* bladder infection (114). (Figure 5A) The adaptive immune responses in the bladder are limited, widely assumed to the restricted ability of mature DCs to capture and present antigens in the bladder (119, 120). Exogenously regulating the DC/NK interaction may be one of the effective strategies to enhance bladder adaptive immune responses.

GBS

GBS is a common commensal of the human genitourinary tract in healthy people (121). Nevertheless, this bacterium can cause life-threatening hazards to pregnant women, the elderly, and immunocompromised individuals (122–124).

When the immune function of the body is compromised, GBS in the urethra will express a variety of virulence factors to damage and adhere to the bladder tissue (122–124). AMPs in the urine are the first line of defense, however, LL-37, one of the AMPs, has no antibacterial effect on GBS (46). On the contrary, the load of GBS increases with the rise of LL-37 (46). Under the action of LL-37, GBS further adheres to the BECs, and this adherence promotes the expression of many cytokines, including IL-8, IL-1β, IL-1α, IL-6, TNF-α, granulocyte-macrophage colony-stimulating factor (GM-CSF) to mediate the occurrence of inflammation and recruit the immune cells including neutrophils, macrophages, and DCs to the infected sites (22, 125, 126). Neutrophils reach the focal point of infection producing anti-infective effects through various biological effects such as phagocytosis and cytokine production (125–128). Macrophages and DCs also make significant contributions to host defenses by secretion of IL-1β and IL-18 through the activation of the NLRP3 inflammasome, deficiency of which has GBS communities increased (129, 130). (Figure 5B) However, immune responses of neutrophils and macrophages can be inhibited by GBS virulence factors, as the cytokines production of macrophages and neutrophils increased when the bladder was infected by the virulence factor capsule sialic acid-deficient GBS (23, 131).

Compared with the anti-bacterial effects of LL-37 on UPEC infection, LL-37 plays an opposite role in GBS infection, which promotes GBS growth and proliferation (46, 47, 132). The role of NLRP3 may also differ between GBS and UPEC infection, as NLRP3-deficient mice were more susceptible to GBS infection and have GBS load increased. Whereas UPEC burden was significantly reduced in NLRP3-deficient BECs (76, 129). As these colonization differences between GBS and UPEC were observed based on the different NLRP3-deficient cells but have not been validated in the same cells and *in vivo* yet, which needs to be further explored (76, 129). Due to the differences in immune responses of the bladder between UPEC and GBS infection, when treating bladder infection caused by GBS, we should adopt different immunomodulation options from that of UPEC.

P.mirabilis

P.mirabilis, which showed high resistance rates to ampicillin, nitrofurantoin, and amoxicillin-clavulanate, is the sixth most common pathogen of uncomplicated UTI (1, 25). When the *P.mirabilis* reaches the mouth of the urethra, it moves up the urethra through the swing of the flagella and reaches the bladder (133). During the ascending process, many immune mediators in the urine including complement (C1q and C3), LL-37, and human β-defensin (hBD) are hydrolyzed by ZapA (Mirabilysin), which is a 54-kDa extracellular proteolytic enzyme with broad-spectrum degradation activity encoded by *P.mirabilis* (26). Similar to the effects on UPEC and *K.pneumoniae*, THP and RNase 7 in the urine resist the adhesion and invasion of *P.mirabilis* to BECs (106, 134). Some *P.mirabilis* survive from THP and RNase 7 and adhere to BECs through fimbriae (135). Once the *P.mirabilis* successfully adhere, a number of leukocytes migrate to the epithelium mediated by the production of c-c chemokine ligand 20 (CCL20), CXCL2, and CCL2 under the stimulation of flagella (136). However, the migration of leukocytes is demonstrated ineffective in clearing *P.mirabilis* (136). (Figure 6A)

There are very few reports on the immune responses to the effective inhibition of *P.mirabilis* in bladder infection. Two broad-spectrum antibacterial mediators, THP and RNase 7, in the urine have been reported to inhibit the growth of *P.mirabilis* (106, 134). However, many immune responses and immune mediators in the urine are suppressed by ZapA (26). In addition, it has been reported that the anti-MrpA (structural subunit of MR/P fimbriae) antibodies in urine and serum can be neutralized by *P.mirabilis* (137). Therefore, the antibacterial immune responses to *P.mirabilis* in bladder infection remain lacking and need more to be explored in the future.

P.aeruginosa

Of all uropathogens in bladder infection, *P.aeruginosa* is a relatively small pathogenic bacterium in UTI, but it has caused great trouble for clinical treatment, as many antibiotics such as topiperacillin-tazobactam, ceftazidime, and cefepime, which are effective against other uropathogens, hardly have effects on *P.aeruginosa* (32). The current research on the immune responses to *P.aeruginosa* in the bladder is extremely limited. Before *P.aeruginosa* adhere to the bladder, the growth of *P.aeruginosa* is firstly affected by iron restriction and THP (34, 138, 139). Surprisingly, the burden of *P.aeruginosa* and histopathological conditions in the bladder and kidney increase under iron-restricted conditions. Consistently, *in vitro* experiments showed that iron-restricted media increases the adhesion of *P.aeruginosa* to the BECs and inhibits macrophage to phagocytose *P.aeruginosa* (138). The reason why iron restriction can aggravate the *P.aeruginosa* bladder infection may be attributed to the enhancement of quorum sensing (QS) signaling molecules under iron deficiency conditions (140, 141). Furthermore, when mice are infected with THP-coated *P.aeruginosa*, the bacterial burden and pathological changes in the kidney are significantly enhanced (139). Therefore, THP and iron restriction have beneficial effects on

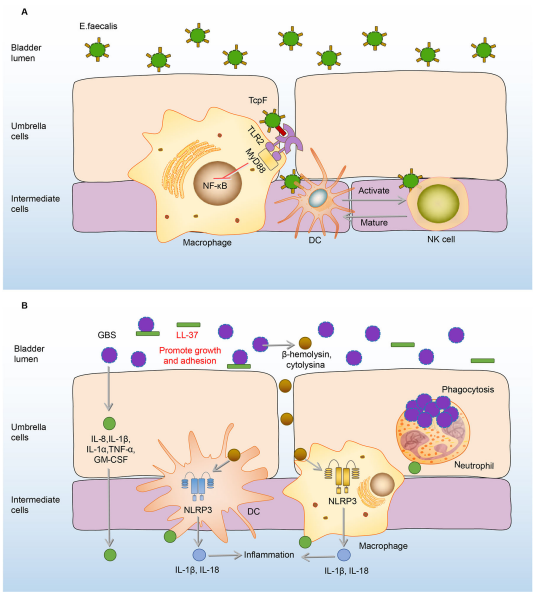

FIGURE 5
Immune responses to *E. faecalis* and GBS in the bladder. **(A)** Initially, RNase 7 in the urine binds to the *E. faecalis* and plays a bactericidal effect. Once *E. faecalis* adheres to BECs, TcpF of which binds to the TIR on macrophages, eliminating downstream MyD88 and NF-kB signals and suppressing the immune responses. However, the proliferation and activation of NK cells are intensified, which promote the maturation and differentiation of DCs. In turn, NK cells can be specifically activated to kill *E. faecalis* through derived effectors signals from infected DCs. **(B)** In the urine, LL-37 sticks to GBS and promotes its growth and adhesion. After adhesion, GBS induces the expression of IL-8, IL-1β, IL-1α, IL-6, TNF-α, GM-CSF to recruit immune cells and mediate inflammation. Macrophages and DCs secrete IL-1β and IL-18 against the GBS infection under the activation of the NLRP3 inflammasome by β-hemolysin/cytolysin of GBS. Neutrophils engulf GBS to play an antibacterial effect. DCs, dendritic cells; *E. faecalis*, *Enterococcus faecalis*; GBS, *Group B Streptococcus*; GM-CSF, granulocyte-macrophage colony-stimulating factor; IL-8, interleukin-8; MyD88, myeloiddifferentiationfactor88; NF-kB, Nuclear factor kappa beta; NK cells, natural killer cells; NLRP3, NOD-like receptor thermal protein domain associated protein 3; RNase 7, ribonuclease 7; TcpF, TLR2-Toll/Interleukin-1 receptor domain-containing protein of *E. Faecalis*.

P.aeruginosa colonization (34, 138, 139). Once the bladder is colonized by *P.aeruginosa*, it will increase the expression of MIP-1α to recruit neutrophils, which can effectively decrease the burden of *P.aeruginosa* in the bladder (142). (Figure 6B)

Many immune responses that have spectral antibacterial effects on other uropathogens have no effects on *P.aeruginosa*, or may even aggravate the infection of *P.aeruginosa*. In addition, many antibiotics, which are effective against other uropathogens, do not affect *P.aeruginosa* bladder infection (32). Hence, it is pretty urgent to continue to explore the effective immune defenses for *P.aeruginosa* in bladder infection so that propose some feasible immunomodulatory interventions.

Candida.

Candida. is a common uropathogenic fungus in UTI, especially in immunocompromised patients (143). Generally speaking, *Candida.* mainly causes disease through its hyphae, *Candida.* adheres to the BECs through the agglutin-like sequence (Als3) glycoprotein structure on the hyphae in the bladder (144, 145). To combat this adhesion process, the THP already present in the bladder urine binds to Als3, thereby inhibiting the adhesion of *Candida.* to the BECs (144). In addition to THP, LL-37 binds to the Xog1p glycoprotein of the *Candida.* cell wall to reduce adhesion to BECs (146, 147). However, once *Candida.* adheres to the BECs, COX-2 will be induced in BECs through the EGFR-ERK/p38-RSK-CREB-1 pathway, the upregulation of which leads to the synthesis of prostaglandins, triggering inflammation (148, 149). (Figure 6C)

Candida. is the only fungus among the nine major uropathogens and the bladder executes different mechanisms of immune responses to *Candida.* from those to bacteria. For example, THP and LL-37 exert an anti-adhesion effect on both *Candida.* and other bacteria, THP targets the hyphae to inhibit the adhesion of *Candida* (144–146).. In bacterial infection, THP targets the fimbriae (52, 91, 134). LL-37 reduces adhesion of the *Candida.* by binding to its glycoprotein, in bacterial infection, LL-37 exerts anti-adhesion by disrupting the bacterial membrane (47, 146).

S.aureus

S.aureus is the most common gram-positive bacteria in hospital-acquired infections, which mainly occur in catheter-induced UTI (150, 151). The immune responses of the bladder to *S.aureus* are blank. However, there are many patients with cystitis caused by *S.aureus*, which is highly resistant to antibiotics (1, 18, 152). It is necessary to carry out research work on the immune responses to *S.aureus* in bladder infection.

Potential individual immunomodulatory interventions

Based on the above summarized immune responses to diverse uropathogens in bladder infection, we deemed that maybe an immune target has antibacterial effects on a variety of uropathogens in bladder infection, and on the other side, some immune mediators play opposite roles in bladder infection (Table 2). In this section, we discuss the potential immunomodulatory interventions for bladder infection caused by different uropathogens.

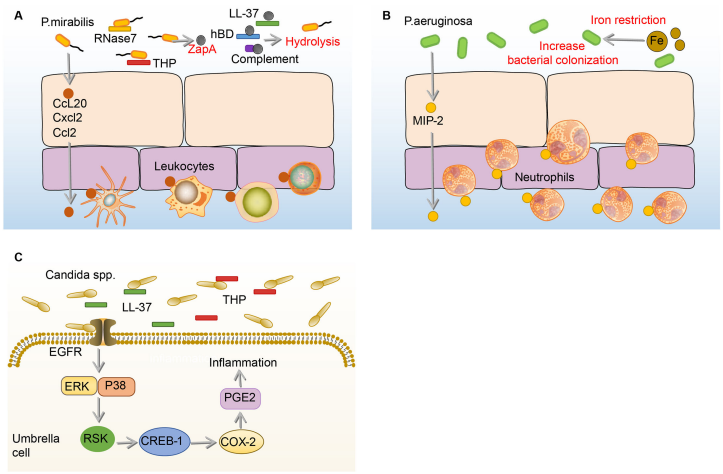

FIGURE 6
Immune responses to *P. mirabilis*, *Paeruginosa* and *Candida* spp. in the bladder. **(A)** Before adhesion, THP and RNase 7 resist the adhesion and invasion of *P.mirabilis* to the bladder, and *P.mirabilis* has countermeasures by expressing extracellular metalloprotease ZapA, which has hydrolytic activity. In addition, ZapA can hydrolyze complement (C1q and C3), LL-37, and human hBD in the urine. Notably, BECs can produce CCL20, CXCL2, and CCL2, and then promote numbers of leukocytes migrate to the epithelium, the specific role of which is not determined. **(B)** Under the iron restriction, *P.aeruginosa* has a stronger colonization ability on BECs. Once *P.aeruginosa* adheres to the BECs, the BECs increase the expression of MIP-1α to recruit neutrophils, which against the bladder infection of *P.aeruginosa*. **(C)** In the urine, THP and LL-37 respectively bind to the Als3 and Xog1p glycoprotein of *Candida* to inhibit adhesion. After *Candida* adhesion, BECs express COX-2 through EGFR-ERK/p38-RSK-CREB-1 pathway, leading to the synthesis of prostaglandins, which mediate the occurrence of inflammation. BECs, bladder epithelial cells; *Candida, Candida spp;* CCL20, c-c chemokine ligand 20; COX-2, cyclooxygenase-2; CREB-1, cAMP-response element-binding protein-1; CXCL2, C-X-C motif chemokine ligand 2; EGFR, epidermal growth factor receptor; ERK, extracellular regulated protein kinases; hBD, β-defensin; MIP-1α, macrophage inflammatory protein-1α; *P.aeruginosa*, *Pseudomonas aeruginosa*; *P. mirabilis*, *Proteus mirabilis*; RNase 7, ribonuclease 7; RSK, ribosomal s6 kinase; THP, tamm-horsfall protein.

Inhibition of adhesion

THP, a broad-spectrum anti-infective protein in bladder infection, has the ability to against many uropathogens, inclusive of UPEC, *K.pneumoniae*, *P.mirabilis*, *S.saprophyticus*, and *Candida* (91, 134, 144, 145, 153, 154). It plays the antibacterial effect mainly by reducing the colonization of uropathogens on BECs, as THP can occupy the binding sites of uropathogens to BECs (91, 134, 144, 145, 153, 154). Therefore, the upregulation of THP may be an excellent intervention option for the bladder infection caused by UPEC, *K.pneumoniae*, *P.mirabilis*, *S.saprophyticus*, and *Candida*. Clinical experiments showed that the level of THP in patients who take cranberry extract orally increases, and the urine from these patients has a stronger inhibitory effect on the adhesion of UPEC (52, 155). However, whether this intervention is effective for bladder infection caused by *P.aeruginosa* is not determined, as the THP can lead to an increase in *P.aeruginosa* load (139). In conclusion, the upregulation of THP is an excellent way to combat the bladder infection of UPEC, *K.pneumoniae*, *S.saprophyticus*, *P.mirabilis*, and *Candida*.

Scavenging of ROS

Over accumulated ROS is involved in the induction of BECs injury and death in bladder infection, but the proper concentration of ROS has antibacterial effects (76, 77, 95, 97–99). Uropathogens including UPEC, *K.pneumoniae*, *S.saprophyticus*, *P.mirabilis*, *P.aeruginosa*, and *Candida*. induce an increase in ROS level in bladder infection (156). Reducing the expression of ROS seems to have a therapeutic effect on UTI (157, 158). The results of a systematic review showed that vitamin C, a drug candidate with antioxidant capacity, has the ability to prevent the occurrence of UTI, and anthocyanins can inhibit ROS to treat UTI caused by *K.pneumoniae* and *P.aeruginosa* (157, 158). Among the anthocyanin extracts of all plants, blueberry is an excellent candidate because of its very rich anthocyanin content (159, 160). We conclude that reducing the content of ROS through the use of antioxidant drugs is a promising intervention for bladder infection.

10.3389/fimmu.2022.953354

TABLE 2 Potential immunomodulatory targets against different uropathogens in bladder infection.

Targets	THP	ROS	Iron restriction	AMPs				Hormones		cAMP	Urothelium repair	Anti-inflammation		Immunization with vaccines	Probitioc interventions
				RNase7	RegIIIγ	LCN2	LL-37	Insulin	estogen			COX-2	NLRP3		
UPEC	√		√	√		√	√	√	√	√	√	√	√	√	√
K.p	√	√	√					√		√				√	√
S.s	√		√	√	√										
E.f								√						√	√
GBS							×	√					×		
P.m	√		√	√										√	
P.a	×	√	×									√			√
Candida.	√						√	√				√			√
S.a								√							

"√" means that this immunomodulatory target has potential therapeutic value, and "×" means that this immunomodulatory target is not recommended; AMPs, antimicrobial peptides; Candida., Candida spp; COX-2, cyclooxygenase-2; *E.f, Enterococcus faecalis*; *GBS, Group B streptococcus*; *K.p, Klebsiella pneumoniae*; LCN2, lipocalin-2; NLRP3, nod-like receptor thermal protein domain associated protein 3; *P.a, Pseudomonas aeruginosa*; *P.m, Proteus mirabilis*; RegIIIγ, regenerating islet-derived 3γ; RNase 7, ribonuclease; ROS, reactive oxygen species; *S.a, Staphylococcus aureus*; *S.s, Staphylococcus saprophyticus*; THP, tamm-horsfall protein.

Iron restriction

Iron restriction, as another broad-spectrum antibacterial method, inhibits the growth of a variety of uropathogens in bladder infection, including UPEC, *K.pneumoniae*, *S.saprophyticus*, and *P.mirabilis* (61, 104, 161–163). Exogenous regulation of iron content in urine is an excellent immune regulation target for the treatment of bladder infection. Animal experiments showed that the dietary restriction of iron significantly reduces the iron content, followed by bacterial burden, bacteriuria, as well as inflammatory responses decreasing in UPEC bladder infection, and the exogenous injection of lactoferrin, an iron-binding glycoprotein, also significantly reduces the UPEC load and the infiltration of neutrophils (164, 165). However, the intervention effects of iron restriction on UTI caused by *P.aeruginosa* are not verified, because iron restriction does not inhibit the growth of *P.aeruginosa*, but increases the bacterial load in the bladder (138). In conclusion, restricting access to iron is a promising intervention for bladder infection caused by UPEC, *K.pneumoniae*, *S.saprophyticus*, and *P.mirabilis*, which may not apply to *P.aeruginosa*.

Increase of AMPs

AMPs are a large class of compounds that participate in a variety of innate immune responses and are considered to be promising compounds to deal with antimicrobial resistance (166). RNase 7 has antibacterial effects on UPEC, *S.saprophyticus*, and *P.mirabilis*, RegIIIγ has antibacterial effects on *S.saprophyticus*, LCN2 has antibacterial effects on UPEC, and LL-37 has antibacterial effects on UPEC and *Candida* (47, 58, 61, 106, 107, 147). Therefore, RNase 7, RegIIIγ, LCN2, and LL-37 may have therapeutic effects against the above uropathogens in bladder infection. Notably, different AMPs and even different segments of the same AMP have different antimicrobial effects. Taking RNase 7 as an example, fragments of RNase 7 have different antibacterial effects on uropathogens, the F:1-97 fragment has the most antibacterial activity against UPEC and *S.saprophyticus*, while all N-terminal fragments except the F:1-45 fragment have the most antibacterial activity against *P.mirabilis* (106). Notably, LL-37 does not have a killing effect on GBS, on the contrary, it will promote GBS bladder infection (46).

Regulation of hormones

Among hormones, insulin has the ability to promote the secretion of RNase 7, RNase4, and LCN2, which are proven to be against bladder infection caused by a variety of uropathogens (167, 168). In addition, insulin reduces the risk factor of blood sugar,

thereby reducing the susceptibility of diabetic patients to bladder infection of UPEC, *K.pneumoniae*, *E.faecalis*, GBS, *S.aureus*, and *Candida* (124, 169–173).. However, a prospective study showed that diabetic patients who used insulin for a long time had a higher risk of UTI than diabetic patients who did not use insulin. The reason for the inconsistency may be that the blood and urine sugar of patients taking insulin is higher than that of patients without taking insulin (174). Insulin may not be suitable for people with low blood sugar, because it can cause hypoglycemia and lead to undesirable consequences such as coma (175). Except for insulin, estrogen also changes the bacterial burden in bladder infection (176–178). Female, compared with male, had lower bacterial burdens and stronger immune responses (178). This may be because of the increase of IL-17 mediated by estrogen, as IL-17 initiates many anti-bacterial pathways, including antimicrobial peptide and chemokine expression and the direct killing effects on bacteria (178–181). Differently, exogenous androgen can increase the burden of UPEC and mediate the development of cystitis into pyelonephritis (176, 177).

Enhancement of intracellular efflux bacteria

cAMP plays an important role in the efflux of UPEC and *K.pneumoniae* from BECs in bladder infection (70, 92). Many drugs, that are proven by US-Food and Drug Administration certification (like Liraglutide, Terbutaline, and so on) can increase the production of cAMP. Liraglutide, a glucagon-like peptide-1 (GLP-1) receptor agonist, is shown to increase cAMP to inhibit the replication of the hepatitis C virus (182). Terbutaline can reduce LPS-induced human pulmonary microvascular endothelial cell damage by increasing cAMP (183). cAMP is proven to be a potential immunomodulatory target for bacterial bladder infection, but there is a lack of research to prove their therapeutic effects, further research is needed (70).

Urothelium repair

BECs play important roles as the first line of defense in bladder infection, because it produces many immune factors to mediate the immune responses, and meanwhile, it prevents the invasion of bacteria into the deep immature epithelium to form QIRs (184). Hyaluronic acid (HA), a high molecular weight glycosaminoglycan, not only induces the production of LCN2 and IL-8 in HA/flagellin-challenged epithelial cells but is also involved in the enhancement of the physical barrier of BECs (185). As clinical data showed that intravesical injection of HA can indeed achieve the purpose of treatment for infected humans (186–188). Similar to HA, clinical trials showed that 25-hydroxyvitamin D3 also has the role of protecting the bladder epithelial integrity in postmenopausal women, as 25-hydroxyvitamin D3 induces expression of occludin and claudin-14, which are the tight junction proteins in the urinary tract (189). In addition to protecting mature epithelial integrity, the measures to promote the regeneration of immature epithelium should be taken into consideration. Briefly, HA, 25-hydroxyvitamin D3 and so on which can repair urothelium are excellent targets to combat the infection of UPEC.

Anti-inflammation

COX-2 and NLRP-3 were shown to favor infections by exacerbating inflammation (76–79, 148, 149, 190). Inhibiting the synthesis of COX-2 or NLRP-3 can protect mice from cystitis induced by uropathogens, but except GBS-induced cystitis, because GBS colonized more in NLRP-3-deficient mice compared with wild type mice (76–79, 129, 148, 149, 190). Therefore, inhibiting inflammation by targeting COX-2 or NLRP-3 theoretically has a certain therapeutic value against uropathogens except for GBS (129). However, a randomized controlled trial with a sample size of 253 showed that targeting COX-2 by using NSAIDs is less effective than antibiotics and may even promote the progression of cystitis to pyelonephritis (191). Another randomized controlled trial with a sample size of 383 also showed that NSAIDs are less effective than antibiotics in the treatment of bladder infections, and may even lead to pyelonephritis and serious adverse events (192). To sum up, although the basic experiments confirmed the value of anti-inflammatory in the intervention of bladder infection, it should be cautious in clinical application for UTI.

Immunization with vaccines

Vaccination holds a promising approach against different microbial bladder infections. Many vaccines designed against individual-specific uropathogens are currently in the stage of basic or clinical trials (193–195). For UPEC bladder infection, there are vaccines targeting type 1 fimbriae, hemolysins, siderophore receptors, cytotoxic necrotizing factor 1 (CNF1), and LPS (194, 196–198). For *P.mirabilis* bladder infection, there are vaccines targeting MR/P fimbriae and hemolysins (199, 200). For *E. faecalis* bladder infection, there is endocarditis- and biofilm-associated (Ebp) fimbriae vaccine (201). To make the vaccines against the diversity of uropathogens, the vaccines can be extracted from a range of uropathogens to form a multivalent vaccine. For example, Urovac (Solco Basel Ltd, Basel, Switzerland) consists of 10 heat-killed uropathogens, including 6 serotypes of UPEC, *P.vulgaris*, *K.pneumoniae*, and *E.faecalis* (202). Although most vaccines have been demonstrated highly efficacious in reducing the incidence and severity of UTI in animal models, there is a lack of large-scale clinical trials to prove their efficacy and safety. As the purpose of vaccination is to induce immune memory of the specific pathogens, the vaccines are effective on the

corresponding uropathogens but not on others. If a broad anti-infective effect is desired in the treatment of bladder infection, then a multivalent vaccine is an option.

Probiotic interventions

Probiotics can inhibit the adherence, growth, and colonization of uropathogens and reduce inflammation in the urinary tract by producing antibacterial substances such as lactic acid and hydrogen peroxide, or by directly competing for the adhesion sites between UPEC and the BECs (203–205). The efficacy and safety of probiotics in the treatment of bladder infection have been confirmed by extensive clinical trials, which include *Lactobacillus rhamnosus*, *Lactobacillus acidophilus*, *Lactobacillus fermentum*, *Lactobacillus reuteri*, *Bifidobacterium bifidum*, and *Bifidobacterium lactis* (206–209). However, different probiotics were demonstrated to have diverse antibacterial effects. *Lactobacillus acidophilus* has an average inhibition zone of 16 mm for UPEC but for *E.faecalis* was 12mm (210). *Lactobacillus salivarius* UCM572 had anti-adhesion effects against UPEC, however, the anti-adhesion effect on other uropathogens was not demonstrated (211). Furthermore, the anti-adhesion effects of different *Lactobacillus* strains against *Candida*, *K.pneumoniae*, *P.aeruginosa*, and *Proteus* were reported to be different (212). Therefore, when probiotics are used to treat different microbial bladder infections, appropriate probiotic strains should be selected according to the specific uropathogens in bladder infection.

Further research

Because of the diverse effects of immunomodulatory interventions on different uropathogens, corresponding immunotherapies should be taken for different uropathogenic bladder infections for better therapeutic effects. However, compared with great advances in the understanding of bladder immune responses trigged by UPEC, understanding of the bladder immune responses caused by other uropathogens remains relatively limited, which results in relatively few individual immunomodulatory options for other uropathogens which we came up with. Further research needs to pay more attention to the immune responses to other uropathogens besides UPEC. In addition, most of the immunomodulatory interventions were proven efficacious in animal models, further clinical research needs to demonstrate the consistency of the effects, and then which will achieve better therapeutic effects in the future.

Conclusion

Antibiotic therapy is the only option for UTI treatment but in recent years it is becoming more limited due to the increasing resistance of UTIs to routinely applied antibiotics. Immunomodulatory interventions have been suggested to be alternatives. However, the bladder executes different immune responses depending on the type of uropathogens, thus one immunomodulatory target has diverse effects on different uropathogens. The similarities and differences in immune responses to the main nine uropathogens in bladder infection were sorted out and comparably analyzed in this Review. To improve the effects of immunomodulatory interventions on different microbial bladder infections, specific uropathogenic bladder infections should adopt corresponding immunomodulatory targets to intervene, and one immunomodulatory intervention can be applied to diverse microbial infections, under the condition that they share the same effective therapeutic targets. Only through individual treatments in different uropathogenic bladder infection by immunomodulatory interventions can achieve better therapeutic results as alternatives for antibiotics in the future.

Author contributions

LL, YL, and HC researched data for the article and wrote the manuscript. HC and XX made substantial contributions to discussions of content, and reviewed and edited the manuscript. All authors contributed to multiple parts of the paper, as well as the final style. All authors contributed to the article and approved the submitted version.

Funding

The authors acknowledge funding received from the Department of Science and Technology of Sichuan Province and Southwest Medical School (2021ZYD0084, 2022NSFSC1381, 2021ZKZD006, and 2021ZKZD004).

Conflict of interest

The authors declare that the research was conducted in the absence of any commercial or financial relationships that could be construed as a potential conflict of interest.

Publisher's note

All claims expressed in this article are solely those of the authors and do not necessarily represent those of their affiliated organizations, or those of the publisher, the editors and the reviewers. Any product that may be evaluated in this article, or claim that may be made by its manufacturer, is not guaranteed or endorsed by the publisher.

References

1. Flores-Mireles AL, Walker JN, Caparon M, Hultgren SJ. Urinary tract infections: Epidemiology, mechanisms of infection and treatment options. *Nat Rev Microbiol* (2015) 13(5):269–84. doi: 10.1038/nrmicro3432

2. Zhu C, Wang DQ, Zi H, Huang Q, Gu JM, Li LY, et al. Epidemiological trends of urinary tract infections, urolithiasis and benign prostatic hyperplasia in 203 countries and territories from 1990 to 2019. *Mil Med Res* (2021) 8(1):64. doi: 10.1186/s40779-021-00359-8

3. Sureshbabu RP, Aramthottil P, Anil N, Sumathy S, Varughese SA, Sreedevi A, et al. Risk factors associated with preterm delivery in singleton pregnancy in a tertiary care hospital in south India: A case control study. *Int J Womens Health* (2021) 13:369–77. doi: 10.2147/IJWH.S282251

4. Lacerda Mariano L, Ingersoll MA. The immune response to infection in the bladder. *Nat Rev Urol* (2020) 17(8):439–58. doi: 10.1038/s41585-020-0350-8

5. Bruxvoort KJ, Bider-Canfield Z, Casey JA, Qian L, Pressman A, Liang AS, et al. Outpatient urinary tract infections in an era of virtual healthcare: Trends from 2008 to 2017. *Clin Infect Dis* (2020) 71(1):100–8. doi: 10.1093/cid/ciz764

6. Sihra N, Goodman A, Zakri R, Sahai A, Malde S. Nonantibiotic prevention and management of recurrent urinary tract infection. *Nat Rev Urol* (2018) 15 (12):750–76. doi: 10.1038/s41585-018-0106-x

7. Gajdacs M, Urban E. Comparative epidemiology and resistance trends of proteae in urinary tract infections of inpatients and outpatients: A 10-year retrospective study. *Antibiotics (Basel)* (2019) 8(3):91. doi: 10.3390/antibiotics8030091

8. Gu J, Song P, Chen X, Yang Z, Zhang X, Bai Y. Comparative study of the bacterial distribution and antimicrobial susceptibility of uropathogens in older and younger patients with urinary stones. *BMC Geriatr* (2022) 22(1):195. doi: 10.1186/s12877-022-02886-y

9. Govindarajan DK, Kandaswamy K. Virulence factors of uropathogens and their role in host pathogen interactions. *Cell Surf* (2022) 8:100075. doi: 10.1016/j.tcsw.2022.100075

10. Subashchandrabose S, Mobley HLT. Virulence and fitness determinants of uropathogenic escherichia coli. *Microbiol Spectr* (2015) 3(4):UTI-0015-2012. doi: 10.1128/microbiolspec.UTI-0015-2012

11. Chathley U, Sharma S, Chhibber S. Lipopolysaccharide-induced resistance in mice against ascending urinary tract infection with klebsiella pneumoniae. *Folia Microbiol (Praha)* (1996) 41(4):373–6. doi: 10.1007/bf02814718

12. Tarkkanen A, Allen B, Williams P, Kauppi M, Haahtela K, Siitonen A, et al. Fimbriation, capsulation, and iron-scavenging systems of klebsiella strains associated with human urinary tract infection. *Infect Immun* (1992) 60(3):1187–92. doi: 10.1128/iai.60.3.1187-1192.1992

13. Li G, Sun S, Zhao ZY, Sun Y. The pathogenicity of rmpa or aerobactin-positive klebsiella pneumoniae in infected mice. *J Int Med Res* (2019) 47(9):4344–52. doi: 10.1177/0300060519863544

14. Kline KA, Ingersoll MA, Nielsen HV, Sakinc T, Henriques-Normark B, Gatermann S, et al. Characterization of a novel murine model of staphylococcus saprophyticus urinary tract infection reveals roles for ssp and sdri in virulence. *Infect Immun* (2010) 78(5):1943–51. doi: 10.1128/IAI.01235-09

15. Ekwealor PA, Ugwu MC, Ezeobi I, Amalukwe G, Ugwu BC, Okezie U, et al. Antimicrobial evaluation of bacterial isolates from urine specimen of patients with complaints of urinary tract infections in awka, Nigeria. *Int J Microbiol* (2016) 2016:9740273. doi: 10.1155/2016/9740273

16. Mortimer TD, Annis DS, O'Neill MB, Bohr LL, Smith TM, Poinar HN, et al. Adaptation in a fibronectin binding autolysin of staphylococcus saprophyticus. *mSphere* (2017) 2(6):e00511-17. doi: 10.1128/mSphere.00511-17

17. Deutch CE. Limited effectiveness of over-the-Counter plant preparations used for the treatment of urinary tract infections as inhibitors of the urease activity from staphylococcus saprophyticus. *J Appl Microbiol* (2017) 122(5):1380–8. doi: 10.1111/jam.13430

18. Juralowicz E, Bartoszko-Tyczkowska A, Tyczkowska-Sieron E, Kurnatowska I. Etiology and bacterial susceptibility to antibiotics in patients with recurrent lower urinary tract infections. *Pol Arch Intern Med* (2020) 130 (5):373–81. doi: 10.20452/pamw.15284

19. Nallapareddy SR, Singh KV, Sillanpaa J, Zhao M, Murray BE. Relative contributions of ebp pili and the collagen adhesin ace to host extracellular matrix protein adherence and experimental urinary tract infection by enterococcus faecalis Og1rf. *Infect Immun* (2011) 79(7):2901–10. doi: 10.1128/IAI.00038-11

20. Xu W, Flores-Mireles AL, Cusumano ZT, Takagi E, Hultgren SJ, Caparon MG. Host and bacterial proteases influence biofilm formation and virulence in a murine model of enterococcal catheter-associated urinary tract infection. *NPJ Biofilms Microbiomes* (2017) 3:28. doi: 10.1038/s41522-017-0036-z

21. Ahmed N, Le Jeune A, Torelli R, Sanguinetti M, Giard J-C, Hartke A, et al. The extracytoplasmic function sigma factor sigv plays a key role in the original model of lysozyme resistance and virulence of enterococcus faecalis. *PloS One* (2010) 5(3):e9658. doi: 10.1371/journal.pone.0009658

22. Kulkarni R, Randis TM, Antala S, Wang A, Amaral FE, Ratner AJ. Beta-Hemolysin/Cytolysin of group b streptococcus enhances host inflammation but is dispensable for establishment of urinary tract infection. *PloS One* (2013) 8(3): e59091. doi: 10.1371/journal.pone.0059091

23. Kline KA, Schwartz DJ, Gilbert NM, Hultgren SJ, Lewis AL. Immune modulation by group b streptococcus influences host susceptibility to urinary tract infection by uropathogenic escherichia coli. *Infect Immun* (2012) 80 (12):4186–94. doi: 10.1128/IAI.00684-12

24. Guo Y, Deng X, Liang Y, Zhang L, Zhao GP, Zhou Y. The draft genomes and investigation of serotype distribution, antimicrobial resistance of group b streptococcus strains isolated from urine in suzhou, China. *Ann Clin Microbiol Antimicrob* (2018) 17(1):28. doi: 10.1186/s12941-018-0280-y

25. Shrestha LB, Baral R, Poudel P, Khanal B. Clinical, etiological and antimicrobial susceptibility profile of pediatric urinary tract infections in a tertiary care hospital of Nepal. *BMC Pediatr* (2019) 19(1):36. doi: 10.1186/s12887-019-1410-1

26. Belas R, Manos J, Suvanasuthi R. Proteus Mirabilis zapa metalloprotease degrades a broad spectrum of substrates, including antimicrobial peptides. *Infect Immun* (2004) 72(9):5159–67. doi: 10.1128/IAI.72.9.5159-5167.2004

27. Scavone P, Villar S, Umpierrez A, Zunino P. Role of Proteus mirabilis Mr/P fimbriae and flagella in adhesion, cytotoxicity and genotoxicity induction in T24 and vero cells. *Pathog Dis* (2015) 73(4):ftv017. doi: 10.1093/femspd/ftv017

28. Nielubowicz GR, Mobley HL. Host-pathogen interactions in urinary tract infection. *Nat Rev Urol* (2010) 7(8):430–41. doi: 10.1038/nrurol.2010.101

29. Dumanski A, Hedelin H, Edin-Liljegren A, Beauchemin D, McLean RJ. Unique ability of the Proteus mirabilis capsule to enhance mineral growth in infectious urinary calculi. *Infect Immun* (1994) 62(7):2998–3003. doi: 10.1128/iai.62.7.2998-3003.1994

30. Himpsl SD, Pearson MM, Arewang CJ, Nusca TD, Sherman DH, Mobley HL. Proteobactin and a yersiniabactin-related siderophore mediate iron acquisition in Proteus mirabilis. *Mol Microbiol* (2010) 78(1):138–57. doi: 10.1111/j.1365-2958.2010.07317.x

31. Yuan F, Huang Z, Yang T, Wang G, Li P, Yang B, et al. Pathogenesis of Proteus mirabilis in catheter-associated urinary tract infections. *Urol Int* (2021) 105 (5-6):354–61. doi: 10.1159/000514097

32. Al-Orphaly M, Hadi HA, Eltayeb FK, Al-Hail H, Samuel BG, Sultan AA, et al. Epidemiology of multidrug-resistant pseudomonas aeruginosa in the middle East and north Africa region. *mSphere* (2021) 6(3):e00202–21. doi: 10.1128/mSphere.00202-21

33. Kroken A, Chen C, Evans D, Yahr T, Fleiszig SJ. Pseudomonas aeruginosathe impact of exos on internalization by epithelial cells is independent of and correlates with bistability of type three secretion system gene expression. *mBio* (2018) 9(3):e00668-18. doi: 10.1128/mBio.00668-18

34. Newman J, Floyd R, Fothergill JL. The contribution of pseudomonas aeruginosa virulence factors and host factors in the establishment of urinary tract infections. *FEMS Microbiol Lett* (2017) 364(15):fnx124. doi: 10.1093/femsle/fnx124

35. Montagut E, Marco M. Biological and clinical significance of quorum sensing alkylquinolones: Current analytical and bioanalytical methods for their quantification. *Anal Bioanal Chem* (2021) 413(18):4599–618. doi: 10.1007/s00216-021-03356-x

36. Gharaghani M, Rezaei-Matehkolaei A, Hardani AK, Zarei Mahmoudabadi A. Genotypic diversity and antifungal susceptibility pattern of candida albicans species isolated from hospitalized paediatric patients with urinary tract infection in Iran. *J Appl Microbiol* (2021) 131(2):1017–27. doi: 10.1111/jam.15006

37. Kauffman C. Diagnosis and management of fungal urinary tract infection. *Infect Dis Clin North Am* (2014) 28(1):61–74. doi: 10.1016/j.idc.2013.09.004

38. Walker JN, Flores-Mireles AL, Pinkner CL, Schreiber H, Joens MS, Park AM, et al. Catheterization alters bladder ecology to potentiate staphylococcus aureus infection of the urinary tract. *Proc Natl Acad Sci U.S.A.* (2017) 114(41): E8721–E30. doi: 10.1073/pnas.1707572114

39. Kot B. Antibiotic resistance among uropathogenic escherichia coli. *Pol J Microbiol* (2019) 68(4):403–15. doi: 10.33073/pjm-2019-048

40. Talan DA, Takhar SS, Krishnadasan A, Mower WR, Pallin DJ, Garg M, et al. Emergence of extended-spectrum beta-lactamase urinary tract infections among hospitalized emergency department patients in the united states. *Ann Emerg Med* (2021) 77(1):32–43. doi: 10.1016/j.annemergmed.2020.08.022

41. Boucher HW, Ambrose PG, Chambers HF, Ebright RH, Jezek A, Murray BE, et al. White paper: Developing antimicrobial drugs for resistant pathogens, narrow-spectrum indications, and unmet needs. *J Infect Dis* (2017) 216(2):228–36. doi: 10.1093/infdis/jix211

42. WHO. Global priority list of antibiotic-resistant bacteria to guide research, discovery, and development of new antibiotics. In: *World health organization* (2017). World Health Organization (Switzerland). Available at: https://www.who.int/news/item/27-02-2017-who-publishes-list-of-bacteria-for-which-new-antibiotics-are-urgently-needed.

43. Abraham SN, Miao Y. The nature of immune responses to urinary tract infections. *Nat Rev Immunol* (2015) 15(10):655–63. doi: 10.1038/nri3887

44. Schwab S, Jobin K, Kurts C. Urinary tract infection: Recent insight into the evolutionary arms race between uropathogenic escherichia coli and our immune system. *Nephrol Dial Transplant* (2017) 32(12):1977–83. doi: 10.1093/ndt/gfx022

45. Ortega Martell JA. Immunology of urinary tract infections. *GMS Infect Dis* (2020) 8:Doc21. doi: 10.3205/id000065

46. Patras KA, Coady A, Babu P, Shing SR, Ha AD, Rooholfada E, et al. Host cathelicidin exacerbates group b streptococcus urinary tract infection. *mSphere* (2020) 5(2):e00932–19. doi: 10.1128/mSphere.00932-19

47. Chromek M, Slamová Z, Bergman P, Kovács L, Podracká L, Ehrén I, et al. The antimicrobial peptide cathelicidin protects the urinary tract against invasive bacterial infection. *Nat Med* (2006) 12(6):636–41. doi: 10.1038/nm1407

48. Wnorowska U, Piktel E, Durnas B, Fiedoruk K, Savage PB, Bucki R. Use of ceragenins as a potential treatment for urinary tract infections. *BMC Infect Dis* (2019) 19(1):369. doi: 10.1186/s12879-019-3994-3

49. Tamadonfar KO, Omattage NS, Spaulding CN, Hultgren SJ. Reaching the end of the line: Urinary tract infections. *Microbiol Spectr* (2019) 7(3):BAI-0014-2019. doi: 10.1128/microbiolspec.BAI-0014-2019

50. Hatton NE, Baumann CG, Fascione MA. Developments in mannose-based treatments for uropathogenic escherichia coli-induced urinary tract infections. *Chembiochem* (2021) 22(4):613–29. doi: 10.1002/cbic.202000406

51. Devuyst O, Olinger E, Rampoldi L. Uromodulin: From physiology to rare and complex kidney disorders. *Nat Rev Nephrol* (2017) 13(9):525–44. doi: 10.1038/nrneph.2017.101

52. Scharf B, Sendker J, Dobrindt U, Hensel A. Influence of cranberry extract on tamm-horsfall protein in human urine and its antiadhesive activity against uropathogenic escherichia coli. *Planta Med* (2019) 85(2):126–38. doi: 10.1055/a-0755-7801

53. Weiss G, Stanisich J, Sauer M, Lin C, Eras J, Zyla D, et al. Architecture and function of human uromodulin filaments in urinary tract infections. *Science* (2020) 369(6506):1005–10. doi: 10.1126/science.aaz9866

54. Pak J, Pu Y, Zhang ZT, Hasty DL, Wu XR. Tamm-horsfall protein binds to type 1 fimbriated escherichia coli and prevents e. coli from binding to uroplakin ia and ib receptors. *J Biol Chem* (2001) 276(13):9924–30. doi: 10.1074/jbc.M008610200

55. Patras KA, Coady A, Olson J, Ali SR, RamachandraRao SP, Kumar S, et al. Tamm-horsfall glycoprotein engages human siglec-9 to modulate neutrophil activation in the urinary tract. *Immunol Cell Biol* (2017) 95(10):960–5. doi: 10.1038/icb.2017.63

56. Behzadi E, Behzadi P. The role of toll-like receptors (Tlrs) in urinary tract infections (Utis). *Cent Eur J Urol* (2016) 69(4):404–10. doi: 10.5173/ceju.2016.871

57. Isaacson B, Hadad T, Glasner A, Gur C, Granot Z, Bachrach G, et al. Stromal cell-derived factor 1 mediates immune cell attraction upon urinary tract infection. *Cell Rep* (2017) 20(1):40–7. doi: 10.1016/j.celrep.2017.06.034

58. Ching CB, Gupta S, Li B, Cortado H, Mayne N, Jackson AR, et al. Interleukin-6/Stat3 signaling has an essential role in the host antimicrobial response to urinary tract infection. *Kidney Int* (2018) 93(6):1320–9. doi: 10.1016/j.kint.2017.12.006

59. Jaillon S, Moalli F, Ragnarsdottir B, Bonavita E, Puthia M, Riva F, et al. The humoral pattern recognition molecule Ptx3 is a key component of innate immunity against urinary tract infection. *Immunity* (2014) 40(4):621–32. doi: 10.1016/j.immuni.2014.02.015

60. Bottek J, Soun C, Lill JK, Dixit A, Thiebes S, Beerlage A-L, et al. Spatial proteomics revealed a Cx3cl1-dependent crosstalk between the urothelium and relocated macrophages through il-6 during an acute bacterial infection in the urinary bladder. *Mucosal Immunol* (2020) 13(4):702–14. doi: 10.1038/s41385-020-0269-7

61. Owusu-Boaitey N, Bauckman KA, Zhang T, Mysorekar IU. Macrophagic control of the response to uropathogenic e. coli infection by regulation of iron retention in an il-6-Dependent manner. *Immun Inflammation Dis* (2016) 4(4):413–26. doi: 10.1002/iid3.123

62. Spencer JD, Schwaderer AL, Wang H, Bartz J, Kline J, Eichler T, et al. Ribonuclease 7, an antimicrobial peptide upregulated during infection, contributes to microbial defense of the human urinary tract. *Kidney Int* (2013) 83(4):615–25. doi: 10.1038/ki.2012.410

63. Eichler T, Bender K, Murtha MJ, Schwartz L, Metheny J, Solden L, et al. Ribonuclease 7 shields the kidney and bladder from invasive uropathogenic escherichia coli infection. *J Am Soc Nephrol* (2019) 30(8):1385–97. doi: 10.1681/ASN.2018090929

64. Pierce K, Eichler T, Mosquera Vasquez C, Schwaderer A, Simoni A, Creacy S, et al. Ribonuclease 7 polymorphism Rs1263872 reduces antimicrobial activity and associates with pediatric urinary tract infections. *J Clin Invest* (2021) 131(22):e149807. doi: 10.1172/jci149807

65. Hirakawa H, Suzue K, Kurabayashi K, Tomita H. The tol-pal system of uropathogenic escherichia coli is responsible for optimal internalization into and aggregation within bladder epithelial cells, colonization of the urinary tract of mice, and bacterial motility. *Front Microbiol* (2019) 10:1827. doi: 10.3389/fmicb.2019.01827

66. Kim W-J, Shea AE, Kim J-H, Daaka Y. Uropathogenic escherichia coli invades bladder epithelial cells by activating kinase networks in host cells. *J Biol Chem* (2018) 293(42):16518–27. doi: 10.1074/jbc.RA118.003499

67. Miao Y, Bist P, Wu J, Zhao Q, Li Q-j, Wan Y, et al. Collaboration between distinct rab small gtpase trafficking circuits mediates bacterial clearance from the bladder epithelium. *Cell Host Microbe* (2017) 22(3):330–42.e4. doi: 10.1016/j.chom.2017.08.002

68. Miao Y, Wu J, Abraham SN. Ubiquitination of innate immune regulator Traf3 orchestrates expulsion of intracellular bacteria by exocyst complex. *Immunity* (2016) 45(1):94–105. doi: 10.1016/j.immuni.2016.06.023

69. Wang C, Bauckman KA, Ross ASB, Symington JW, Ligon MM, Scholtes G, et al. A non-canonical autophagy-dependent role of the Atg16l1(T300a) variant in urothelial vesicular trafficking and uropathogenic escherichia coli persistence. *Autophagy* (2019) 15(3):527–42. doi: 10.1080/15548627.2018.1535290

70. Song J, Bishop B, Li G, Grady R, Stapleton A, Abraham SN. Tlr4-mediated expulsion of bacteria from infected bladder epithelial cells. *Proc Natl Acad Sci U.S.A.* (2009) 106(35):14966–71. doi: 10.1073/pnas.0900527106

71. Miao Y, Li G, Zhang X, Xu H, Abraham SN. A trp channel senses lysosome neutralization by pathogens to trigger their expulsion. *Cell* (2015) 161(6):1306–19. doi: 10.1016/j.cell.2015.05.009

72. Duell BL, Carey AJ, Tan CK, Cui X, Webb RI, Totsika M, et al. Innate transcriptional networks activated in bladder in response to uropathogenic escherichia coli drive diverse biological pathways and rapid synthesis of il-10 for defense against bacterial urinary tract infection. *J Immunol* (2012) 188(2):781–92. doi: 10.4049/jimmunol.1101231

73. Ingersoll MA, Kline KA, Nielsen HV, Hultgren SJ. G-Csf induction early in uropathogenic escherichia coli infection of the urinary tract modulates host immunity. *Cell Microbiol* (2008) 10(12):2568–78. doi: 10.1111/j.1462-5822.2008.01230.x

74. Sivick KE, Schaller MA, Smith SN, Mobley HL. The innate immune response to uropathogenic escherichia coli involves il-17a in a murine model of urinary tract infection. *J Immunol* (2010) 184(4):2065–75. doi: 10.4049/jimmunol.0902386

75. Schiwon M, Weisheit C, Franken L, Gutweiler S, Dixit A, Meyer-Schwesinger C, et al. Crosstalk between sentinel and helper macrophages permits neutrophil migration into infected uroepithelium. *Cell* (2014) 156(3):456–68. doi: 10.1016/j.cell.2014.01.006

76. Demirel I, Persson A, Brauner A, Sarndahl E, Kruse R, Persson K. Activation of the Nlrp3 inflammasome pathway by uropathogenic escherichia coli is virulence factor-dependent and influences colonization of bladder epithelial cells. *Front Cell Infect Microbiol* (2018) 8:81. doi: 10.3389/fcimb.2018.00081

77. Wu Z, Li Y, Liu Q, Liu Y, Chen L, Zhao H, et al. Pyroptosis engagement and bladder urothelial cell-derived exosomes recruit mast cells and induce barrier dysfunction of bladder urothelium after uropathogenic E.Coli infection. *Am J Physiol Cell Physiol* (2019) 317(3):C544–C55. doi: 10.1152/ajpcell.00102.2019

78. Hannan TJ, Roberts PL, Riehl TE, van der Post S, Binkley JM, Schwartz DJ, et al. Inhibition of cyclooxygenase-2 prevents chronic and recurrent cystitis. *EBioMedicine* (2014) 1(1):46–57. doi: 10.1016/j.ebiom.2014.10.011

79. Chen T, Tsai J, Huang H, Teng C, Chien S, Kuo H, et al. Regulation of cyclooxygenase-2 expression in human bladder epithelial cells infected with type I fimbriated uropathogenic e. coli. *Cell Microbiol* (2011) 13(11):1703–13. doi: 10.1111/j.1462-5822.2011.01650.x

80. Himpsl SD, Shea AE, Zora J, Stocki JA, Foreman D, Alteri CJ, et al. The oxidative fumarase fumc is a key contributor for e. coli fitness under iron-limitation and during uti. *PloS Pathog* (2020) 16(2):e1008382. doi: 10.1371/journal.ppat.1008382

81. Bessaiah H, Pokharel P, Habouria H, Houle S, Dozois CM. Yqhg contributes to oxidative stress resistance and virulence of uropathogenic escherichia coli and identification of other genes altering expression of type 1 fimbriae. *Front Cell Infect Microbiol* (2019) 9:312. doi: 10.3389/fcimb.2019.00312

82. Sharma K, Thacker VV, Dhar N, Clapes Cabrer M, Dubois A, Signorino-Gelo F, et al. Early invasion of the bladder wall by solitary bacteria protects upec from antibiotics and neutrophil swarms in an organoid model. *Cell Rep* (2021) 36 (3):109351. doi: 10.1016/j.celrep.2021.109351

83. Hicks RM. The mammalian urinary bladder: An accommodating organ. *Biol Rev Camb Philos Soc* (1975) 50(2):215–46. doi: 10.1111/j.1469-185x.1975.tb01057.x

84. Wu J, Hayes BW, Phoenix C, Macias GS, Miao Y, Choi HW, et al. A highly polarized Th2 bladder response to infection promotes epithelial repair at the expense of preventing new infections. *Nat Immunol* (2020) 21(6):671–83. doi: 10.1038/s41590-020-0688-3

85. Liu C, Tate T, Batourina E, Truschel ST, Potter S, Adam M, et al. Pparg promotes differentiation and regulates mitochondrial gene expression in bladder epithelial cells. *Nat Commun* (2019) 10(1):4589. doi: 10.1038/s41467-019-12332-0

86. Shin K, Lee J, Guo N, Kim J, Lim A, Qu L, et al. Hedgehog/Wnt feedback supports regenerative proliferation of epithelial stem cells in bladder. *Nature* (2011) 472(7341):110–4. doi: 10.1038/nature09851

87. Bohnenpoll T, Wittern AB, Mamo TM, Weiss AC, Rudat C, Kleppa MJ, et al. A shh-Foxf1-Bmp4 signaling axis regulating growth and differentiation of epithelial and mesenchymal tissues in ureter development. *PloS Genet* (2017) 13(8): e1006951. doi: 10.1371/journal.pgen.1006951

88. Alfouzan W, Dhar R, Abdo NM, Alali WQ, Rabaan AA. Epidemiology and microbiological profile of common healthcare associated infections among patients in the intensive care unit of a general hospital in Kuwait: A retrospective observational study. *J Epidemiol Glob Health* (2021) 3:302–9. doi: 10.2991/jegh.k.210524.001

89. Chang Y, Jeon K, Lee SM, Cho YJ, Kim YS, Chong YP, et al. The distribution of multidrug-resistant microorganisms and treatment status of hospital-acquired Pneumonia/Ventilator-associated pneumonia in adult intensive care units: A prospective cohort observational study. *J Korean Med Sci* (2021) 36(41):e251. doi: 10.3346/jkms.2021.36.e251

90. Wang G, Zhao G, Chao X, Xie L, Wang H. The characteristic of virulence, biofilm and antibiotic resistance of klebsiella pneumoniae. *Int J Environ Res Public Health* (2020) 17(17):6278. doi: 10.3390/ijerph17176278

91. Raffi HS, Bates JMJr., Laszik Z, Kumar S. Tamm-horsfall protein acts as a general host-defense factor against bacterial cystitis. *Am J Nephrol* (2005) 25 (6):570–8. doi: 10.1159/000088990

92. Song J, Bishop B, Li G, Duncan M, Abraham SN. Tlr4-initiated and camp-mediated abrogation of bacterial invasion of the bladder. *Proc Natl Acad Sci U.S.A.* (2007) 1(4):287–98. doi: 10.1016/j.chom.2007.05.007

93. Nanduri R, Furusawa T, Bustin M. Biological functions of hmgn chromosomal proteins. *Int J Mol Sci* (2020) 21(2):449. doi: 10.3390/ijms21020449

94. Wu G, Cao Y, Fan B, Zheng F, Gao X, Liu N, et al. High-mobility group protein N2 (Hmgn2) inhibited the internalization of klebsiella pneumoniae into cultured bladder epithelial cells. *Acta Biochim Biophys Sin (Shanghai)* (2011) 43 (9):680–7. doi: 10.1093/abbs/gmr064

95. Lu H, Wu Q, Yang H. Duox2 promotes the elimination of the klebsiella pneumoniae strain K5 from T24 cells through the reactive oxygen species pathway. *Int J Mol Med* (2015) 36(2):551–8. doi: 10.3892/ijmm.2015.2234

96. Dang PM, Rolas L, El-Benna J. The dual role of reactive oxygen species-generating nicotinamide adenine dinucleotide phosphate oxidases in gastrointestinal inflammation and therapeutic perspectives. *Antioxid Redox Signal* (2020) 33(5):354–73. doi: 10.1089/ars.2020.8018

97. Aviello G, Knaus UG. Nadph oxidases and ros signaling in the gastrointestinal tract. *Mucosal Immunol* (2018) 11(4):1011–23. doi: 10.1038/s41385-018-0021-8

98. Van Acker H, Coenye T. The role of reactive oxygen species in antibiotic-mediated killing of bacteria. *Trends Microbiol* (2017) 25(6):456–66. doi: 10.1016/j.tim.2016.12.008

99. Pinegin B, Vorobjeva N, Pashenkov M, Chernyak B. The role of mitochondrial ros in antibacterial immunity. *J Cell Physiol* (2018) 233(5):3745–54. doi: 10.1002/jcp.26117

100. Gerlach G, Clegg S, Allen BL. Identification and characterization of the genes encoding the type 3 and type 1 fimbrial adhesins of klebsiella pneumoniae. *J Bacteriol* (1989) 171(3):1262–70. doi: 10.1128/jb.171.3.1262-1270.1989

101. Rosen DA, Pinkner JS, Walker JN, Elam JS, Jones JM, Hultgren SJ. Molecular variations in klebsiella pneumoniae and escherichia coli fimh affect function and pathogenesis in the urinary tract. *Infect Immun* (2008) 76(7):3346–56. doi: 10.1128/IAI.00340-08

102. Rosen DA, Pinkner JS, Jones JM, Walker JN, Clegg S, Hultgren SJ. Utilization of an intracellular bacterial community pathway in klebsiella pneumoniae urinary tract infection and the effects of fimk on type 1 pilus expression. *Infection Immun* (2008) 76(7):3337–45. doi: 10.1128/iai.00090-08

103. Ehlers S, Merrill SA. Staphylococcus saprophyticus. In: *Statpearls*. Treasure Island (FL: StatPearls Publishing Copyright © 2022, StatPearls Publishing LLC (2022).

104. Souza BSV, Silva KCS, Parente AFA, Borges CL, Paccez JD, Pereira M, et al. The influence of ph on staphylococcus saprophyticus iron metabolism and the production of siderophores. *Microbes Infection* (2019) 21(10):456–63. doi: 10.1016/j.micinf.2019.04.008

105. Böswald L, Matzek D, Kienzle E, Popper B. Influence of strain and diet on urinary ph in laboratory mice. *Anim (Basel)* (2021) 11(3):702. doi: 10.3390/ani11030702

106. Wang H, Schwaderer AL, Kline J, Spencer JD, Kline D, Hains DS. Contribution of structural domains to the activity of ribonuclease 7 against uropathogenic bacteria. *Antimicrobial Agents Chemother* (2012) 57(2):766–74. doi: 10.1128/aac.01378-12

107. Spencer JD, Jackson AR, Li B, Ching CB, Vonau M, Easterling RS, et al. Expression and significance of the Hip/Pap and regiiigamma antimicrobial peptides during mammalian urinary tract infection. *PloS One* (2015) 10(12): e0144024. doi: 10.1371/journal.pone.0144024

108. Fan H, Wang Y, Zhang X, Chen J, Zhou Q, Yu Z, et al. Ginsenoside compound K ameliorates imiquimod-induced psoriasis-like dermatitis through inhibiting Reg3a/Regiiigamma expression in keratinocytes. *Biochem Biophys Res Commun* (2019) 515(4):665–71. doi: 10.1016/j.bbrc.2019.06.007

109. Lai Y, Li D, Li C, Muehleisen B, Radek KA, Park HJ, et al. The antimicrobial protein Reg3a regulates keratinocyte proliferation and differentiation after skin injury. *Immunity* (2012) 37(1):74–84. doi: 10.1016/j.immuni.2012.04.010

110. Chen Y, Lu H, Liu Q, Huang G, Lim CP, Zhang L, et al. Function of grim-19, a mitochondrial respiratory chain complex I protein, in innate immunity. *J Biol Chem* (2012) 287(32):27227–35. doi: 10.1074/jbc.M112.340315

111. Nallar SC, Kalvakolanu DV. Grim-19: A master regulator of cytokine induced tumor suppression, metastasis and energy metabolism. *Cytokine Growth Factor Rev* (2017) 33:1–18. doi: 10.1016/j.cytogfr.2016.09.001

112. Bhola P, Mvelase NR, Balakrishna Y, Mlisana KP, Swe Swe-Han K. Antimicrobial susceptibility patterns of uropathogens isolated from pregnant women in kwazulu-natal province: 2011 - 2016. *S Afr Med J* (2020) 110(9):872–6. doi: 10.7196/SAMJ.2020.v110i9.14468

113. Kraemer TD, Quintanar Haro OD, Domann E, Chakraborty T, Tchatalbachev S. The tir domain containing locus ofenterococcus faecalisis predominant among urinary tract infection isolates and downregulates host inflammatory response. *Int J Microbiol* (2014) 2014:1–9. doi: 10.1155/2014/918143

114. Kathirvel S, Mani M, Gopala Krishnan GK, Sethumadhavan A, Vijayalakshmi T, Ponnan SM, et al. Molecular characterization of enterococcus faecalis isolates from urinary tract infection and interaction between enterococcus faecalis encountered dendritic and natural killer cells. *Microb Pathog* (2020) 140:103944. doi: 10.1016/j.micpath.2019.103944

115. Cai S, Zhu G, Cen X, Bi J, Zhang J, Tang X, et al. Synthesis, structure-activity relationships and preliminary mechanism study of n-benzylideneaniline derivatives as potential Tlr2 inhibitors. *Bioorg Med Chem* (2018) 26(8):2041–50. doi: 10.1016/j.bmc.2018.03.001

116. Munoz MD, Gutierrez LJ, Delignat S, Russick J, Gomez Mejiba SE, Lacroix-Desmazes S, et al. The nitrone spin trap 5,5dimethyl1pyrroline noxide binds to toll-like receptor-2-Tir-Bb-Loop domain and dampens downstream inflammatory signaling. *Biochim Biophys Acta Mol Basis Dis* (2019) 1865 (6):1152–9. doi: 10.1016/j.bbadis.2019.01.005

117. Zou J, Baghdayan AS, Payne SJ, Shankar N. A tir domain protein from e. faecalis attenuates Myd88-mediated signaling and nf-kappab activation. *PloS One* (2014) 9(11):e112010. doi: 10.1371/journal.pone.0112010

118. Tien BYQ, Goh HMS, Chong KKL, Bhaduri-Tagore S, Holec S, Dress R, et al. Enterococcus faecalis promotes innate immune suppression and polymicrobial catheter-associated urinary tract infection. *Infection Immun* (2017) 85(12):e00378–17. doi: 10.1128/iai.00378-17

119. Gause WC, Mora-Bau G, Platt AM, van Rooijen N, Randolph GJ, Albert ML, et al. Macrophages subvert adaptive immunity to urinary tract infection. *PloS Pathog* (2015) 11(7):e1005044. doi: 10.1371/journal.ppat.1005044

120. Chan Cheryl Y, St. John Ashley L, Abraham Soman N. Mast cell interleukin-10 drives localized tolerance in chronic bladder infection. *Immunity* (2013) 38(2):349–59. doi: 10.1016/j.immuni.2012.10.019

121. Jalalifar S, Havaei SA, Motallebirad T, Moghim S, Fazeli H, Esfahani BN. Determination of surface proteins profile, capsular genotyping, and antibiotic susceptibility patterns of group b streptococcus isolated from urinary tract infection of Iranian patients. *BMC Res Notes* (2019) 12(1):437. doi: 10.1186/s13104-019-4428-4

122. Ulett KB, Benjamin WHJr., Zhuo F, Xiao M, Kong F, Gilbert GL, et al. Diversity of group b streptococcus serotypes causing urinary tract infection in adults. *J Clin Microbiol* (2009) 47(7):2055–60. doi: 10.1128/JCM.00154-09

123. Girma W, Yimer N, Kassa T, Yesuf E. Group b streptococcus recto-vaginal colonization in near-term pregnant women, southwest Ethiopia. *Ethiop J Health Sci* (2020) 30(5):687–96. doi: 10.4314/ejhs.v30i5.7

124. John PP, Baker BC, Paudel S, Nassour L, Cagle H, Kulkarni R. Exposure to moderate glycosuria induces virulence of group b streptococcus. *J Infect Dis* (2021) 223(5):843–7. doi: 10.1093/infdis/jiaa443

125. Leclercq SY, Sullivan MJ, Ipe DS, Smith JP, Cripps AW, Ulett GC. Pathogenesis of streptococcus urinary tract infection depends on bacterial strain and β-Hemolysin/Cytolysin that mediates cytotoxicity, cytokine synthesis, inflammation and virulence. *Sci Rep* (2016) 6(1):29000. doi: 10.1038/srep29000

126. Ulett GC, Webb RI, Ulett KB, Cui X, Benjamin WH, Crowley M, et al. Group b streptococcus (Gbs) urinary tract infection involves binding of gbs to bladder uroepithelium and potent but gbs-specific induction of interleukin 1alpha. *J Infect Dis* (2010) 201(6):866–70. doi: 10.1086/650696

127. Burgener SS, Schroder K. Neutrophil extracellular traps in host defense. *Cold Spring Harb Perspect Biol* (2020) 12(7):a037028. doi: 10.1101/cshperspect.a037028

128. Tsai CY, Hsieh SC, Liu CW, Lu CS, Wu CH, Liao HT, et al. Cross-talk among polymorphonuclear neutrophils, immune, and non-immune cells *Via* released cytokines, granule proteins, microvesicles, and neutrophil extracellular trap formation: A novel concept of biology and pathobiology for neutrophils. *Int J Mol Sci* (2021) 22(6):3119. doi: 10.3390/ijms22063119

129. Costa A, Gupta R, Signorino G, Malara A, Cardile F, Biondo C, et al. Activation of the Nlrp3 inflammasome by group b streptococci. *J Immunol* (2012) 188(4):1953–60. doi: 10.4049/jimmunol.1102543

130. Tsai CM, Riestra AM, Ali SR, Fong JJ, Liu JZ, Hughes G, et al. Siglec-14 enhances Nlrp3-inflammasome activation in macrophages. *J Innate Immun* (2020) 12(4):333–43. doi: 10.1159/000504323

131. Kline KA, Schwartz DJ, Lewis WG, Hultgren SJ, Lewis AL, Camilli A. Immune activation and suppression by group b streptococcus in a murine model of urinary tract infection. *Infection Immun* (2011) 79(9):3588–95. doi: 10.1128/iai.00122-11

132. Babikir IH, Abugroun EA, Bilal NE, Alghasham AA, Abdalla EE, Adam I. The impact of cathelicidin, the human antimicrobial peptide ll-37 in urinary tract infections. *BMC Infect Dis* (2018) 18(1):17. doi: 10.1186/s12879-017-2901-z

133. Pearson MM. Methods for studying swarming and swimming motility. *Methods Mol Biol* (2019) 2021:15–25. doi: 10.1007/978-1-4939-9601-8_3

134. Raffi HS, Bates JMJr., Laszik Z, Kumar S. Tamm-horsfall protein protects against urinary tract infection by Proteus mirabilis. *J Urol* (2009) 181(5):2332–8. doi: 10.1016/j.juro.2009.01.014

135. Armbruster CE, Mobley HLT, Pearson MM. Pathogenesis of Proteus mirabilis infection. *EcoSal Plus* (2018) 8(1):ESP-0009-2017. doi: 10.1128/ecosalplus.ESP-0009-2017

136. Umpiérrez A, Scavone P, Romanin D, Marqués JM, Chabalgoity JA, Rumbo M, et al. Innate immune responses to Proteus mirabilis flagellin in the urinary tract. *Microbes Infection* (2013) 15(10-11):688–96. doi: 10.1016/j.micinf.2013.06.007

137. Scavone P, Umpierrez A, Rial A, Chabalgoity JA, Zunino P. Native flagellin does not protect mice against an experimental Proteus mirabilis ascending urinary tract infection and neutralizes the protective effect of mrpa fimbrial protein. *Antonie Van Leeuwenhoek* (2014) 105(6):1139–48. doi: 10.1007/s10482-014-0175-7

138. Mittal R, Sharma S, Chhibber S, Harjai K. Iron dictates the virulence of pseudomonas aeruginosa in urinary tract infections. *J Biomed Sci* (2008) 15(6):731–41. doi: 10.1007/s11373-008-9274-7

139. Harjai K, Mittal R, Chhibber S, Sharma S. Contribution of tamm–horsfall protein to virulence of pseudomonas aeruginosa in urinary tract infection. *Microbes Infection* (2005) 7(1):132–7. doi: 10.1016/j.micinf.2004.09.005

140. Sun F, Li N, Wang L, Feng H, Shen D, Wang M. Iron interferes with quorum sensing-mediated cooperation in pseudomonas aeruginosa by affecting the expression of ppyr and mext, in addition to rhlr. *J Microbiol* (2020) 58(11):938–44. doi: 10.1007/s12275-020-0264-4

141. Montagut EJ, Marco MP. Biological and clinical significance of quorum sensing alkylquinolones: Current analytical and bioanalytical methods for their quantification. *Anal Bioanal Chem* (2021) 18:4599–618. doi: 10.1007/s00216-021-03356-x

142. Mittal R, Chhibber S, Sharma S, Harjai KJM. Macrophage inflammatory protein-2, neutrophil recruitment and bacterial persistence in an experimental mouse model of urinary tract infection. *Microbes Infect* (2004) 6(14):1326–32. doi: 10.1016/j.micinf.2004.08.008

143. Poloni JAT, Rotta LN. Urine sediment findings and the immune response to pathologies in fungal urinary tract infections caused by candida spp. *J Fungi (Basel)* (2020) 6(4):245. doi: 10.3390/jof6040245

144. Coady A, Ramos AR, Olson J, Nizet V, Patras KA, Deepe GS. Tamm-horsfall protein protects the urinary tract againstcandida albicans. *Infection Immun* (2018) 86(12):e00451–18. doi: 10.1128/iai.00451-18

145. Chen H, Zhou X, Ren B, Cheng L. The regulation of hyphae growth in candida albicans. *Virulence* (2020) 11(1):337–48. doi: 10.1080/21505594.2020.1748930

146. Tsai PW, Yang CY, Chang HT, Lan CY. Human antimicrobial peptide ll-37 inhibits adhesion of candida albicans by interacting with yeast cell-wall carbohydrates. *PloS One* (2011) 6(3):e17755. doi: 10.1371/journal.pone.0017755

147. Arkowitz RA, Tsai P-W, Yang C-Y, Chang H-T, Lan C-Y. Characterizing the role of cell-wall β-1,3-Exoglucanase Xog1p in candida albicans adhesion by the human antimicrobial peptide ll-37. *PloS One* (2011) 6(6):e21394. doi: 10.1371/journal.pone.0021394

148. Wang S-H, Wang S-C, Chen P-C, Wang S-T, Liu Y-W. Induction of cyclooxygenase-2 gene bycandida albicansthrough egfr, erk, and P38 pathways in human urinary epithelium. *Med Mycol* (2016) 3:314–22. doi: 10.1093/mmy/myw082

149. Mahesh G, Anil Kumar K, Reddanna P. Overview on the discovery and development of anti-inflammatory drugs: Should the focus be on synthesis or degradation of Pge2? *J Inflammation Res* (2021) 14:253–63. doi: 10.2147/JIR.S278514

150. Rafa E, Walaszek MZ, Walaszek MJ, Domanski A, Rozanska A. The incidence of healthcare-associated infections, their clinical forms, and microbiological agents in intensive care units in southern Poland in a multicentre study from 2016 to 2019. *Int J Environ Res Public Health* (2021) 18(5):2238. doi: 10.3390/ijerph18052238

151. Litwin A, Fedorowicz O, Duszynska W. Characteristics of microbial factors of healthcare-associated infections including multidrug-resistant pathogens and antibiotic consumption at the university intensive care unit in Poland in the years 2011-2018. *Int J Environ Res Public Health* (2020) 17(19):6943. doi: 10.3390/ijerph17196943

152. Bazaid AS, Saeed A, Alrashidi A, Alrashidi A, Alshaghdali K, AH S, et al. Antimicrobial surveillance for bacterial uropathogens in ha'il, Saudi Arabia: A five-year multicenter retrospective study. *Infect Drug Resist* (2021) 14:1455–65. doi: 10.2147/IDR.S299846

153. Orskov I, Ferencz A, Orskov FJL. Tamm-horsfall protein or uromucoid is the normal urinary slime that traps type 1 fimbriated escherichia coli. *Lancet* (1980) 1(8173):887. doi: 10.1016/s0140-6736(80)91396-3

154. Schaeffer C, Devuyst O, Rampoldi L. Uromodulin: Roles in health and disease. *Annu Rev Physiol* (2021) 83:477–501. doi: 10.1146/annurev-physiol-031620-092817

155. Scharf B, Schmidt TJ, Rabbani S, Stork C, Dobrindt U, Sendker J, et al. Antiadhesive natural products against uropathogenic e. coli: What can we learn from cranberry extract? *J Ethnopharmacol* (2020) 257:112889. doi: 10.1016/j.jep.2020.112889

156. Kurutas EB, Ciragil P, Gul M, Kilinc M. The effects of oxidative stress in urinary tract infection. *Mediators Inflammation* (2005) 2005(4):242–4. doi: 10.1155/MI.2005.242

157. Cerezo AB, Cătunescu GM, González MM-P, Hornedo-Ortega R, Pop CR, Rusu CC, et al. Anthocyanins in blueberries grown in hot climate exert strong antioxidant activity and may be effective against urinary tract bacteria. *Antioxidants* (2020) 9(6):478. doi: 10.3390/antiox9060478

158. Ghouri F, Hollywood A, Ryan K. A systematic review of non-antibiotic measures for the prevention of urinary tract infections in pregnancy. *BMC Pregnancy Childbirth* (2018) 18(1):99. doi: 10.1186/s12884-018-1732-2

159. Kalt W, Cassidy A, Howard LR, Krikorian R, Stull AJ, Tremblay F, et al. Recent research on the health benefits of blueberries and their anthocyanins. *Adv Nutr* (2020) 11(2):224–36. doi: 10.1093/advances/nmz065

160. Wu X, Beecher G, Holden J, Haytowitz D, Gebhardt S, Prior RL, et al. Concentrations of anthocyanins in common foods in the united states and estimation of normal consumption. *J Agric Food Chem* (2006) 54(11):4069–75. doi: 10.1021/jf060300l

161. Lima A, Zunino P, D'Alessandro B, Piccini C. An iron-regulated outer-membrane protein of Proteus mirabilis is a haem receptor that plays an important role in urinary tract infection and in *in vivo* growth. *J Med Microbiol* (2007) 56(12):1600–7. doi: 10.1099/jmm.0.47320-0

162. Robinson AE, Lowe JE, Koh E-I, Henderson JP. Uropathogenic enterobacteria use the yersiniabactin metallophore system to acquire nickel. *J Biol Chem* (2018) 293(39):14953–61. doi: 10.1074/jbc.RA118.004483

163. Dogan O, Vatansever C, Atac N, Albayrak O, Karahuseyinoglu S, Sahin OE, et al. Virulence determinants of colistin-resistant k. pneumoniae high-risk clones. *Biol (Basel)* (2021) 10(5):436. doi: 10.3390/biology10050436

164. Patras KA, Ha AD, Rooholfada E, Olson J, Ramachandra Rao SP, Lin AE, et al. Augmentation of urinary lactoferrin enhances host innate immune clearance

of uropathogenic escherichia coli. *J Innate Immun* (2019) 11(6):481–95. doi: 10.1159/000499342

165. Bauckman K, Matsuda R, Higgins C, DeBosch B, Wang C, Mysorekar IU. Dietary restriction of iron availability attenuates upec pathogenesis in a mouse model of urinary tract infection. *Am J Physiol Renal Physiol* (2019) 316(5):F814–F22. doi: 10.1152/ajprenal.00133.2018

166. Annunziato G, Costantino G. Antimicrobial peptides (Amps): A patent review (2015-2020). *Expert Opin Ther Pat* (2020) 30(12):931–47. doi: 10.1080/13543776.2020.1851679

167. Eichler TE, Becknell B, Easterling RS, Ingraham SE, Cohen DM, Schwaderer AL, et al. Insulin and the phosphatidylinositol 3-kinase signaling pathway regulate ribonuclease 7 expression in the human urinary tract. *Kidney Int* (2016) 90(3):568–79. doi: 10.1016/j.kint.2016.04.025

168. Murtha M, Eichler T, Bender K, Metheny J, Li B, Schwaderer A, et al. Insulin receptor signaling regulates renal collecting duct and intercalated cell antibacterial defenses. *J Clin Invest* (2018) 128(12):5634–46. doi: 10.1172/jci98595

169. Ho C-H, Fan C-K, Wu C-C, Yu H-J, Liu H-T, Chen K-C, et al. Enhanced uropathogenic escherichia coli-induced infection in uroepithelial cells by sugar through tlr-4 and Jak/Stat1 signaling pathways. *J Microbiol Immunol Infection* (2019) 2:193–205. doi: 10.1016/j.jmii.2019.05.008

170. Esmailzadeh A, Zarrinfar H, Fata A, Sen T. High prevalence of candiduria due to non-albicans candida species among diabetic patients: A matter of concern? *J Clin Lab Anal* (2018) 32(4):e22343. doi: 10.1002/jcla.22343

171. Saenkham P, Jennings-Gee J, Hanson B, Kock ND, Adams LG, Subashchandrabose S. Hyperglucosuria induced by dapagliflozin augments bacterial colonization in the murine urinary tract. *Diabetes Obes Metab* (2020) 22(9):1548–55. doi: 10.1111/dom.14064

172. Mama M, Manilal A, Gezmu T, Kidanewold A, Gosa F, Gebresilasie A. Prevalence and associated factors of urinary tract infections among diabetic patients in arba minch hospital, arba minch province, south Ethiopia. *Turk J Urol* (2019) 45(1):56–62. doi: 10.5152/tud.2018.32855

173. Giannakopoulos X, Sakkas H, Ragos V, Tsiambas E, Bozidis P, M Evangelou A, et al. Impact of enterococcal urinary tract infections in immunocompromised - neoplastic patients. *J BUON* (2019) 24(5):1768–75.

174. Al-Rubeaan KA, Moharram O, Al-Naqeb D, Hassan A, Rafiullah MR. Prevalence of urinary tract infection and risk factors among Saudi patients with diabetes. *World J Urol* (2013) 31(3):573–8. doi: 10.1007/s00345-012-0934-x

175. Amiel SA. The consequences of hypoglycaemia. *Diabetologia* (2021) 64 (5):963–70. doi: 10.1007/s00125-020-05366-3

176. Olson PD, Hruska KA, Hunstad DA. Androgens enhance Male urinary tract infection severity in a new model. *J Am Soc Nephrol* (2016) 27(6):1625–34. doi: 10.1681/ASN.2015030327

177. Olson PD, McLellan LK, Hreha TN, Liu A, Briden KE, Hruska KA, et al. Androgen exposure potentiates formation of intratubular communities and renal abscesses by escherichia coli. *Kidney Int* (2018) 94(3):502–13. doi: 10.1016/j.kint.2018.04.023

178. Zychlinsky Scharff A, Rousseau M, Lacerda Mariano L, Canton T, Consiglio C, Albert M, et al. Sex differences in il-17 contribute to chronicity in Male versus female urinary tract infection. *JCI Insight* (2019) 5:e122998. doi: 10.1172/jci.insight.122998

179. Papotto PH, Ribot JC, Silva-Santos B. Il-17+ Γδ T cells as kick-starters of inflammation. *Nat Immunol* (2017) 18(6):604–11. doi: 10.1038/ni.3726

180. Veldhoen M. Interleukin 17 is a Chief orchestrator of immunity. *Nat Immunol* (2017) 18(6):612–21. doi: 10.1038/ni.3742

181. Baldwin CL, Yirsaw A, Gillespie A, Le Page L, Zhang F, Damani-Yokota P, et al. Gammadelta T cells in livestock: Responses to pathogens and vaccine potential. *Transbound Emerg Dis* (2020) 67 Suppl 2:119–28. doi: 10.1111/tbed.13328

182. Lee MY, Chen WC, Hsu WH, Chen SC, Lee JC. Liraglutide inhibits hepatitis c virus replication through an amp activated protein kinase dependent mechanism. *Int J Mol Sci* (2019) 20(18):4569. doi: 10.3390/ijms20184569

183. Duan X, Yang Y, Yang A, Zhao Y, Fan F, Niu L, et al. Terbutaline attenuates lps-induced injury of pulmonary microvascular endothelial cells by Camp/Epac signaling. *Drug Dev Res* (2021) 83(3):699–707. doi: 10.1002/ddr.21901

184. Wu J, Miao Y, Abraham SN. The multiple antibacterial activities of the bladder epithelium. *Ann Transl Med* (2017) 5(2):35. doi: 10.21037/atm.2016.12.71

185. Mowbray C, Shams S, Chung G, Stanton A, Aldridge P, Suchenko A, et al. High molecular weight hyaluronic acid: A two-pronged protectant against infection of the urogenital tract? *Clin Trans Immunol* (2018) 7(6):e1021. doi: 10.1002/cti2.1021

186. Damiano R, Quarto G, Bava I, Ucciero G, De Domenico R, Palumbo MI, et al. Prevention of recurrent urinary tract infections by intravesical administration of hyaluronic acid and chondroitin sulphate: A placebo-controlled randomised trial. *Eur Urol* (2011) 59(4):645–51. doi: 10.1016/j.eururo.2010.12.039

187. Cicione A, Cantiello F, Ucciero G, Salonia A, Torella M, De Sio M, et al. Intravesical treatment with highly-concentrated hyaluronic acid and chondroitin sulphate in patients with recurrent urinary tract infections: Results from a multicentre survey. *Can Urological Assoc J* (2014) 8(9-10):E721–7. doi: 10.5489/cuaj.1989

188. De Vita D, Giordano S. Effectiveness of intravesical hyaluronic Acid/Chondroitin sulfate in recurrent bacterial cystitis: A randomized study. *Int Urogynecol J* (2012) 23(12):1707–13. doi: 10.1007/s00192-012-1794-z

189. Mohanty S, Kamolvit W, Hertting O, Brauner A. Vitamin d strengthens the bladder epithelial barrier by inducing tight junction proteins during e. coli urinary tract infection. *Cell Tissue Res* (2020) 380(3):669–73. doi: 10.1007/s00441-019-03162-z

190. Ambite I, Puthia M, Nagy K, Cafaro C, Nadeem A, Butler DS, et al. Molecular basis of acute cystitis reveals susceptibility genes and immunotherapeutic targets. *PloS Pathog* (2016) 12(10):e1005848. doi: 10.1371/journal.ppat.1005848

191. Kronenberg A, Butikofer L, Odutayo A, Muhlemann K, da Costa BR, Battaglia M, et al. Symptomatic treatment of uncomplicated lower urinary tract infections in the ambulatory setting: Randomised, double blind trial. *BMJ* (2017) 359:j4784. doi: 10.1136/bmj.j4784

192. Vik I, Bollestad M, Grude N, Baerheim A, Damsgaard E, Neumark T, et al. Ibuprofen versus pivmecillinam for uncomplicated urinary tract infection in women-a double-blind, randomized non-inferiority trial. *PloS Med* (2018) 15(5): e1002569. doi: 10.1371/journal.pmed.1002569

193. Poolman JT, Wacker M. Extraintestinal pathogenic escherichia coli, a common human pathogen: Challenges for vaccine development and progress in the field. *J Infect Dis* (2016) 213(1):6–13. doi: 10.1093/infdis/jiv429

194. O'Brien VP, Hannan TJ, Nielsen HV, Hultgren SJ. Drug and vaccine development for the treatment and prevention of urinary tract infections. *Microbiol Spectr* (2016) 4(1):UTI-0013-2012. doi: 10.1128/microbiolspec.UTI-0013-2012

195. Aziminia N, Hadjipavlou M, Philippou Y, Pandian SS, Malde S, Hammadeh MY. Vaccines for the prevention of recurrent urinary tract infections: A systematic review. *BJU Int* (2019) 123(5):753–68. doi: 10.1111/bju.14606

196. Hasanzadeh S, Farokhi M, Habibi M, Shokrgozar MA, Ahangari Cohan R, Rezaei F, et al. Silk fibroin nanoadjuvant as a promising vaccine carrier to deliver the FimH-IutA antigen for urinary tract infection. *ACS Biomater Sci Eng* (2020) 6 (8):4573–82. doi: 10.1021/acsbiomaterials.0c00736

197. Frick-Cheng AE, Sintsova A, Smith SN, Pirani A, Snitkin ES, Mobley HLT. Ferric citrate uptake is a virulence factor in uropathogenic escherichia coli. *mBio* (2022) 13(3):e0103522. doi: 10.1128/mbio.01035-22

198. Huttner A, Hatz C, van den Dobbelsteen G, Abbanat D, Hornacek A, Frölich R, et al. Safety, immunogenicity, and preliminary clinical efficacy of a vaccine against extraintestinal pathogenic escherichia coli in women with a history of recurrent urinary tract infection: A randomised, single-blind, placebo-controlled phase 1b trial. *Lancet Infect Dis* (2017) 17(5):528–37. doi: 10.1016/S1473-3099(17)30108-1

199. Habibi M, Asadi Karam MR, Bouzari S. Construction and evaluation of the immune protection of a recombinant divalent protein composed of the MrpA from MR/P fimbriae and flagellin of Proteus mirabilis strain against urinary tract infection. *Microb Pathog* (2018) 117:348–55. doi: 10.1016/j.micpath.2018.02.023

200. Alamuri P, Eaton KA, Himpsl SD, Smith SN, Mobley HL. Vaccination with proteus toxic agglutinin, a hemolysin-independent cytotoxin *in vivo*, protects against Proteus mirabilis urinary tract infection. *Infect Immun* (2009) 77(2):632–41. doi: 10.1128/IAI.01050-08

201. Flores-Mireles AL, Pinkner JS, Caparon MG, Hultgren SJ. EbpA vaccine antibodies block binding of enterococcus faecalis to fibrinogen to prevent catheter-associated bladder infection in mice. *Sci Transl Med* (2014) 6(254):254ra127. doi: 10.1126/scitranslmed.3009384

202. Grischke EM, Rüttgers H. Treatment of bacterial infections of the female urinary tract by immunization of the patients. *Urol Int* (1987) 42(5):338–41. doi: 10.1159/000281988

203. Osset J, Bartolomé RM, García E, Andreu A. Assessment of the capacity of lactobacillus to inhibit the growth of uropathogens and block their adhesion to vaginal epithelial cells. *J Infect Dis* (2001) 183(3):485–91. doi: 10.1086/318070

204. Mastromarino P, Brigidi P, Macchia S, Maggi L, Pirovano F, Trinchieri V, et al. Characterization and selection of vaginal lactobacillus strains for the preparation of vaginal tablets. *J Appl Microbiol* (2002) 93(5):884–93. doi: 10.1046/j.1365-2672.2002.01759.x

205. Barrons R, Tassone D. Use of lactobacillus probiotics for bacterial genitourinary infections in women: A review. *Clin Ther* (2008) 30(3):453–68. doi: 10.1016/j.clinthera.2008.03.013

206. Sadeghi-Bojd S, Naghshizadian R, Mazaheri M, Ghane Sharbaf F, Assadi F. Efficacy of probiotic prophylaxis after the first febrile urinary tract infection in children with normal urinary tracts. *J Pediatr Infect Dis Soc* (2020) 9(3):305–10. doi: 10.1093/jpids/piz025

207. Stapleton AE, Au-Yeung M, Hooton TM, Fredricks DN, Roberts PL, Czaja CA, et al. Randomized, placebo-controlled phase 2 trial of a lactobacillus crispatus probiotic given intravaginally for prevention of recurrent urinary tract infection. *Clin Infect Dis* (2011) 52(10):1212–7. doi: 10.1093/cid/cir183

208. Forster CS, Hsieh MH, Cabana MD. Perspectives from the society for pediatric research: Probiotic use in urinary tract infections, atopic dermatitis, and antibiotic-associated diarrhea: An overview. *Pediatr Res* (2021) 90(2):315–27. doi: 10.1038/s41390-020-01298-1

209. Aragón IM, Herrera-Imbroda B, Queipo-Ortuño MI, Castillo E, Del Moral JS, Gómez-Millán J, et al. The urinary tract microbiome in health and disease. *Eur Urol Focus* (2018) 4(1):128–38. doi: 10.1016/j.euf.2016.11.001

210. Shim YH, Lee SJ, Lee JW. Antimicrobial activity of lactobacillus strains against uropathogens. *Pediatr Int* (2016) 58(10):1009–13. doi: 10.1111/ped.12949

211. de Llano DG, Arroyo A, Cárdenas N, Rodríguez JM, Moreno-Arribas MV, Bartolomé B. Strain-specific inhibition of the adherence of uropathogenic bacteria to bladder cells by probiotic lactobacillus spp. *Pathog Dis* (2017) 75(4):ftx043. doi: 10.1093/femspd/ftx043

212. Manzoor A, Ul-Haq I, Baig S, Qazi JI, Seratlic S. Efficacy of locally isolated lactic acid bacteria against antibiotic-resistant uropathogens. *Jundishapur J Microbiol* (2016) 9(1):e18952. doi: 10.5812/jjm.18952

Glossary

Aas	a hemagglutinin-autolysinadhesin
AC-3	adenylyl cyclase-3
Als	agglutinin-like sequence
AMPs	antimicrobial peptides
anti-MrpA	structural subunit of MR/P fimbriae
BECs	bladder epithelial cells;
bH/C	b-hemolysin/cytolysin
cAMP	cyclic adenosine monophosphate;
Candida.	Candida spp.
CCL20	C-C chemokine ligand 20
ClfA/B	Clumping Factors A and B
CNF1	cytotoxic necrotizing factor 1
COX-2	cyclooxygenase-2
CREB-1	cAMP-response element-binding protein-1;
CXCL1	C-X-C motif chemokine ligand 1
CXCL2	C-X-C motif chemokine ligand 2
CXCL5	C-X-C otif chemokine ligand 5
CX3CL1	CX3-C motif chemokine 1
CXCR4	CXC-motif chemokine receptor 4
DCs	dendritic cells
Ebp	endocarditis- and biofilm-associated
E. coli	Escherichia coli
E.f	Enterococcus faecalis
E.faecalis	Enterococcus faecalis
EGF	epidermal growth factor
EGFR	epidermal growth factor receptor
ERK	extracellular regulated protein kinases
Esp	enterococcal surface protein;
ExoU/T/S	exoenzyme U/T/S
F1C pili	type 1-like immunological group C pili
GBS	Group B Streptococcus
GLP-1	glucagon-like peptide-1
GM-CSF	granulocyte-macrophage colony-stimulating factor
GRIM-19	genes associated with retinoid-IFN-induced mortality-19
HA	Hyaluronic acid;
hBD	human b-defensin
HlyA	a-hemolysin
HMGN2	high-mobility group protein N2
HpmA	haemolysin
IBCs	intracellular bacterial communities;
LCN2	lipocalin-2
IDSA	Infectious Disease Society of America
IGF-1	insulin-like growth factors-1
IL-1	interleukin-1
IL-6	interleukin 6
IL-8	interleukin-8
INF-g	interferon-g
JNK	c-Jun-NH2-terminal kinase

(Continued)

Continued

K.p	Klebsiella pneumoniae
K. pneumoniae	Klebsiella pneumoniae
INF-g	interferon-g
LPS	lipopolysaccharide
MIP-1	macrophage inflammatory protein-1
MIP-1a	macrophage inflammatory protein-1a
MR/P pili	mannose-resistant Proteus-like
MyD88	myeloiddifferentiationfactor88;
NF-kB	Nuclear factor kappa beta
NK cells	natural killer cells
NLRP3	NOD-like receptor thermal protein domain associated protein 3
P.a	Pseudomonas aeruginosa
PAMP	pathogen-associated molecular pattern;
PAR2	Protease-activated receptor 2
PKA	protein kinase A
P.m	Proteus mirabilis
Pparg	peroxisome proliferator-activated receptor-g
P pili	pyelonephritis-associated pili
Pta	Proteus toxic agglutinin
PTX3	Pentraxins
QIRs	quiescent intracellular reservoirs
QS	quorum sensing;
RegIIIg	regenerating islet-derived 3g
RNase 7	ribonuclease 7
ROS	Reactive oxygen species
RSK	ribosomal s6 kinase
S.a	Staphylococcus aureus
SDF-1	stromal cell-derived factor1
SdrI	a surface-associated collagen-binding protein
SHH	sonic hedgehog
Siglec-9	sialic acid-binding Ig-like lectin-9;
SigV	extracytoplasmic function sigma factor
S.s	Staphylococcus saprophyticus
Ssp	a surface-associated lipase
SssF	S. saprophyticus surface protein F
Stat3	signal transducers and activators of transcription 3;
TcpF	TLR2-Toll/Interleukin-1 receptor domain-containing protein of E. Faecalis
TGF-a	transforming growth factor-a
THP	Tamm-Horsfall protein
TIR	TLR2-Toll/interleukin-1 receptor
TLR4	toll-like receptor 4;
TNF-a	tumor necrosis factor-a
TRPML3	transient receptor potential 3;
UafB	a cell wall-anchored protein
UPEC	Uropathogenic Escherichia coli;
UTI	Urinary tract infection
WHO	World Health Organization
ZapA	an extracellular metalloprotease, Mirabilysin.

frontiers | Frontiers in Immunology

TYPE Original Research
PUBLISHED 20 September 2022
DOI 10.3389/fimmu.2022.970725

Check for updates

OPEN ACCESS

EDITED BY
Paola Massari,
Tufts University, United States

REVIEWED BY
Sara Ahmadi Badi,
Pasteur Institute of Iran, Iran
Qiong Liu,
Nanchang University, China
Mariola J. Edelmann,
University of Florida, United States

*CORRESPONDENCE
Maria Kaparakis-Liaskos
m.liaskos@latrobe.edu.au

SPECIALTY SECTION
This article was submitted to Microbial Immunology, a section of the journal Frontiers in Immunology

RECEIVED 16 June 2022
ACCEPTED 22 August 2022
PUBLISHED 20 September 2022

CITATION
Gilmore WJ, Johnston EL, Bitto NJ, Zavan L, O'Brien-Simpson N, Hill AF and Kaparakis-Liaskos M (2022) *Bacteroides fragilis* outer membrane vesicles preferentially activate innate immune receptors compared to their parent bacteria.
Front. Immunol. 13:970725.
doi: 10.3389/fimmu.2022.970725

COPYRIGHT
© 2022 Gilmore, Johnston, Bitto, Zavan, O'Brien-Simpson, Hill and Kaparakis-Liaskos. This is an open-access article distributed under the terms of the Creative Commons Attribution License (CC BY). The use, distribution or reproduction in other forums is permitted, provided the original author(s) and the copyright owner(s) are credited and that the original publication in this journal is cited, in accordance with accepted academic practice. No use, distribution or reproduction is permitted which does not comply with these terms.

Bacteroides fragilis outer membrane vesicles preferentially activate innate immune receptors compared to their parent bacteria

William J. Gilmore[1,2], Ella L. Johnston[1,2], Natalie J. Bitto[1,2], Lauren Zavan[1,2], Neil O'Brien-Simpson[3], Andrew F. Hill[2,4,5] and Maria Kaparakis-Liaskos[1,2]*

[1]Department of Microbiology, Anatomy, Physiology and Pharmacology, School of Agriculture, Biomedicine and Environment, La Trobe University, Melbourne, VIC, Australia, [2]Research Centre for Extracellular Vesicles, School of Agriculture, Biomedicine and Environment, La Trobe University, Melbourne, VIC, Australia, [3]ACTV Research Group, Centre for Oral Health Research, Royal Dental Hospital, Melbourne Dental School, The University of Melbourne, Melbourne, VIC, Australia, [4]Department of Biochemistry and Chemistry, School of Agriculture, Biomedicine and Environment, La Trobe University, Melbourne, VIC, Australia, [5]Institute for Health and Sport, Victoria University, Melbourne, VIC, Australia

The release of bacterial membrane vesicles (BMVs) has become recognized as a key mechanism used by both pathogenic and commensal bacteria to activate innate immune responses in the host and mediate immunity. Outer membrane vesicles (OMVs) produced by Gram-negative bacteria can harbor various immunogenic cargo that includes proteins, nucleic acids and peptidoglycan, and the composition of OMVs strongly influences their ability to activate host innate immune receptors. Although various Gram-negative pathogens can produce OMVs that are enriched in immunogenic cargo compared to their parent bacteria, the ability of OMVs produced by commensal organisms to be enriched with immunostimulatory contents is only recently becoming known. In this study, we investigated the cargo associated with OMVs produced by the intestinal commensal *Bacteroides fragilis* and determined their ability to activate host innate immune receptors. Analysis of *B. fragilis* OMVs revealed that they packaged various biological cargo including proteins, DNA, RNA, lipopolysaccharides (LPS) and peptidoglycan, and that this cargo could be enriched in OMVs compared to their parent bacteria. We visualized the entry of *B. fragilis* OMVs into intestinal epithelial cells, in addition to the ability of *B. fragilis* OMVs to transport bacterial RNA and peptidoglycan cargo into Caco-2 epithelial cells. Using HEK-Blue reporter cell lines, we identified that *B. fragilis* OMVs could activate host Toll-like receptors (TLR)-2, TLR4, TLR7 and nucleotide-binding oligomerization domain-containing protein 1 (NOD1), whereas *B. fragilis* bacteria could only induce the activation of TLR2. Overall, our data demonstrates that *B. fragilis* OMVs activate a broader range of host innate immune receptors compared to their parent bacteria due to their enrichment of biological cargo and their ability to transport this cargo directly

into host epithelial cells. These findings indicate that the secretion of OMVs by *B. fragilis* may facilitate immune crosstalk with host epithelial cells at the gastrointestinal surface and suggests that OMVs produced by commensal bacteria may preferentially activate host innate immune receptors at the mucosal gastrointestinal tract.

KEYWORDS

bacterial membrane vesicles, outer membrane vesicles (OMVs), *Bacteroides fragilis*, TLRs, NOD1, innate immunity, epithelial cells, Commensals

Introduction

Bacterial membrane vesicles (BMVs) are nanoparticles released by both pathogenic and non-pathogenic bacteria as part of their normal growth. BMVs are referred to as outer membrane vesicles (OMVs) or membrane vesicles (MVs), if produced by Gram-negative or Gram-positive bacteria, respectively. BMVs contain a range of biological and immunogenic cargo originating from their parent bacteria which includes proteins (1), DNA (2), RNA (3), lipids (4) and peptidoglycan (5, 6), and also lipopolysaccharides (LPS) if produced by Gram-negative bacteria (7). In addition to containing a range of biological cargo, pathogen-derived BMVs can also harbor virulence effectors and immunostimulatory molecules derived from their parent bacteria, enabling them to enhance pathogenesis in the host (8). Due to the diverse range of biological cargo associated with BMVs, they can activate a wide range of host pattern recognition receptors (PRRs) which include Toll-like receptors (TLRs) at the host cell surface, or they can enter host cells and deliver their cargo to intracellular TLRs or nucleotide-binding oligomerisation domain-containing protein (NOD) receptors to mediate inflammation in the host (8). More recently, it has been demonstrated that BMVs produced by pathogenic bacteria may also be enriched in specific cargo compared to their parent bacteria which can include toxins (9), proteins (7), LPS (7), peptidoglycan (6), lipids (4), DNA (10), and RNA (11), and that the differential enrichment of cargo into pathogen-derived BMVs can enhance their immunostimulatory or immunomodulatory functions (12). Therefore, pathogen-derived BMVs are immunogenic, and can be enriched in cargo that facilitates pathogenesis independently of their parent bacteria.

In addition to pathogen-derived BMVs that can elicit immune responses in the host (8), commensal bacteria and their secreted BMVs can also be immunostimulatory or immunomodulatory in the host (13). Recently, the gut microbiota has emerged as a key player in regulating host immune responses, and one mechanism by which they do this is *via* the secretion of immunomodulatory BMVs (13). A large body of evidence now demonstrates that microbiota-derived BMVs contain diverse bacterial cargo including proteins (14–19), RNA (18, 20) and peptidoglycan (21), and that they can deliver their cargo to host cells to activate PRRs and drive immune responses (22–28). One important member of the gut microbiota is *Bacteroides fragilis*, which constitutes 1-2% of the normal intestinal microflora (29), and has the ability to modulate host immunity by mediating IL-10 production as a result of detection of its polysaccharide A (PSA) capsule by TLR2 (30–32). It also was identified that *B. fragilis* OMVs contain PSA and can modulate host immunity, as a result of TLR2 activation and the secretion of IL-10, to ultimately confer protection against colitis in murine models of disease (22, 25). *B. fragilis* OMVs can also contain proteins and lipid A (15), however, it is unclear whether other immunostimulatory bacterial components such as nucleic acids or peptidoglycan are also present in *B. fragilis* OMVs, and their ability to activate innate immune receptors remains unknown.

In this study, we examined the immunogenic cargo associated with *B. fragilis* OMVs and investigated their ability to enter host epithelial cells and activate PRRs. We showed that *B. fragilis* OMVs contain proteins, DNA, RNA, LPS and peptidoglycan. Additionally, we identified that *B. fragilis* OMVs could enter host intestinal epithelial cells and transport their peptidoglycan and RNA cargo intracellularly, rendering this cargo accessible to intracellular PRRs. Moreover, due to the cargo they packaged and their ability to enter host cells, we identified that *B. fragilis* OMVs were able to activate cell-surface receptors TLR2 and TLR4, as well as intracellular PRRs TLR7 and NOD1, in a dose-dependent manner. In comparison, *B. fragilis* bacteria were only able to activate TLR2 and did not activate any other PRRs examined. Collectively, our data demonstrates that *B. fragilis* OMVs are laden with potentially immunogenic cargo that enables them to activate a broader range of PRRs compared to their parent bacteria. These findings highlight the importance of OMV secretion by the commensal *B. fragilis* in maintaining intercellular communication at the mucosal epithelial cell surface.

Materials and methods

Bacterial culturing conditions

Bacteroides fragilis strain NCTC 9343 was cultured as previously described (33). Briefly, *B. fragilis* was cultured using Horse Blood Agar medium consisting of Blood Agar Base No. 2 (Oxoid, USA) supplemented with 8% (v/v) horse blood (Australian Ethical Biologicals, Australia), or using Brain Heart Infusion (BHI) broth (BD Biosciences, USA) supplemented with 5 µg/ml Hemin (Sigma-Aldrich, USA) with shaking at 120 rpm. Cultures were grown at 37°C in anaerobic conditions using an AnaeroGen 2.5L sachet (Oxoid, USA) and an AnaeroJar 2.5L anaerobic jar (Oxoid, USA).

Isolation of *B. fragilis* OMVs

B. fragilis OMVs were isolated using our established methods of OMV isolation (5, 6, 12, 34–36). Briefly, BHI broth was inoculated using an overnight *B. fragilis* culture at a starting optical density (O.D. $_{600\ nm}$) of 0.05 and grown at 37°C with shaking for 16 h to stationary phase of growth (O.D. $_{600\ nm}$ of approximately 1.8-2.0) using anaerobic conditions. Bacteria were pelleted by centrifugation at 3, 800 × g for 1 h at 4°C, and the supernatant was subsequently filtered using a 0.22µm polyethersulfone (PES) filter (Nalgene, USA) to remove any remaining bacteria. OMVs contained within bacterial free supernatants were concentrated by tangential flow filtration using a VivaFlow 200 PES crossflow cassette with a 10 kDa molecular weight cut-off filter (Sartorius, Australia), and then pelleted by ultracentrifugation at 100, 000 × g for 2 h at 4°C using a P28S rotor in a CP100NX ultracentrifuge (Hitachi, Japan). The resulting OMV pellets were resuspended in Dulbecco's phosphate-buffered saline (DPBS; Gibco, USA) and stored at -80°C until further purified.

Purification of *B. fragilis* OMVs

B. fragilis OMVs were purified by OptiPrep (60% iodixanol (v/v); Sigma-Aldrich, USA) density gradient ultracentrifugation as previously described (6, 12, 35, 36). In brief, OMV samples were adjusted to 45% (v/v) OptiPrep in 2ml DPBS and were then overlaid with a discontinuous OptiPrep gradient containing 2ml each of 40%, 35%, 30%, 25% and 20% OptiPrep (v/v) in DPBS. The OptiPrep gradient was subjected to ultracentrifugation at 100, 000 × g for 16 h at 4°C. Twelve fractions (1 ml each) were collected, each fraction was washed with 10 volumes of DPBS by ultracentrifugation at 100, 000 × g for 2 h at 4°C, and then resuspended in DPBS. Fractions 3 to 9 containing purified OMVs were pooled and washed using ultracentrifugation at 100,000 × g for 2 h at 4°C and the purity of OMV preparations was confirmed using Transmission electron microscopy (TEM). Purified OMVs were stored at -80°C until required.

Nanoparticle tracking analysis (NTA)

Quantification of purified OMVs was performed using ZetaView™ Nanoparticle Tracking Analysis (NTA; Particle Metrix, Germany) as previously described (6). Briefly, OMVs were diluted in DPBS to a concentration of 50 - 200 particles per field of view. NTA measurements of OMV samples were performed using a 488 nm 40 mW laser and CMOS camera by observing 11 cell positions at 25°C with 60 frames captured per position. Analysis was then performed using ZetaView software version 8.05.14 SP7 (minimum brightness: 30, maximum brightness: 255, minimum area: 5, maximum area: 1000, minimum trace length: 15). The average of three biological replicates was calculated and plotted as particle size versus particles per ml using GraphPad Prism v9.3.1.

Transmission electron microscopy (TEM)

TEM sample preparation was performed as previously described (5, 35). Briefly, OMVs were coated onto carbon-coated 400 mesh copper grids (ProSciTech, Australia) for 10 min, fixed in 1% (w/v) glutaraldehyde (Sigma-Aldrich, USA) and negatively-stained with 2% (w/v) uranyl-acetate (ProSciTech, Australia). OMV samples were then coated with 2% (w/v) methyl-cellulose (Sigma-Aldrich, USA) in 0.4% (w/v) uranyl acetate. Samples were air dried and viewed using a JEM-2100 transmission electron microscope (JEOL, Japan) operated at 200 kV using a Valeta 4 MP CCD camera (Emsis, Germany).

Quantification of the cargo associated with *B. fragilis* OMVs and *B. fragilis* bacteria

The protein cargo associated with *B. fragilis* OMVs was quantified using Qubit protein assay (Invitrogen, USA) using a Qubit 3.0 Fluorometer, according to the manufacturer's instructions.

OMV-associated DNA was quantified using Qubit broad-range DNA assay. Briefly, OMVs were incubated with 4U Turbo DNase (Invitrogen, USA) at 37°C for 1 h to degrade extra-vesicular DNA, according to the manufacturer's rigorous DNA degradation protocol. Alternatively, OMVs were incubated at 37°C for 1 h with DPBS as a control. To confirm DNase activity, *B. fragilis* genomic DNA was extracted using the Wizard Genomic DNA Purification Kit (Promega, USA) and incubated with DNase as a control. DNA associated with

OMVs and controls was quantified using a Qubit 3.0 Fluorometer, according to the manufacturer's instructions.

OMV associated RNA was quantified using the Qubit high-sensitivity assay. Briefly, OMVs were incubated with 10 pg/µl RNase A (Invitrogen, USA) at 37°C for 1 h as previously described (37), or OMVs were incubated with DPBS as a control. To confirm the efficiency of RNase, *B. fragilis* RNA was extracted using the Isolate II RNA Mini Kit (Bioline, UK) and incubated with RNase as a control. RNA in samples was quantified using a Qubit 3.0 Fluorometer, according to the manufacturer's instructions.

OMV-associated peptidoglycan was quantified as described previously (5, 6, 38). Briefly, OMV samples and L-18 muramyldipeptide (MDP) standards (Invivogen, USA) were adjusted to a volume of 0.5 ml in 1M NaOH and incubated at 38°C for 30 min. Samples were then incubated with 0.5 ml of 0.5M H_2SO_4 and 5 ml concentrated H_2SO_4 at 95°C for 5 min. Samples were cooled immediately under running water, followed by the addition of 50 µl $CuSO_4$ (4% w/v) and 100 µl of 1.5% (w/v) 4-phenylphenol (dissolved in 96% (v/v) ethanol) and incubated at 30°C for 30 min. Absorbance was measured at 560 nm using a spectrophotometer and the amount of peptidoglycan associated with *B. fragilis* OMVs was determined using the MDP standard curve.

LPS associated with OMVs was quantified using the Pierce Chromogenic Endotoxin Quant kit, according to the manufacturer's instructions (Thermo Scientific, USA). Briefly, OMV samples and LPS standards were adjusted to a volume of 50 µl and incubated with 50 µl limulus amoebocyte lysate for 9 min. Chromogenic substrate solution was added and samples were incubated for 6 min at 37°C, then the reaction was stopped by the addition of 25% (v/v) acetic acid. Absorbance was measured at 405 nm using a CLARIOstar plate reader (BMG Labtech, Germany) and the amount of LPS associated with 10^8 OMVs was quantified using the standard curve (0.1-1.0 EU/ml), according to the manufacturer's instructions. Each assay was performed in technical triplicate.

Detection of protein, LPS and peptidoglycan cargo associated with *B. fragilis* OMVs and *B. fragilis* bacteria

To detect proteins associated with either *B. fragilis* OMVs or *B. fragilis* bacteria, samples were boiled at 95°C for 5 min in 1x NuPAGE LDS sample buffer (Invitrogen, USA) and 1x NuPAGE Reducing Agent (Invitrogen, USA). Samples were normalized by an equivalent amount of protein and were separated by SDS-PAGE as previously described (6). Proteins associated with *B. fragilis* OMVs and *B. fragilis* bacteria were detected by staining SDS-PAGE gels using Sypro Ruby (Invitrogen, USA), according to the manufacturer's instructions, and visualized at 560 nm using a ChemiDoc image system (Bio-Rad Laboratories, USA).

Peptidoglycan associated with *B. fragilis* OMVs and their parent bacteria was detected by Western immunoblot, as described previously (6). In brief, 10 µg of *B. fragilis* OMVs and *B. fragilis* bacterial samples were separated by SDS-PAGE, transferred to a 0.2 µm polyvinylidene difluoride membrane and then blocked using 5% (w/v) bovine serum albumin (BSA; Sigma-Aldrich, USA) in Tris-buffered saline containing 0.05% (v/v) Tween (TBS-T). The membrane was then incubated with an anti-peptidoglycan mouse monoclonal antibody (Bio-Rad Laboratories, USA; clone number 3F6B3, 1:1,000 dilution), washed and then incubated with goat anti-mouse IgG HRP antibody (Invitrogen, USA, 1:5,000 dilution). The membranes were then washed, developed using Clarity Western ECL Substrate (Bio-Rad Laboratories, USA) and imaged using a GE Amersham imager 600 (GE Life Sciences, UK).

To detect LPS associated with *B. fragilis* OMVs and their parent bacteria, samples (10 µg protein) were first incubated with proteinase K (10 µM; Invitrogen, USA), or DPBS as a control, for 90 min at 37°C. Samples were then resuspended in 1x NuPAGE LDS sample buffer and 1x NuPAGE Reducing Agent and separated by SDS-PAGE. Next, to visualize LPS, SDS-PAGE gels were stained using ProQ Emerald 300 LPS stain kit (Invitrogen, USA), according to the manufacturer's instructions. Briefly, samples were fixed [50% methanol (v/v), 5% acetic acid (v/v)] for 90 min, oxidized using periodic acid containing 3% acetic acid (v/v) for 30 min, and stained with ProQ Emerald stain for 2 h. SDS-PAGE gels were then washed using 3% acetic acid (v/v), and LPS was visualized at 300 nm using a ChemiDoc image system (Bio-Rad Laboratories). To determine the amount of protein associated with these samples, SDS-PAGE gels were then counterstained using Sypro Ruby protein stain and visualized at 560 nm.

Cell culture and stimulations

Human intestinal epithelial cells (Caco-2) were routinely cultured as previously described (39). In brief, Caco-2 cells were cultured in high-glucose Dulbecco's modified eagle medium (DMEM; Gibco, USA) supplemented with 10% (v/v) fetal calf serum (FCS; Gibco, USA), 1% (v/v) L-glutamine (Gibco, USA), 1% (v/v) penicillin-streptomycin (Gibco, USA), 1% non-essential amino acids (Gibco, USA) and 25mM HEPES (Gibco, USA). HEK-Blue null cells and HEK-Blue hTLR2, hTLR4, hTLR7, hTLR8, hTLR9, hNOD1 and hNOD2 cells (Invivogen, USA) were maintained in DMEM supplemented with 10% (v/v) FCS, 1% (v/v) L-glutamine, 1% (v/v) penicillin-streptomycin and selective antibiotics required for each individual cell line as described previously (6, 40). All cell lines were cultured at 37°C with 5% CO_2.

To perform HEK-Blue assays, HEK-Blue cells were seeded in 96-well plates (Greiner, Germany) at a density of 1×10^5 cells per well in 200 µl culture media and cultured to approximately 80-90% confluence. *B. fragilis* bacteria were cultured for 16 h and washed with PBS, then added to HEK-Blue cells at an increasing multiplicity of infection (MOI) for 18 h. Alternatively, *B. fragilis* bacteria were heat-killed at 95°C for 45 min as previously described (41), before their addition to HEK-Blue cells at an increasing MOI for 18 h. Viable counts were performed on live and heat-killed *B. fragilis* bacteria by enumerating serial dilutions spread on horse blood agar and cultured overnight at 37°C using anaerobic conditions. Additionally, HEK-Blue cells were either stimulated with an increasing MOI of purified *B. fragilis* OMVs for 18 h, or not-stimulated as negative controls. Positive controls for each cell line included: 50 ng/ml Pam3CSK4 (Pam3CysSerLys4) for TLR2 cells (Invivogen, USA), 6.25 ng/ml LPS for TLR4 cells (Invivogen, USA), 1 pg/ml R848 (resiquimod) for TLR7 and TLR8 cells (Invivogen, USA), 5 nM CpG ODN for TLR9 cells (Invivogen, USA), 100ng/ml TriDap for NOD1 cells (Invivogen, USA) and 0.001 pg/ml L18-MDP for NOD2 cells (Invivogen, USA). After 24 h, 20 µl of cell culture supernatant was transferred to a fresh 96-well plate and incubated with 180 µl of QUANTI-Blue solution (Invivogen, USA) at 37°C. SEAP activity was measured at 625 nm using a CLARIOstar plate reader (BMG Labtech, Germany).

MTT cell viability assay

The viability of HEK-Blue cells following 18 h stimulation with either live or heat-killed bacteria, or not-stimulated as controls, was determined using the MTT Cell Proliferation Kit (Abcam, UK), according to the manufacturer's protocol. Briefly, HEK-Blue cell lines (Null, hTLR2, hTLR4, hTLR7 and hNOD1) were seeded at 1×10^5 cells per well in 96-well plates and stimulated with either live or heat-killed *B. fragilis* bacteria at an MOI of 1,000 for 18 h. Culture media was then replaced with DMEM containing 100 µg/ml gentamicin for 2 h. The media was then replaced with 50 µl MTT reagent in 50 µl DMEM for 3 h followed by adding 150 µl MTT solvent for 15 minutes with shaking. Absorbance was measured at 590 nm using a CLARIOstar plate reader (BMG Labtech, Germany).

Fluorescent labelling of OMVs and OMV-associated cargo

B. fragilis OMVs were labelled using Vybrant DiI (10 µM; Invitrogen, USA) as described previously (6, 10, 42–44). Briefly, OMVs were adjusted to 1.2×10^{12} OMVs per ml in 100 µl of DPBS and stained with DiI for 30 min at 37°C with gentle agitation. The RNA content of OMVs was labelled by incubating with Syto RNASelect (1µM; Invitrogen, USA) for 60 min with gentle agitation, as previously described (43–45). The peptidoglycan content of *B. fragilis* OMVs was labelled using BODIPY-FL vancomycin (4 ng/ml; Invitrogen, USA) and non-labelled vancomycin (4 ng/ml; Sigma-Aldrich, USA) for 20 min, as previously described (42). An equivalent amount of each fluorescent stain in DPBS (in the absence of OMVs) was used as a negative control. Excess DiI, Syto RNASelect or BODIPY-FL vancomycin dye were removed by washing OMVs and controls four times with 4 ml DPBS using a 10 kDa centrifugal filtration unit (Merck Millipore, Germany).

Examining OMV entry into host cells by confocal microscopy

To visualise OMV entry into host cells, Caco-2 cells were seeded on 18mm round coverslips (Marienfeld, Germany) in 12-well plates at a density of 3×10^5 cells per well in 1ml of media for 24 h. Caco-2 cells were stimulated with either DiI, BODIPY-FL or Syto RNASelect-labelled *B. fragilis* OMVs for 4 h at an MOI of 4×10^5 OMVs per cell, or each respective stain in DPBS as a control. Following incubation, cells were washed three times with DPBS, and extracellular fluorescence was quenched with 0.025% (v/v) Trypan blue as previously described (34). Cells were fixed using 4% paraformaldehyde (Sigma-Aldrich, USA) and blocked using 1% BSA (w/v) in DPBS. Cell nuclei and cellular actin were stained with 4',6-diamidino-2-phenylindole dilactate (DAPI; Merck, Germany) and Alexa Fluor 680 phalloidin (Invitrogen, USA), respectively. Samples were then mounted using VectaShield mounting medium (Vector Laboratories, USA) and imaged using a Zeiss 780 PicoQuant confocal microscope (Zeiss, Germany) using a 63x/1.4NA oil objective at $1024 \times 1024 \times 32$ bit per channel. Image analysis was performed using Imaris x64 v9.5.0 (Bitplane, Switzerland). Three biological replicates of Caco-2 cells stimulated with OMVs, labelled with each individual stain, were examined. Three fields of view were imaged for each treatment containing a minimum of 10 cells per field of view.

Statistical analysis

All statistical analyses were performed using GraphPad Prism software v9.3.1. Qubit quantification experiments were analysed using an unpaired *t*-test. HEK-Blue experiments were analysed using an unpaired *t*-test or one-way ANOVA with Dunnett's multiple comparisons test, as indicated. Differences were considered statistically significant when $^*p < 0.05$, $^{**}p < 0.01$, $^{***}p < 0.001$, $^{****}p < 0.0001$.

Results

B. fragilis OMVs contain DNA, RNA, protein, LPS, and peptidoglycan

B. fragilis OMVs contain a range of cargo including polysaccharides (22), proteins (15, 16, 46) and LPS (15). However, it remains unclear if *B. fragilis* OMVs also contain other biological cargo including peptidoglycan and nucleic acids. *B. fragilis* OMVs were isolated and purified to examine their biological cargo composition, as well as their size and morphology. Examination of purified *B. fragilis* OMVs using transmission electron microscopy (TEM) and Nanoparticle Tracking Analysis (NTA) revealed that they were heterogeneous in size, with the predominant population of OMVs being approximately 135 nm in diameter (Figures 1A, B). Next, we quantified the amount of protein, DNA, RNA, peptidoglycan and LPS cargo associated with *B. fragilis* OMVs (Figures 1C–G). Having previously shown that there is variability in the quantification of OMV-associated cargo based on the type of protein assay used and the method used to normalise BMV number (35), we quantified the biological cargo associated with OMVs and represented the quantity of cargo per 10^9 OMVs (Figures 1C–G). Quantification of the cargo associated with 10^9 *B. fragilis* OMVs revealed that they contained protein, DNA and RNA (Figures 1C–E). Furthermore, degradation of extra-vesicular DNA using DNase, or RNA using RNase, revealed that the majority of DNA and RNA was protected from degradation and was therefore predominantly located within OMVs (Figures 1D, E). We also identified that *B. fragilis* OMVs contained peptidoglycan, with approximately 600 ng of peptidoglycan associated with 10^9 OMVs (Figure 1F), in addition to LPS with approximately 38 endotoxin units (EU) of LPS per 10^9 OMVs (Figure 1G). Collectively, these findings demonstrate that *B. fragilis* OMVs contain a diverse range of biological cargo including protein, DNA, RNA, peptidoglycan and LPS.

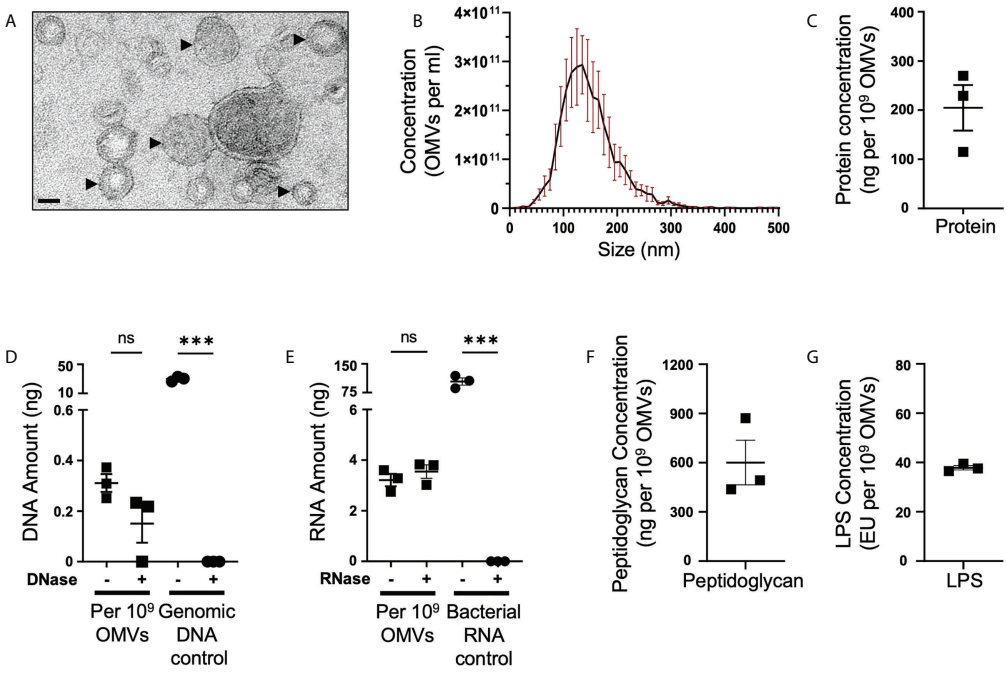

FIGURE 1
B fragilis OMVs are heterogenous in size and morphology, and harbour protein, DNA, RNA, peptidoglycan and LPS cargo. **(A)** Purified *B. fragilis* OMVs were visualized using transmission electron microscopy (TEM). OMVs are indicated by black arrows. Images are representative of three biological replicates (Scale bar = 100 nm). **(B)** The size distribution of *B. fragilis* OMVs was determined using ZetaView Nanoparticle Tracking Analysis. Data shows the mean (black line) ± SEM (red error bars) of three biological replicates. **(C)** Quantification of OMV-associated protein, per 10^9 *B. fragilis* OMVs, using Qubit fluorometric analysis. Data shows the mean ± SEM of three biological replicates. **(D)** Quantification of DNA associated with DNase-treated (+) or non-treated (-) *B. fragilis* OMVs using Qubit fluorometric analysis. *B. fragilis* genomic DNA (Genomic DNA control), either treated with DNase (+) or non-treated (-), was used as a control for DNase activity. Shown is the mean ± SEM of three biological replicates. ns, not significant, ***p < 0.001 (unpaired *t*-test). **(E)** Quantification of RNA associated with RNase-treated (+) or non-treated (-) *B. fragilis* OMVs using Qubit fluorometric analysis. *B. fragilis* bacterial RNA (Bacterial RNA control), either treated with RNase (+) or not-treated (-), was used as a control for RNase activity. Shown is the mean ± SEM of three biological replicates. ns, not significant, ***p < 0.001 (unpaired *t*-test). **(F)** Quantification of the peptidoglycan cargo associated with 10^9 *B. fragilis* OMVs. Shown is the mean ± SEM of three biological replicates. **(G)** LPS associated with 10^9 *B. fragilis* OMVs was quantified using the Pierce™ Chromogenic Endotoxin Quant kit. Data represents the mean ± SEM of three biological replicates.

B. fragilis OMVs have an altered cargo composition compared to their parent bacteria

We have previously demonstrated that BMVs produced by Gram-negative and Gram-positive bacteria contain cargo that differs from their parent bacterium, suggesting that bacteria can preferentially package or enrich biological cargo in their BMVs (6, 12). Furthermore, we showed that enrichment of biological cargo within BMVs can have a profound effect on their subsequent biological functions, when compared to their parent bacteria and to BMVs produced during different stages of bacterial growth, indicating that selective cargo packaging into BMVs regulates their functions (12). As *B. fragilis* OMVs contain protein, DNA, RNA, LPS and peptidoglycan, we next investigated if *B. fragilis* OMVs were enriched in biological cargo compared to their parent bacteria. Examination of the overall protein profiles of *B. fragilis* OMVs by SDS-PAGE revealed that a range of predominant protein bands, including those at approximately 125 kDa, 75 kDa, 30 kDa and 17 kDa, were enriched in *B. fragilis* OMVs compared to their parent bacteria (Figure 2A, arrows). Similarly, some protein bands present in *B. fragilis* bacteria, such as bands of approximately 60 and 45 kDa, were not equally prominent in OMVs (Figure 2A, stars), suggesting that there is selective cargo packaging of protein into *B. fragilis* OMVs.

We next detected the presence of peptidoglycan within OMVs and bacterial samples by Western immunoblot. Examination of an equivalent amount of *B. fragilis* OMVs and bacteria, normalized by protein amount, revealed that OMVs were enriched in peptidoglycan, evidenced by a prominent band of approximately 10 kDa, compared to their parent bacteria (Figure 2B). These differences in peptidoglycan profiles suggest differences in peptidoglycan packaging into OMVs compared to their parent bacteria, similar to what we have previously observed in MVs produced by the Gram-positive pathogen *S. aureus* (6).

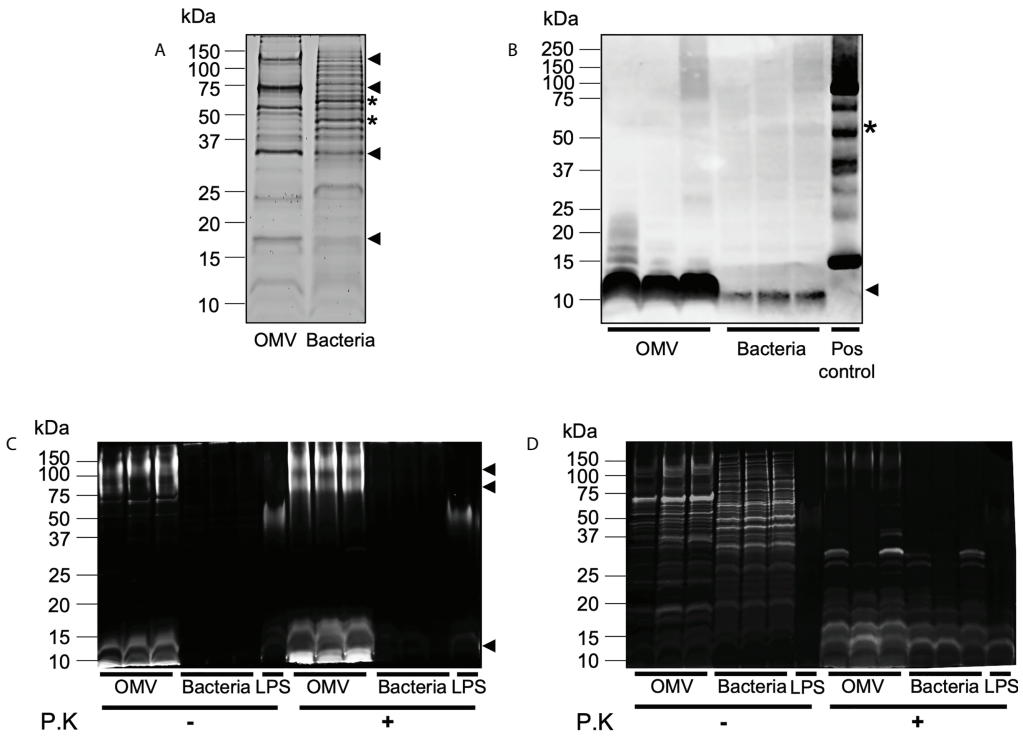

FIGURE 2
B. fragilis OMVs are enriched in protein, peptidoglycan and LPS cargo compared to their parent bacteria. **(A)** *B. fragilis* OMVs (10 µg) and *B. fragilis* bacteria (10 µg) were separated using SDS-PAGE and their protein cargo was stained using Sypro Ruby. Data is representative of three biological replicates. **(B)** The presence of peptidoglycan cargo associated with *B. fragilis* OMVs (10 µg) and *B. fragilis* bacteria (10 µg) was detected using Western immunoblot using an anti-peptidoglycan antibody. Peptidoglycan was used as a positive control (Pos control). Data shows three biological samples of *B. fragilis* OMVs and *B. fragilis* bacteria and is representative of three experiments. **(C)** *B. fragilis* OMVs and *B. fragilis* bacteria were treated with Proteinase K (P.K) (+) or not treated as controls (-), and their LPS cargo was detected by staining with ProQ Emerald 300 LPS stain. **(D)** ProQ Emerald-stained SDS-PAGE gels were counterstained with the protein-specific stain Sypro Ruby. Data in panel C and D represents three independent biological samples of *B. fragilis* OMVs and *B. fragilis* bacteria and is representative of three independent experiments. In all panels **(A–D)**, black arrows represent cargo that is enriched in OMVs compared to bacteria, stars represent cargo that is less abundant in OMVs compared to bacteria.

Although it was previously reported that there were no structural differences between the lipid A LPS moiety of *B. fragilis* and their OMVs (15), the relative abundance of LPS cargo in *B. fragilis* OMVs compared to their parent bacteria remains unknown. To address this, we examined the LPS profiles of *B. fragilis* OMVs compared to their parent bacteria using SDS-PAGE, loaded with equivalent protein amounts, and visualized LPS using the ProQ Emerald stain (Figure 2C). LPS moieties of approximately 100 kDa, 75 kDa and 10 kDa were prominent in *B. fragilis* OMVs, however these moieties were less evident in *B. fragilis* bacterial samples, suggesting that LPS was enriched in OMVs compared to their parent bacteria (Figure 2C). The higher molecular weight staining (approximately 75 to 100 kDa) in the *B. fragilis* OMV samples suggests the presence of LPS. In contrast, the low molecular weight smear (10 kDa) may represent lipooligosaccharide (LOS) or lipid A components (Figure 2C), as described previously (40). Additionally, both high and low molecular weight smears were resistant to proteinase K degradation (Figure 2C) and were not visualized by Sypro Ruby staining (Figure 2D), validating that these bands were representative of LPS. Taken together, these data demonstrate that *B. fragilis* OMVs harbor a range of biological cargo that includes proteins, peptidoglycan, and LPS and that there are differences in the preferential packaging of these immunostimulatory cargo into OMVs compared to their parent bacteria, which may ultimately alter their ability to activate host PRRs.

B. fragilis OMVs activate TLR2 and TLR4 responses compared to their parent bacteria that can only activate TLR2

Having revealed that *B. fragilis* OMVs contain various biological cargo with distinct differences in their cargo composition compared to their parent bacteria (Figures 2A–D), we sought to determine if there was a difference in the ability of *B. fragilis* OMVs and their parent bacteria to activate host PRRs. To address this, HEK-Blue reporter cells that express either human TLR2 or TLR4, or control HEK-Blue null cells, were stimulated with an increasing dose of either *B. fragilis* OMVs, live *B. fragilis* bacteria, or heat killed *B. fragilis* bacteria as a control. First, we identified that *B. fragilis* OMVs as well as live or heat-killed bacteria were unable to induce the activation of HEK-Blue null cells (Figures 3A–D; Supplementary Figure 1A). However, both *B. fragilis* OMVs and their parent bacteria activated TLR2 in a dose-dependent manner (Figures 3A, B), consistent with previous reports (22, 32). OMV-mediated TLR2 activation occurred at an MOI as low as approximately 80 OMVs per cell ($p < 0.01$), suggesting that OMVs can readily activate TLR2 (Figure 3A). Next, we investigated whether *B. fragilis* and their OMVs could activate TLR4, and observed dose-dependent activation of TLR4 by *B. fragilis* OMVs, which occurred at MOI as low as approximately 625 OMVs per cell ($p < 0.01$) (Figure 3C). However, we did not observe any TLR4 activation in response to stimulation with live *B. fragilis* bacteria at any of the concentrations examined, suggesting that there is a difference in the TLR4 immunostimulatory abilities of *B. fragilis* OMVs compared to their parent bacteria (Figure 3D). Similarly, heat-killed *B. fragilis* bacteria also activated TLR2 but not TLR4-expressing HEK-Blue cells (Supplementary Figures 1B, C), identifying that the inability of *B. fragilis* to activate TLR4 was independent of bacterial viability or potential cytotoxic effects mediated by live bacteria on host cells. We also confirmed the viability of HEK-Blue null cells and TLR2 and TLR4 expressing HEK-Blue cells following stimulation with either live or heat killed *B. fragilis* bacteria at maximal MOI (Supplementary Figures 1D–F), validating that the lack of TLR4 activation in response to stimulation with live *B. fragilis* bacteria was not due to a decrease in HEK-Blue cell viability. Overall, these data demonstrate that *B. fragilis* OMVs activate both TLR2 and TLR4, whereas live and heat killed *B. fragilis* bacteria can only activate TLR2, suggesting that the immunogenic cargo of *B. fragilis* OMVs may enhance their ability to activate TLR4 compared to their parent bacteria.

B. fragilis OMVs can enter host intestinal epithelial cells and deliver peptidoglycan and RNA intracellularly

We next investigated the ability of *B. fragilis* OMVs to enter and deliver their immunogenic cargo, including peptidoglycan and RNA, to host epithelial cells. First, we confirmed the ability of *B. fragilis* OMVs to enter human intestinal epithelial cells (Caco-2). To do this, DiI-labelled *B. fragilis* OMVs were incubated with Caco-2 cells for 4 hours, and the ability of OMVs to enter epithelial cells was determined by confocal microscopy (Figure 4A). Examination revealed that *B. fragilis* OMVs were capable of entering Caco-2 epithelial cells, and therefore able to deliver their immunogenic cargo intracellularly to host cells (Figure 4A).

We have previously shown that *Helicobacter pylori* OMVs contain peptidoglycan, and that they can deliver their peptidoglycan cargo into host epithelial cells, resulting in the activation of the cytoplasmic host innate immune receptor NOD1 and the induction of an innate immune response (5, 42). As *B. fragilis* OMVs also contain peptidoglycan (Figures 1, 2), we next investigated the ability of *B. fragilis* OMVs to deliver their peptidoglycan cargo intracellularly to host epithelial cells. To do this, peptidoglycan associated with *B. fragilis* OMVs was fluorescently labelled using BODIPY-FL vancomycin, and the ability of fluorescently-labelled *B. fragilis* OMVs to enter Caco-2 cells was determined using confocal microscopy (Figure 4B). We

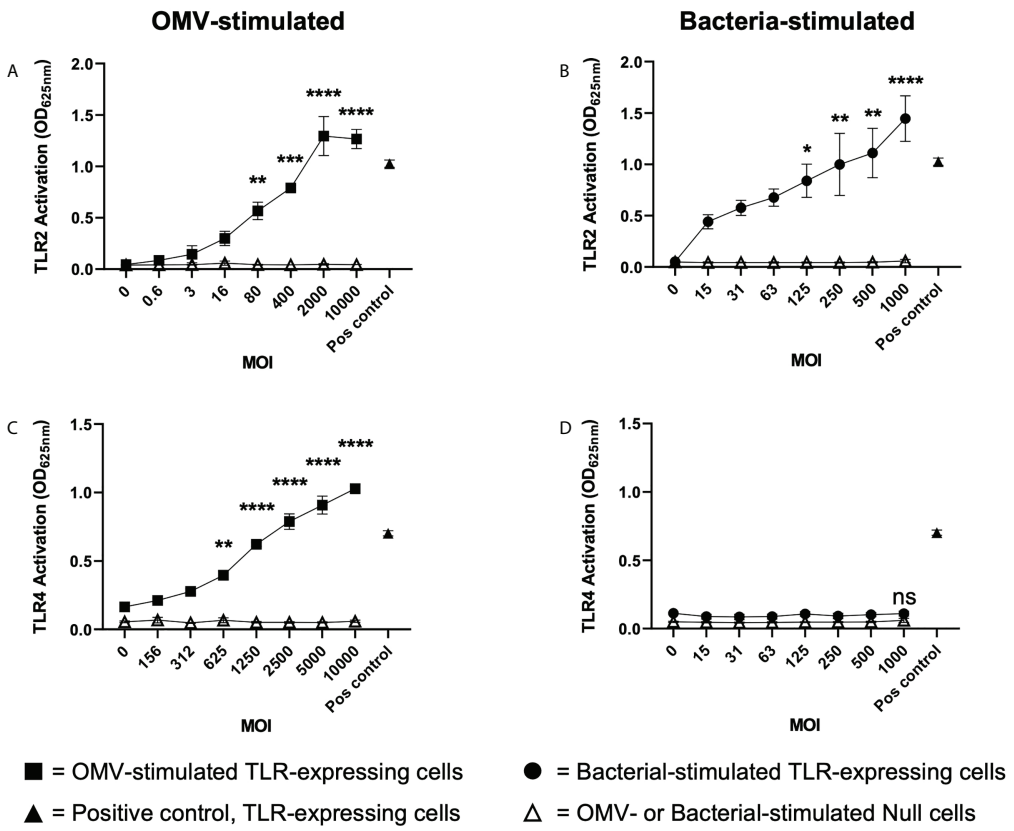

FIGURE 3
B. fragilis OMVs activate TLR2 and TLR4 compared to their parent bacteria which only activate TLR2. **(A, B)** TLR2 and **(C, D)** TLR4 expressing HEK-Blue cells were stimulated with either *B. fragilis* OMVs (**A**, **C**, squares) or *B fragilis* bacteria (**B**, **D**, circles) at an increasing multiplicity of infection (MOI) for 18 hours. In all panels, open triangles indicate stimulation of the HEK-Blue null cell line with either OMVs **(A, C)** or bacteria **(B, D)** in each assay, filled triangles indicate positive controls for each respective cell line. Data represents mean ± SEM of three biological replicates. ns = not significant, *p < 0.05, **p < 0.01, ***p < 0.001, ****p < 0.0001 (One-way ANOVA with Dunnett's multiple comparisons test, compared to non-stimulated controls).

found that BODIPY-FL-labelled *B. fragilis* OMVs entered Caco-2 epithelial cells and were therefore capable of delivering their fluorescently-labelled peptidoglycan intracellularly (Figure 4B).

Pathogen-derived BMVs can also mediate the intracellular delivery of bacterial RNA to host cells, resulting in the induction of innate immunity (6, 37, 44, 47, 48). However, the ability of commensal-derived BMVs to deliver RNA cargo into host cells remains to be elucidated. Therefore, we next examined the ability of *B. fragilis* OMVs to deliver their RNA cargo intracellularly to intestinal epithelial cells. To do this, RNA associated with *B. fragilis* OMVs was labelled using Syto RNASelect. *B. fragilis* OMVs containing fluorescently-labelled RNA were incubated with Caco-2 cells and examined by confocal microscopy, revealing that *B. fragilis* OMVs could deliver RNA intracellularly to Caco-2 cells (Figure 4C). As a control for the non-specific uptake of DiI, BODIPY-FL vancomycin or Syto RNASelect, Caco-2 cells were incubated with each respective stain resuspended in DPBS in the absence of OMVs and examined by confocal microscopy, revealing a lack of each fluorescent stain intracellularly (Figure 4, controls). These findings reveal that *B. fragilis* OMVs can enter host epithelial cells to deliver their cargo, that includes peptidoglycan and RNA.

B. fragilis OMVs activate NOD1 and TLR7 responses, whereas their parent bacteria cannot

We next investigated the ability of *B. fragilis* OMVs to activate the intracellular receptors for peptidoglycan, NOD1 and NOD2, which detect unique components of bacterial peptidoglycan. Specifically, NOD1 detects D-glutamyl-meso-diaminopimelic acid found predominantly in Gram-negative bacteria (49), whereas NOD2 detects muramyl dipeptide found in peptidoglycan of both Gram-negative and Gram-positive bacteria (50). To investigate the immune-stimulating potential

10.3389/fimmu.2022.970725

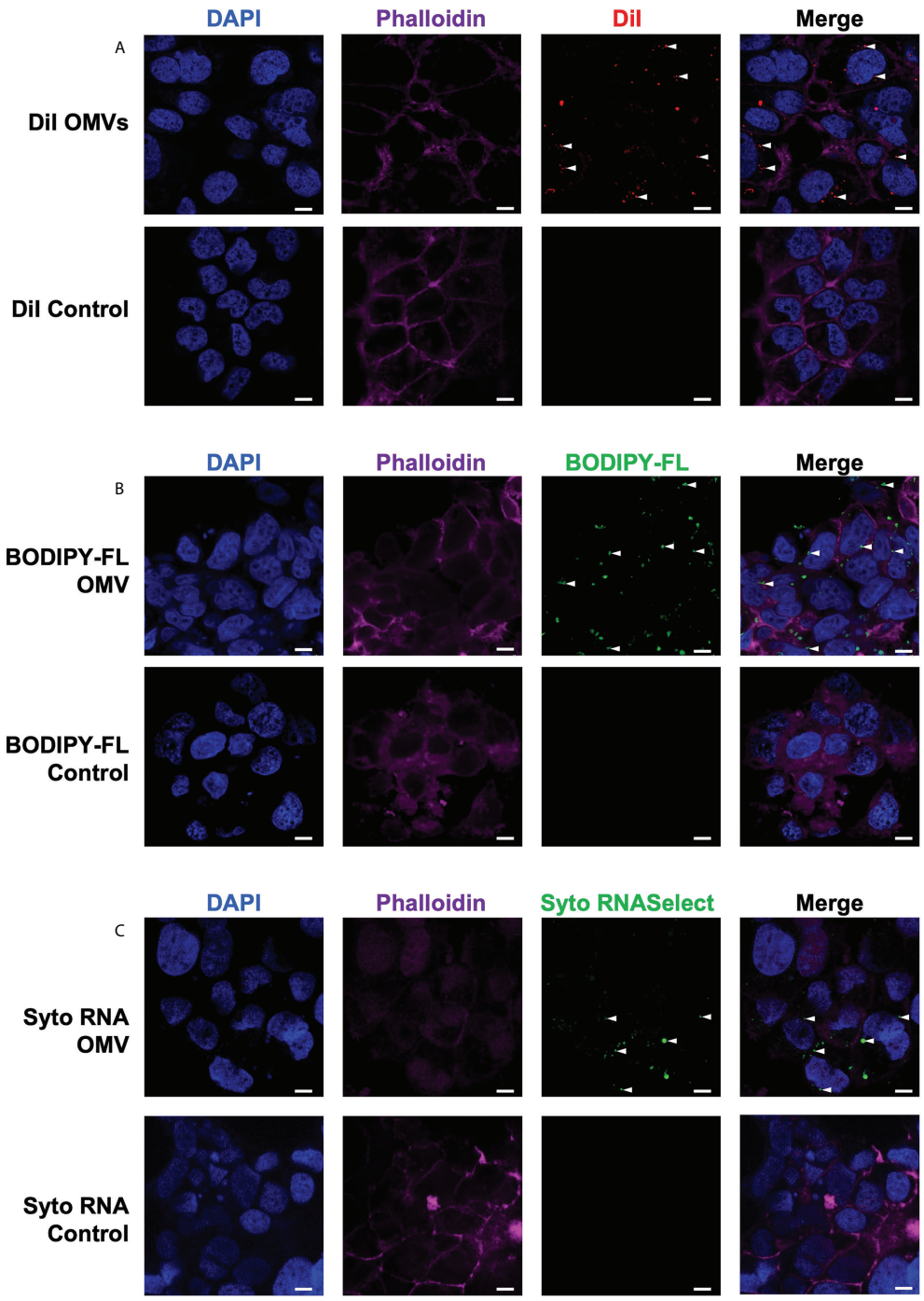

FIGURE 4
B fragilis OMVs enter host intestinal epithelial cells and transport their peptidoglycan and RNA cargo intracellularly. The **(A)** lipid (DiI; red), **(B)** peptidoglycan (BODIPY-FL vancomycin; green) and **(C)** RNA (Syto RNASelect; green) cargo associated with *B. fragilis* OMVs was fluorescently labelled. Fluorescently labelled *B. fragilis* OMVs were then incubated with Caco-2 cells for 4 hours, and OMV entry was visualized by confocal microscopy. Cell nuclei and cellular actin were visualized by staining with DAPI (blue) or Phalloidin (magenta). Intracellular *B. fragilis* OMVs are indicated by white arrows. DPBS containing each respective stain (Control) were incubated with Caco-2 cells to control for the non-specific uptake of each fluorescent stain by host cells. Images are representative of three biological replicates of Caco-2 cells stimulated with each type of fluorescently-labelled *B. fragilis* OMVs. Scale bar = 10 μm.

of peptidoglycan delivered by *B. fragilis* OMVs, HEK-Blue cells expressing human NOD1 were stimulated with an increasing dose of *B. fragilis* OMVs or *B. fragilis* bacteria (Figures 5A, B). We found that stimulation of NOD1-expressing HEK-Blue cells with an MOI of 2×10^7 OMVs per cell resulted in significant activation of NOD1 compared to non-stimulated controls ($p < 0.05$) (Figure 5A). Based on our quantification of peptidoglycan associated with OMVs (Figure 1D), this corresponded to approximately 12 ng of peptidoglycan associated with 2×10^7 OMVs resulting in the activation of NOD1 (Figure 5A). In comparison, we observed that NOD1 was not activated by *B. fragilis* bacteria at any MOI examined in this study, indicating that there are differences in the ability of *B. fragilis* and their OMVs to activate NOD1 (Figure 5B). We next characterized the ability of OMVs to activate NOD2, which has been previously reported to have a role in the detection of *B. fragilis* OMVs by bone marrow-derived dendritic cells (25, 50). However, we did not observe any significant activation of NOD2-expressing HEK-Blue cells by either *B. fragilis* OMVs or *B. fragilis* bacteria at any of MOI examined in this study (Figures 5C, D). Furthermore, heat-killed bacteria did not activate either NOD1 or NOD2, and the inability of *B. fragilis* bacteria to activate NOD1 signaling compared to OMVs was not due to a reduction in host cell viability (Supplementary Figures 2A–C).

Having determined that *B. fragilis* OMVs harbor both DNA and RNA cargo (Figures 1D, E) and that RNA associated with B. *fragilis* OMVs can enter epithelial cells (Figure 4C), we next investigated their ability to activate the RNA receptors TLR7 and TLR8, and TLR9 that detects bacterial DNA. To address this, TLR7, TLR8 and TLR9 expressing HEK-Blue cells were stimulated with an increasing dose of *B. fragilis* OMVs or their parent bacteria (Figures 5E–J). Stimulation of TLR7 expressing HEK-Blue cells with an increasing dose of *B. fragilis* OMVs resulted in significant activation of TLR7 compared to non-stimulated controls, with a minimum MOI of approximately 5×10^5 OMVs per cell being required to induce TLR7 activation ($p < 0.05$) (Figure 5E). In contrast, live and heat killed *B. fragilis* bacteria could not activate TLR7 at any concentration examined in this study (Figure 5F, Supplementary Figure 3A). Furthermore, the inability of live or heat killed *B. fragilis* to activate TLR7 compared to OMVs was not due to impairing the viability of HEK-Blue cells expressing TLR7 (Supplementary Figure 3B). We also found that neither *B. fragilis* OMVs, nor live or heat-killed *B. fragilis* bacteria were able to induce the activation of TLR8 (Figures 5G, H, Supplementary Figure 3C), suggesting that *B. fragilis* bacteria were unable to activate either TLR7 or TLR8, and that RNA associated with *B. fragilis* OMVs preferentially activated TLR7 compared to TLR8 (Figure 5E). This is in contrast to what we have previously observed using *S. aureus* MVs, where an equivalent amount of RNA-containing *S. aureus* MVs could activate both TLR7 and TLR8 (6). Moreover, we found that live and heat killed *B. fragilis* bacteria and their OMVs could not activate TLR9 responses at all MOIs examined (Figures 5I, J, Supplementary Figure 3D). The inability of *B. fragilis* OMVs to activate TLR9 responses may be attributed to them having approximately ten-fold less DNA (0.311ng per 10^9 OMVs) than RNA (3.21ng per 10^9 OMVs) content (Figures 1D, E) and therefore, the amount of DNA delivered by *B. fragilis* OMVs may be insufficient to induce TLR9 activation. Moreover, NF-κB activity was not observed in the negative control HEK-Blue null cell line in response to stimulation with *B. fragilis* OMVs or bacteria, revealing that the delivery of bacterial cargo by *B. fragilis* OMVs is essential for their ability to activate the intracellular receptors NOD1 and TLR7 (Figure 5).

Taken together, our data identify the ability of the intestinal commensal *B. fragilis* to package protein, DNA, RNA, peptidoglycan and LPS into their OMVs, and that there is enrichment of immunogenic cargo in *B. fragilis* OMVs. Furthermore, we show the ability of enriched *B. fragilis* OMV-associated cargo to be delivered intracellularly to host cells, which ultimately enables *B. fragilis* OMVs to preferentially activate a broader range of innate immune receptors compared to their parent bacteria. Moreover, these findings identify novel mechanisms of selective immune activation mediated by *B. fragilis* OMVs at the host epithelial cells surface *via* preferential activation of TLR4, TLR7 and NOD1.

Discussion

The immunostimulatory functions of BMVs depend upon the specific cargo they contain and their ability to deliver this cargo to host cells. BMVs produced by both pathogens and commensals can package various biological cargo including nucleic acids, proteins, LPS and peptidoglycan. Furthermore, pathogen-derived BMVs can be enriched in immunostimulatory cargo, enabling them to activate host PRRs and drive immune responses in the host. However, the enrichment of immunostimulatory cargo in commensal-derived BMVs compared to their parent bacteria, and their subsequent ability to deliver this cargo and activate innate immune receptors is not equally well characterized. The findings of this study reveal that OMVs produced by the commensal *B. fragilis* contain protein, nucleic acids, LPS and peptidoglycan and are enriched in LPS, peptidoglycan and proteins compared to their parent bacterium (Figures 1, 2). Additionally, we show that *B. fragilis* OMVs can enter intestinal epithelial cells to deliver their RNA and peptidoglycan cargo intracellularly (Figure 4). Moreover, the enrichment of peptidoglycan, LPS and protein cargo into *B. fragilis* OMVs, in addition to their ability to deliver their cargo into host epithelial cells, enables them to activate a more diverse range of PRRs which includes TLR4, TLR7 and NOD1 compared to their parent bacteria (Figures 3, 5). Collectively, our findings identify the enrichment of select cargo into *B. fragilis*

10.3389/fimmu.2022.970725

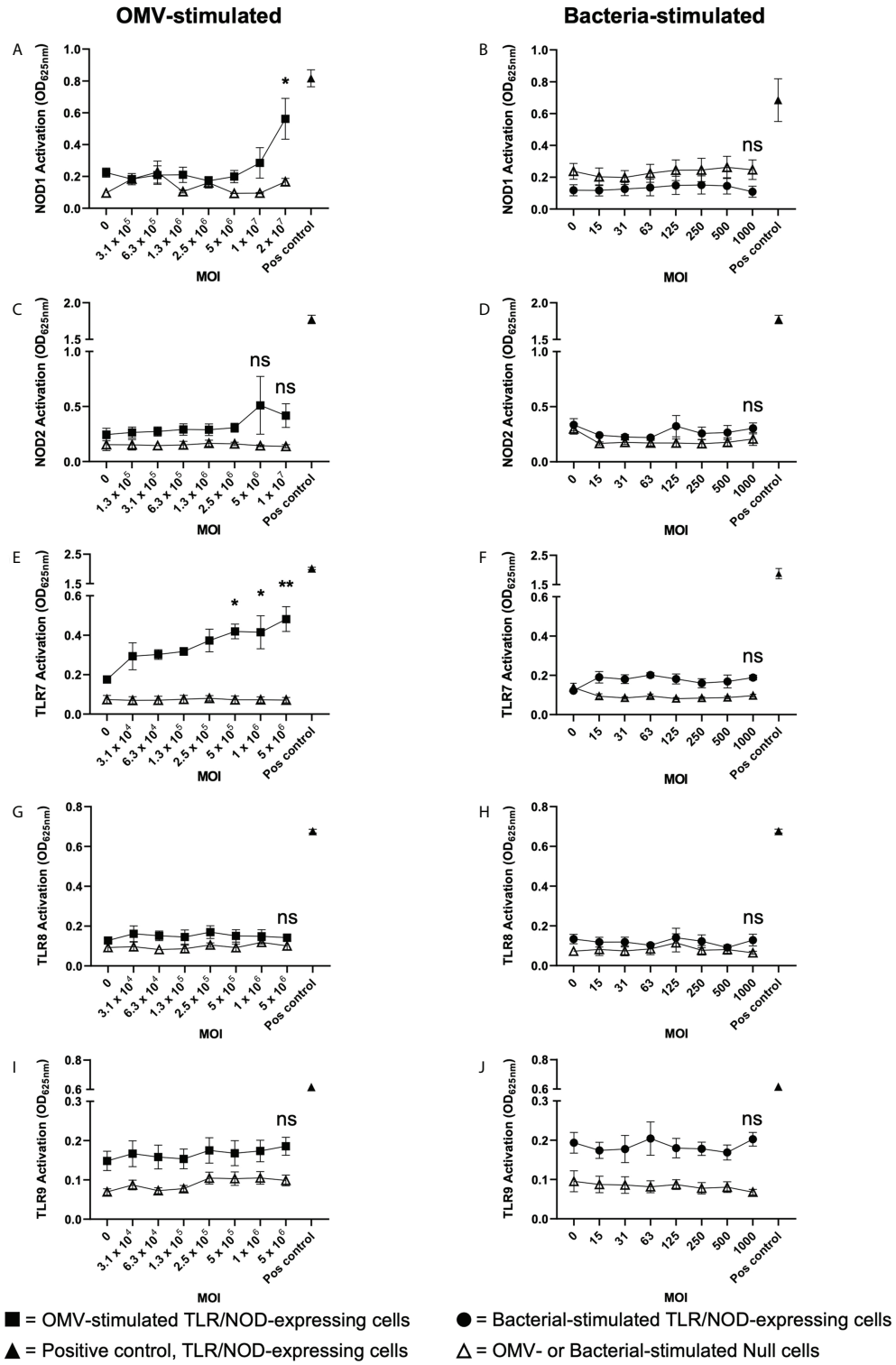

FIGURE 5
B fragilis OMVs activate NOD1 and TLR7 whereas *B fragilis* bacteria cannot. **(A, B)** NOD1, **(C, D)** NOD2, **(E, F)** TLR7, **(G, H)** TLR8 and **(I, J)** TLR9 expressing HEK-Blue cells were stimulated with an increasing MOI of either *B. fragilis* OMVs (**A**, **C**, **E**, **G**, **I**, squares) or *B. fragilis* bacteria (**B**, **D**, **F**, **H**, **J**, circles) for 18 hours. Open triangles indicate stimulation of the HEK-Blue null cell line with either *B. fragilis* OMVs or *B. fragilis* bacteria as a negative control in each assay. Filled triangles indicate positive controls for each respective cell line. Data represents mean ± SEM of three biological replicates. ns=not significant, *p < 0.05, **p < 0.01. (One-way ANOVA with Dunnett's multiple comparisons test, compared to non-stimulated controls).

OMVs that subsequently results in their ability to activate a broader range of host innate immune receptors compared to their parent bacteria, revealing that *B. fragilis* OMVs may function to increase the potential for commensal-host crosstalk at the intestinal epithelial barrier.

In this study, we investigated the type and quantity of biological cargo associated with *B. fragilis* OMVs and determined their ability to activate host innate immune receptors compared to their parent bacteria. Our data revealed that *B. fragilis* OMVs contain a wide range of biological cargo consisting of protein, LPS, peptidoglycan, DNA and RNA (Figure 1). Interestingly, *B. fragilis* OMVs contained approximately ten-fold more RNA than DNA (Figures 1D, E), which is consistent with previous studies identifying that MVs derived from the Gram-positive commensals *Lactobacillus reuteri* (20) and *Lactobacillus casei* (18) also packaged significantly more RNA than DNA. While the RNA associated with pathogen-derived BMVs is becoming increasingly recognized as being able to activate innate immune receptors and to modulate cellular functions when delivered into host cells (37, 51), knowledge regarding the immunostimulatory and immunomodulatory abilities of RNA delivered by commensal-derived BMVs is limited, highlighting that future research endeavors should focus on broadening our understanding of their functions.

Our data show that *B. fragilis* OMVs were enriched with protein cargo compared to their parent bacterium (Figure 2A). In agreement with our findings, a previous study examining the proteome of *B. fragilis* OMVs found that they were enriched in acidic proteases and sugar-hydrolysing glycosidases, which facilitated the catabolism and acquisition of environmental nutrients and were thought to ameliorate the establishment and composition of the gut microbiota (15). Moreover, while selective protein packaging into pathogen-derived BMVs has been shown to promote pathogen colonisation or survival (52, 53), proteins enriched in BMVs produced by various pathogens also have important roles in facilitating bacterial pathogenesis and promoting the development of inflammatory host immune responses (12, 52–55), further supporting the notion that bacteria can regulate the proteome of their OMVs to modulate their functions.

We also observed the enrichment of LPS into *B. fragilis* OMVs compared to their parent bacteria (Figure 2C). Although ProQ Emerald stain used in this study cannot discriminate between different LPS isoforms at the molecular level, the LPS enriched in *B. fragilis* OMVs was characteristic of both larger LPS species, as well as smaller LPS, LOS or lipid A species (Figure 2C). Consequently, we observed that *B. fragilis* OMVs, but not their parent bacteria, induced dose-dependent activation of TLR4, the host immune receptor responsible for the detection of LPS. Therefore, our findings suggest that the enrichment of LPS into *B. fragilis* OMVs enhances their ability to activate TLR4 compared to their parent bacteria. In agreement with our findings, a previous study showed that long-chain LPS moieties could be enriched in *Porphyromonas gingivalis* OMVs compared to their parent bacteria (7). Moreover, it was also reported that OMVs produced by wild-type *Neisseria meningitidis* strains induced stronger TLR4 responses compared to OMVs produced by LPS-depleted strains, demonstrating that OMVs containing more LPS were more readily able to induce the activation of TLR4-mediated immune responses (56). Collectively, these studies support our findings that LPS can be enriched in *B. fragilis* OMVs which may contribute to their enhanced capacity to mediate TLR4 signaling compared to their parent bacteria.

In addition to examining the ability of *B. fragilis* OMVs to preferentially activate host cell surface expressed TLRs, we also investigated the ability of *B. fragilis* OMVs to enter epithelial cells, rendering their cargo accessible to intracellular PRRs, and their subsequent ability to activate these cytoplasmic PRRs. Using previously validated methods to label BMVs and their associated peptidoglycan and RNA cargo, we demonstrated that *B. fragilis* OMVs entered intestinal epithelial cells and delivered their fluorescently-labelled peptidoglycan and RNA cargo intracellularly (Figure 4). Considering that *B. fragilis* bacteria are non-invasive and do not readily secrete immunostimulatory effector molecules *via* a known secretion system (57, 58), OMVs are emerging as a novel secretion mechanism utilized by *B. fragilis* to deliver immunostimulatory cargo into the cytoplasm of host epithelial cells. Consistent with our findings, a previous study reported the ability of OMVs produced by the closely related *Bacteroides thetaiotaomicron* to enter intestinal epithelial cells using both Caco-2 cells and small intestinal organoid models of OMV entry (59). The entry of *B. fragilis* OMVs into intestinal epithelial cells has not been well described, however previous studies have reported the uptake of *B. fragilis* OMVs by host dendritic cells *ex vivo*, which was thought to facilitate the activation of the cytoplasmic NOD2 immune receptor (22, 25). Additionally, OMVs produced by commensal and probiotic strains of *Escherichia coli* were also found to enter intestinal epithelial cells, whereby fluorescent labelling of their peptidoglycan cargo demonstrated the intracellular delivery of peptidoglycan and the subsequent activation of NOD1-dependent immune responses (21). In contrast to the limited studies reporting the delivery of commensal-derived peptidoglycan into host cells *via* BMVs, there are numerous studies reporting the ability of BMVs produced by pathogens including *H. pylori*, *Vibrio cholerae* and *Aggregatibacter actinomycetemcomitans* to contain peptidoglycan and induce the activation of NOD1- or NOD2-dependent immune responses upon their entry into host epithelial cells (5, 42, 60–62). The BMV-mediated delivery of bacterial RNA to host cells has been also observed for pathogen-derived BMVs (37, 44, 48), resulting in the activation of intracellular detectors of microbial RNA, TLR7 and TLR8 (6, 40), but this has not been characterized in the context of commensal-derived BMVs. Therefore, our findings identify

that *B. fragilis* can deliver bacterial RNA to host epithelial cells *via* OMVs and suggests the possibility that other commensal organisms may also be capable of potentially delivering bacterial-derived RNA into host cells *via* this mechanism, and this forms the basis of future studies. Collectively, these findings demonstrate that *B. fragilis* OMVs enter intestinal epithelial cells to deliver peptidoglycan and RNA cargo intracellularly, resulting in the activation of their respective cytoplasmic PRRs.

Having shown that *B. fragilis* OMVs are enriched in peptidoglycan (Figure 2), as well as their ability to deliver this cargo intracellularly (Figure 4), we demonstrated that *B. fragilis* OMVs can activate NOD1, the intracellular receptor for Gram-negative peptidoglycan (Figure 5A). However, in contrast to a previous study reporting that *B. fragilis* OMVs activated NOD2 following phagocytosis by dendritic cells (25), *B. fragilis* OMVs did not activate NOD2 in our epithelial HEK-Blue cell model of PRR activation. This may be explained by the differences in OMV entry between phagocytic dendritic cells compared to non-phagocytic epithelial cells (63), in addition to the increased expression of NOD2 by cells of myeloid origin (64). Furthermore, *B. fragilis* OMVs activated the intracellular RNA receptor, TLR7, but did not activate TLR8 which can also detect microbial RNA. Whilst human TLR7 and TLR8 are both responsible for the detection of single-stranded RNA compounds, and can be activated by RNA delivered by *S. aureus* MVs into host epithelial cells (6), evidence suggests that TLR7 may have greater ligand sensitivity than TLR8 (65), thus providing a potential explanation as to why we did not see TLR8 activation by *B. fragilis* OMVs in our study. In addition, we did not observe TLR9 activation in response to stimulation with *B. fragilis* OMVs at any MOI examined in this study, which suggests that the amount of DNA delivered by *B. fragilis* OMVs may not have been sufficient to mediate TLR9 activation (35). We have previously shown that BMVs produced by different strains of a bacterial species vary in their amount of DNA and RNA cargo and therefore differ in their ability to activate their respective TLRs (35). Therefore, although we did not see activation of TLR8 and TLR9 by *B. fragilis* OMVs in our study, we cannot exclude the possibility that stimulation of these cells with an increased amount of OMVs, or with OMVs produced by a different *B. fragilis* strain that harbor a greater concentration of DNA and RNA, may activate these TLRs.

Most importantly, the findings of our study revealed that *B. fragilis* bacteria did not induce the activation of any intracellular receptor tested in this study, which may be due to the bacterium being unable to directly deliver their biological cargo intracellularly. Therefore, the ability of the commensal *B. fragilis* to produce OMVs that mediate the activation of intracellular receptors NOD1 and TLR7 enables *B. fragilis* to activate a broader range of immune receptors at the epithelium. Collectively these findings suggest that OMV secretion by *B. fragilis* is a novel mechanism used by this bacterium to increase their potential to mediate immune crosstalk at the intestinal epithelium.

Overall, our findings identify that *B. fragilis* OMVs are enriched in immunostimulatory cargo and can transport this cargo directly into host epithelial cells to preferentially activate host PRRs compared to their parent bacteria. Furthermore, whilst previous studies have recognized the immunomodulatory properties of commensal bacteria or their BMVs, this study compares and provides evidence of key differences in the abilities of *B. fragilis* OMVs and *B. fragilis* bacteria to activate host TLRs and NODs. Therefore, OMVs emerge as a novel secretion mechanism used by *B. fragilis* and potentially other non-invasive commensal bacteria to mediate TLR and NOD activation in epithelial cells. In this way, commensal-derived BMVs may directly contribute to immune activation or modulation at the intestinal mucosal surface. Further research elucidating the composition and ability of other commensal and microbiota-derived BMVs to selectively deliver immunogenic cargo, and to activate and signal *via* host innate immune receptors is needed to improve our understanding of their contribution to maintaining homeostasis in the gastrointestinal niche.

Data availability statement

The original contributions presented in the study are included in the article/Supplementary Material. Further inquiries can be directed to the corresponding author.

Author contributions

All authors performed the research. WG, EJ, AFH and MK-L wrote the manuscript. All authors contributed to the article and approved the submitted version.

Funding

This work was supported by an Australian Research Council Discovery Grant (MK-L and AFH, Grant number DP190101655) and by the LIMS Bioimaging Platform (La Trobe University, Australia). MK-L is supported by a veski Inspiring Women Fellowship.

Conflict of interest

The authors declare that the research was conducted in the absence of any commercial or financial relationships that could be construed as a potential conflict of interest.

Publisher's note

All claims expressed in this article are solely those of the authors and do not necessarily represent those of their affiliated organizations, or those of the publisher, the editors and the reviewers. Any product that may be evaluated in this article, or claim that may be made by its manufacturer, is not guaranteed or endorsed by the publisher.

Supplementary material

The Supplementary Material for this article can be found online at: https://www.frontiersin.org/articles/10.3389/fimmu.2022.970725/full#supplementary-material

SUPPLEMENTARY FIGURE 1
Live and heat-killed *B. fragilis* bacteria activate TLR2, but not TLR4, without reducing host cell viability. HEK-Blue **(A)** null cells as well as **(B)** TLR2 and **(C)** TLR4 expressing HEK-Blue cells were stimulated with an increasing dose of either live (closed circles) or heat-killed (open circles) *B. fragilis* bacteria for 18 hours. Triangles represent positive controls for each respective cell line. Data represents mean ± SEM of three biological replicates. ns = not significant, *p < 0.05 (Unpaired *t*-test). **(D)** HEK-Blue null cells as well as **(E)** TLR2 and **(F)** TLR4 expressing HEK-Blue cells were stimulated with either live or heat-killed *B. fragilis* bacteria (MOI 1,000) for 18 hours, and cell viability was measured using MTT Assay. Non-stimulated cells (NS) were used as a control. Data represents mean ± SEM of at least three biological replicates. ns = not significant (One-way ANOVA with Tukey's multiple comparisons test).

SUPPLEMENTARY FIGURE 2
Live and heat-killed *B. fragilis* bacteria do not activate NOD1 or NOD2, and do not decrease the viability of NOD1-expressing cells. HEK-Blue cells expressing **(A)** NOD1 or **(B)** NOD2 were stimulated with an increasing dose of either live (closed circles) or heat-killed (open circles) *B. fragilis* bacteria for 18 hours. Triangles represent positive controls for each respective cell line. Data represents mean ± SEM of three biological replicates. ns = not significant (Unpaired *t*-test). **(C)** The viability of NOD1-expressing HEK-Blue cells following 18 hours stimulation with either live or heat-killed *B. fragilis* bacteria (MOI 1,000) was measured by MTT Assay. Non-stimulated cells (NS) were used as a control. Data represents mean ± SEM of four biological replicates. ns = not significant (One-way ANOVA with Tukey's multiple comparisons test).

SUPPLEMENTARY FIGURE 3
Live and heat-killed *B. fragilis* bacteria do not activate TLR7, TLR8 or TLR9, and do not decrease the viability of TLR7-expressing cells. HEK-Blue cells expressing **(A)** TLR7, **(C)** TLR8 or **(D)** TLR9 were stimulated with an increasing dose of either live (closed circles) or heat-killed (open circles) *B. fragilis* bacteria for 18 hours. Triangles represent positive controls for each respective cell line. Data represents mean ± SEM of three biological replicates. ns = not significant, (Unpaired *t*-test). **(B)** The viability of TLR7-expressing HEK-Blue cells following 18 hours stimulation with either live or heat-killed *B. fragilis* bacteria (MOI 1,000) was measured by MTT Assay. Non-stimulated cells (NS) were used as a control. Data represents mean ± SEM of four biological replicates. ns = not significant (One-way ANOVA with Tukey's multiple comparisons test).

References

1. Horstman AL, Kuehn MJ. Enterotoxigenic *Escherichia coli* secretes active heat-labile enterotoxin *via* outer membrane vesicles. *J Biol Chem* (2000) 275 (17):12489–96. doi: 10.1074/jbc.275.17.12489

2. Kadurugamuwa JL, Beveridge TJ. Virulence factors are released from *Pseudomonas aeruginosa* in association with membrane vesicles during normal growth and exposure to gentamicin: a novel mechanism of enzyme secretion. *J Bacteriol* (1995) 177(14):3998–4008. doi: 10.1128/jb.177.14.3998-4008.1995

3. Sjöström AE, Sandblad L, Uhlin BE, Wai SN. Membrane vesicle-mediated release of bacterial RNA. *Sci Rep* (2015) 5:15329. doi: 10.1038/srep15329

4. Roier S, Zingl FG, Cakar F, Durakovic S, Kohl P, Eichmann TO, et al. A novel mechanism for the biogenesis of outer membrane vesicles in gram-negative bacteria. *Nat Commun* (2016) 7:10515. doi: 10.1038/ncomms10515

5. Kaparakis M, Turnbull L, Carneiro L, Firth S, Coleman HA, Parkington HC, et al. Bacterial membrane vesicles deliver peptidoglycan to NOD1 in epithelial cells. *Cell Microbiol* (2010) 12(3):372–85. doi: 10.1111/j.1462-5822.2009.01404.x

6. Bitto NJ, Cheng L, Johnston EL, Pathirana R, Phan TK, Poon IKH, et al. *Staphylococcus aureus* membrane vesicles contain immunostimulatory DNA, RNA and peptidoglycan that activate innate immune receptors and induce autophagy. *J Extracell Vesicles* (2021) 10(6):e12080. doi: 10.1002/jev2.12080

7. Haurat MF, Aduse-Opoku J, Rangarajan M, Dorobantu L, Gray MR, Curtis MA, et al. Selective sorting of cargo proteins into bacterial membrane vesicles. *J Biol Chem* (2011) 286(2):1269–76. doi: 10.1074/jbc.M110.185744

8. Kaparakis-Liaskos M, Ferrero RL. Immune modulation by bacterial outer membrane vesicles. *Nat Rev Immunol* (2015) 15(6):375–87. doi: 10.1038/nri3837

9. Kato S, Kowashi Y, Demuth DR. Outer membrane-like vesicles secreted by *Actinobacillus actinomycetemcomitans* are enriched in leukotoxin. *Microb Pathog* (2002) 32(1):1–13. doi: 10.1006/mpat.2001.0474

10. Bitto NJ, Chapman R, Pidot S, Costin A, Lo C, Choi J, et al. Bacterial membrane vesicles transport their DNA cargo into host cells. *Sci Rep* (2017) 7 (1):7072. doi: 10.1038/s41598-017-07288-4

11. Resch U, Tsatsaronis JA, Le Rhun A, Stübiger G, Rohde M, Kasvandik S, et al. A two-component regulatory system impacts extracellular membrane-derived vesicle production in group a *Streptococcus*. *mBio* (2016) 7(6):e00207-16. doi: 10.1128/mBio.00207-16

12. Zavan L, Bitto NJ, Johnston EL, Greening DW, Kaparakis-Liaskos M. *Helicobacter pylori* growth stage determines the size, protein composition, and preferential cargo packaging of outer membrane vesicles. *Proteomics* (2019) 19(1-2):e1800209. doi: 10.1002/pmic.201800209

13. Díaz-Garrido N, Badia J, Baldomà L. Microbiota-derived extracellular vesicles in interkingdom communication in the gut. *J Extracell Vesicles* (2021) 10 (13):e12161. doi: 10.1002/jev2.12161

14. Aguilera L, Toloza L, Giménez R, Odena A, Oliveira E, Aguilar J, et al. Proteomic analysis of outer membrane vesicles from the probiotic strain. *Escherichia coli* Nissle 1917. *Proteomics* (2014) 14(2-3):222–9. doi: 10.1002/pmic.201300328

15. Elhenawy W, Debelyy MO, Feldman MF. Preferential packing of acidic glycosidases and proteases into *Bacteroides* outer membrane vesicles. *mBio* (2014) 5(2):e00909-14. doi: 10.1128/mBio.00909-14

16. Zakharzhevskaya NB, Vanyushkina AA, Altukhov IA, Shavarda AL, Butenko IO, Rakitina DV, et al. Outer membrane vesicles secreted by pathogenic and nonpathogenic *Bacteroides fragilis* represent different metabolic activities. *Sci Rep* (2017) 7(1):5008. doi: 10.1038/s41598-017-05264-6

17. Hong J, Dauros-Singorenko P, Whitcombe A, Payne L, Blenkiron C, Phillips A, et al. Analysis of the *Escherichia coli* extracellular vesicle proteome identifies markers of purity and culture conditions. *J Extracell Vesicles* (2019) 8(1):1632099. doi: 10.1080/20013078.2019.1632099

18. Domínguez Rubio AP, Martínez JH, Martínez Casillas DC, Coluccio Leskow F, Piuri M, Pérez OE. *Lactobacillus casei* BL23 produces microvesicles carrying proteins that have been associated with its probiotic effect. *Front Microbiol* (2017) 8:1783. doi: 10.3389/fmicb.2017.01783

19. Li M, Lee K, Hsu M, Nau G, Mylonakis E, Ramratnam B. *Lactobacillus*-derived extracellular vesicles enhance host immune responses against vancomycin-resistant enterococci. *BMC Microbiol* (2017) 17(1):66. doi: 10.1186/s12866-017-0977-7

20. Hu R, Lin H, Wang M, Zhao Y, Liu H, Min Y, et al. *Lactobacillus reuteri*-derived extracellular vesicles maintain intestinal immune homeostasis against lipopolysaccharide-induced inflammatory responses in broilers. *J Anim Sci Biotechnol* (2021) 12(1):25. doi: 10.1186/s40104-020-00532-4

21. Cañas MA, Fábrega MJ, Giménez R, Badia J, Baldomà L. Outer membrane vesicles from probiotic and commensal *Escherichia coli* activate NOD1-mediated immune responses in intestinal epithelial cells. *Front Microbiol* (2018) 9:498. doi: 10.3389/fmicb.2018.00498

22. Shen Y, Giardino Torchia ML, Lawson GW, Karp CL, Ashwell JD, Mazmanian SK. Outer membrane vesicles of a human commensal mediate immune regulation and disease protection. *Cell Host Microbe* (2012) 12(4):509–20. doi: 10.1016/j.chom.2012.08.004

23. Kang CS, Ban M, Choi EJ, Moon HG, Jeon JS, Kim DK, et al. Extracellular vesicles derived from gut microbiota, especially *Akkermansia muciniphila*, protect the progression of dextran sulfate sodium-induced colitis. *PLoS One* (2013) 8(10): e76520. doi: 10.1371/journal.pone.0076520

24. Al-Nedawi K, Mian MF, Hossain N, Karimi K, Mao YK, Forsythe P, et al. Gut commensal microvesicles reproduce parent bacterial signals to host immune and enteric nervous systems. *FASEB J* (2015) 29(2):684–95. doi: 10.1096/fj.14-259721

25. Chu H, Khosravi A, Kusumawardhani IP, Kwon AH, Vasconcelos AC, Cunha LD, et al. Gene-microbiota interactions contribute to the pathogenesis of inflammatory bowel disease. *Science* (2016) 352(6289):1116–20. doi: 10.1126/science.aad9948

26. Seo MK, Park EJ, Ko SY, Choi EW, Kim S. Therapeutic effects of kefir grain *Lactobacillus*-derived extracellular vesicles in mice with 2,4,6-trinitrobenzene sulfonic acid-induced inflammatory bowel disease. *J Dairy Sci* (2018) 101 (10):8662–71. doi: 10.3168/jds.2018-15014

27. Maerz JK, Steimle A, Lange A, Bender A, Fehrenbacher B, Frick JS. Outer membrane vesicles blebbing contributes to *B. vulgatus* mpk-mediated immune response silencing. *Gut Microbes* (2018) 9(1):1–12. doi: 10.1080/19490976.2017.1344810

28. Diaz-Garrido N, Fábrega M-J, Vera R, Giménez R, Badia J, Baldomà L. Membrane vesicles from the probiotic nissle 1917 and gut resident *Escherichia coli* strains distinctly modulate human dendritic cells and subsequent T cell responses. *J Funct Foods* (2019) 61:103495. doi: 10.1016/j.jff.2019.103495

29. Sears CL, Geis AL, Housseau F. *Bacteroides fragilis* subverts mucosal biology: from symbiont to colon carcinogenesis. *J Clin Invest* (2014) 124 (10):4166–72. doi: 10.1172/jci72334

30. Round JL, Mazmanian SK. Inducible Foxp3+ regulatory T-cell development by a commensal bacterium of the intestinal microbiota. *Proc Natl Acad Sci USA* (2010) 107(27):12204–9. doi: 10.1073/pnas.0909122107

31. Mazmanian SK, Round JL, Kasper DL. A microbial symbiosis factor prevents intestinal inflammatory disease. *Nature* (2008) 453(7195):620–5. doi: 10.1038/nature07008

32. Round JL, Lee SM, Li J, Tran G, Jabri B, Chatila TA, et al. The toll-like receptor 2 pathway establishes colonization by a commensal of the human microbiota. *Science* (2011) 332(6032):974–7. doi: 10.1126/science.1206095

33. Stentz R, Horn N, Cross K, Salt L, Brearley C, Livermore DM, et al. Cephalosporinases associated with outer membrane vesicles released by *Bacteroides* spp. protect gut pathogens and commensals against β-lactam antibiotics. *J Antimicrob Chemother* (2015) 70(3):701–9. doi: 10.1093/jac/dku466

34. Turner L, Bitto NJ, Steer DL, Lo C, D'Costa K, Ramm G, et al. *Helicobacter pylori* outer membrane vesicle size determines their mechanisms of host cell entry and protein content. *Front Immunol* (2018) 9:1466. doi: 10.3389/fimmu.2018.01466

35. Bitto NJ, Zavan L, Johnston EL, Stinear TP, Hill AF, Kaparakis-Liaskos M. Considerations for the analysis of bacterial membrane vesicles: Methods of vesicle production and quantification can influence biological and experimental outcomes. *Microbiol Spectr.* (2021) 9(3):e0127321. doi: 10.1128/Spectrum.01273-21

36. Bitto NJ, Kaparakis-Liaskos M. Methods of bacterial membrane vesicle production, purification, quantification, and examination of their immunogenic functions. *Methods Mol Biol* (2022) 2523:43–61. doi: 10.1007/978-1-0716-2449-4_4

37. Koeppen K, Hampton TH, Jarek M, Scharfe M, Gerber SA, Mielcarz DW, et al. A novel mechanism of host-pathogen interaction through sRNA in bacterial outer membrane vesicles. *PLoS Pathog* (2016) 12(6):e1005672. doi: 10.1371/journal.ppat.1005672

38. Hadzija O. A simple method for the quantitative determination of muramic acid. *Anal Biochem* (1974) 60(2):512–7. doi: 10.1016/0003-2697(74)90261-9

39. Cañas MA, Giménez R, Fábrega MJ, Toloza L, Baldomà L, Badia J. Outer membrane vesicles from the probiotic *Escherichia coli* Nissle 1917 and the commensal ECOR12 enter intestinal epithelial cells *via* clathrin-dependent endocytosis and elicit differential effects on DNA damage. *PLoS One* (2016) 11 (8):e0160374. doi: 10.1371/journal.pone.0160374

40. Cecil JD, O'Brien-Simpson NM, Lenzo JC, Holden JA, Chen YY, Singleton W, et al. Differential responses of pattern recognition receptors to outer membrane vesicles of three periodontal pathogens. *PLoS One* (2016) 11(4):e0151967. doi: 10.1371/journal.pone.0151967

41. Alhawi M, Stewart J, Erridge C, Patrick S, Poxton IR. *Bacteroides fragilis* signals through toll-like receptor (TLR) 2 and not through TLR4. *J Med Microbiol* (2009) 58(Pt 8):1015–22. doi: 10.1099/jmm.0.009936-0

42. Irving AT, Mimuro H, Kufer TA, Lo C, Wheeler R, Turner LJ, et al. The immune receptor NOD1 and kinase RIP2 interact with bacterial peptidoglycan on early endosomes to promote autophagy and inflammatory signaling. *Cell Host Microbe* (2014) 15(5):623–35. doi: 10.1016/j.chom.2014.04.001

43. Choi JW, Kim SC, Hong SH, Lee HJ. Secretable small RNAs *via* outer membrane vesicles in periodontal pathogens. *J Dent Res* (2017) 96(4):458–66. doi: 10.1177/0022034516685071

44. Rodriguez BV, Kuehn MJ. *Staphylococcus aureus* secretes immunomodulatory RNA and DNA *via* membrane vesicles. *Sci Rep* (2020) 10 (1):18293. doi: 10.1038/s41598-020-75108-3

45. Nicola AM, Frases S, Casadevall A. Lipophilic dye staining of *Cryptococcus neoformans* extracellular vesicles and capsule. *Eukaryot Cell* (2009) 8(9):1373–80. doi: 10.1128/ec.00044-09

46. Nakayama-Imaohji H, Hirota K, Yamasaki H, Yoneda S, Nariya H, Suzuki M, et al. DNA Inversion regulates outer membrane vesicle production in. *Bacteroides fragilis*. *PLoS One* (2016) 11(2):e0148887. doi: 10.1371/journal.pone.0148887

47. Ha JY, Choi SY, Lee JH, Hong SH, Lee HJ. Delivery of periodontopathogenic extracellular vesicles to brain monocytes and microglial IL-6 promotion by RNA cargo. *Front Mol Biosci* (2020) 7:596366. doi: 10.3389/fmolb.2020.596366

48. Zhang H, Zhang Y, Song Z, Li R, Ruan H, Liu Q, et al. sncRNAs packaged by *Helicobacter pylori* outer membrane vesicles attenuate IL-8 secretion in human cells. *Int J Med Microbiol* (2020) 310(1):151356. doi: 10.1016/j.ijmm.2019.151356

49. Girardin SE, Boneca IG, Carneiro LA, Antignac A, Jéhanno M, Viala J, et al. Nod1 detects a unique muropeptide from gram-negative bacterial peptidoglycan. *Science* (2003) 300(5625):1584–7. doi: 10.1126/science.1084677

50. Girardin SE, Boneca IG, Viala J, Chamaillard M, Labigne A, Thomas G, et al. Nod2 is a general sensor of peptidoglycan through muramyl dipeptide (MDP) detection. *J Biol Chem* (2003) 278(11):8869–72. doi: 10.1074/jbc.C200651200

51. Dauros-Singorenko P, Hong J, Swift S, Phillips A, Blenkiron C. Effect of the extracellular vesicle RNA cargo from uropathogenic *Escherichia coli* on bladder cells. *Front Mol Biosci* (2020) 7:580913. doi: 10.3389/fmolb.2020.580913

52. Jang KS, Sweredoski MJ, Graham RL, Hess S, Clemons WM Jr. Comprehensive proteomic profiling of outer membrane vesicles from *Campylobacter jejuni*. *J Proteomics* (2014) 98:90–8. doi: 10.1016/j.jprot.2013.12.014

53. Lee EY, Bang JY, Park GW, Choi DS, Kang JS, Kim HJ, et al. Global proteomic profiling of native outer membrane vesicles derived from *Escherichia coli*. *Proteomics* (2007) 7(17):3143–53. doi: 10.1002/pmic.200700196

54. Deo P, Chow SH, Hay ID, Kleifeld O, Costin A, Elgass KD, et al. Outer membrane vesicles from *Neisseria gonorrhoeae* target PorB to mitochondria and induce apoptosis. *PLoS Pathog* (2018) 14(3):e1006945. doi: 10.1371/journal.ppat.1006945

55. Kwon SO, Gho YS, Lee JC, Kim SI. Proteome analysis of outer membrane vesicles from a clinical *Acinetobacter baumannii* isolate. *FEMS Microbiol Lett* (2009) 297(2):150–6. doi: 10.1111/j.1574-6968.2009.01669.x

56. Zariri A, Beskers J, van de Waterbeemd B, Hamstra HJ, Bindels TH, van Riet E, et al. Meningococcal outer membrane vesicle composition-dependent activation of the innate immune response. *Infect Immun* (2016) 84(10):3024–33. doi: 10.1128/iai.00635-16

57. Chatzidaki-Livanis M, Geva-Zatorsky N, Comstock LE. *Bacteroides fragilis* type VI secretion systems use novel effector and immunity proteins to antagonize human gut bacteroidales species. *Proc Natl Acad Sci USA* (2016) 113(13):3627–32. doi: 10.1073/pnas.1522510113

58. Coyne MJ, Roelofs KG, Comstock LE. Type VI secretion systems of human gut bacteroidales segregate into three genetic architectures, two of which are contained on mobile genetic elements. *BMC Genomics* (2016) 17:58. doi: 10.1186/s12864-016-2377-z

59. Jones EJ, Booth C, Fonseca S, Parker A, Cross K, Miquel-Clopés A, et al. The uptake, trafficking, and biodistribution of *Bacteroides thetaiotaomicron* generated outer membrane vesicles. *Front Microbiol* (2020) 11:57. doi: 10.3389/fmicb.2020.00057

60. Thay B, Damm A, Kufer TA, Wai SN, Oscarsson J. *Aggregatibacter actinomycetemcomitans* outer membrane vesicles are internalized in human host cells and trigger NOD1- and NOD2-dependent NF-κB activation. *Infect Immun* (2014) 82(10):4034–46. doi: 10.1128/iai.01980-14

61. Bielig H, Rompikuntal PK, Dongre M, Zurek B, Lindmark B, Ramstedt M, et al. NOD-like receptor activation by outer membrane vesicles from *Vibrio cholerae* non-O1 non-O139 strains is modulated by the quorum-sensing regulator HapR. *Infect Immun* (2011) 79(4):1418–27. doi: 10.1128/iai.00754-10

62. Johnston EL, Heras B, Kufer TA, Kaparakis-Liaskos M. Detection of bacterial membrane vesicles by NOD-like receptors. *Int J Mol Sci* (2021) 22 (3):1005. doi: 10.3390/ijms22031005

63. O'Donoghue EJ, Krachler AM. Mechanisms of outer membrane vesicle entry into host cells. *Cell Microbiol* (2016) 18(11):1508–17. doi: 10.1111/cmi.12655

64. Ogura Y, Inohara N, Benito A, Chen FF, Yamaoka S, Nunez G. Nod2, a Nod1/Apaf-1 family member that is restricted to monocytes and activates NF-kappaB. *J Biol Chem* (2001) 276(7):4812–8. doi: 10.1074/jbc.M008072200

65. Jurk M, Heil F, Vollmer J, Schetter C, Krieg AM, Wagner H, et al. Human TLR7 or TLR8 independently confer responsiveness to the antiviral compound r-848. *Nat Immunol* (2002) 3(6):499. doi: 10.1038/ni0602-499

frontiers | Frontiers in Immunology

TYPE Review
PUBLISHED 27 September 2022
DOI 10.3389/fimmu.2022.971048

Check for updates

OPEN ACCESS

EDITED BY
Mario M. D'Elios,
University of Florence, Italy

REVIEWED BY
Guojun Wu,
Rutgers, The State University of New Jersey, United States
Chiara Della Bella,
University of Florence, Italy
Nagaja Capitani,
University of Siena, Italy

*CORRESPONDENCE
Maria Jelinic
m.jelinic@latrobe.edu.au

†These authors share first authorship

SPECIALTY SECTION
This article was submitted to Microbial Immunology, a section of the journal Frontiers in Immunology

RECEIVED 16 June 2022
ACCEPTED 16 August 2022
PUBLISHED 27 September 2022

CITATION
Brettle H, Tran V, Drummond GR, Franks AE, Petrovski S, Vinh A and Jelinic M (2022) Sex hormones, intestinal inflammation, and the gut microbiome: Major influencers of the sexual dimorphisms in obesity. *Front. Immunol.* 13:971048. doi: 10.3389/fimmu.2022.971048

COPYRIGHT
© 2022 Brettle, Tran, Drummond, Franks, Petrovski, Vinh and Jelinic. This is an open-access article distributed under the terms of the Creative Commons Attribution License (CC BY). The use, distribution or reproduction in other forums is permitted, provided the original author(s) and the copyright owner(s) are credited and that the original publication in this journal is cited, in accordance with accepted academic practice. No use, distribution or reproduction is permitted which does not comply with these terms.

Sex hormones, intestinal inflammation, and the gut microbiome: Major influencers of the sexual dimorphisms in obesity

Holly Brettle[1†], Vivian Tran[1†], Grant R. Drummond[1], Ashley E. Franks[2], Steve Petrovski[1], Antony Vinh[1] and Maria Jelinic[1*]

[1]Centre for Cardiovascular Biology and Disease Research, Department of Microbiology, Anatomy Physiology and Pharmacology, School of Agriculture, Biomedicine and Environment, La Trobe University, Bundoora, VIC, Australia, [2]Department of Microbiology, Anatomy Physiology and Pharmacology, School of Agriculture, Biomedicine and Environment, La Trobe University, Bundoora, VIC, Australia

Obesity is defined as the excessive accumulation of body fat and is associated with an increased risk of developing major health problems such as cardiovascular disease, diabetes and stroke. There are clear sexual dimorphisms in the epidemiology, pathophysiology and sequelae of obesity and its accompanying metabolic disorders, with females often better protected compared to males. This protection has predominantly been attributed to the female sex hormone estrogen and differences in fat distribution. More recently, the sexual dimorphisms of obesity have also been attributed to the differences in the composition and function of the gut microbiota, and the intestinal immune system. This review will comprehensively summarize the pre-clinical and clinical evidence for these sexual dimorphisms and discuss the interplay between sex hormones, intestinal inflammation and the gut microbiome in obesity. Major gaps and limitations of this rapidly growing area of research will also be highlighted in this review.

KEYWORDS

leukocytes, obesity, gut microbiota, estrogen (17β-estradiol), testosterone

Introduction

Obesity is a globally increasing pandemic affecting all ages, ethnicities, sexes, and socio-economic groups. The prevalence of obesity has tripled in the last forty years now affecting ~30% of adults worldwide (1). Obesity is the excessive accumulation of body fat and is associated with an increased risk of developing major health problems such as

cardiovascular disease, diabetes and stroke (2). The most used standard in identifying overweight and obesity is a body mass index (BMI; body weight (kg)/height (m) ^{2}) > 25 kg/m^2 classified as overweight and > 30 as obese (3). It is important to note, that while these are the most widely reported BMI cutoffs, they are only relevant to Caucasians. The BMI cutoffs for obesity for other racial and ethnic categories vary to these values (4). For example, the cutoffs for South Asian populations are slightly lower with a BMI > 23 are classified as overweight and > 25 as obese (3). Concomitant metabolic disturbances of obesity include low-grade chronic inflammation, metabolic endotoxemia, hypertension, dyslipidemia, hyperglycemia, and insulin resistance (5). Interestingly, there are clear sexual dimorphisms in the epidemiology and pathophysiology of obesity and its accompanying metabolic disorders. Generally, females are better protected compared to males – this phenomenon will be discussed in much more detail throughout this review (6). Protection in females has been attributed to various biological processes, that will be the focus of this review, such as the influence of adipose distribution, sex hormones, sex chromosomes, the gut microbiota and the intestinal immune system (7–10).

Adipose tissue biology in obesity

Obesity is instigated by a chronic imbalance of increased energy intake and/or reduced energy expenditure (1). This increases adiposity, a key driver in the development of obesity and the consequential inflammatory state (11). Adipocytes are the predominant cell type in adipose tissue. However, a variety of other cell types also reside in fat beds including leukocytes, endothelial cells and fibroblasts (12). Adipose is a major source of both inflammatory and hormonal signals, and thus is becoming recognized as an endocrine organ in its own right (12). Adipocytes are traditionally classified as either white or brown (12). White adipocytes are particularly important in the storage of energy, whereas brown adipocytes are primarily involved in thermoregulation (via non-shivering thermogenesis) (12). In obesity, where there is a persistent excess of energy, white adipocytes undergo hypertrophy and proliferate to adapt to the accumulation of triglycerides (13). As a result, white adipocytes promote a chronic inflammatory response by secreting pro-inflammatory cytokines such as tumor necrosis factor alpha (TNF-α), interleukin-6 (IL-6), and interleukin-1 beta (IL-1β) (14). This pro-inflammatory phenotype is further compounded by a reduction in the release of anti-inflammatory molecules by obesogenic adipose (15). Ultimately, these changes aid the infiltration of pro-inflammatory immune cells into the adipose tissue and surrounding organs (16). Unsurprisingly, in obesity, white adipose tissue provokes dyslipidemia, insulin resistance and hyperglycemia further exacerbating the dysregulation of whole-body energy homeostasis (16) (Figure 1). Importantly, the changes in adipocyte biology and the subsequent downstream metabolic processes in obesity significantly differ between the sexes and therefore, serve as a major source for the sexual dimorphism of obesity (17).

Sexual dimorphisms in adipose tissue distribution, sex hormones and sex chromosomes

Historically, females have been grossly underrepresented in clinical trials and pre-clinical research. Part of this sex bias in research is the result of an early misconception that men and women are the same. We now know that men and women are unique on a cellular level, and in the setting of obesity there are major sexual dimorphisms. Obesity is slightly more common in females. However, compared to males, females are protected from many of the metabolic disturbances and sequalae that are associated with disease progression in obesity (18, 19). These sexual dimorphisms are also reflected in experimental animal models of diet-induced obesity (19). Male rodents experience an earlier onset and greater degree of obesity, as well as more prevalent concomitant risk factors compared to their female counterparts (such as hyperglycemia, hyperinsulinemia and hypertension) (20, 21). Interestingly, older female animals, or those which model a post-menopause stage (i.e., ovariectomized) are less protected than young females with intact ovaries (22). This correlates with human epidemiology of obesity, whereby men and post-menopausal women are at the greatest risk of developing complications of obesity (23). Collectively, this supports the notion that sex hormones in pre-menopausal women are protective in the setting of obesity. Indeed, sex hormones, such as estrogen, testosterone and androgens are related to the regulation of energy metabolism, food intake and body weight in humans (22, 24). Estrogen is of particular importance and well-established to be protective against cardiometabolic disorders such as obesity, hypertension, and diabetes (25).

The correlation between adipose tissue distribution, sex hormones and the concomitant metabolic disturbances of obesity are well defined (Figure 2), and visceral adiposity is a known driver in the progression of disease in obesity (26). The distribution of adipose tissue throughout the body differs between men and women (27–29). Women have a greater degree of subcutaneous fat ('gynoid' pattern), primarily in the gluteofemoral region. Whereas adipose tissue in men is predominantly seen in the abdominal area ('android' pattern) as visceral fat (30, 31). The sexual bias of these effects has been reported in both rodent models of obesity and in a clinical setting. Male mice on a high fat diet are at a higher risk of developing a pro-inflammatory profile (visceral inflammation,

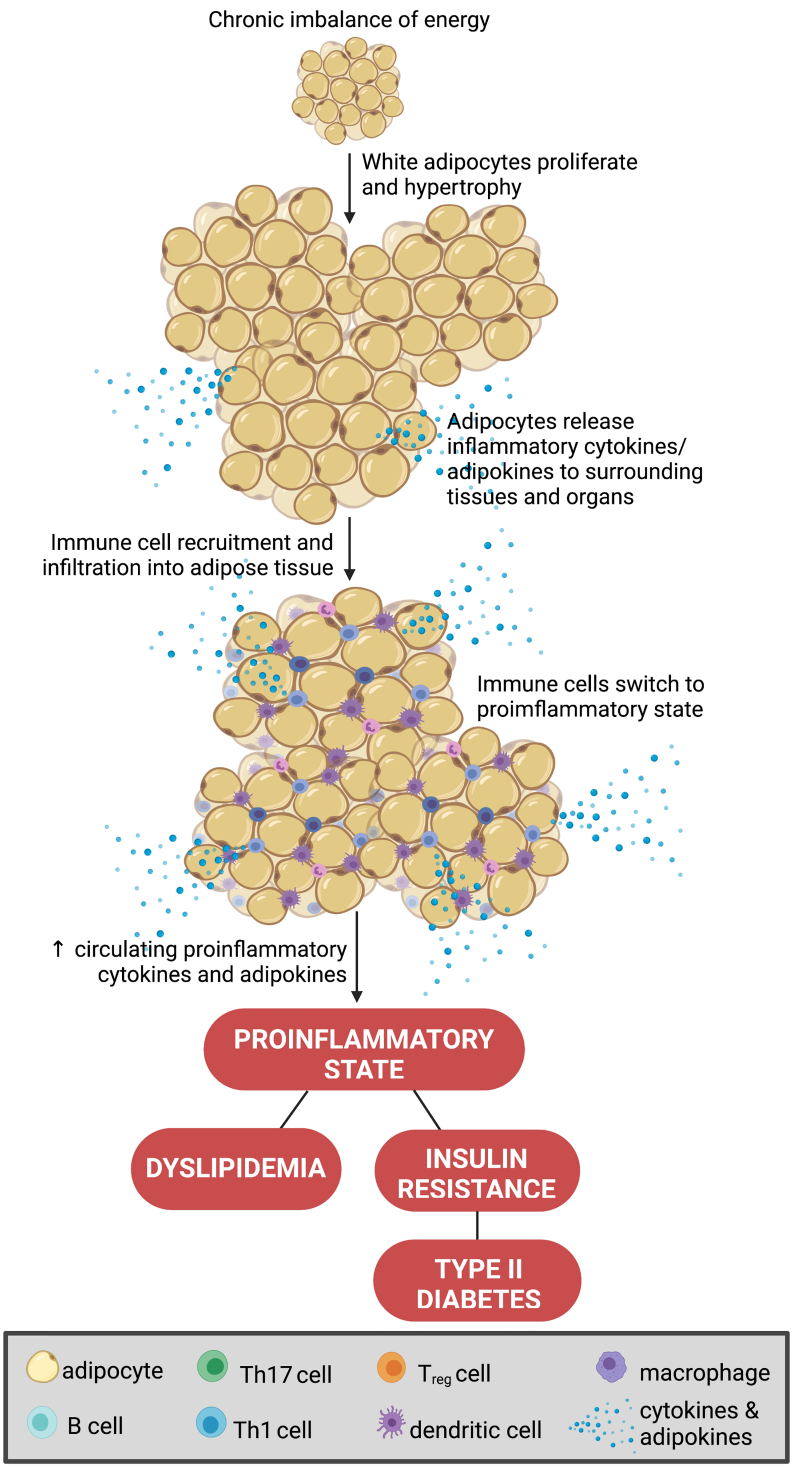

FIGURE 1
Adipocyte biology in obesity. A chronic imbalance of increased energy intake and or reduced energy expenditure increases adiposity, *via* hypertrophy and proliferation of white adipocytes. This promotes the secretion of pro-inflammatory cytokines (i.e., tumor necrosis factor alpha (TNF-α), interleukin 6 (IL-6), IL-1β, and IL-10) to aid the infiltration of pro-inflammatory immune cells into the adipose tissue and surrounding organs (16). This process promotes dyslipidemia, insulin resistance and hyperglycemia further exacerbating the dysregulation of whole-body energy homeostasis. Created with BioRender.com.

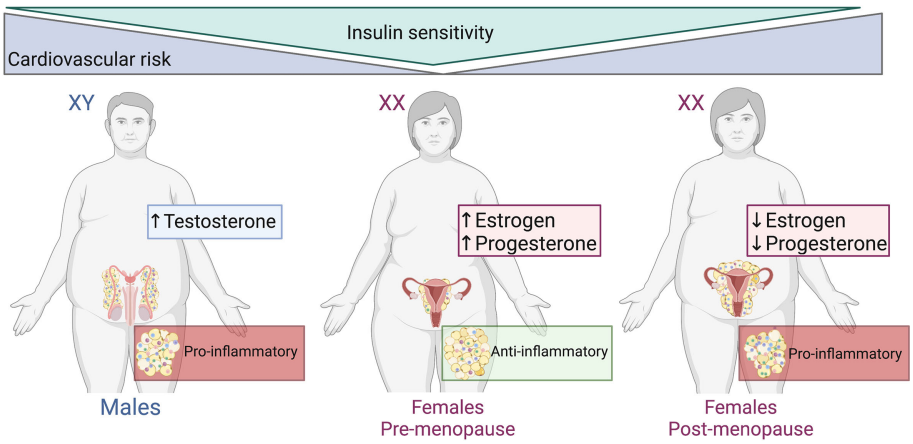

FIGURE 2
Adipose tissue distribution, sex hormones and metabolic disturbances of obesity. Males and post-menopausal females have increased cardiovascular risk, abdominal/visceral obesity and reduced insulin subcutaneous adipose distribution compared to pre-menopausal females. The adipose tissue within males and post-menopausal females is more pro-inflammatory than that of pre-menopausal females. Created with BioRender.com.

glucose intolerance, insulin resistance and hyperinsulinemia) when compared to their female counterparts (32, 33). Increased visceral adiposity in men exacerbates the secretion of pro-inflammatory molecules into systemic circulation which produces a knock-on effect whereby the risk of cardiovascular events is markedly increased. This was observed in the European Health Examination Survey in Luxembourg (34). Interestingly, the Netherlands Epidemiology of Obesity Study reported that visceral adipose tissue distribution was more strongly associated with cardiometabolic risk factors in obese females than in obese males (35). The differences observed in these two studies may be due to the Netherlands study including only obese participants, whereas in the Luxembourg study the BMI of participants ranged from <20 to >35 kg/m^2.

Pre- and post-menopausal studies in women emphasize the role of estrogen in the distribution of adipose tissue by which intra-abdominal visceral fat is increased in post-menopausal women (25, 36–38). With this shift in fat distribution, post-menopausal women undergo metabolic alterations. Lipoprotein lipase activity increases and lipolysis decreases with the fall of estrogen and increased androgenicity is induced during the transition to menopause (36). Ovariectomy in rodents is commonly used as a model of estrogen depletion that occurs in humans. White adipose inflammation is increased and comparable to a male-like phenotype of inflammatory gene expression in ovariectomized mice (39). Despite this pro-inflammatory profile, there were no differences in adipocyte size and total adiposity between ovariectomized and sham mice. This suggests that ovarian hormones are not important in the expansion or apoptosis of adipocytes (39).

In addition to the detrimental effects of visceral adipose, studies also report striking protective effects of gluteofemoral subcutaneous adipose tissue (40). Specifically, increased gluteofemoral mass is associated with lower arterial calcification, arterial stiffness, improved blood lipid levels and atherosclerotic protection (41). While the precise protective mechanisms remain unclear, gluteofemoral adipose has an active role in fatty acid uptake and release by 'trapping' excessive fatty acids, preventing lipid accumulation and lipotoxicity (41–43). Lipolysis relative to energy expenditure is therefore higher in women. Other studies link the protective effects of gluteofemoral adipose with the secretion of anti-inflammatory molecules such as adipokines (41).

Sex chromosomes are another crucial contributing factor to the sexual dimorphisms of adipose tissue distribution and the subsequent metabolic complications of obesity. Female gonads typically occur in individuals with XX chromosomes and male gonads in those with XY chromosomes (44). In a unique mouse model, gonadectomized male and female mice carrying XX chromosome complements developed worse obesity disease outcomes than gonadectomized mice carrying the XY chromosome complements (i.e. increased adiposity, increased satiety, and elevated lipid and insulin levels) (45). Gonadectomized mice carrying XO and XXY chromosome complements revealed that the differences between the XX and XY mice due to the additional X chromosome (or "X chromosome dosage") rather than the lack of a Y chromosome. Indeed, several genes that escape X chromosome inactivation are highly expressed in adipose and liver tissues – both of which are key regulators of metabolism. Thus, the X chromosome may be an important factor in addition to gonads/sex hormones that causes sex differences in obesity and metabolism (45).

Human sex chromosome anomalies also exist such as Klinefelter syndrome (XXY) and Turner syndrome (XO) (46). In Klinefelter syndrome, the most common sex chromosome disorder in men, patients typically present with hypergonadotropic hypogonadism and infertility, with a 5-fold higher incidence in metabolic syndrome, stemming from hypogonadism and low testosterone levels, affecting adiposity and different metabolic traits (47). Turner syndrome patients (the most common sex disorder observed in females, whereby one of the X chromosomes are partially or completely missing) have dramatically reduced gonadal hormone levels. These patients also lack protection against abdominal obesity and have a 4-fold increase in risk for type 2 diabetes (48). Notably, the presence of XX and XY chromosomes influence the developmental path between sexes and gonadal hormones. This ultimately affects the gene expression that may underpin the differences in obesity and metabolism observed between males and females. Although largely attributed to sex hormones and sex chromosomes, the sexual dimorphism of obesity has also been partially credited to sex differences in the microflora residing in our intestines.

The gut microbiota: A key player in health and disease

The gut microbiota is made up of trillions of complex and dynamic microorganisms living within the intestines and working symbiotically with their host for essential metabolic functions (49). Dietary carbohydrates are fermented by the gut microbiota generating short chain fatty acids (SCFA) as by-products, primarily acetate, butyrate and propionate (50). A higher abundance of SCFA, particularly butyrate, is associated with reduced intestinal inflammation and offers protection against the development of insulin resistance and obesity (51, 52). Additionally, there are certain beneficial, anti-inflammatory bacterial species that respond well to fiber rich diets such as *Akkermansia muciniphila, Bifidobacterium* spp., *Prevotella* spp., and *Veillonella* spp. forming a favored environment in terms of functionality and immunity (53). Other by-products of the gut microbiota include energy metabolites including pyruvic, citric, fumaric and malic acid (54, 55). These organic acids aid in digestion, immunity, and specifically in preventing the growth of pathogenic bacteria and thus, offer further protection for their host (56, 57).

In addition to aiding in the digestion of foods to produce favorable by-products, the gut microbiota also has an important role in stimulating and regulating hormone production (58). Previous studies show significant correlations between sex steroid levels (i.e., estrogen, progesterone, and testosterone) and gut microbiota composition (7, 59–61). These studies of the interactions between sex hormones and the gut microbiota revealed sexual dimorphisms in the composition of the gut microbiota which will be discussed later. Another crucial function of the gut microbiota is the maintenance of the intestinal immune system response and its tolerance to the bacterial community (62). Due to their close proximity, it is essential that the gut microbiota and intestinal immune system tolerate one another (62). The interaction between the immune system and gut microbiota is a recognized key player in the development of cardiometabolic diseases and will be discussed in detail later in this review. The next section of the review will focus on the role of the gut microbiota in regulating metabolic functions, particularly in the context of diseases such as obesity and other cardiometabolic diseases (63).

The gut microbiota clearly influences the health of its host and various disease states are associated with “dysbiosis” of the gut microbiota (i.e. an altered composition or functionality). However, dysbiosis is often disease-specific and not consistent between different studies. This is likely due to environmental factors such as diet, lifestyle and drugs being major determinants of gut microbiome composition. Consequently, the gut microbiome is highly individualized which makes it difficult to define what constitutes a healthy microbiome (64). Thus, both clinical and experimental studies should be replicated in independent locations to maximize reproducibility and translatability of findings (65). Moreover, it is largely unclear if gut dysbiosis is a cause or the consequence of disease, highlighting the need for further studies defining the molecular mechanisms by which altered microbiomes cause disease. A recent study built a machine learning model that included both human variables and gut microbiota to try to infer gut microbiota and disease associations more accurately (66).

Despite the striking variations in findings between studies, one of the most consistent findings of intestinal dysbiosis in the setting of disease is the loss of microbiota diversity (67, 68). A highly diverse microbiota is thought to be crucial to good gut health as it is more resilient against pathogens, has a greater functionally complex community and builds a stronger and more stable immune system (69–71). Therefore, reduced gut microbiome diversity is most likely detrimental in disease due to a subsequent loss of microbial community function. Many studies have highlighted that microbial community composition is less important than microbial community function. Therefore, increased microbial diversity can be both beneficial or detrimental, more context is often required for accurate interpretation. For example, germ-free mice lacking a microbiome (and thus lack microbiome diversity), but are protected diet-induced obesity, compared to mice with a gut microbiota (72). Ultimately, making conclusions based on microbiota diversity alone has limited value, and should be avoided.

Major shifts in gut microbiota in obesity

Dysbiosis is a particularly common consequence of a poor diet – a common factor in obesity (73). Diets have a marked influence on the gut microbiota, for example, diets low in fiber and rich in bad fats can modify the bacterial population in as little as 24 hours (74, 75). Diet-induced obesity in animal models is often used to mimic metabolic disturbances and the concomitant gut dysbiosis seen in humans (76, 77). Typically, obesogenic diets include high fat and/or high sugar contents with variations in the types of fat and sugar as well as differences in the duration of diet regimes (77, 78). Importantly, the gut microbiome also influences the concomitant metabolic disturbances of obesity. Oral antibiotic treatment (ampicillin) improves glucose tolerance in high fat diet-fed obese mice. These 'protective' effects of antibiotics in obesity are only effective in early life, suggesting that the plasticity of the gut microbiome reduces with age (79, 80).

Gut microbiota dysbiosis describes the imbalance of microorganisms within the gut resulting in metabolic disturbances in the body and contributing to the development of obesity (81, 82). Overall, dysbiosis can be identified by the loss of beneficial bacteria, the increased abundance of harmful bacteria and a loss of compositional and functional diversity (83). Notably, an emphasis has been placed on the status of the Firmicutes: Bacteroidetes ratio, two dominant phyla in the gut microbiota, and how these phyla alter with disease (84). Many studies conclude that disease states such as obesity are associated with an increase in the abundance of the Firmicutes phyla and a decrease in the abundance of the Bacteroidetes phyla (85–87). Moreover, this phenomenon has proven to be reversible with weight loss (88). While the majority of studies report increased Firmicutes : Bacteroidetes ratios in obesity, it is important to highlight that this is not always the case, and contrasting findings have become more common in recent years. For example, in a recent small cohort study of Beijing volunteers the ratio of Firmicutes/Bacteroidetes decreased significantly in people with obesity (89). Larger studies have also reported similar findings (90). Unfortunately, the Firmicutes: Bacteroidetes ratio is not a robust marker of obesity-related microbiome dysbiosis and many of the studies interpreting changes to the Firmicutes: Bacteroidetes ratio are drastically underpowered (91).

A more accurate approach may be to detect obesity-related changes to the genus, family and species levels within the gut microbiome (54). Beneficial bacteria such as *Akkermansia muciniphila* and members of the *Bifidobacterium* genus have a negative correlation in the development of obesity (92, 93). The beneficial effects of *A. muciniphila* on the intestinal epithelial barrier have long been reported, as it a highly effective mucin-degrading bacterium, with the ability to use various enzyme combinations to hydrolyze up to 85% of mucin structures within the gut (94). A reduction in *A. muciniphila* is associated with increased intestinal permeability or a "leaky gut" – a hallmark of gut dysbiosis in obesity (95). Intestinal permeability allows leakage of water, proteins and other endotoxic molecules such as lipopolysaccharide (LPS) into systemic circulation with the ability to reach other organs and tissues (96). High circulating levels of LPS, termed metabolic endotoxemia, promotes further inflammation, weight gain and diabetes in experimental animals and humans (97). Recent studies have explored the possibility of using *A. muciniphila-associated therapies* as a next-generation treatment for obesity (98). Opposingly, harmful bacteria such as the those from the *Desulfovibrio*, *Fusobacterium* and *Bilophila* genera are positively correlated with obesity (92, 93, 99).

The metabolic and hormonal consequences of gut dysbiosis in obesity

Harmful bacteria within the gut have specified mechanisms that can be destructive to the host. For example, members of the *Desulfovibrio* genus and other sulphate-reducing bacteria induce apoptosis of cells on the intestinal epithelial barrier allowing barrier degradation (100). Additionally, the abundance of gram-negative bacteria increases, with endotoxic lipopolysaccharide (LPS) in their outer membrane (101). LPS then gains access into systemic circulation due to the increased permeability of the epithelial barrier (102). The combination of an increase in harmful bacteria, the decrease in beneficial bacteria, and an increased concentration of pro-inflammatory cytokines within the intestines causes degradation of tight junction proteins between cells allowing LPS and other molecules into underlying tissues and thus, increasing intestinal inflammation (100, 103, 104). Some studies have explored the therapeutic potential of targeting this increase in harmful bacteria in obesity. Alteration of the gut microbiota *via* antibiotics in mice with diet-induced obesity inhibits weight gain, increases lipid oxidation, thermogenesis, and adiponectin gene expression in epididymal adipose tissue. Increases in these molecular pathways likely inhibit fat synthesis and promote a "leaner" phenotype (105). Advances in metagenomics and metabolomics revealed new associations between microbial-derived metabolites (i.e. LPS, short chain fatty acids (SCFAs), ethanol, trimethylamine (TMA), and bile acids) and obesity.

Bile acids are a class of amphipathic steroids synthesized in the liver from cholesterol and metabolized by the gut microbiota. Bile acids facilitate intestinal fat absorption but also modulate glucose, lipid and energy metabolism, intestinal integrity and immunity (106). While there are some discrepancies between studies, circulating bile acid levels are generally positively correlated with obesity. Importantly, microbiome-derived bile acid species have different signaling functions to liver-derived

species. There is a growing body of evidence suggesting a link between the microbiome – an important player in bile acid metabolism – and bile acid levels/composition in obesity (106). Fecal microbiota transplantation (FMT; from a single lean donor) in obese, metabolically uncompromised patients had sustained shifts in microbiomes and bile acid levels toward those of the donor (107). Like much of the microbiome research to date, further studies are still needed to establish whether there is causality, as these "beneficial" changes were not associated with weight loss or changes to glucose metabolism.

To date, numerous studies suggest that gut microbiomes influence eating behavior in humans and animals. Appetite-related hormones such leptin (inhibits appetite) and ghrelin (promotes appetite) are produced by peripheral organs, including gut and adipose tissue. Changes to specific microbial compositions have reported effects on these hormones, and *vice versa*. For example, in obese and non-obese humans, higher circulating leptin concentrations are associated with reduced gut microbiome diversity (108). Moreover, *in vivo* and *in vitro* studies showed that the translocation of living gut microbiota to adipose tissues in obese patients with increased intestinal permeability inhibits leptin signaling (109). Alternatively, the gut microbiota may modulate appetite *via* grehlin. In another study, treatment with SCFAs, lactate, or bacterial supernatants to promote gut microbiome health attenuated ghrelin-mediated signaling (110).

Clearly, whilst gut dysbiosis has been consistently reported in obesity, the severity, and subsequent consequences of dysbiosis vary among obese individuals depend on many factors, which likely explains inconsistent findings between studies (111, 112). One such factor that has more recently been recognized to influence the gut microbiota is an individual's sex.

Sexual dimorphisms and gut microbiota

The impact of the gut microbiota and its influence on the development of obesity has been well documented. However, one aspect that was overlooked in earlier research is the effect of sex. Many studies have investigated the impact of the gut microbiota by altering variables such as diet, lifestyle, and drugs but it is important to recognize that the gut microbiota is different for males and females prior to any manipulations (113). Sequencing the microbial community of prepubescent male and female mice does not show any separation between sexes indicating that sex differences are influenced by gonadal-derived sex hormones and puberty (59, 114). Typically, in mice, the female gut microbiota more closely resembles that of prepubescent males, or castrated males, rather than age-matched males (59, 115). Furthermore, the diversity differs between sexes, with males having a lower species richness and evenness compared to females of the same age in mice models (116). As well as differences in diversity, both animal and human studies show clear variance in the abundance of specific bacteria being higher in one sex compared to the other (113, 117–119). The distinct differences in the male and female gut microbiota, for both animal and human models, inevitably generate differences in metabolic processes and therefore, differences in dysbiosis and the protection or susceptibility to metabolic diseases including obesity (56, 115, 120).

It is well-established that sex steroid hormones are the major drivers of sexual dimorphisms in males and females however, whether there is the strong interaction between sex hormones and gut microbiota is still unclear (59). An observational study that compared the microbiota of men and women with higher serum hormone levels to those with low hormone levels suggests that sex hormones do indeed influence the gut microbiota (121). Higher levels of hormones were associated with a greater diversity in the gut community compared to those with lower hormone levels in both sexes. Moreover, bacteria such as those from the *Acinetobacter, Ruminococcus* and *Megamonas* genus were significantly associated with testosterone levels in men and *Slackia* and *Butyricimonas* were significantly associated with estradiol levels in women (121). Gut microbial transplants to the opposite sex have also been used to determine the hormonal association (10). In these studies females receiving male donor gut microbiota, not only showed higher levels of gut inflammation (a common sign of obesity and cardiometabolic disease) but also resulted in raised testosterone levels (10, 115).

The gut microbiota has also been shown to directly influence sex hormone levels in animal studies using microbial transplants between germ-free mice and mice of opposite sex (7, 10, 122). Colonizing germ-free mice with gut microbiota increases the levels of circulating androgens and begins the development of immune and protective pathways (7, 59). However, there is also evidence that sex hormones can also influence the gut microbiome. Inoculating germ-free mice with human male donor gut microbiota results in males and females harboring these microorganisms differently (122). In female mice, the gut microbiota significantly differed from the matched males and donor, with a higher bacterial diversity (122). Collectively, these studies indicate that there is likely a two-way communication between systemic sex hormones and the gut microbiome, whereby both factors impact one another.

The interactions between sex hormones and gut microbiota have also been studied in animal models using hormone and gonadectomy treatments (61, 101). Estradiol, the most common form of estrogen, is used in hormone treatments to remedy the loss of ovarian estrogen typically seen in menopausal women (123). High fat diet-fed female mice treated with estradiol are protected from cardiometabolic disease (reduced weight gain, improved glucose tolerance and insulin sensitivity) when compared to untreated high fat diet-fed female mice (61). Moreover, estradiol alters the gut microbiota by slowing the

increase in Firmicutes: Bacteroidetes ratio that is usually seen in high fat diet-fed mice (61). Interestingly, sequencing of the gut microbiome of these mice revealed that bacteria from the *S24-7* and *Ruminococcaceae* families, known to generate beneficial SCFA, were in higher abundance in estradiol-treated mice, compared to untreated mice (61). The benefits of estradiol treatment are not limited to just females. Male mice treated with estradiol have a reduced susceptibility to gut epithelial permeability, inflammation and weight gain compared to untreated males (101, 124).

Sexual dimorphisms of the gut microbiota in obesity

As previously discussed, the female sex is also protected from the development of metabolic disturbances in obesity, and the gut microbiota responds differently to diet based on sex (summarized in Table 1). This was demonstrated in overweight and obese adults undergoing either a high protein or low-fat weight loss intervention diet (125). Changes in the gut microbiota occurred not only in diet-specific manner but also differed based on sex (125). Additionally, in animal models of obesity, high fat/high sugar diet-fed mice, demonstrated that females respond slower to the biological adverse effects of the diet as well as differentiating in the composition of the gut microbiota, compared to males (126). The increased Firmicutes: Bacteroidetes ratio typically seen in the development of obesity and metabolic disease is significantly slower in female mice (127). Moreover, differences in the abundance of specific genera are also observed in metabolic syndrome patients. Higher abundances of *Veillonella*, *Methanobrevibacter, Acidaminococcus, Clostridium, Roseburia* and *Faecalibacterium* genera in males, whereas genera such as *Bilophila, Ruminococcus* and *Bacteroides* were greater in females (68, 82). In the male gut microbiota for example, *Veillonella* genera are found in higher abundance in children with type 1 diabetes however, *Roseburia* genera is found to improve metabolic alterations brought on by high fat diets (128, 129). Likewise, for females, *Bilophila* genera aggravates metabolic dysfunction however, *Bacteroides* genera has numerous metabolic benefits on the host (130, 131). These findings suggest that it is not simply the abundance of specific bacteria in the gut microbiota that determine health and disease within the host.

In addition to the sexual dimorphism in response to poor "Western-style" diets, the sex-specific response to beneficial diet supplementations have also been studied (132, 133). Beneficial fiber compounds, including pre- and probiotics, can attenuate the unfavorable effects of the diet by shaping the gut microbiota (93). The addition of prebiotic fibers, such as oligofructose, significantly increases beneficial gut bacteria in healthy and gnotobiotic female, but not male mice, such as *Bacteroides* and *Bifidobacterium* genera and *A. muciniphila* (122, 134). Furthermore, probiotic treatments also adjust the gut microbiota differently for males and females (135). Administration of *Lactobacillus reuteri* increased the abundance of the Bacteroidetes phylum and decreased Firmicutes

TABLE 1 Summary of human and mouse studies investigating the sexual dimorphisms of intestinal microbiota in obesity.

Model	Age	Physiological effects	Main findings	Ref
4-months of either moderately high-protein or LFD in patients with BMI > 25kg/m^2	N/A	Weight loss: ↓ BMI, total & visceral fat, BP, total glucose, LDL cholesterol, leptin, and insulin regardless of diet or sex.	Weight loss-related changes to the intestinal microbiota occurred in a sex- and diet-specific manner.	(125)
Men & post-menopausal women, split based on BMI, following either a Mediterranean or low-fat diet.	♂: 61.2 ±1.3y ♀: 60.3 ±1.4y	N/A: study did not compare physiological parameters between sexes or groups.	Obesity influenced sex differences in gut microbiota. ♂: ↓ *Bacteroides* abundance with ↑ BMI; ↑ *Methanobrevibacter* abundance *(vs.* ♀) regardless of BMI. ♀: ↔ *Bacteroides* abundance with ↑ BMI; ↑ *Bilophila* abundance *(vs.* ♂) regardless of BMI.	(82)
C57BL/6 mice fed either a NCD or HFD (60% fat) for 20 weeks.	8 weeks old	♂: ↑ weight gain for the first 7 weeks on HFD *vs.* ♀. No sex differences following this timepoint.	Sex differences existed in diversity and structure of the gut microbiota at baseline. Gender-specific changes to gut microbiota occurred following HFD.	(113)
C57BL/6 mice fed either a LFLS (10% total fat) or HFHS (45% total fat) for 14 weeks.	8 weeks old	♂: HFHS ↑ weight gain and plasma leptin *vs.* ♀ HFHS mice.	Significant differences in gut microbiota between males and females in both LFLS and HFHS groups. Diet-induced changes to Firmicutes differed between males and females for certain genera.	(126)
C57BL/6 mice fed either a LFD (10% total fat) or HFD (60% total fat) for 20 weeks.	6 weeks old	HFD increased body weight in males and females however, males developed obesity much earlier than female mice.	♂: HFD ↓ Bacteroidetes, Proteobacteria & Tenericutes; ↑ Firmicutes. LFD ↓ Proteobacteria & Tenericutes; ↑ Bacteroidetes; ↔ Firmicutes. ♀: HFD ↓ Firmicutes & Tenericutes; ↑ "others"; ↔ Bacteroidetes. LFD ↓ Firmicutes & Tenericutes; ↑ Bacteroidetes & "others".	(127)

BMI, body mass index; BP, blood pressure; HFD, high fat diet; HFHS, high fat, high sugar diet; LDL, low-density lipoprotein; LFD, low fat diet; LFLS, low fat, low sugar diet; N/A, not applicable; NCD, normal control diet; ref, reference.
♂, male; ♀, female; ↑, increased; ↓, decreased; ↔, unchanged.

in healthy female mice, but showed opposite effects in healthy male mice (135). Given the differences at the phylum level, this also incurred significant differences at the genus level. Females had a significantly greater abundance of *Bacteroides, Prevotella* and *Lactobacillus*, but males had a higher abundance of *Clostridium* (135). These findings not only illustrate that the female gut microbiota has a stronger protection against the adversities of poor diet, but also that the male and female gut microbiota respond differently to the effect of beneficial supplements and how they harbor their microbial communities. The explanation for the sexual dimorphisms in gut microbial composition and function, in both healthy and metabolically disturbed subjects, comes full circle and back to differences in sex steroid hormones and inflammatory responses.

Gonadectomy surgery can be used to eliminate sex steroid hormones and therefore, also be used to study the interactions between sex hormones and the gut microbiota in obesity. In ovariectomized obese female mice, the Firmicutes phyla dominated the gut microbiota community which is commonly seen in obese and high fat diet-fed mice and the sequenced gut community of ovariectomized female mice more closely resembles that of male mice (101, 136). Furthermore, when treating ovariectomized female mice and male mice with estrogen the microbial composition resembles that of non-ovariectomized female mice (101). Similar to ovariectomized mice and the reduction in estrogen, is the changes occurring to the gut microbiota with menopause (137). Studies have shown that the gut microbiota of post-menopausal women reveal higher abundances of Firmicutes compared to both pre-menopausal women and age-matched males (137). These findings reveal that sex and sex hormones, specifically in the presence of obesity, strongly guide the shape of the gut microbiota. In addition to the sexual dimorphism existing within the gut microbiota and obesity, research has revealed that sex-based differences of obesity are also associated with the immune system specifically within the gut (Figure 3).

Sexual dimorphism of intestinal inflammation

Obesity is commonly accompanied with low-grade systemic inflammation which is a key driver of the subsequent comorbidities of obesity due to higher concentrations of endotoxic molecules (i.e., LPS from bacteria) and in circulation increased adiposity increasing cytokines such as TNF-α, IL-1, and IL-6 (138, 139). Many studies in obesity have concentrated on visceral adipose tissue as the driving force of inflammation however, inflammation within the intestinal tract precedes both adipose tissue inflammation and obese characteristics such as weight gain (138). This finding is of particular importance as a significant proportion of the systemic innate and adaptive immune cells within the body (70%) reside within the intestinal tract (140). To our knowledge, the sexual dimorphisms of the intestinal immune system in the setting of obesity has not been researched in a preclinical setting. However, studies have identified sex differences in healthy individuals (141, 142). For example, in the lamina propria layer of the intestines female have higher immune activation and higher $CD4^+$ and $CD8^+$ T cell counts in compared to males (141).

Another crucial mediator of the sexual dimorphisms in intestinal immunity is the gut microbiota. Due to their close proximity, the interplay between the gut microbiota and intestinal immune system is well-established as shaping and developing one another (143). This is highlighted in studies using germ-free mice, which lack a gut microbiota. The consequence of this is poorly developed intestinal lymphatic tissue (Peyer's patches) and immune cell populations (144). Moreover, the sex differences of intestinal immunity in autoimmune disease settings are abolished in germ-free mice, suggesting that the sex bias in immunity is driven by sex differences in the microbiome rather than sex hormones (59, 115).

As mentioned previously, females have a stronger intestinal immune response compared to males and this influence of the gut microbiota on this must also be considered (145). Therefore, the sexual dimorphisms of the gut microbiota and in particular, the difference in biomarkers of obesity such as the Firmicutes: Bacteroidetes phyla and taxa abundance difference likely drive the discrepancies in the intestinal immune system of males and females (127). For example, the Firmicutes phyla are the predominant producers of butyrate, a known anti-inflammatory molecular metabolite (146). Therefore, the increased Firmicutes abundance typical of obese males (compared to obese females), elevates butyrate production, which could suppress the intestinal immune response in males. Alternatively, the Bacteroidetes phyla, generally seen in higher abundance in obese females compared to obese males, are gram-negative bacteria (147). Gram-negative bacteria contain LPS in their outer membrane thus, an increased abundance of these taxa, and subsequent increased circulating LPS, correlates with a stronger intestinal immune response (147).

Although a stronger immune response is associated with an increased inflammatory profile, this may be beneficial in the context of obesity and intestinal inflammation. For example, females are superior in eliminating pathogenic and opportunistic bacteria (possibly obesity-related bacteria) present in the gut, which might be a by-product of their enhanced immune response. The enhanced immune response in females may very well be the factor that protects or delays the development of obesity-related metabolic disturbances in females (148). In the opposing manner, the intestinal immune response is relatively smaller in males, thus allowing the manifestation of deleterious microorganisms and thus, possibly exacerbating the disease development of obesity.

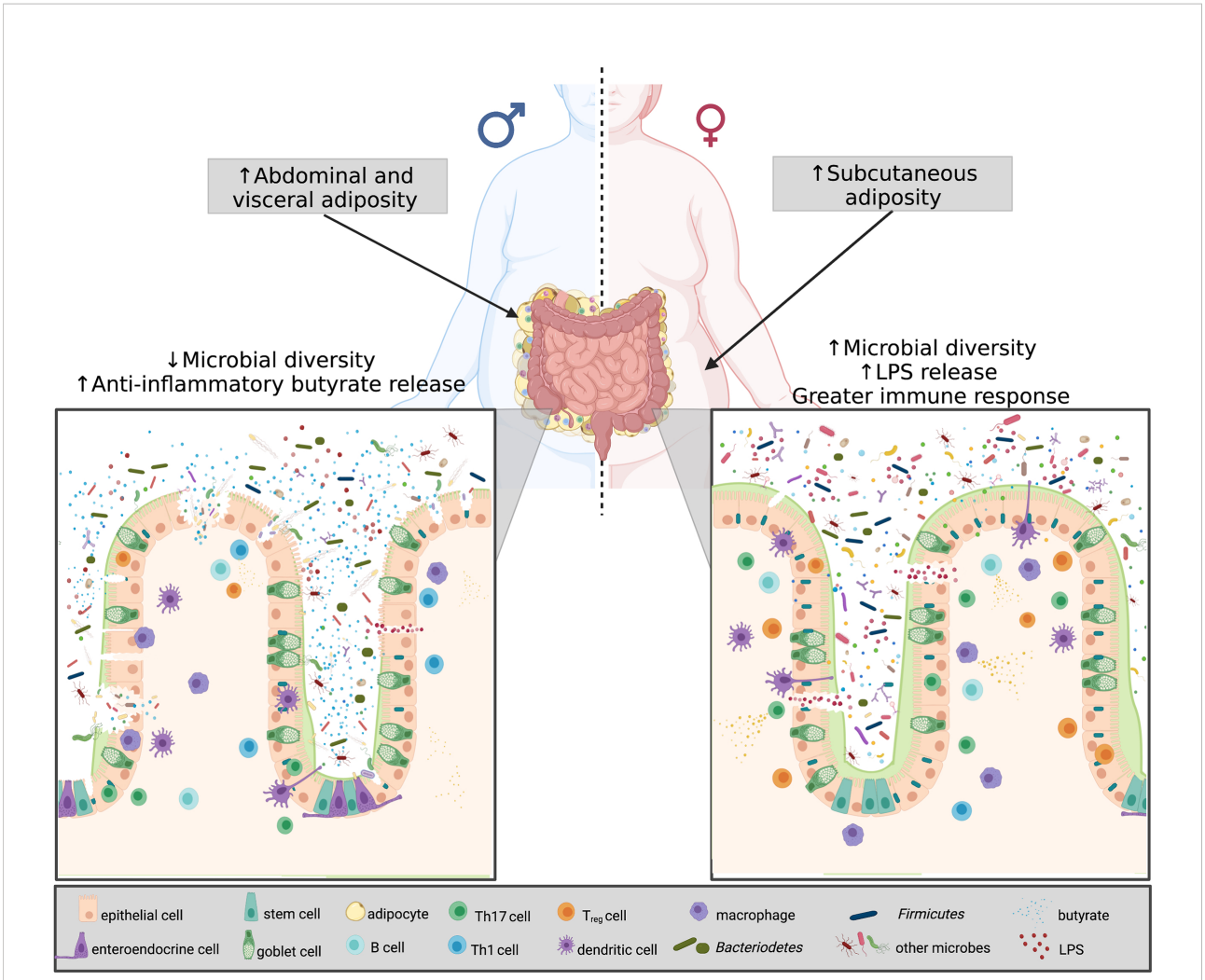

FIGURE 3
Microbial diversity, sex hormones and chromosomes in obesity. Differences in sex-based characteristics are modulated by a variety of factors. Women have a greater degree of subcutaneous fat, whereas males predominantly accumulate visceral fat. In obesity, the shift in the Firmicutes: Bacteroidetes determines disease severity. Obese males have less species richness, and testosterone was found to be associated with increased Firmicutes, thus more anti-inflammatory butyrate release. Obese females, on the other hand, despite having greater microbial diversity, have an increase estradiol and Bacteroidetes, resulting in greater LPS release, thus eliciting a greater immune response. Created with BioRender.com.

Conclusion

The sexual dimorphisms in the epidemiology and pathophysiology of obesity put males and post-menopausal women at the greatest risk of metabolic disturbances and end-organ damage. Although several factors such as sex hormones, sex chromosomes and fat distribution serve as a basis for these sexual dimorphisms, they can also be attributed to differences in the composition and function of the gut microbiota and the intestinal immune response. Both the gut microbiota and immune system are well-documented influencers of the development of obesity however, the important role that sex plays in this relationship is often overlooked. The "give-and-take" relationship each of these three factors have on one another is an important consideration for future studies (Figure 4). Moreover, the vast majority of studies to date are purely associative. More studies that assess causality are needed to unequivocally identify which harmful gut bacteria and or specific gut microbiome imbalances cause obesity. Importantly, it is crucial that these causal studies firstly consider the sex differences in the gut microbiota prior to commencing the study; and secondly, assess the role that sex plays throughout the treatment that will influence the study outcomes. In addition to this, the sex differences in the intestinal immune response in obesity must also be considered in future studies. Very few studies examine both the microbiome and intestinal immune

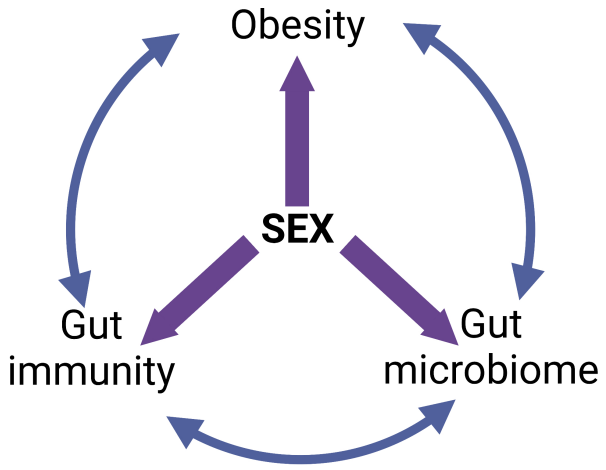

FIGURE 4
The "give-and-take" relationships between obesity, intestinal immunity, gut microbiome and sex. Created with BioRender.com.

response. Finally, due to the sexual dimorphisms that exist in both the gut microbiota and intestinal immune response, it is crucial that females – both pre- and post-menopausal – are represented in research studies to the same extent as males for findings and future treatments to be valid in both sexes.

Author contributions

HB wrote the first draft of the manuscript. VT, AV and MJ wrote sections of the manuscript. HB, VT and MJ created the figures. All authors contributed to manuscript revision, read, and approved the submitted version.

Funding

HB and VT were funded by Australian Research Training Scholarships. MJ was funded by a joint NHMRC and National Heart Foundation Early Career Fellowship (GNT1146314 and 101943, respectively).

Conflict of interest

The authors declare that the research was conducted in the absence of any commercial or financial relationships that could be construed as a potential conflict of interest.

Publisher's note

All claims expressed in this article are solely those of the authors and do not necessarily represent those of their affiliated organizations, or those of the publisher, the editors and the reviewers. Any product that may be evaluated in this article, or claim that may be made by its manufacturer, is not guaranteed or endorsed by the publisher.

References

1. World Health Organization. Overweight and Obesity. (2021). Available at: https://www.who.int/news-room/fact-sheets/detail/obesity-and-overweight

2. Heymsfield SB, Longo DL, Wadden TA. Mechanisms, pathophysiology, and management of obesity. *N Engl J Med* (2017) 376:254–66. doi: 10.1056/NEJMra1514009

3. Smith KB, Smith MS. Obesity statistics. *Prim Care Clin Office Pract* (2016) 43:121–35. doi: 10.1016/j.pop.2015.10.001

4. Caleyachetty R, Barber TM, Mohammed NI, Cappuccio FP, Hardy R, Mathur R, et al. Ethnicity-specific BMI cutoffs for obesity based on type 2 diabetes risk in England: A population-based cohort study. *Lancet Diabetes Endocrinol* (2021) 9:419–26. doi: 10.1016/S2213-8587(21)00088-7

5. Chrostowska M, Szyndler A, Hoffmann M, Narkiewicz K. Impact of obesity on cardiovascular health. *Best Pract Res Clin Endocrinol Metab* (2013) 27:147–56. doi: 10.1016/j.beem.2013.01.004

6. Palmer BF, Clegg DJ. The sexual dimorphism of obesity. *Mol Cell Endocrinol* (2015) 402:113–9. doi: 10.1016/j.mce.2014.11.029

7. Org E, Mehrabian M, Parks BW, Shipkova P, Liu X, Drake TA, et al. Sex differences and hormonal effects on gut microbiota composition in mice. *Gut Microbes* (2016) 7:313–22. doi: 10.1080/19490976.2016.1203502

8. Dean R, Mank JE. The role of sex chromosomes in sexual dimorphism: discordance between molecular and phenotypic data. *J Evol Biol* (2014) 27:1443–53. doi: 10.1111/jeb.12345

9. Elderman M, van Beek A, Brandsma E, de Haan B, Savelkoul H, de Vos P, et al. Sex impacts Th1 cells, tregs, and DCs in both intestinal and systemic immunity in a mouse strain and location-dependent manner. *Biol Sex Differ* (2016) 7:21. doi: 10.1186/s13293-016-0075-9

10. Fransen F, van Beek AA, Borghuis T, Meijer B, Hugenholtz F, van der Gaast-de Jongh C, et al. The impact of gut microbiota on gender-specific differences in immunity. *Front Immunol* (2017) 8:754. doi: 10.3389/fimmu.2017.00754

11. Zheng C, Yang Q, Cao J, Xie N, Liu K, Shou P, et al. Local proliferation initiates macrophage accumulation in adipose tissue during obesity. *Cell Death Dis* (2016) 7:e2167. doi: 10.1038/cddis.2016.54

12. Chakraborty A, Barajas S, Lammoglia GM, Reyna AJ, Morley TS, Johnson JA, et al. Vascular endothelial growth factor-d (VEGF-d) overexpression and lymphatic expansion in murine adipose tissue improves metabolism in obesity. *Am J Pathol* (2019) 189:924–39. doi: 10.1016/j.ajpath.2018.12.008

13. Muir LA, Neeley CK, Meyer KA, Baker NA, Brosius AM, Washabaugh AR, et al. Adipose tissue fibrosis, hypertrophy, and hyperplasia: Correlations with diabetes in human obesity. *Obes (Silver Spring)* (2016) 24:597–605. doi: 10.1002/oby.21377

14. Kang YE, Kim JM, Joung KH, Lee JH, You BR, Choi MJ, et al. The roles of adipokines, proinflammatory cytokines, and adipose tissue macrophages in obesity-associated insulin resistance in modest obesity and early metabolic dysfunction. *PLoS One* (2016) 11:e0154003. doi: 10.1371/journal.pone.0154003

15. Ouchi N, Parker JL, Lugus JJ, Walsh K. Adipokines in inflammation and metabolic disease. *Nat Immunol* (2011) 11:85–97. doi: 10.1038/nri2921

16. Brestoff JR, Artis D. Immune regulation of metabolic homeostasis in health and disease. *Cell* (2015) 161:146–60. doi: 10.1016/j.cell.2015.02.022

17. Link JC, Reue K. Genetic basis for sex differences in obesity and lipid metabolism. *Annu Rev Nutr* (2017) 37:225–45. doi: 10.1146/annurev-nutr-071816-064827

18. Kanter R, Caballero B. Global gender disparities in obesity: A review. *Adv Nutr* (2012) 3:491–8. doi: 10.3945/an.112.002063

19. Hong J, Stubbins RE, Smith RR, Harvey AE, Nunez NP. Differential susceptibility to obesity between male, female and ovariectomized female mice. *Nutr J* (2009) 8:11. doi: 10.1186/1475-2891-8-11

20. Arcones AC, Cruces-Sande M, Ramos P, Mayor FJr., Murga C. Sex differences in high fat diet-induced metabolic alterations correlate with changes in the modulation of GRK2 levels. *Cells* (2019) 8(11):1464. doi: 10.3390/cells8111464

21. Hwang LL, Wang CH, Li TL, Chang SD, Lin LC, Chen CP, et al. Sex differences in high-fat diet-induced obesity, metabolic alterations and learning, and synaptic plasticity deficits in mice. *Obes (Silver Spring)* (2010) 18:463–9. doi: 10.1038/oby.2009.273

22. Sharma G, Mauvais-Jarvis F, Prossnitz ER. Roles of G protein-coupled estrogen receptor GPER in metabolic regulation. *J Steroid Biochem Mol Biol* (2018) 176:31–7. doi: 10.1016/j.jsbmb.2017.02.012

23. Pradhan AD. Sex differences in the metabolic syndrome: implications for cardiovascular health in women. *Clin Chem* (2014) 60:44–52. doi: 10.1373/clinchem.2013.202549

24. Bianchi VE, Locatelli V. Testosterone a key factor in gender related metabolic syndrome. *Obes Rev* (2018) 19:557–75. doi: 10.1111/obr.12633

25. Shi H, Clegg DJ. Sex differences in the regulation of body weight. *Physiol Behav* (2009) 97:199–204. doi: 10.1016/j.physbeh.2009.02.017

26. Hetemaki N, Savolainen-Peltonen H, Tikkanen MJ, Wang F, Paatela H, Hamalainen E, et al. Estrogen metabolism in abdominal subcutaneous and visceral adipose tissue in postmenopausal women. *J Clin Endocrinol Metab* (2017) 102:4588–95. doi: 10.1210/jc.2017-01474

27. Bjorntrop P. Body fat distribution, insulin resistance, and metabolic diseases. *J Nutr* (1997) 13:795–803. doi: 10.1016/S0899-9007(97)00191-3

28. Gruzdeva O, Borodkina D, Uchasova E, Dyleva Y, Barbarash O. Localization of fat depots and cardiovascular risk. *Lipids Health Dis* (2018) 17:218. doi: 10.1186/s12944-018-0856-8

29. Rask-Andersen M, Karlsson T, Ek WE, Johansson A. Genome-wide association study of body fat distribution identifies adiposity loci and sex-specific genetic effects. *Nat Commun* (2019) 10:339. doi: 10.1038/s41467-018-08000-4

30. Jelavic MM, Babic Z, Pintaric H. The importance of two metabolic syndrome diagnostic criteria and body fat distribution in predicting clinical severity and prognosis of acute myocardial infarction. *Arch Med Sci* (2017) 13:795–806. doi: 10.5114/aoms.2016.59703

31. Ladeiras-Lopes R, Sampaio F, Bettencourt N, Fontes-Carvalho R, Ferreira N, Leite-Moreira A, et al. The ratio between visceral and subcutaneous abdominal fat assessed by computed tomography is an independent predictor of mortality and cardiac events. *Rev Esp Cardiol* (2017) 70:331–7. doi: 10.1016/j.recesp.2016.09.006

32. Pettersson US, Walden TB, Carlsson PO, Jansson L, Phillipson M. Female mice are protected against high-fat diet induced metabolic syndrome and increase the regulatory T cell population in adipose tissue. *PloS One* (2012) 7:e46057. doi: 10.1371/journal.pone.0046057

33. Christensen RH, von Scholten BJ, Hansen CS, Jensen MT, Vilsboll T, Rossing P, et al. Epicardial adipose tissue predicts incident cardiovascular disease and mortality in patients with type 2 diabetes. *Cardiovasc Diabetol* (2019) 18:114. doi: 10.1186/s12933-019-0917-y

34. Ruiz-Castell M, Samouda H, Bocquet V, Fagherazzi G, Stranges S, Huiart L. Estimated visceral adiposity is associated with risk of cardiometabolic conditions in a population based study. *Sci Rep* (2021) 11:9121. doi: 10.1038/s41598-021-88587-9

35. Elffers TW, de Mutsert R, Lamb HJ, de Roos A, Willems van Dijk K, Rosendaal FR, et al. Body fat distribution, in particular visceral fat, is associated with cardiometabolic risk factors in obese women. *PLoS One* (2017) 12:e0185403. doi: 10.1371/journal.pone.0185403

36. Toth MJ, Tchernof A, Sites CK, Poehlman ET. Effect of menopausal status on body composition and abdominal fat distribution. *Int J Obes* (2000) 24:226–31. doi: 10.1038/sj.ijo.0801118

37. Chen GC, Arthur R, Iyengar NM, Kamensky V, Xue X, Wassertheil-Smoller S, et al. Association between regional body fat and cardiovascular disease risk among postmenopausal women with normal body mass index. *Eur Heart J* (2019) 40:2849–55. doi: 10.1093/eurheartj/ehz391

38. Karvonen-Gutierrez C, Kim C. Association of mid-life changes in body size, body composition and obesity status with the menopausal transition. *Healthcare (Basel)* (2016) 4(3):42. doi: 10.3390/healthcare4030042

39. Vieira Potter VJ, Strissel KJ, Xie C, Chang E, Bennett G, Defuria J, et al. Adipose tissue inflammation and reduced insulin sensitivity in ovariectomized mice occurs in the absence of increased adiposity. *Endocrinology* (2012) 153:4266–77. doi: 10.1210/en.2011-2006

40. Giannini A, Montt-Guevara M, Shortrede JE, Palla G, Chedraui P, Genazzani AR, et al. Metabolic syndrome and excessive body weight in peri- and postmenopausal women. In: *Postmenopausal diseases and disorders*. Cham: Springer (2019).

41. Manolopoulos KN, Karpe F, Frayn KN. Gluteofemoral body fat as a determinant of metabolic health. *Int J Obes (Lond)* (2010) 34:949–59. doi: 10.1038/ijo.2009.286

42. Lee JW, Kim SY, Lee HJ, Han SW, Lee JE, Lee SM. Prognostic significance of abdominal-to-Gluteofemoral adipose tissue distribution in patients with breast cancer. *J Clin Med* (2019) 8(9):1358. doi: 10.3390/jcm8091358

43. Lotta LA, Wittemans LBL, Zuber V, Stewart ID, Sharp SJ, Luan J, et al. Association of genetic variants related to gluteofemoral vs abdominal fat distribution with type 2 diabetes, coronary disease, and cardiovascular risk factors. *JAMA* (2018) 320:2553–63. doi: 10.1001/jama.2018.19329

44. Link JC, Chen X, Arnold AP, Reue K. Metabolic impact of sex chromosomes. *Adipocyte* (2013) 2:74–9. doi: 10.4161/adip.23320

45. Chen X, McClusky R, Chen J, Beaven SW, Tontonoz P, Arnold AP, et al. The number of x chromosomes causes sex differences in adiposity in mice. *PLoS Genet* (2012) 8:e1002709. doi: 10.1371/journal.pgen.1002709

46. Zore T, Palafox M, Reue K. Sex differences in obesity, lipid metabolism, and inflammation-a role for the sex chromosomes? *Mol Metab* (2018) 15:35–44. doi: 10.1016/j.molmet.2018.04.003

47. Bojesen A, Host C, Gravholt CH. Klinefelter's syndrome, type 2 diabetes and the metabolic syndrome: the impact of body composition. *Mol Hum Reprod* (2010) 16:396–401. doi: 10.1093/molehr/gaq016

48. Baldin AD, Siviero-Miachon AA, Fabbri T, de Lemos-Marini SH, Spinola-Castro AM, Baptista MT, et al. Turner syndrome and metabolic derangements: another example of fetal programming. *Early Hum Dev* (2012) 88:99–102. doi: 10.1016/j.earlhumdev.2011.07.014

49. Lloyd-Price J, Abu-Ali G, Huttenhower C. The healthy human microbiome. *Genome Med* (2016) 8:51. doi: 10.1186/s13073-016-0307-y

50. Chen Y, Chang SKC, Zhang Y, Hsu CY, Nannapaneni R. Gut microbiota and short chain fatty acid composition as affected by legume type and processing methods as assessed by simulated *in vitro* digestion assays. *Food Chem* (2020) 312:126040. doi: 10.1016/j.foodchem.2019.126040

51. Jiminez JA, Uwiera TC, Abbott DW, Uwiera RRE, Inglis GD. Butyrate supplementation at high concentrations alters enteric bacterial communities and reduces intestinal inflammation in mice infected with citrobacter rodentium. *mSphere* (2017) 2(4):e00243-17. doi: 10.1128/mSphere.00243-17

52. Mollica MP, Mattace Raso G, Cavaliere G, Trinchese G, De Filippo C, Aceto S, et al. Butyrate regulates liver mitochondrial function, efficiency, and dynamics in insulin-resistant obese mice. *Diabetes* (2017) 66:1405–18. doi: 10.2337/db16-0924

53. Velikonja A, Lipoglavsek L, Zorec M, Orel R, Avgustin G. Alterations in gut microbiota composition and metabolic parameters after dietary intervention with barley beta glucans in patients with high risk for metabolic syndrome development. *Anaerobe* (2019) 55:67–77. doi: 10.1016/j.anaerobe.2018.11.002

54. Khan MJ, Gerasimidis K, Edwards CA, Shaikh MG. Role of gut microbiota in the aetiology of obesity: Proposed mechanisms and review of the literature. *J Obes* (2016) 2016:7353642. doi: 10.1155/2016/7353642

55. Yadav S, Jha R. Strategies to modulate the intestinal microbiota and their effects on nutrient utilization, performance, and health of poultry. *J Anim Sci Biotechnol* (2019) 10:2. doi: 10.1186/s40104-018-0310-9

56. Elderman M, de Vos P, Faas M. Role of microbiota in sexually dimorphic immunity. *Front Immunol* (2018) 9:1018. doi: 10.3389/fimmu.2018.01018

57. Shimizu K, Yamada T, Ogura H, Mohri T, Kiguchi T, Fujimi S, et al. Synbiotics modulate gut microbiota and reduce enteritis and ventilator-associated pneumonia in patients with sepsis: A randomized controlled trial. *J Crit Care* (2018) 22:239. doi: 10.1186/s13054-018-2167-x

58. Li JY, Chassaing B, Tyagi AM, Vaccaro C, Luo T, Adams J, et al. Sex steroid deficiency-associated bone loss is microbiota dependent and prevented by probiotics. *J Clin Invest* (2016) 126:2049–63. doi: 10.1172/JCI86062

59. Yurkovetskiy L, Burrows M, Khan AA, Graham L, Volchkov P, Becker L, et al. Gender bias in autoimmunity is influenced by microbiota. *Immunity* (2013) 39:400–12. doi: 10.1016/j.immuni.2013.08.013

60. Cross TL, Kasahara K, Rey FE. Sexual dimorphism of cardiometabolic dysfunction: Gut microbiome in the play? *Mol Metab* (2018) 15:70–81. doi: 10.1016/j.molmet.2018.05.016

61. Acharya KD, Gao X, Bless EP, Chen J, Tetel MJ. Estradiol and high fat diet associate with changes in gut microbiota in female ob/ob mice. *Sci Rep* (2019) 9:20192. doi: 10.1038/s41598-019-56723-1

62. Ottman N, Ruokolainen L, Suomalainen A, Sinkko H, Karisola P, Lehtimaki J, et al. Soil exposure modifies the gut microbiota and supports immune tolerance in a mouse model. *J Allergy Clin Immunol* (2019) 143:1198–206.e12. doi: 10.1016/j.jaci.2018.06.024

63. Li X, Watanabe K, Kimura I. Gut microbiota dysbiosis drives and implies novel therapeutic strategies for diabetes mellitus and related metabolic diseases. *Front Immunol* (2017) 8:1882. doi: 10.3389/fimmu.2017.01882

64. McBurney MI, Davis C, Fraser CM, Schneeman BO, Huttenhower C, Verbeke K, et al. Establishing what constitutes a healthy human gut microbiome: State of the science, regulatory considerations, and future directions. *J Nutr* (2019) 149:1882–95. doi: 10.1093/jn/nxz154

65. Marques FZ, Jama HA, Tsyganov K, Gill PA, Rhys-Jones D, Muralitharan RR, et al. Guidelines for transparency on gut microbiome studies in essential and experimental hypertension. *Hypertension* (2019) 74:1279–93. doi: 10.1161/HYPERTENSIONAHA.119.13079

66. Zhu C, Wang X, Li J, Jiang R, Chen H, Chen T, et al. Determine independent gut microbiota-diseases association by eliminating the effects of human lifestyle factors. *BMC Microbiol* (2022) 22:4. doi: 10.1186/s12866-021-02414-9

67. Brüssow H. Problems with the concept of gut microbiota dysbiosis. *Microbial Biotechnol* (2020) 13:423–34. doi: 10.1111/1751-7915.13479

68. Santos-Marcos JA, Perez-Jimenez F, Camargo A. The role of diet and intestinal microbiota in the development of metabolic syndrome. *J Nutr Biochem* (2019) 70:1–27. doi: 10.1016/j.jnutbio.2019.03.017

69. Linninge C, Xu J, Bahl MI, Ahrne S, Molin G. Lactobacillus fermentum and lactobacillus plantarum increased gut microbiota diversity and functionality, and mitigated enterobacteriaceae, in a mouse model. *Benef Microbes* (2019) 10:413–24. doi: 10.3920/BM2018.0074

70. Jakobsson HE, Abrahamsson TR, Jenmalm MC, Harris K, Quince C, Jernberg C, et al. Decreased gut microbiota diversity, delayed bacteroidetes colonisation and reduced Th1 responses in infants delivered by caesarean section. *Gut* (2014) 63:559–66. doi: 10.1136/gutjnl-2012-303249

71. Wang H, Hong T, Li N, Zang B, Wu X. Soluble dietary fiber improves energy homeostasis in obese mice by remodeling the gut microbiota. *Biochem Biophys Res Commun* (2018) 498:146–51. doi: 10.1016/j.bbrc.2018.02.017

72. Bäckhed F, Manchester JK, Semenkovich CF, Gordon JI. Mechanisms underlying the resistance to diet-induced obesity in germ-free mice. *Proc Natl Acad Sci* (2007) 104:979–84. doi: 10.1073/pnas.0605374104

73. McFadyen T, Chai LK, Wyse R, Kingsland M, Yoong SL, Clinton-McHarg T, et al. Strategies to improve the implementation of policies, practices or programmes in sporting organisations targeting poor diet, physical inactivity, obesity, risky alcohol use or tobacco use: A systematic review. *BMJ Open* (2018) 8:e019151. doi: 10.1136/bmjopen-2017-019151

74. Kulecka M, Paziewska A, Zeber-Lubecka N, Ambrozkiewicz F, Kopczynski M, Kuklinska U, et al. Prolonged transfer of feces from the lean mice modulates gut microbiota in obese mice. *Nutr Metab* (2016) 13:57. doi: 10.1186/s12986-016-0116-8

75. Razavi AC, Potts KS, Kelly TN, Bazzano LA. Sex, gut microbiome, and cardiovascular disease risk. *Biol Sex Differ* (2019) 10:29. doi: 10.1186/s13293-019-0240-z

76. Pindjakova J, Sartini C, Lo Re O, Rappa F, Coupe B, Lelouvier B, et al. Gut dysbiosis and adaptive immune response in diet-induced obesity vs. systemic inflammation. *Front Microbiol* (2017) 8:1157. doi: 10.3389/fmicb.2017.01157

77. Panchal SK, Brown L. Rodent models for metabolic syndrome research. *J BioMed Biotechnol* (2011) 2011:351982. doi: 10.1155/2011/351982

78. Gilbert ER, Fu Z, Liu D. Development of a nongenetic mouse model of type 2 diabetes. *Exp Diabetes Res* (2011) 2011:416254. doi: 10.1155/2011/416254

79. Rune I, Hansen CH, Ellekilde M, Nielsen DS, Skovgaard K, Rolin BC, et al. Ampicillin-improved glucose tolerance in diet-induced obese C57BL/6NTac mice is age dependent. *J Diabetes Res* (2013) 2013:319321. doi: 10.1155/2013/319321

80. Cho I, Yamanishi S, Cox L, Methe BA, Zavadil J, Li K, et al. Antibiotics in early life alter the murine colonic microbiome and adiposity. *Nature* (2012) 488:621–6. doi: 10.1038/nature11400

81. Levy M, Kolodziejczyk AA, Thaiss CA, Elinav E. Dysbiosis and the immune system. *Nat Rev Immunol* (2017) 17:219–32. doi: 10.1038/nri.2017.7

82. Haro C, Rangel-Zuniga OA, Alcala-Diaz JF, Gomez-Delgado F, Perez-Martinez P, Delgado-Lista J, et al. Intestinal microbiota is influenced by gender and body mass index. *PloS One* (2016) 11:e0154090. doi: 10.1371/journal.pone.0154090

83. DeGruttola AK, Low D, Mizoguchi A, Mizoguchi E. Current understanding of dysbiosis in disease in human and animal models. *Inflammation Bowel Dis* (2016) 22:1137–50. doi: 10.1097/MIB.0000000000000750

84. Human Microbiome Project Consortium. Structure, function and diversity of the healthy human microbiome. *Nature* (2012) 486:207–14. doi: 10.1038/nature11234

85. Patrone V, Vajana E, Minuti A, Callegari ML, Federico A, Loguercio C, et al. Postoperative changes in fecal bacterial communities and fermentation products in obese patients undergoing bilio-intestinal bypass. *Front Microbiol* (2016) 7:200. doi: 10.3389/fmicb.2016.00200

86. Ley RE, Turnbaugh PJ, Klein S, Gordon JI. Human gut microbes associated with obesity. *Nature* (2006) 444:1022–3. doi: 10.1038/4441022a

87. Palmas V, Pisanu S, Madau V, Casula E, Deledda A, Cusano R, et al. Gut microbiota markers associated with obesity and overweight in Italian adults. *Sci Rep* (2021) 11:5532. doi: 10.1038/s41598-021-84928-w

88. Ulker I, Yildiran H. The effects of bariatric surgery on gut microbiota in patients with obesity: A review of the literature. *Biosci Microb Food Health* (2019) 38:3–9. doi: 10.12938/bmfh.18-018

89. Duan M, Wang Y, Zhang Q, Zou R, Guo M, Zheng H. Characteristics of gut microbiota in people with obesity. *PloS One* (2021) 16:e0255446. doi: 10.1371/journal.pone.0255446

90. Schwiertz A, Taras D, Schäfer K, Beijer S, Bos NA, Donus C, et al. Microbiota and SCFA in lean and overweight healthy subjects. *Obes (Silver Spring)* (2010) 18:190–5. doi: 10.1038/oby.2009.167

91. Magne F, Gotteland M, Gauthier L, Zazueta A, Pesoa S, Navarrete P, et al. The Firmicutes/Bacteroidetes ratio: A relevant marker of gut dysbiosis in obese patients? *Nutrients* (2020) 12(5):1474. doi: 10.3390/nu12051474

92. Schneeberger M, Everard A, Gomez-Valades AG, Matamoros S, Ramirez S, Delzenne NM, et al. Akkermansia muciniphila inversely correlates with the onset of inflammation, altered adipose tissue metabolism and metabolic disorders during obesity in mice. *Sci Rep* (2015) 5:16643. doi: 10.1038/srep16643

93. Wang J, Tang H, Zhang C, Zhao Y, Derrien M, Rocher E, et al. Modulation of gut microbiota during probiotic-mediated attenuation of metabolic syndrome in high fat diet-fed mice. *ISME J* (2015) 9:1–15. doi: 10.1038/ismej.2014.99

94. Trastoy B, Naegeli A, Anso I, Sjögren J, Guerin ME. Structural basis of mammalian mucin processing by the human gut O-glycopeptidase OgpA from akkermansia muciniphila. *Nat Commun* (2020) 11:4844. doi: 10.1038/s41467-020-18696-y

95. Chelakkot C, Choi Y, Kim DK, Park HT, Ghim J, Kwon Y, et al. Akkermansia muciniphila-derived extracellular vesicles influence gut permeability through the regulation of tight junctions. *Exp Mol Med* (2018) 50:e450. doi: 10.1038/emm.2017.282

96. Stenman LK, Burcelin R, Lahtinen S. Establishing a causal link between gut microbes, body weight gain and glucose metabolism in humans - towards treatment with probiotics. *Benef Microbes* (2016) 7:11–22. doi: 10.3920/BM2015.0069

97. Gruber L, Kisling S, Lichti P, Martin FP, May S, Klingenspor M, et al. High fat diet accelerates pathogenesis of murine crohn's disease-like ileitis independently of obesity. *PloS One* (2013) 8:e71661. doi: 10.1371/journal.pone.0071661

98. Xu Y, Wang N, Tan HY, Li S, Zhang C, Feng Y. Function of akkermansia muciniphila in obesity: Interactions with lipid metabolism, immune response and gut systems. *Front Microbiol* (2020) 11:219. doi: 10.3389/fmicb.2020.00219

99. Si X, Shang W, Zhou Z, Strappe P, Wang B, Bird A, et al. Gut microbiome-induced shift of acetate to butyrate positively manages dysbiosis in high fat diet. *Mol Nutr Food Res* (2018) 62:1700670. doi: 10.1002/mnfr.201700670

100. Coutinho C, Coutinho-Silva R, Zinkevich V, Pearce CB, Ojcius DM, Beech I. Sulphate-reducing bacteria from ulcerative colitis patients induce apoptosis of gastrointestinal epithelial cells. *Microb Pathog* (2017) 112:126–34. doi: 10.1016/j.micpath.2017.09.054

101. Kaliannan K, Robertson RC, Murphy K, Stanton C, Kang C, Wang B, et al. Estrogen-mediated gut microbiome alterations influence sexual dimorphism in metabolic syndrome in mice. *Microbiome* (2018) 6:205. doi: 10.1186/s40168-018-0587-0

102. Nighot M, Al-Sadi R, Guo S, Rawat M, Nighot P, Watterson MD, et al. Lipopolysaccharide-induced increase in intestinal epithelial tight permeability is mediated by toll-like receptor 4/myeloid differentiation primary response 88 (MyD88) activation of myosin light chain kinase expression. *Am J Pathol* (2017) 187:2698–710. doi: 10.1016/j.ajpath.2017.08.005

103. Shin J, Noh JR, Chang DH, Kim YH, Kim MH, Lee ES, et al. Elucidation of akkermansia muciniphila probiotic traits driven by mucin depletion. *Front Microbiol* (2019) 10:1137. doi: 10.3389/fmicb.2019.01137

104. Kawano M, Miyoshi M, Ogawa A, Sakai F, Kadooka Y. Lactobacillus gasseri SBT2055 inhibits adipose tissue inflammation and intestinal permeability in mice fed a high-fat diet. *J Nutr Sci* (2016) 5:e23. doi: 10.1017/jns.2016.12

105. Yao H, Fan C, Lu Y, Fan X, Xia L, Li P, et al. Alteration of gut microbiota affects expression of adiponectin and resistin through modifying DNA methylation in high-fat diet-induced obese mice. *Genes Nutr* (2020) 15:12. doi: 10.1186/s12263-020-00671-3

106. Li R, Andreu-Sánchez S, Kuipers F, Fu J. Gut microbiome and bile acids in obesity-related diseases. *Best Pract Res Clin Endocrinol Metab* (2021) 35:101493. doi: 10.1016/j.beem.2021.101493

107. Allegretti JR, Kassam Z, Mullish BH, Chiang A, Carrellas M, Hurtado J, et al. Effects of fecal microbiota transplantation with oral capsules in obese patients. *Clin Gastroenterol Hepatol* (2020) 18:855–863.e2. doi: 10.1016/j.cgh.2019.07.006

108. Le Chatelier E, Nielsen T, Qin J, Prifti E, Hildebrand F, Falony G, et al. Richness of human gut microbiome correlates with metabolic markers. *Nature* (2013) 500:541–6. doi: 10.1038/nature12506

109. Massier L, Chakaroun R, Tabei S, Crane A, Didt KD, Fallmann J, et al. Adipose tissue derived bacteria are associated with inflammation in obesity and type 2 diabetes. *Gut* (2020) 69:1796–806. doi: 10.1136/gutjnl-2019-320118

110. Torres-Fuentes C, Golubeva AV, Zhdanov AV, Wallace S, Arboleya S, Papkovsky DB, et al. Short-chain fatty acids and microbiota metabolites attenuate ghrelin receptor signaling. *FASEB J* (2019) 33:13546–59. doi: 10.1096/fj.201901433R

111. Rothschild D, Weissbrod O, Barkan E, Kurilshikov A, Korem T, Zeevi D, et al. Environment dominates over host genetics in shaping human gut microbiota. *Nature* (2018) 555:210–5. doi: 10.1038/nature25973

112. Davenport ER. Genetic variation shapes murine gut microbiota *via* immunity. *Trends Immunol* (2020) 41:1–3. doi: 10.1016/j.it.2019.11.009

113. Bridgewater LC, Zhang C, Wu Y, Hu W, Zhang Q, Wang J, et al. Gender-based differences in host behavior and gut microbiota composition in response to high fat diet and stress in a mouse model. *Sci Rep* (2017) 7:10776. doi: 10.1038/s41598-017-11069-4

114. Steegenga WT, Mischke M, Lute C, Boekschoten MV, Pruis MGM, Lendvai A, et al. Sexually dimorphic characteristics of the small intestine and colon of prepubescent C57BL/6 mice. *Biol Sex Differ* (2014) 5:1–17. doi: 10.1186/s13293-014-0011-9

115. Markle J, Frank D, Mortin-Toth S, Robertson CE, Feazel LM, Rolle-Kampczyk U, et al. Sex differences in the gut microbiome drive hormone-dependent regulation of autoimmunity. *Science* (2013) 339:1084–8. doi: 10.1126/science.1233521

116. Kozik AJ, Nakatsu CH, Chun H, Jones-Hall YL. Age, sex, and TNF associated differences in the gut microbiota of mice and their impact on acute TNBS colitis. *Exp Mol Pathol* (2017) 103:311–9. doi: 10.1016/j.yexmp.2017.11.014

117. Suzuki Y, Ikeda K, Sakuma K, Kawai S, Sawaki K, Asahara T, et al. Association between yogurt consumption and intestinal microbiota in healthy young adults differs by host gender. *Front Microbiol* (2017) 8:847. doi: 10.3389/fmicb.2017.00847

118. Mueller S, Saunier K, Hanisch C, Norin E, Alm L, Midtvedt T, et al. Differences in fecal microbiota in different European study populations in relation to age, gender, and country: A cross-sectional study. *Appl Environ Microbiol* (2006) 72:1027–33. doi: 10.1128/AEM.72.2.1027-1033.2006

119. Takagi T, Naito Y, Inoue R, Kashiwagi S, Uchiyama K, Mizushima K, et al. Differences in gut microbiota associated with age, sex, and stool consistency in healthy Japanese subjects. *J Gastroenterol* (2019) 54:53–63. doi: 10.1007/s00535-018-1488-5

120. Faith JJ, McNulty NP, Rey FE, Gordon JI. Predicting a human gut microbiota's response to diet in gnotobiotic mice. *Science* (2011) 333:101–4. doi: 10.1126/science.1206025

121. Shin JH, Park YH, Sim M, Kim SA, Joung H, Shin DM. Serum level of sex steroid hormone is associated with diversity and profiles of human gut microbiome. *Res Microbiol* (2019) 170:192–201. doi: 10.1016/j.resmic.2019.03.003

122. Wang JJ, Wang J, Pang XY, Zhao LP, Tian L, Wang XP. Sex differences in colonization of gut microbiota from a man with short-term vegetarian and inulin-supplemented diet in germ-free mice. *Sci Rep* (2016) 6:36137. doi: 10.1038/srep36137

123. Baber RJ, Panay N, Fenton AI.M.S.W. Group. 2016 IMS recommendations on women's midlife health and menopause hormone therapy. *Climacteric* (2016) 19:109–50. doi: 10.3109/13697137.2015.1129166

124. Garratt M, Lagerborg KA, Tsai YM, Galecki A, Jain M, Miller RA. Male Lifespan extension with 17-alpha estradiol is linked to a sex-specific metabolomic response modulated by gonadal hormones in mice. *Aging Cell* (2018) 17:e12786. doi: 10.1111/acel.12786

125. Cuevas-Sierra A, Romo-Hualde A, Aranaz P, Goni L, Cuervo M, Martinez JA, et al. Diet- and sex-related changes of gut microbiota composition and functional profiles after 4 months of weight loss intervention. *Eur J Nutr* (2021) 60:3279–301. doi: 10.1007/s00394-021-02508-0

126. Daly CM, Saxena J, Singh J, Bullard MR, Bondy EO, Saxena A, et al. Sex differences in response to a high fat, high sucrose diet in both the gut microbiome and hypothalamic astrocytes and microglia. *Nutr Neurosci* (2020) 25(2):321–35. doi: 10.1080/1028415X.2020.1752996

127. Qin Y, Roberts JD, Grimm SA, Lih FB, Deterding LJ, Li R, et al. An obesity-associated gut microbiome reprograms the intestinal epigenome and leads to altered colonic gene expression. *Genome Biol* (2018) 19:7. doi: 10.1186/s13059-018-1389-1

128. Vesth T, Ozen A, Andersen SC, Kaas RS, Lukjancenko O, Bohlin J, et al. Veillonella, firmicutes: Microbes disguised as gram negatives. *Stand Genom Sci* (2013) 9:431–48. doi: 10.4056/sigs.2981345

129. Neyrinck AM, Possemiers S, Verstraete W, De Backer F, Cani PD, Delzenne NM. Dietary modulation of clostridial cluster XIVa gut bacteria (Roseburia spp.) by chitin-glucan fiber improves host metabolic alterations induced by high-fat diet in mice. *J Nutr Biochem* (2012) 23:51–9. doi: 10.1016/j.jnutbio.2010.10.008

130. Natividad JM, Lamas B, Pham HP, Michel ML, Rainteau D, Bridonneau C, et al. Bilophila wadsworthia aggravates high fat diet induced metabolic dysfunctions in mice. *Nat Commun* (2018) 9:2802. doi: 10.1038/s41467-018-05249-7

131. Wexler AG, Goodman AL. An insider's perspective: Bacteroides as a window into the microbiome. *Nat Microbiol* (2017) 2:17026. doi: 10.1038/nmicrobiol.2017.26

132. Roopchand DE, Carmody RN, Kuhn P, Moskal K, Rojas-Silva P, Turnbaugh PJ, et al. Dietary polyphenols promote growth of the gut bacterium akkermansia muciniphila and attenuate high-fat diet–induced metabolic syndrome. *Diabetes* (2015) 64:2847–58. doi: 10.2337/db14-1916

133. Zhu G, Ma F, Wang G, Wang Y, Zhao J, Zhang H, et al. Bifidobacteria attenuate the development of metabolic disorders, with inter- and intra-species differences. *Food Funct* (2018) 9:3509–22. doi: 10.1039/C8FO00100F

134. Shastri P, McCarville J, Kalmokoff M, Brooks SP, Green-Johnson JM. Sex differences in gut fermentation and immune parameters in rats fed an oligofructose-supplemented diet. *Biol Sex Differ* (2015) 6:13. doi: 10.1186/s13293-015-0031-0

135. He J, Wang W, Wu Z, Pan D, Guo Y, Cai Z, et al. Effect of lactobacillus reuteri on intestinal microbiota and immune parameters: Involvement of sex differences. *J Funct Foods* (2019) 53:36–43. doi: 10.1016/j.jff.2018.12.010

136. Choi S, Hwang YJ, Shin MJ, Yi H. Difference in the gut microbiome between ovariectomy-induced obesity and diet-induced obesity. *J Microbiol Biotechnol* (2017) 27:2228–36. doi: 10.4014/jmb.1710.10001

137. Santos-Marcos JA, Rangel-Zuniga OA, Jimenez-Lucena R, Quintana-Navarro GM, Garcia-Carpintero S, Malagon MM, et al. Influence of gender and menopausal status on gut microbiota. *Maturitas* (2018) 116:43–53. doi: 10.1016/j.maturitas.2018.07.008

138. Ding S, Lund PK. Role of intestinal inflammation as an early event in obesity and insulin resistance. *Curr Opin Clin Nutr Metab Care* (2011) 14:328–33. doi: 10.1097/MCO.0b013e3283478727

139. Winer DA, Luck H, Tsai S, Winer S. The intestinal immune system in obesity and insulin resistance. *Cell Metab* (2016) 23:413–26. doi: 10.1016/j.cmet.2016.01.003

140. Vancamelbeke M, Vermeire S. The intestinal barrier: A fundamental role in health and disease. *Expert Rev Gastroenterol Hepatol* (2017) 11:821–34. doi: 10.1080/17474124.2017.1343143

141. Sankaran-Walters S, Macal M, Grishina I, Nagy L, Goulart L, Coolidge K, et al. Sex differences matter in the gut: Effect on mucosal immune activation and inflammation. *Biol Sex Differ* (2013) 4:1–12. doi: 10.1186/2042-6410-4-10

142. Houghton LA, Heitkemper M, Crowell M, Emmanuel A, Halpert A, McRoberts JA, et al. Age, gender and women's health and the patient. *Gastroenterology* (2016) S0016-5085(16)00183-9. doi: 10.1053/j.gastro.2016.02.017

143. Ciampolillo A. Metabolic syndrome and gut microbiota: There is a gender difference? *Ital J Gend-Specif Med* (2019) 5:21–6. doi: 10.1723/3148.31295

144. Fiebiger U, Bereswill S, Heimesaat MM. Dissecting the interplay between intestinal microbiota and host immunity in health and disease: Lessons learned from germfree and gnotobiotic animal models. *Eur J Microbiol Immunol* (2016) 6:253–71. doi: 10.1556/1886.2016.00036

145. Vemuri R, Sylvia KE, Klein SL, Forster SC, Plebanski M, Eri R, et al. The microgenderome revealed: Sex differences in bidirectional interactions between the microbiota, hormones, immunity and disease susceptibility. *Semin Immunopathol* (2019) 41:265–75. doi: 10.1007/s00281-018-0716-7

146. Postler TS, Ghosh S. Understanding the holobiont: How microbial metabolites affect human health and shape the immune system. *Cell Metab* (2017) 26:110–30. doi: 10.1016/j.cmet.2017.05.008

147. Wu S, Pan L, Liao H, Yao W, Shen N, Chen C, et al. High-fat diet increased NADPH-oxidase-related oxidative stress and aggravated LPS-induced intestine injury. *Life Sci* (2020) 253:117539. doi: 10.1016/j.lfs.2020.117539

148. Mulak A, Tache Y, Larauche M. Sex hormones in the modulation of irritable bowel syndrome. *World J Gastroenterol* (2014) 20:2433–48. doi: 10.3748/wjg.v20.i10.2433

frontiers | Frontiers in Immunology

TYPE Original Research
PUBLISHED 28 September 2022
DOI 10.3389/fimmu.2022.946929

Check for updates

OPEN ACCESS

EDITED BY
Maria Kaparakis-Liaskos,
La Trobe University, Australia

REVIEWED BY
Bum-Joon Kim,
College of Medicine, Seoul National University, South Korea
Mary O'Sullivan,
Trinity College Dublin, Ireland

*CORRESPONDENCE
Seungwha Paik
swpaik11@cnu.ac.kr
Eun-Kyeong Jo
hayoungj@cnu.ac.kr

SPECIALTY SECTION
This article was submitted to Microbial Immunology, a section of the journal Frontiers in Immunology

RECEIVED 18 May 2022
ACCEPTED 07 September 2022
PUBLISHED 28 September 2022

CITATION
Paik S, Kim KT, Kim IS, Kim YJ, Kim HJ, Choi S, Kim H-J and Jo E-K (2022) Mycobacterial acyl carrier protein suppresses TFEB activation and upregulates miR-155 to inhibit host defense. *Front. Immunol.* 13:946929. doi: 10.3389/fimmu.2022.946929

COPYRIGHT
© 2022 Paik, Kim, Kim, Kim, Kim, Choi, Kim and Jo. This is an open-access article distributed under the terms of the Creative Commons Attribution License (CC BY). The use, distribution or reproduction in other forums is permitted, provided the original author(s) and the copyright owner(s) are credited and that the original publication in this journal is cited, in accordance with accepted academic practice. No use, distribution or reproduction is permitted which does not comply with these terms.

Mycobacterial acyl carrier protein suppresses TFEB activation and upregulates miR-155 to inhibit host defense

Seungwha Paik[1,2]*, Kyeong Tae Kim[1,2,3], In Soo Kim[1,2,3], Young Jae Kim[1,2,3], Hyeon Ji Kim[1,2,3], Seunga Choi[1,2], Hwa-Jung Kim[1,2,3] and Eun-Kyeong Jo[1,2,3]*

[1]Department of Microbiology, Chungnam National University School of Medicine, Daejeon, South Korea, [2]Department of Medical Science, Chungnam National University School of Medicine, Daejeon, South Korea, [3]Infection Control Convergence Research Center, Chungnam National University School of Medicine, Daejeon, South Korea

Mycobacterial acyl carrier protein (AcpM; Rv2244), a key protein involved in *Mycobacterium tuberculosis* (Mtb) mycolic acid production, has been shown to suppress host cell death during mycobacterial infection. This study reports that mycobacterial AcpM works as an effector to subvert host defense and promote bacterial growth by increasing microRNA (miRNA)-155-5p expression. In murine bone marrow-derived macrophages (BMDMs), AcpM protein prevented transcription factor EB (TFEB) from translocating to the nucleus in BMDMs, which likely inhibited transcriptional activation of several autophagy and lysosomal genes. Although AcpM did not suppress autophagic flux in BMDMs, AcpM reduced Mtb and LAMP1 co-localization indicating that AcpM inhibits phagolysosomal fusion during Mtb infection. Mechanistically, AcpM boosted the Akt-mTOR pathway in BMDMs by upregulating miRNA-155-5p, a SHIP1-targeting miRNA. When miRNA-155-5p expression was inhibited in BMDMs, AcpM-induced increased intracellular survival of Mtb was suppressed. In addition, AcpM overexpression significantly reduced mycobacterial clearance in C3HeB/FeJ mice infected with recombinant *M. smegmatis* strains. Collectively, our findings point to AcpM as a novel mycobacterial effector to regulate antimicrobial host defense and a potential new therapeutic target for Mtb infection.

KEYWORDS

***Mycobacterium tuberculosis*, transcription factor EB, phagosome-lysosome fusion, microRNA-155-5p, acyl carrier protein, bone marrow-derived macrophages**

Introduction

Tuberculosis (TB) is a worldwide infectious disease that has claimed many lives, and the fight against TB still faces many challenges. According to the World Health Organization's global TB report 2020, TB caused an estimated 10 million new cases and 1.5 million deaths in 2020, making it the second most deadly infectious disease caused by a single pathogen after COVID-19. *Mycobacterium tuberculosis* (Mtb), the bacteria that causes tuberculosis, has a variety of defense mechanisms to evade the host's innate immune system, including autophagy, apoptosis, and inflammation (1). Mtb can also survive as a latent infection for a long time in alveolar macrophages, making it resistant to anti-TB drugs and difficult to eradicate (2). To control Mtb, it's crucial to understand the dynamics of the host-pathogen interaction. To date, several mycobacterial factors, such as SapM (3), ESAT-6/CFP-10 (4), nuoG (5), Eis (6), LprG (7), PE_PGRS47 (8), SecA2 (9, 10), LprE (11), PknG (12), and phthiocerol dimycocerosates (PDIM) (13), are known to influence how Mtb suppresses host defenses through modulating various innate immune strategies against Mtb in host immune cells. Nonetheless, new mycobacterial components that alter the host's innate immune response must be discovered to better understand the molecular mechanisms underlying mycobacterial pathogenesis and develop new therapeutic targets.

Mtb requires a unique acyl carrier protein (AcpM), the second most glycosylated protein involved in mycolic acid biosynthesis (14). Mycolic acids, which protect Mtb from the host environment while also eluting virulence, are one of the most important components of the mycobacterial cell wall (15). AcpM interacts with PptT, which transfers 4′-phosphopantetheine (Ppt) from coenzyme A (CoA) to AcpM in Mtb for mycolic acid synthesis (16). According to a recent study, a small compound called "8918" inhibited PptT action by binding to the Ppt pocket in the active site, resulting in selective antimicrobial activity comparable to rifampin (17). These findings raise concerns about the intrinsic properties of the AcpM and how they affect Mtb virulence. Although AcpM is essential for Mtb growth by producing lipid-rich cell walls, little is known about its immunological properties in host-pathogen interactions.

This study investigated the mechanisms by which the AcpM protein prevents nuclear translocation of transcription factor EB (TFEB) and phagosomal maturation in host macrophages. AcpM appeared to inhibit autophagy in bone marrow-derived macrophages (BMDMs) by lowering the LC3 I to II ratio; however, it did not affect autophagic flux in BMDMs. Rather than this, AcpM markedly reduced nuclear translocation of TFEB and several autophagy-related genes including lysosomal-associated membrane protein 1 (*Lamp1*), which was regulated by TFEB, in macrophages. Moreover, AcpM activated the protein kinase B (Akt) pathway, which is associated with Mtb survival in host cells, by inducing miR-155, which targets SH2-domain-containing inositol 5-phosphatase 1 (SHIP1) (18). AcpM prevented Mtb from fusing with lysosomes in BMDMs, thus increasing Mtb intracellular survival (ICS). Finally, in the lung lysates of recombinant *M. smegmatis*-infected mice, AcpM overexpression increased Mtb colony-forming unit (CFU) levels while decreasing several autophagy and lysosomal genes.

Taken together, these findings help us to explore the relationship between the host immune response and mycobacterial infection in terms of Mtb AcpM, revealing its potential as a target for novel tuberculosis therapies.

Materials and methods

Animals and ethics statement

Female C57BL/6 and BALB/c mice were purchased from Samtako Bio (Gyeonggi-do, Korea) at 6–7 weeks of age, and C3HeB/FeJ mice were obtained from the Jackson Laboratory (Bar Harbor, ME, USA). Mice were maintained under specific pathogen-free conditions. All animal experimental methods and procedures were performed following the relevant ethical guidelines and regulations approved by the Institutional Research and Ethics Committee at Chungnam National University, School of Medicine (202009A-CNU-155; Daejeon, Korea) and the guidelines of the Korean Food and Drug Administration.

Cell culture

Bone marrow cells were isolated from C57BL/6 mice (6-8 weeks old) and cultured in Dulbecco's modified Eagle's medium (DMEM; Lonza, Walkersville, USA) containing 10% fetal bovine serum (FBS; Gibco, NY, USA) and antibiotics (Lonza). Differentiating for 4–5 days in the presence of 25 μg/ml of recombinant mouse macrophage colony-stimulating factor (M-CSF) (R&D Systems) in a 37°C humidified atmosphere containing 5% CO_2 produced primary BMDMs. Approximately 4 x 10^5 cells/well in the 24-well cell culture plate (SPL Life Science Co., Gyeonggi-do, Korea) or 2 x 10^5 cells/well in the 48-well cell culture plate (Corning, NY, USA) were used for the entire *in-vitro* analysis.

Preparation of recombinant AcpM protein and anti-AcpM antibody

Recombinant AcpM protein was prepared according to the previous study (19). Briefly, mycobacterial *acpM* was amplified from genomic DNA of Mtb H37Rv ATCC 27294 using the forward (5'-CATATGCCTGTCACTCAGGAAGAAATC-3') and reverse primers (5'-AAGCTTCTTGGACTCGG CCTCAAGCCT-3'), and the PCR product was inserted into

the pET-22b (+) vector (Novagen, Madison, WI, USA). The recombinant plasmids were transformed into *E. coli* BL21 cells by heat-shocking for 1 min at 42 °C. Cell disruption was used to obtain the overexpressed AcpM protein, which was then purified using NI-NTA resin. The purified recombinant protein was dialyzed and incubated with polymyxin B-agarose (Sigma Chemical Co.) to remove residual endotoxin. The purified endotoxin-free AcpM was filter sterilized and kept frozen at -80°C until use. To collect anti-AcpM antibodies, BALB/c mice were injected three times intraperitoneally with purified AcpM (25 μg per mouse) emulsified in incomplete Freund's adjuvant. One week after the final immunization, serum was collected and stored frozen until use with proper dilution.

Construction of recombinant *M. smegmatis* strains

Mycobacterial *acpM* was amplified from genomic DNA of Mtb H37Rv ATCC 27294 using the forward (*Nde*I site, 5'-CATATGCCTGTCACTCAGGAAGAAATC-3') and reverse primers (*Hin*dIII site, 5'-AAGCTTCTTGGACTCGG CCTCAAGCCT-3') as in the previous study (19). Then, amplified *acpM* was inserted into the pVV16 vector to create pVV16_AcpM. The pVV16 (vector only) and pVV16_AcpM plasmids were electroporated into suspensions of *M. smegmatis* mc^2155 competent cells at 2.5 kV, 1,000 Ω, and 25 μF using a Gene Pulser (Bio-Rad, San Diego, CA, USA) to construct Ms_Vec and Ms_AcpM, respectively. Western blot image of AcpM expression in Ms_Vec and Ms_AcpM using anti-AcpM antibody was presented in Supplementary Figure S1.

Western blot analysis

BMDMs cultured in 24-well cell culture plates were lysed in 150 μl of radioimmunoprecipitation assay (RIPA) buffer (LPS solution, CBR002) added with protease and phosphatase inhibitor cocktail (Roche, Mannheim, Germany). The whole mouse lung was homogenized in 1 ml of PBS containing 0.05% Tween 80 (PBST) and then half of the homogenates were centrifuged and lysed in 500 μl of RIPA buffer containing protease and phosphatase inhibitor cocktail. The cell lysates were mixed with Protein 5X Sample Buffer (ELPIS BIOTECH, EBA-1052) and boiled for 10 min. Prepared protein extracts were separated by SDS-polyacrylamide gel electrophoresis (PAGE) and then transferred to polyvinylidene difluoride (PVDF; Millipore, Burlington, MA, USA) membranes. The membranes were then blocked using 1X blocking solution (Biofact) for 1 h at room temperature (RT) and then incubated overnight with primary antibodies at 4 °C. After washing with tris-buffered saline supplemented with 0.1% Tween 20 (TBST), the membranes were incubated with the secondary antibodies for 1 h at RT. Immunoblotting was performed using an enhanced chemiluminescence reagent (Millipore, WBKL S0500) and a UVitec Alliance mini-chemiluminescence device (UVitec, Rugby, UK). The densitometric values were calculated using ImageJ software and data were normalized to loading controls shown in the figures. Bafilomycin A1 (B1793) was purchased from Sigma-Aldrich (St. Louis, MO, USA) The primary and secondary antibodies used were as follows: Anti-p62 (1:1000 diluted; P0067) and anti-LC3 (1:1000 diluted; L8918) antibodies were purchased from Sigma-Aldrich. anti-LAMP1 (1:1000 diluted; sc-20011) was purchased from Santa Cruz Biotechnology (Dallas, TX, USA), Anti-β-actin (1:2000 diluted; 5125s), anti-phospho-mTOR (1:1000 diluted; 2971s), anti-mTOR (1:1000 diluted; 2983s), anti-phospho-Akt (1:1000 diluted; 4060s), anti-Akt (1:1000 diluted; 9272s), anti-TFEB (1:1000 diluted; 4240s), anti-ATG5 (1:1000 diluted; 12994s), anit-SHIP1 (1:1000 diluted; 2728s), anti-FOXO3a (1:1000 diluted; 12829s), anti-mouse IgG (1:5000 diluted; 7076s), and anti-rabbit IgG (1:5000 diluted; 7074s) antibodies were purchased from Cell Signaling Technology (Danvers, MA, USA).

Bacterial strains and culture

Mtb H37Rv was kindly provided by Dr. R. L. Friedman (University of Arizona, Tucson, AZ, USA). Mtb was grown at 37 °C with shaking in Middlebrook 7H9 broth (Difco, Paris, France) supplemented with 0.5% glycerol, 0.05% Tween-80 (Sigma-Aldrich), and oleic albumin dextrose catalase (OADC; BD Biosciences). Mtb-expressing enhanced red fluorescent protein (Mtb-ERFP) and recombinant *M. smegmatis* strains were grown in Middlebrook 7H9 medium supplemented with OADC and 50 μg/ml kanamycin (Sigma-Aldrich). Bacterial strains were then harvested by centrifugation at 3000 rates per min for 30 min and the pellets were resuspended in ice-cold phosphate-buffered saline (PBS). All mycobacterial suspensions were aliquoted and stored at −80 °C until just before use. For all experiments, mid-log-phase bacteria (O.D = 0.6) were used. The number of CFUs of the inoculum was verified by serially diluting and plating on Middlebrook 7H10 agar (Difco).

Immunofluorescence analysis

BMDMs were cultured on coverslips in 24-well cell culture plates. After the appropriate infection or treatment, cells were washed twice with PBS, fixed with 4% paraformaldehyde for 15 min, and permeabilized with 0.25% Triton X-100 (Sigma-Aldrich) for 10 min. Cells were incubated with anti-TFEB antibody (1:400 diluted; Bethyl Laboratories, A303-673A) or anti-LAMP1 Ab (1:400 diluted; Santa Cruz Biotechnology, SC-19992) overnight at 4°C. Cells were washed with PBS to remove excess primary antibodies and then incubated with secondary

anti-rabbit or anti-rat IgG-Alexa Fluor 488 Ab (1:400 diluted; Invitrogen, A11008 or A11006) for 1 h at RT. Nuclei were stained using Fluoromount-G™, with DAPI mounting medium (Thermo Fisher Scientific, 00-4959-52). Immunofluorescence images were acquired using a confocal laser-scanning microscope (Zeiss, LSM-900). Quantification of TFEB-nuclear translocation was performed by manual calculation and the degree of colocalization between Mtb-ERFP and LAMP-1 was analyzed using the JACoP plugin of the ImageJ software.

Total RNA extraction and sequencing

Total RNA from BMDMs was isolated using QIAzol lysis reagent (Qiagen, Hilden, Germany) and miRNeasy Mini Kits (Qiagen) according to the manufacturer's instructions. RNA quality was assessed by Agilent 2100 bioanalyzer using the RNA 6000 Pico Chip (Agilent Technologies, CA, USA), and quantification was performed using a NanoDrop 2000 Spectrophotometer system (Thermo Fisher Scientific, MA, USA). For messenger RNA-sequencing (mRNA-seq), the library was constructed using QuantSeq 3' mRNA-Seq Library Prep Kit (Lexogen, Wien, Austria) according to the manufacturer's instructions. In brief, each sample was prepared with 500 ng of total RNA, an oligo-dT primer with an Illumina-compatible sequence at its 5' end was hybridized with the RNA, and reverse transcription was performed. After degradation of the RNA template, second-strand synthesis was initiated by a random primer with an Illumina-compatible linker sequence at its 5' end. The double-stranded library was purified using magnetic beads to remove all reaction components and amplified to add the complete adapter sequences required for cluster generation. The finished library was purified from PCR components, and then high-throughput sequencing was performed as single-end 75 sequencings using NextSeq 500 (Illumina, CA, USA). For micro RNA-sequencing (miRNA-seq), the construction of the library was performed using the NEBNext Multiplex Small RNA Library Prep kit (New England BioLabs, MA, USA) according to the manufacturer's instructions. Briefly, for library construction, total RNA from each sample was used 1 μg to ligate the adaptors, and then cDNA was synthesized using reverse-transcriptase with adaptor-specific primers. PCR was performed for library amplification, and libraries were cleaned up using QIAquick PCR Purification Kit (Qiagen) and AMPure XP beads (Beckman Coulter, CA, USA). The Agilent 2100 Bioanalyzer instrument assessed the yield and size distribution of the small RNA libraries for the High-sensitivity DNA Assay (Agilent Technologies). The NextSeq500 system produced High-throughput sequences to single-end 75 sequencings (Illumina).

All raw reads received the quality check using BBduk, a tool in the BBMap package (https://sourceforge.net/projects/bbmap), to remove low-quality bases (< Q20). The remaining reads from QuantSeq 3' mRNA-Seq and miRNA-seq were mapped to the mouse mm10 genome reference and mature miRNA sequences of the miRBase database (20) using Bowtie2 software (21), respectively. Read counts of genes were calculated with Bedtools (22) and the raw counts were transformed into counts per million (CPM) for exclusion of very lowly expressed genes using edgeR (version 3.36.0) (23). Genes with one or more log2-CPM in at least two samples were kept for further analysis. Next, normalization factors were calculated with the trimmed mean of M-values (TMM) method using the calcNormFactors function in edgeR. For Z-score normalization, the TMM-adjusted log CPM counts were calculated, and Gaussian normalization was performed. To identify differentially expressed genes (DEGs), gene expression levels were statistically tested between groups using the glmFit and glmLRT functions embedded in the edgeR package. Benjamini and Hochberg's false discovery rate (FDR) method was used to correct for multiple testing. Genes with the fold change over two and the significance (adjusted p-value) below 0.01 were considered DEGs. The binding site between miRNA and the 3' untranslated region (UTR) of target mRNA was predicted by miRWalk 3.0 at http://mirwalk.umm.uni-heidelberg.de/ (last accessed February 2022).

Quantitative real-time PCR

For mRNA expression analysis, total RNA from BMDMs cultured in 48-well cell culture plates or mouse lung tissue homogenates was extracted using TRIzol reagent (Invitrogen; 15596026) according to the manufacturer's instructions, followed by RNA quantitation and assessment using QIAxpert (Qiagen). Complement DNA from total RNA was synthesized using the reverse transcription master premix (ELPIS Biotech; EBT-1515c) as manufacturer's instruction. Two-step quantitative real-time PCR (qRT-PCR) was carried out using cDNA, primers, and Rotor-Gene SYBR Green PCR Kit (Qiagen, 204074). Reactions were run on a Rotor-Gene Q 2plex system (Qiagen, 9001620). The samples were amplified for 40 cycles as follows: 95°C for 5 s and 60°C for 10 s. Data were expressed as relative fold changes using the 2-ΔΔ threshold cycle (Ct) method with *β-actin* (BMDMs) or *Gapdh* (lung tissue homogenates) as an internal control gene. The primer sequences used are shown in Supplementary Table 1.

For miRNA expression analysis, total RNA from BMDMs cultured in 48-well cell culture plates was isolated using QIAzol lysis reagent (Qiagen, 79306) and miRNeasy Mini Kits (Qiagen, 217004) according to the manufacturer's instructions. Next, cDNA from total RNA was synthesized using miScript II RT Kits (Qiagen, 218161) by the manufacturer's instructions. Three-step qRT-PCR was performed using the miScript SYBR Green

PCR Kit (Qiagen, 218073), and samples were amplified for 50 cycles as follows: 95°C for 15 s, 55°C for 30 s, and 72°C for 30 s. Small nuclear RNA (RNU6-6P RNA; Qiagen, MS00033740) was used for the normalization of the expression of miR-155-3p and miR-155-5p. The primer sequences used are shown in Supplementary Table 2.

Transient transfection

BMDMs cultured in 48-well cell culture plates were transiently transfected with a miRNA mimic negative control (20 nM), miR-155-5p mimic (20 nM), miRNA inhibitor negative control (100 nM), or miR-155-5p inhibitor (100 nM) using the Lipofectamine 3000 Transfection Kit (Invitrogen, L3000-008) according to the manufacturer's instructions. Genolution (Seoul, South Korea) provided the miR-155-5p mimic (5′-UUAAUGCUAAUUGUGAUAGGGGU-3′) and miR-155-5p inhibitor (5′-ACCCCUAUCACAAUUAGCAUUAA-3′), and Ambion (Austin, TX, USA) provided the miRNA mimic negative control (4464058) and inhibitor negative control (4464076).

Colony-forming unit assay

BMDMs cultured in 48-well cell culture plates were transiently transfected with miRNA inhibitor negative control or miR-155-5p inhibitor before infecting with Mtb H37Rv at a multiplicity of infection (MOI) of 3 for 4 h. The infected cells were washed with PBS to remove extracellular bacteria and further incubated in the fresh medium for the indicated periods. Cells were then lysed in sterile distilled water for 30 min, serially diluted with PBS, and plated on the Middlebrook 7H10 agar plates containing OADC. Plates were incubated for 2-3 weeks at 37°C and colonies were enumerated to assess intracellular bacterial viability.

In-vivo analysis with recombinant *M. smegmatis* strains

Frozen bacterial cells were centrifuged after thawing, and the pellet was resuspended in PBST. After anesthetizing C3HeB/FeJ mice, 1×10^6 CFU/mouse of Ms_Vec or Ms_AcpM were inoculated intranasally. At the indicated times after infection, mice were euthanized and the lungs were collected to assess the bacterial burden. Lung tissues were homogenized using a tissue homogenizer (Omni International Inc., Warrenton, VA, USA) in PBST. Serial dilutions of the homogenates were planted in 7H10 agar plates, and colonies were counted after 3-4 days of incubation at 37°C.

Statistical analysis

All of the experiments were repeated as indicated in figure legends, with consistent results. An unpaired Student's t-test was used to determine the significance of differences between two groups, and an one-way analysis of variance (ANOVA) followed by Tukey's multiple comparison test was used to determine the significance of differences among three or more groups using Prism® software version 8 (GraphPad Software, San Diego, CA, USA). Data are expressed as means ± standard deviation (SD) or standard error of the mean (SEM); statistical significance was defined as $^*p < 0.05$, $^{**}p < 0.01$, and $^{***}p < 0.001$.

Results

AcpM inhibits TFEB expression and its nuclear translocation

To find the key molecule governing the host defense in AcpM-treated BMDMs, mRNA-seq analysis was performed (Figure 1A; Supplementary Table 3). Several autophagy-related genes, including *Tfeb*, were significantly downregulated in AcpM-treated BMDMs (AcpM) when compared to untreated cells (Un) (Figure 1A). Since TFEB is known to play a pivotal role in the regulation of lysosomal biogenesis and autophagy (24), qRT-PCR and western blot analysis were conducted to confirm its relative expression. Over time, AcpM treatment reduced the gene (Figure 1B) and protein (Figure 1C) levels of TFEB. Furthermore, AcpM treatment effectively suppressed the nuclear translocation of TFEB. The degree of TFEB in the nucleus reduced at early time points after AcpM addition in BMDMs, as shown by confocal images with TFEB staining in green (Figure 1D).

AcpM suppresses the expression of numerous autophagy and lysosomal genes in the TFEB downstream pathway

TFEB enters the nucleus to function as a transcription factor inducing lysosomal biogenesis. Since AcpM blocks its nuclear translocation (Figure 1D), various genes related to autophagy or lysosomal activity were thought to decrease with AcpM treatment in BMDMs. In detail, AcpM treatment significantly reduced the levels of *Lamp1*, *Lamp2*, autophagy-related gene 5 (*Atg5*), *Atg 7*, and several *Tfeb* downstream genes such as *Uvrag* and *Vps11* over time (Figure 2A). AcpM also significantly suppressed the expression of *Rap7a*, *Gabarap*, *Beclin-1* (*Becn1*), and damage-regulated autophagy modulator 2 (*Dram2*) at most

10.3389/fimmu.2022.946929

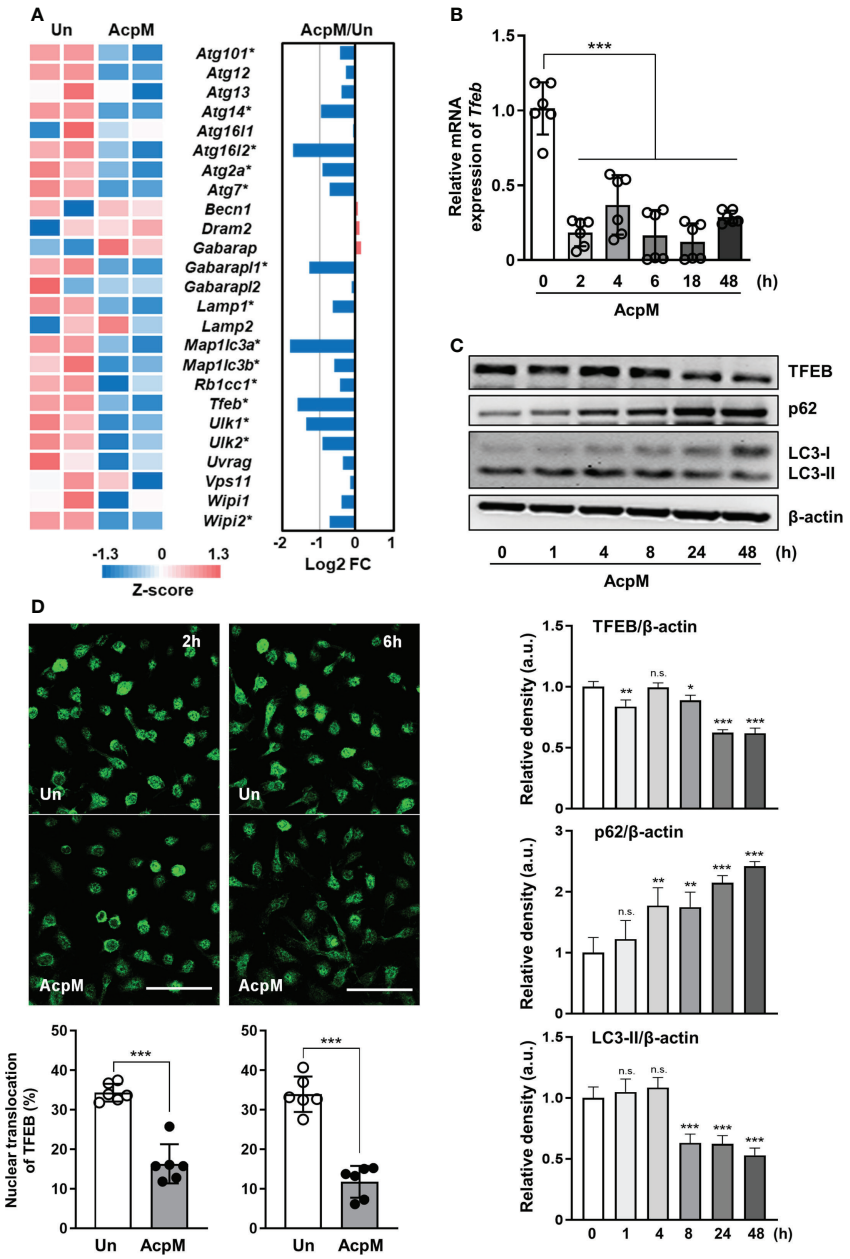

FIGURE 1
AcpM suppresses TFEB expression and its nuclear translocation. **(A)** A heatmap and a bar graph showing the expression of autophagy-associated genes in the AcpM-treated (AcpM, 10 μg/ml for 18 h) and untreated (Un) BMDMs. The left panel heatmap shows relative expression levels for each gene with Z-scores. The bar graph in the right panel depicts the fold change (FC). Gene names with an asterisk indicate statistical significance (FDR < 0.01). **(B, C)** BMDMs were treated with recombinant AcpM (10 μg/ml) for indicated times, and the harvested cells were subjected to either qRT-PCR analysis to measure *Tfeb* mRNA gene expression **(B)** or immunoblot analysis to measure TFEB protein expression **(C)**. One representative image, (**C**, upper panel) and the densitometric analysis (**C**, lower panel) of immunoblots were presented. **(D)** BMDMs treated with recombinant AcpM (10 μg/ml) for 2 or 6 h were harvested and stained with TFEB (green). Then the cells were subjected to confocal microscopy. Representative confocal images (Scale bar: 50 μm) from each group were presented. Statistical analysis was determined with an unpaired *t*-test or one-way ANOVA and presented as means ± SD from at least three independent experiments performed. *$p < 0.05$; **$p < 0.01$; ***$p < 0.001$. a.u., arbitrary unit; n.s., not significant; Un, untreated; AcpM, AcpM-treated.

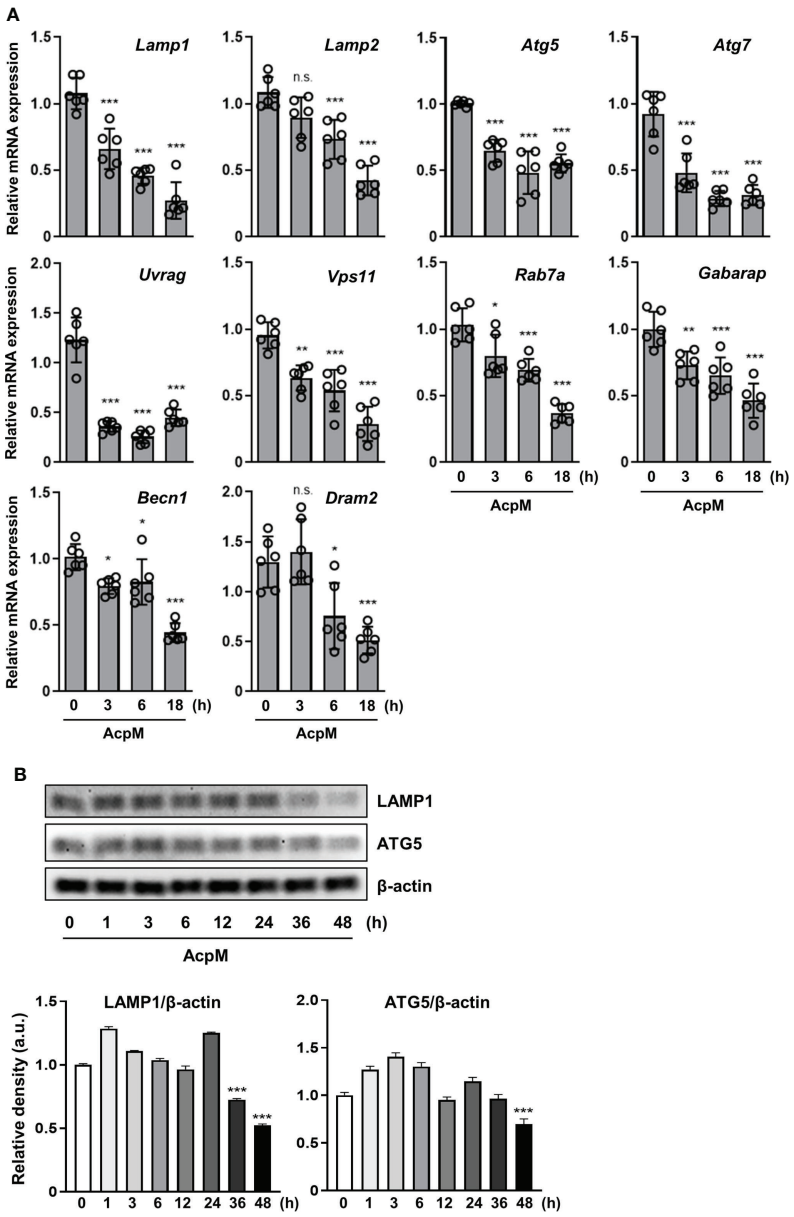

FIGURE 2
AcpM suppresses various autophagy and lysosomal genes. **(A)** BMDMs were treated with recombinant AcpM (10 μg/ml) for the indicated times. Total RNAs extracted from the cells were then subjected to qRT-PCR analysis to measure the expression of autophagic/lysosomal genes. **(B)** BMDMs treated with recombinant AcpM (10 μg/ml) for the indicated times were harvested, lysed, and subjected to immunoblot analysis to measure the LAMP1 and ATG5 expression. The representative image (upper panel) and the densitometric analysis (lower panel) of protein bands were presented. Statistical analysis was determined with one-way ANOVA and presented as means ± SD from at least three independent experiments performed. *$p < 0.05$; **$p < 0.01$; ***$p < 0.001$. a.u., arbitrary unit; n.s., not significant.

time points (Figure 2A). Moreover, both LAMP1 and ATG5 protein levels in BMDMs were significantly reduced at 48 h after AcpM treatment (Figure 2B). Collectively, AcpM addition blocks nuclear translocation of TFEB, thereby downregulating the expression of various autophagy and lysosomal genes in BMDMs.

AcpM inhibits LC3-II/LC3-I ratio, but does not affect autophagic flux in murine macrophages

To determine whether AcpM affected autophagy in murine BMDMs, p62 and LC3 levels were validated by western blotting.

AcpM treatment increased p62 while decreasing the LC3-II band over time (Figure 3A). To confirm the effect of AcpM in autophagic flux, the vacuolar type H^+-ATPase (V-ATPase) inhibitor bafilomycin A1 (Baf-A1) was used. Baf-A1 was added 1 h before AcpM treatment to inhibit the lysosomal activity. After 8 h and 24 h, LC3-II bands in the AcpM-treated cells showed a significant difference in Baf-A1-untreated and -treated conditions, indicating that AcpM had no effect on the basal autophagic flux (Figure 3B). Furthermore, at 24 h after AcpM treatment, p62 levels were higher in Baf-A1-treated cells than in Baf-A1-untreated cells, implying that p62 accumulation in AcpM-treated conditions is not due to a block in autophagic flux. These findings indicate that, while AcpM inhibits LC3-II/LC3-I ratio over time, it has no effect on autophagic flux in BMDMs.

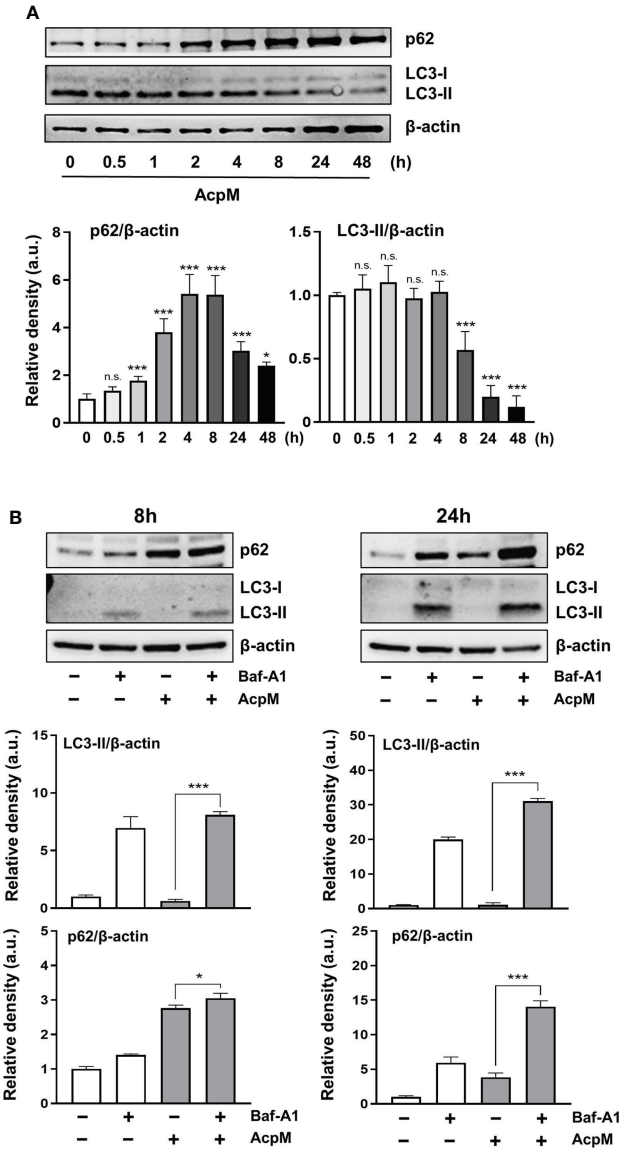

FIGURE 3
AcpM has no effect on autophagic flux in macrophages. **(A)** BMDMs were treated with recombinant AcpM (10 μg/ml) for the indicated times and the cell lysates were subjected to immunoblot analysis. One representative image (upper panel) and the densitometric analysis of the protein bands (lower panel) were presented. **(B)** BMDMs were pretreated with or without Baf-A1 (50 nM) for 1 h and then followed by AcpM (10 μg/ml) treatment. After 8h or 24 h, cells were harvested and subjected to immunoblot analysis with cell lysates. One representative image (upper panel) and the densitometric analysis (lower panel) of immunoblots were presented. Statistical analysis was determined with an one-way ANOVA and presented as means ± SD from at least three independent experiments performed. *$p < 0.05$; ***$p < 0.001$. a.u., arbitrary unit; n.s., not significant.

AcpM suppresses phagosomal maturation of Mtb during infection

The next question was whether adding AcpM protein to Mtb-infected macrophages would affect phagosomal maturation. BMDMs were infected with an Mtb-ERFP strain, which was followed by AcpM treatment in fresh media. The cells were then stained with LAMP1 antibody to visualize lysosomes in confocal microscopy analysis. The colocalizing rate between Mtb and LAMP1 was significantly lower in the AcpM-treated conditions than in the untreated group (Figure 4). Therefore, AcpM helps Mtb circumvent phagosomal maturation by blocking phagosome and lysosome fusion.

AcpM induces Akt-mTOR signaling *via* upregulating SHIP1-targeting miR-155-5p expression

Previous studies have highlighted the importance of miRNAs in the regulation of host immune response (25–27). To see if AcpM was involved in the increase of specific miRNAs, miRNA-seq analysis was performed. The expression rates of miRNA-155p-3p and miRNA-155p-5p were the highest among the miRNAs that showed a significant change in the miRNA-seq analysis of AcpM-treated BMDMs when compared to untreated cells (Figure 5A, Supplementary Table 4). However, the qRT-PCR analysis revealed that miR-155-5p increased more than tenfold with increasing AcpM concentration in BMDMs, while miR-155-3p showed no significant change (Figure 5B). Previous studies showed that SHIP1 prevented Akt phosphorylation, thus blocking the Akt-mTOR pathway (18, 28). Also, as miR-155 was shown to target SHIP1 from an earlier study (Figure 5C) (29), the gene expression and protein amount of SHIP1 was investigated under AcpM treatment in BMDMs. At 3 and 6 h-post AcpM treatment, *Ship1* expressions analyzed with two different primers were significantly suppressed (Figure 5D). In western blot analysis, total SHIP1 expression was also significantly reduced from 3 to 18 h after AcpM administration, which was accompanied by an increase in phosphorylation of Akt and mTOR (Figure 5E). Along with increased Akt phosphorylation, there was also a reduction in FOXO3 levels (Figure 5E). To further demonstrate the ability of AcpM-induced miR-155-5p to regulate SHIP1 expression, miR-155-5p mimic and inhibitor (m155 and i155, respectively), as well as negative controls of miRNA mimic and inhibitor (mNC and iNC, respectively), were transfected into BMDMs. It was discovered that either m155 transfection or AcpM addition suppressed SHIP1 effectively and that i155 transfection could counteract AcpM-induced miR-155-5p expression and restore SHIP1 levels (Figure 5F). Overall, these findings suggest that AcpM-induced miR-155-5p plays a role in Akt-mTOR activation by targeting SHIP1.

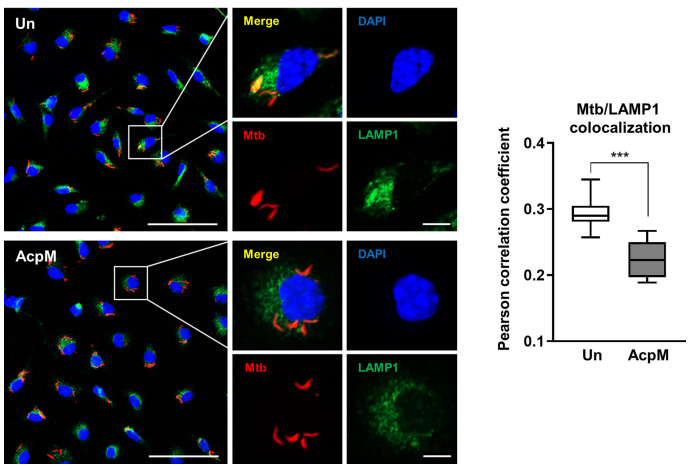

FIGURE 4
AcpM inhibits phagosome-lysosome fusion of Mtb. BMDMs were infected with Mtb-ERFP (MOI 5) for 4 h and then incubated with or without AcpM (10 μg/ml) in the freshly changed media for 4 h. Cells were stained with anti-LAMP1 (green) antibody and DAPI (blue) to visualize fluorescent images using Zeiss LSM-900 confocal microscopy (Scale bar: 50 μm for field views, 5 μm for single cell images). The colocalization rates between Mtb-ERFP and LAMP1 were assessed by calculating Pearson correlation coefficient from 12-15 field images (at least 80 cells per image). Statistical analysis was determined with an unpaired *t*-test and presented as means ± SD from at least three independent experiments performed. ***$p < 0.001$. Un, untreated; AcpM, AcpM-treated.

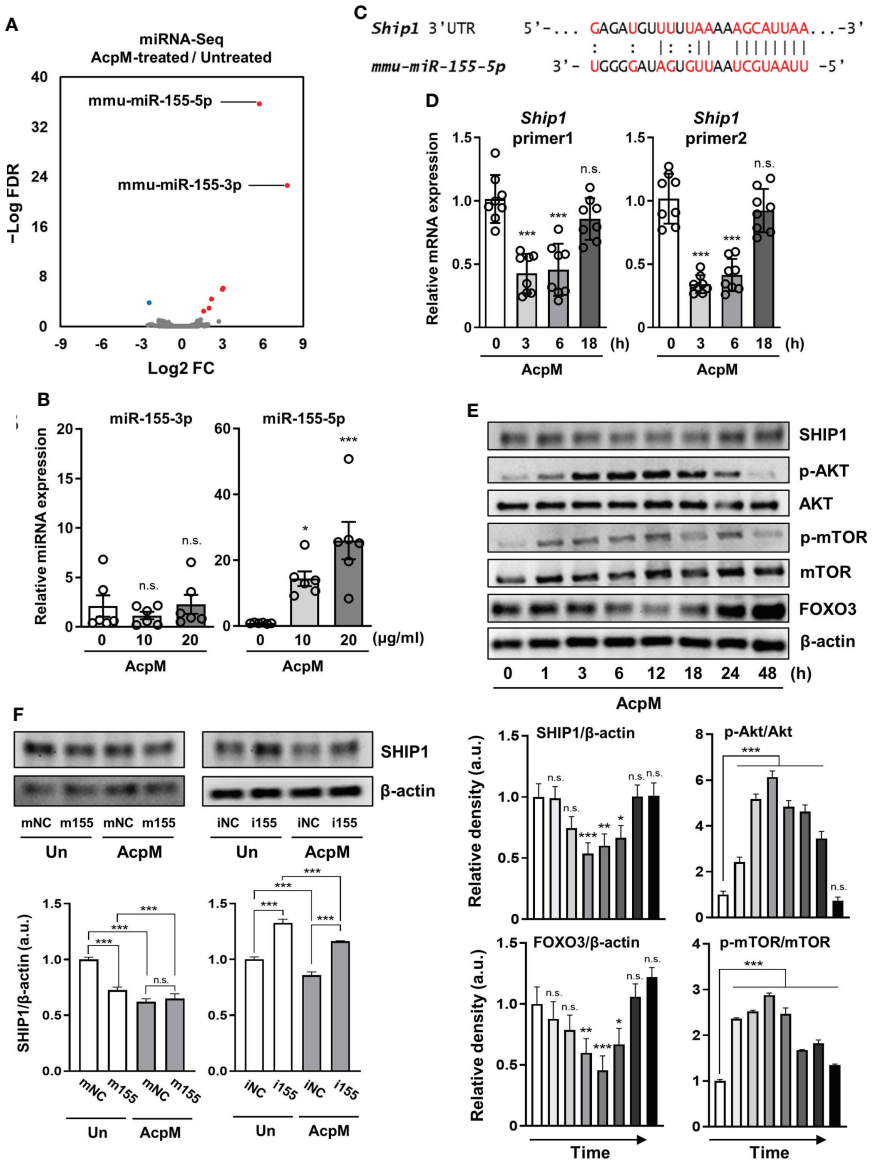

FIGURE 5
AcpM suppresses SHIP1 by increasing miR-155 expression. **(A)** A volcano plot representing differentially expressed miRNAs with the log2-fold change (FC) plotted against the negative log10 false discovery rate (FDR) for the AcpM-treated group compared to the untreated group. Red and blue dots indicate upregulated and downregulated genes, respectively. **(B)** BMDMs were treated with recombinant AcpM (10 or 20 μg/ml) for 8 h and the cell lysates were subjected to qRT-PCR analysis to measure the miR-155-3p and miR-155-5p expression. **(C)** The 3′ UTR of *ship1* mRNA is shown schematically, along with the relative location of the mouse miR-155-5p binding site. **(D, E)** BMDMs were treated with recombinant AcpM (10 μg/ml) for indicated times, and the harvested cells were subjected to either qRT-PCR analysis to determine the gene expression of *Ship1* **(D)** or immunoblot analysis to measure the expression of SHIP1 and SHIP1-downstream signaling molecules **(E)**. The representative image (**E**, upper panel) and the densitometric analysis (**E**, lower panel) of protein bands were presented. **(F)** BMDMs were transfected with mNC, m155, iNC, or i155, then further treated for 8 h with recombinant AcpM (10 μg/ml). Cells were lysed and subjected to immunoblot analysis to determine the SHIP1 protein level. The representative image (upper panel) and the densitometric analysis (lower panel) of SHIP1 bands were presented. Statistical analysis was determined with an unpaired *t*-test or one-way ANOVA and presented as means ± SD from at least three independent experiments performed. $*p < 0.05$; $**p < 0.01$; $***p < 0.001$. a.u., arbitrary unit; n.s., not significant; mNC, negative control of miR-155-5p mimic; m155, miR-155-5p mimic; iNC, negative control of miR-155-5p inhibitor; i155, miR-155-5p inhibitor. Un, untreated; AcpM, AcpM-treated.

AcpM promotes Mtb intracellular survival by inducing the expression of miR-155-5p

Because AcpM inhibited Mtb fusion with lysosomes (Figure 4), Mtb ICS was thought to be increased. As expected, the Mtb CFU level was significantly higher in BMDMs 3 days after AcpM treatment than in the untreated group (Un) (Figure 6A). Furthermore, when i155-transfected groups were compared to iNC-transfected groups, CFU level in the AcpM-treated groups was significantly reduced (Figure 6B). Relative miR-155-5p expression in the same experimental settings as in Figure 6B revealed a positive correlation between the miR-155-5p and the Mtb CFU levels in BMDMs (Figure 6C). According to the findings, AcpM is thought to promote Mtb survival in BMDMs by upregulating miR-155-5p expression.

AcpM overexpression enhances *in-vivo* survival of *M. smegmatis* in C3HeB/FeJ mice

To evaluate the effect of AcpM secretion *in-vivo*, recombinant *M. smegmatis* strains overexpressing AcpM (Ms_AcpM) and a vector plasmid carrying control (Ms_Vec) were used. C3HeB/FeJ mice were challenged with either Ms_Vec or Ms_AcpM *via* nasal route and sacrificed at 1, 4, and 7 days post-infection (dpi). One day after infection, there was no significant difference in CFU levels between lung lysates from two recombinant strains-infected mice, indicating that an equal amount of strains was properly administered through the nasal airways (Figure 7A). However, the viability of Ms_AcpM was significantly higher than that of Ms_Vec at 4 and 7 dpi (Figure 7A), suggesting that AcpM overexpression improves *M. smegmatis in-vivo* survival. Interestingly, qRT-PCR analysis of the samples obtained from the same mice revealed a decrease in several autophagy and lysosomal genes including *Tfeb* (Figure 7B). These data suggest that AcpM overexpression helps *M. smegmatis* survival in mouse lungs, possibly by altering TFEB downstream pathways as shown in murine macrophages.

Discussion

In this study, AcpM, an essential protein for Mtb survival and mycolic acid synthesis (30), was newly discovered as a mycobacterial effector for pathogenesis through blocking TFEB activation and increasing miR-155-5p expression. A schematic summary of the AcpM's suggested mode of action was presented in Figure 8. Previously, the apoptosis inhibiting feature of AcpM was also described (19). In murine BMDM settings, AcpM did not directly affect autophagic flux, but significantly suppressed

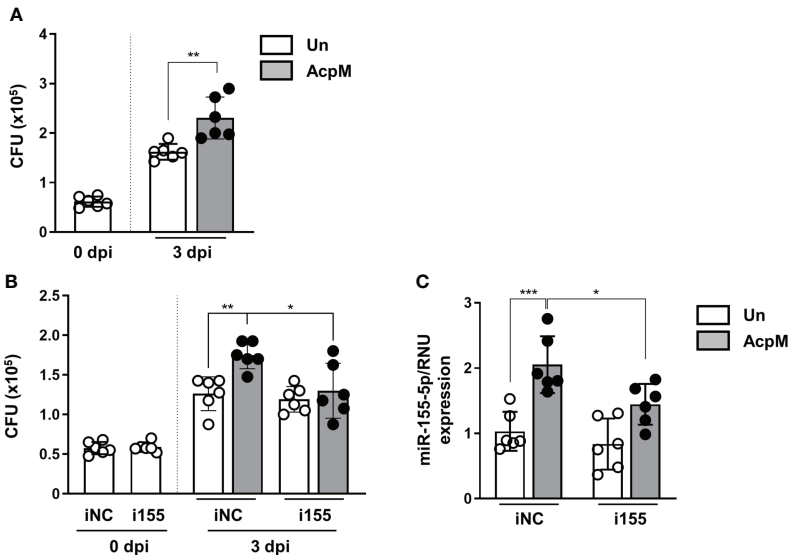

FIGURE 6
AcpM increases intracellular survival of Mtb by miR-155 upregulation. **(A)** BMDMs were infected with Mtb H37Rv (MOI 3) for 4 h and treated with recombinant AcpM (10 μg/ml) in the fresh media. After 3 days, cells were lysed and subjected to a CFU assay to explore the intracellular survival of Mtb. **(B, C)** BMDMs were transfected with either iNC or i155, then infected with Mtb H37Rv (MOI 3) for 4 h before treating recombinant AcpM (10 g/ml) in fresh media. Cells were lysed and subjected to CFU assay at the indicated times **(B)** or qRT-PCR after 18 h **(C)**. Statistical analysis was determined with an unpaired *t*-test and presented as means ± SD from at least three independent experiments performed. *$p < 0.05$; **$p < 0.01$; ***$p < 0.001$. iNC, negative control of miR-155-5p inhibitor; i155, miR-155-5p inhibitor. Un, untreated; AcpM, AcpM-treated.

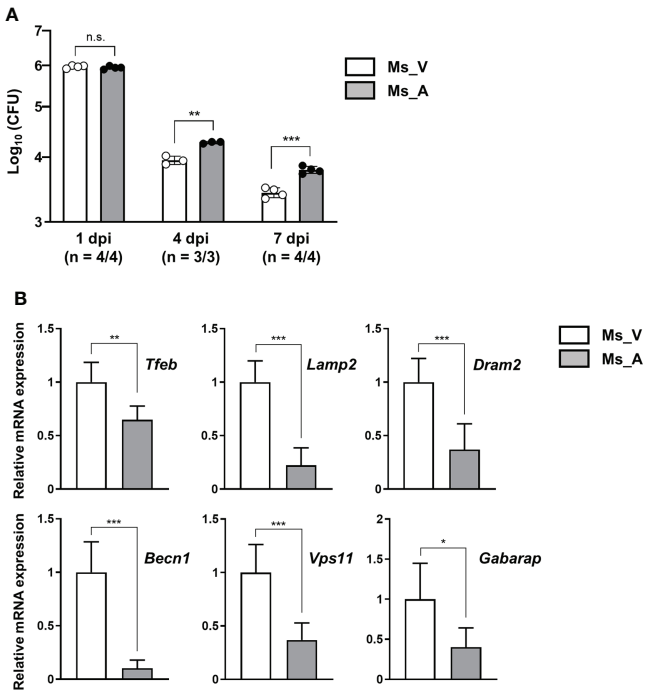

FIGURE 7
AcpM overexpression increases the survival of *M. smegmatis in-vivo*. **(A)** C3HeB/FeJ mice (n = 22) were intranasally infected with recombinant *M. smegmatis* strains Ms_AcpM (n = 11) or Ms_Vec (n = 11) and euthanized at the indicated times after infection (1, 4, or 7 dpi). The lungs were resected from mice to assess the bacterial burden by CFU assay. **(B)** Lung lysates from two randomly selected mice from each group were analyzed in triplicate using qRT-PCR to evaluate the expression level of autophagic/lysosomal genes at 7 dpi. Statistical significances were calculated with an unpaired *t*-test. Data are presented as mean ± SD. $^{*}P < 0.05$; $^{**}P < 0.01$; $^{***}P < 0.001$; a.u., arbitrary unit; n.s., not significant; CFU, colony-forming unit; dpi, days post-infection; Ms_V, Ms_Vec-infected; Ms_A, Ms_AcpM-infected.

multiple autophagy gene expression, which may influence host defense pathways in an autophagy-independent manner. Importantly, we found that the mRNA and protein expression of LAMP1, which is regulated by TFEB (31), was down-regulated by AcpM, suggesting that AcpM affects lysosomal biogenesis during Mtb infection. In addition, our data highlights the AcpM function in the elevation of miR-155-5p, which was shown to target SHIP1 (29, 32, 33). Previous studies showed that SHIP1 plays an essential role in the activation of Akt pathway, thereby enhancing intracellular Mtb survival (18). In addition, miR-155 can target FOXO3 (34), which is associated with the gene expression of multiple autophagy-related genes such as *Atg5*, *Atg12*, *Becn1*, *Lc3* and *Bnip3* (35, 36). However, the role of Mtb-induced miR-155 expression in regulating host defense in the early stages of infection has sparked debate. Wang et al. reported that miR-155 induced autophagy to eliminate intracellular mycobacteria by targeting Ras homolog enriched in brain (Rheb) in RAW264.7 cells (37). Indeed, the miR-155 level is elevated in both Mtb-infected macrophages (37) and active TB patients (38). On the other hand, Rothchild et al. demonstrated that miR-155 promoted Mtb survival in BMDMs through targeting SHIP1 in the early stages of infection, even though it also activated Mtb-specific T cell function in the adaptive immune response to effectively reduce bacterial survival in the late stages of infection (28). Kumar et al. also discovered that overexpression of miR-155 reduced the expression of BTB and CNC homology 1 (BACH1) and SHIP1, allowing Mtb to survive in macrophages (18). These results show a partial correlation with ours that miR-155 favors mycobacterial survival in macrophages by targeting SHIP1-Akt axis. Although the role of miR-155 in host defense regulation varies depending on the host cell type or bacterial strain, it appears that miR-155 inhibits antimicrobial host defense in macrophages in the early stages of infection.

TFEB is known as a master regulator of lysosomal biogenesis (24). Previous research reported that the suppression of the Akt-mTOR pathway enhances nuclear translocation of TFEB to induce transcriptional activation of lysosomal and autophagy-related genes (39, 40). According to our findings, AcpM increased Akt and mTOR phosphorylation (Figure 5E) while decreasing TFEB expression and its nuclear translocation (Figure 1), which likely leads to the downregulation of autophagy and lysosomal genes (Figure 2). Recent studies showed that TFEB activation is critically involved in the

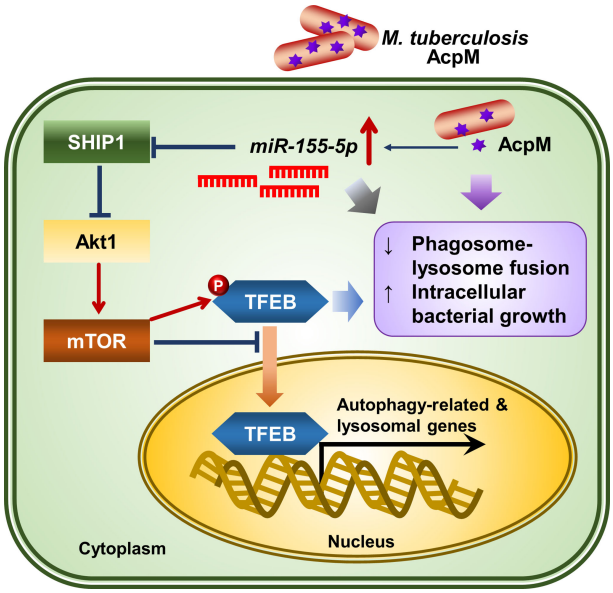

FIGURE 8
The proposed mechanism of action of AcpM in Mtb-infected macrophages. AcpM promotes the expression of miR-155, which targets SHIP1 to activate the Akt/mTOR pathway. The activated Akt/mTOR signaling pathway inhibits TFEB nuclear translocation and reduces the expression of autophagy and lysosomal genes, which is likely to induce antimicrobial defense in macrophages. AcpM also improves intracellular mycobacterial survival by inhibiting phagosome-lysosome fusion.

regulatory node of antimicrobial responses against Mtb in macrophages (41–43). Importantly, we found that AcpM did not affect the induction of autophagy or activation of autophagic flux when treated with Baf-A1 in basal conditions at both 8 h and 24 h after AcpM treatment (Figure 3). Thus, the AcpM's role in the suppression of antimicrobial responses against Mtb infection seems to be associated with the inhibition of TFEB, but not directly related to the suppression of autophagy. In addition, a recent study revealed that TFEB activation is required for the induction of mitochondrial itaconate synthesis to control intracellular bacterial growth (44, 45), suggesting the critical function of TFEB in terms of antimicrobial defense in macrophages. Future studies will clarify whether AcpM is involved in the regulation of immunometabolic remodeling in macrophages to further affect TFEB-induced antimicrobial responses during Mtb infection.

We also found that AcpM increased miR-155 production, which targets SHIP1 to prevent its negative regulation on Akt phosphorylation, resulting in the increased Mtb survival in host cells. Because AcpM-induced miR-155-5p upregulates the Akt/mTOR pathway by targeting SHIP1, it is supposed that miR-155-5p-mediated Akt/mTOR activation leads to the suppression of TFEB activation. Since the level of miR-155 is related to the virulence of infected mycobacterial strains (18, 37), the present data is important to show the function of AcpM as an inducer of miR-155 to further regulate the host protective responses during infection. In this regard, identifying other mycobacterial factors that stimulate miR-155 expression and elucidating the exact mechanism of how mycobacteria activate miR-155 production would help us better understand mycobacterial pathogenesis.

To further understand the function of AcpM during mycobacterial infection, an attempt was made to construct an AcpM-conditional knockout system using the Mtb H37Rv strain. However, we were unable to achieve it, most likely due to the AcpM's essential role in Mtb survival. Thus, *M. smegmatis* strains, Ms_AcpM and Ms_Vec, were used to test if AcpM overexpression could increase the number of surviving bacteria in lung tissues of infected mice. Because *M. smegmatis* strains are non-pathogenic, they have little tolerance for the host's innate immune system. To slow down the declining survival rate of recombinant *M. smegmatis* strains, an *in-vivo* challenge was conducted using C3HeB/FeJ mice (46). As a result, CFU levels of Ms_AcpM were significantly higher than that of Ms_Vec, implying that AcpM overexpression improves the survival of *M. smegmatis in-vivo* (Figure 7A). Thus, AcpM expressed in mycobacteria is likely to suppress the *tfeb* and *tfeb*-downstream autophagy-related gene expression in the lung tissues in the same way that recombinant AcpM protein does in macrophages.

Recently, a small molecule called "8918," which selectively binds to PptT, was discovered to have anti-tuberculosis efficacy comparable to rifampin, a first-line anti-tuberculosis drug (17). In addition, a newly discovered Ppt hydrolase, PptH, which removes Ppt from AcpM, made Mtb more sensitive to 8918, even when PptT was only partially inhibited (17). Therefore, it's

possible to believe that Mtb virulence is influenced by the formation and maintenance of holo-AcpM. Finding small chemical compounds that can selectively target AcpM could be helpful in the development of new anti-mycobacterial drugs.

In summary, AcpM's role in modulating antimicrobial host defense was revealed in this work. AcpM was discovered to effectively reduce TFEB nuclear translocation and downregulate the expression of autophagy and lysosomal genes in macrophages. In addition, AcpM-mediated miR-155-5p activated the Akt/mTOR pathway by targeting SHIP1. AcpM also improved intracellular mycobacterial survival by reducing phagosome-lysosome fusion. These findings highlight the importance of understanding host-pathogen interactions in the context of the Mtb virulence factors and provoke future studies targeting AcpM to expand the development of novel Mtb therapeutics.

Data availability statement

All mRNA-seq and miRNA-seq data generated in this study are available through the NCBI Gene Expression Omnibus through accession numbers SRR18614842-SRR18614845 and SRR18615277-SRR18615280 under BioProject PRJNA823491.

Ethics statement

The animal study was reviewed and approved by Institutional Research and Ethics Committee at Chungnam National University, School of Medicine (202009A-CNU-155; Daejeon, Korea).

Author contributions

SP was in charge of the majority of the data processing and analysis. SP, KK, IK, YK, and H-JK carried out the experiments and data analysis. SP and SC constructed and purified the recombinant AcpM protein and the *M. smegmatis* strains used in this study. SP, KK, IK, and YK wrote the manuscript, which was then peer-reviewed by H-JK and E-KJ. SP and E-KJ guided and supervised the work. All authors contributed to the article and approved the submitted version.

Funding

This work was supported by the National Research Foundation of Korea (NRF) grant funded by the Korean government (MSIT) (No. 2021R1C1C2006968 and 2017R1A5A2015385).

Acknowledgments

We are grateful to Prof. Sung Jae Shin (Yonsei University, Korea) and Prof. Jin Kyung Kim (Keimyung University, Korea) for providing and harvesting Mtb-ERFP, respectively.

Conflict of interest

The authors declare that the research was conducted in the absence of any commercial or financial relationships that could be construed as a potential conflict of interest.

Publisher's note

All claims expressed in this article are solely those of the authors and do not necessarily represent those of their affiliated organizations, or those of the publisher, the editors and the reviewers. Any product that may be evaluated in this article, or claim that may be made by its manufacturer, is not guaranteed or endorsed by the publisher.

Supplementary material

The Supplementary Material for this article can be found online at: https://www.frontiersin.org/articles/10.3389/fimmu.2022.946929/full#supplementary-material

References

1. Liu CH, Liu H, Ge B. Innate immunity in tuberculosis: Host defense vs pathogen evasion. *Cell Mol Immunol* (2017) 14(12):963–75. doi: 10.1038/cmi.2017.88

2. Gengenbacher M, Kaufmann SH. *Mycobacterium tuberculosis*: Success through dormancy. *FEMS Microbiol Rev* (2012) 36(3):514–32. doi: 10.1111/j.1574-6976.2012.00331.x

3. Vergne I, Chua J, Lee HH, Lucas M, Belisle J, Deretic V. Mechanism of phagolysosome biogenesis block by viable *Mycobacterium tuberculosis*. *Proc Natl Acad Sci USA* (2005) 102(11):4033–8. doi: 10.1073/pnas.0409716102

4. Tan T, Lee WL, Alexander DC, Grinstein S, Liu J. The ESAT-6/CFP-10 secretion system of *Mycobacterium marinum* modulates phagosome maturation. *Cell Microbiol* (2006) 8(9):1417–29. doi: 10.1111/j.1462-5822.2006.00721.x

5. Velmurugan K, Chen B, Miller JL, Azogue S, Gurses S, Hsu T, et al. *Mycobacterium tuberculosis nuoG* is a virulence gene that inhibits apoptosis of infected host cells. *PLoS Pathog* (2007) 3(7):e110. doi: 10.1371/journal.ppat.0030110

6. Shin DM, Jeon BY, Lee HM, Jin HS, Yuk JM, Song CH, et al. *Mycobacterium tuberculosis* eis regulates autophagy, inflammation, and cell death through redox-

dependent signaling. *PLoS Pathog* (2010) 6(12):e1001230. doi: 10.1371/journal.ppat.1001230

7. Shukla S, Richardson ET, Athman JJ, Shi L, Wearsch PA, McDonald D, et al. *Mycobacterium tuberculosis* lipoprotein LprG binds lipoarabinomannan and determines its cell envelope localization to control phagolysosomal fusion. *PLoS Pathog* (2014) 10(10):e1004471. doi: 10.1371/journal.ppat.1004471

8. Saini NK, Baena A, Ng TW, Venkataswamy MM, Kennedy SC, Kunnath-Velayudhan S, et al. Suppression of autophagy and antigen presentation by *Mycobacterium tuberculosis* PE_PGRS47. *Nat Microbiol* (2016) 1(9):16133. doi: 10.1038/nmicrobiol.2016.133

9. Hinchey J, Lee S, Jeon BY, Basaraba RJ, Venkataswamy MM, Chen B, et al. Enhanced priming of adaptive immunity by a proapoptotic mutant of *Mycobacterium tuberculosis*. *J Clin Invest* (2007) 117(8):2279–88. doi: 10.1172/JCI31947

10. Zulauf KE, Sullivan JT, Braunstein M. The SecA2 pathway of *Mycobacterium tuberculosis* exports effectors that work in concert to arrest phagosome and autophagosome maturation. *PLoS Pathog* (2018) 14(4): e1007011. doi: 10.1371/journal.ppat.1007011

11. Padhi A, Pattnaik K, Biswas M, Jagadeb M, Behera A, Sonawane A. *Mycobacterium tuberculosis* LprE suppresses TLR2-dependent cathelicidin and autophagy expression to enhance bacterial survival in macrophages. *J Immunol* (2019) 203(10):2665–78. doi: 10.4049/jimmunol.1801301

12. Ge P, Lei Z, Yu Y, Lu Z, Qiang L, Chai Q, et al. *M. tuberculosis* PknG manipulates host autophagy flux to promote pathogen intracellular survival. *Autophagy* (2021), 18(3):576–94. doi: 10.1080/15548627.2021.1938912

13. Quigley J, Hughitt VK, Velikovsky CA, Mariuzza RA, El-Sayed NM, Briken V. The cell wall lipid PDIM contributes to phagosomal escape and host cell exit of *Mycobacterium tuberculosis*. *mBio* (2017) 8(2):e00148-17. doi: 10.1128/mBio.00148-17

14. Birhanu AG, Yimer SA, Kalayou S, Riaz T, Zegeye ED, Holm-Hansen C, et al. Ample glycosylation in membrane and cell envelope proteins may explain the phenotypic diversity and virulence in the *Mycobacterium tuberculosis* complex. *Sci Rep* (2019) 9(1):2927. doi: 10.1038/s41598-019-39654-9

15. Verschoor JA, Baird MS, Grooten J. Towards understanding the functional diversity of cell wall mycolic acids of *Mycobacterium tuberculosis*. *Prog Lipid Res* (2012) 51(4):325–39. doi: 10.1016/j.plipres.2012.05.002

16. Zimhony O, Schwarz A, Raitses-Gurevich M, Peleg Y, Dym O, Albeck S, et al. AcpM, the meromycolate extension acyl carrier protein of *Mycobacterium tuberculosis*, is activated by the 4'-phosphopantetheinyl transferase PptT, a potential target of the multistep mycolic acid biosynthesis. *Biochemistry* (2015) 54(14):2360–71. doi: 10.1021/bi501444e

17. Ballinger E, Mosior J, Hartman T, Burns-Huang K, Gold B, Morris R, et al. Opposing reactions in coenzyme a metabolism sensitize *Mycobacterium tuberculosis* to enzyme inhibition. *Science* (2019) 363(6426):eaau8959. doi: 10.1126/science.aau8959

18. Kumar R, Halder P, Sahu SK, Kumar M, Kumari M, Jana K, et al. Identification of a novel role of ESAT-6-dependent miR-155 induction during infection of macrophages with *Mycobacterium tuberculosis*. *Cell Microbiol* (2012) 14(10):1620–31. doi: 10.1111/j.1462-5822.2012.01827.x

19. Paik S, Choi S, Lee KI, Back YW, Son YJ, Jo EK, et al. *Mycobacterium tuberculosis* acyl carrier protein inhibits macrophage apoptotic death by modulating the reactive oxygen species/c-jun n-terminal kinase pathway. *Microbes Infect* (2019) 21(1):40–9. doi: 10.1016/j.micinf.2018.06.005

20. Kozomara A, Birgaoanu M, Griffiths-Jones S. Mirbase: From microRNA sequences to function. *Nucleic Acids Res* (2019) 47(D1):D155–62. doi: 10.1093/nar/gky1141

21. Langmead B, Salzberg SL. Fast gapped-read alignment with bowtie 2. *Nat Methods* (2012) 9(4):357–9. doi: 10.1038/nmeth.1923

22. Quinlan AR, Hall IM. Bedtools: A flexible suite of utilities for comparing genomic features. *Bioinformatics* (2010) 26(6):841–2. doi: 10.1093/bioinformatics/btq033

23. Robinson MD, McCarthy DJ, Smyth GK. Edger: A bioconductor package for differential expression analysis of digital gene expression data. *Bioinformatics* (2010) 26(1):139–40. doi: 10.1093/bioinformatics/btp616

24. Settembre C, Di Malta C, Polito VA, Garcia Arencibia M, Vetrini F, Erdin S, et al. TFEB links autophagy to lysosomal biogenesis. *Science* (2011) 332 (6036):1429–33. doi: 10.1126/science.1204592

25. Su Z, Yang Z, Xu Y, Chen Y, Yu Q. MicroRNAs in apoptosis, autophagy and necroptosis. *Oncotarget* (2015) 6(11):8474–90. doi: 10.18632/oncotarget.3523

26. Gozuacik D, Akkoc Y, Ozturk DG, Kocak M. Autophagy-regulating microRNAs and cancer. *Front Oncol* (2017) 7:65. doi: 10.3389/fonc.2017.00065

27. Aguilar C, Mano M, Eulalio A. MicroRNAs at the host-bacteria interface: Host defense or bacterial offense. *Trends Microbiol* (2019) 27(3):206–18. doi: 10.1016/j.tim.2018.10.011

28. Rothchild AC, Sissons JR, Shafiani S, Plaisier C, Min D, Mai D, et al. MiR-155-regulated molecular network orchestrates cell fate in the innate and adaptive immune response to *Mycobacterium tuberculosis*. *Proc Natl Acad Sci U.S.A.* (2016) 113(41):E6172–E81. doi: 10.1073/pnas.1608255113

29. O'Connell RM, Chaudhuri AA, Rao DS, Baltimore D. Inositol phosphatase SHIP1 is a primary target of miR-155. *Proc Natl Acad Sci USA* (2009) 106 (17):7113–8. doi: 10.1073/pnas.0902636106

30. Kremer L, Nampoothiri KM, Lesjean S, Dover LG, Graham S, Betts J, et al. Biochemical characterization of acyl carrier protein (AcpM) and malonyl-CoA : AcpM transacylase (mtFabD), two major components of *Mycobacterium tuberculosis* fatty acid synthase II. *J Biol Chem* (2001) 276(30):27967–74. doi: 10.1074/jbc.M103687200

31. Pan HY, Alamri AH, Valapala M. Nutrient deprivation and lysosomal stress induce activation of TFEB in retinal pigment epithelial cells. *Cell Mol Biol Lett* (2019) 24:33. doi: 10.1186/s11658-019-0159-8

32. Wang J, Wu M, Wen J, Yang K, Li M, Zhan X, et al. MicroRNA-155 induction by *Mycobacterium bovis* BCG enhances ROS production through targeting SHIP1. *Mol Immunol* (2014) 62(1):29–36. doi: 10.1016/j.molimm.2014.05.012

33. Rouquette-Jazdanian AK, Kortum RL, Li W, Merrill RK, Nguyen PH, Samelson LE, et al. MiR-155 controls lymphoproliferation in LAT mutant mice by restraining T-cell apoptosis *via* SHIP-1/mTOR and PAK1/FOXO3/BIM pathways. *PLoS One* (2015) 10(6):e0131823. doi: 10.1371/journal.pone.0131823

34. Huang J, Jiao J, Xu W, Zhao H, Zhang C, Shi Y, et al. MiR-155 is upregulated in patients with active tuberculosis and inhibits apoptosis of monocytes by targeting FOXO3. *Mol Med Rep* (2015) 12(5):7102–8. doi: 10.3892/mmr.2015.4250

35. Mammucari C, Milan G, Romanello V, Masiero E, Rudolf R, Del Piccolo P, et al. FOXO3 controls autophagy in skeletal muscle *in vivo*. *Cell Metab* (2007) 6 (6):458–71. doi: 10.1016/j.cmet.2007.11.001

36. Chen Y, Lv L, Pi H, Qin W, Chen J, Guo D, et al. Dihydromyricetin protects against liver ischemia/reperfusion induced apoptosis *via* activation of FOXO3a-mediated autophagy. *Oncotarget* (2016) 7(47):76508–22. doi: 10.18632/oncotarget.12894

37. Wang J, Yang K, Zhou L, Minhaowu, Wu Y, Zhu M, et al. MicroRNA-155 promotes autophagy to eliminate intracellular mycobacteria by targeting rheb. *PLoS Pathog* (2013) 9(10):e1003697. doi: 10.1371/journal.ppat.1003697

38. Wu J, Lu C, Diao N, Zhang S, Wang S, Wang F, et al. Analysis of microRNA expression profiling identifies miR-155 and miR-155* as potential diagnostic markers for active tuberculosis: A preliminary study. *Hum Immunol* (2012) 73 (1):31–7. doi: 10.1016/j.humimm.2011.10.003

39. Settembre C, Zoncu R, Medina DL, Vetrini F, Erdin S, Erdin S, et al. A lysosome-to-nucleus signalling mechanism senses and regulates the lysosome *via* mTOR and TFEB. *EMBO J* (2012) 31(5):1095–108. doi: 10.1038/emboj.2012.32

40. Puertollano R, Ferguson SM, Brugarolas J, Ballabio A. The complex relationship between TFEB transcription factor phosphorylation and subcellular localization. *EMBO J* (2018) 37(11):e98804. doi: 10.15252/embj.201798804

41. Kumar S, Jain A, Choi SW, da Silva GPD, Allers L, Mudd MH, et al. Mammalian Atg8 proteins and the autophagy factor IRGM control mTOR and TFEB at a regulatory node critical for responses to pathogens. *Nat Cell Biol* (2020) 22(8):973–85. doi: 10.1038/s41556-020-0549-1

42. Singh N, Kansal P, Ahmad Z, Baid N, Kushwaha H, Khatri N, et al. Antimycobacterial effect of IFNG (interferon gamma)-induced autophagy depends on HMOX1 (heme oxygenase 1)-mediated increase in intracellular calcium levels and modulation of PPP3/calcineurin-TFEB (transcription factor EB) axis. *Autophagy* (2018) 14(6):972–91. doi: 10.1080/15548627.2018.1436936

43. Kim YS, Lee HM, Kim JK, Yang CS, Kim TS, Jung M, et al. PPAR-alpha activation mediates innate host defense through induction of TFEB and lipid catabolism. *J Immunol* (2017) 198(8):3283–95. doi: 10.4049/jimmunol.1601920

44. Schuster EM, Epple MW, Glaser KM, Mihlan M, Lucht K, Zimmermann JA, et al. TFEB induces mitochondrial itaconate synthesis to suppress bacterial growth in macrophages. *Nat Metab* (2022) 4(7):856–66. doi: 10.1038/s42255-022-00605-w

45. Martina JA, Puertollano R. The IRG1/itaconate/TFEB axis: A new weapon in macrophage antibacterial defense. *Mol Cell* (2022) 82(15):2732–4. doi: 10.1016/j.molcel.2022.06.009

46. Driver ER, Ryan GJ, Hoff DR, Irwin SM, Basaraba RJ, Kramnik I, et al. Evaluation of a mouse model of necrotic granuloma formation using C3HeB/FeJ mice for testing of drugs against *Mycobacterium tuberculosis*. *Antimicrob Agents Chemother* (2012) 56(6):3181–95. doi: 10.1128/AAC.00217-12

frontiers | Frontiers in Immunology

TYPE Original Research
PUBLISHED 29 September 2022
DOI 10.3389/fimmu.2022.974604

Check for updates

OPEN ACCESS

EDITED BY
Marina De Bernard,
University of Padua, Italy

REVIEWED BY
Carmen Amaro,
University of Valencia, Spain
Yongbo Bao,
Zhejiang Wanli University, China

*CORRESPONDENCE
Songlin Chen
chensl@ysfri.ac.cn

†These authors have contributed equally to this work

SPECIALTY SECTION
This article was submitted to Microbial Immunology, a section of the journal Frontiers in Immunology

RECEIVED 21 June 2022
ACCEPTED 05 September 2022
PUBLISHED 29 September 2022

CITATION
Zhou Q, Chen Y, Chen Z, Wang L, Ma X, Wang J, Zhang Q and Chen S (2022) Genomics and transcriptomics reveal new molecular mechanism of vibriosis resistance in fish. *Front. Immunol.* 13:974604. doi: 10.3389/fimmu.2022.974604

COPYRIGHT
© 2022 Zhou, Chen, Chen, Wang, Ma, Wang, Zhang and Chen. This is an open-access article distributed under the terms of the Creative Commons Attribution License (CC BY). The use, distribution or reproduction in other forums is permitted, provided the original author(s) and the copyright owner(s) are credited and that the original publication in this journal is cited, in accordance with accepted academic practice. No use, distribution or reproduction is permitted which does not comply with these terms.

Genomics and transcriptomics reveal new molecular mechanism of vibriosis resistance in fish

Qian Zhou[1,2,3†], Yadong Chen[1†], Zhangfan Chen[1], Lei Wang[1], Xinran Ma[1], Jie Wang[1], Qihao Zhang[1] and Songlin Chen[1,2,3,4*]

[1]Yellow Sea Fisheries Research Institute, Chinese Academy of Fishery Sciences; Key Laboratory for Sustainable Development of Marine Fisheries, Ministry of Agriculture, Qingdao, China, [2]Laboratory for Marine Fisheries Science and Food Production Processes, Pilot National Laboratory for Marine Science and Technology, Qingdao, China, [3]Shandong Key Laboratory for Marine Fishery Biotechnology and Genetic Breeding, Qingdao, China, [4]College of Life Science, Qingdao University, Qingdao, China

Infectious diseases have caused dramatic production decline and economic loss for fish aquaculture. However, the poor understanding of fish disease resistance severely hampered disease prevention. Chinese tongue sole (*Cynoglossus semilaevis*) is an important economic flatfish suffering from vibriosis. Here we used genomic, transcriptomic and experimental approaches to investigate the molecular genetic mechanisms underlying fish vibriosis resistance. A genome-wide comparison revealed that the genes under selective sweeps were enriched for glycosaminoglycan (GAG) chondroitin sulfate (CS)/dermatan sulfate (DS) metabolism. Transcriptomic analyses prioritized synergic gene expression patterns in this pathway, which may lead to an increased CS/DS content in the resistant family. Further experimental evidence showed that carbohydrate sulfotransferases 12 (Chst12), a key enzyme for CS/DS biosynthesis, has a direct antibacterial activity. To the best of our knowledge, this is the first report that the *chst12* gene has a bactericidal effect. In addition, CS/DS is a major component of the extracellular matrix (ECM) and the selection signatures and fine-tuned gene expressions of ECM-receptor interaction genes indicated a modification in the ECM structure with an enhancement of the barrier function. Furthermore, functional studies conducted on Col6a2, encoding a collagen gene which constitutes the ECM, pointed to that it may act as a cellular receptor for *Vibrio* pathogens, thus plays an important role for the *Vibrio* invasion. Taken together, these findings provide new insights into the molecular protective mechanism underlying vibriosis resistance in fish, which offers crucial genomic resources for the resistant germplasm breeding and infectious disease control in fish culturing.

KEYWORDS

vibriosis resistance, molecular mechanism, selective sweep, RNA-Seq, fish disease control, *Cynoglossus semilaevis*

Introduction

Currently, the global food production and security is facing great challenges. Aquaculture plays an increasingly important role in nutrition and food supply. However, infectious diseases are recognized as a major cause of mortality and constitute a major global threat for the production of fish farming (1), and the success and sustainability of fish aquaculture largely depends on the control of diseases (2). Genetic breeding of fish with improved diseases resistance remains a highly sought-after objective in aquaculture (3), providing effective and long-term control over disease problem. To achieve the selective breeding and disease control, it is important to understand the molecular mechanisms determining the resistance of fish to pathogenic microbes.

Conceptually, "disease resistance" refers to the host's ability to reduce pathogen invasion (limitation of pathogen entry into the targe tissue and replication) (1), which in fish encompasses a variety of mechanisms including maintenance of epithelial barriers and the mucus coat; nonspecific cellular factors such as phagocytosis by macrophages and neutrophils; nonspecific humoral factors such as lysozyme, complement, and transferrin; and specific humoral and cellular immunity (4). A number of studies have documented the genetic variations and genes associated with disease resistance in fish. Quantitative trait locus (QTL) mappings and genome-wide association studies (GWAS) allowed detection of the single-nucleotide polymorphisms (SNPs) and genes associated with disease resistance in many fish, such as Atlantic salmon, rainbow trout (2, 5) and Chinese tongue sole (6). Comparative transcriptome analyses of resistant and susceptible fish upon pathogenic infections indicated that transcriptional responses induced by various pathogens generally involved essentially the same genes and pathways in immune systems, such as complement, immune signaling transduction pathways and a number of enzymes and chemokines among Atlantic salmon (7, 8), rainbow trout (9), common carp (10) and Chinese tongue sole (11). While these studies have shown that the resistant and susceptible fish have different genetic architecture and distinct molecular responses after temporary infections, a crucial question that how the fish disease resistance emerges and why the resistant fish can resist the pathogenic infections remains poorly resolved.

Vibriosis, caused by the *Vibrio* genera species such as *V. anguillarum*, *V. alginolyticus*, *V. harveyi*, and *V. splendidus*, is one of the most detrimental infectious diseases for various marine fish and invertebrate. Outbreaks of vibriosis result to 50-100% mortalities in different fish. Chinese tongues sole (*Cynoglossus semilaevis*) is an important and widely cultivated economic flatfish species with delicious taste and superior nutritive value, which is recorded as one of the nine varieties in the national marine fish industry technology system of China (https://www.cafs.ac.cn/info/1024/38584.htm). *C. semilaevis* has suffered from striking production decline caused by its dominant bacterial pathogen *V. harveyi*. In our previous work, we have conducted a successive selective breeding for more than 10 years and produced robust *C. semilaevis* families with high vibriosis resistance (12). This constant selection practice provides a unique opportunity for tracing the evolutionary and molecular basis underlying the acquisition of vibriosis resistance in fish, using the pre-selection and post-selection individuals. It is proposed that divergence in both gene sequence frequencies and gene expressions underpin the phenotypic evolution (13). Combining multiple approaches will lead to cross information, allowing a dissection of the genetic mechanisms of resistance to infections, and contribute to the identification of potential targets of selection for improved resistance (14).

The objective of this study was the identification of the genetic determinants of resistance to vibriosis using the species *C. semilaevis* as a model. With this objective, we sequenced, analyzed and compared the genomes and transcriptomes of selected resistant and sensitive fish. Both the genomic and transcriptomic divergence highlighted the functional potentials of CS/DS metabolism and ECM-receptor interaction in the vibriosis resistance. Additionally, we characterized the expression and defensive functions of crucial genes in the host defense against the bacterial pathogens. These results demonstrated that the selection pressure has acted on specific genes and pathways in mediating the bacterial adhesion and invasion, which may largely account for the improved vibriosis resistance.

Results and discussion

Genome-wide selective sweeps and genes relevant to vibriosis resistance

The selection pressure finally acts on phenotype. To accurately detect the genomic signatures of the selection associated with vibriosis resistance, we measured the genome-wide variations between 74 pre-selection and 108 post-selection *C. semilaevis*. From the genome resequencing data, we detected 3,768,965 single nucleotide polymorphisms (SNPs), among which 1,600,893 SNPs were located in the genic regions, including 51,901 nonsynonymous, 131,463 synonymous and 1,417,529 intronic SNPs. In addition, 2,142,956, 9,050 and 15,254 SNPs were located in intergenic, upstream and downstream and unknown regions, respectively (Supplementary Table S1).

The result of PCA indicated that the pre-selection and post-selection individuals were separately clustered (Figure 1A), which was in line with the phylogenetic relationship revealed by the Neighbor-Joining (NJ) tree (Supplementary Figure S1A). Some individuals in the two groups were overlap clustered. A possible reason is that all the fish were originated from a

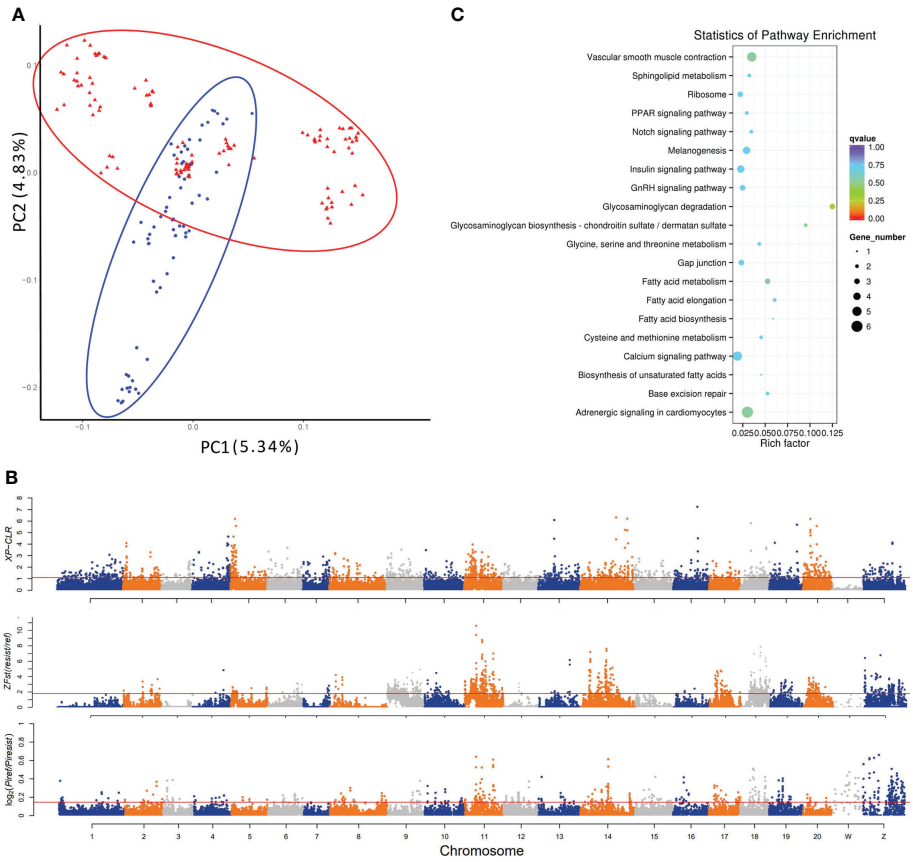

FIGURE 1
Genetic divergence and genome-wide identification of selective sweeps for vibriosis resistance in *C. semilaevis*. A total of 3,768,965 SNPs (MAF > 5%, missing rate < 10%) identified from 182 samples were used. **(A)** PCA shows a genetic divergence between pre-selected (*ref*) and post-selected (*resist*) individuals. The first and second dimensional coordinates are plotted. Pre-selected and post-selected individuals are shown in blue and red colors, respectively. **(B)** Distributions of XP-CLR, *Z* (F_{ST}) and $\theta\pi$ (in $\log_2$ ($\theta\pi$ ratio ($\theta\pi_{ref}/\theta\pi_{resist}$)) values calculated using a 40 kb sliding window with a step size of 20 kb. The dashed horizontal lines correspond to the top 5% values of each measurement (where XP-CLR was 1.10, $Z(F_{ST})$ was 1.82, and $\log_2$ ($\theta\pi$ ratio) was 0.1455). **(C)** Top 20 enriched KEGG pathways for the 207 genes under selective sweep, which were simultaneously identified by XP-CLR, *Z* (F_{ST}) and $\log_2$ [$\theta\pi$ ratio ($\theta\pi_{ref}/\theta\pi_{resist}$)].

relatively small ancestral breeding population, thus some individuals might have a close genetic relationship. This may also partially explain why in the PCA result, the PC2 mainly discriminates the pre- and post-selection individuals. In addition, the genetic stratification was further confirmed using STRUCTURE program, which identified the optimal number of the genetic clusters when the K was set to 2 (Supplementary Figure S1B). These results indicated a genetic divergence correlating with the selection to vibriosis resistance in *C. semilaevis*.

The selected genomic regions are expected to have a reduced allele frequency, elevated differentiation, and lower genetic diversity between genetically diverged groups. To detect the genomic regions and genes with selection signatures, we screened the genome using three distinct metrics of selective sweeps, including XP-CLR, F_{ST} and nucleotide diversity. First, the XP-CLR approach identified a total of 39.5 Mb genomic regions with selective sweep signals, harboring 2011 gene (XP-CLR value greater than 1.1 (top 5%)) (Figure 1B). These genes were enriched in 7 KEGG pathways, including "melanogenesis", "calcium signaling pathway", "tight junction", "phagosome", "GAG degradation", "vascular smooth muscle contraction" and "gap junction" ($p < 0.05$) (Supplementary Table S2). In addition, calculation of z transformation of F_{ST} (top 5%, empirical $F_{ST} \geq 1.82$) identified 170 selective sweeps in a total length of 45.12 Mb (Figure 1B). In these regions, we retrieved 2057 genes that were annotated with KEGG pathways such as "lysine degradation", "notch signaling pathway" and "lysosome" ($p < 0.05$) (Supplementary Table S2). Furthermore, we constructed a genome-wide empirical distribution of the $\log_2$ ($\theta\pi$ ratio ($\theta\pi_{ref}/\theta\pi_{resist}$)) between the pre-selection (ref) and post-selection (resist) groups, and identified 288 selective sweeps (52.98 Mb) that had reduced nucleotide diversity in the post-selection group (5% right tail, where $\log_2(\theta_\pi$ ratio) was 0.145)

(Figure 1B). These regions harbored 2302 genes that were overrepresented in various metabolic and signaling pathways such as "phosphatidylinositol signaling system" and "RIG-I-like receptor signaling pathway" ($p < 0.05$) (Supplementary Table S2).

We found that most of the selective sweeps were distinctly identified or slightly overlapped, and a total of 5.24 Mb genome sequences were simultaneously identified by the three metrics. A total of 207 genes were in these shared selective sweeps (Supplementary Table S3), which were most overrepresented in "GAG degradation" and "GAG biosynthesis-chondroitin sulfate (CS)/dermatan sulfate (DS)" ($p < 0.05$) (Table 1; Figure 1C). CS/DS are representative sulfated GAGs that are widespread on cell surfaces and are abundant in the ECM, where they have essential functions in tissue development and homeostasis and are among the first host macromolecules encountered by infectious agents (15). These results indicated that mutations affecting genes in the CS/DS metabolism pathways may underlie the changes in the vibriosis resistance and provided clues for the functional characterization of the genes responsible for this trait.

Transcriptional differences between the resistant and susceptible groups

Variation in gene expression patterns often plays a key role in the evolution of many complex phenotypes. To explore whether the gene expressions, especially those in the CS/DS metabolism, were regulated, we performed RNA-seq comparisons in gill and skin between the resistant and susceptible families. Both gill and skin are the surface tissues that directly encounter outside stimulations and act as the first line of defense against pathogens.

A total of 653 and 1421 differentially expressed genes (DEGs) were identified in gill and skin, respectively (Supplementary Figure S2). The DEGs included 367 and 1001 down-expressed, and 286 and 420 up-expressed in gill and skin of the resistant family, respectively. The discovery of more than 1000 transcriptional divergent genes indicated that the resistance against vibriosis in *C. semilaevis* might be controlled by multiple genes. This is in line with the results in fish and mammals that a few genes with large range of immune responses control host defense against foreign organisms (16). Moreover, KEGG analyses allowed an identification of the DEGs significantly enriched for "ECM-receptor interaction" in gill, and in "complement and coagulation cascades", "cardiac muscle contraction", "starch and sucrose metabolism" and "aminoacyl-tRNA biosynthesis" in skin (adjusted $p < 0.05$) (Figure 2; Supplementary Table S4).

Interestingly, we observed that the up- and down-expressed genes in gill were enriched for "GAG biosynthesis-CS/DS" and "GAG degradation", respectively (Figure 2; Supplementary Table S5), indicating that the metabolism of CS/DS might be under distinguished regulations between the resistant and susceptible families. These transcriptomic results are as would be predicted from results of the selective sweep analyses, indicating that the artificial selection has substantially changed the genes and gene expressions in the CS/DS metabolism, which may contribute to drive the vibriosis resistance evolution.

CS/DS is a major component of the ECM, which is mainly composed of water, proteins, and polysaccharides. It is notable that the DEGs in both gill and skin were enriched in "ECM-receptor interaction" (Figure 2; Supplementary Table S5, S6), which participates in a wide variety of cellular functions including the homeostasis, inflammation, and response to bacterial infection (17). Our results indicated that this pathway and the involved DEGs might link tightly to the improvement of vibriosis resistance.

CS/DS metabolism and chst12 gene in vibriosis resistance

Both the selective sweep and transcriptomic analyses pinpointed a conspicuous connection of the biosynthesis and degradation of CS/DS to the evolution of vibriosis resistance (Figure 1C, Figure 2). CS/DS has a number of useful biological properties for tissue integration including anti-inflammatory activity, water and nutrient absorption, improved wound healing and biological activity that may help to restore arthritic joint function (18). Previous studies have demonstrated that several pathogens including parasites, bacteria, and viruses can utilize cell surface CS/DS chains to

TABLE 1 Enriched KEGG pathways for the genes in selective sweeps simultaneously identified by XP-CLR, F_{ST} and nucleotide diversity measurements.

#Term	ID	p-Value	qValue
Glycosaminoglycan degradation	dre00531	0.004092	0.286472
Glycosaminoglycan biosynthesis - chondroitin sulfate/dermatan sulfate	dre00532	0.031101	0.534791
Vascular smooth muscle contraction	dre04270	0.033716	0.534791
Fatty acid metabolism	dre01212	0.035902	0.534791
Adrenergic signaling in cardiomyocytes	dre04261	0.038199	0.534791

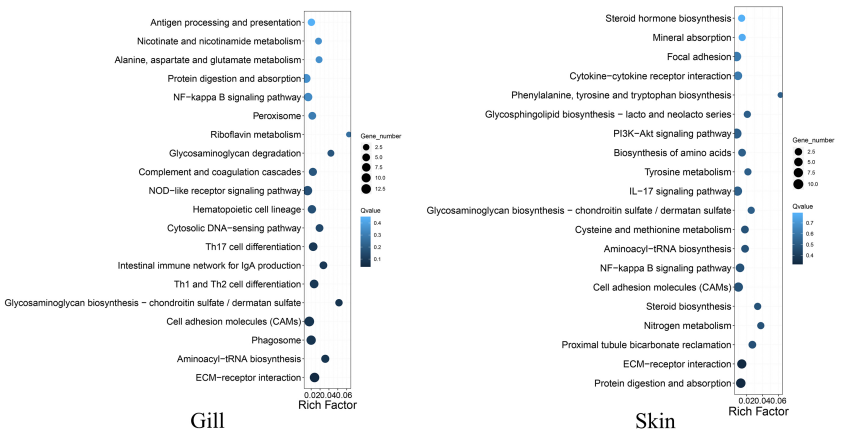

FIGURE 2
Top 20 KEGG pathways enrichments for the DEGs between the resistant and susceptible families of *C. semilaevis*.

attach to and infect host cells (15). For example, CS chains rich in E units can serve as a cell surface receptor in the case of herpes simplex virus (HSV) infection (19). In addition, it has been reported that CS can activate the NF-κB transcription factor in antigen presenting cells and this pro-inflammatory immune response of CS was largely dependent on its molecular size and the degree of acetylation (20).

The tissue CS/DS content depends on both synthesis and degradation of these molecules. Our RNA-seq data showed that *chst12*, *chst15* and *chst11-like* genes exhibited significantly elevated expressions in the resistant families (Figure 3A, left panel). On the contrary, most of the genes pivotal for CS/DS degradation, including alpha-iduronidase (*idua*), arylsulfatase B-like (*arsb-like*) and hyaluronidase-5-like (*hyal5*) were lower-expressed (Figure 3A, right panel). Therefore, not only increased biosynthesis, but also decreased their degradation may contribute to increase the CS/DS content in the resistant family. At genetic level, three genes including *chst15*, *arsb* and *idua*, which have undergone selective sweep, are critically important for the CS metabolism (Figure 3B). For example, *arsb* is required for the hydrolysis of 4-sulfates of the *N*-acetyl-d-galactosamine-4-sulfate units of CS and DS. Therefore, the genetic changes on these genes may have facilitated the regulation in gene expressions and the evolution of the resistance to vibriosis.

The carbohydrate sulfotransferase (Chst) are key enzymes that can catalyze the transfer of sulfate to position 4 of the N-acetylgalactosamine (GalNAc) residue of CS/DS and play a key role in tissue remodeling (21). The Chst12 is one of the CS structure modifying sulfotransferases, which can effectively regulate the levels of CS synthesis (5). Previous studies showed that inhibition of CHST12 promoted inflammation in human bone diseases (22). In zebrafish, Chst12 and other CS/DS modification enzymes are differentially expressed while CS/DS structure varies significantly during development (23). However, very few studies have investigated the role of the sulfotransferase in the host defense against pathogens. Here we first explored the expression characteristics of *chst12* upon bacterial stimulation *in vitro* and *in vivo*. Results showed that the expression of *chst12* was robustly stimulated by lipopolysaccharide (LPS) in both the skin and kidney cells ($p < 0.05$), whereas its response to PBS was modest (Figure 3C). Using the tissue samples removed from the *V. harveyi* infected fish, we observed that the expression of *chst12* varied significantly after the infection. Specifically, in both skin and spleen, the transcript levels of *chst12* gradually increased from 24 hours post infection (hpi), reaching the peak at 72 hpi ($p < 0.05$). In kidney, the peak of expression level appeared at 96 hpi ($p < 0.05$). In gill, intestine and liver, a decreased expression occurred at 12 hpi and maintained at a low level till 96 hpi (Figure 3D). These results indicated that the infection may stimulate the expressions of *chst12* in skin, kidney and spleen, while the expressions in gill and intestine were inhibited. The differential expression patterns in different tissues also indicated that *chst12* gene is a highly responsive gene to the infection of *V. harveyi*, and that CHST12 may play roles in both mucosal and systemic immune processes against the bacterial invasion. Further studies need to be performed to illustrate the specific function of *chst12* gene in the immune responses in different tissues.

We further constructed the Chst12 recombinant protein using *Pichia pastoris* KM71. The molecular weight of the recombinant Chst12 was about 28-30 kDa, which was verified by 12% SDS-PAGE (Figure 3E). Using the Oxford cup method, we found that recombinant Chst12 had an obvious inhibitory ability against both *V. harveyi* and *Edwardsiella tarda* (Figure 3F). Thus, *chst12* gene might play dual roles in the vibriosis resistance both indirectly, by regulating the CS/DS biosynthesis and directly, by inhibiting the bacterial growth. To the best of our knowledge, this is the

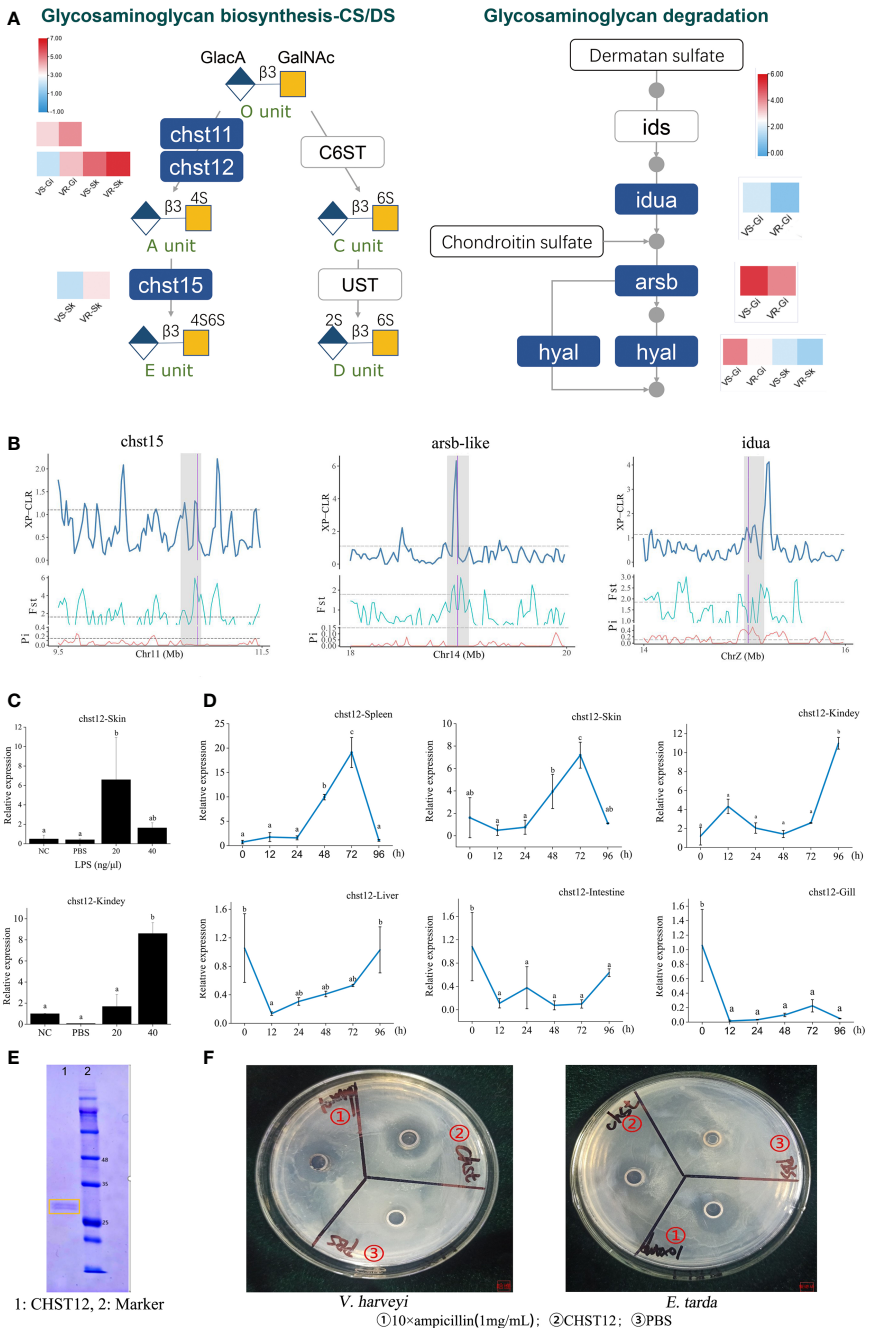

FIGURE 3
Identification of glycosaminoglycan CS/DS metabolism that contribute to improvement of vibriosis resistance. **(A)** Schematic diagram of pathways for biosynthesis (right panel) and degradation (left panel) of CS/DS chains. Heatmaps show the significantly different expression levels of the genes in the resistant (VR) and susceptible (VS) families. Gi: gill, Sk: skin. Ids: iduronate 2-sulfatase; Ust: uronyl 2-O-sulfotransferase; C6ST: chondroitin 6-O-sulfotransferase-1. O unit: GlacA-GalNAc, A unit: GlacA-GalNAc(4S), C unit: GlacA-GalNAc(6S), D unit: GlacA(2S)-GalNAc(6S), E unit: GlacA-GalNAc(4S, 6S). 2S, 4S, and 6S represent the 2-O-, 4-O-, and 6-O-sulfate group, respectively. GalNAc: *N*-acetylgalactosamine, GlcA: glucuronic acid. **(B)** *chst15*, *arsb-like* and *iuda* genes in glysosaminoglycan metabolism pathways were embedded in selective sweeps. The XP-CLR, F_{ST} and $\theta\pi$ ratio values are plotted. Genomic regions located above the dashed line (corresponding to the top 5% values) were termed as strong selective sweeps for the post-selection individuals (grey regions). The boundaries of genes are marked in purple. **(C)** Relative expression levels of *chst12* gene after LPS stimulation, with respect to its background expression levels in kidney and skin cells, respectively. Cells were treated with LPS at 28°C for 2h. **(D)** Time-course relative expressions of *chst12* gene in skin, gill, spleen, liver, kidney and intestine after *V. harveyi* infection. Data are means ± S.D., representing average values of three replicates. Different words indicate significant differences ($p < 0.05$). **(E)** Analysis of recombinant Chst12 by 12% SDS-PAGE. **(F)** Antimicrobial activity of recombinant Chst12 against *V. harveyi* and *E. tarda* using Oxford cup method.

10.3389/fimmu.2022.974604

first report that the *chst12* gene has significant bactericidal impact upon infectious bacterial pathogens. Previous studies have shown that the Chst proteins may play important regulatory roles in a variety of human disease and cancers (24). In addition, evidence showed that Chst genes had the antiviral function and enhanced resistance to white spot syndrome virus in *Procambarus clarkii* (25). Taken together, we identified Chst12 as a significant CHST member which plays an anti-infection role in vibriosis resistance. These results demonstrated that the artificial selection for vibriosis resistance has likely acted at least partly on the genes for CS/DS metabolism, in which the defenses preventing the establishment and invasion of pathogens are caused mainly by fine-tuned modulation of CS/DS and gene antibacterial activity.

ECM-receptor interaction in vibriosis resistance

The genetic and transcriptomic analyses also presented an emphasis on the functional potential of "ECM-receptor interaction" in the vibriosis resistance (Figure 2), involving 15 ECM genes under the selective sweeps, and 16 and 20 DEGs in gill and skin, respectively (Figure 4A; Supplementary Table S7). The intersection of DEGs and selection genes consisted of seven genes, including *col6a2*, *col9a2*, *col28a*, *lamb3*, *fndc7*, *cav3* and *itgb1* (Figure 4A).

ECM composing of several protein components, such as collagen (Col), laminin (Ln), fibronectin, is a complex and dynamic structure that provides the scaffold and surface where complex interactions between invading pathogens, host tissues and immune cells occur (26). A study in oyster has reported that the responses to *Vibrio tasmaniensis* LGP32 infection was characterized by genes in ECM remodeling and other four categories (27). Accumulating evidence have shown that bacterial pathogens bind to different ECM proteins and adhesive matrix molecules, to effectively establish tissue adherence and invasion (28). In this context, Lnα2 acts as a bridge between the host cell and the pathogens, including group B *Streptococcus*, and *Staphylococcus aureus* (29). Similarly, fibronectin has been reported to have a bridging function in the invasion of *S. aureus* (30).

We found that different types of ECM genes systematically exhibited different expression patterns. For example, the Ln protein family comprising about 20 glycoproteins, assemble into a cross-linked web and interweave with the type IV collagen network in basement membranes (31). The Ln-5 (α3β3γ2) isoform is the dominant form that are distributed in the skin in vertebrates. We observed that all the lnα3, β3 and γ2 genes showed higher expressions in the resistant family (Figure 4A), which may indicate an enhanced ECM structure as a physical barrier against the vibrio invasion.

Collagens, constituting of different types that can be subdivided into fibril-forming collagens, network-forming collagens, fibril-associated collagen with interrupted triple helices (FACIT), transmembrane collagens and finally multiplexins. A recent study for steelhead trout (*Oncorhynchus mykiss*) reported that the resistant fish have a different response to parasite infection at the tissue level with the collagenous stratum compactum acting as a barrier preventing parasite spreading (32). We found that the network-forming collagens (type IV collagen) *col4a4* and *col4a5*, which are the major nonfibril structural component of basement membranes, were up-expressed in skin tissue of the resistant families; The fibril-associated collagens with interruptions in their triple helices (FACITs), such as *col6a2*, *col6a3*, *col12a1* and *col28a1* showed down-expressions in skin tissue; All the fibril-forming collagens (e.g., types I, II, III collagen) levels were not different (Figure 4A).

In addition, several other collagen related genes were also differentially expressed. For instance, procollagen galactosyltransferase 1-like, which is involved in the biosynthesis of collagen type IV and facilitates the formation of collagen triple helix, was up-expressed (Figure 4A). The collagenase 3-like gene, which encodes an enzyme that degrades a variety of ECM proteins, including fibronectin, laminin and types III, IV, IX, and X collagen, was also up-regulated (Figure 4A). Therefore, the fine-tuned expressions of these ECM genes indicated ECM remodeling and an alteration in the ECM architecture, which may lead to an enhancement of the barrier function. Furthermore, we measured the expression patterns of three ECM genes including *col6a2*, *col28a* and collagenase3, in response to LPS stimulation in skin cells. All these genes exhibited significant decreased levels with LPS with a higher concentration (40 μg/μL) ($p < 0.05$) (Figure 4B), suggesting that they are responsive to bacterial simulations.

The first event in bacterial invasion requires attachment of the bacteria to the host cells. Pathogens usually take advantage of existing receptor proteins to facilitate opportunistic penetration in hosts. To identify the candidate receptor protein for *Vibrio* species, we exploited the role of an ECM gene *col6a2*, which was down-expressed in both gill and skin of the resistant family, in mediating the bacterial adhesion to host cell. First, to assess whether bacteria can bind to Col6a2, we mixed the recombinant Col6a2 protein with different *Vibrio* pathogens, including *V. parahaemolyticus*, *V. anguillarum* and *V. harveyi*. After removing the unbound Col6a2 protein, the bindings were measured using Western Blot analysis. Clear target bands were detected in all cases (Figure 4C), indicating that these Vibrio pathogens could directly bind to Col6a2 protein. In addition, bacteria-cell adhesion assays based on transfected *col6a2* in HEK293T cells showed that the number of adherent bacteria were significantly increased after the transfection, suggesting that the overexpression of Col6a2 could significantly improve the adhesions of all the three *Vibrio* species to HEK293T cells (Figure 4D). These results showed the Col6a2 had extracellular adhesion activity to *V. parahaemolyticus*, *V. anguillarum* and

10.3389/fimmu.2022.974604

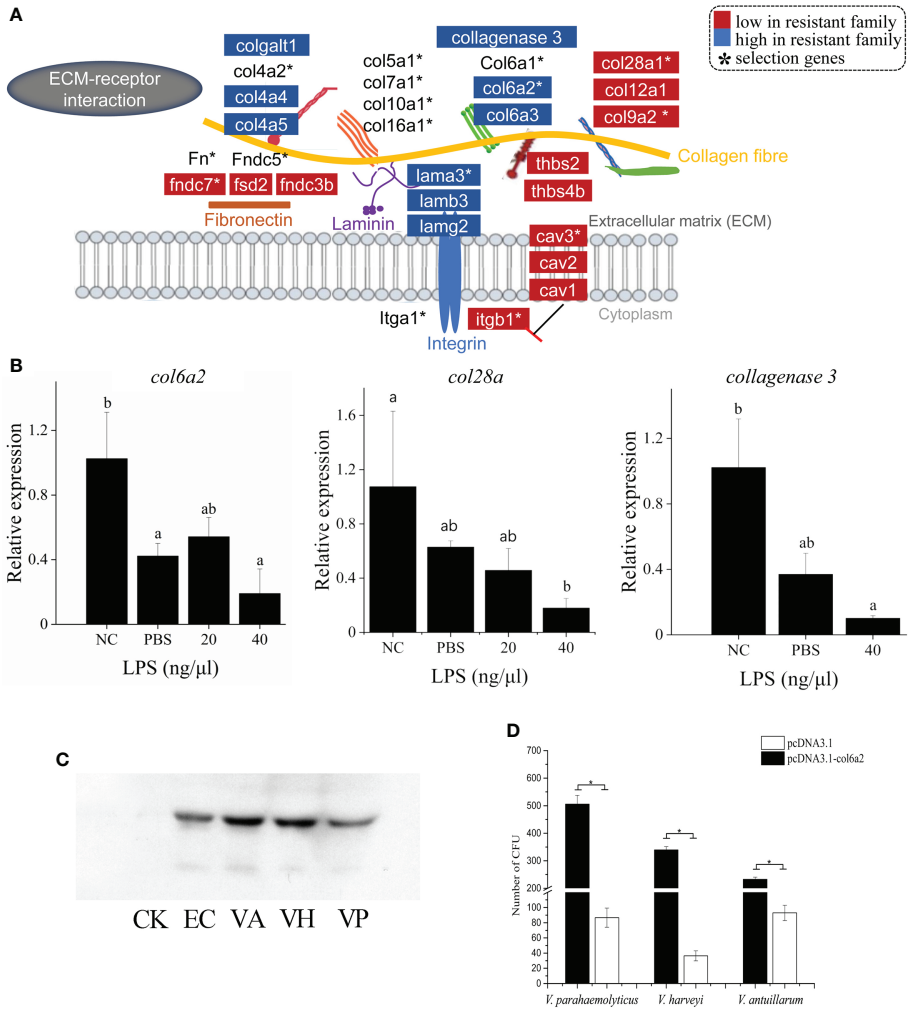

FIGURE 4
ECM-receptor interaction has strong associations with vibriosis resistance and identification of Col6a2 as a *Vibrio* receptor for *C. semilaevis*. **(A)** Schematic of the genetic and transcriptomic divergence in ECM-receptor interaction. Red and blue colors indicate the lower and higher expressed genes in the resistant family compared to susceptible family ($p < 0.05$). * indicates the genes under selective sweeps. **(B)** Relative expressions of *col6a2*, *col28a* and collagenase 3 gene in skin and kidney cells after LPS stimulation. Cells were treated with 20 and 40 ng/μL LPS at 28°C for 2h. The alphabets a, b and c indicate significantly different expressions among the samples ($P < 0.05$). **(C)** Western Blot analysis showed that Col6a2 binds to three *Vibrio* pathogens, including *V. anguillarum*, (*VA*); *V. harveyi*, (*VH*); *V. parahaemolyticus*, (*VP*); *E. coli* (EC) and control (CK). **(D)** Transfections of HEK293T cells with *col6a2* enhanced the *Vibrio* adhesions. * indicate significant differences ($p < 0.05$) of the transfected versus untransfected cells using one-way ANOVA.

V. harveyi, thus may act as a *Vibrio* acceptor that can enhance the bacterial-cell adhesions. Taken together, our data validated that Col6a2 may play a bridging role between the *Vibrio* pathogens and the host cell, and the differential expression patterns of the *col6a2* between the resistant and susceptible families may partly account for their different resistance to *Vibrio* infection.

Together with the multiple levels of evidence and previous study linking ECM genes as a preferred target for Gram-negative bacterial adhesion (29, 30), our data suggest that modulation of ECM structure might be an important tissue protective mechanism contributing to vibriosis resistance. We identified Col6a2 as a receptor for *Vibrio* pathogens, and its lower abundance may limit the *Vibrio* adhesion and invasion in the resistant family.

Conclusions

In this study, we presented the genomic selective signatures and transcriptomic divergence underlying the vibriosis resistance for the *C. semilaevis*. Our results revealed that the selection pressure for resisting *Vibrio* infection may preferentially target genes in the CS/DS metabolism and ECM-receptor interaction pathways, both of which work in mediating

bacterial adhesions and invasions and act as the first barrier of the host defense system. Furthermore, we characterized *chst12* and *col6a2* as critical genes with important functional implications for defense against bacterial infections. These results demonstrated that *C. semilaevi* evolved tissue protective mechanisms as a first defense line preventing invasive vibrio diseases. Our findings provide critical genetic resources facilitating breeding, as well as important knowledge to improve the prevention and treatment of fish infectious diseases.

Materials and methods

Selective breeding and sample preparation

The selective breeding of the vibriosis resistant and susceptible families for *C. semilaevis* were performed as previously described (12). Briefly, we first identified the genetic sex of parental fish by a sex-specific AFLP marker (33), and constructed full-sib families by strip spawning. Each family was tagged with visible implant elastomers and reared in several common tanks under a flow-through system. The pedigree information of each family was precisely recoded to trace their lineages. When fish reached at average size of 10-12 cm, challenge tests were performed by intraperitoneal injection with a medial lethal dose (LD_{50}) of *V. harveyi* ATCC 33843 (12, 34). We recorded the mortality of each family, and the families with a survival rate > 80% and < 30% were considered as Vibrio resistant (VR) and susceptible (VS) families, respectively.

The artificial selections have been performed for successive five generations, and the generated VR and VS families were used for transcriptomic sequencing and comparison. We also sampled the fish in the challenge experiment to analyze their time-course immune responses after *V. harveyi* infection. In addition, to identify the genomic divergence and signatures of selective sweeps underlying the resistance variation, we conducted genome resequencing for 182 tongue soles, including 74 tongue soles from the pre-selection breeding population and 108 fish from the post-selection resistant families, which were sampled in 2012 and 2018, respectively.

Genome re-sequencing and genotyping

Genomic DNA was extracted from the fins using DNeasy Blood & Tissue Kit (Qiagen, Germany). PE libraries with an insert distance of 300 bp were constructed according to the standard protocol (Illumina, USA). The sequencing was performed on Illumina HiSeq platform, producing raw reads in 2×150 bp. The low quality reads were detected and filtered using QC-Chain (35). Finally, the resequencing of the 182 fish yielded a total of 1.39 Tb high-quality data with an average sequencing depth of 13.8 × (Supplementary Table S8).

We used the BWA software (36) to align the clean reads to the reference genome (NCBI Accession No. GCA_000523025.1), with an average mapping rate of 97.79% (Supplementary Table S8). The variants calling was performed with SAMtools (37) and GATK (38) with default parameters, respectively. SNPs identified by both the methods were retained for further analysis. Then the SNPs with minor allele frequency (MAF) > 0.05 and missing rate < 10%, and no departure from Hardy-Weinberg equilibrium ($p < 0.001$) were used for further analyses.

SNP annotation

We used ANNOVAR (39) to annotate the SNPs as coding regions, UTRs, upstream or downstream regions (within 1 kb region from the transcription start or stop site), and intergenic regions. Exonic SNPs were further categorized into synonymous (causing no amino acid changes), nonsynonymous (causing amino acid changes), stop gain or stop loss ones. The SNPs-related genes were functional annotated by KEGG database using BLAST.

Population structure analysis

Principal-component analysis (PCA) of the genetic divergence between the pre-selection and post-selection individuals was performed using GCTA (40) and the first two dimensional coordinates were plotted. An individual-based neighbor-joining tree was constructed using TreeBest (v1.9.2) (41) according to a *p*-distance matrix with a bootstrap value of 1,000. The genetic structure was also examined using the software STRUCTURE (38), setting the pre-defined genetic clusters (K) from 2 to 5. We ran the analysis with 10,000 iterations.

Genome-wide scan of selective sweeps

To detect the candidate selected regions between the pre-selection (original, ORI) and post-selection (resistant, RES) fish, we firstly used a cross-population composite likelihood approach XP-CLR (Chen et al., 2010) to compare the allele frequency distributions with parameters of "-w1 0.005 100 100 –p0 CHR# 0.8". Then we used the program VCFtools (v0.1.14) (42) to estimate the fixation index (F_{ST}) and the nucleotide diversity ($\theta\pi$), which was represented by the $\log_2(\theta\pi$ ratio) of $\theta\pi_{ORI}/\theta\pi_{RES}$, throughout the whole genome. A 40 kb non-overlapping window with a step size of 20 kb, was used to screen the whole genome and the windows containing more

than 10 SNPs were retained. Adjacent windows were merged into a single selective sweep if their distance was less than 200 kb. The windows with top 5% of the maximum XP-CLR, F_{ST} and $\log_2(\theta\pi$ ratio) values were deemed as candidate significant selective sweeps and genes in these regions were defined as selection genes. Additionally, the selection genes locating in the overlapping selective sweeps identified by the three metrics were subjected to KEGG and GO enrichment analyses.

RNA-seq and comparative transcriptomic analyses

To characterize and compare the gene expression patterns, we collected gill and skin tissues from the resistant and susceptible families, respectively. Three replicates for each tissue samples were used for total RNA extraction with TRIzol (Invitrogen, USA). Pair-ended (PE) RNA-seq libraries were constructed using the Truseq mRNA stranded RNA-Seq Library Prep Kit (Illumina, USA) according to the standard protocol. Sequencing of the 30 libraries was conducted with a BGI-Seq500 sequencing platform, generating raw reads with a read length of 2 × 100 bp and an insert size of 350 bp. The quality control of the raw data was performed with RNA-QC-Chain (43) to remove the ambiguous N's, adaptor reads, low quality reads with more than 20% of the bases having a quality score < 20. Finally, we obtained 62.26-79.69 million raw reads per sample, amounting to a total of 86.47 Gb clean data (Supplementary Table S9). The raw reads were deposited at the NCBI sequence read archive (SRA) under project number PRJNA785712.

We aligned the clean reads to the reference genome of *C. semilaevis* (NCBI Accession No. GCA_000523025.1) using BWA (36). The mapping rates varied from 83.9% to 93.1%, averaging 88.6% (Supplementary Table S9). Fragments per kilobase per million mapped sequence reads (FPKMs) value for each gene was calculated with RSEM (v1.2.12) (44). Then we used NOIseq (45) to detect the DEGs, which were defined following the criteria of $|\log_2(\text{Fold Change})| \geq 1$, with a probability ≥ 0.9. Hierarchical heatmaps of the gene expression levels were constructed with Euclidean distance using the Cluster (v3.0) (46).

KEGG enrichment analyses

We conducted KEGG and GO enrichment analyses using phyper in R software, with *Danio rerio* (dre) as the reference species for the KEGG analyses. KEGG pathways and GO terms with *p*-values less than 0.05 were considered enriched, and with FDR of the *p*-value (*q*-value) less than 0.05 to be significantly enriched.

Cell culture and LPS treatment

The skin and kidney cells were cultured using similar methods as previously described (47). Briefly, the cells were derived from the corresponding tissues of the tongue sole, and were maintained at 24°C in L-15 medium with 20% fetal bovine serum (FBS), 100 IU/mL penicillin and 100 μg/mL streptomycin. Cells were subcultured over 3-4 days using standard procedures, and then plated on 12-well culture plates at a density of 3×10^5/well to form a complete monolayer (34). After 24 h, LPS (Sigma-Aldrich, USA) was added to reach final concentrations of 20 and 40 ng/μL, respectively. The control group was treated with PBS. The cells were sampled for RNA isolation at 24 h post treatment.

V. harveyi challenge experiment

To investigate the time-course transcriptomic responses to *V. harveyi* infection *in vivo*, we performed a *V. harveyi* challenge test as previously described (34). Briefly, Around 50 fish were intraperitoneal injected with 1.0×10^4 CFU of a 24 h bacterial culture. Another 50 fish were injected with PBS as the control group. Five individuals were sampled at 0, 12, 24, 48, 72 and 96 hours post infection (hpi). Skin and gill tissues were removed and used for RNA extraction and qPCR analyses.

Quantitative real-time PCR

Total RNAs were extracted using Trizol and reverse transcribed into cDNA with the PrimeScript™ RT reagent Kit with gDNA Eraser (Takara, Japan). The gene expression levels were measured with quantitative real-time PCR (qPCR) using the 7500 Real-Time PCR System (Applied Biosystems, USA). The reaction system consisted of 1 × SYBR Premix Ex Taq, 200 nM each primer, 1 × ROX Reference Dye II (Takara, Japan) and 1 μL of the cDNA template in a final volume of 20 μL, with three replicates for each sample. The PCR conditions were performed as 95 °C for 30 s, followed by 40 cycles for 5 s at 95 °C, and 60 °C for 33 s. The relative expression was analyzed with the $2^{-\Delta\Delta Ct}$ method and the statistical significance ($p < 0.05$) was determined by one-way analysis of variance (one-way ANOVA), followed by a two-sided Dunnett's *post hoc* test.

Recombinant protein expression and purification in *Pichia pastoris*

Based on the information of Chst12 and optimal codons of *Pichia pastoris*, codon optimized *chst12* gene sequence was synthesized and cloned into pMV vector by the Beijing Genomics Institute. The plasmid containing the codon optimized *chst12*

sequence was named pMV-chst12. Then, a pair of primer 9k-chst12F/9k-chst12R was synthesized and used to amplify the target sequence. The product was ligated into the linearized vector pPIC9k precut with *EcoRI* and *NotI* to construct the recombinant plasmid. The resulting constructs pPIC9k-Chst12 was transformed into the *E. coli* DH5α and verified by sequencing. The recombinant plasmid pPIC9k-Chst12 was extracted and linearized with *SalI* followed by transformation with *Pichia pastoris* host strain KM71 using PEG1000 method (48).

The cDNA encoding CDS without signal peptide of Col6a2 was amplified and cloned into T1 vector, and then transformed into *E. coli* DH5α. The *col6a2* with HIS tag was inserted into pic9K Vector (*EcoRI* site) with the help of ClonExpress® Ultra One Step Cloning Kit (Vazyme, China). The positive clones were confirmed using sequencing, the recombinant expression plasmid was extracted and transformed into GS115 using Quick & Easy Yeast Transformation Mix (Takara, Japan).

Transformants were selected for their ability to grow on histidine-deficient minimal dextrose agar plates. In addition, isolation of genomic DNA was performed, and PCR amplifications were then carried out to select positive clones according to Invitrogen's recommendations with a pair of primers (5'AOX1/3'AOX1). For each positive clone, small-scale expression trials were initially performed to identify the most productive transformants and secretion of Chst12 was determined by SDS-PAGE using 10% (w/v) separating gel and 5% (w/v) stacking gel at 96 h after induction with methanol. After treatment with methanol at the final concentration of 1% for 4 days, the cells were pelleted out from the culture medium by centrifugation at 8,000 r/min for 10 min at 4 °C. The supernatant was used to purify the recombinant Chst12 by affinity chromatography using Ni-NTA-agarose resin (49). The purified protein was identified by 12% SDS-PAGE. Primer sequences were listed in Supplementary Table S10.

Antibacterial assay

The antibacterial activity of recombinant protein was tested by the Oxford-cup method. The *V. harveyi* ATCC 33843 and *E. tarda* H1 were cultured in LB medium to OD600 nm = 0.5, and then take 100 μL to spread LB plate. Then placed the sterilized Oxford cups vertically on the surface of the plates. 100 μL 1 mg/mL Ampicillin, 50 μg/mL recombinant protein and PBS were filled into the cups respectively. The plates were cultivated at 37° C for 12 h and then halo of growth inhibition were observed.

Bacteria adhesion to recombinant Col6a2 protein

Three pathogenic *Vibrio* species, including *V. parahaemolyticus, V. anguillarum*, and *V. harveyi*, were cultivated overnight. Then 900 μL bacteria were then combined with 100 μL of recombinant Col6a2 protein and incubated at room temperature (25°C) for 40 min. After centrifugated at 2,000 rpm for 1 min, the precipitate was recovered and submitted to Western blot after being centrifuged at 2,000 rpm for 2 min. SDS-PAGE was used to separate the samples, which were then transferred to the nitrocellulose filter membrane (300 mA for 40 min). The membrane was blocked for 2 h with 5% (w/v) nonfat milk, washed three times with TBST (TBS containing 0.05 percent Tween-20), and then incubated overnight at 4°C with mouse anti-His-tag antibody (the primary antibody, diluted 1: 1000), followed by 1 h incubation with goat anti-mouse HRP-conjugated IgG (the secondary antibody, diluted 1: 1000). After that, the protein was stained with DAB (3, 3'-diaminobenzidine) solution for 10 min. The primary and secondary antibodies were purchased from Beyotime Biotechnology (China).

Bacteria-cell adhesion assays

Human embryonic kidney cell line HEK293T were purchased from Procell (China) and were routinely cultured following American Type Culture Collection (ATCC) culturing conditions, in Dulbecco's modified Eagle medium (supplemented with 10% Foetal Bovine Serum and 1% penicillin/streptomycin) at 37°C with 5% CO_2. The plasmids pcDNA3.1-col6a2 (GFP-tagged) was constructed and used for the overexpression of Col6a2. The transfections of recombinant vector (pcDNA3.1-col6a2) were performed using Lipo8000™ transfection reagent (2 μg DNA and 6 μL Lipo8000) (Beyotime Biotechnology, China). After transfection, the cells were treated with 500 μg/mL G418 for 4 weeks to obtain stable cell lines. All treated samples were observed and captured under Nikon ECLIPSE TE 2000-U fluorescence microscope.

The bacterial and cell adhesion assays were then performed. Briefly, 2×10^5 HEK293T cells per well were seeded into 24-well plates. After culturing overnight, the plates were gently washed with PBS to remove the non-adherent cells. Then 50 μL of the diluted bacteria (10^2-10^3 CFU/mL) was mixed into the cell well and incubated for 30 min. After that, the plates were gently washed with PBS to remove the non-adherent bacteria. The attached cells were then gently harvested with Cell Scrapers and transferred to coated plates with LB for *V. parahaemolyticus* RIMD 2210633 and *V. anguillarum* PF4-E2-R4, and with trypticase soy broth for *V. harveyi* ATCC 33843. After being cultured at 28 °C or 37 °C for 12 h, the colonies were counted with Gel-Pro Analyze v4.0 (Media Cybernetics, USA). Statistical significance ($p < 0.05$) was determined by one-way ANOVA.

Data availability statement

The datasets presented in this study can be found in online repositories. The names of the repository/repositories and

accession number(s) can be found below: https://www.ncbi.nlm.nih.gov/, PRJNA542202.

Ethics statement

The animal study was reviewed and approved by the Animal Care and Use Committee of the Chinese Academy of Fishery Sciences.

Author contributions

QZ and SC conceived the study and designed the analytical strategy. QZ, LW, and QHZ performed animal work and prepared biological samples. QZ analyzed the data. YC performed the cell culture, recombinant protein expression and cDNA transfection experiment. ZC, XM, and JW performed the qPCR experiments. QZ and SC wrote the manuscript. All authors contributed to the article and approved the submitted version.

Funding

This work was supported by National Natural Science Foundation of China (grant number 31973006); Central Public-interest Scientific Institution Basal Research Fund, CAFS [grant number 2020TD20] and Taishan Scholar Climbing Project of Shandong Province of China.

Conflict of interest

The authors declare that the research was conducted in the absence of any commercial or financial relationships that could be construed as a potential conflict of interest.

Publisher's note

All claims expressed in this article are solely those of the authors and do not necessarily represent those of their affiliated organizations, or those of the publisher, the editors and the reviewers. Any product that may be evaluated in this article, or claim that may be made by its manufacturer, is not guaranteed or endorsed by the publisher.

Supplementary material

The Supplementary Material for this article can be found online at: https://www.frontiersin.org/articles/10.3389/fimmu.2022.974604/full#supplementary-material

References

1. Robinson NA, Gjedrem T, Quillet E. Chapter 2 - Improvement of disease resistance by genetic methods. In: Jeney G, editor. *Fish diseases*. Academic Press Salt Lake City (2017). p. 21–50.

2. Yáñez J, Houston RD, Newman S. Genetics and genomics of disease resistance in salmonid species. *Front Genet* (2014) 5:415. doi: 10.3389/fgene.2014.00415

3. Houston RD, Bean TP, Macqueen DJ, Gundappa MK, Jin YH, Jenkins TL, et al. Harnessing genomics to fast-track genetic improvement in aquaculture. *Nat Rev Genet* (2020) 21:389–409. doi: 10.1038/s41576-020-0227-y

4. Blazer, Vicki S. "Nutrition and disease resistance in fish". Annual Review of Fish Diseases. (1992) 309:323.

5. Izumikawa T, Koike T, Kitagawa H. Chondroitin 4-O-sulfotransferase-2 regulates the number of chondroitin sulfate chains initiated by chondroitin n-acetylgalactosaminyltransferase-1. *Biochem J* (2012) 441:697–705. doi: 10.1042/BJ20111472

6. Zhou Q, Su Q, Li YZ, Liu Y, Wang L, Lu S. Genome-wide association mapping and gene expression analyses reveal genetic mechanisms of disease resistance variations in Cynoglossus semilaevis. *Frontiers in Genetics* (2019) 10:1167. doi: 10.3389/fgene.2019.01167

7. Robledo D, Taggart JB, Ireland JH, McAndrew BJ, Starkey WG, Haley CS, et al. Gene expression comparison of resistant and susceptible Atlantic salmon fry challenged with infectious pancreatic necrosis virus reveals a marked contrast in immune response. *BMC Genomics* (2016) 17:279. doi: 10.1186/s12864-016-2600-y

8. Robledo D, Gutiérrez AP, Barría A, Yáñez JM, Houston RD. Gene expression response to Sea lice in Atlantic salmon skin: RNA sequencing comparison between resistant and susceptible animals. *Front Genet* (2018) 9:287. doi: 10.3389/fgene.2018.00287

9. Langevin C, Blanco M, Martin SA, Jouneau L, Bernardet JF, Houel A, et al. Transcriptional responses of resistant and susceptible fish clones to the bacterial pathogen flavobacterium psychrophilum. *PloS One* (2012) 7:e39126. doi: 10.1371/journal.pone.0039126

10. Tadmor-Levi R, Doron-Faigenboim A, Marcos-Hadad E, Petit J, Hulata G, Forlenza M, et al. Different transcriptional response between susceptible and resistant common carp (Cyprinus carpio) fish hints on the mechanism of CyHV-3 disease resistance. *BMC Genomics* (2019) 20:1019. doi: 10.1186/s12864-019-6391-9

11. Xu H, Xu X, Li X, Wang L, Cheng J, Zhou Q. Comparative transcriptome profiling of immune response against Vibrio harveyi infection in Chinese tongue sole. *Scientific Data* (2019) 6(1):224. doi: 10.1038/s41597-019-0231-2

12. Li Y, Wang L, Yang Y, Li X, Dai H, Chen S. Genetic analysis of disease resistance to vibrio harveyi by challenge test in Chinese tongue sole (Cynoglossus semilaevis). *Aquaculture* (2019) 503:430–5. doi: 10.1016/j.aquaculture.2019.01.011

13. Groen SC, Calic I, Joly-Lopez Z, Platts AE, Choi JY, Natividad M, et al. The strength and pattern of natural selection on gene expression in rice. *Nature* (2020) 578:572–6. doi: 10.1038/s41586-020-1997-2

14. Fraslin C, Quillet E, Rochat T, Dechamp N, Bernardet JF, Collet B, et al. Combining multiple approaches and models to dissect the genetic architecture of resistance to infections in fish. *Front Genet* (2020) 11:677. doi: 10.3389/fgene.2020.00677

15. Mikami T, Kitagawa H. Biosynthesis and function of chondroitin sulfate. *Biochim Biophys Acta* (2013) 1830:4719–33. doi: 10.1016/j.bbagen.2013.06.006

16. Breuer K, Foroushani AK, Laird MR, Chen C, Sribnaia A, Lo R, et al. InnateDB: systems biology of innate immunity and beyond–recent updates and continuing curation. *Nucleic Acids Res* (2013) 41:D1228–1233. doi: 10.1093/nar/gks1147

17. Boyd DF, Thomas PG. Towards integrating extracellular matrix and immunological pathways. *Cytokine* (2017) 98:79–86. doi: 10.1016/j.cyto.2017.03.004

18. Wang DA, Varghese S, Sharma B, Strehin I, Fermanian S, Gorham J, et al. Multifunctional chondroitin sulphate for cartilage tissue-biomaterial integration. *Nat Mater* (2007) 6:385–92. doi: 10.1038/nmat1890

19. Uyama T, Ishida M, Izumikawa T, Trybala E, Tufaro F, Bergstrom T, et al. Chondroitin 4-O-sulfotransferase-1 regulates e disaccharide expression of chondroitin sulfate required for herpes simplex virus infectivity. *J Biol Chem* (2006) 281:38668–74. doi: 10.1074/jbc.M609320200

20. Zhang W, Sun F, Niu H, Wang Q, Duan J. Mechanistic insights into cellular immunity of chondroitin sulfate a and its zwitterionic n-deacetylated derivatives. *Carbohydr Polym* (2015) 123:331–8. doi: 10.1016/j.carbpol.2015.01.059

21. Bowman KG, Bertozzi CR. Carbohydrate sulfotransferases: mediators of extracellular communication. *Chem Biol* (1999) 6:R9–R22. doi: 10.1016/S1074-5521(99)80014-3

22. Han J, Li D, Qu C, Wang D, Wang L, Guo X, et al. Altered expression of chondroitin sulfate structure modifying sulfotransferases in the articular cartilage from adult osteoarthritis and kashin-beck disease. *Osteoarthritis Cartilage* (2017) 25:1372–5. doi: 10.1016/j.joca.2017.02.803

23. Habicher J, Haitina T, Eriksson I, Holmborn K, Dierker T, Ahlberg PE, et al. Chondroitin / dermatan sulfate modification enzymes in zebrafish development. *PloS One* (2015) 10:e0121957. doi: 10.1371/journal.pone.0121957

24. Klüppel M.. The roles of chondroitin-4-sulfotransferase-1 in development and disease. *Prog Mol Biol Transl Sci* (2010) 93:113–132. doi: 10.1016/S1877-1173(10)93006-8

25. Zhang L, Shi R, Ouyang H, Li Y. Cloning and characterization of chst11 from Procambarus clarkii involved in the host immune response of white spot syndrome virus and Aeromonas hydrophila. *Fish Shellfish Immunol* (2020) 106:82–91. doi: 10.1016/j.fsi.2020.04.020

26. Singh B, Fleury C, Jalalvand F, Riesbeck K. Human pathogens utilize host extracellular matrix proteins laminin and collagen for adhesion and invasion of the host. *FEMS Microbiol Rev* (2012) 36:1122–80. doi: 10.1111/j.1574-6976.2012.00340.x

27. Rubio T, Oyanedel D, Labreuche Y, Toulza E, Luo X, Bruto M, et al. Species-specific mechanisms of cytotoxicity toward immune cells determine the successful outcome of vibrio infections. *Proc Natl Acad Sci U.S.A.* (2019) 116:14238–47. doi: 10.1073/pnas.1905747116

28. Pizarro-Cerdá J, Cossart P. Bacterial adhesion and entry into host cells. *Cell* (2006) 124:715–27. doi: 10.1016/j.cell.2006.02.012

29. van Wijk XM, Döhrmann S, Hallström BM, Li S, Voldborg BG, Meng BX, et al. Whole-genome sequencing of invasion-resistant cells identifies laminin α2 as a host factor for bacterial invasion. *mBio* (2017) 8(1):e02128-16. doi: 10.1128/mBio.02128-16

30. Fowler T, Wann ER, Joh D, Johansson S, Foster TJ, Höök M. Cellular invasion by staphylococcus aureus involves a fibronectin bridge between the bacterial fibronectin-binding MSCRAMMs and host cell beta1 integrins. *Eur J Cell Biol* (2000) 79:672–9. doi: 10.1078/0171-9335-00104

31. Yue B. Biology of the extracellular matrix: an overview. *J Glaucoma* (2014) 23:S20–23. doi: 10.1097/IJG.0000000000000108

32. Barrett DE, Estensoro I, Sitja-Bobadilla A, Bartholomew JL. Intestinal transcriptomic and histologic profiling reveals tissue repair mechanisms underlying resistance to the parasite ceratonova shasta. *Pathogens* (2021) 10(9):1179. doi: 10.3390/pathogens10091179

33. Chen SL, Li J, Deng SP, Tian YS, Wang QY, Zhuang ZM, et al. Isolation of female-specific AFLP markers and molecular identification of genetic sex in half-smooth tongue sole (Cynoglossus semilaevis). *Mar Biotechnol (NY)* (2007) 9:273–80. doi: 10.1007/s10126-006-6081-x

34. Chen Z, Wang L, Xu X, Zhou Q, Wang J, Chen Y, et al. Molecular cloning and immune characterization of CIITA in artificially challenged Chinese tongue sole (Cynoglossus semilaevis) with vibrio harveyi. *Dev Comp Immunol* (2021) 121:104091. doi: 10.1016/j.dci.2021.104091

35. Zhou Q, Su X, Wang A, Xu J, Ning K. QC-Chain: fast and holistic quality control method for next-generation sequencing data. *PloS One* (2013) 8:e60234. doi: 10.1371/journal.pone.0060234

36. Li H, Durbin R. Fast and accurate short read alignment with burrows-wheeler transform. *Bioinformatics* (2009) 25:1754–60. doi: 10.1093/bioinformatics/btp324

37. Li H, Handsaker B, Wysoker A, Fennell T, Ruan J, Homer N, et al. The sequence Alignment/Map (SAM) format and SAMtools. *Transplant Proc* (2009) 25:1653–4. doi: 10.1093/bioinformatics/btp352

38. McKenna A, Hanna M, Banks E, Sivachenko A, Cibulskis K, Kernytsky A, et al. The genome analysis toolkit: a MapReduce framework for analyzing next-generation DNA sequencing data. *Genome Res* (2010) 20:1297–303. doi: 10.1101/gr.107524.110

39. Wang K, Li M, Hakonarson H. ANNOVAR: functional annotation of genetic variants from high-throughput sequencing data. *Nucleic Acids Res* (2010) 38:e164. doi: 10.1093/nar/gkq603

40. Yang J, Lee SH, Goddard ME, Visscher PM. GCTA: a tool for genome-wide complex trait analysis. *Am J Hum Genet* (2011) 88:76–82. doi: 10.1016/j.ajhg.2010.11.011

41. Li H, Coghlan A, Ruan J, Coin LJ, Heriche JK, Osmotherly L, et al. TreeFam: a curated database of phylogenetic trees of animal gene families. *Nucleic Acids Res* (2006) 34:D572–580. doi: 10.1093/nar/gkj118

42. Danecek P, Auton A, Abecasis G, Albers CA, Banks E, DePristo MA, et al. The variant call format and VCFtools. *Bioinformatics* (2011) 27:2156–8. doi: 10.1093/bioinformatics/btr330

43. Zhou Q, Su X, Jing G, Chen S, Ning K. RNA-QC-chain: comprehensive and fast quality control for RNA-seq data. *BMC Genomics* (2018) 19:144. doi: 10.1186/s12864-018-4503-6

44. Dewey CN, Bo L. RSEM: accurate transcript quantification from RNA-seq data with or without a reference genome. *BMC Bioinf* (2011) 12:323–3. doi: 10.1186/1471-2105-12-323

45. Tarazona S, García F, Ferrer A, Dopazo J, Conesa A. NOIseq: a RNA-seq differential expression method robust for sequencing depth biases. *Univ Southampton* (2012) 17:18. doi: 10.14806/ej.17.B.265

46. Eisen MB, Spellman PT, Brown PO, Botstein D. Cluster analysis and display of genome-wide expression patterns. *Proc Natl Acad Sci U.S.A.* (1998) 95:14863–8. doi: 10.1073/pnas.95.25.14863

47. Zheng Y, Wang N, Xie MS, Sha ZX, Chen SL. Establishment and characterization of a new fish cell line from head kidney of half-smooth tongue sole (Cynoglossus semilaevis). *Fish Physiol Biochem* (2012) 38:1635–43. doi: 10.1007/s10695-012-9660-y

48. Zhang J, Li F, Wang Z, Xiang J. Expression, purification, and characterization of recombinant Chinese shrimp crustin-like protein (CruFc) in *Pichia pastoris*. *Biotechnol Lett* (2007) 29:813–7. doi: 10.1007/s10529-007-9317-6

49. Sun Y, Zhang J, Wang S. Heterologous expression and efficient secretion of chitosanase from *Microbacterium* sp in *Escherichia coli*. *Indian J Microbiol* (2015) 55:194–9. doi: 10.1007/s12088-014-0505-5

Frontiers in Immunology

Explores novel approaches and diagnoses to treat immune disorders.

The official journal of the International Union of Immunological Societies (IUIS) and the most cited in its field, leading the way for research across basic, translational and clinical immunology.

Discover the latest Research Topics

See more →

Frontiers

Avenue du Tribunal-Fédéral 34
1005 Lausanne, Switzerland
frontiersin.org

Contact us

+41 (0)21 510 17 00
frontiersin.org/about/contact